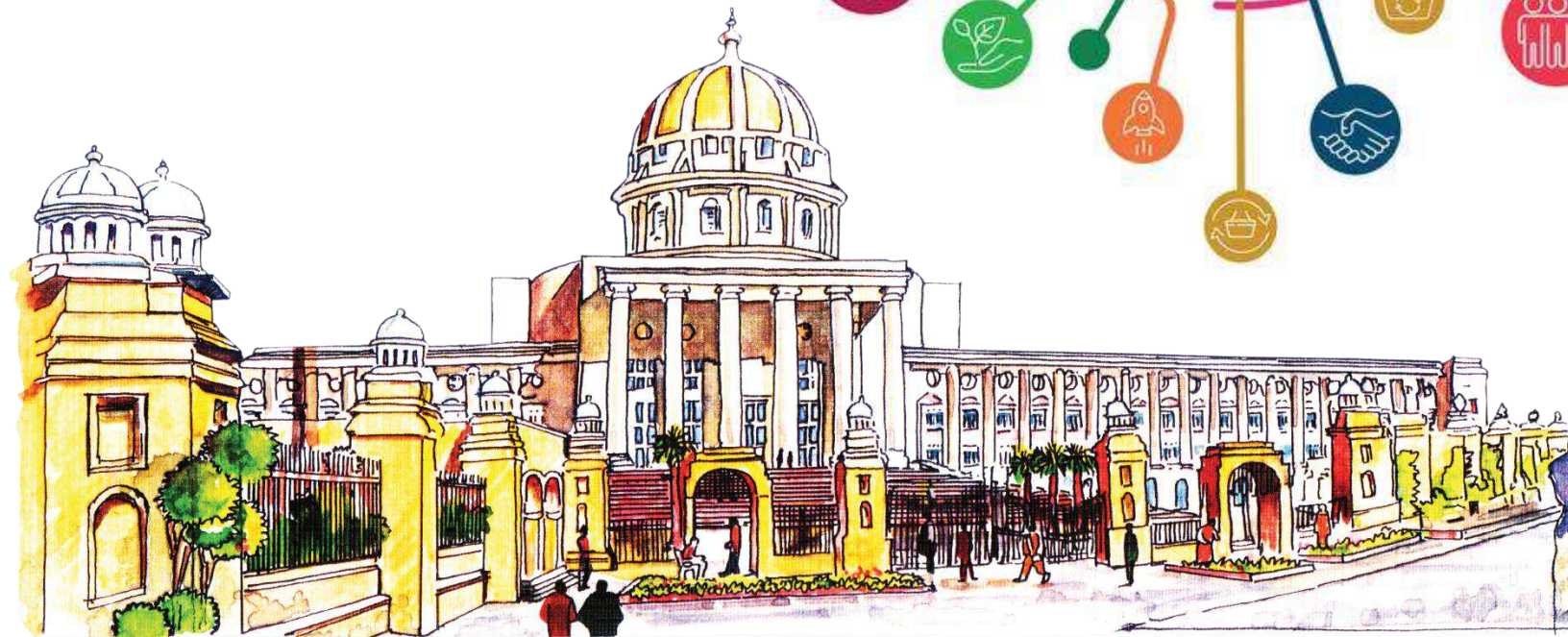




MANIPAL UNIVERSITY
JAIPUR

SDG 15



SUSTAINABLE DEVELOPMENT GOALS

REPORT 2023

15 LIFE ON LAND





MUJ organizes afforestation and biodiversity conservation drives within the campus. The university's eco-club organizes tree plantation drives, and initiatives to preserve flora and fauna of the region are actively encouraged. Research on sustainable agricultural and conservation practices are promoted, demonstrating commitment towards terrestrial ecosystems conservation and biodiversity.



Contents

1. Academics
2. Research
3. Events
4. Collaborations



ACADEMICS



Program/Courses offered in





Sr. No.	Course code	Name of course	Web link of Scheme
1	HA1131	Food Production Lab -I	https://jaipur.manipal.edu/content/dam/manipal/muj/fom/documents/hotelmanagement-eventlist/BHM%20Course%20Structure_2023-27.pdf
2	HA1201	Food Production Foundation -II	https://jaipur.manipal.edu/content/dam/manipal/muj/fom/documents/hotelmanagement-eventlist/BHM%20Course%20Structure_2023-27.pdf
3	HA1231	Food Production Lab -II 0	https://jaipur.manipal.edu/content/dam/manipal/muj/fom/documents/hotelmanagement-eventlist/BHM%20Course%20Structure_2023-27.pdf
4	HA2103	Accommodation Management -I	https://jaipur.manipal.edu/content/dam/manipal/muj/fom/documents/hotelmanagement-eventlist/BHM%20Course%20Structure_2023-27.pdf
5	HA2202	Food &. Beverage Management	https://jaipur.manipal.edu/content/dam/manipal/muj/fom/documents/hotelmanagement-eventlist/BHM%20Course%20Structure_2023-27.pdf
6	HA2133	Accommodation Management Lab 0	https://jaipur.manipal.edu/content/dam/manipal/muj/fom/documents/hotelmanagement-eventlist/BHM%20Course%20Structure_2023-27.pdf
7	HA1203	Travel Agency & Tour Operations	https://jaipur.manipal.edu/content/dam/manipal/muj/fom/documents/hotelmanagement-eventlist/BHM%20Course%20Structure_2023-27.pdf
8	HA4101	Safety, Security and Travel Documentation	https://jaipur.manipal.edu/content/dam/manipal/muj/fom/documents/hotelmanagement-eventlist/BHM%20Course%20Structure_2023-27.pdf
9	HA4102	Hospitality Organizational Behavior	https://jaipur.manipal.edu/content/dam/manipal/muj/fom/documents/hotelmanagement-eventlist/BHM%20Course%20Structure_2023-27.pdf



DIRECTORATE OF STUDENTS' WELFARE

Workshop on MENSTRUAL HEALTH AND HYGIENE

ENVIRO CLUB

Department of Biosciences

OFFLINE EVENT

Date of Event (2nd November 2023)

(11:30 AM to 2:00 PM)

(AB1 Room No.105)

Index

S.No	Activity Heads	Page no.
1.	Introduction of the Event	3
2.	Objective of the Event	3
3.	Beneficiaries of the Event	3
4.	Brief Description of the event	3
5.	Photographs	4-5
6.	Brochure or creative of the event	5
7.	Schedule of the Event	6
8.	Attendance of the Event	6

- **Introduction of the Event**

ENVIRO CLUB organized a ‘**MENSTRUAL HYGIENE AND HEALTH**’ on the 2nd of November 2023. To debunk all the myths and raise awareness for proper hygiene and proper use of sanitary pads.

This event is arranged to break the stigma and form a supporting community.

This event is a collaboration with “Saukhyam” an organization for reusable pads and an initiative started by Sri Mata Amritanandamayi Devi.

- **Objectives of the Event**

- To raise awareness about menstrual hygiene, debunk myths, and promote the use of sustainable sanitary products like reusable pads. It's also aimed at creating a supportive community where these topics can be openly discussed. A truly commendable initiative
- Primarily, it aims to debunk myths surrounding menstrual hygiene, promoting proper sanitary practices. It also seeks to break societal stigmas and create a supportive community where these topics can be discussed openly. Lastly, by partnering with "Saukhyam", the event promotes the use of reusable pads, contributing to environmental sustainability. It's an all-round initiative for health, awareness, and environment.
- To empower people with knowledge and understanding about menstrual hygiene, which is often misunderstood or misrepresented in society. By providing factual and practical information, the event could help to change attitudes and behaviors, leading to better health outcomes and greater equality. And let's not forget the environmental aspect - by promoting the use of reusable pads, the event is also contributing to the fight against plastic waste and promoting sustainability.

- **Beneficiaries of the Event**

- MUJ students and Staff

- **Brief Description of the event**

On the 2nd of November, 2023, the Enviro Club organized a comprehensive workshop on Menstrual Health and Hygiene at Venue AB1, 105. The event featured various segments, including the formal welcome of esteemed guests and attendees, followed by the introduction of Saukhyam and its representative, Ms. Divya Rai.

During her presentation, Ms. Rai enlightened the audience about the paramount importance of menstrual health. She provided insights into Saukhyam's unique approach to manufacturing eco-friendly and biodegradable menstrual pads, utilizing banana fiber. Emphasizing their commitment to sustainability, Ms. Rai highlighted the absence of harmful chemicals in Saukhyam pads.

Furthermore, Ms. Rai elucidated the intricate process involved in crafting these pads and offered detailed instructions on their correct usage. The informative session aimed at raising awareness about sustainable menstrual products proved to be educative for both staff members and students in attendance.

Taking the initiative a step further, Ms. Divya Rai, in collaboration with Dr. Monika Sogani, the faculty coordinator of Enviro Club, decided to randomly distribute samples of Saukhyam pads

among the audience. This strategic move aimed to encourage firsthand experiences and gather genuine feedback from the participants, fostering a dialogue on the efficacy of sustainable sanitary options.

In summary, the Menstrual Health and Hygiene workshop hosted by the Enviro Club served as a platform for introducing Saukhyam and promoting awareness about eco-friendly menstrual pads. The event not only contributed to the dissemination of crucial information but also allowed for practical engagement through the distribution of samples, benefiting both the academic community and staff members alike.

- **Photographs**



- **Brochure or Creative of the Event**



MANIPAL UNIVERSITY
JAIPUR



ENVIRO CLUB



Department of Biosciences

in collaboration with

Department of ECE

and

Atal Incubation Center MUJ,

DIRECTORATE OF STUDENT WELFARE (DSW)

Presents

Awareness Workshop on

Menstrual Health & Hygiene



Speaker : Ms. Divya Rai

(Director, Outreach Programs Saukhyam Reusable Pads.)

Date : 2nd November 2023

Time : 11:30 AM Onwards

Venue : AB1, 105

Convenor :

Dr. Monika Sogani

(Sr. Associate Professor, Department of Biosciences)

(Faculty Coordinator, Enviro club, MUJ)

Dr. Deepika Bansal

(Assistant Professor Department of ECE)



NOV 2
@
11:30 AM

BETTER FOR OUR SEAS, TREES,
OUR BODIES AND OUR WALLETS



DITCHING DISPOSABLES



BEAUTIFUL



BANANA FIBER
SUPER ABSORBENT

NATURAL



AWARDED BY
NITI AAYOG

ESSENTIAL

FOR A MORE WHOLESOME
PERIOD EXPERIENCE

Organiser: **ENVIRO CLUB**

WITH REUSABLE MENSTRUAL PADS



WE COMBAT
CLIMATE CHANGE



SAFEGUARD OUR
HEALTH



SAVE NEARLY
HALF A LAKH OF RUPEES !

To learn more, we invite you to attend our awareness workshop

saukhyampads.org | +91 8971042444 | info@saukhyampads.org

Contact: (Enviro Club) 7807866869

- **Schedule of the event**

2nd November 2023 from 11:30 AM onwards

- **Attendance of the event:**

S No.	Name	Reg. no	Course	Year
1	vanshita	221014003	msc biotech	2
2	bhoomika	221014010	msc biotech	2
3	aditi	221014008	msc biotech	2
4	nandini	211003001	bsc hons microbio	3
5	mrunal	211003007	bsc hons microbio	3
6	ayush	211003012	bsc hons microbio	3
7	durgesh	229302418	btech cse iot	2
8	ankit	221014016	msc biotech	2
9	pranav	229303145	btech cse iot	2
10	rijul	229311015	btech cse iot	2
11	arohi	221014006	msc biotech	2
12	priti	221014004	msc biotech	2
13	tribhuvan	221015077	bca	2
14	megha	23fa10bsp00017	bsc hons psychology	1
15	ayushi	23FM10BBA00184	BBA	1
16	SYLVIA	211003009	BSC microbiology	3
17	Bhumi	23FM10BBA00210	bba	1
18	Simran wadhvani	23FM10BBA00201	BBA	1
19	kusum	23fm20MBA0029	MBA	1
20	NEHA SINGH	23FM20MBA00035	MBA	1
21	Anushka Kesarwani	220903014	bcom hons	2
22	Nidhi Mehata	220903068	bcom hons	2

and all female MIS staff of MUJ (Approx 100).



Assistant Director, DSW

**DIRECTOR STUDENT WELFARE & PROCTOR
MANIPAL UNIVERSITY, JAIPUR**

MUJ/DSW/Student Clubs/2023/Biotech Club MUJ/9thSeptember'23



DIRECTORATE OF STUDENTS' WELFARE

IMPORTANCE OF GUT MICROBE IN HUMAN HEALTH AND DISEASE

Biotech Club, Manipal University Jaipur

Date of Event (9th September 2023)

(Platform: Google Meet)

Index

S.No.	Activity Heads	Page no.
1.	Introduction of the Event	3
2.	Objective of the Event	3
3.	Beneficiaries of the Event	3
4.	Brief Description of the event	3
5.	Photographs	4
6.	Brochure or creative of the event	6
7.	Schedule of the Event	7
8.	Attendance of the Event	7
9.	Event link	9

1. Introduction of the Event

The Biotech Club, Manipal University Jaipur organized an online Bio wellness session on 9th September'23. The convenor – Dr. Mousumi Debnath, Faculty Coordinator, Biotech Club, invited: Mr. Surendra K Chikara, founder and CEO of Bione Ventures Pvt. Ltd., Bengaluru, Mr. Prabhat Nath Jha, professor, BITS Pilani.

This Bio wellness session was organised for students to understand the importance of gut microbes in human health and diseases caused by them. Measures for keeping the body healthy and be deprived of diseases were discussed in meeting.

2. Objectives of the Event

- To increase the awareness about the various microbes found inside the human body, especially the gut and their roles in human health and how can they affect humans due to poor and malnourished diet.
- To discover how minor dietary adjustments can elevate the quality of these microorganisms serves as a catalyst, inspiring students to embrace healthier dietary choices and cultivate a wholesome lifestyle
- To understand the measures implemented to maintain body and keep state of mind healthy
- Understanding the wellness of gut and its environment and with help of an online test called “MyMicroBiome Test”

3. Beneficiaries of the Event

- MUJ students
- BITS PILANI students

4. Brief Description of the event

The Biotech Club at Manipal University Jaipur successfully hosted an enlightening online webinar titled "Importance Of Gut Microbes in Human Health and Diseases," skillfully guided by our esteemed faculty coordinator, Dr. Mousumi Debnath, from the Department of Biosciences. We were honored to welcome the distinguished guest, Mr. Surendra K Chikara, who graced the event with his expertise. The session commenced with an insightful opening address by Dr. Mousumi, setting the stage for an engaging and informative gathering. Dr. Surendra then assumed the role of guest lecturer, sharing his expertise and knowledge with our students.

He delivered a comprehensive presentation, elucidating the pivotal role of gut microbes in human health and disease. Dr. Surendra delved into the diverse array of microbes residing within the human body and the intricate relationship they share with our dietary choices. He expounded on the profound connections between gut microbes, diabetes, and obesity, emphasizing the transformative potential of personalized dietary recommendations in rejuvenating gut health. Dr. Surendra also introduced us to the innovative concept of the MyMicroBiome Test, a tool for analyzing gut health and tailoring balanced diets to maintain its well-being.

The session culminated in an engaging Q&A session, where Dr. Surendra K Chikara addressed students' inquiries, covering topics such as nutrition, gut health-related health issues, and dietary recommendations for nurturing and sustaining a healthy gut. In

closing, heartfelt gratitude was extended to all participants, speakers, and organizers for their invaluable contributions.

The online webinar proved to be an enriching and informative guide to holistic health, leaving a lasting impact on all those who attended.

5. Photographs



Figure 1 Introduction to Speakers



Figure 2 Explanation of topic by Dr. Surendra K Chikara

What is Microbiome

- The human body is host to a vast number of microbes, including bacteria, fungi and viruses, terms as microbiomes
 - ~100 trillion microbes in human intestine
 - 3.3 million nr-genes (150X).
 - 300-1200 species of bacteria in GUT
 - Control almost all body functions
- Microbiome is unique to each person like its DNA
- Importance of GUT Microbiome has been ignored till recently in context to management of chronic disease in human.

www.bione.in

Surendra K is presenting

The Importance of the MICROBIOME by the Numbers

- 90%** - 90% of all diseases are linked to the gut and health of the microbiome.
- 10-100 trillion** - Trillions of organisms (microbes) exist in each person's gut. The number of microbes in the gut is the same as the number of cells in the human body.
- >10,000** - The number of different species of microbes that have been identified in the human body.
- 10X** - The number of microbes in the gut is 10 times more than the number of cells in the human body.
- 100 to 1** - The number of microbes in the gut is 100 times more than the number of cells in the human body.
- 3.3 million** - The number of genes in the human gut microbiome.
- 22,000** - The number of genes in the human genome.
- 80%-90%** - The number of genes in the human gut microbiome is 80-90% of the number of genes in the human genome.
- 99.9%** - The number of genes in the human gut microbiome is 99.9% of the number of genes in the human genome.

Figure 3 Presentation by Mr. Chikara

Zoom meeting grid showing participants:

- Surendra K (Video on)
- Pallavi (Video off)
- Prabhat Nath Jha (Video off)
- You (Video off)
- Mousumi (Video on)
- M (Video off)
- 73 others (Video off)

Figure 4 Final address/ Vote of thanks

6. Brochure or Creative of the Event



**MANIPAL UNIVERSITY
JAIPUR**
(University under Section 2(f) of the UGC Act)



BITS Pilani
Full. Dist. (Incl. Hyderabad)



G20
भारत 2023 INDIA



Biotech Club



MICROBIOLOGISTS SOCIETY OF INDIA
Microbes for Better Tomorrow



AACSB
ACCREDITED

Live Webinar organised by

**DEPARTMENT OF BIOSCIENCES MUJ,
BIOTECH CLUB &
DEPARTMENT OF BIOLOGICAL SCIENCES,
BITS PILANI**

Academia-Industry collaboration

ON

**IMPORTANCE OF GUT MICROBIOME IN
HUMAN HEALTH AND DISEASE**





9th September 2023



4 PM ONWARDS

SCAN TO REGISTER



Conveyors

DR. MOUSUMI DEBNATH
FACULTY COORDINATOR BIOTECH CLUB
DEPARTMENT OF BIOSCIENCES,
MANIPAL UNIVERSITY JAIPUR

PROF. PRABHAT NATH JHA
DEPARTMENT OF BIOLOGICAL SCIENCES,
BITS PILANI, PILANI CAMPUS

OUR SPEAKER:
DR. SURENDRA KUMAR CHIKARA
FOUNDER AND CEO
BIONE VENTURES PVT. LTD.
BENGALURU, KARNATAKA

.....

STUDENT COORDINATORS
ANSHULIKA SAXENA (7080114443)
ANVARSHU GOPAL (9506542226)

7. SCHEDULE OF THE EVENT:

The event was on the 9th September 2023 from 4:00 AM- 5:30 PM on Google Meet.

8. ATTENDANCE OF THE EVENT:

S.No.	Name	Registration No.
1.	Anshulika Saxena	211002053
2.	Prachi Jain	221002016
3.	Anvarshu Gopal	211002011
4.	Anuj Kumar	221002063
5.	Divyanshu Joshi	221002056
6.	Arindam Yadav	221003015
7.	Anshi Agarwal	211002008
8.	Yashvardhan Gupta	221002012
9.	Tanya Barua	221002065
10.	Mohammad Aman	221003012
11.	Poorvi Sharma	221002074
12.	Vaishali Shahi	23FS10BIO00056
13.	Tushar Pareek	23FS10BIO00040
14.	Aishwarya Jaiswal	23FS20MBO00014
15.	Pari Tayal	23FS10BIO00049
16.	Simran maharshi	23FS20MBO00022
17.	Garima	23FS20MBO00011
18.	Nikita	23FS20MBO00018
19.	Prashant pradhan	23FS20MBO00015
20.	Tanishka	23FS10BIO00048

21.	Riya ranjan	23FS10MIC00009
22.	Akshara Alex	23FS10BIO00022
23.	Priya Agarwal	23FS10BIO00042
24.	Pragya Chauhan	23FS10BIO00006
25.	Kanushree Rathore	23FS10BIO00055
26.	Juhi Garg	23FS10BIO00036
27.	Aishwarya Rai Saxena	23FS10BIO00065
28.	Radhika Rathore	23FS20MBO00008
29.	Lavanya	23FS20MBO00002
30.	Faizan Khan	23FS10BIO00009
31.	Shreyas M Iyer	2020PHXF0005P
32.	Simran Khushwaha	2018PHXF0406P
33.	Muskan Yadav	211002040
34.	Rochita Bani	211002039
35.	Samrat Banerjee	211003008
36.	Priya sharma	2023PHXP0001P
37.	Abhimanyu kumar	2023PHXP0002P
38.	Shivani Tiwari	211002002
39.	Sakshi Gupta	2023H1290008P
40.	Dikshita Aneja	231051005
41.	Siddharth	2020B1A31392P
42.	Yasaswini Reddy S	2020B1A71892P
43.	Harsh khandan	2020B1A40601P
44.	Anisha Saini	f2021B1TS2072P

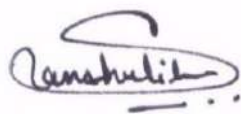
45.	Ayush	2020B1A70623P
46.	Archi Jain	2020B1A71380P
47.	Ameya Aglawe	2020B1A41913P
48.	Suhani Gupta	23FE10CSB00027
49.	Adya	23FS10BIO00067
50.	Sahil Kumar	23FS10BIO00046
51.	Namrata Yadav	23FS10BIO00032
52.	Anukriti sharma	23FS10BIO00052
53.	Ragini Singh Thakur	23FS10BIO00051
54.	Akash Chandra	211002036
55.	Avyakt Garg	2020B1A71902P
56.	Sahaj Tandi	2020B1A31904P
57.	Sylvia Parveen	211003009
58.	Anushka Singh	211002003
59.	Divya	211002056
60.	Gourav verma	2FS10BIO00017
61.	Kashish jain	230115700
62.	Gaurav Jetlie	23FS10MIC00003
93.	Thati Ameta	23FS10BIO00031
64.	Abhishek	2020B1A81914P
65.	Saksham Kumar	23FS10BIO00059
66.	Rohan Sharda	2020B1A31610P
67.	Nitya gupta	23FS10BIO00039
68.	Jaspreet Marwaha	23FS10MIC00011

69.	Tejas Sangale	23FE10BTE00034
70.	Aditi Mukherjee	230106036
71.	Garima	230111382
72.	Asmi Dhadiwal	23FE10BTE00013
73.	Sheryl	23FS10BIO00021
74.	Krishnendra Singh	23FS10BIO00014
75.	Soumya	23FS10BIO00002
76.	Sakshi Nirmal	211002060
77.	Stephenie Namchyö	230108439
78.	Bhumika Agarwal	23FS10MIC00010
79.	Arun Ramanathan	2020B1A41907P
80.	Ishpreet Singh	2020B1A40651P
81.	Nihal Panchal	23FS10BIO00010
82.	Shivali Sharma	23FS10MIC00012
83.	Jayraj Kuntal	23FS10BIO00018
84.	Samarth Trivedi	2020B1A71605P
85.	Gautam chikkara	MT230007
86.	Vanisha Sharma	230201821
87.	Harshita	211003011
88.	Smita Dey	2019PHXF0419P
89.	Sanyam Gupta	2020B1A31910P
90.	Mona singh	23FS10BIO00035
91.	Avinash Gautam	RU2119424
92.	Jyoti yadav	BU0210257546

93.	Gargi	23FS20MBO00026
94.	Anirudha Kumar Sahu	2018PHXF0408P
95.	Deeya Pradhan	23FS10BIO00023
96.	Jigyasha Rishu	23FS10BIO00012
97.	Mariyam khan	23FS10BIO00027
98.	Soubhik Ghosh	221002009
99.	Aditi Rathore	221002036
100.	Tanisha Singh	221002003

9.POST EVENT LINK:

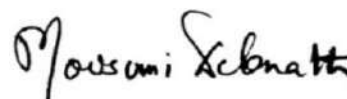
<https://meet.google.com/okc-uans-dpd>



Anshulika Saxena

President, Biotech Club MUJ

Signature of the Student Coordinator



Dr. Mousumi Debnath

School of Basic Sciences

Signature of the Faculty Coordinator





**MANIPAL UNIVERSITY
JAIPUR**

Department of Interior Design

FACULTY OF DESIGN

Make & Take

Kokedama

Hands-on Workshop

22/11/2023



Content of Report

1. Introduction of the Event
2. Objective of the Event
3. Beneficiaries of the Event
4. Details of the Guests
5. Brief Description of the event
6. Photographs
7. Poster of an Event
8. Schedule of the Event
9. Attendance of the Event
10. Link of the event



1. Introduction of the Event

The Department of Interior Design, Faculty of Design at Manipal University Jaipur organized a Kokedama Workshop on 22.11.2023, as a part of the curriculum for 3rd-year B.Des (ID) students. This workshop was conducted under the subject Interior Landscape (ID3105) to provide students with a practical, hands-on experience in the art of preparing Kokedamas. Along with 3rd year B. Des students, this workshop is open for all Manipal University Jaipur students (Diploma, Undergraduate and Postgraduate), Research Scholars, Academicians, Faculty Housing Women, And Industry Professionals with fees of Rs 300/- that included all the materials.

An introduction and demonstration to Kokedama was given by Ms. Geeta Ahluwalia, General Secretary, Kitchen Garden Association, Jaipur. Kitchen Garden Association is an all women lead non-profit organisation in Jaipur. Ar. Sneh Singh (HoD Interior Design) along with Ar. Megha Prabhu K (Asst. Professor, Interior Design) conducted a hands-on 'Make & Take' Kokedama Workshop.

2. Objective of the Event

- Provide 3rd-year B. Des (ID) students with a hands-on experience in the preparation of Kokedamas.
- Enhance the understanding of interior landscaping principles among participants and foster practical skills in crafting Kokedamas, focusing on plant selection, soil composition, and wrapping techniques.
- Facilitate knowledge exchange and collaboration among participants from diverse academic backgrounds, including students, research scholars, academicians, and industry professionals.
- Encourage creativity and innovation in Interior Design through the exploration of Japanese moss ball planters.
- Provide a platform for participants to engage in a Q&A session, allowing for a deeper understanding of the art of Kokedama.
- Create a supportive and inclusive learning environment for all attendees, fostering a sense of community and collaboration within Manipal University Jaipur.



3. Beneficiaries of the Event

The workshop was open to a diverse audience, including 3rd-year B.Des(ID) students, students from other programs (Diploma, Undergraduate, and Postgraduate) at Manipal University Jaipur, research scholars, academicians, Faculty Housing Women, and industry professionals. The inclusive nature of the workshop aimed to foster collaboration and knowledge exchange among participants.

4. Details of the Guests

The honoured guest for the event was Ms. Geeta Ahluwalia, the Secretary of the Kitchen Garden Association Jaipur. Kitchen Garden Association is an all women lead non-profit organisation in Jaipur. Ms. Ahuwalia's expertise in the field brought a valuable perspective to the workshop, and her presence added significant value to the overall learning experience for the participants.

5. Brief Description of the event

The Kokedama workshop provided a unique opportunity for participants to explore the creative and technical aspects of crafting Kokedamas, which are Japanese moss ball planters. The event kicked off with a warm welcome to all attendees, followed by an insightful introduction to the art of Kokedama and its relevance in interior design.

Participants were guided through the step-by-step process of creating their own Kokedamas, emphasizing the selection of suitable plants, soil composition, and wrapping techniques. Ms. Ahuwalia shared her expertise and provided practical tips, enriching the learning experience for everyone involved.

6. Photographs of the Event



Introduction and Demonstration given by Expert, Ms. Geeta Ahluwalia



Demonstration of Kokedama given by Expert, Ms. Geeta Ahluwalia



Participants showcasing their works

7. Poster of the event



The poster features a green background with large leaf graphics. At the top left is the Manipal University Jaipur logo. At the top right are two icons: '11 SUSTAINABLE CITIES AND COMMUNITIES' and '15 LIFE ON LAND'. The central image shows a person's hands planting a green plant into a moss ball. Below this image is a text box with the following text: 'DEPARTMENT OF INTERIOR DESIGN, FACULTY OF DESIGN IS ORGANISING A HANDS-ON WORKSHOP ON'. The main title 'Kokedama' is in a large, elegant font, followed by the subtitle 'Make & Take Interior Landscape'. A paragraph describes Kokedama as a traditional Japanese art form. Below this are two columns of text: 'List of Materials provided to you:' with a bulleted list, and 'Expert Lecture on:' with a bulleted list. To the right of these lists is a section for 'Details of the Workshop:' with icons for date, time, venue, and registration fee. At the bottom left, there is a call to action to register by 19.11.2023 and a QR code for a Google Form. At the bottom right is a QR code.

MANIPAL UNIVERSITY
JAIPUR

11 SUSTAINABLE CITIES AND COMMUNITIES

15 LIFE ON LAND

DEPARTMENT OF INTERIOR DESIGN,
FACULTY OF DESIGN
IS
ORGANISING A HANDS-ON WORKSHOP ON

Kokedama

Make & Take Interior Landscape

Kokedama, a traditional Japanese art form, transforms plants into living sculptures, encased in moss and twine, suspended like hanging gardens – a harmonious blend of nature and artistry, where plants seem to defy gravity. These captivating green orbs bring an enchanting touch of Zen to any space, inviting serenity and connection with the natural world.

List of Materials provided to you:

- Plants: Ferns and Pothos
- Soil Mix: Peat moss and Clay Soil
- Sheet Moss
- Twine or String
- Scissors
- Plastic Wrap
- Decorative Accent: Miniature figurines

Expert Lecture on:

- How to make Kokedama
- The creative process
- The benefits and aftercare

In collaboration with the Kitchen Garden Association.
It is an all-women-led Non-Profit Organization.

Details of the Workshop:

 Date: 22nd November 2023

 Time: 10:30 am onwards

 Venue: Porch Area, First Floor, Administrative Building

 Registration Fee: Rs. 300
(Inclusive of all materials)

REGISTER YOUR SPOT BY 19.11.2023!
VISIT THE QR CODE FOR GOOGLE FORM



8. Schedule of the event

'Make & Take' Kokedama Workshop 22 November 2023, Wednesday	
Porch Area, 1 st Floor, Administration Building, MUJ	
Time	Event
09:30 am	Registration and Reporting
10:30 am	Welcome address by Ar. Megha Prabhu Karkala Introduction of the Guest Address by Dean, Prof. (Dr.) Madhura Yadav, Dean, FoD
10:45 am	Expert Lecture and Introduction to Kokedama by Ms. Geeta Ahuwalia
11:00 am	Practical Session: Crafting Kokedamas
11:30 am	Making Kokedamas by students
12:45 pm	Completion of Kokedamas and Q&A Session
01:00 pm	Felicitation of Ms. Geeta Ahuwalia and Closing Remarks
01:15 pm	Group Photographs and Exhibition of Students works

9. Attendance of the Event

Sl.No	Participate Name	Participant	Department	Registration No.
1	Kashish Kriplani	Student	B.Des (Interior Design)	210606041
2	Kartik Totla	Student	B.Des (Interior Design)	210606011
3	Aakash Singh	Student	B.Des (Interior Design)	210501007
4	Garima Vijaycharan	Student	B.Des (Interior Design)	210606021
5	Kumari Anjali	Student	B.Des (Interior Design)	210606008
6	Himanshi Sharma	Student	B.Des (Interior Design)	210606028
7	Esha Giri	Student	B.Des (Interior Design)	210606031
8	Anisha Chopra	Student	B.Des (Interior Design)	210606020
9	Rutu Shah	Student	B.Des (Interior Design)	210606007
10	Anushka Rai	Student	B.Des (Interior Design)	210606019
11	Rishika	Student	B.Des (Interior Design)	210606029
12	Paridhi Verma	Student	B.Des (Interior Design)	210606017
13	Naman	Student	B.Des (Interior Design)	210606013
14	Diya Ramchandani	Student	B.Des (Interior Design)	210606039
15	Krishangee Goyal	Student	B.Des (Interior Design)	210606026
16	Avinash Yadav	Student	B.Des (Interior Design)	210606047
17	Himanshi Yadav	Student	B.Des (Interior Design)	210606014
18	Hridyanshi Vyas	Student	B.Des (Interior Design)	210606018
19	Khushi Bhargava	Student	B.Des (Interior Design)	210606010
20	Madhu Tanwar	Student	B.Des (Interior Design)	210606027
21	Riddhi Agarwal	Student	B.Des (Interior Design)	210606038
22	Michelle Earnest	Student	B.Des (Interior Design)	210606043



MANIPAL UNIVERSITY JAIPUR

23	Pooja Jain	Student	B.Des (Interior Design)	23fd10bid00020
24	Shreshtha Gaur	Student	B.Des (Interior Design)	210606012
25	Geetika Gupta	Student	B.Des (Interior Design)	210606037
26	Manya Agarwal	Student	B.Des (Interior Design)	210606015
27	Riya	Student	B.Des (Interior Design)	210606035
28	Ananya Thakan	Student	B.Des (Interior Design)	210606006
29	Devanshi Jain	Student	B.Des (Interior Design)	210606046
30	Drishti Sharma	Student	B.Des (Interior Design)	210606045
31	Sejal Sharma	Student	B.Des (Interior Design)	210606023
32	Samarth Gandhi	Student	B.Des (Interior Design)	210606003
33	Saija Tanya	Student	B.Des (Interior Design)	210606044
34	Garvit Garg	Student	B.Des (Interior Design)	210606001
35	Shruti Dubey	Student	B.Des (Interior Design)	210606022
36	Keshav Katta	Student	B.Des (Interior Design)	210606005
37	Grishma Korjani	Student	B.Des (Interior Design)	210606016
38	Shweta Sharma	Non-Teaching Staff	Non- Teaching Staff	MUJ1134
39	Megha Prabhu Karkala	Assistant Professor	Faculty of Design	MUJ1434
40	Smriti Saraswat	Assistant Professor	Faculty of Design	MUJ1248
41	Dr. Shilpi Gupta	Assistant Professor	Department of Economics	MUJ0403
42	Malini G Prabhu	Faculty Housing Member	Faculty Housing Member	NA
43	Rajendar Kumar	Non-Teaching Staff	GSA	MUJ1300
44	Reetika Choudary	Non-Teaching Staff	Admission Department	MUJ1406
45	Priyanka Samarth	Non-Teaching Staff	Admission Department	MUJ1408
46	Panchami Sharma	Non-Teaching Staff	HR Department	MUJ11002438
47	Kusuma Jinka	Faculty Housing Member	Faculty Housing Member	NA
48	Madan	Non-Teaching Staff	GSA	
49	Gopal	Non-Teaching Staff	GSA	
50	Kush Jee Kamal	Assistant Professor	Faculty of Design	MUJ1714
51	Man Mohan Mehta	Non-Teaching Staff	Admission Department	MUJ0170



MANIPAL UNIVERSITY JAIPUR

Manipal University Jaipur				
Department of Interior Design I FOD				
II Year III Semester - ID3105-Interior Landscape				
KOKEDAMA WORKSHOP - 22.11.2023				
Sl. No.	ROLL No.	NAME	SIGN	
1	210606001	GARVIT GARG		
2	210606003	SAMARTH GANDHI		
3	210606004	VISHVA SAMIRBHAI DAVE	- ABSENT -	
6	210606005	KESHAV KATTA		
5	210606006	ANANYA THAKAN		
6	210606007	RUTU DILIP KUMAR SHAH		
7	210606008	KUMARI ANJALI		
8	210606010	KHUSHI BHARGAVA		
9	210606011	KARTIK TOTLA		
10	210606012	SHRESHTHA GAUR		
11	210606013	NAMAN HODKASIA	- ABSENT -	
12	210606014	HIMANSHI YADAV		
13	210606015	MANYA AGARWAL		
14	210606016	GRISHMA KORJANI		
15	210606017	PARIDHI VERMA		
16	210606018	HRIDIYANSHI VIRESH VYAS		
17	210606019	ANUSHKA RAI		
18	210606020	ANISHA CHOPRA		
19	210606021	GARIMA VIJAY CHARAN		
20	210606022	SHRUTI DUBEY		
21	210606023	SEJAL SHARMA		
22	210606026	KRISHANGEE GOYAL		
23	210606027	MADHU TANWAR		
24	210606028	HIMANSHI SHARMA		
25	210606029	RISHIKA		
26	210606031	ESHA GIRI		
27	210606034	KREETI YADAV	- ABSENT -	
28	210606035	RIYA GAUTAM ROY		
29	210606036	HRIDAY SINGH	- ABSENT -	
30	210606037	GEETIKA GUPTA		
31	210606038	RIDDHI AGARWAL		
32	210606039	DIYA RAMCHANDANI		
33	210606041	KASHISH KRIPLANI		
34	210606043	MICHELLE EARNEST		
35	210606044	SAIJA TANYA		
36	210606045	DRISHTI SHARMA		
37	210606046	DEVANSHI JAIN		
38	210606047	AVINASH YADAV		
39	210501007	AKASH		

Manipal University Jaipur				
Department of Interior Design				
Faculty of Design				
KOKEDAMA WORKSHOP - 22.11.2023				
Sl. No.	MUJ ID/ Roll No	NAME	Department	SIGN
1	MUJ1300	Rajendra Kumar	GS/SP	
2	MUJ1406	Reetika Choudhary	Admission	
3	MUJ1408	Rajendra Kumar	Admission	
6				
5	MUJ1002438	Panchami Sharma	HR	
6	FH member	Malini G Prabhakar	Faculty Housing	Malini Prabhakar
7	FH member	Kusuma Jinka	Faculty Housing	
8	MUJ403	Dr. Shilpa Gupta	Executive	
9		Nadun	GS	
10		Copul	GS	
11	MUJ134	Shobha Sharma	Senior- Personal Assistant	
12	MUJ1719	Kushal Karna	IP	
13	MUJ5072	Man Melom Melom	Administration	Man M
14				

10. Link of MUJ social media page

LinkedIn: <https://www.linkedin.com/feed/update/urn:li:activity:7134914090002526208>

Facebook:

- <https://www.facebook.com/share/p/veNm8xBHeCEpUkJh/?mibextid=WC7FNe>
- <https://www.facebook.com/share/p/SESHp8BN95zt4VCP/?mibextid=WC7FNe>

Instagram:

- https://www.instagram.com/p/C0JntI-LnvS/?utm_source=ig_web_copy_link&igshid=MzRIODBiNWFIZA==
- https://www.instagram.com/p/C0Jwf4orIKQ/?utm_source=ig_web_copy_link&igshid=MzRIODBiNWFIZA==

Head, Department of Interior Design
SP&D, Faculty of Design
Manipal University Jaipur



**MANIPAL UNIVERSITY
JAIPUR**

Department of Interior Design

FACULTY OF DESIGN

Make & Take

Kokedama

Hands-on Workshop

22/11/2023



Content of Report

1. Introduction of the Event
2. Objective of the Event
3. Beneficiaries of the Event
4. Details of the Guests
5. Brief Description of the event
6. Photographs
7. Poster of an Event
8. Schedule of the Event
9. Attendance of the Event
10. Link of the event



1. Introduction of the Event

The Department of Interior Design, Faculty of Design at Manipal University Jaipur organized a Kokedama Workshop on 22.11.2023, as a part of the curriculum for 3rd-year B.Des (ID) students. This workshop was conducted under the subject Interior Landscape (ID3105) to provide students with a practical, hands-on experience in the art of preparing Kokedamas. Along with 3rd year B. Des students, this workshop is open for all Manipal University Jaipur students (Diploma, Undergraduate and Postgraduate), Research Scholars, Academicians, Faculty Housing Women, And Industry Professionals with fees of Rs 300/- that included all the materials.

An introduction and demonstration to Kokedama was given by Ms. Geeta Ahluwalia, General Secretary, Kitchen Garden Association, Jaipur. Kitchen Garden Association is an all women lead non-profit organisation in Jaipur. Ar. Sneh Singh (HoD Interior Design) along with Ar. Megha Prabhu K (Asst. Professor, Interior Design) conducted a hands-on 'Make & Take' Kokedama Workshop.

2. Objective of the Event

- Provide 3rd-year B. Des (ID) students with a hands-on experience in the preparation of Kokedamas.
- Enhance the understanding of interior landscaping principles among participants and foster practical skills in crafting Kokedamas, focusing on plant selection, soil composition, and wrapping techniques.
- Facilitate knowledge exchange and collaboration among participants from diverse academic backgrounds, including students, research scholars, academicians, and industry professionals.
- Encourage creativity and innovation in Interior Design through the exploration of Japanese moss ball planters.
- Provide a platform for participants to engage in a Q&A session, allowing for a deeper understanding of the art of Kokedama.
- Create a supportive and inclusive learning environment for all attendees, fostering a sense of community and collaboration within Manipal University Jaipur.



3. Beneficiaries of the Event

The workshop was open to a diverse audience, including 3rd-year B.Des(ID) students, students from other programs (Diploma, Undergraduate, and Postgraduate) at Manipal University Jaipur, research scholars, academicians, Faculty Housing Women, and industry professionals. The inclusive nature of the workshop aimed to foster collaboration and knowledge exchange among participants.

4. Details of the Guests

The honoured guest for the event was Ms. Geeta Ahluwalia, the Secretary of the Kitchen Garden Association Jaipur. Kitchen Garden Association is an all women lead non-profit organisation in Jaipur. Ms. Ahuwalia's expertise in the field brought a valuable perspective to the workshop, and her presence added significant value to the overall learning experience for the participants.

5. Brief Description of the event

The Kokedama workshop provided a unique opportunity for participants to explore the creative and technical aspects of crafting Kokedamas, which are Japanese moss ball planters. The event kicked off with a warm welcome to all attendees, followed by an insightful introduction to the art of Kokedama and its relevance in interior design.

Participants were guided through the step-by-step process of creating their own Kokedamas, emphasizing the selection of suitable plants, soil composition, and wrapping techniques. Ms. Ahuwalia shared her expertise and provided practical tips, enriching the learning experience for everyone involved.

6. Photographs of the Event



Introduction and Demonstration given by Expert, Ms. Geeta Ahluwalia



Demonstration of Kokedama given by Expert, Ms. Geeta Ahluwalia



Participants showcasing their works

7. Poster of the event



The poster features a green background with large leaf graphics. At the top left is the Manipal University Jaipur logo. At the top right are two icons: '11 SUSTAINABLE CITIES AND COMMUNITIES' and '15 LIFE ON LAND'. The central image shows a person's hands planting a green plant into a moss ball. Below this image is a white text box with the following text: 'DEPARTMENT OF INTERIOR DESIGN, FACULTY OF DESIGN IS ORGANISING A HANDS-ON WORKSHOP ON'. Below the text box is the title 'Kokedama' in a large, elegant font, followed by the subtitle 'Make & Take Interior Landscape'. A paragraph of text describes Kokedama as a traditional Japanese art form. Below this are two columns of text: 'List of Materials provided to you:' with a bulleted list, and 'Expert Lecture on:' with a bulleted list. To the right of these lists is a vertical line, followed by text about the Kitchen Garden Association and workshop details. At the bottom left, there is a registration deadline and a QR code link. At the bottom right, there is a QR code.

MANIPAL UNIVERSITY
JAIPUR

11 SUSTAINABLE CITIES AND COMMUNITIES

15 LIFE ON LAND

DEPARTMENT OF INTERIOR DESIGN,
FACULTY OF DESIGN
IS
ORGANISING A HANDS-ON WORKSHOP ON

Kokedama

Make & Take Interior Landscape

Kokedama, a traditional Japanese art form, transforms plants into living sculptures, encased in moss and twine, suspended like hanging gardens – a harmonious blend of nature and artistry, where plants seem to defy gravity. These captivating green orbs bring an enchanting touch of Zen to any space, inviting serenity and connection with the natural world.

List of Materials provided to you:

- Plants: Ferns and Pothos
- Soil Mix: Peat moss and Clay Soil
- Sheet Moss
- Twine or String
- Scissors
- Plastic Wrap
- Decorative Accent: Miniature figurines

Expert Lecture on:

- How to make Kokedama
- The creative process
- The benefits and aftercare

In collaboration with the Kitchen Garden Association.
It is an all-women-led Non-Profit Organization.

Details of the Workshop:

 Date: 22nd November 2023

 Time: 10:30 am onwards

 Venue: Porch Area, First Floor, Administrative Building

 Registration Fee: Rs. 300
(Inclusive of all materials)

REGISTER YOUR SPOT BY 19.11.2023!
VISIT THE QR CODE FOR GOOGLE FORM



8. Schedule of the event

'Make & Take' Kokedama Workshop 22 November 2023, Wednesday	
Porch Area, 1 st Floor, Administration Building, MUJ	
Time	Event
09:30 am	Registration and Reporting
10:30 am	Welcome address by Ar. Megha Prabhu Karkala Introduction of the Guest Address by Dean, Prof. (Dr.) Madhura Yadav, Dean, FoD
10:45 am	Expert Lecture and Introduction to Kokedama by Ms. Geeta Ahuwalia
11:00 am	Practical Session: Crafting Kokedamas
11:30 am	Making Kokedamas by students
12:45 pm	Completion of Kokedamas and Q&A Session
01:00 pm	Felicitation of Ms. Geeta Ahuwalia and Closing Remarks
01:15 pm	Group Photographs and Exhibition of Students works

9. Attendance of the Event

Sl.No	Participate Name	Participant	Department	Registration No.
1	Kashish Kriplani	Student	B.Des (Interior Design)	210606041
2	Kartik Totla	Student	B.Des (Interior Design)	210606011
3	Aakash Singh	Student	B.Des (Interior Design)	210501007
4	Garima Vijaycharan	Student	B.Des (Interior Design)	210606021
5	Kumari Anjali	Student	B.Des (Interior Design)	210606008
6	Himanshi Sharma	Student	B.Des (Interior Design)	210606028
7	Esha Giri	Student	B.Des (Interior Design)	210606031
8	Anisha Chopra	Student	B.Des (Interior Design)	210606020
9	Rutu Shah	Student	B.Des (Interior Design)	210606007
10	Anushka Rai	Student	B.Des (Interior Design)	210606019
11	Rishika	Student	B.Des (Interior Design)	210606029
12	Paridhi Verma	Student	B.Des (Interior Design)	210606017
13	Naman	Student	B.Des (Interior Design)	210606013
14	Diya Ramchandani	Student	B.Des (Interior Design)	210606039
15	Krishangee Goyal	Student	B.Des (Interior Design)	210606026
16	Avinash Yadav	Student	B.Des (Interior Design)	210606047
17	Himanshi Yadav	Student	B.Des (Interior Design)	210606014
18	Hridyanshi Vyas	Student	B.Des (Interior Design)	210606018
19	Khushi Bhargava	Student	B.Des (Interior Design)	210606010
20	Madhu Tanwar	Student	B.Des (Interior Design)	210606027
21	Riddhi Agarwal	Student	B.Des (Interior Design)	210606038
22	Michelle Earnest	Student	B.Des (Interior Design)	210606043



MANIPAL UNIVERSITY JAIPUR

23	Pooja Jain	Student	B.Des (Interior Design)	23fd10bid00020
24	Shreshtha Gaur	Student	B.Des (Interior Design)	210606012
25	Geetika Gupta	Student	B.Des (Interior Design)	210606037
26	Manya Agarwal	Student	B.Des (Interior Design)	210606015
27	Riya	Student	B.Des (Interior Design)	210606035
28	Ananya Thakan	Student	B.Des (Interior Design)	210606006
29	Devanshi Jain	Student	B.Des (Interior Design)	210606046
30	Drishti Sharma	Student	B.Des (Interior Design)	210606045
31	Sejal Sharma	Student	B.Des (Interior Design)	210606023
32	Samarth Gandhi	Student	B.Des (Interior Design)	210606003
33	Saija Tanya	Student	B.Des (Interior Design)	210606044
34	Garvit Garg	Student	B.Des (Interior Design)	210606001
35	Shruti Dubey	Student	B.Des (Interior Design)	210606022
36	Keshav Katta	Student	B.Des (Interior Design)	210606005
37	Grishma Korjani	Student	B.Des (Interior Design)	210606016
38	Shweta Sharma	Non-Teaching Staff	Non- Teaching Staff	MUJ1134
39	Megha Prabhu Karkala	Assistant Professor	Faculty of Design	MUJ1434
40	Smriti Saraswat	Assistant Professor	Faculty of Design	MUJ1248
41	Dr. Shilpi Gupta	Assistant Professor	Department of Economics	MUJ0403
42	Malini G Prabhu	Faculty Housing Member	Faculty Housing Member	NA
43	Rajendar Kumar	Non-Teaching Staff	GSA	MUJ1300
44	Reetika Choudary	Non-Teaching Staff	Admission Department	MUJ1406
45	Priyanka Samarth	Non-Teaching Staff	Admission Department	MUJ1408
46	Panchami Sharma	Non-Teaching Staff	HR Department	MUJ11002438
47	Kusuma Jinka	Faculty Housing Member	Faculty Housing Member	NA
48	Madan	Non-Teaching Staff	GSA	
49	Gopal	Non-Teaching Staff	GSA	
50	Kush Jee Kamal	Assistant Professor	Faculty of Design	MUJ1714
51	Man Mohan Mehta	Non-Teaching Staff	Admission Department	MUJ0170



MANIPAL UNIVERSITY JAIPUR

Manipal University Jaipur				
Department of Interior Design I FOD				
II Year III Semester - ID3105-Interior Landscape				
KOKEDAMA WORKSHOP - 22.11.2023				
Sl. No.	ROLL No.	NAME	SIGN	
1	210606001	GARVIT GARG		
2	210606003	SAMARTH GANDHI		
3	210606004	VISHVA SAMIRBHAI DAVE	- ABSENT -	
6	210606005	KESHAV KATTA		
5	210606006	ANANYA THAKAN		
6	210606007	RUTU DILIP KUMAR SHAH		
7	210606008	KUMARI ANJALI		
8	210606010	KHUSHI BHARGAVA		
9	210606011	KARTIK TOTLA		
10	210606012	SHRESHTHA GAUR		
11	210606013	NAMAN HODKASIA	- ABSENT -	
12	210606014	HIMANSHI YADAV		
13	210606015	MANYA AGARWAL		
14	210606016	GRISHMA KORJANI		
15	210606017	PARIDHI VERMA		
16	210606018	HRIDIYANSHI VIRESH VYAS		
17	210606019	ANUSHKA RAI		
18	210606020	ANISHA CHOPRA		
19	210606021	GARIMA VIJAY CHARAN		
20	210606022	SHRUTI DUBEY		
21	210606023	SEJAL SHARMA		
22	210606026	KRISHANGEE GOYAL		
23	210606027	MADHU TANWAR		
24	210606028	HIMANSHI SHARMA		
25	210606029	RISHIKA		
26	210606031	ESHA GIRI		
27	210606034	KREETI YADAV	- ABSENT -	
28	210606035	RIYA GAUTAM ROY		
29	210606036	HRIDAY SINGH	- ABSENT -	
30	210606037	GEETIKA GUPTA		
31	210606038	RIDDHI AGARWAL		
32	210606039	DIYA RAMCHANDANI		
33	210606041	KASHISH KRIPLANI		
34	210606043	MICHELLE EARNEST		
35	210606044	SAIJA TANYA		
36	210606045	DRISHTI SHARMA		
37	210606046	DEVANSHI JAIN		
38	210606047	AVINASH YADAV		
39	210501007	AKASH		

Manipal University Jaipur				
Department of Interior Design				
Faculty of Design				
KOKEDAMA WORKSHOP - 22.11.2023				
Sl. No.	MUJ ID/ Roll No	NAME	Department	SIGN
1	MUJ1300	Rajendra Kumar	GS/SP	
2	MUJ1406	Reetika Choudhary	Admission	
3	MUJ1408	Rajendra Kumar	Admission	
6				
5	MUJ1002438	Panchani Sharma	HR	
6	FH member	Malini G Prabhakar	Faculty Housing	Malini Prabhakar
7	FH member	Kusuma Jinka	Faculty Housing	
8	MUJ403	Dr. Shilpa Gupta	Executive	
9		Nadun	GS	
10		Chopal	GS	
11	MUJ134	Shobha Sharma	Senior - Personal Assistant	
12	MUJ1719	Kushal Karna	IP	
13	MUJ5072	Man Melom Melom	Administration	Man M
14				

10. Link of MUJ social media page

LinkedIn: <https://www.linkedin.com/feed/update/urn:li:activity:7134914090002526208>

Facebook:

- <https://www.facebook.com/share/p/veNm8xBHeCEpUkJh/?mibextid=WC7FNe>
- <https://www.facebook.com/share/p/SESHp8BN95zt4VCP/?mibextid=WC7FNe>

Instagram:

- https://www.instagram.com/p/C0JntI-LnvS/?utm_source=ig_web_copy_link&igshid=MzRIODBiNWFIZA==
- https://www.instagram.com/p/C0Jwf4orIKQ/?utm_source=ig_web_copy_link&igshid=MzRIODBiNWFIZA==

Head, Department of Interior Design
SP&D, Faculty of Design
Manipal University Jaipur



RESEARCH

Summary for Manipal University Jaipur 15

Manipal University Jaipur

2021 to 2023 ▾

Research performance within SDG 15: Life on Land (2023)

Entity: Manipal University Jaipur · Within: All subject areas (ASJC) · Year range: 2021 to 2023 · Data source: Scopus, up to 30 Oct 2024

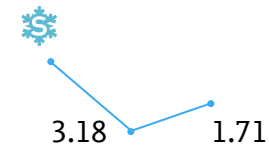
33

Scholarly Output 



1.71

Field-Weighted Citation Impact 



3

International Collaboration 



573

Views Count

388

Citation Count 

Collaboration summary within SDG 15: Life on Land (2023)

Entity: Manipal University Jaipur · Within: All subject areas (ASJC) · Year range: 2021 to 2023 · Data source: Scopus, up to 30 Oct 2024

International Collaboration

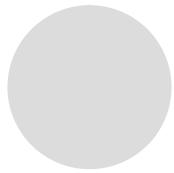
Publications co-authored with Institutions in other countries/regions



Manipal University Jaipur
9.1%

Academic-Corporate Collaboration


Publications with both academic and corporate affiliations

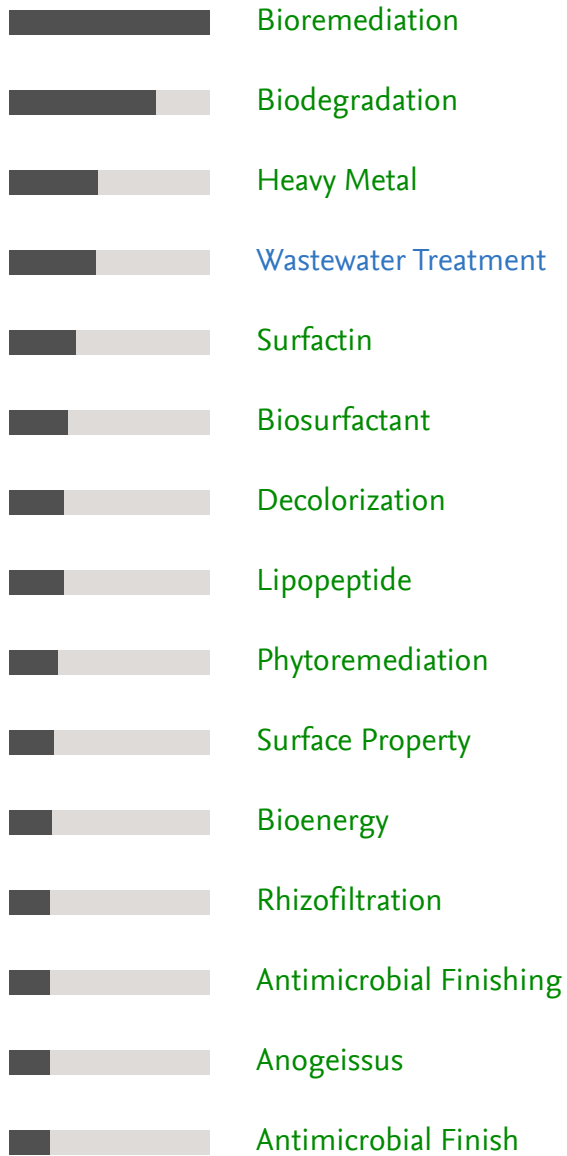


Manipal University Jaipur
0.0%

Top keyphrases within SDG 15: Life on Land (2023)

Entity: Manipal University Jaipur · Within: All subject areas (ASJC) · Year range: 2021 to 2023 · Data source: Scopus, up to 30 Oct 2024

Top keyphrases by  relevance





EVENTS



MUJ/DSW/Society Connect/ 31 Oct 2023



MANIPAL UNIVERSITY
JAIPUR

DIRECTORATE OF STUDENT'S WELFARE

(SOCIETY CONNECT)

And

Faculty of Management and Commerce

Department of Business Administration

Activity on

SWACH BHARAT

OCTOBER 31, 2023

1. Introduction of the Event

School of Business and Commerce in collaboration with Directorate of Student Welfare (NCC, NSS) and Rotaract Club (Rotary Bapu Nagar) organized a “Awareness on Environment Protection” on October 31, 2023. 40 students and 2 faculty members participated in the campaign. The event took place in Dehmi Kalan hamlet.

2. Objective of the Event

The aim of the campaign was to raise awareness about plantation and Environmental Protection.

3. Beneficiaries of the Event

Through this initiative, students and villagers had better communication and understanding of the situation.

4. Details of the Guests

The event was laid by the students of BBA, BBA(BA), IMBA and Club Members of Rotaract Club MUJ

5. Brief Description of the event

School of Business and Commerce, Department of Business Administration in collaboration with Directorate of Student Welfare, Directorate of sports and NCC, NSS organized a plantation drive for creating awareness on environment protection on 31st October 2023. 20 students and 2 faculty members participated in the drive. The group visited various houses in the Begas Village Road and planted saplings and encouraged villagers to take care about environment and newly planted saplings. Students also learned various communication skills and interactive skills with the villagers.

6. Photographs



Fig 1 Students at Begus Village for Plantation



Fig 2 Students doing Plantation.

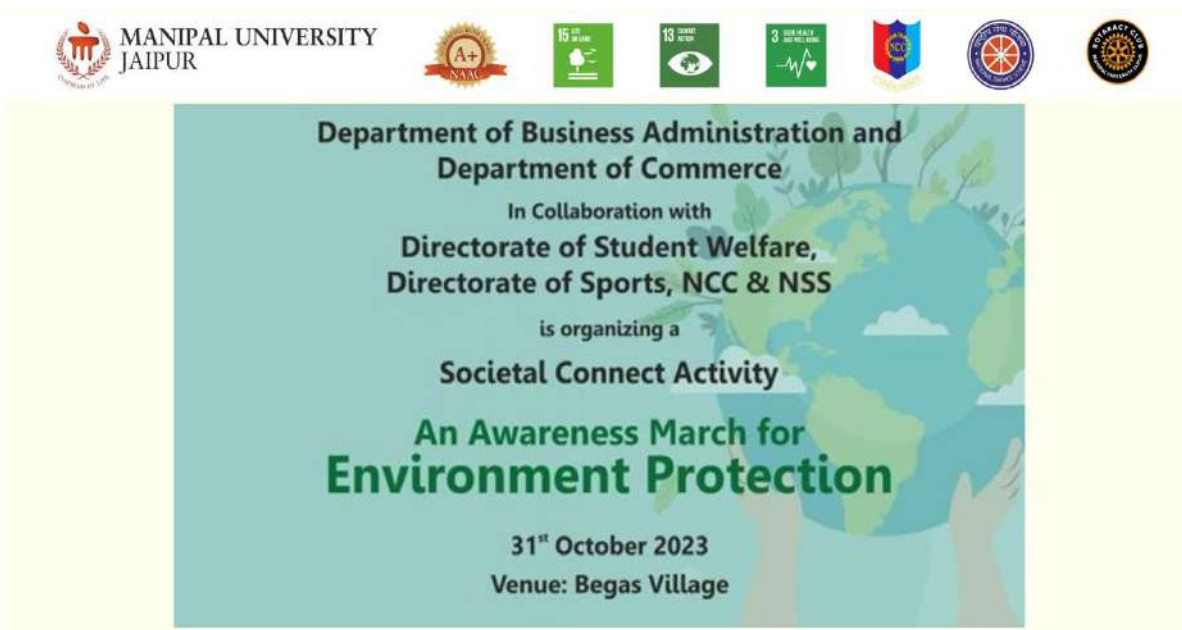


Fig 2 Students & Faculty doing Plantation.



Fig 4 Students & Faculty doing Plantation.

7. Brochure or creative of the event



8. Schedule of the Event

The event took place on October 31, 2023

9. Attendance of the Event (60 student)

Sr. No	Registration No	Attendee Name	Name of Institution
1	23FM10BBA00197	VIPUL SHARMA	Manipal University Jaipur
2	23FM10BBA00198	MUKUND MAHESHWARI	Manipal University Jaipur
3	23FM10BBA00199	ROSHAN GUPTA	Manipal University Jaipur
4	23FM10BBA00200	VANSH MULCHANDANI	Manipal University Jaipur
5	23FM10BBA00227	PAWAN POTALIYA	Manipal University Jaipur
6	23FM10BBA00232	AKSHAT KUMARCHOUDHARY	Manipal University Jaipur
7	23FM10BBA00233	DHAIRYA BANSAL	Manipal University Jaipur
8	23FM10BBA00230	YASH ARORA	Manipal University Jaipur
9	23FA10BSP00028	Anupama Rustagi	Manipal Univesrity Jaipur
10	23FE10CCE00085	Siddhartha tiwari	Manipal Univesrity Jaipur
11	23FA10BAP00002	Tanisha Mathur	Manipal Univesrity Jaipur
12	23FD10BFD00009	Mariya Shabbir Baiwala	Manipal Univesrity Jaipur
13	23FE10CDS00224	Harsh Ajmera	Manipal Univesrity Jaipur
14	23fe10cds00125	Suryanshi Singh	Manipal Univesrity Jaipur
15	23fs10mat00009	Malavika ramdas	Manipal Univesrity Jaipur
16	221007021	Arshi Jain	Manipal Univesrity Jaipur
17	23FE10CSE00137	Stuti Dixit	Manipal Univesrity Jaipur
18	23fe10cii00094	Aarohi Tyagi	Manipal Univesrity Jaipur
19	23FE10CSE00152	Gautam Kakkar	Manipal Univesrity Jaipur



20	23FE10CSE00318	Krish Ray	Manipal Univesrity Jaipur
21	23FE10CII00076	KriiSSH Marwaha	Manipal Univesrity Jaipur
22	229310321	Shiv Rajput	Manipal Univesrity Jaipur
23	23FS10BIO00051	Ragini Singh Thakur	Manipal Univesrity Jaipur
24	23FS10BIO00052	Anukriti sharma	Manipal Univesrity Jaipur
25	220901073	Diya Mittal	Manipal Univesrity Jaipur
26	23FE10CSE00081	Smmayan Gupta	Manipal Univesrity Jaipur
27	229309083	Raghav Gupta	Manipal Univesrity Jaipur
28	23FE10CDS00397	Hrishita Singh Timaney	Manipal Univesrity Jaipur
29	23FE10ITE00203	Sarah Sharda	Manipal Univesrity Jaipur
30	23fa10bsp00025	Jasleen kaur	Manipal Univesrity Jaipur
31	23FA10BSP00039	Jiya Kumar	Manipal Univesrity Jaipur
32	23FA10BSP00004	Aarya Mahale	Manipal Univesrity Jaipur
33	220606020	Chaarvi Kumar	Manipal Univesrity Jaipur
34	23fa10bsp00058	Kashvi Mahajan	Manipal Univesrity Jaipur
35	229301095	Shaurya Singh	Manipal Univesrity Jaipur
36	23fe10ece00024	Kushagra agrawal	Manipal Univesrity Jaipur
37	23FA10BSP00017	Megha Sharma	Manipal Univesrity Jaipur
38	23FM10BBA00162	Alina Nadeem	Manipal Univesrity Jaipur
39	23FM10BBA00178	Avishi Akhaury	Manipal Univesrity Jaipur
40	221007004	Urvi Thakare	Manipal Univesrity Jaipur
41	23FA10BAP00027	Natasha Joan Menezes	Manipal Univesrity Jaipur
42	23FA10BLE00004	Tanisha chaturvedi	Manipal Univesrity Jaipur
43	23fe10cai00579	Arjun Malhotra	Manipal Univesrity Jaipur
44	23FE10CAI00352	Maanyata Aul	Manipal Univesrity Jaipur
45	220901322	Divyanshi Singh	Manipal Univesrity Jaipur
46	229310412	Jatin Verma	Manipal Univesrity Jaipur
47	229301094	Yashovardhan Pratap Singh	Manipal Univesrity Jaipur
48	23FM10BBA00348	Niska kedia	Manipal Univesrity Jaipur
49	221105005	Dhruv Nair	Manipal Univesrity Jaipur
50	23FM10BBA00170	Shambhavi Agrawal	Manipal Univesrity Jaipur
51	23FE10CDS00241	Armaan Setia	Manipal Univesrity Jaipur
52	23FE10CAI00105	Mritunjay Singh	Manipal Univesrity Jaipur
53	229311075	Aarna Tyagi	Manipal Univesrity Jaipur
54	229302051	Prince jindal	Manipal Univesrity Jaipur
55	23FA10BHE00035	Taneesha puri	Manipal Univesrity Jaipur
56	220903033	Suhani Jain	Manipal Univesrity Jaipur
57	220901391	Dipika Agarwal	Manipal Univesrity Jaipur
58	229310222	Aayush Sharma	Manipal Univesrity Jaipur
59	221003007	Yachna Jain	Manipal Univesrity Jaipur
60	220901002	Anshu jangir	Manipal Univesrity Jaipur



(Hemant Kumar)
Assistant Director, Society Connect
Directorate of Student's Welfare

DIRECTOR STUDENT WELFARE & PROCTOR
MANIPAL UNIVERSITY, JAIPUR

Dr Narendra Singh Bhati Ho

HOD, BBA

(Prof. AD Vyas)

Director, Directorate of Student's Welfare



MUJ/DSW/Student Clubs/2023/MUJ ACM/02.04.2023



MANIPAL UNIVERSITY
JAIPUR

DIRECTORATE OF STUDENTS' WELFARE

AutoBots

MUJ ACM SIGBED Student Chapter OFFLINE EVENT

Date of Event

2nd April, 2023

(5:00 PM onwards)

Index

S.No.	Activity Heads	Page no.
1.	Introduction of the Event	3
2.	Objective of the Event	3
3.	Beneficiaries of the Event	3
4.	Brief Description of the event	3
5.	Photographs	4
6.	Brochure or creative of the event	5
7.	Schedule of the Event	6
8.	Attendance of the Event	6
9.	Signatures Student Coordinator, Club President, Faculty Coordinator (with Department Name and contact number)	7

1. Introduction of the Event

The MUJ ACM SIGBED Student Chapter brings to you "AutoBots". This event is being presented to the public with the intention of providing a platform for enthusiasts to showcase their knowledge and skills in the field of IOT and Robotics.

This is an event that utilizes Robot building and programming skills of the participants to overcome a set of challenges and allow them to showcase their potential typically in the field of embedded systems.

2. Objectives of the Event

- Encourage students to showcase innovative ideas and solutions to real world problems.
- Encourage students to showcase their creativity and demonstrate their ability to think and outside the box
- Encourage students to network with like-minded people.

3. Beneficiaries of the Event

- Students of Manipal University, Jaipur
- Members of MUJ ACM Student Chapter
- Members of MUJ ACM SIGAI Chapter
- Members of MUJ ACM SIGBED Chapter

4. Brief Description of the event

AutoBots is a robot building competition that is based on IoT technology. The event required participants to have knowledge of robotics and IoT technologies. The robots were designed using IoT technologies, such as sensors, microcontrollers, and other peripherals, which enable them to navigate through the track and overcome obstacles. The proceedings started at 5 o'clock. The participants were allowed dry runs and test their robots on the course. The deadline to perform dry runs was till 8pm. The teams were informed of the event's regulations and grading procedures during a briefing session. The participating teams had to put the robot together, programme it to move through several checkpoints, and make sure it doesn't run into any walls as it moves through the track. With few wall collisions and restarts, 12 teams raced for the fastest lap time on the track. At 10:00 pm, the event's results were released.

5. Photograph



6. Brochure or Creative of the event







AUTOBOTS



2ND APRIL
PRIZEPOOL : 7K
VENUE : AB 1 GALLERY

CONTACT:
PUSHKAL GARG : 7303221508
SAAMARTH MISHRA : 9919201610

7. Schedule of the event

S.no	Event	Date	Time
1.	Commencement	2 nd April 2023	5:00pm-9:00pm
2.	Judgement	2 nd April 2023	9:00pm-9:30pm

8. Attendance of the event:

S No	Name of the Participants
1	Naad Dantale
2	Vansh Kumar Singh
3	Vansh Kumar Singh
4	Shivam Raj Dubey
5	Jaskaran Singh Taneja
6	Rishabh Bachani
7	Varun Lall Srivastava
8	Ayush Jaiswal
9	Aryan Gupta
10	Prithvi Singh
11	ADITYA KUMAR MISHRA
12	Yash Prasd
13	Aryan Garv
14	Priyansh Goel
15	Anurag Bijalwan
16	Anushka Shreya
17	Devansh Goel
18	Varun Lall Srivastava
19	Aryan Mishal
20	Pratyush Kumar Debata
21	Yaduvir
22	Aayush singh
23	ANGSHUMAN KUMAR MAHATO
24	Nekunj Khanna
25	Rachit Mehwala
26	Kumar Kartikay Shankar
27	Aryan Mishal
28	Harshit Agarwal
29	Abhyam
30	Tushar goyal
31	Naman jain
32	Adwait Sumedh Deshpande
33	Kamya Singh
34	Sairaj Sirsat
35	Hanis Gori
36	Sugam Nema



Umang

Umang
Chairperson
MUJ ACM SIGBED Student Chapter

Shiva Prasad H C

Dr. Shiva Prasad HC
Director SAMM
School of Automobile, Mechanical
& Mechatronics

	<p><i>Sanchit Anand</i></p> <p>Dr. Sanchit Anand Assistant Professor, Assistant Director DSW</p>
--	---



MUJ/DSW/Student Clubs/2023/Coreografia/1stApril2023



MANIPAL UNIVERSITY
JAIPUR

DIRECTORATE OF STUDENTS' WELFARE

Ecstasy

Cultural Event

Coreografia – The Official Dance Society of MUJ

OFFLINE EVENT

Venue: Dr. TMA Pai Auditorium

Date of Event (1st and 2nd April 2023)

Index

S.No.	Activity Heads	Page no.
1.	Introduction of the Event	3
2.	Objective of the Event	3
3.	Beneficiaries of the Event	3
4.	Brief Description of the event	3-4
5.	Photographs	4
6.	Brochure or creative of the event	5
7.	Schedule of the Event	5
8.	Attendance of the Event	6-7
9.	Link of MUJ website	7

1. Introduction of the Event

Dancing is more than just knowing how to move the body; it is an expression of one's deepest thoughts and emotions. We are excited to present the second edition of Ecstasy, a dynamic and vibrant celebration of the art of dance. This in-house event will bring together dancers and dance enthusiasts of all levels and backgrounds, featuring a diverse range of performances by professional and amateur dancers. Attendees will have the opportunity to learn new dance styles, connect with other dance enthusiasts, and experience the joy and excitement of live dance performances. Ecstasy will be held in Manipal University Jaipur campus, on 1st and 2nd April 2023.

2. Objectives of the Event

- To help fellow students to grow not only in dance but grow as a professional.
- To help the students in improving self-confidence, adapt to different situations, to improve in teamwork as well as in leadership
- To help the students to learn and improve upon themselves and mainly to help the students nurture their passion and give them opportunities where they can showcase their talent.

3. Beneficiaries of the Event

- All students of Manipal University Jaipur

4. Brief Description of the event

Coreografia presents Ecstasy, a 2-day event that celebrated dance in its true form. This event comprised of 4 teams that battled it out in a series of dance competitions spread across 2 days, mainly being Solo, Duet and Battle. The 4 team leaders got a fixed number of credits and had to sit through an auction to select their team members. The events were as follows:

Day 1 – Solo

There were two categories to this event, Solo Western and Solo Classical. The event took place in Dr. TMA Pai Auditorium.

Day 1 – Battle

This was a hip hop based 4v4 battle. The battle took place in Campus, in Academic Block-1 Lobby. The battle was judged on musicality, beat sense, flow levels, and other technical aspects.

Day 2 – Duets

This was an all-style Duet competition which took place in Dr. TMA Pai Auditorium.

The winners and the winning team were announced on the last day, during a cultural event, which was the closing event of Ecstasy.

5. Photographs



6. Brochure or Creative of the Event



7. Schedule of the event

Desk setup for participation starts	6th March 2023, 6PM
Desk setup for participation ends	16th March 2023, 9PM
Road to Ecstasy	
<ul style="list-style-type: none"> • Auction 	18th March 2023, 6PM
<ul style="list-style-type: none"> • Desk setup and minor activities 	20th March to 26th March 2023
<ul style="list-style-type: none"> • Flash mob with flex reveal 	27th March 2023, 7:30PM
<ul style="list-style-type: none"> • Inter-club performances 	29th March 2023, 7:30PM
Ecstasy Day 1 - Inauguration	1st April 2023, 11AM
Ecstasy Day 1 - Solo Dance Competition	1st April 2023, 12PM
Ecstasy Day 1 - Battle	1st April 2023, 5:30PM
Ecstasy Day 2 - Duet Dance Competition	2nd April 2023, 12PM
Cultural Event	2nd April 2023, 6:30PM

8. Attendance of the event: Total attendee: 112

Timestamp	Name	Registration Number	Year
3/16/2023 16:17:34	AANYA MITTAL	229310435	1st
3/16/2023 17:12:53	Charvi Solanki	221015168	1st year
3/16/2023 17:17:15	Sanchi Mishra	229303029	First
3/16/2023 18:13:04	Manjul Varshney	219302057	2nd
3/16/2023 18:55:57	Shreya chouhan	229311258	1st
3/16/2023 19:45:50	Ananya Gupta	220606008	1st Year
3/16/2023 20:57:49	Bhoomi Gupta	229301707	1st
3/16/2023 22:09:46	Ishita sharma	229303237	First
3/16/2023 22:20:17	M.yagna	229303220	2nd sem
3/16/2023 22:21:11	Yash Chowdhary	229311060	1st
3/16/2023 23:06:33	Shruti dubey	210606022	2nd
3/16/2023 23:24:54	Navyaa Jain	219310202	2nd
3/16/2023 23:26:47	Priyasha SINGH	209302050	3
3/17/2023 2:21:35	Kanishka Kasana	229301231	1st
3/17/2023 12:11:25	Kirti Jain	220803009	1
3/17/2023 13:10:28	Bhavya sharma	220606032	1
3/17/2023 13:18:04	Harindra Singh	229302325	1st
3/17/2023 14:04:31	Anant Khemka	209301508	3rd
3/17/2023 14:40:09	Anisha	221016049	1st year
3/17/2023 18:33:42	Twinkle Khatwa	221007050	First
3/17/2023 18:59:34	Khushi verma	211004006	2nd
3/17/2023 19:28:39	Srishti Jaiswal	229302008	1st year
3/18/2023 12:32:50	Devika Kaimal	229301514	1st
3/18/2023 15:06:19	Shruti Sunthwal	229309147	1st year
3/18/2023 19:43:20	Stuti Saxena	229310263	1st
3/18/2023 20:01:52	Nupur Palav	209202061	3rd
3/18/2023 20:18:26	Mehma singh	220801003	1
3/18/2023 20:59:53	Anvenshi garg	220901428	1st
3/18/2023 22:19:00	Devyanish Mishra	229302594	1st year
3/18/2023 23:01:26	Naman sharma	221305001	1 st year
3/19/2023 18:17:33	Mahi Kulshresth	229310362	First year
3/19/2023 18:26:25	Devyani Ghildiyal	229301091	1
3/19/2023 20:30:09	Sandali Singh	229301803	1st
3/19/2023 20:48:19	Ayonija	229302173	1
3/19/2023 20:52:26	Yashni yogeesh poojary	221305061	1 st
3/19/2023 21:05:07	Swarna Jain	229301247	1st
3/19/2023 21:11:39	Ushasi Bhattacharya	221103011	1st year
3/19/2023 21:19:58	AMAN SHARMA	229303298	2026
3/19/2023 21:37:17	Harsh Thakur	229301722	1st year
3/19/2023 21:41:47	Mayank Maheshwari	229309030	1st year
3/19/2023 21:44:00	Vitika Vora	219309114	2nd
3/19/2023 21:58:27	Shreya Yogesh shedge	229310170	1 st
3/19/2023 22:05:53	Himanshi Punjabi	211007042	2nd
3/19/2023 23:13:19	Vedika Gupta	221007014	1
3/20/2023 21:07:46	Satvika Arora	229310274	1st
3/20/2023 22:38:29	Priyanshu Saini	209301418	3rd
3/21/2023 12:37:11	Shreja Shekhar	229302536	1st
3/21/2023 12:38:48	Simran Chhipa	221015104	1st
3/21/2023 16:18:16	Sakshi anjana	221101027	1st
3/21/2023 16:39:21	Anushka singh	229301760	1st
3/21/2023 16:45:00	Tulsi Ghonshette	221016067	1st
3/21/2023 16:48:16	Tanisha Mishra	229303442	2023
3/21/2023 16:50:11	Shristi Krishna	229301311	1st
3/21/2023 16:51:34	Paridhi Rawat	221201037	1st year
3/21/2023 17:12:53	Udisha Jaiswal	229303196	1st year
3/21/2023 17:17:15	Shreya Gupta	229302230	1st year
3/21/2023 18:13:04	Muskan Gupta	229302508	First
3/21/2023 18:55:57	Saloni singh	229301405	1

3/21/2023 19:45:50	Shivambika Bhati	201301051	2026
3/21/2023 20:57:49	Ishika gandhi	220901355	1st year
3/21/2023 22:09:46	Yuvraj Singh Chouhan	229102008	1
3/21/2023 22:20:17	Tanisha yadav	229303277	1st
3/21/2023 22:21:11	Sarvi Agarwal	229301372	1st
3/21/2023 23:06:33	Arshia	229301779	1st
3/21/2023 23:24:54	Tvisha Khanna	229301606	1
3/21/2023 23:26:47	Nayani Jindal	229311253	1st
3/22/2023 2:21:35	Aryan Agrawal	229302124	1st
3/22/2023 12:11:25	Ananda Chaturvedi	229302457	1st year
3/22/2023 13:10:28	ISHANK BANSAL	229302220	1st
3/22/2023 13:18:04	Pratishtha singh	211002044	2nd
3/22/2023 14:04:31	Shubham Kukreti	229302422	1st
3/22/2023 14:40:09	Kartik Dubey	229303040	1st
3/22/2023 18:33:42	Anushka Das	229310232	1
3/22/2023 18:59:34	Sushank Choudhary	229302339	1st
3/22/2023 19:28:39	Sunny Jayaswal	229301061	1st
3/22/2023 12:32:50	Saksham Arun	229311032	1st
3/22/2023 15:06:19	Sanskriti Jha	229301120	1st
3/22/2023 19:43:20	Deepanshu poonia	229310103	1styear
3/22/2023 20:01:52	Priyanshi Garg	229311224	1 st
3/22/2023 20:18:26	Nikita Sharma	229301413	First
3/22/2023 20:59:53	Naman	229302321	1st year
3/22/2023 22:19:00	Parth	229301241	1st
3/22/2023 23:01:26	Goutham R Varma	229309042	1st
3/22/2023 23:02:33	Milind	219301778	2003
3/22/2023 23:03:25	Suraj Chaudhary	229309234	1
3/22/2023 23:04:09	Isha Gupta	221103065	1st yera
3/22/2023 23:05:19	Sanidhya Mehta	229303449	1st
3/22/2023 23:06:26	Ridhi Agrawal	220901043	1
3/22/2023 23:07:07	Sujal jain	229309038	1st
3/22/2023 23:11:39	Shreyas Kumar	229310403	1st Year
3/22/2023 23:19:58	Aryan singh	229303356	1st
3/22/2023 23:20:17	Anushka Sharma	229302020	1
3/22/2023 23:21:47	Vidit Sood	229301097	1st
3/22/2023 23:22:00	Shashank Saraswat	219310301	2nd
3/22/2023 23:23:27	Shashank	229303430	1st
3/22/2023 23:25:53	Aaron Sequeira	219302100	2023
3/22/2023 23:26:19	Hiten Gehlot	219302018	2nd year
3/22/2023 23:27:46	Harsh Upadhyay	229302547	1st
3/22/2023 23:28:29	Aryan Sharma	219309105	2nd
3/22/2023 23:29:11	Tiya Gandhi	220606025	1year
3/22/2023 23:30:48	Shikha wadhvani	221103035	1
3/22/2023 23:31:16	Eishana B	229311199	1st
3/22/2023 23:32:21	Yashika khattri	229302074	1st
3/22/2023 23:33:00	Yash Sharma	229309194	1st year
3/22/2023 23:34:16	Bhavya sharma	220606032	1
3/22/2023 23:35:11	Lipika	229301292	1
3/22/2023 23:35:48	Shreyasi ray	229302125	1
3/22/2023 23:36:16	Ishika sazena	229302183	1
3/22/2023 23:33:21	maahin khan	229302496	1
3/22/2023 23:34:00	arvind nair	229301393	1
3/22/2023 23:34:16	shagun verma	229303024	1
3/22/2023 23:50:11	saksham chanana	229301116	1

9. Post event link: NA



Raghav Handoo

General Secretary, Coreografia, MUJ

Signature of the Student Coordinator

Mr. Hemant Kumar

Department of Mechatronics

Signature of the Faculty Coordinator



MANIPAL UNIVERSITY
JAIPUR

FACULTY OF ENGINEERING

**DEPARTMENT OF CIVIL ENGINEERING
AND
DEPARTMENT OF ARTIFICIAL INTELLIGENCE MACHINE LEARNING**

Prepared a Report

On an event

“Basic Life Support”
20 October, 2023

Venue: Smt. Sharada Pai Auditorium

Organized By:

**Dr. Meena Sharma
Dr. Puneet Mittal**

Table of Contents



S. No.	Contents	Page No.
1.	Introduction of the Event	3
2.	Objective of the Event	3
3.	Beneficiaries of the Event.....	3
4.	Details of the Guest.....	3
5.	Brief Description of the Event.....	4
6.	Geo Tagged Photographs.....	5
7.	Brochure or creative of the event.....	6
8.	Schedule of the event.....	7
9.	Attendance of the event.....	7
10.	Feedback of the Event.....	8



1. Introduction of the Event

Basic Life Support (BLS) is a critical set of skills and actions that can be performed by bystanders or healthcare providers to sustain or revive a person's life in the event of a cardiac arrest or other life-threatening emergencies. BLS techniques primarily focus on maintaining an open airway, providing effective chest compressions, and ensuring proper ventilation, with the goal of oxygenating the brain and vital organs until more advanced medical care can be administered. The primary purpose of this training was to empower participants with the ability to recognize and respond effectively to life-threatening emergencies, particularly cardiac arrests. Participants learnt how to provide immediate care until professional medical assistance arrives, and in some cases, actions alone could be the difference between life and death.

In a world that urgently requires sustainable solutions, this training directly addresses the Sustainable Development Goal (SDG) set by the United Nations, particularly:

SDG 3 (Good Health and Well Being): To Ensure healthy lives and promote well-being for all at all ages.

2. Objective of the Event

- Understand the importance of early recognition and activation of the emergency response system.
- Develop proficiency in providing high-quality chest compressions.
- Acquire the knowledge to assess and respond to various emergency scenarios, including choking and sudden cardiac arrest.

3. Beneficiaries of the Event

Faculty Members of Manipal University Jaipur.

4. Details of the Guest

Dr. Ravi Prakash Chaudhary is the Associate Director and HOD of Emergency Medicine at Manipal Hospital Jaipur. He treats and devises diagnosis plans for patients from all walks of life and of all ages. He is very compassionate and empathetic for his patients. He has done MBBS from JLN medical College, Ajmer and Masters in Emergency Medicine from GWU-USA. He is having experience of 10 years in the field of emergency medicine.



5. Brief Description of the event

Introduction to BLS: The training commenced with an overview of the importance of BLS and its role in saving lives during cardiac and respiratory emergencies.

CPR: Dr. Prakash provided detailed instruction on performing cardiopulmonary resuscitation (CPR) on adults. He emphasized the importance of chest compressions, rescue breaths, and the correct compression-to-ventilation ratio. The training included hands-only CPR techniques, focusing on uninterrupted chest compressions to maximize the chances of survival.

Practical Demonstrations: Dr. Prakash conducted practical demonstrations, allowing participants to practice BLS skills on manikins and receive feedback on their technique.

Choking Relief: Dr. Prakash demonstrated techniques for relieving choking in conscious and unconscious adults, children, and infants.

Recognition of Heart Attacks and Strokes: Participants learned to recognize the signs and symptoms of heart attacks and strokes, along with the appropriate steps to take in these emergencies.

Chain of Survival: Dr. Prakash discussed the concept of the "Chain of Survival" and how each link in the chain is crucial for improving survival rates in cardiac emergencies.

Q&A and Scenario-Based Learning: The session encouraged active participation through interactive discussions, question-and-answer sessions, and scenario-based learning to simulate real-life situations.


6. Geo Tagged Photographs








7. Brochure or creative of the event




**Department of Civil Engineering
&
Department of Artificial Intelligence and Machine Learning
in collaboration with
Manipal Hospital Jaipur
is organizing Training Session on**


“Basic Life Support Training (BLS)”




Trainer:
Dr. Ravi Prakash
M.B.B.S.; M.E.M. (GWU -USA), EPHM (IIM CALCUTTA)
PG.D.G.M. (UK); PG.D.D.M.(MAMC); PG.D.H.H.M.; PG.D.M.L.S.
Sr. Consultant, Associate Director and Head of Department,
Department of Emergency Medicine


Chief Patron	Patron	Co Patrons		
Mr. S. Vaitheeswaran Chairperson, MUJ	Dr. G K Prabhu President, MUJ	Dr. Thammaiah CS Pro President, MUJ	Dr. Nitu Bhatnagar Registrar, MUJ	Prof. Arun Shanbhag Dean (FoE)
Organizers				
Dr. Bhavna Tripathi Director, SCCE (FoE)	Dr. Sandeep Chaurasia Director, SCSE	Dr. Santosh Kumar Vishwakarma Head, AIML		
Conveners				
Prof. Arun Shanbhag Dean (FoE)	Prof. Meena Kumari Prof & Head, Civil Engg.	Dr. Puneet Mittal Associate Prof., AIML		


 **20th Oct.2023**

 **10:30 am – 12:30 pm**

 **Smt. Sharda Pai Auditorium**

Scan Code for
Registration







8. Schedule of the event (insert in the report)

Date: 20 October, 2023

Time: 10:30 am – 12:30 pm

Mode: Offline

9. Attendance of the Event

Total attendees: 66

S.No.	Name	MUJ ID	Department
1	MUJ1591	Dr. Preeti Narooka	AIML
2	MUJ0527	Sandeep Chaurasia	CSE
3	MUJ1160	Dr. Sumit Dhariwal	IT
4	MUJ1571	Dr. Puneet Mittal	AIML
5	MUJ1185	Dhananya Kumar Singh	IT
6	MUJ1517	Surbhi Sharma	CSE
7	MUJ1376	Dr Sakshi Shringi	COMPUTER SCIENCE ENGINEERING
8	MUJ1604	Dr. Sukhwinder Sharma	DATA SCIENCE & ENGINEERING
9	MUJ1698	Dr. Amit Kumar Sharma	COMPUTER AND COMMUNICATION ENGINEERING
10	MUJ1599	Dr. Mohit Agarwal	CCE
11	MUJ1183	Anil Kumar	CSE
12	MUJ1544	Dr Gireesh Kumar	COMPUTER SCIENCE AND ENGINEERING
13	MUJ1689	Dr. Sandeep Singh	DEPT. OF COMPUTER AND COMMUNICATION ENGINEERING
14	MUJ1550	Dr Mayank Namdev	COMPUTER SCIENCE & ENGINEERING
15	MUJ1047	Santosh Kumar Vishwakarma	ARTIFICIAL INTELLIGENCE AND MACHINE LEARNING
16	MUJ1628	Dr Nidhi Vyas	DOE
17	MUJ1090	Vivek Sharma	CCE
18	MUJ1038	Dr. Amit Kumar Bairwa	CSE-AIML
19	MUJ1664	Priya	AIML
20	MUJ0660	Anita Shrotriya	COMPUTER SCIENCE & ENGINEERING
21	MUJ1563	Manish Rai	AIML
22	MUJ1444	Shubh Lakshmi Agrwal	AIML
23	MUJ1417	Dr. Yadendra Singh	AIML
24	MUJ 1533	Dr. Ankur Pandey	CSE
25	MUJ0719	Dr Ginika Mahajan	DSE
26	MUJ1497	Dr Sushila	CSE
27	MUJ1606	Dr Saurav Mishra	IT
28		Dr Sayar Singh Shikhawat	CSE
29		Dr Laxmi Poonia	MATHS
30	MUJ1547	Upendar Singh	AIML
31	MUJ1542	Dr Praneet	CSE
32	MUJ1539	Dr Neetu Gupta	CSE



33	MUJ1631	Yaquika Sharma	DOE COMMERCE
34	MUJ1569	Dr Hemlata	AIML
35		Rs Bhasar	CCE
36	MUJCONO67	Rayaz Khan	J&MC
37		Dipati	NURSING
38	MUJ1638	Jaydeep Kishore	AIML
39	MUJ1598	Mr Vivek	AIML
40		Bhawani	PHD SCHOLAR
41	MUJ1562	Dr Dibakar Sinha	CSE
42	MUJ1581	Pramod Rathore	CCE
43	MUJ0499	Dr Arvind	CSE
44	MUJ1599	Dr Mohit Agarwal	SCSE
45	MUJ1471	Dr Ankur Jain	MATHS
46	MUJ1678	Abhishek Kesarwani	AIML
47	MUJ1680	Surendra Solanki	AIML
48	MUJ175	Santoshi	CSE
49	MUJ16	Nema Sikawar	CCE
50	MUJ1549	Dr Pooja	CCE
51	MUJ1246	Dr Varun	AIML
52	MUJ1662	Atul Verma	CSE
53	MUJ31823	Dipati	NURSING
54		Sameer	NURSING
55		Rakesh	NURSING
56	MUJ0711	Arjun Singh	CCE
57	MUJ1040	Vijay Kr Sharma	CCE
58	MUJ1396	Shikha Chaudhary	IT
59	MUJ1516	Rajat Goel	CSE
60	MUJ0155	Sandeep Joshi	CSE
61	MUJ0366	Anamika Jain	MATHEMATICS AND STATISTICS
62	MUJ1151	Dr Deepika Shekawat	AIML
63	MUJ0446	Dr. Meena Kumari	CIVIL
64	MUJ0575	Dr. Tej Bahadur	CIVIL
65	MUJ0495	Mr. Sagar Gupta	CIVIL
66	MUJ0764	Dr. Rudhra Halder	CIVIL

10. Feedback report of the Event

The Basic Life Support training conducted by Dr. Ravi Prakash was highly informative and beneficial for all attendees. Participants left with a heightened sense of confidence in their ability to respond effectively to life-threatening emergencies. The comprehensive content, hands-on practice, and expert guidance provided by Dr. Prakash made this training a resounding success.

21/10/2023

Seal and Signature of Head with date



DIRECTORATE OF STUDENT'S WELFARE

(SOCIETY CONNECT)

And

FACULTY OF ENGINEERING

SCHOOL OF COMPUTER SCIENCE & ENGINEERING

**DEPARTMENT OF COMPUTER SCIENCE &
ENGINEERING**

Organized

A Training Session

on

“Basic Life Support”

15 December, 2023

Venue: TMA Pai Auditorium, AB2



Table of Contents

Sl.No.	Contents	Page No.
1.	Introduction of the Event	3
2.	Objective of the Event	3
3.	Beneficiaries of the Event.....	3
4.	Brief Description of the Event.....	4
5.	Geo Tagged Photographs.....	6
6.	Brochure or creative of the event.....	9
7.	Schedule of the event.....	10
8.	Attendance of the event.....	11
9.	Feedback of the Event.....	

1. Introduction of the Event

Basic Life Support (BLS) is a critical set of skills and actions that can be performed by bystanders or healthcare providers to sustain or revive a person's life in the event of a cardiac arrest or other life-threatening emergencies. BLS techniques primarily focus on maintaining an open airway, providing effective chest compressions, and ensuring proper ventilation, with the goal of oxygenating the brain and vital organs until more advanced medical care can be administered. The primary purpose of this training was to empower participants with the ability to recognize and respond effectively to life-threatening emergencies, particularly cardiac arrests. Participants learnt how to provide immediate care until professional medical assistance arrives, and in some cases, actions alone could be the difference between life and death.

Department of Computer Science and Engineering organized an initiative for quality education (SDG Goal 3-**Good Health and Well Being**) in collaboration with Directorate of Student's Welfare (NSS, NCC) and Rotaract Club MUJ. To Ensure healthy lives and promote well-being for all at all ages.

2. Objective of the Event

- Understand the importance of early recognition and activation of the emergency response system.
- Develop proficiency in providing high-quality chest compressions.
- Acquire the knowledge to assess and respond to various emergency scenarios, including choking and sudden cardiac arrest.

3. Beneficiaries of the Event

Staff and Faculty Members of Manipal University Jaipur.

4. Details of the Guest

Dr. Ravi Prakash Chaudhary is the Associate Director and HOD of Emergency Medicine at Manipal Hospital Jaipur. He treats and devises diagnosis plans for patients from all walks of life and of all ages. He is very compassionate and empathetic for his patients. He has done MBBS from JLN medical College, Ajmer and Masters in Emergency Medicine from GWU-USA. He is having experience of 10 years in the field of emergency medicine.

5. Brief Description of the event

Introduction to BLS: The training commenced with an overview of the importance of BLS and its role in saving lives during cardiac and respiratory emergencies.

CPR: Dr. Prakash provided detailed instruction on performing cardiopulmonary resuscitation (CPR) on adults. He emphasized the importance of chest compressions, rescue breaths, and the correct compression-to-ventilation ratio. The training included hands-only CPR techniques, focusing on uninterrupted chest compressions to maximize the chances of survival.

Practical Demonstrations: Dr. Prakash conducted practical demonstrations, allowing participants to practice BLS skills on manikins and receive feedback on their technique.

Choking Relief: Dr. Prakash demonstrated techniques for relieving choking in conscious and unconscious adults, children, and infants.

Recognition of Heart Attacks and Strokes: Participants learned to recognize the signs and symptoms of heart attacks and strokes, along with the appropriate steps to take in these emergencies.

Chain of Survival: Dr. Prakash discussed the concept of the "Chain of Survival" and how each link in the chain is crucial for improving survival rates in cardiac emergencies.

Fits (Seizures):

Dr. Prakash addressed the recognition and appropriate response to seizures, including providing a safe environment and support for the affected individual.

Animal Bites and Stings:

Information was provided on the initial first aid steps for treating bites and stings, along with guidelines for seeking medical attention.

Burns:

Types of burns, their severity, and the immediate steps to be taken for burn victims were discussed. Participants learned how to assess burn injuries and administer appropriate first aid.

Nosebleeds (Epistaxis):

Practical guidance was given on managing nosebleeds, including proper positioning and pressure application techniques.

Fractures and Sprains:

Dr. Prakash covered the basics of recognizing and providing initial care for fractures and sprains, emphasizing the importance of immobilization.

Basic Wound Care:

The training included instruction on cleaning and dressing wounds to prevent infection and promote healing.

Medical Emergencies:

Recognition and initial response to various medical emergencies, such as diabetic emergencies and allergic reactions, were discussed.

Q&A and Scenario-Based Learning: The session encouraged active participation through interactive discussions, question-and-answer sessions, and scenario-based learning to simulate real-life situations.

6. Geo Tagged Photographs



Image 1: Doctor giving the session about the Basic Life Support

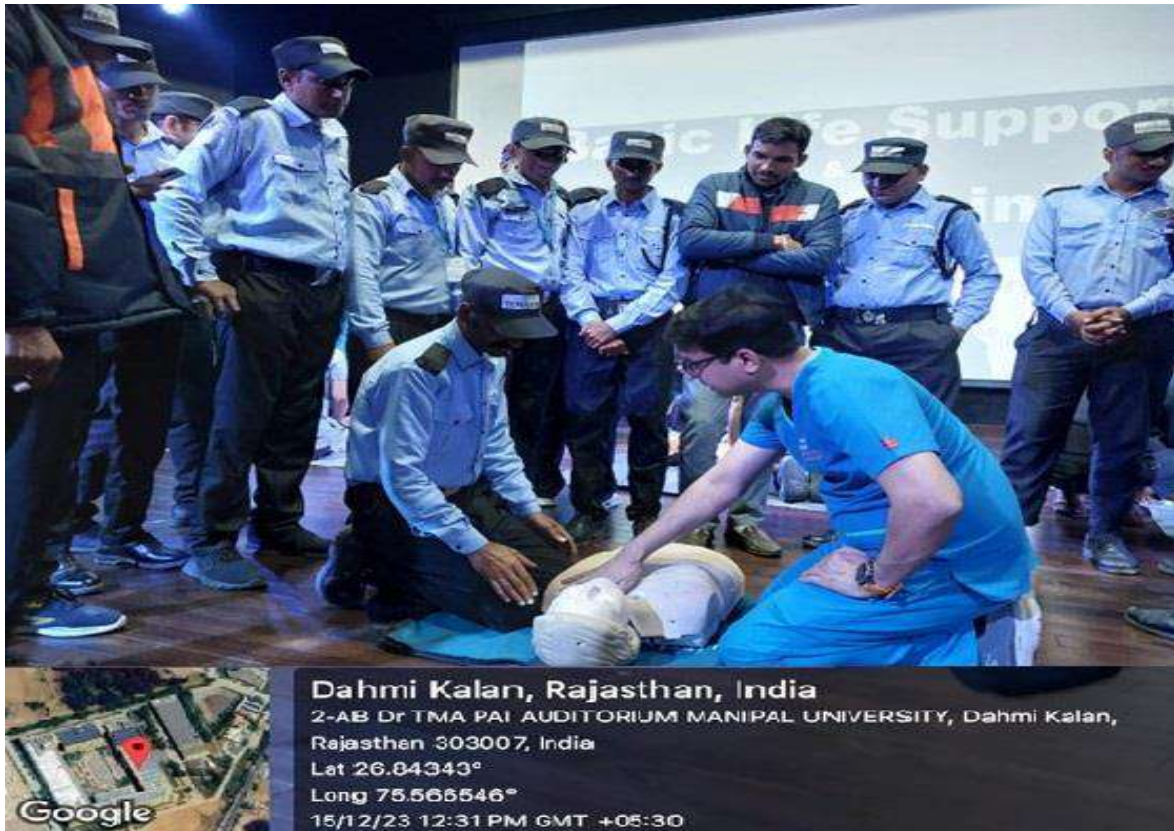


Image 2: Doctor giving the session about the Basic Life Support



Image 3: Session strength listening the lecture.



Image 4: Registrar MUJ Felicitating the invited Dr. Ravi Prakash

7. Brochure or creative of the event

MANIPAL UNIVERSITY JAIPUR **manipalhospitals** **NAAC A+** **SUSTAINABLE DEVELOPMENT GOALS**

(University under Section 2(f) of the UGC Act) **LIFE'S ON** **3 GOOD HEALTH AND WELL-BEING**

Basic Life Support + Training

Organized by
School of Computer Science and Engineering
and
HR Section
in association with
Manipal Hospital Jaipur

Friday, 15 December, 2023 11:00 am onwards
Dr TMA Pai Auditorium

Speaker:
Dr. Ravi Prakash
M.B.B.S., M.E.M. (GWU -USA), EPHM (IIM CALCUTTA)
P.G.D.G.M. (UK); P.G.D.D.M.(MAMC); P.G.D.H.H.M., P.G.D.M.L.S.
Consultant and Head Of Department
Department of Emergency Medicine,
Manipal Hospital, Jaipur

Chief Patron **Patron** **Co-Patrons**

Mr. S. Vaitheeswaran
Chairperson, MUJ

Dr. G K Prabhu
President, MUJ

Cmde.(Dr.) Jawahar M Jangir
Pro President, MUJ

Dr. Nitu Bhatnagar
Registrar, MUJ

Dr. Arun Shanbhag
Dean, FoE, MUJ



8. Schedule of the event

Date: 15 December, 2023

Time: 11:00 am – 03:00 pm

Mode: Offline

9. Attendance of the Event

Total attendees: Students (113)

S.NO.	Reg No	Name	Institute Name
1	23FE10CAI00360	shaivi adesh	Manipal University Jaipur
2	23FE10CAI00487	Dev Sharma	Manipal University Jaipur
3	23FS20MBO00001	Ankita Singh	Manipal University Jaipur
4	23FA20MCP00005	Ayushi Pushkarna	Manipal University Jaipur
5	23FE10CSE00186	Akshita Sai Pery	Manipal University Jaipur
6	23FE10CSE00766	Akshat Tiwari	Manipal University Jaipur
7	23FE10CSE00435	HARSHIT ATTRI	Manipal University Jaipur
8	23FE10CAI00028	VALLURI SRI AASRITHA	Manipal University Jaipur
9	23FE10CDS00483	Kritika Magnani	Manipal University Jaipur
10	23FE10CDS00528	VANSHIKA VISHNAWAT	Manipal University Jaipur
11	23FE10CSE00043	KRITI RASTOGI	Manipal University Jaipur
12	23FE10CII00034	Trisha shanvi	Manipal University Jaipur
13	23FE10ITE00199	Ayush Singh	Manipal University Jaipur
14	23FE10CCE00034	KRISHNA GOEL	Manipal University Jaipur
15	23FE10AEE00008	Kisna Rana	Manipal University Jaipur
16	23FE10CSE00077	Akriti Chauhan	Manipal University Jaipur
17	23FE10CAI00548	Poorti Swarup	Manipal University Jaipur
18	23FE10CSE00005	Suhana Kaushik	Manipal University Jaipur
19	23FA10BSP00024	Lavanya Choudhary	Manipal University Jaipur
20	23FA10BSP00046	Rafia	Manipal University Jaipur
21	23FA10BHE00012	Nausheen broca	Manipal University Jaipur
22	23FE10CCE00057	Mohit kumhar	Manipal University Jaipur
23	23fe10cse00395	Samriddhi Sharma	Manipal University Jaipur
24	23FE10CSE00699	Nancy	Manipal University Jaipur
25	23FE10ITE00015	Janhvi Soni	Manipal University Jaipur
26	23FE10ITE00185	Aryaman Singh	Manipal University Jaipur
27	23FE10CSE00039	Priyal Kansal	Manipal University Jaipur
28	23FE10CSE00643	KSHITIJ VERMA	Manipal University Jaipur
29	23FE10CDS00235	Anika sharma	Manipal University Jaipur
30	23FE10CII00109	Satvik Ahuja	Manipal University Jaipur
31	23FE10CDS00208	Ananya Srivastava	Manipal University Jaipur
32	23FE10CSE00222	Taarunya Aggarwal	Manipal University Jaipur
33	23FM10IBA00010	Harshit singh	Manipal University Jaipur
34	23FE10ITE00277	Aayushi Singh	Manipal University Jaipur
35	23FM10BBA00341	Pallavi Dhaibhai	Manipal University Jaipur

36	23fd10bar00004	Aadhya mahajan	Manipal University Jaipur
37	23FE10CDS00423	Purvi Sharma	Manipal University Jaipur
38	23FE10ITE00021	Mounil Kankhara	Manipal University Jaipur
39	23FE10ITE00178	Pranav Prakash	Manipal University Jaipur
40	23FE10ITE00079	Amisha anand	Manipal University Jaipur
41	23FE10CAI00360	shaivi adesh	Manipal University Jaipur
42	23FE10CSE00060	Amay Garg	Manipal University Jaipur
43	23FE10CDS00177	Manas Mathur	Manipal University Jaipur
44	23fe10bte00029	Saloni kamal	Manipal University Jaipur
45	23FE10CSE00508	Dev Dhawan	Manipal University Jaipur
46	23fe10cii00035	Bhargavi Anand	Manipal University Jaipur
47	23FA10BSP00028	Anupama Rustagi	Manipal University Jaipur
48	23FE10CCE00085	Siddhartha tiwari	Manipal University Jaipur
49	23FA10BAP00002	Tanisha Mathur	Manipal University Jaipur
50	23FD10BFD00009	Mariya Shabbir Baiwala	Manipal University Jaipur
51	23FE10CDS00224	Harsh Ajmera	Manipal University Jaipur
52	23fe10cds00125	Suryanshi Singh	Manipal University Jaipur
53	23fs10mat00009	Malavika ramdas	Manipal University Jaipur
54	23FE10CSE00137	Stuti Dixit	Manipal University Jaipur
55	23fe10cii00094	Aarohi Tyagi	Manipal University Jaipur
56	23FE10CSE00152	Gautam Kakkar	Manipal University Jaipur
57	23FE10CSE00318	Krish Ray	Manipal University Jaipur
58	23FE10CII00076	Kriish Marwaha	Manipal University Jaipur
59	23FS10BIO00051	Ragini Singh Thakur	Manipal University Jaipur
60	23FS10BIO00052	Anukriti sharma	Manipal University Jaipur
61	23FE10CSE00081	Smmayan Gupta	Manipal University Jaipur
62	23FE10CDS00397	Hrishita Singh Timaney	Manipal University Jaipur
63	23FE10ITE00203	Sarah Sharda	Manipal University Jaipur
64	23fa10bsp00025	Jasleen kaur	Manipal University Jaipur
65	23FA10BSP00039	Jiya Kumar	Manipal University Jaipur
66	23FA10BSP00004	Aarya Mahale	Manipal University Jaipur
67	23fa10bsp00058	Kashvi Mahajan	Manipal University Jaipur
68	23fe10ece00024	Kushagra agrawal	Manipal University Jaipur
69	23FA10BSP00017	Megha Sharma	Manipal University Jaipur
70	23FM10BBA00162	Alina Nadeem	Manipal University Jaipur
71	23FM10BBA00178	Avishi Akhaury	Manipal University Jaipur
72	23FA10BAP00027	Natasha Joan Menezes	Manipal University Jaipur
73	23FA10BLE00004	Tanisha chaturvedi	Manipal University Jaipur
74	23fe10cai00579	Arjun Malhotra	Manipal University Jaipur
75	23FE10CAI00352	Maanyata Aul	Manipal University Jaipur
76	23FM10BBA00348	Niska kedia	Manipal University Jaipur
77	23FM10BBA00170	Shambhavi Agrawal	Manipal University Jaipur
78	23FE10CDS00241	Armaan Setia	Manipal University Jaipur
79	23FE10CAI00105	Mritunjay Singh	Manipal University Jaipur
80	23FA10BHE00035	Taneesha puri	Manipal University Jaipur
81	23FE10CDS00284	Anant Barjatya	Manipal University Jaipur

82	23fa10bsp00047	Vartika Agarwal	Manipal University Jaipur
83	23FA10BSP00041	Kali Vithlani	Manipal University Jaipur
84	23FM10BBA00030	Harshal Saini	Manipal University Jaipur
85	23FE10CSE00746	Daksh Sharma	Manipal University Jaipur
86	23FS10BIO00034	PC Rahul	Manipal University Jaipur
87	23FA10BSP00005	Teshant arora	Manipal University Jaipur
88	23fe10cse00479	Arushi Singh	Manipal University Jaipur
89	23FM10BBA00130	Riddhima Gupta	Manipal University Jaipur
90	23fe10cse00290	Harshit chadha	Manipal University Jaipur
91	23FS10BCA00234	Anila Jayanson George	Manipal University Jaipur
92	23FS10BCA00234	Anamika Gandhi	Manipal University Jaipur
93	23FE10CAI00485	Kakul Rawat	Manipal University Jaipur
94	23FE10CSE00795	Anwasha jain	Manipal University Jaipur
95	23FE10CSE00094	Satya Agrawal	Manipal University Jaipur
96	23FE10CCE00079	Lakshya Verma	Manipal University Jaipur
97	23fe10cse00122	Shritama Acharyee	Manipal University Jaipur
98	23FE10CSE00344	Aakash kushwaha	Manipal University Jaipur
99	23FE10CSE00414	Ananya Khandelwal	Manipal University Jaipur
100	23FA10BSP00049	Aarushi Thora	Manipal University Jaipur
101	23fe10cii00012	Nishant Prasad	Manipal University Jaipur
102	23FE10CSE00195	Vaishnavi karelia	Manipal University Jaipur
103	23FE10CAI00282	isha nagpal	Manipal University Jaipur
104	23FM10BBA00168	Aarchi Chhabra	Manipal University Jaipur
105	23FM20MBA00015	Apurva Gupta	Manipal University Jaipur
106	219402024	Puneet Sharma	Manipal University Jaipur
107	221015107	Munesh	Manipal University Jaipur
108	221002065	Tanya Barua	Manipal University Jaipur
109	23FA10BAP00033	Dipal gupta	Manipal University Jaipur
110	23FL10IBL00040	Shinjini Bansal	Manipal University Jaipur
111	229310012	Pragati Pandey	Manipal University Jaipur
112	23FE10ITE00212	Eshaan Tushar Bobdey	Manipal University Jaipur
113	23FE10CSE00507	Manalee Tamrakar	Manipal University Jaipur

Manipal University Jaipur
School of Computer Science and Engineering
Training on Basic Life Support (BLS)
Date : 15/12/2023 Venue: Dr. TMA Pai Auditorium

S. NO.	MUJ ID	NAME	DEPARTMENT	SIGNATURE
1	MUJ1459	Dr. Pragya Vaishnav	CA	
2	MUJ1718	Arpana Sinhal	Comp. App	
3	MUJ1664	Dr. Priya Goyal	AIML	
4	MUJ1544	Dr. Gaurav Kumar	CSE	
5	MUJ1196	Dr. Anil Agrawal	DCA	
6	MUJ1563	Manish Raj	AIML	
7	MUJ1690	Suresh Chandra	AIML	
8	MUJ1523	Dr. Sayan Singh Shrivastava	CSE	
9	MUJ1454	Dr. Sufabrata Roy	CSE	
10		Shirna George	HR	
11	MUJ1376	Dr. SAKSHI SHRINGI	CSE	
12	MUJ1234	Dr. Neelam Chaudhary	CSE	
13	MUJ1571	Dr. Krunal Mehta	AIML	
14		सविता	H.K.	
15		मीना	H.K.	
16		कान्ता	H.K.	
17		सीमा	H.K.	
18		कान्तावती	H.K.	
19		हेमलता	H.K.	
20		मुखा	H.K.	
21		डोमा	H.K.	
22		किरा	H.K.	
23		सुमन	H.K.	
24		उडी	H.K.	
25		ममता	H.K.	
26		सुनिता	H.K.	
27		संद्या	H.K.	
28		इनारवी	H.K.	
29		दिरा	H.K.	
30		सुनिता	H.K.	
31		मीना	H.K.	
32		आशा	H.K.	



MANIPAL UNIVERSITY
JAIPUR

Manipal University Jaipur
School of Computer Science and Engineering
Training on Basic Life Support (BLS)

Date : 15/12/2023

Venue: Dr. TMA Pal Auditorium

S. NO.	MUJ ID	NAME	DEPARTMENT	SIGNATURE
34	DH036	Deepak kumar	Terrier	[Signature]
35	AM160	Ajay Yadav	Terrier	[Signature]
36	RN777	RICHHAR Mehta	Terrier	[Signature]
37	SZ072	Shay Singh	Terrier	[Signature]
38	DG888	Devedet Rajput	Terrier	[Signature]
39	NF678	Nand Lal Bairwa	GDPA Terrier	Nand Lal Bairwa
40	Gn162	Guram Kanwar	Terrier	Guram Kanwar
41	HJ966	Heena Choudhary	Terrier	[Signature]
42		ASHA RANI Choudhary	Terrier	[Signature]
43			Terrier	[Signature]
44	0100R1	RANVIR SINGH		[Signature]
45	VD972	Vinod Kumar Verma	Terrier	[Signature]
46	ML929	mahesh kumar	Terrier	[Signature]
47	SY552	Satyam Narayan Meena	Terrier	[Signature]
48	DH089	Deval Goyal	Terrier	[Signature]
49	O369	omesh kumar Goyal	Terrier	[Signature]
50	RN815	Rajneesh kumar Meena	Terrier	Rajneesh
51	MUJ1459	Ashish Sharma	CSE	[Signature]
52	MUJ1542	Dr. Pramod Saurabh	CSE	[Signature]
53	MUJ1388	Dr. Rishav Dubey	LSE	[Signature]
54	MUJ0499	Dr. Arvind Kumar	CSE	[Signature]
55	MUJ1516	Dr. Rajat Goyal	CSE	[Signature]
56	MUJ1497	Dr. Surbha Vishi	CSE	[Signature]
57	MUJ1402	Dr. Amit Goyal	CSE	[Signature]
58	MUJ1562	D. Dibakar Singh	CSE	[Signature]
59	MUJ0744	Dr. Ridhi Gupta	CSE	[Signature]
60	MUJ1541	Upendra Singh	AIML	[Signature]
61	MUJ1661	Bhawanee sharma	CCE	[Signature]
62	MUJ1561	Dr. Hemlata	AIML	[Signature]
63	MUJ1664	Dr. Pooja Goyal	AIML	[Signature]
64	MUJ1036	Dr. Sonu R. Goyal	CCE	[Signature]
65	MUJ1421	Shikha Chandra	CSE	[Signature]
66	MUJ1234	Dr. Neelam Chaptor	LSE	[Signature]

Manipal University Jaipur
School of Computer Science and Engineering
Training on Basic Life Support (BLS)

Date : 15/12/2023 Venue: Dr. TMA Pai Auditorium

S. NO.	MUJ ID	NAME	DEPARTMENT	SIGNATURE
166	MUJ1340	Suresh Kumar Prajapati	Finance	Suresh
167	MUJ1321	Jawan Kumar	Help desk	Jawan
168	MUJ1306	Deepak Wadhawan	Registration	Deepak
169	MUJ1347	Sumar Singh	VC office	Sumar
170	MUJ1539	Prakash Singh	Admission	Prakash
171	" 1346	Suresh Kumar Sharma	V.C OFFICE	Suresh
172	" 1302	Lokesh Kumar Verma	MUJ Store	Lokesh
173	" 1282	Ramkishan Sharma	Carpenter	Ramkishan
174	" 1288	Siddhant C. Jat	MUJ Store	Siddhant
175		Kundan	Coordinator	Kundan
176		अमित	अमित	अमित
177		अमित		अमित
178		अमित		अमित
179		अमित		अमित
180		अमित		अमित
181	MUJ1288	Pradeep Sharma	main.	Pradeep
182	quest	Surgeon Garg	H.K. Exe.	Surgeon
183	quest	Shivraj Singh	H.K. Exe.	Shivraj
184		Pawan Kumar Patodiya	Outlet	Pawan
185		Rajesh Kumar Rajput	Outlet	Rajesh
186	quest	Ramkishan Mishra	Kitchen	Ramkishan
187		Ramkishan	Kitchen	Ramkishan
188	Security	Rukma Chaudhary	Security	Rukma
189	MUJ1468	PRIVANKA SAMBHA	ADMISSION	Privanka
190	MUJ1404	PARUL KANWAR	Arts	Parul
191	MUJ0403	Dr. Shilpi Gupta (Resol.)	Economics	Shilpi
192	-	Devanshi Kapoor	Economics	Devanshi
193	MUJ1702	Vaishali Chauhan	CSE	Vaishali
194	MUJ1691	Dr. Monika Jyotiya	Comp. Application	Monika
195	MUJ-1416	Ranveer Singh Shekhar	SB C	Ranveer
196	09 R5	matchand	Security	Matchand
197	073RT	MUKTAR SINGH	- -	Muktar
198				

10. Feedback report of the Event

The Basic Life Support training conducted by Dr. Ravi Prakash was highly informative and beneficial for all attendees. Participants left with a heightened sense of confidence in their ability to respond effectively to life-threatening emergencies. The comprehensive content, hands-on practice, and expert guidance provided by Dr. Prakash made this training a resounding success.

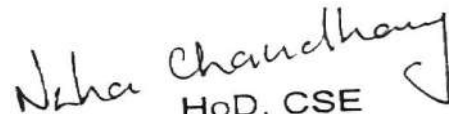


(Hemant Kumar)

Assistant Director, Society Connect

Directorate of Student's Welfare

DIRECTOR STUDENT WELFARE & PROCTOR
MANIPAL UNIVERSITY, JAIPUR


HO D, CSE
MANIPAL UNIVERSITY
JAIPUR-303007

Seal and Signature of Head with date



(Prof. AD Vyas)

Director, Directorate of Student's Welfare



**MANIPAL UNIVERSITY
JAIPUR**

Faculty of Management and Commerce

Department of Business Administration

Societal Connect Activity on

Bird Nest Installation

NOVEMBER 30, 2023



**Head
Department of Business Administration
Manipal University Jaipur**

1. Introduction of the Event

Introduction of the Event: School of Business and Commerce organized a activity to install bird nests in the nearby village on November 30, 2023. 5 students and 1 faculty member participated in the campaign. The event took place in nearby village of Manipal university.

2. Objective of the Event

The primary objective of the event was to promote environmental awareness and conservation by actively contributing to the well-being of local bird populations. Through the installation of bird nests, the aim was to create a sustainable habitat for birds in the nearby village, fostering biodiversity and ecological balance.

3. Beneficiaries of the Event

The beneficiaries of the event included the local bird species in the nearby village. By providing suitable nesting spaces, the initiative sought to enhance the living conditions for birds, contributing to the overall ecosystem health. Additionally, the participating students gained hands-on experience in environmental stewardship.

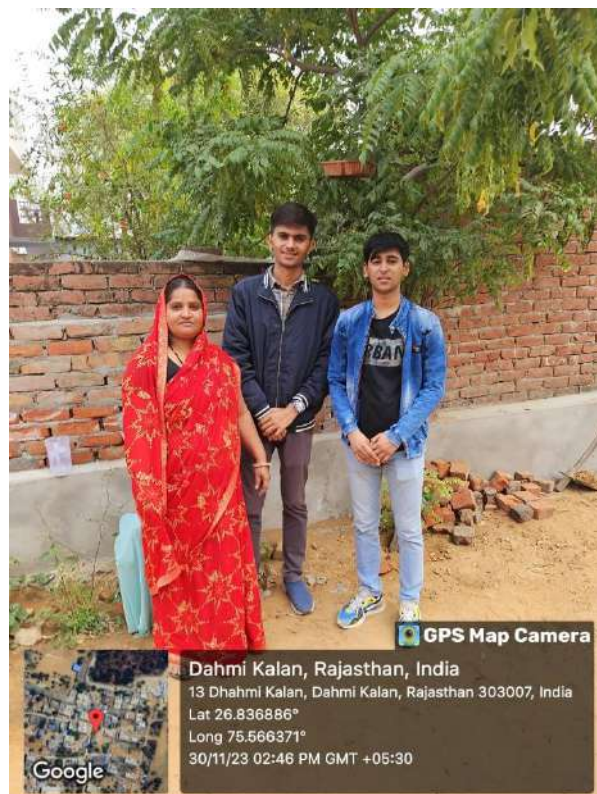
4. Details of the Guests

The event was laid by the students of BBA.

5. Brief Description of the event

The activity involved the installation of bird nests in the nearby village of Manipal University, with students and faculty members actively engaging in the process. Participants worked together to strategically place the nests, considering the local ecology and the needs of various bird species. The event not only contributed to the local environment but also provided a unique learning experience for the students, emphasizing the importance of hands-on conservation efforts. Overall, the initiative aimed to create a positive impact on the local ecosystem while instilling a sense of environmental responsibility among the participants.

6. Photographs





 **GPS Map Camera**

Dahmi Kalan, Rajasthan, India

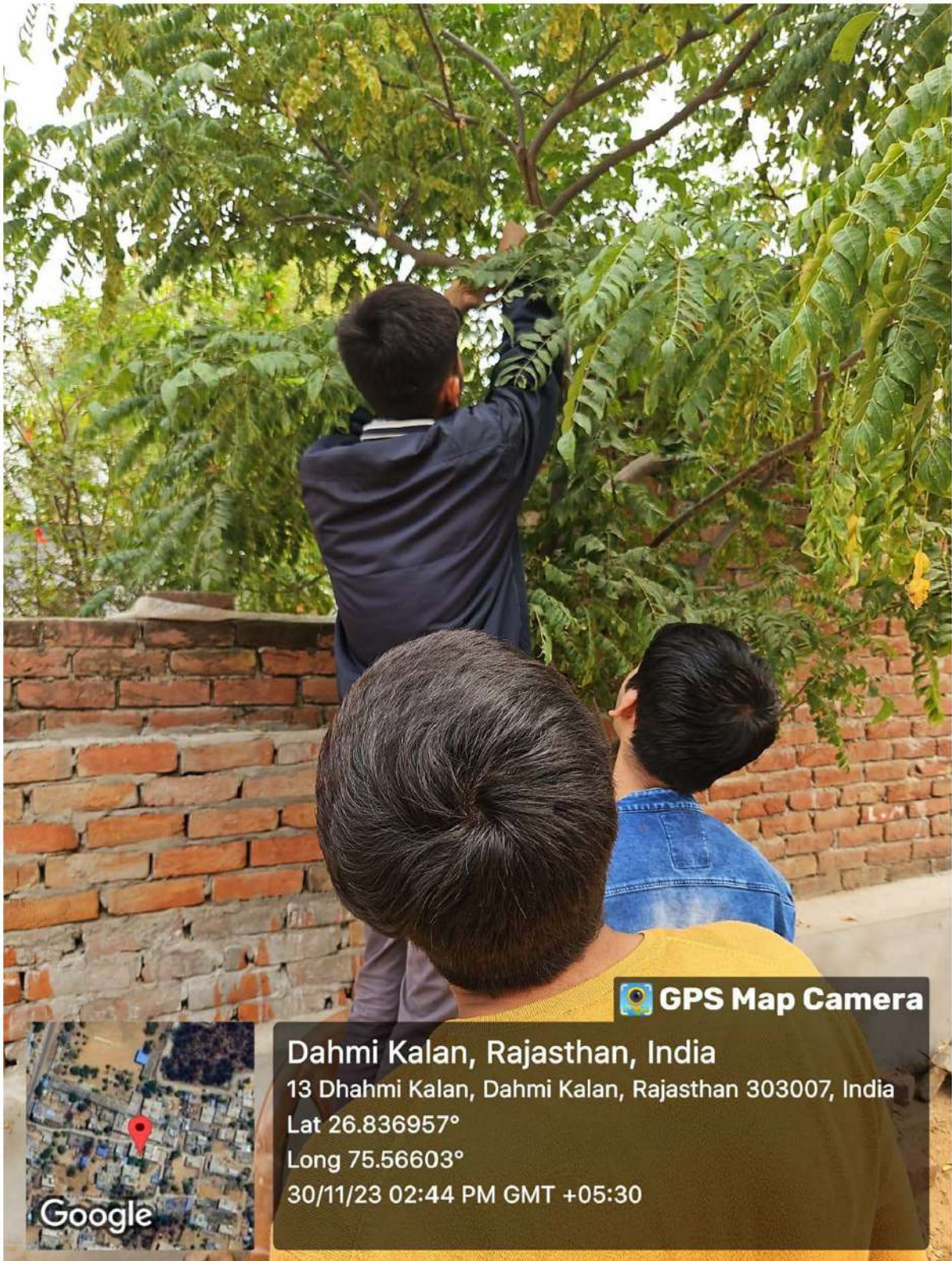
13 Dhahmi Kalan, Dahmi Kalan, Rajasthan 303007, India

Lat 26.836886°

Long 75.566371°


30/11/23 02:45 PM GMT +05:30









 **GPS Map Camera**

Dahmi Kalan, Rajasthan, India
13 Dhahmi Kalan, Dahmi Kalan, Rajasthan 303007, India
Lat 26.837003°
Long 75.566019°
30/11/23 02:40 PM GMT +05:30












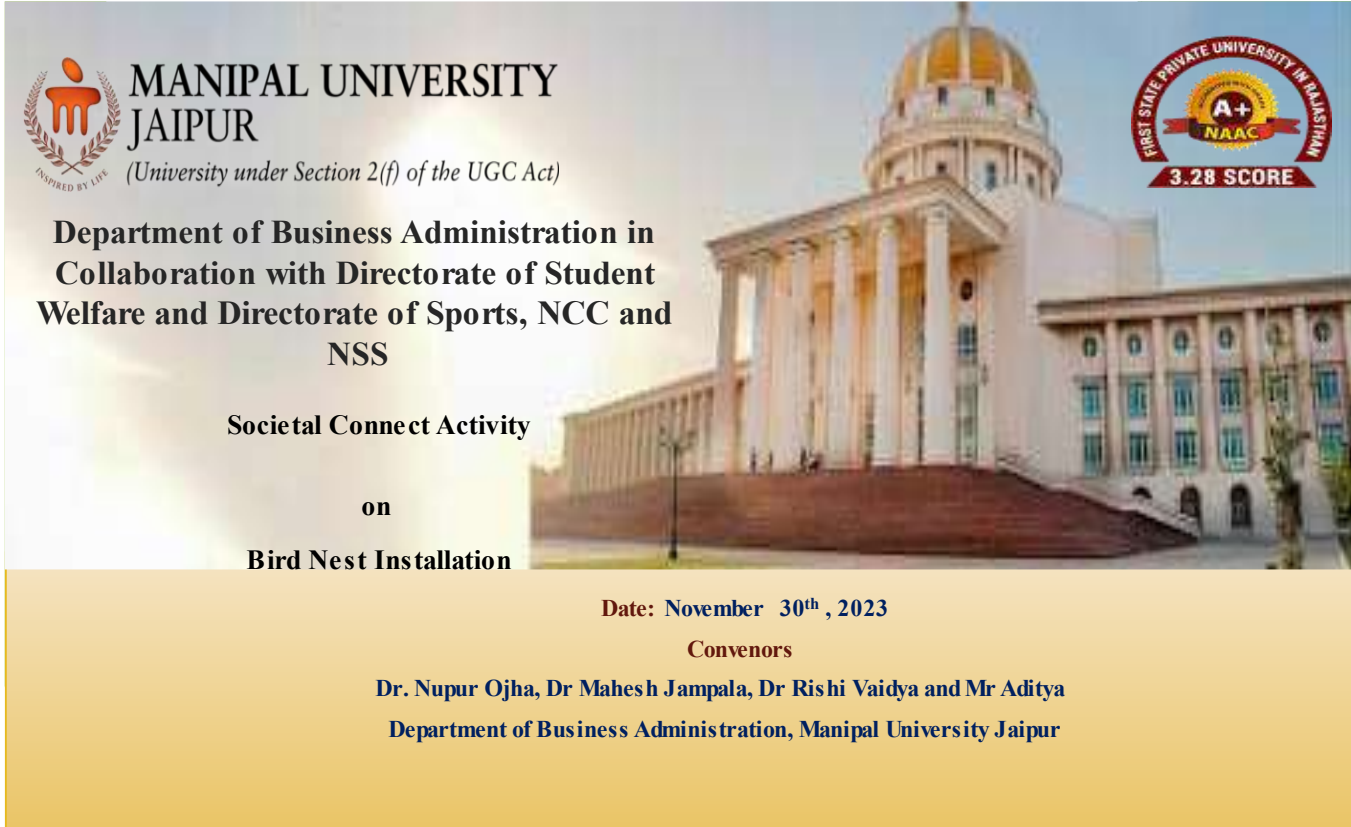
 **GPS Map Camera**


Dahmi Kalan, Rajasthan, India
RHP8+X24, Dahmi Kalan, Rajasthan 303007, India
Lat 26.836853°
Long 75.565522°
30/11/23 02:33 PM GMT +05:30






7. Brochure or creative of the event



 **MANIPAL UNIVERSITY**
JAIPUR
(University under Section 2(f) of the UGC Act)



**Department of Business Administration in
Collaboration with Directorate of Student
Welfare and Directorate of Sports, NCC and
NSS**

Societal Connect Activity

on

Bird Nest Installation

Date: November 30th, 2023


Convenors
Dr. Nupur Ojha, Dr Mahesh Jampala, Dr Rishi Vaidya and Mr Aditya
Department of Business Administration, Manipal University Jaipur

8. Schedule of the Event

The event took place on November 30, 2023

9. Attendance of the Event

Sr. No	Name of Institution	Registration Number/ Employee Code	Attendee Name
1	Manipal University Jaipur	MUJ0099	Dr. Mahesh Jampala
2	Manipal University Jaipur	MUJ1538	Dr Rishi Vaidya
3	Manipal University Jaipur	MUJ0623	Dr. Nupur Ojha
4	Manipal University Jaipur	MUJ1490	Mr. Aditya Dhiman
5	Manipal University Jaipur	23FM10BBA00204	DINESH CHOUDHARY
6	Manipal University Jaipur	23FM10BBA00200	VANSH MULCHANDANI
7	Manipal University Jaipur	23FM10BBA00214	GOPAL BISHNOI
8	Manipal University Jaipur	23FM10BBA00215	AKSHAT SHARMA
9	Manipal University Jaipur	23FM10BBA00216	KHUSHWANT SANKHLA
10	Manipal University Jaipur	23FM10BBA00205	AYUSHMAN GUPTA


Head
Department of Business Administration
Manipal University Jaipur

MUJ/DSW/Society Connect/Oct 2023/02



MANIPAL UNIVERSITY
JAIPUR

DIRECTORATE OF STUDENT'S WELFARE

(SOCIETY CONNECT)

#DAANUTSAV 2023

CLEANLINESS DRIVE

(GANDHI JAYANTI)

2nd October 2023



Index

S.No.	Activity Heads	Page no.
1.	Introduction of the Event	1
2.	Objective of the Event	1
3.	Beneficiaries of the Event	1
4.	Brief Description of the event	1
5.	Photographs	2-3
6.	Brochure or creative of the event	4-5
7.	Schedule of the Event	6
8.	Attendance of the Event	6-8
9.	Feedback of the Event	8
10.	Link of MUJ website	8

1. Introduction of the Event

A clean India would be the best tribute India could pay to Mahatma Gandhi on his 150-birth anniversary in 2019," said Shri Narendra Modi as he launched the Swachh Bharat Mission at Rajpath in New Delhi. On 2nd October 2014, Swachh Bharat Mission was launched throughout the length and breadth of the country as a national movement. The campaign aims to achieve the vision of a 'Clean India'. In this direction, "*Cleanliness Drive*" is organized on 2nd October 2023 at the nearby village called Dehmi kalan at 9 Am morning. The importance of Swachh Bharat Abhiyan has been discussed with local people and vendor. The whole team of Faculty and students advised the local people and vendors to put dustbin near the village. Team also interacted with the students at school and discussed the swachhatha hi seva and Swachh Bharat Mission. This drive is organized by Rotaract Club of MUJ on the auspicious occasion of Gandhi Jayanti and DAAN UTSAV 2023 i.e 2nd October from 9 in the morning. The drive was conducted to help clean our surroundings and the betterment of the environment.

2. Objective of the Event

- Promote the value of cleanliness
- Discipline and respect for the environment
- Spreading word about the need for cleanliness and hygiene
- Sensitizing people about the importance of cleanliness

3. Beneficiaries of the Event

Community, students of MUJ

4. Brief Description of the event

The Cleanliness Drive took place on 2nd October, the birth anniversary of Mahatma Gandhi and the 4th anniversary of Swachh Bharat Abhiyan. On the account of DAAN UTSAV 2023, Rotaract Club organized this event in Dahmi Kalan Village. Students participated with enthusiasm throughout the drive. Everyone gathered at 9 a.m. to depart for the drive. Everyone helped each other to clean up the area and dispose the waste properly.

The drive helped instill the importance of cleanliness and hygiene in the environment and how we, as regular people, can help maintain it.

5. Photographs of the event



Image 1 Cleanliness Drive at Dahmi Kalan



Image 2 Cleaning drive at near School



Image 3 Rotaract Club Srtuents participating in the drive



Image 4 Students participating in the drive.

6. Brochure or creative of the event



MANIPAL UNIVERSITY
JAIPUR







**Directorate of Student's Welfare
Society Connect**

Rotaract Club

DAANUTSAV 2023

CLEANLINESS DRIVE



स्वच्छ भारत
एक कदम स्वच्छता की ओर



Gandhi Jayanti
2023

Date: 2 OCT 2023
Time : 9 AM to 12 noon
Venue : Dehmi Kalan Village, Jaipur

#DAANUTSAV 2023- Cleanliness Drive

7. Schedule of the event

S.NO.	Name of the Event	Time	Place
1.	Cleanliness Drive	9:00 AM	Dehmi Kalan Village

8. Attendance of the Event (insert in the document only)

Total attendee- 70

S.NO.	Registration Number	Name	Institute Name
1	229302644	Ankur kumar	Manipal University Jaipur
2	229311104	Shashwat Kumar	Manipal University Jaipur
3	229301221	Rubhav Bahirwani	Manipal University Jaipur
4	229302571	Shreya Kumari	Manipal University Jaipur
5	23FE10CAI00360	shaivi adesh	Manipal University Jaipur
6	23FE10CAI00487	Dev Sharma	Manipal University Jaipur
7	229310059	Aditya Yadav	Manipal University Jaipur
8	23FS20MBO00001	Ankita Singh	Manipal University Jaipur
9	23FA20MCP00005	Ayushi Pushkarna	Manipal University Jaipur
10	23FE10CSE00186	Akshita Sai Pery	Manipal University Jaipur
11	23FE10CSE00766	Akshat Tiwari	Manipal University Jaipur



12	23FE10CSE00435	HARSHIT ATTRI	Manipal University Jaipur
13	229310269	Sneha Bhatia	Manipal University Jaipur
14	229303005	Nidhi Verma	Manipal University Jaipur
15	221007075	Preetika Sharma	Manipal University Jaipur
16	23FE10CAI00028	VALLURI SRI AASRITHA	Manipal University Jaipur
17	23FE10CDS00483	Kritika Magnani	Manipal University Jaipur
18	23FE10CDS00528	VANSHIKA VISHNAWAT	Manipal University Jaipur
19	23FE10CSE00043	KRITI RASTOGI	Manipal University Jaipur
20	23FE10CII00034	Trisha shanvi	Manipal University Jaipur
21	23FE10ITE00199	Ayush Singh	Manipal University Jaipur
22	23FE10CCE00034	KRISHNA GOEL	Manipal University Jaipur
23	23FE10AEE00008	Kisna Rana	Manipal University Jaipur
24	23FE10CSE00077	Akriti Chauhan	Manipal University Jaipur
25	23FE10CAI00548	Poorti Swarup	Manipal University Jaipur
26	23FE10CSE00005	Suhana Kaushik	Manipal University Jaipur
27	23FA10BSP00024	Lavanya Choudhary	Manipal University Jaipur
28	23FA10BSP00046	Rafia	Manipal University Jaipur
29	23FA10BHE00012	Nausheen broca	Manipal University Jaipur
30	221007020	Ayushi Mittal	Manipal University Jaipur
31	23FE10CCE00057	Mohit kumhar	Manipal University Jaipur
32	23fe10cse00395	Samriddhi Sharma	Manipal University Jaipur
33	23FE10CSE00699	Nancy	Manipal University Jaipur
34	23FE10ITE00015	Janhvi Soni	Manipal University Jaipur
35	23FE10ITE00185	Aryaman Singh	Manipal University Jaipur
36	23FE10CSE00039	Priyal Kansal	Manipal University Jaipur
37	221002064	shweta mishra	Manipal University Jaipur
38	23FE10CSE00643	KSHITIJ VERMA	Manipal University Jaipur
39	23FE10CDS00235	Anika sharma	Manipal University Jaipur
40	23FE10CII00109	Satvik Ahuja	Manipal University Jaipur
41	23FE10CDS00208	Ananya Srivastava	Manipal University Jaipur
42	23FE10CSE00222	Taarunya Aggarwal	Manipal University Jaipur
43	23FM10IBA00010	Harshit singh	Manipal University Jaipur
44	23FE10ITE00277	Aayushi Singh	Manipal University Jaipur
45	229302160	Parth johar	Manipal University Jaipur
46	23FM10BBA00341	Pallavi Dhaibhai	Manipal University Jaipur
47	23fd10bar00004	Aadhya mahajan	Manipal University Jaipur
48	23FE10CDS00423	Purvi Sharma	Manipal University Jaipur
49	23FE10ITE00021	Mounil Kankhara	Manipal University Jaipur
50	23FE10ITE00178	Pranav Prakash	Manipal University Jaipur
51	23FE10ITE00079	Amisha anand	Manipal University Jaipur
52	23FE10CAI00360	shaivi adesh	Manipal University Jaipur
53	23FE10CSE00060	Amay Garg	Manipal University Jaipur
54	23FE10CDS00177	Manas Mathur	Manipal University Jaipur
55	23fe10bte00029	Saloni kamal	Manipal University Jaipur
56	23FE10CSE00508	Dev Dhawan	Manipal University Jaipur

57	23fe10cii00035	Bhargavi Anand	Manipal University Jaipur
58	220606004	Pranjal Puri	Manipal University Jaipur
59	23FA10BSP00028	Anupama Rustagi	Manipal University Jaipur
60	23FE10CCE00085	Siddhartha tiwari	Manipal University Jaipur
61	23FA10BAP00002	Tanisha Mathur	Manipal University Jaipur
62	23FD10BFD00009	Mariya Shabbir Baiwala	Manipal University Jaipur
63	23FE10CDS00224	Harsh Ajmera	Manipal University Jaipur
64	23fe10cds00125	Suryanshi Singh	Manipal University Jaipur
65	23fs10mat00009	Malavika ramdas	Manipal University Jaipur
66	221007021	Arshi Jain	Manipal University Jaipur
67	23FE10CSE00137	Stuti Dixit	Manipal University Jaipur
68	23fe10cii00094	Aarohi Tyagi	Manipal University Jaipur
69	23FE10CSE00152	Gautam Kakkar	Manipal University Jaipur
70	23FE10CSE00318	Krish Ray	Manipal University Jaipur

9. Feedback of the Event

The students participated enthusiastically and helped to spread message for cleanliness.



(Hemant Kumar)

Assistant Director, Society Connect

Directorate of Student's Welfare



(Prof. AD Vyas)

Director, Directorate of Student's Welfare

DIRECTOR STUDENT WELFARE & PROCTOR
MANIPAL UNIVERSITY, JAIPUR



MUJ/DSW/Society Connect/ Oct2023/03



MANIPAL UNIVERSITY
JAIPUR

DIRECTORATE OF STUDENT'S WELFARE

(SOCIETY CONNECT)

#DAANUTSAV 2023

Plantation Drive

3rd October 2023

Date: 3rd October 2023



Index

S.No.	Activity Heads	Page no.
1.	Introduction of the Event	1
2.	Objective of the Event	1
3.	Beneficiaries of the Event	1
4.	Brief Description of the event	1
5.	Photographs	2-4
6.	Brochure or creative of the event	5-6
7.	Schedule of the Event	6
8.	Attendance of the Event	6-9
9.	Feedback of the Event	9
10.	Link of MUJ website	9



1. Introduction of the Event

“A nation that destroys its soils destroys itself. Forests are the lungs of our land, purifying the air and giving fresh strength to our people.” Trees are indispensable for life. Man can't live without trees. However, the present condition of forests in the world, especially developing countries is pathetic and miserable. Forests are the source of life. They are the giving angels. They give man oxygen, rains, wood, fruit, make the world look so beautiful, yet the sinister man kills them! Who will be more inhumane than man himself? Cutting of forests ultimately endangers man's own existence. Trees are important to the environment; they recycle water and process carbon dioxide in the atmosphere through photosynthesis. They are the world's full-time purifiers of air and water. Their cutting will disturb the natural water cycles which will lead to the shortage of fresh water in the water reserves of the world.

Rotaract Green Club under Society Connect organized a Plantation Drive on account of DAAN UTSAV 2031. It took place on the 3rd of October from 10 a.m. Students were taken to the Mahatma Gandhi School, Begus for the drive. The drive aimed to instill a sense of discipline and respect for the environment while doing our part.

2. Objective of the Event

- Spread awareness on the importance of afforestation
- Direct students' mind in constructive activities
- Contribution to the society
- Promote tree planting
- Create awareness regarding importance of ecology
- Attempt at reducing pollution and improve green ambience

3. Beneficiaries of the Event

Community

4. Brief Description of the event

Rotaract Green Club organized the Plantation Drive on the 3rd October at 9 a.m. on account of DAAN UTSAV 2023. The drive's main aim was to direct student's mind

in constructive activities with the positive outcome through the facilitation of contributing to the nature and environment.

It also aimed at spreading awareness about the effects of global warming and the positive effects of planting trees. The students gathered on campus to go to the Mahatma Gandhi School, Begus.

The students participated in the drive enthusiastically and helped each other in planting the saplings. All the saplings were planted in the school ground by students. Participants were highly energetic to make the event a big success. A spirit of teamwork, exchange of ideas and enthusiasm of the participants especially among the students could be seen. Pictures were taken. The drive was successfully conducted by planting 40-50 saplings.

5. Photographs of the event



Image 1. Students and Faculty planting saplings



Image 2 Students participating in the Drive.



Students participating in the Drive.



Image 4 Giving the manure to the newly plant samplings

6. Brochure or creative of the event



Plantation Drive

7. Schedule of the event

S.NO.	Name of the Event	Time	Place
1.	Plantation Drive	10:00 AM	Mahatma Gandhi School (English Medium) Begus.

A bus from MUJ was taken to the school in the morning.

8. Attendance of the Event

Total attendee- 67

S.No.	Reg. NO.	Name of Students	Institute Name
1	23FE10ITE00079	Amisha anand	Manipal University Jaipur
2	23FE10CAI00360	shaivi adesh	Manipal University Jaipur
3	23FE10CSE00060	Amay Garg	Manipal University Jaipur
4	23FE10CDS00177	Manas Mathur	Manipal University Jaipur
5	23fe10bte00029	Saloni kamal	Manipal University Jaipur
6	23FE10CSE00508	Dev Dhawan	Manipal University Jaipur
7	23fe10cii00035	Bhargavi Anand	Manipal University Jaipur
8	220606004	Pranjal Puri	Manipal University Jaipur
9	23FA10BSP00028	Anupama Rustagi	Manipal University Jaipur
10	23FE10CCE00085	Siddhartha tiwari	Manipal University Jaipur
11	23FA10BAP00002	Tanisha Mathur	Manipal University Jaipur
12	23FD10BFD00009	Mariya Shabbir Baiwala	Manipal University Jaipur
13	23FE10CDS00224	Harsh Ajmera	Manipal University Jaipur
14	23fe10cds00125	Suryanshi Singh	Manipal University Jaipur
15	23fs10mat00009	Malavika ramdas	Manipal University Jaipur
16	221007021	Arshi Jain	Manipal University Jaipur
17	23FE10CSE00137	Stuti Dixit	Manipal University Jaipur
18	23fe10cii00094	Aarohi Tyagi	Manipal University Jaipur
19	23FE10CSE00152	Gautam Kakkar	Manipal University Jaipur
20	23FE10CSE00318	Krish Ray	Manipal University Jaipur
21	23FE10CII00076	Kriissh Marwaha	Manipal University Jaipur
22	229310321	Shiv Rajput	Manipal University Jaipur
23	23FS10BIO00051	Ragini Singh Thakur	Manipal University Jaipur
24	23FS10BIO00052	Anukriti sharma	Manipal University Jaipur
25	220901073	Diya Mittal	Manipal University Jaipur
26	23FE10CSE00081	Smmayan Gupta	Manipal University Jaipur
27	229309083	Raghav Gupta	Manipal University Jaipur
28	23FE10CDS00397	Hrishita Singh Timaney	Manipal University Jaipur
29	23FE10ITE00203	Sarah Sharda	Manipal University Jaipur
30	23fa10bsp00025	Jasleen kaur	Manipal University Jaipur

31	23FA10BSP00039	Jiya Kumar	Manipal University Jaipur
32	23FA10BSP00004	Aarya Mahale	Manipal University Jaipur
33	220606020	Chaarvi Kumar	Manipal University Jaipur
34	23fa10bsp00058	Kashvi Mahajan	Manipal University Jaipur
35	229301095	Shaurya Singh	Manipal University Jaipur
36	23fe10ece00024	Kushagra agrawal	Manipal University Jaipur
37	23FA10BSP00017	Megha Sharma	Manipal University Jaipur
38	23FM10BBA00162	Alina Nadeem	Manipal University Jaipur
39	23FM10BBA00178	Avishi Akhaury	Manipal University Jaipur
40	221007004	Urvi Thakare	Manipal University Jaipur
41	23FA10BAP00027	Natasha Joan Menezes	Manipal University Jaipur
42	23FA10BLE00004	Tanisha chaturvedi	Manipal University Jaipur
43	23fe10cai00579	Arjun Malhotra	Manipal University Jaipur
44	23FE10CAI00352	Maanyata Aul	Manipal University Jaipur
45	220901322	Divyanshi Singh	Manipal University Jaipur
46	229310412	Jatin Verma	Manipal University Jaipur
47	229301094	Yashovardhan Pratap Singh	Manipal University Jaipur
48	23FM10BBA00348	Niska kedia	Manipal University Jaipur
49	221105005	Dhruv Nair	Manipal University Jaipur
50	23FM10BBA00170	Shambhavi Agrawal	Manipal University Jaipur
51	23FE10CDS00241	Armaan Setia	Manipal University Jaipur
52	23FE10CAI00105	Mritunjay Singh	Manipal University Jaipur
53	229311075	Aarna Tyagi	Manipal University Jaipur
54	229302051	Prince jindal	Manipal University Jaipur
55	23FA10BHE00035	Taneesha puri	Manipal University Jaipur
56	220903033	Suhani Jain	Manipal University Jaipur
57	220901391	Dipika Agarwal	Manipal University Jaipur
58	229310222	Aayush Sharma	Manipal University Jaipur
59	221003007	Yachna Jain	Manipal University Jaipur
60	220901002	Anshu jangir	Manipal University Jaipur
61	23FE10CDS00284	Anant Barjatya	Manipal University Jaipur
62	221015074	Rupal Sharma	Manipal University Jaipur
63	23fa10bsp00047	Vartika Agarwal	Manipal University Jaipur
64	23FA10BSP00041	Kali Vithlani	Manipal University Jaipur
65	23FM10BBA00030	Harshal Saini	Manipal University Jaipur
66	23FE10CSE00746	Daksh Sharma	Manipal University Jaipur
67	23FS10BIO00034	PC Rahul	Manipal University Jaipur

9. Feedback of the Event:- The students participated enthusiastically.



(Hemant Kumar)

Assistant Director, Society Connect

Directorate of Student's Welfare

(Prof. AD Vyas)

Director, Directorate of Student's Welfare

DIRECTOR STUDENT WELFARE & PROCTOR
MANIPAL UNIVERSITY, JAIPUR



MANIPAL UNIVERSITY
JAIPUR



MUJ/Q&C/DSW/SC/1.01



MANIPAL UNIVERSITY
JAIPUR

DIRECTORATE OF STUDENT'S WELFARE

(SOCIETY CONNECT)

And

Faculty of Science

Department of Chemistry

Presents

Plantation Drive

OCTOBER 26, 2023

Venue : Dabar Ki Dhani



1. Introduction of the Event

School of Basic science in collaboration with Directorate of Student Welfare, NCC, NSS organized a “Plantation Drive” on October 26, 2023. The societal connect outreach activity on by planting the small plants. Program is organized by the Department of Chemistry in collaboration with Department of Student welfare (DSW) under the guidance of Mr. Hemant Kumar (Assistant Director, DSW), Dr. Rahul Shrivastava (Head, Department of Chemistry) and Dr Meenakshi Pilia (Departmental coordinator, DSW). The mention activity held at a Government School, Dabar ki Dhani, near Manipal University Jaipur on Thursday, 26th October 2023.

2. Objective of the Event

The focal point of this event was to spread awareness among school students with respect to their environment and also motivate the students towards to work their endeavors via the power of knowledge and education.

3. Beneficiaries of the Event

Through this initiative, students and villagers had better communication and understanding of the situation.

4. Details of the Guests

The event was laid by the students of BBA, BBA(BA), IMBA

Rotary Club Jaipur Bapu Nagar

Rotary started with the vision of one man — Paul Harris. The Chicago attorney formed the Rotary Club of Chicago on 23 February 1905, so professionals with diverse backgrounds could exchange ideas and form meaningful, lifelong friendships.

Over time, Rotary’s reach and vision gradually extended to humanitarian service. Members have a long track record of addressing challenges in their communities and around the world.

Rotary is a global network of 1.4 million neighbors, friends, leaders, and problem-solvers who see a world where people unite and take action to create lasting change – across the globe, in our communities, and in ourselves. They provide service to others, promote integrity, and advance world understanding, goodwill, and peace through our fellowship of business, professional, and community leaders. We collaborate with community leaders who want to get to work on projects that have a real, lasting impact on people’s lives. We connect passionate people with diverse perspectives to exchange

ideas, forge lifelong friendships, and, above all, take action to change the world.

5. Brief Description of the event

The Department of Chemistry organized a societal connect outreach activity on Plantation in collaboration with the Department of Student Welfare (DSW) under the supervision of Mr. Hemant Kumar (Assistant Director, DSW), Dr. Rahul Shrivastava (Head, Department of Chemistry) and Dr. Meenakshi Pilonia (Departmental coordinator, DSW). The mentioned activity was held at a Govt. school, Dabar ki Dhani, near Manipal University Jaipur on Thursday, 26th October 2023.

6. Photographs



Image 1 : Students with faculty at School for the Career Awareness



Image 2: Students of school during the plantation drive



Image 3: Team of MUJ Students at DABAR ki Dani School

7. Brochure or creative of the event



8. Schedule of the Event

The event took place on October 26, 2023

9. Attendance of the Event (50)

S. No.	Name	Registration No	Name of Institution
1	Rakshanda Singhal	211051012	Manipal University Jaipur
2	Vartika Vaishya	211051015	Manipal University Jaipur
3	Shakir Sisodia	201022604	Manipal University Jaipur
4	Govind Gupta	170703601	Manipal University Jaipur
5	Kanika Taneja	211004002	Manipal University Jaipur
6	Avani Kothari	221004004	Manipal University Jaipur
7	Pranjalee Ghosh	221004002	Manipal University Jaipur
8	Kishika Arora	221004003	Manipal University Jaipur
9	Aman Kumar	221004001	Manipal University Jaipur



10	Khushi Verma	211004006	Manipal University Jaipur
11	Karunya Papney	211004004	Manipal University Jaipur
12	Ankita Kumawat	211004003	Manipal University Jaipur
13	Supriyo	23FS20MCH00004	Manipal University Jaipur
14	Anjali Yadav	23FS20MCH00001	Manipal University Jaipur
15	Divya Sharma	23FS20MCH00003	Manipal University Jaipur
16	Vaibhav Anand	221013001	Manipal University Jaipur
17	Dipesh Gehlot	221013002	Manipal University Jaipur
18	Suman Yadav	221013003	Manipal University Jaipur
19	Ashish Sharma	221013004	Manipal University Jaipur
20	Ishan Jain	229310159	Manipal University Jaipur
21	Ishika Jain	229310410	Manipal University Jaipur
22	Aditi Singh Parihar	219311171	Manipal University Jaipur
23	Utkarsh Shukla	229301763	Manipal University Jaipur
24	Vedika	221007014	Manipal University Jaipur
25	Honey Trivedi	229302207	Manipal University Jaipur
26	Shaurya Nandwani	229301726	Manipal University Jaipur
27	Shreyas Bhati	229301374	Manipal University Jaipur
28	Aditya Mishra	229310237	Manipal University Jaipur
29	Aaryan kale	229303031	Manipal University Jaipur
30	Mustansir kanchwala	220903021	Manipal University Jaipur
31	Sahil Kalra	229303321	Manipal University Jaipur
32	Krishang Goel	229309035	Manipal University Jaipur
33	Anand Mandlik	229310162	Manipal University Jaipur
34	Aryan Sachdeva	229301438	Manipal University Jaipur
35	Ansh manawat	229301712	Manipal University Jaipur
36	Utkarsh Jha	220901009	Manipal University Jaipur
37	ria chauhan	229301253	Manipal University Jaipur
38	Ishita Sharma	229303237	Manipal University Jaipur
39	Ajinkya wagh	229310003	Manipal University Jaipur
40	Kritika Pahuja	229310048	Manipal University Jaipur
41	Ishan Aaditya	229303314	Manipal University Jaipur
42	Jiya Thakur	229309176	Manipal University Jaipur
43	Utsav Acharjya	229301358	Manipal University Jaipur
44	Kanishka Chaudhary	229202010	Manipal University Jaipur
45	Sameeksha	229310311	Manipal University Jaipur
46	Taarush Kathuria	229301462	Manipal University Jaipur
47	Ankit Kumar Tiwari	229309098	Manipal University Jaipur
48	Hanis Gori	229310131	Manipal University Jaipur
49	Aditya Prakash Sinha	229310189	Manipal University Jaipur
50	Lakshita Agrawal	229301455	Manipal University Jaipur



(Hemant Kumar)
Assistant Director, Society Connect
Directorate of Student's Welfare

DIRECTOR STUDENT WELFARE & PROCTOR
MANIPAL UNIVERSITY, JAIPUR

(Prof. AD Vyas)
Director, Directorate of Student's Welfare



MANIPAL UNIVERSITY
JAIPUR



MUJ/Q&C/021/F/1.01



MANIPAL UNIVERSITY
JAIPUR

DIRECTORATE OF STUDENT'S WELFARE

(SOCIETY CONNECT)

And

Faculty of Management and Commerce

Department of Business Administration

Presents

SWACH BHARAT

OCTOBER 25, 2023



1. Introduction of the Event

School of Business and Commerce in collaboration with Directorate of Student Welfare, Directorate of sports and NCC, NSS organized a “SWACH BHARAT” on October 25, 2023. 52 students participated in the campaign. The event took place in Dehmi Kalan hamlet.

2. Objective of the Event

The aim of the campaign was to raise awareness about Waste Segregation and encourage education on the SWACH BHARAT.

3. Beneficiaries of the Event

Through this initiative, students and villagers had better communication and understanding of the situation.

4. Details of the Guests

The event was laid by the students of BBA, BBA(BA), IMBA

Rotary Club Jaipur Bapu Nagar

Rotary started with the vision of one man — Paul Harris. The Chicago attorney formed the Rotary Club of Chicago on 23 February 1905, so professionals with diverse backgrounds could exchange ideas and form meaningful, lifelong friendships.

Over time, Rotary’s reach and vision gradually extended to humanitarian service. Members have a long track record of addressing challenges in their communities and around the world.

Rotary is a global network of 1.4 million neighbors, friends, leaders, and problem-solvers who see a world where people unite and take action to create lasting change – across the globe, in our communities, and in ourselves. They provide service to others, promote integrity, and advance world understanding, goodwill, and peace through our fellowship of business, professional, and community leaders. We collaborate with community leaders who want to get to work on projects that have a real, lasting impact on people’s lives. We connect passionate people with diverse perspectives to exchange ideas, forge lifelong friendships, and, above all, take action to change the world.

5. Brief Description of the event

The event was initiated to make students aware of their surroundings with respect to Waste and its consequences on the local community. The students went on a rally in groups, holding posters on Wet Waste and Dry Waste. They were chanting slogans “Alag Karo Alag Karo” Gila aur Sukha Kachara Alag Karo, to make the local community aware of the Waste Segregation process.

6. Photographs

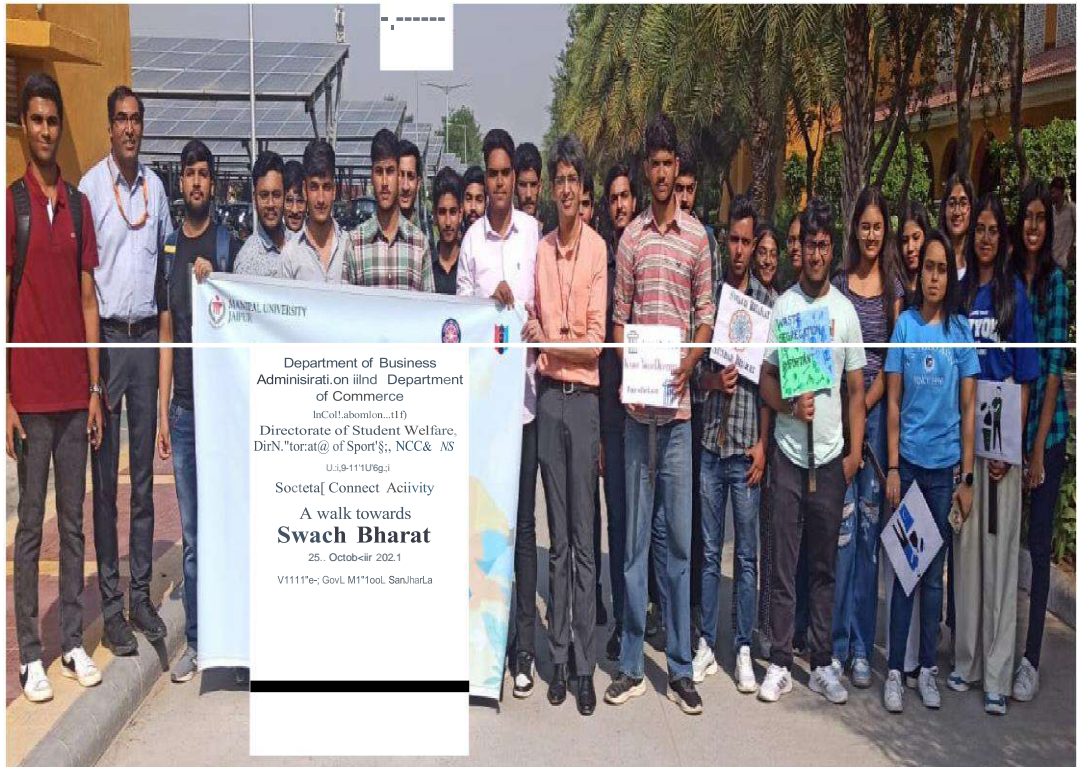


Image 1 : Students with faculty



Image 2: Students walking with the Rally through the Village



Image 3: Team of MUJ Students at Village for Rally

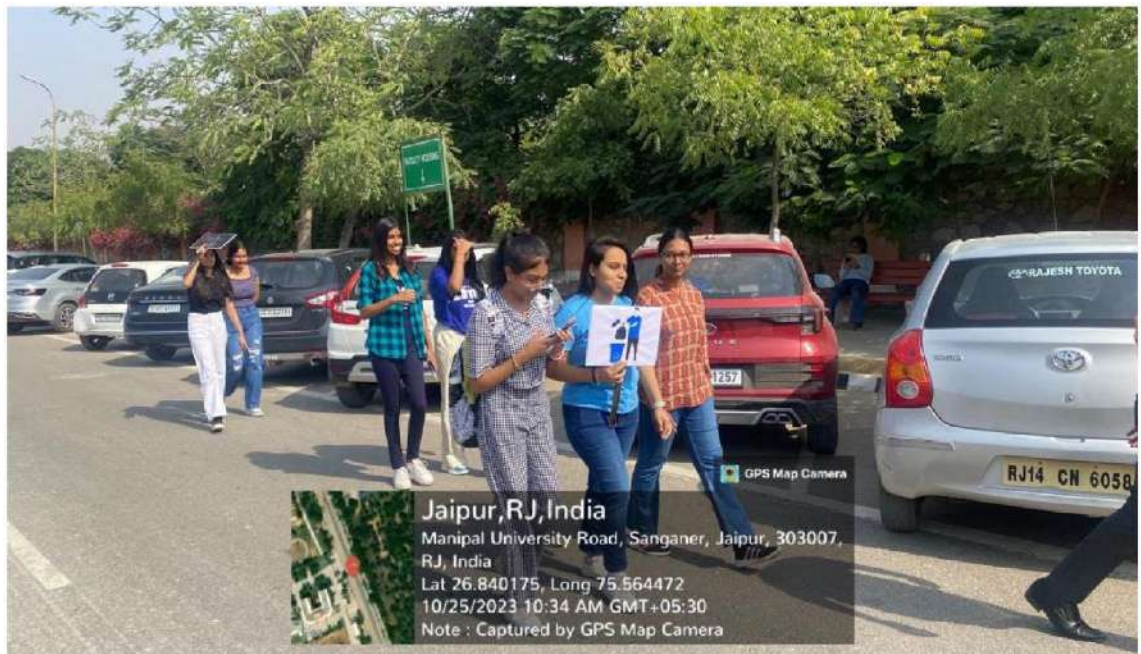


Image 4: Team of MUJ Students at Village for Rally

7. Brochure or creative of the event



8. Schedule of the Event

The event took place on October 25, 2023

9. Attendance of the Event

Sr. No	Name of Institution	Registration No	Attendee Name
1	Manipal University Jaipur	23FM10BBA00122	Naresh Choudhary
2	Manipal University Jaipur	23FM10BBA00123	Prem Singhrathore
3	Manipal University Jaipur	23FM10BBA00124	Yash Vardhansingh
4	Manipal University Jaipur	23FM10BBA00125	Krishna Snair
5	Manipal University Jaipur	23FM10BBA00126	Viyom Gupta
6	Manipal University Jaipur	23FM10BBA00127	Aditya Singh shekhawat
7	Manipal University Jaipur	23FM10BBA00128	Sheikh Tabish ahmed
8	Manipal University Jaipur	23FM10BBA00129	Bhavesh Aggarwal
9	Manipal University Jaipur	23FM10BBA00130	Riddhima Gupta
10	Manipal University Jaipur	23FM10BBA00131	Ishita Sharma
11	Manipal University Jaipur	23FM10BBA00132	Akshat Sharma
12	Manipal University Jaipur	23FM10BBA00133	Preksha Sood
13	Manipal University Jaipur	23FM10BBA00134	Tanisha Agarwal
14	Manipal University Jaipur	23FM10BBA00135	Ram Avtarchouhan



15	Manipal University Jaipur	23FM10BBA00136	Sourabh Shekhawat
16	Manipal University Jaipur	23FM10BBA00137	Abhishek Jain
17	Manipal University Jaipur	23FM10BBA00138	Priyanshu Yadav
18	Manipal University Jaipur	23FM10BBA00139	Riddhi Charan
19	Manipal University Jaipur	23FM10BBA00140	Akhil
20	Manipal University Jaipur	23FM10BBA00141	Shaily Kushwaha
21	Manipal University Jaipur	23FM10BBA00142	Deep Mittal
22	Manipal University Jaipur	23FM10BBA00143	Rahul Choudhary
23	Manipal University Jaipur	23FM10BBA00144	Ronil Joshi
24	Manipal University Jaipur	23FM10BBA00145	Arihant Jaisawal
25	Manipal University Jaipur	23FM10BBA00146	Ayush Kumarthakur
26	Manipal University Jaipur	23FM10BBA00147	Angad Yadav
27	Manipal University Jaipur	23FM10BBA00148	Shashank Chaudhary
28	Manipal University Jaipur	23FM10BBA00149	Khushi Gupta
29	Manipal University Jaipur	23FM10BBA00150	Garvita Rathore
30	Manipal University Jaipur	23FM10BBA00151	Anirban Bhattacharyya
31	Manipal University Jaipur	23FM10BBA00152	Keshav Badthuniya
32	Manipal University Jaipur	23FM10BBA00153	Yash Saini
33	Manipal University Jaipur	23FM10BBA00154	Vineet Kumar
34	Manipal University Jaipur	23FM10BBA00155	Bhavuk Parashar
35	Manipal University Jaipur	23FM10BBA00156	Mohit Oshu
36	Manipal University Jaipur	23FM10BBA00157	Honey Chandnani
37	Manipal University Jaipur	23FM10BBA00158	Veer Singh
38	Manipal University Jaipur	23FM10BBA00159	Naman Kriplani
39	Manipal University Jaipur	23FM10BBA00160	Himanshu Yogesh Mittal
40	Manipal University Jaipur	23FM10BBA00161	Amogh Goyal
41	Manipal University Jaipur	23FM10BBA00162	Alina Nadeem
42	Manipal University Jaipur	23FM10BBA00163	Prince Gandhi
43	Manipal University Jaipur	23FM10BBA00164	Devansh Devansh Tiwari
43	Manipal University Jaipur	221016048	Aarohi
44	Manipal University Jaipur	229301387	Soham maskara
45	Manipal University Jaipur	229301650	Karan Kapoor
46	Manipal University Jaipur	229301552	MONIL SHAH
47	Manipal University Jaipur	229311009	Krittika Wadhawan
48	Manipal University Jaipur	229301034	Maulik Mehrotra
49	Manipal University Jaipur	229302340	Shreya Saihgai
50	Manipal University Jaipur	229302257	Yash Dhruv
51	Manipal University Jaipur	229302641	Pankaj Patel
52	Manipal University Jaipur	229310250	Amrit Raj
53	Manipal University Jaipur	220901154	Mehul rawat
54	Manipal University Jaipur	221201002	Palak chawla
55	Manipal University Jaipur	229309070	Pranav Banker
56	Manipal University Jaipur	229303128	Mahi Bhardwaj
57	Manipal University Jaipur	229303305	Karshh Divekar
58	Manipal University Jaipur	229310242	Ashmit



59	Manipal University Jaipur	229301681	Armaan Deep Singh Bedi
60	Manipal University Jaipur	229302281	Shriyam Singh Tiwari
61	Manipal University Jaipur	229301130	Shreyansh Reddy
62	Manipal University Jaipur	220901032	Raj Singh
63	Manipal University Jaipur	211103077	Sanmai Pathak
64	Manipal University Jaipur	211103075	Anvesha Shekhar
65	Manipal University Jaipur	219311129	Shubham Yadav
66	Manipal University Jaipur	221201033	Divanshi Gupta
67	Manipal University Jaipur	229310052	Lakshya Khandelwal
68	Manipal University Jaipur	229303191	Krishang Shukla
69	Manipal University Jaipur	221305050	Baibhav Bhanu Naithani
70	Manipal University Jaipur	229302371	Rishika Bhagawati
71	Manipal University Jaipur	229311168	Rudra Nayyar
72	Manipal University Jaipur	229311024	Shivam Singh
73	Manipal University Jaipur	229311289	puneet more
74	Manipal University Jaipur	229310200	Nainish Mane
75	Manipal University Jaipur	229310153	Diksha M
76	Manipal University Jaipur	221007068	Akshita Pandey
77	Manipal University Jaipur	229309068	Rahul Trivedi
78	Manipal University Jaipur	229309052	Raez Mohammed K P

Dr Narendra Singh Bhati HoD, BBA

(Hemant Kumar)
Assistant Director, Society Connect
Directorate of Student's Welfare

DIRECTOR STUDENT WELFARE & PROCTOR
MANIPAL UNIVERSITY, JAIPUR

(Prof. AD Vyas)

Director, Directorate of Student's Welfare



MANIPAL UNIVERSITY
JAIPUR

FACULTY OF ARTS

SCHOOL OF HUMANITIES AND SOCIAL SCIENCES

DEPARTMENT OF ARTS

Tree plantation Drive

Social outreach event in collaboration with DSW and NCC

06/09/2023



Index

1. Introduction of the Event
2. Objective of the Event
3. Beneficiaries of the Event
4. Details of the Guests
5. Brief Description of the event
6. Geo-tagged Photographs
7. Brochure or creative of the event
8. Schedule of the Event
9. Attendance of the Event
10. News Publication
11. Feedback of the Event
12. Link of MUJ website

1. Introduction of the Event

The Department of Arts in collaboration with the DSW (NCC and NSS) organized a tree plantation drive with a number of BA(Liberal Arts) students.

2. Objective of the Event (bullet points or about 50 words)

To make the students aware of the importance of tree plantation.

3. Beneficiaries of the Event

Government school, Begas, an adopted school of MUJ

4. Brief Description of the event

The Department of Arts in collaboration with the DSW (NCC and NSS) organized a tree plantation drive with a number of BA(Liberal Arts) students. The objective of the event was to make the students aware of the importance of tree plantation.

5. Photographs



Students engaged in a tree plantation drive in the government school, Begas



MUJ students with the government school students



MUJ department students during the plantation drive

6. Brochure or creative of the event (insert in the document only)

8x4.5 feet



7. Schedule of the event (insert in the report)

6th September, 11:00 a.m. to 12:00 p.m.

8. Attendance of the Event (insert in the document only)

Total attendee-16

Sr. No	Name of Institution	Place of Institution	Name of Attendee	Name of Dept
1.	MUJ	Jaipur	Chandravardhan	Arts
2.	MUJ	Jaipur	Kumesh Mishra	Arts
3.	MUJ	Jaipur	Soumya Pareek Dhanushree	Arts
4.	MUJ	Jaipur		Arts
5.	MUJ	Jaipur	Karan Mallick	Arts
6.	MUJ	Jaipur	Vanshika Agarwal	Arts
7.	MUJ	Jaipur	Prithviraj	Arts
8.	MUJ	Jaipur	Akshatt Singh	Arts
9.	MUJ	Jaipur	Dhruv Nair	Arts
10.	MUJ	Jaipur	Krishna	Arts
11.	MUJ	Jaipur	Gaury	Arts
12.	MUJ	Jaipur	Sudeepti Dhruv Dahiya	Arts
13.	MUJ	Jaipur	Aditi Panigrahi	Arts
14.	MUJ	Jaipur	Aradhya Khandelwal	Arts
15.	MUJ	Jaipur	Komal Chadha	Arts
16.	MUJ	Jaipur	Kkritika Khandelwal Pragya Sharma	Arts
17.	MUJ	Jaipur	Prachi Randhawa	Arts
18.	MUJ	Jaipur	Gurmehr Singh	Arts
19.	MUJ	Jaipur	Himmat di Charan	Arts
20.	MUJ	Jaipur	Sameer Khan	Arts
21.	MUJ	Jaipur	Ananya Thakur	Arts
22.	MUJ	Jaipur	Harshita Das	Arts
23.	MUJ	Jaipur	Manan Sharma	Arts



24.	MUJ	Jaipur	Surendra Singh	Arts
25.	MUJ	Jaipur	Joy Tak	Arts
26.	MUJ	Jaipur	Soumya harna	Arts
27.	MUJ	Jaipur	Deepak	Arts
28.	MUJ	Jaipur	Anup Choudhary	Arts
29.	MUJ	Jaipur	Prithviraj Hada	Arts
30.	MUJ	Jaipur	Tanisha Vashisht	Arts



9. **Link of MUJ website stating the event is uploaded on website**

<https://jaipur.manipal.edu/muj/news-events/events-list.html>

Dr. Mani Sachdev
Head, Department of Arts
Manipal University Jaipur

15.9.23

Seal and Signature of HOD

DIRECTOR STUDENT WELFARE & PROCTOR
MANIPAL UNIVERSITY, JAIPUR

(Prof. AD Vyas)

Director, Directorate of Student's Welfare




**MANIPAL UNIVERSITY
JAIPUR**

FACULTY OF DESIGN

**International Conference on Sustainable Development for
Heritage and Built Environment**

22/06/2023 – 23/06/2023


Head, Department of Interior Design
SD&A, Faculty of Design
Manipal University Jaipur



Content of Report

1. Introduction of the Event
2. Objective of the Event
3. Beneficiaries of the Event
4. Brief Description of the event
5. Photographs
6. Poster of an Event
7. Schedule of the Event
8. Attendance of the Event

1. Introduction of the Event

The conference is inspired from the critical challenge of human, environmental, heritage and built sustainability concerning the present and future generations in a global-scale context. This theme emphasizes the strong foundation that is provided by using research to inform our everyday practices, policies, and analytical approaches. This interdisciplinary forum is for scholars, teachers, and practitioners from the built environment professional discipline who share an interest in—and concern for— sustainability in an holistic perspective, where environmental, cultural, economic and social concerns intersect. It will provide a platform for various individuals to connect the past and present and develop solutions to a more universal and environmentally friendly approach towards built environment.

The conference will include topics such as

- (i) Sustainable approach to design in built environment,
- (ii) Sustainability & built Heritage,
- (iii) Conserving Built Heritage,
- (iv) Sustainable Policies for Environmental and Infrastructure Planning,
- (v) Earth and Environmental Planning & Design

2. Objective of the Event

This conference was a gathering of minds dedicated to addressing the pressing challenges of sustainability that affect our world today and tomorrow. It recognized that sustainability is a multifaceted concept that requires interdisciplinary collaboration and rigorous research. By bringing together scholars, educators, and practitioners, the conference facilitated the exchange of ideas and the development of solutions that promote a more sustainable, resilient, and environmentally friendly built environment.

3. Beneficiary of the event

This interdisciplinary forum is for scholars, teachers, and practitioners from the built environment professional discipline who share an interest in—and concern for— sustainability in an holistic perspective, where environmental, cultural, economic and social concerns intersect.

4. Brief Description of the event

The conference was hosted by Department of Interior Design and School of Architecture and Design, Faculty of Design at Manipal University Jaipur. This interactive and engaging event is tailored exclusively for our researchers, as part of our commitment to foster continuous learning, future research opportunities. The presentations focused on sustainability as the prime agenda and paved way for the researchers to present their work at an international level.

5. Photographs of the Event



Snippets of the Conference

6. Poster of the event



**MANIPAL UNIVERSITY
JAIPUR**
(University under Section 2(i) of the UGC Act)

School of Architecture and
Design and Department of
Interior Design

International Conference
on
**“Sustainable
Development for
Heritage and Built
Environment”**

22nd June – 23rd June 2023

Venue:
Manipal University Jaipur/ Hybrid
Mode

About the University
The Manipal Education Group, with its heritage of excellence in higher education for over 60 years, launched Manipal University Jaipur (MUJ) in 2011. MUJ is affiliated by University Grants Commission, Association of Indian Universities, Council of Architecture, Bar Council of India and All India council of technical education. MUJ is the first university in the state of Rajasthan, accredited as A+ (3.28) grade by NAAC. The university offers courses in different disciplines like Architecture, Interior Design, Fashion Design, Applied arts, Engineering, Management, Hospitality, Humanities & Social Sciences, Journalism and Mass communication, Basic Sciences, Law, Business & Commerce.

Organizing Committee
Patron:
Dr. G. K. Prabhu (President, MUJ)
Co - Patrons
Dr. Thammaiah Chekkera (Pro-President, MUJ)
Dr. Nitu Bhatnagar (Registrar, MUJ)
Chair:
Dr. Madhura Yadav (Dean, FoD, MUJ)
Dr. J.P. Sampath Kumar (Director, SD&A, MUJ)
Convenors:
Dr. Richa Jagatramka (Assist. Prof., ID-SD&A)
Ar. Raunak Prasad (Assist. Prof., SA&D)
Coordinators:
Ar. Megha Prabhu (Assist. Prof., ID-SD&A)
Ar. Himangshu Kedia (Assist. Prof., ID-SD&A)
Ar. Akshay Gupta (Assist. Prof., SA&D)
Ar. Ashutosh Saini (Assist. Prof., SA&D)

About the Conference
The conference will include topics such as

- (i) Sustainable approach to design in built environment,
- (ii) Sustainability & built Heritage,
- (iii) Conserving Built Heritage,
- (iv) Sustainable Policies for Environmental and Infrastructure Planning,
- (v) Earth and Environmental Planning & Design.

Participants will gain exposure and insight To various sustainable approaches to sustain the heritage as well as define the built environment. It will provide a platform for various individuals to connect the past and present and develop solutions to a more universal and environmentally friendly approach towards built environment.

Submission Deadline:
Call for Papers – 23rd Feb 2023
Abstract Submission – 30th March 2023
Acceptance Notification – 7th April 2023
Full paper Submission – 23rd April 2023

Publication –
Conference proceedings with IOP
Conference Series: Earth and Environmental Science (SCOPUS Indexed)

Notable Speakers

1. Dr. Ranjith Dayaranthe , Associate Professor, Asian School of Architecture, Australia
2. Dr. Muge Belek Fialho Teixeira, Queensland University of Technology.
3. Dr. Shikha Jain, Director, DRONAH
4. Dr. Rajat Gupta, Oxford Brookes, Director, Dept. of sustainable development
5. Ar. Chitra Vishwanath, Biome Bangalore.

Conference Fees :
Students 9500 INR
Academicians & professional 10500 INR

For International Participants
Students - 150 USD
Academicians & professional – 180 USD

For additional Information contact –
richa.jagatramka@jaipur.manipal.edu
raunak.prasad@jaipur.manipal.edu

7. Schedule of the event

Time	Event	Speaker
11:00 – 11:30 AM	Opening speech	Dr Richa Jagatramka
11: 30 – 11:35 AM	Welcome address	Dr Madhura Yadav
11: 35 – 11:45 AM	Introduction of international speaker	Ar Himangshu Kedia
11: 45 AM – 12:45 PM	Presentation by Dr Muge	Dr Muge
12: 45 – 01:00 PM	Q & A session	
01:00 – 01:05PM	Vote of Thanks	Ar. Himangshu Kedia

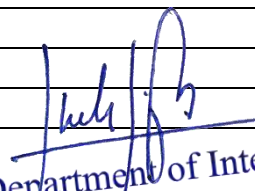
Meeting Link :

https://teams.microsoft.com/l/meetup-join/19%3ameeting_MmRjNjZiN2ltMTc1NS00YmJlTkwMTltMzBiYTVjNTIOYTRh%40thread.v2/0?context=%7b%22tid%22%3a%227d0726e8-bf4b-4ac1-99f1-010fb11f1d3f%22%2c%22oid%22%3a%2216be8839-914f-456c-9836-e6b3ba8fa2f9%22%7d

8. Attendance of the Event

Total attendees – 28 participants from MUJ and outside

Sl.no	Name	Organisation
1	Dr. Richa Jagatramka	FOD
2	Megha Prabhu K	FOD
3	Dr. Sampath Kumar Padmanabha Jinka	FOD
4	Dr. Madhura Yadav	FOD
5	Dr. Anantkumar Dada Ozarkar	FOD
6	Dr. Subhash Chandra Devrath	FOD
7	Nisha Nelson	FOD
8	Preethi Agrawal	Practicing Architect and PhD scholar
9	NITIKA TORVI	Christ University
10	Subhadha B	Christ University
11	Himangshu Kedia	FOD
12	Rushikesh Kolte	MNIT
13	Dr. Sunanda Kapoor	FOD
14	Ananya Tripathi	AKTU - GCA
15	Kinzalk Chauhan	FOD
16	Ritu Sharma	FOS – Phd Scholar
17	Rimjhim Swami	FOD
18	Ayushi Sharma	FOD
19	Apoorva Agarwal	FOD
20	Muge Fialho Leandro Alves Teixeira	QUT Australia
21	Deeksha	MNIT
22	Siddharth Mishra	FOD
23	Akshay Gupta	FOD
24	Ritu Sharma	FOD
25	Neha Saxena	FOD
26	Antima Kuda	MAHE Dubai
27	Raunak Prasad	FOD
28	Ashutosh Saini	FOD


Head, Department of Interior Design
SD&A, Faculty of Design
Manipal University Jaipur



MANIPAL UNIVERSITY
JAIPUR



MUJ/DSW/Society Connect/ Oct2023/03



MANIPAL UNIVERSITY
JAIPUR

DIRECTORATE OF STUDENT'S WELFARE

(SOCIETY CONNECT)

#DAANUTSAV 2023

Plantation Drive

3rd October 2023

Date: 3rd October 2023



Index

S.No.	Activity Heads	Page no.
1.	Introduction of the Event	1
2.	Objective of the Event	1
3.	Beneficiaries of the Event	1
4.	Brief Description of the event	1
5.	Photographs	2-4
6.	Brochure or creative of the event	5-6
7.	Schedule of the Event	6
8.	Attendance of the Event	6-9
9.	Feedback of the Event	9
10.	Link of MUJ website	9

1. Introduction of the Event

“A nation that destroys its soils destroys itself. Forests are the lungs of our land, purifying the air and giving fresh strength to our people. ” Trees are indispensable for life. Man can't live without trees. However, the present condition of forests in the world, especially developing countries is pathetic and miserable. Forests are the source of life. They are the giving angels. They give man oxygen, rains, wood, fruit, make the world look so beautiful, yet the sinister man kills them! Who will be more inhumane than man himself? Cutting of forests ultimately endangers man's own existence. Trees are important to the environment; they recycle water and process carbon dioxide in the atmosphere through photosynthesis. They are the world's full-time purifiers of air and water. Their cutting will disturb the natural water cycles which will lead to the shortage of fresh water in the water reserves of the world.

Rotaract Green Club under Society Connect organized a Plantation Drive on account of DAAN UTSAV 2031. It took place on the 3rd of October from 10 a.m. Students were taken to the Mahatma Gandhi School, Begus for the drive. The drive aimed to instill a sense of discipline and respect for the environment while doing our part.

2. Objective of the Event

- Spread awareness on the importance of afforestation
- Direct students' mind in constructive activities
- Contribution to the society
- Promote tree planting
- Create awareness regarding importance of ecology
- Attempt at reducing pollution and improve green ambience

3. Beneficiaries of the Event

Community

4. Brief Description of the event

Rotaract Green Club organized the Plantation Drive on the 3rd October at 9 a.m. on account of DAAN UTSAV 2023. The drive's main aim was to direct student's mind

in constructive activities with the positive outcome through the facilitation of contributing to the nature and environment.

It also aimed at spreading awareness about the effects of global warming and the positive effects of planting trees. The students gathered on campus to go to the Mahatma Gandhi School, Begus.

The students participated in the drive enthusiastically and helped each other in planting the saplings. All the saplings were planted in the school ground by students. Participants were highly energetic to make the event a big success. A spirit of teamwork, exchange of ideas and enthusiasm of the participants especially among the students could be seen. Pictures were taken. The drive was successfully conducted by planting 40-50 saplings.

5. Photographs of the event



Image 1. Students and Faculty planting saplings



Image 2 Students participating in the Drive.



Students participating in the Drive.





Image 4 Giving the manure to the newly plant samplings

6. Brochure or creative of the event





MANIPAL UNIVERSITY
JAIPUR

















**Directorate of Students' Welfare
Society Connect**

ROTARACT CLUB

Presents

#DAANUTSAV2023

PLANTATION DRIVE

Date: 3rd October, 2023 Time: 10:00 AM

Venue: Govt. Senior Secondary School, Sanjhariya, Jaipur

Plantation Drive

7. Schedule of the event

S.NO.	Name of the Event	Time	Place
1.	Plantation Drive	10:00 AM	Mahatma Gandhi School (English Medium) Begus.

A bus from MUJ was taken to the school in the morning.

8. Attendance of the Event

Total attendee- 67

S.No.	Reg. NO.	Name of Students	Institute Name
1	23FE10ITE00079	Amisha anand	Manipal University Jaipur
2	23FE10CAI00360	shaivi adesh	Manipal University Jaipur
3	23FE10CSE00060	Amay Garg	Manipal University Jaipur
4	23FE10CDS00177	Manas Mathur	Manipal University Jaipur
5	23fe10bte00029	Saloni kamal	Manipal University Jaipur
6	23FE10CSE00508	Dev Dhawan	Manipal University Jaipur
7	23fe10cii00035	Bhargavi Anand	Manipal University Jaipur
8	220606004	Pranjal Puri	Manipal University Jaipur
9	23FA10BSP00028	Anupama Rustagi	Manipal University Jaipur
10	23FE10CCE00085	Siddhartha tiwari	Manipal University Jaipur
11	23FA10BAP00002	Tanisha Mathur	Manipal University Jaipur
12	23FD10BFD00009	Mariya Shabbir Baiwala	Manipal University Jaipur
13	23FE10CDS00224	Harsh Ajmera	Manipal University Jaipur
14	23fe10cds00125	Suryanshi Singh	Manipal University Jaipur
15	23fs10mat00009	Malavika ramdas	Manipal University Jaipur
16	221007021	Arshi Jain	Manipal University Jaipur
17	23FE10CSE00137	Stuti Dixit	Manipal University Jaipur
18	23fe10cii00094	Aarohi Tyagi	Manipal University Jaipur
19	23FE10CSE00152	Gautam Kakkar	Manipal University Jaipur
20	23FE10CSE00318	Krish Ray	Manipal University Jaipur
21	23FE10CII00076	Kriissh Marwaha	Manipal University Jaipur
22	229310321	Shiv Rajput	Manipal University Jaipur
23	23FS10BIO00051	Ragini Singh Thakur	Manipal University Jaipur
24	23FS10BIO00052	Anukriti sharma	Manipal University Jaipur
25	220901073	Diya Mittal	Manipal University Jaipur
26	23FE10CSE00081	Smmayan Gupta	Manipal University Jaipur
27	229309083	Raghav Gupta	Manipal University Jaipur
28	23FE10CDS00397	Hrishita Singh Timaney	Manipal University Jaipur
29	23FE10ITE00203	Sarah Sharda	Manipal University Jaipur
30	23fa10bsp00025	Jasleen kaur	Manipal University Jaipur

31	23FA10BSP00039	Jiya Kumar	Manipal University Jaipur
32	23FA10BSP00004	Aarya Mahale	Manipal University Jaipur
33	220606020	Chaarvi Kumar	Manipal University Jaipur
34	23fa10bsp00058	Kashvi Mahajan	Manipal University Jaipur
35	229301095	Shaurya Singh	Manipal University Jaipur
36	23fe10ece00024	Kushagra agrawal	Manipal University Jaipur
37	23FA10BSP00017	Megha Sharma	Manipal University Jaipur
38	23FM10BBA00162	Alina Nadeem	Manipal University Jaipur
39	23FM10BBA00178	Avishi Akhaury	Manipal University Jaipur
40	221007004	Urvi Thakare	Manipal University Jaipur
41	23FA10BAP00027	Natasha Joan Menezes	Manipal University Jaipur
42	23FA10BLE00004	Tanisha chaturvedi	Manipal University Jaipur
43	23fe10cai00579	Arjun Malhotra	Manipal University Jaipur
44	23FE10CAI00352	Maanyata Aul	Manipal University Jaipur
45	220901322	Divyanshi Singh	Manipal University Jaipur
46	229310412	Jatin Verma	Manipal University Jaipur
47	229301094	Yashovardhan Pratap Singh	Manipal University Jaipur
48	23FM10BBA00348	Niska kedia	Manipal University Jaipur
49	221105005	Dhruv Nair	Manipal University Jaipur
50	23FM10BBA00170	Shambhavi Agrawal	Manipal University Jaipur
51	23FE10CDS00241	Armaan Setia	Manipal University Jaipur
52	23FE10CAI00105	Mritunjay Singh	Manipal University Jaipur
53	229311075	Aarna Tyagi	Manipal University Jaipur
54	229302051	Prince jindal	Manipal University Jaipur
55	23FA10BHE00035	Taneesha puri	Manipal University Jaipur
56	220903033	Suhani Jain	Manipal University Jaipur
57	220901391	Dipika Agarwal	Manipal University Jaipur
58	229310222	Aayush Sharma	Manipal University Jaipur
59	221003007	Yachna Jain	Manipal University Jaipur
60	220901002	Anshu jangir	Manipal University Jaipur
61	23FE10CDS00284	Anant Barjatya	Manipal University Jaipur
62	221015074	Rupal Sharma	Manipal University Jaipur
63	23fa10bsp00047	Vartika Agarwal	Manipal University Jaipur
64	23FA10BSP00041	Kali Vithlani	Manipal University Jaipur
65	23FM10BBA00030	Harshal Saini	Manipal University Jaipur
66	23FE10CSE00746	Daksh Sharma	Manipal University Jaipur
67	23FS10BIO00034	PC Rahul	Manipal University Jaipur

9. Feedback of the Event:- The students participated enthusiastically.



(Hemant Kumar)

Assistant Director, Society Connect

Directorate of Student's Welfare

(Prof. AD Vyas)

Director, Directorate of Student's Welfare

DIRECTOR STUDENT WELFARE & PROCTOR
MANIPAL UNIVERSITY, JAIPUR



MANIPAL UNIVERSITY
JAIPUR

MUJ/Q&C/DSW/SC/1.01



MANIPAL UNIVERSITY
JAIPUR

DIRECTORATE OF STUDENT'S WELFARE

(SOCIETY CONNECT)

And

Faculty of Science

Department of Chemistry

Presents

Plantation Drive

OCTOBER 26, 2023

Venue : Dabar Ki Dhani

1. Introduction of the Event

School of Basic science in collaboration with Directorate of Student Welfare, NCC, NSS organized a “Plantation Drive” on October 26, 2023. The societal connect outreach activity on by planting the small plants. Program is organized by the Department of Chemistry in collaboration with Department of Student welfare (DSW) under the guidance of Mr. Hemant Kumar (Assistant Director, DSW), Dr. Rahul Shrivastava (Head, Department of Chemistry) and Dr Meenakshi Pilonia (Departmental coordinator, DSW). The mention activity held at a Government School, Dabar ki Dhani, near Manipal University Jaipur on Thursday, 26th October 2023.

2. Objective of the Event

The focal point of this event was to spread awareness among school students with respect to their environment and also motivate the students towards to work their endeavors via the power of knowledge and education.

3. Beneficiaries of the Event

Through this initiative, students and villagers had better communication and understanding of the situation.

4. Details of the Guests

The event was laid by the students of BBA, BBA(BA), IMBA

Rotary Club Jaipur Bapu Nagar

Rotary started with the vision of one man — Paul Harris. The Chicago attorney formed the Rotary Club of Chicago on 23 February 1905, so professionals with diverse backgrounds could exchange ideas and form meaningful, lifelong friendships.

Over time, Rotary’s reach and vision gradually extended to humanitarian service. Members have a long track record of addressing challenges in their communities and around the world.

Rotary is a global network of 1.4 million neighbors, friends, leaders, and problem-solvers who see a world where people unite and take action to create lasting change – across the globe, in our communities, and in ourselves. They provide service to others, promote integrity, and advance world understanding, goodwill, and peace through our fellowship of business, professional, and community leaders. We collaborate with community leaders who want to get to work on projects that have a real, lasting impact on people’s lives. We connect passionate people with diverse perspectives to exchange

ideas, forge lifelong friendships, and, above all, take action to change the world.

5. Brief Description of the event

The Department of Chemistry organized a societal connect outreach activity on Plantation in collaboration with the Department of Student Welfare (DSW) under the supervision of Mr. Hemant Kumar (Assistant Director, DSW), Dr. Rahul Shrivastava (Head, Department of Chemistry) and Dr. Meenakshi Pilonia (Departmental coordinator, DSW). The mentioned activity was held at a Govt. school, Dabar ki Dhani, near Manipal University Jaipur on Thursday, 26th October 2023.

6. Photographs



Image 1 : Students with faculty at School for the Career Awareness



Image 2: Students of school during the plantation drive



Image 3: Team of MUJ Students at DABAR ki Dani School

7. Brochure or creative of the event



8. Schedule of the Event

The event took place on October 26, 2023

9. Attendance of the Event (50)

S. No.	Name	Registration No	Name of Institution
1	Rakshanda Singhal	211051012	Manipal University Jaipur
2	Vartika Vaishya	211051015	Manipal University Jaipur
3	Shakir Sisodia	201022604	Manipal University Jaipur
4	Govind Gupta	170703601	Manipal University Jaipur
5	Kanika Taneja	211004002	Manipal University Jaipur
6	Avani Kothari	221004004	Manipal University Jaipur
7	Pranjalee Ghosh	221004002	Manipal University Jaipur
8	Kishika Arora	221004003	Manipal University Jaipur
9	Aman Kumar	221004001	Manipal University Jaipur

10	Khushi Verma	211004006	Manipal University Jaipur
11	Karunya Papney	211004004	Manipal University Jaipur
12	Ankita Kumawat	211004003	Manipal University Jaipur
13	Supriyo	23FS20MCH00004	Manipal University Jaipur
14	Anjali Yadav	23FS20MCH00001	Manipal University Jaipur
15	Divya Sharma	23FS20MCH00003	Manipal University Jaipur
16	Vaibhav Anand	221013001	Manipal University Jaipur
17	Dipesh Gehlot	221013002	Manipal University Jaipur
18	Suman Yadav	221013003	Manipal University Jaipur
19	Ashish Sharma	221013004	Manipal University Jaipur
20	Ishan Jain	229310159	Manipal University Jaipur
21	Ishika Jain	229310410	Manipal University Jaipur
22	Aditi Singh Parihar	219311171	Manipal University Jaipur
23	Utkarsh Shukla	229301763	Manipal University Jaipur
24	Vedika	221007014	Manipal University Jaipur
25	Honey Trivedi	229302207	Manipal University Jaipur
26	Shaurya Nandwani	229301726	Manipal University Jaipur
27	Shreyas Bhati	229301374	Manipal University Jaipur
28	Aditya Mishra	229310237	Manipal University Jaipur
29	Aaryan kale	229303031	Manipal University Jaipur
30	Mustansir kanchwala	220903021	Manipal University Jaipur
31	Sahil Kalra	229303321	Manipal University Jaipur
32	Krishang Goel	229309035	Manipal University Jaipur
33	Anand Mandlik	229310162	Manipal University Jaipur
34	Aryan Sachdeva	229301438	Manipal University Jaipur
35	Ansh manawat	229301712	Manipal University Jaipur
36	Utkarsh Jha	220901009	Manipal University Jaipur
37	ria chauhan	229301253	Manipal University Jaipur
38	Ishita Sharma	229303237	Manipal University Jaipur
39	Ajinkya wagh	229310003	Manipal University Jaipur
40	Kritika Pahuja	229310048	Manipal University Jaipur
41	Ishan Aaditya	229303314	Manipal University Jaipur
42	Jiya Thakur	229309176	Manipal University Jaipur
43	Utsav Acharjya	229301358	Manipal University Jaipur
44	Kanishka Chaudhary	229202010	Manipal University Jaipur
45	Sameeksha	229310311	Manipal University Jaipur
46	Taarush Kathuria	229301462	Manipal University Jaipur
47	Ankit Kumar Tiwari	229309098	Manipal University Jaipur
48	Hanis Gori	229310131	Manipal University Jaipur
49	Aditya Prakash Sinha	229310189	Manipal University Jaipur
50	Lakshita Agrawal	229301455	Manipal University Jaipur



(Hemant Kumar)
Assistant Director, Society Connect
Directorate of Student's Welfare



(Prof. AD Vyas)
Director, Directorate of Student's Welfare

DIRECTOR STUDENT WELFARE & PROCTOR
MANIPAL UNIVERSITY, JAIPUR



**MANIPAL UNIVERSITY
JAIPUR**

Faculty of Management and Commerce

Department of Business Administration

Societal Connect Activity on

Bird Nest Installation

NOVEMBER 30, 2023



**Head
Department of Business Administration
Manipal University Jaipur**

1. Introduction of the Event

Introduction of the Event: School of Business and Commerce organized a activity to install bird nests in the nearby village on November 30, 2023. 5 students and 1 faculty member participated in the campaign. The event took place in nearby village of Manipal university.

2. Objective of the Event

The primary objective of the event was to promote environmental awareness and conservation by actively contributing to the well-being of local bird populations. Through the installation of bird nests, the aim was to create a sustainable habitat for birds in the nearby village, fostering biodiversity and ecological balance.

3. Beneficiaries of the Event

The beneficiaries of the event included the local bird species in the nearby village. By providing suitable nesting spaces, the initiative sought to enhance the living conditions for birds, contributing to the overall ecosystem health. Additionally, the participating students gained hands-on experience in environmental stewardship.

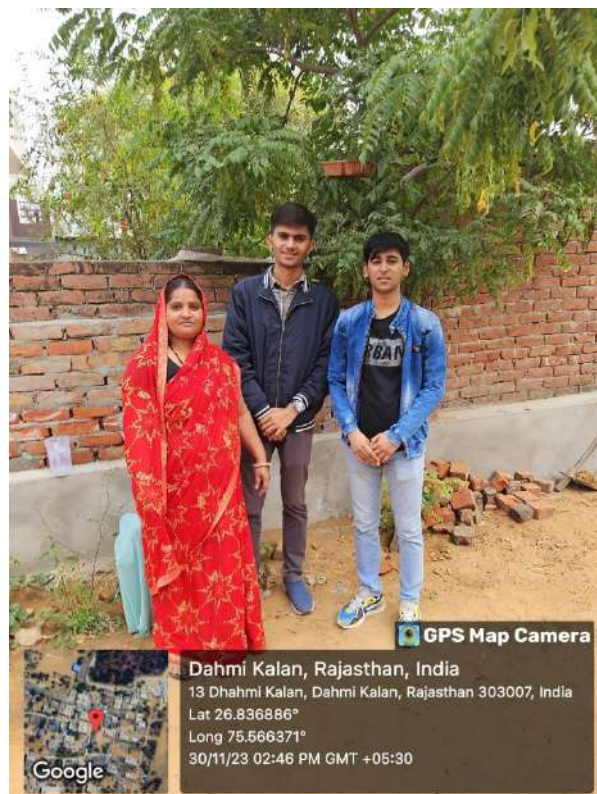
4. Details of the Guests

The event was laid by the students of BBA.


5. Brief Description of the event

The activity involved the installation of bird nests in the nearby village of Manipal University, with students and faculty members actively engaging in the process. Participants worked together to strategically place the nests, considering the local ecology and the needs of various bird species. The event not only contributed to the local environment but also provided a unique learning experience for the students, emphasizing the importance of hands-on conservation efforts. Overall, the initiative aimed to create a positive impact on the local ecosystem while instilling a sense of environmental responsibility among the participants.

6. Photographs





 **GPS Map Camera**

Dahmi Kalan, Rajasthan, India
13 Dhahmi Kalan, Dahmi Kalan, Rajasthan 303007, India
Lat 26.836886°
Long 75.566371°
30/11/23 02:45 PM GMT +05:30





 **GPS Map Camera**

Dahmi Kalan, Rajasthan, India

13 Dhahmi Kalan, Dahmi Kalan, Rajasthan 303007, India

Lat 26.836957°

Long 75.56603°

30/11/23 02:44 PM GMT +05:30





 **GPS Map Camera**

Dahmi Kalan, Rajasthan, India
13 Dhahmi Kalan, Dahmi Kalan, Rajasthan 303007, India
Lat 26.836995°
Long 75.566008°
30/11/23 02:41 PM GMT +05:30



Google




 **GPS Map Camera**

Dahmi Kalan, Rajasthan, India
13 Dhahmi Kalan, Dahmi Kalan, Rajasthan 303007, India
Lat 26.837003°
Long 75.566019°
30/11/23 02:40 PM GMT +05:30





 **GPS Map Camera**

Dahmi Kalan, Rajasthan, India
13 Dhahmi Kalan, Dahmi Kalan, Rajasthan 303007, India
Lat 26.837006°
Long 75.566008°
30/11/23 02:39 PM GMT +05:30



Google




 **GPS Map Camera**

Dahmi Kalan, Rajasthan, India
Unnamed Road, Dahmi Kalan, Rajasthan 303007, India
Lat 26.836785°
Long 75.565537°
30/11/23 02:35 PM GMT +05:30






 **GPS Map Camera**

Dahmi Kalan, Rajasthan, India
Unnamed Road, Dahmi Kalan, Rajasthan 303007, India
Lat 26.836798°
Long 75.565526°
30/11/23 02:34 PM GMT +05:30



Google




 **GPS Map Camera**

Dahmi Kalan, Rajasthan, India
RHP8+X24, Dahmi Kalan, Rajasthan 303007, India
Lat 26.836853°
Long 75.565522°
30/11/23 02:33 PM GMT +05:30





 **GPS Map Camera**



Dahmi Kalan, Rajasthan, India

RHP8+X24, Dahmi Kalan, Rajasthan 303007, India

Lat 26.837056°

Long 75.565398°

30/11/23 02:31 PM GMT +05:30

7. Brochure or creative of the event

MANIPAL UNIVERSITY JAIPUR
(University under Section 2(f) of the UGC Act)

Department of Business Administration in Collaboration with Directorate of Student Welfare and Directorate of Sports, NCC and NSS

Societal Connect Activity

on

Bird Nest Installation

Date: November 30th, 2023

Convenors
Dr. Nupur Ojha, Dr Mahesh Jampala, Dr Rishi Vaidya and Mr Aditya
Department of Business Administration, Manipal University Jaipur

8. Schedule of the Event

The event took place on November 30, 2023

9. Attendance of the Event

Sr. No	Name of Institution	Registration Number/ Employee Code	Attendee Name
1	Manipal University Jaipur	MUJ0099	Dr. Mahesh Jampala
2	Manipal University Jaipur	MUJ1538	Dr Rishi Vaidya
3	Manipal University Jaipur	MUJ0623	Dr. Nupur Ojha
4	Manipal University Jaipur	MUJ1490	Mr. Aditya Dhiman
5	Manipal University Jaipur	23FM10BBA00204	DINESH CHOUDHARY
6	Manipal University Jaipur	23FM10BBA00200	VANSH MULCHANDANI
7	Manipal University Jaipur	23FM10BBA00214	GOPAL BISHNOI
8	Manipal University Jaipur	23FM10BBA00215	AKSHAT SHARMA
9	Manipal University Jaipur	23FM10BBA00216	KHUSHWANT SANKHLA
10	Manipal University Jaipur	23FM10BBA00205	AYUSHMAN GUPTA


Head
Department of Business Administration
Manipal University Jaipur



**MANIPAL UNIVERSITY
JAIPUR**



**MANIPAL UNIVERSITY
JAIPUR**

FACULTY OF ARTS

SCHOOL OF HUMANITIES AND SOCIAL SCIENCES

DEPARTMENT OF ECONOMICS

COMMUNITY OUTREACH VISIT

Date of Event- October 31, 2023



Content of Report (index)

1. Introduction of the Event
2. Objective of the Event
3. Beneficiaries of the Event
4. Details of the Guests
5. Brief Description of the event
6. Geo-tagged Photographs
7. Brochure or creative of the event
8. Schedule of the Event
9. Attendance of the Event
10. News Publication
11. Feedback of the Event
12. Link of MUJ website

1. Introduction of the Event

The practical knowledge about the subject is of immense importance for the students of B.A, Economics (Hons.), M.A. Economics (Hons.), and as such apart from regular classroom teaching there is a strong case for exposing them to innovative and practical outdoor sessions/visits to the nearby areas & projects. Taking this pedagogy of teaching, a one day visit to the renowned Laporiya village and interaction with **Padma Shree Laxman Singh** was planned to closely to observe how the water stressed Laporiya village became self-sufficient in water with all the efforts of **Laxman Singh Ji**. He has been awarded the Padma Shree for his significant contribution to the field of saving water and the environment for the last 40 years. He changed the picture of more than 50 villages with the technique of saving water and the campaign launched for it. He recharged the ponds with the Chowka technique to save water and pastures.

To take insights into his dedication, efforts, and commitments, this visit was planned for students to interact with him so that the **environmental sustainability** thought will sustain forever with **Gen-Z** and they will transfer the same to **Gen-Alpha**.

2. Objective of the Event

Water is a finite and shared resource. As well as being a basic human right and fundamental to healthy ecosystems, water is vital to the functioning of the global economy. However, increasing demand and competition, climate change and pollution are putting pressure on global water resources, creating risks for business and society. To experience the outstanding achievements and gain practical knowledge about environmental economics, an academic visit to “Laporiya village, near Dudu” is organized for the betterment and knowledge enhancement of the students.

3. Beneficiaries of the Event

Students and faculty members of Manipal University Jaipur.

4. Details of the Guests

The President of India has awarded Shri Laxman Singh Ji Padma Shree for his commendable work of reviving the Chowka system, a traditional water harvesting method in Rajasthan. He has founded the NGO Gram Vikas Navyuvak Mandal Laporiya (GVNML). The efforts of Sh. Laxman Singh Ji has borne fruits in a drought-ridden small village (Lapodiya), 80 km from Jaipur.

5. Brief Description of the event

It was an expert lecture on Syllogism of knowledge of economics, entrepreneurial and data skills: Unpack the Why? by Mr. Abhishek Jain, EY, Senior project consultant E & Y. The aim of the lecture is to provide economic knowledge, entrepreneurial skill with basic data analytics knowledge and skills when it comes to leveraging data while growing their businesses, regardless of their respective industries. Student's always be in prisoners dilemma of Why?

Photographs

3 to 5 geotagged photographs of the event or screenshots of the event (if online) with captions



Mr Laxaman Singh Ji discussing the importance of ecosystem



Mr Laxaman Singh Ji Addressing the students



The Village well



Taking a short break, Mr Lakshman Singh Ji, faculties and students

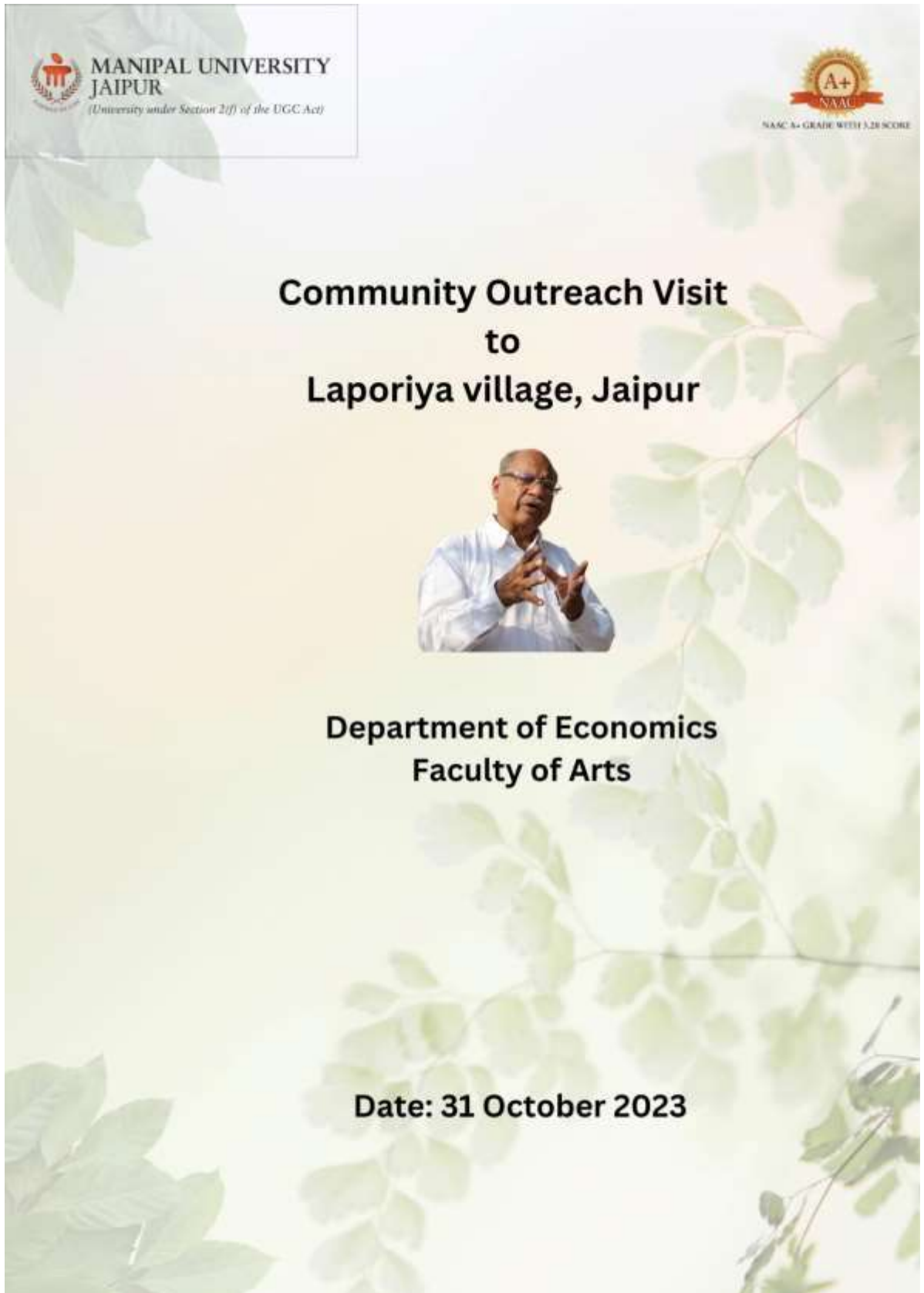


Mr Singh (centre) discussing the young mind's learnings and impressions in his house at the end of the visit.



The students, Mr Lakshman Singh (towards right in white) and Dr Shilpi Gupta, outside his house.

6. Brochure or creative of the event (insert in the document only)



The brochure cover features a light green background with a faint pattern of leaves. In the top left corner, there is a white box containing the Manipal University Jaipur logo and the text "MANIPAL UNIVERSITY JAIPUR (University under Section 2(f) of the UGC Act)". In the top right corner, there is a gold NAAC A+ logo with the text "NAAC A+ GRADE WITH 3.28 SCORE". The main title is centered and reads "Community Outreach Visit to Lajoriya village, Jaipur". Below the title is a photograph of a man in a white shirt, gesturing with his hands. Underneath the photo, the text reads "Department of Economics Faculty of Arts". At the bottom, the date "Date: 31 October 2023" is displayed.

7. Schedule of the event (insert in the report)

Date of the event –October 31, 2023 7:30 AM

8. Attendance of the Event (insert in the document only)

Total attendee-

Registration No.	Name of the Students	Column1	Column2
211101046	Akshay	P	
211101035	Anubhav	p	
211101003	Dakshita	P	
211101043	Gaurav basniwal	P	
211101050	Gaurav kumar	P	
211101013	Saarthak tiwari	P	
211101042	Praseeda	P	
211101004	Rishita	P	
211101006	Shivangi	P	
211101015	Sumriddhi	P	
211101040	Yash	P	
211101041	Yashi	P	
211101039	Anushka	P	
211101007	Utkarsh	P	
211101044	Riti	P	
211101021	Paritosh	P	
211101028	Divya surana	P	
211101025	Atharv	P	
23FA20MEA00004	Santanu Bhowmick	P	
23FA20MEA00007	Anubhav Joshi	P	
23FA20MEA00005	Bhumita Yadav	P	
23FA20MEA00006	Shweta Choudhary	P	
23FA20MEA00003	Medini Choudhary	A	Unwell
23FA20MEA00002	Nisha Choudhary	A	Unwell
231151001	Devanshi Kapoor	P	
Dr. Shilpi Gupta	Associate professor - Department of Economics	P	
Mr. Apoorva Saxena	Head, community Radio Station	P	
Mr. Parul Kanwar	Jr. Assistant SHSS	P	



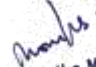
News Publication- News printed in newspaper or online links (if any) for news – insert images)

NA

9. Feedback report of the Event

Students experienced Padam Shree Laxman Singh Ji's dedication, efforts, and commitments, and take away from him the **environmental sustainability** thought which will sustain forever with **Gen-Z** and they will transfer the same to **Gen-Alpha**.

10. Link of MUJ website stating the event is uploaded on website


Dr. Monika Mathur
Head, Department of Economics
Manipal University Jaipur

Seal and Signature of Head with date



**MANIPAL UNIVERSITY
JAIPUR**

MUJ/Q&C/22/F/1.01

Event Report Format



**MANIPAL UNIVERSITY
JAIPUR**

FACULTY OF ARTS

SCHOOL OF HUMANITIES AND SOCIAL SCIENCES

DEPARTMENT OF ARTS

Tree plantation Drive

Social outreach event in collaboration with DSW and NCC

06/09/2023



Index

1. Introduction of the Event
2. Objective of the Event
3. Beneficiaries of the Event
4. Details of the Guests
5. Brief Description of the event
6. Geo-tagged Photographs
7. Brochure or creative of the event
8. Schedule of the Event
9. Attendance of the Event
10. News Publication
11. Feedback of the Event
12. Link of MUJ website



1. Introduction of the Event

The Department of Arts in collaboration with the DSW (NCC and NSS) organized a tree plantation drive with a number of BA(Liberal Arts) students.

2. Objective of the Event (bullet points or about 50 words)

To make the students aware of the importance of tree plantation.

3. Beneficiaries of the Event

Government school, Begas, an adopted school of MUJ

4. Brief Description of the event

The Department of Arts in collaboration with the DSW (NCC and NSS) organized a tree plantation drive with a number of BA(Liberal Arts) students. The objective of the event was to make the students aware of the importance of tree plantation.

5. Photographs



Students engaged in a tree plantation drive in the government school, Begas



MUJ students with the government school students



MUJ department students during the plantation drive

6. Brochure or creative of the event (insert in the document only)

8x4.5 feet



7. Schedule of the event (insert in the report)

6th September, 11:00 a.m. to 12:00 p.m.

8. Attendance of the Event (insert in the document only)

Total attendee-16

Sr. No	Name of Institution	Place of Institution	Name of Attendee	Name of Dept
1.	MUJ	Jaipur	Chandravardhan	Arts
2.	MUJ	Jaipur	Kumesh Mishra	Arts
3.	MUJ	Jaipur	Soumya Pareek Dhanushree	Arts
4.	MUJ	Jaipur		Arts
5.	MUJ	Jaipur	Karan Mallick	Arts
6.	MUJ	Jaipur	Vanshika Agarwal	Arts
7.	MUJ	Jaipur	Prithviraj	Arts
8.	MUJ	Jaipur	Akshatt Singh	Arts
9.	MUJ	Jaipur	Dhruv Nair	Arts
10.	MUJ	Jaipur	Krishna	Arts
11.	MUJ	Jaipur	Gaury	Arts
12.	MUJ	Jaipur	Sudeepti Dhruv Dahiya	Arts
13.	MUJ	Jaipur	Aditi Panigrahi	Arts
14.	MUJ	Jaipur	Aradhya Khandelwal	Arts
15.	MUJ	Jaipur	Komal Chadha	Arts
16.	MUJ	Jaipur	Kkritika Khandelwal Pragya Sharma	Arts
17.	MUJ	Jaipur	Prachi Randhawa	Arts
18.	MUJ	Jaipur	Gurmehr Singh	Arts
19.	MUJ	Jaipur	Himmat di Charan	Arts
20.	MUJ	Jaipur	Sameer Khan	Arts
21.	MUJ	Jaipur	Ananya Thakur	Arts
22.	MUJ	Jaipur	Harshita Das	Arts
23.	MUJ	Jaipur	Manan Sharma	Arts



24.	MUJ	Jaipur	Surendra Singh	Arts
25.	MUJ	Jaipur	Joy Tak	Arts
26.	MUJ	Jaipur	Soumya harna	Arts
27.	MUJ	Jaipur	Deepak	Arts
28.	MUJ	Jaipur	Anup Choudhary	Arts
29.	MUJ	Jaipur	Prithviraj Hada	Arts
30.	MUJ	Jaipur	Tanisha Vashisht	Arts

9. Link of MUJ website stating the event is uploaded on website

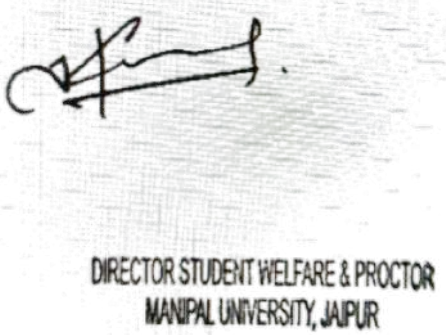
<https://jaipur.manipal.edu/muj/news-events/events-list.html>



Dr. Mani Sachdev
Head, Department of Arts
Manipal University Jaipur

15.9.23

Seal and Signature of HOD



DIRECTOR STUDENT WELFARE & PROCTOR
MANIPAL UNIVERSITY, JAIPUR



(Prof. AD Vyas)

Director, Directorate of Student's Welfare



COLLABORATIONS



OPEN

Climate trends and maize production nexus in Mississippi: empirical evidence from ARDL modelling

Ramandeep Kumar Sharma¹, Jagmandeep Dhillon^{1✉}, Pushp Kumar², Raju Bheemanahalli¹, Xiaofei Li³, Michael S. Cox¹ & Krishna N. Reddy⁴

Climate change poses a significant threat to agriculture. However, climatic trends and their impact on Mississippi (MS) maize (*Zea mays* L.) are unknown. The objectives were to: (i) analyze trends in climatic variables (1970 to 2020) using Mann–Kendall and Sen slope method, (ii) quantify the impact of climate change on maize yield in short and long run using the auto-regressive distributive lag (ARDL) model, and (iii) categorize the critical months for maize-climate link using Pearson's correlation matrix. The climatic variables considered were maximum temperature (Tmax), minimum temperature (Tmin), diurnal temperature range (DTR), precipitation (PT), relative humidity (RH), and carbon emissions (CO₂). The pre-analysis, post-analysis, and model robustness statistical tests were verified, and all conditions were met. A significant upward trend in Tmax (0.13 °C/decade), Tmin (0.27 °C/decade), and CO₂ (5.1 units/decade), and a downward trend in DTR (−0.15 °C/decade) were noted. The PT and RH insignificantly increased by 4.32 mm and 0.11% per decade, respectively. The ARDL model explained 76.6% of the total variations in maize yield. Notably, the maize yield had a negative correlation with Tmax for June, and July, with PT in August, and with DTR for June, July, and August, whereas a positive correlation was noted with Tmin in June, July, and August. Overall, a unit change in Tmax reduced the maize yield by 7.39% and 26.33%, and a unit change in PT reduced it by 0.65% and 2.69% in the short and long run, respectively. However, a unit change in Tmin, and CO₂ emissions increased maize yield by 20.68% and 0.63% in the long run with no short run effect. Overall, it is imperative to reassess the agronomic management strategies, developing and testing cultivars adaptable to the revealed climatic trend, with ability to withstand severe weather conditions in ensuring sustainable maize production.

Maize is the most important cereal, known as the “queen of cereals¹.” The United States (US) is the leading producer, followed by China, Brazil, and Argentina². The US contributes 32% to global production, and 60% of total production is exported². Within the US, Mississippi (MS) is the state that contributes 748.3 million USD annually to national maize revenue³. Mississippi has 0.64 million acres under maize cultivation⁴. Mississippi has eight of the total twelve soil types, 60% of cropland is irrigated (by center pivot and furrow), and maize is grown on raised beds^{5,6}. Mississippi has registered its maize yield progressing at a faster annual growth rate than the US for the past two decades⁷. As a result, MS actual maize yield surpassed the US in 2000; the current yields for MS and the US are 12.51 and 11.87 Mg ha^{−1}, respectively⁴. Over the past half-century, MS has experienced a rapid increase (173%) in the harvested acres for maize compared to the US average (47%)⁴. More intriguingly, MS maize still has a considerable yield gap of 2 to 5.6 Mg ha^{−1}, or 14 to 31%, at the state level when compared to the highest achievable yield under best management practices⁷. Closing these yield gaps is critical for economic benefits, reducing food prices, and consequently improving food security⁸. Strategies to close existing yield gaps via research necessitate a broader understanding of the causal factors and their extent on variations in crop yield⁹.

The factors that govern crop production and its variability include genetics, environment, and management such as soil properties, and agronomic management for instance fertilization, irrigation, tillage, planting dates,

¹Department of Plant and Soil Sciences, Mississippi State University, Mississippi, USA. ²Department of Economics, Manipal University Jaipur, Dharam Kalan, Rajasthan, India. ³Department of Agricultural Economics, Mississippi State University, Mississippi, USA. ⁴Crop Production Systems Research Unit, United States Department of Agriculture (USDA)-Agricultural Research Service (ARS), Stoneville, MS, USA. ✉email: jagman.dhillon@msstate.edu

row-to-row width, planting population, planting time, depth, etc.,^{10,11}. However, amongst all, the climate is noted to be the major uncontrollable contributor affecting crop production, with the proven potential to explain up to or even greater than 60% of the global crop yield variations¹². Numerous studies on wheat (*Triticum aestivum* L.)^{13–16}, maize^{17–19} and rice (*Oryza sativa* L.)^{20,21} has demonstrated a consensus on crop-climate link in cereals. Based on region-specific studies, the crop-climate association was found to be strong, ranging 22–60%, 40–71.3%, and 67–92% in wheat, maize, and rice, respectively. The same has been confirmed by global studies for other crops as well^{22–25}. Specifically, in maize, Rizzo et al.²⁶ attempted to separate climate, management, and genetic factors and deduced that climate change (48%) explained most of the yield variation, followed by management (39%), and genetics (13%). Given the alarming rate of future climate warming, almost 1.5 °C upsurge, precipitation (PT) irregularities (24–40%) combined with increased carbon emissions, the coefficient of yield dependability on climate is expected to rise further by 47% in 2050²⁷.

Climatic trends induce biotic and abiotic stresses in plants by controlling microclimates around them, and influence evapotranspiration, gas exchange, resource use efficiency, plant-microbe relations, phenological processes, crop performance, and finally yield²⁸. The severity of crop-climate links is determined by the magnitude and trend of change of climatic variables, which vary by region, and such estimates for MS are lacking²⁹. Mississippi is in a climatically vulnerable southeastern region of the US, and has a significant agro-economic impact^{30,31}. Also, Mississippi agriculture relies on reduced capital investments and infrastructural inputs, removing several choices for combating climate-related negative consequences^{32,33}. Even so, only a few climate-crop studies were conducted so far for MS^{34–37}, and even fewer on maize^{21,38,39}. Therefore, the current study is aimed at calculating (i) the trend in climatic variables, namely, daily maximum temperature (Tmax), daily minimum temperature (Tmin), diurnal temperature range (DTR), precipitation (PT), carbon emissions (CO₂), and relative humidity (RH) in MS during 1970–2020, and (ii) impact of change in these variables on MS maize yield. The novelty of this study lies in investigating climatic variables other than just temperatures and PT, monthly investigations of trends in climatic variables, pinpointing crucial months impacting maize and employing econometric method for the first time to explore crop-climate link in MS.

Methodology

A detailed step-by-step outline of the various methodologies used to accomplish the study's objectives is displayed in Fig. 1. The sections below provide a detailed discussion on the various methodology components, including data, study model specifications, and the estimation procedures involved.

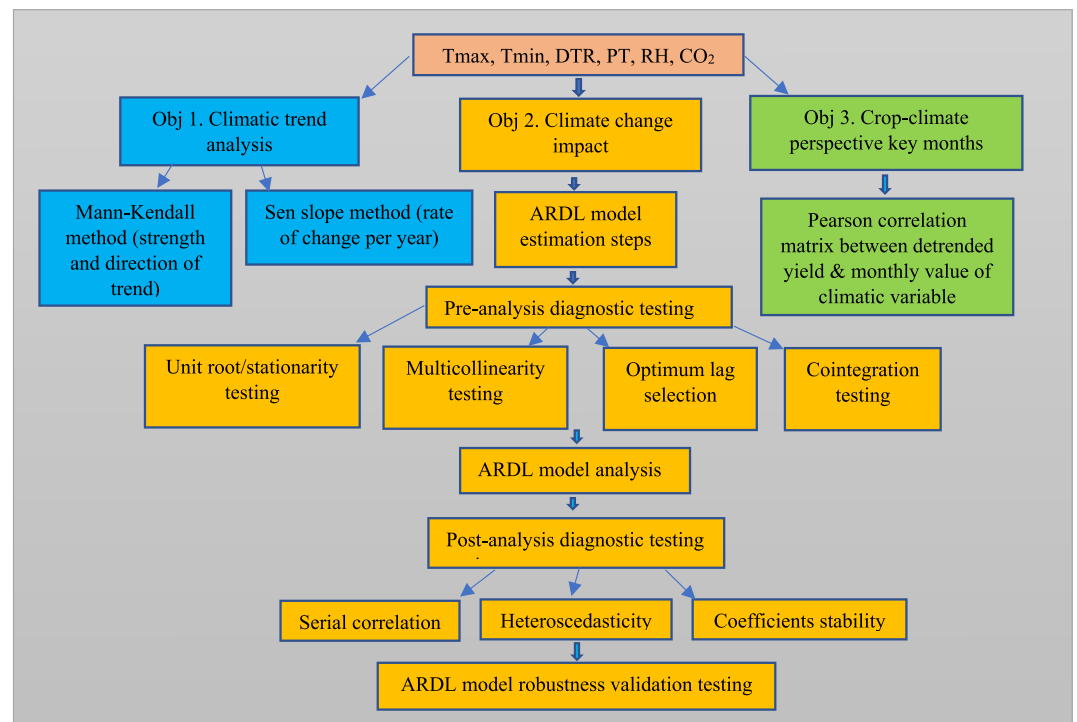


Figure 1. A step-by-step flowchart outlining the detailed methodology for the three different objectives. The first objective—estimating the trend for each of the six climatic variables—maximum temperature (Tmax), minimum temperature (Tmin), diurnal range (DTR), precipitation (PT), relative humidity (RH), and carbon dioxide emissions (CO₂)—is shown in blue boxes on the left, the second objective—quantifying the overall impact of climatic variables on maize yield—are shown in yellow boxes in the middle, and the third objective workflow—identifying the key months for crop-climate linkage—are shown in green boxes on the right.

Data

The present study utilized the past 50 years of time-series dataset for MS (Fig. 2), from 1970 to 2020 similarly to previous studies^{12,40–42}.

As per World Meteorological Organization guidelines, 30 years (at minimum) dataset is recommended for climatic trend computations⁴³. The response variable was maize yield, and the explanatory variables were Tmax, Tmin, DTR, PT, RH and CO₂ (Fig. 1). Harvested area (HA) was included as an input control variable as suggested by Jan et al.⁴⁴. Moreover, following Chandio et al.⁴⁰, the Tmax, Tmin, DTR, and RH were averaged, and PT was totaled to maize growing season (MGS) for analyzing the impact of growing season anomalies. Also, the monthly averaged data of each variable was utilized to compute the month-wise climatic impact on maize. The MGS (March–September) was taken as per the USDA harvesting and planting dates handbook. The data on CO₂ was available on a yearly average basis. The data were gathered from the USDA-NASS repository (<https://www.nass.usda.gov/>) for yield, National Oceanic and Atmospheric Administration (NOAA) database (<https://www.noaa.gov/>) for Tmax, Tmin, DTR, and PT, PRISM database (<https://prism.oregonstate.edu/comparisons/>) for RH, and US energy information administration (<https://www.eia.gov/environment/emissions/state/>) for CO₂. There is a vast literature authenticating the use of time series data and the aforesaid data sources for crop-climate estimations^{45–48}.

Econometric model specification

The two-dimensional effects of climate change on crops include a short-term effect that is directly impacting the yield in the current and subsequent (residual effect) years^{49,50}. This immediate effect accumulates to build the foundation for permanent effects, referred to as long-term effects, that ultimately influence the soil-forming processes, soil properties, microbial buildups in the soil, and nutrient-use abilities^{51–53}. Therefore, the study evaluated both the short and long-term relationships between the variables using the widely used auto-regressive distributive lag (ARDL) bound-testing method^{44,54–58}. The ARDL model is preferred over other statistical methods because it can efficiently run the analysis for both short-term and long-term relationships simultaneously at *ceteris paribus* keeping all other variables unchanged⁵⁵. Moreover, the ARDL model accounts for previous year inputs/factors influencing the current year yield, by incorporating the “lag length” component in its functionality⁵⁹. These factors could be residual effects of previous year fertilization especially if a granular form is applied, late season excessive rainfall, or maybe rollover effects of previous crop rotation^{60,61}. By regressing the lag values of the regressors against the regressand, the lag length feature statistically advises the ARDL model on how far back in time it needs to go to capture the residual effect^{62,63}. The ARDL model works well regardless of the integration level of the time series data *i.e.*, level (I = 0), at first difference (I = 1), or combination of I (0), and I (1)⁵⁶. The ARDL approach is robust against endogeneity issues, which arises when the dependent variable tends to correlate with the error term in the regression model⁶⁴, reducing residual correlation, and small sample sizes⁵⁴. The ARDL has an intrinsic feature of error correction model (ECM) that estimates the pace (% per year) with which the short-term effects transfer cumulatively to form permanent basis for the long-term effects⁵⁴. The following linear equation was used to evaluate short-term and long-term association of mentioned variables:

$$Y = f(Tmax, Tmin, DTR, Prec, RH, CO_2, HA) \quad (1)$$

The natural log form variables are suggested for time series data to smoothen multicollinearity and instability issues if any⁵⁶.

$$\begin{aligned} \ln Y_t = & \beta_0 + \beta_1 \ln(Tmax)_t + \beta_2 \ln(Tmin)_t + \beta_3 \ln(DTR)_t + \beta_4 \ln(PT)_t \\ & + \beta_5 \ln(RH)_t + \beta_6 \ln(CO_2)_t + \beta_7 \ln(HA)_t + \varepsilon_t \end{aligned} \quad (2)$$



Figure 2. The study area (Mississippi state) highlighted on the USA map.

where, Y_t is maize yield (Mg ha^{-1}) in year t . Tmax, Tmin, and DTR are in ($^{\circ}\text{C}$), PT in (mm), RH in (%), CO_2 in metric ton, HA is maize harvested in hectares, β_0 is intercept, and $\beta_1, \beta_2, \beta_3, \beta_4, \beta_5, \beta_6, \beta_7$ are coefficients of slopes in the function, and ε_t is error term in time t .

Auto-regressive distributive lag (ARDL) bound test approach

The ARDL model equation adopted in similar previous studies^{44,55,57}, is used here as follow:

$$\begin{aligned} \Delta \ln Y_{it} = & \alpha_0 + \sum_{i=1}^n \alpha_1 \Delta \ln(Y)_{t-i} + \sum_{i=1}^n \alpha_2 \Delta \ln(\text{Tmax})_{t-i} \\ & + \sum_{i=1}^n \alpha_3 \Delta \ln(\text{Tmin})_{t-i} + \sum_{i=1}^n \alpha_4 \Delta \ln(\text{DTR})_{t-i} + \sum_{i=1}^n \alpha_5 \Delta \ln(\text{PT})_{t-i} \\ & + \sum_{i=1}^n \alpha_6 \Delta \ln(\text{CO}_2)_{t-i} + \sum_{i=1}^n \alpha_7 \Delta \ln(\text{RH})_{t-i} + \sum_{i=1}^n \alpha_8 \Delta \ln(\text{HA})_{t-i} \\ & + \sum_{i=1}^n \gamma_1 \Delta \ln(Y)_{t-i} + \sum_{i=1}^n \gamma_2 \Delta \ln(\text{Tmax})_{t-i} + \sum_{i=1}^n \gamma_3 \Delta \ln(\text{Tmin})_{t-i} \\ & + \sum_{i=1}^n \gamma_4 \Delta \ln(\text{DTR})_{t-i} + \sum_{i=1}^n \gamma_5 \Delta \ln(\text{PT})_{t-i} + \sum_{i=1}^n \delta_6 \Delta \ln(\text{CO}_2)_{t-i} \\ & + \sum_{i=1}^n \gamma_7 \Delta \ln(\text{RH})_{t-i} + \sum_{i=1}^n \gamma_8 \Delta \ln(\text{HA})_{t-i} + \emptyset(\text{ECT})_{t-i} + \varepsilon_t \end{aligned} \quad (3)$$

where Y is maize yield, t is the time in year, i is the lag order with n is the highest lag value, α_0 is the intercept, Δ denotes the first differencing, ε_t is the error term, α_1 to α_8 represents coefficients of long term cointegration for different variables, γ_1 to γ_8 are short term coefficients for different variables, ECT is the error correction term and \emptyset is its coefficient which determines the pace (% per year) by which short term climatic impacts cumulatively transfer to form basis for permanent long term effects.

The first differencing, as suggested in previous studies^{23,65}, was applied as a technique to detrend the maize yield to account for the other yield impacting unobserved factors such as advancement in agricultural technology, progression of the adjustments in growers according to the management recommendations, and the infrastructural developments. The data on aforesaid factors was not available. Detrending is widely used in literature to exclude (minimize) the impact of such unobserved variables and to capture the sole impact of climate variables on crop yields^{23,65}.

Climatic trend analysis

The Mann-Kendall test^{66,67} and Sen slope method⁶⁸ were employed to time series (1970–2020) data for all study variables to establish the trend on both monthly and growing seasonal timescale (Mar-Sep). Both these non-parametric tests are recommended by the World Meteorological Organization for climatic trend estimation⁶⁹. The Kendall tau computes the direction and strength of the trend where positive sign of the coefficient indicates increasing (upward), negative sign signifies decreasing (downward) trend, and the magnitude of 0–0.25 (weak), 0.26–0.50 (fair), 0.51–0.75 (moderate), and values above 0.76 (strong) signifies the strength of the trend^{70–72}. However, the Sen slope coefficient indicates the rate of change per year. For more detailed understanding on methodology of both these tests, readers are suggested to read Gocic and Trajkovic⁷³ or Gujree et al.⁷⁴ procedures.

Estimation procedures

Unit tests

Units root problem arise when the mean, variances, and co-variances are time dependent or non-constant during the study timeframe⁷⁵. Usually, unit root problems (non-stationarity) exist with time series data, if it exists, can cause spurious regression⁷⁶. When a single coefficient fails to accurately reflect the true relationship between the study variables, false regression occurs, and the conclusions drawn may be untrue⁷⁶. Hence, the Augmented Dickey-Fuller (ADF)⁷⁷ and the Phillips–Perron tests (PP)⁷⁸ unit root tests were performed. The results revealed that all the variables were stationary at level or first differencing, fulfilling the assumption of ARDL bound testing model (Table 1A).

Multicollinearity testing

Analyses involving multiple variables may be susceptible to multicollinearity due to the propensity of variables to become correlated with one another⁷⁹. To avoid overfitting in a regression model caused by multicollinearity, either the variables exhibiting it should be eliminated, or it needs to be verified that the data is free of multicollinearity, using tests such as the variance inflation factor (VIF) test and tolerance test⁸⁰. The present study performed both these tests and found that the VIF value (3.45) and tolerance value (0.30) were within the permissible limits (Table 1B); VIF < 10 and tolerance value (TOV) > 0.1^{42,79,80}, confirmed that multicollinearity was not an issue with the dataset (Table 1B).

Variables	ADF		PP		
	Level	First difference	Level	First difference	
(A) Unit root test results following Augmented Dickey-Fuller (ADF) and Phillips-Perron (PP) tests of variables including maximum temperature (Tmax), minimum temperature (Tmin), carbon dioxide emission (CO ₂), harvested area (HA), precipitation (PT), and maize grain yield (Y)					
Tmax	-6.276***		-10.036***		
Tmin	-6.340***		-10.580***		
CO ₂	-2.256	-8.400***	-2.264	-8.357***	
HA	-3.237	-8.323***	-3.170	-10.284***	
PT	-6.317***		-6.287***		
Y	-7.058***		-7.054***		
Variable	Variance inflation factor (VIF)	Tolerance value (TOV)			
(B) Multicollinearity test results based on variance inflation factor (VIF) and tolerance value (TOV) tests of variables including maximum temperature (Tmax), minimum temperature (Tmin), carbon dioxide emission (CO ₂), harvested area (HA), and precipitation (PT)					
Tmax	4.512	0.221			
Tmin	4.126	0.242			
CO ₂	3.207	0.312			
PT	2.475	0.404			
HA	2.937	0.340			
Mean value	3.451	0.304			
Lag	SMLR	FPE	AIC	SIC	HQ
(C) Model's lag selection criterion using sequential modified statistics test (SMLR), final prediction error (FPE) test, Akaike information criterion (AIC) method, Schwarz information criterion (SIC) method, and Hannan-Quinn information criterion (HQ) method					
0	NA	8.36e-13	-10.783	-10.544	-10.693
1	177.455	4.28e-14	-13.768	-12.099*	-13.142*
2	37.853	7.06e-14	-13.350	-10.249	-12.188
3	26.476*	3.42e-14*	-14.295*	-9.7631	-12.597
4	67.775	7.43e-14	-13.990	-8.0276	-11.756
Test Statistic	Value	Significance (%)	Level I (0)	First difference I (1)	
(D) The ARDL bounds cointegration test results					
F-statistic	7.228	10	2.08	3	
		5	2.39	3.38	
		1	3.06	4.15	

Table 1. Pre-analysis diagnostic testing. “***” shows the significance level at 1%. *Indicates lag order selected by the criterion, SMLR: sequential modified likelihood ratio test statistic, FPE: Final prediction error, AIC: Akaike information criterion, SC: Schwarz information criterion, HQ: Hannan-Quinn information criterion, and each test at 5% level of significance.

Optimum lag selection

The ARDL model can determine the number of prior years to include in the model for regressing the explanatory variables (including their lag values) against the regressand (current year yield) by using the optimal lag number, to incorporate the previous years' residual effects on current year maize yield⁵⁵. The study used statistical tests such as Sequential modified likelihood ratio (SMLR) test, final prediction error (FPE) test, Akaike information criterion (AIC) method, Schwarz information criterion (SIC) method, and Hannan-Quinn information criterion (HQ) method, as guided by Agbenyo et al.⁵⁷, and Warsame et al.⁵⁵, to select optimum lag length for the model.

The appropriate lag length for the ARDL model was determined to be three (Table 1C), based on the minimum value generated by majority of the tests (SMLR, FPE, and AIC) utilized. The lag length of three signifies that the previous three years data needs to be considered to regress against the regressand for capturing residual effects.

Cointegration testing

The Wald F-test was used for the null and alternative hypotheses testing after running a regression to check for the existence of cointegration between regressors and regressand⁴⁴. The two types of threshold values were produced, the upper bound threshold values were termed I (1), and the lower bound threshold values were termed I (0). The null hypothesis is accepted if the Wald F-statistics value is less than the lower bound (at I = 0) threshold value, indicating no relationship present between the regressand and regressors⁴¹. However, the null hypothesis is rejected if the Wald F-statistics value is higher than the upper bound (at I = 1) threshold value, indicating the presence of a relationship between the regressand and regressors⁴¹. The Wald F-test value (Table 1D) was estimated as 7.228, which, at the 1% significance level, was higher than the upper critical limit (4.15). The absence

of cointegration was thus ruled out as the null hypothesis, and the presence of cointegration was determined at a 1% level of significance.

Post analysis diagnostic tests, and sensitivity/robustness check of ARDL model

After the ARDL model estimation, the study performed Breusch–Godfrey LM test (for serial correlation check), Breusch–Pagan–Godfrey test (for heteroscedasticity check), and cumulative sum (CUSUM) and cumulative sum of squares (CUSUMSQ) of recursive residuals tests (for stability check of the model coefficients), as suggested by the previous studies⁵⁸.

The results confirmed that the functional model was free from serial correlation and heteroskedasticity (mis-specifications) issues (Table 2A). The CUSUM and CUSUMSQ test graphs found that the parameter plot lines were consistent, stable, and stayed within critical bounds at the 5% level of significance (Figs. 3 and 4). Hence, confirming the accuracy and stability of short and long run model coefficients that affected the MS maize yield from 1970 to 2020. The CUSUM test can identify systematic, whereas the CUSUMSQ test identifies rapid and drastic variations from the constancy of the model coefficients⁸¹.

After confirming the ARDL model's goodness of fit and predictive effectiveness by running post-analysis diagnostic tests, the sensitivity analysis was carried out using the fully modified ordinary least square (FMOLS) model to examine the robustness of the ARDL model functionality in long run. The FMOLS model showed that Tmax and PT had a negative impact on maize yield while Tmin and CO₂ had a positive impact (Table 2B). These results are consistent with the long-run coefficients of the ARDL model, further validating the robustness of the model recommendations.

Test	Statistics	Probability		
(A) Diagnostic test results following Breusch–Pagan–Godfrey test, Breusch–Godfrey LM test, cumulative sum (CUSUM) and cumulative sum of squares (CUSUMSQ) of recursive residuals tests, for the error terms of the regression equation obtained based on the ARDL model output				
BPG test for Heteroskedasticity	0.532	0.919		
BG LM test for Serial Correlation	0.841	0.443		
CUSUM	Stable	Figure 3		
CUSUM Squares	Stable	Figure 4		
Variable	Coefficient	Std. error	t-Statistic	Prob
(B) Results of fully modified ordinary least square (FMOLS) model for confirming the robustness and validation of the study model				
Tmax	– 14.133	4.073	– 3.469***	0.001
Tmin	7.735	2.524	3.064***	0.004
CO ₂	1.374	0.574	2.396**	0.021
HA	0.252	0.115	2.180**	0.035
PT	– 1.253	0.438	– 2.858***	0.007
C	26.614	10.959	2.429**	0.019
R-square	0.828			
Adjusted R-square	0.808			

Table 2. Post analysis diagnostic testing. Tmax represents maximum temperature, Tmin: minimum temperature, CO₂: carbon emissions, HA: harvested acres for maize, and PT: precipitation.

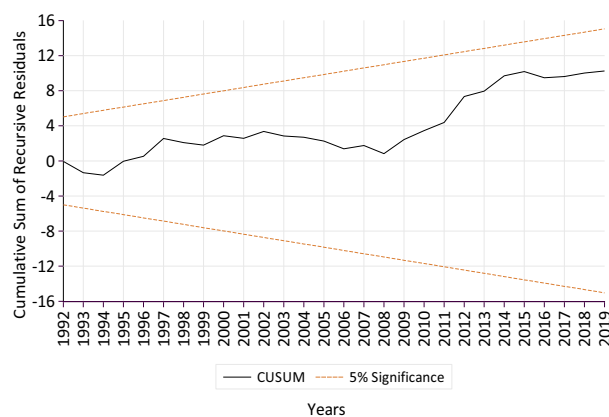


Figure 3. Cumulative sum (CUSUM) plot of recursive residuals of ARDL model with 95% confidence interval around the null.

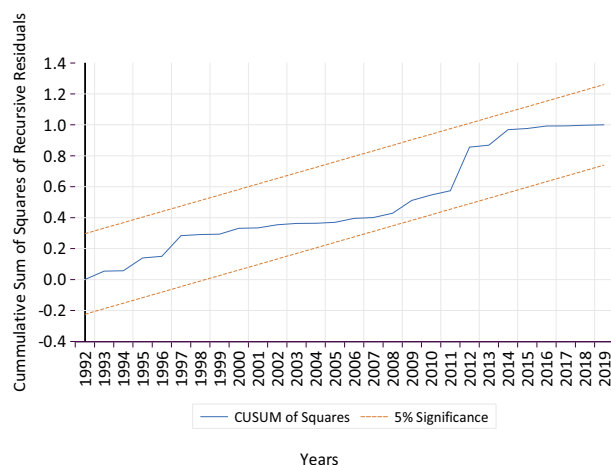


Figure 4. Cumulative sum (CUSUM) of squares Plot for recursive residuals of ARDL model with 95% confidence interval around the null.

Pearson’s coefficient of correlation matrix

Pearson’s coefficient of correlation between detrended (first differenced) yield and monthly averaged value of each climatic variable, as suggested by Eck et al.⁸², was calculated. Based on the strength of correlation, the months that had the greatest impact on maize yield were pinpointed.

Results and discussions

The final regression fit equation used by the ARDL was a reduced model, which excluded DTR and RH since they were found to be non-significant and reducing the overall predictive efficiency of the model. Hence, the pre and post diagnostic tests (Tables 1, 2)—all of which were based on the ARDL model’s assumptions—were only carried out for the variables that were part of the ARDL model. However, all variables were included for climatic trend analysis, and for calculating the Pearson’s correlation between detrended (first differenced) yield and monthly averaged values of climatic variables (Tables 3 and 4B).

Climatic trend analysis

Tmax increased by 0.13 °C per decade in MGS, while Tmin increased by 0.27 °C per decade, which is 107.67% faster than Tmax (Table 3). Other studies have found similar unsymmetric Tmin-Tmax warming rates^{83–86}.

Series/test	Tmax		Tmin		DTR		PT		RH		CO ₂	
	Kendall tau	Sen slope	Kendall tau	Sen slope	Kendall tau	Sen slope	Kendall tau	Sen slope	Kendall tau	Sen slope	Kendall tau	Sen slope
March	0.139	0.032	0.146	0.030	0.012	0.001	-0.095	-0.193	0.047	0.021	-	-
April	0.014	0.003	0.101	0.015	-0.078	-0.008	0.090	0.194	0.157	0.060	-	-
May	0.103	0.012	0.178	0.022	-0.092	-0.009	-0.087	-0.183	0.003	0.000	-	-
June	0.051*	0.007*	0.373***	0.035***	-0.261**	-0.028**	0.095	0.163	0.125	0.036	-	-
July	-0.006	-0.001	0.262**	0.024**	-0.401***	-0.031***	0.119	0.147	0.068	0.022	-	-
August	0.066*	0.009*	0.299**	0.027**	-0.201*	-0.019*	0.158	0.269	-0.009	-0.004	-	-
September	0.143	0.021	0.183	0.027	0.006	0.001	-0.063	-0.112	-0.110	-0.060	-	-
MGS	0.176*	0.013*	0.422***	0.027***	-0.252**	-0.015**	0.057	0.432	0.027	0.011	0.669***	0.514***
Mean	28.56 °C		16.02 °C		12.54 °C		48.49 mm		66.73%		53.58 million metric tons (Mmt)	

Table 3. The summarized results of the Mann–Kendall test and the Sen slope method for trend estimation of variables including maximum temperature (Tmax), minimum temperature (Tmin), diurnal temperature range (DTR), precipitation (PT), relative humidity (RH), and carbon dioxide emission (CO₂) in Mississippi from 1970 to 2020. Kendall tau negative (-) value signifies downward (decreasing) trend, and positive (+) value indicates upward (increasing) trend with its value ranging between -1 and 1, and its absolute value signifies the strength of the trend. As the absolute value of Kendall tau approach 1, the strength of the trend becomes strong. The Sen slope value represents the rate of change (of variable) per year. Kendall tau is a pure number (unitless) as it is a correlation coefficient and Sen slope units are °C/year (for Tmax, Tmin, and DTR), mm/year (for PT), percentage/year (for RH), and Mmt/year (for CO₂). The negative (-) value of Sen slope means the rate of decrease per year while the positive (+) value represents the rate of increase per year. Significance: “*” $p < 0.05$, “**” $p < 0.01$, and “***” $p < 0.001$.

Variable	Coefficient	Std. Error	t-Statistic	Prob	
(A) Calculated ARDL model estimates for short and long run effects of Tmax, Tmin, CO ₂ , HA, and PT on maize yield (dependent variable)					
ARDL model long run effects					
Tmax	-26.330	9.169	-2.872***	0.008	
Tmin	20.684	6.731	3.073***	0.005	
CO ₂	0.629	0.976	0.644**	0.032	
HA	0.155	0.154	1.007	0.323	
PT	-2.696	0.983	-2.742**	0.011	
ARDL model short run effects					
Tmax	-7.392	2.074	-3.563***	0.001	
Tmin	2.361	1.340	1.760	0.091	
CO ₂	-0.061	0.623	-0.098	0.922	
HA	0.018	0.093	0.198	0.844	
PT	-0.645	0.249	-2.587**	0.016	
C	44.329	25.660	1.728**	0.096	
ECM	-0.302	0.038	-7.892***	0.000	
R square	0.834				
Adjusted R square	0.766				
Climatic variables					
Growing season months	Tmax	Tmin	DTR	PT	RH
(B) Pearson's correlation matrix between the first differenced (detrended) yield and climatic variables (Tmax, Tmin, DTR, PT, RH) based on each month of MGS					
March	0.248	0.228	0.013	-0.251	0.103
April	0.062	0.129	-0.107	0.024	0.248
May	0.173	0.240	-0.123	-0.143	-0.024
June	-0.001**	0.485***	-0.420**	0.267	0.226
July	-0.159***	0.314*	-0.472***	0.132	0.190
August	-0.000	0.354**	-0.319*	-0.323*	0.022
September	0.213	0.231	-0.019	-0.098	-0.126

Table 4. Impact of climate change on maize yield. “*” $p < 0.05$, “**” $p < 0.01$, and “***” $p < 0.001$. Tmax represents maximum temperature, Tmin: minimum temperature, DTR: diurnal temperature range, CO₂: carbon emissions, HA: harvested acres for maize, PT: precipitation, and ECM: error correction model. Significance codes: “*” $p < 0.05$, “**” $p < 0.01$, and “***” $p < 0.001$.

There was an upward trend for Tmax for MGS, specifically for June and August, but it was weak, as magnitude of correlation strength was less than 0.25 (Fig. 5A; Table 3). July was the only month that experienced a Tmax decreasing trend (Fig. 5A), yet non-significant (Table 3).

In contrast, MGS shows an upward trend for Tmin, increasing by 0.27 °C per decade in the last five decades (Fig. 5B; Table 3). Tmin warming rates ranged between 0.24 and 0.35 °C per decade in June, July, and August of MGS (Table 3). June, Tmin had the greatest rise, adding 0.35 °C per decade to global warming (Table 3). The equivalent rising trends were seen by Eck et al.⁸² and Sharma et al.⁸⁷ in MGSs in the southeastern part of the US.

In recent years, the DTR (Tmax-Tmin) has been recognized as another climatic variable that is essential for diagnosis, particularly under rising unsymmetrical warming scenarios^{88,89}. There was a downward trend for DTR in June, July, and MGS, and a weak trend for August (Fig. 5C). In MGS, the DTR decreased by 0.15 °C per decade, but in June, July, and August, it decreased by 0.19–0.31 °C per decade (Table 3). These rates are comparable with the computations of Sun et al.⁹⁰ for the other maize-growing regions.

Precipitation and RH, neither for MGS nor for any other month were found to indicate a significant trend line (Figs. 5D, 6A), although numerically, a negative trend was noted in March, May, and September for PT and August and September for RH (Table 3).

A moderately strong and significant upward trend and an annual increase rate of 0.51 units was noted for CO₂ (Fig. 6B; Table 3). The same is corroborated by Rahman⁹¹ and Wu et al.⁹² previously in the context of direction and strength, and by Ainsworth et al.⁹³ in the context of rate of increase.

The climatic impact on maize

The Tmax was found to have a significant negative effect on maize yield in both the short and long run (Table 4A). More specifically, every 1 °C rise in Tmax reduced the maize yield by 7.39% and 26.33% in the short and long run, respectively (Table 4A).

On further downscaling the analysis to monthly basis to capture the effect of within season variability, it was noted that the monthly averaged Tmax of June and July had a significantly negative correlation with maize yield (Table 4B). This indicates that Tmax in June and July (reproductive-early grain filling stages) contributed the

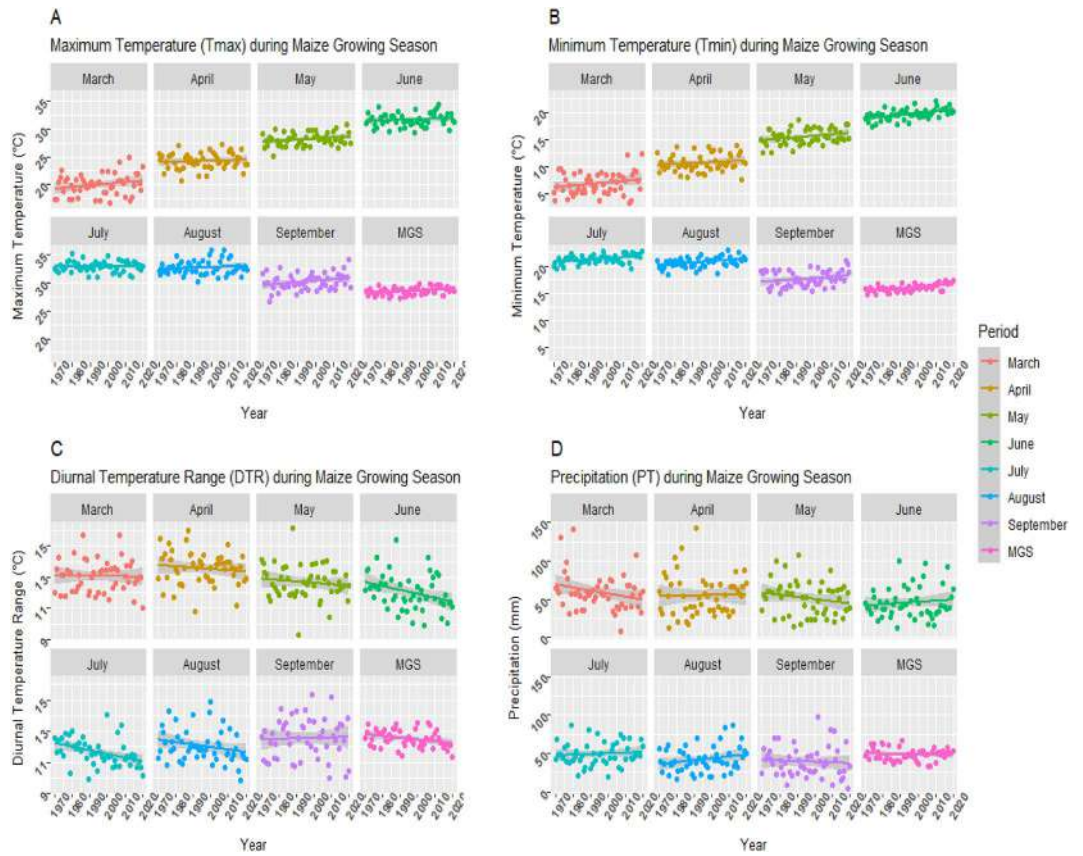


Figure 5. Trend lines for Tmax (A), Tmin (B), DTR (C), and precipitation (D) for maize growing season (MGS) and its individual months from 1970 to 2020 in Mississippi. Each figure is faceted by months from March to September and average of all months all together in MGS.

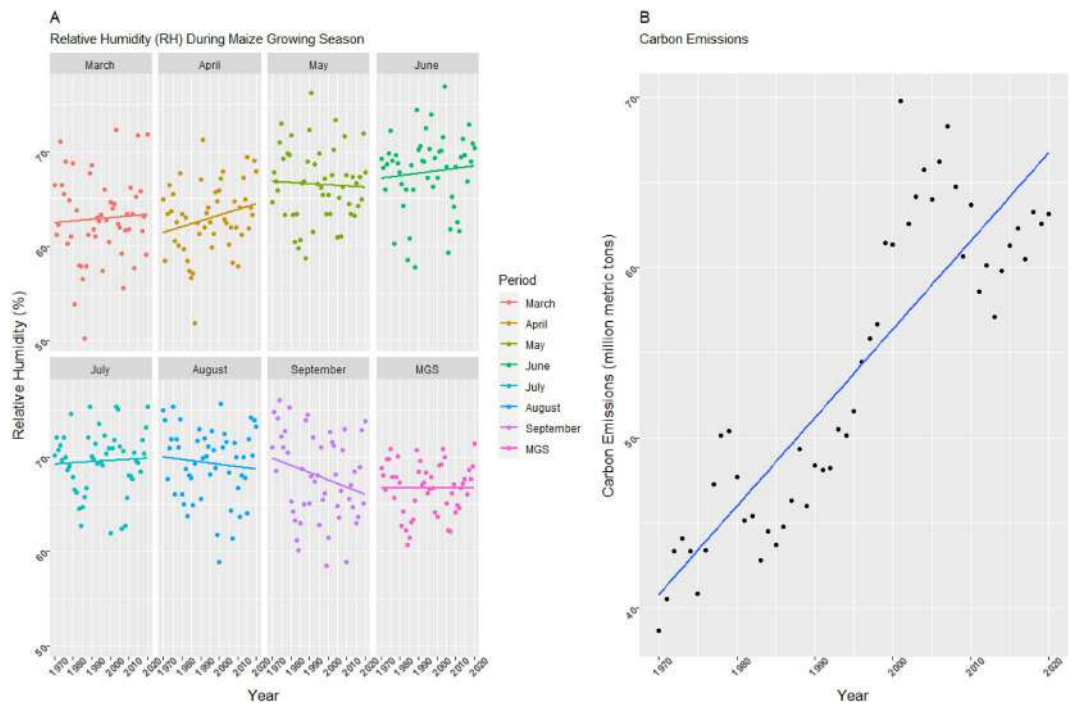


Figure 6. (A) Trend lines for relative humidity for maize growing season (MGS) and its individual months from 1970 to 2020 in Mississippi. (B) Trend line for CO₂ emissions for years from 1970 to 2020 in Mississippi. Figure A is faceted by months from March to September and average of all months all together in MGS.

most to yield loss in MS. This is because in reproductive stage, stress-induced plant dysfunction has irreparable harm on kernel development and yield which is not the case with the vegetative phase^{94,95}. These findings are consistent with those of Kucharik and Serbin¹⁷ in the context of highly correlated months with respect to maize growing season and to those of Lobell and Field²³, and Wu et al.⁹² in the context of Tmax's adverse effects. Hu and Buyanovsky⁹⁶ reported that maize needs both a warming trend with temperatures higher than average in April and May to provide better conditions for germination and emergence and a cooling trend with temperatures lower than average in June–August to promote reproductive success and, consequently, yield. This statement is largely agreed with by Lobell and Asner⁹⁷ as well. However, MS had not seen any significant warming trend in April and May; instead, it showed an unfavorable significant warming trend in June and August (Table 3). Contrary to favorable conditions, MS was observed to have temperatures that were below average (28.56 °C) in April (24.24 °C) and May (28.13 °C) and above average in June (31.66 °C) and August (32.78 °C) (Table 3). The Mid-MGS (*i.e.*, the beginning reproductive stage) coincides with June and July (hotter climate), which affects tasseling and grain filling, thereby yield, and is sensitive to additional warming^{98,99}. Furthermore, the average Tmax (28.56 °C) noted in MS for MGS (Table 3) has already surpassed the optimal temperature (26.40 °C) for maize¹⁰⁰, and is rapidly approaching 29 °C, which is damaging to maize¹⁰¹. The main reason is that after surpassing 29 °C^{101,102} or 30 °C¹⁰³, processes such as anthesis-silking, assimilates production, translocation of resources during reproductive and grain filling are hampered. Temperature beyond this range has been linked to impaired pollen structure, decreased sugar (energy) levels upon anthesis, and retarded pollen shedding, all of which negatively affect pollen germination ability and fertilization¹⁰⁴. More recent studies found that short duration of Tmax episodes during anthesis can cause significant reduction in pollen germination (30%), kernel number (72%), kernel weight (10%), and stomatal conductivity (52%) in maize^{105,106}. Further at the biochemical level, the activity of the enzymes involved in converting atmospheric CO₂ to glucose or other key photosynthesis-related molecules were found to be disrupted by elevated temperatures¹⁰⁷. In worst case scenario at higher temperatures, a yield loss could reach 34–80%^{87,108}.

A 1 °C rise in Tmin increased maize productivity by 20.68% over the long run, indicating a significant and positive effect on maize yield in MS (Table 4A). Several other maize-growing regions have shown that yields respond to Tmin^{87,109–111}. Tmin warming was also shown to be advantageous to maize yield in the short run, while the impact was not significant (Table 4A). Although there has not yet been an agreement regarding the physiological effects of Tmin on plants as there is an inclination of the crop-climate research towards the Tmax or Tavg and overlooking the Tmin^{112,113}. The current study's findings on the positive association of Tmin and maize yield were supported by evidence from the literature, which included studies using statistical modeling^{87,114–121} as well as simulation-based studies^{122,123}. This is attributable to the fact that the increased Tmin speeds up night-time respiration, resulting in carbohydrates losses¹²⁴. However, this carbon starvation enhances the following day photosynthetic rate to more than make up for the losses brought on by the accelerated night-time respiration, increasing overall plant productivity^{125,126}. Consequently, the amassed dry matter from various plant tissues starts remobilizing toward grain, increasing maize kernel weight, and hence, the yield¹²⁷. Also, the increased Tmin is believed to impart conducive conditions for germination, emergence, seedling growth, grain filling (during night-time), and milk-maturity stage in maize¹¹⁰. More importantly, according to Badu-Apraku et al.¹²⁷, Cairns et al.¹²⁸, and Sanchez et al.¹⁰⁰, all the beneficial mechanisms of Tmin mentioned above only prevail when the Tavg is below 25 °C or 26.40 °C. The Tavg for the current study was found to be 22.29 °C (Table 3). Furthermore, a similar case of Tavg of less than 25 °C was observed in all studies that supported the current findings, specifically at 21.2 °C and 24.4 °C in Liu et al.¹¹⁶ and Shammi and Meng³⁶. Contrarily, the studies that found negative effects of Tmin on maize yield were all found to have been carried out at Tavg of more than 25 °C¹²⁹. For example, Wang et al.¹³⁰ tested at Tavg (27–31 °C), Liu et al.¹³¹ tested at Tavg (25–35 °C), Suwa et al.¹³² at Tavg (31 °C), and Wilhelm et al.¹³³ at 29.5 °C and observed negative Tmin-yield impact in maize. Furthermore, it was noted that June, July, and August demonstrated a significant and positive correlation between Tmin and detrended yield (Table 4B). This suggests that warmer nights in June, July, and August are beneficial for maize yields in MS, but there is no evidence that this beneficial effect offsets the detrimental effect of Tmax during the same months. Chen et al.¹¹⁰ also noted 1 °C Tmin warming during May/September improved maize yield by 303/284 kg ha⁻¹. Reilly¹³⁴, Izaurralde et al.¹³⁵, and Reilly et al.¹³⁶ also realized the positive effects of warming on maize yield. Also, according to Schlenker and Roberts¹³⁷, Lobell et al.¹³⁸, and Lobell et al.¹³⁹, yield reductions are expected when temperature surpasses 30 °C, which was not the case with this study (Table 3). So far, the curve of Tmin has never reached the point at which it can cause the Tavg to pass above the optimal range and negatively affect maize yield.

According to the model's long-run estimation, the rising trend in CO₂ emissions had a positive and significant impact on maize yield (Table 4A). Ahsan et al.¹⁴⁰ and Chandio et al.⁴⁰ also realized similar yield improvements due to CO₂ emissions. However, it was discovered that the impact of CO₂ emissions on maize yield in the short run was not significant (Table 4A), and this is consistent with Warsame et al.⁵⁵ and Anapalli et al.³⁸ studies, focused on MS. Specifically, every unit increase in CO₂ emissions resulted in a long-term improvement in maize yield of 0.62% (Table 4A). Similar reports of 0.23% and 0.70% yield increases were noted by Asfew and Bedemo⁵⁶ and Mahrous¹⁴¹ where they quantified the positive effects of increased CO₂ emissions. However, Islam et al.¹⁴² estimated that under current climate change scenarios, these CO₂ emissions-driven yield increments might reach 3.5 to 12.8% at the rate of 1.80% every decade¹⁴³. The upsides of elevated CO₂ on maize yield are due to its effects on plant physiology, growth, and biochemistry, through diminished stomatal conductivity and enhanced photosynthetic rates^{144–147}. The decreased stomatal conductance reduces water loss thereby increasing water use efficiency, especially in drought-stress conditions^{148,149}. The rise in atmospheric CO₂ levels increases the intercellular CO₂ concentration (Ci) and thus, photosynthetic rate (A)¹⁵⁰. However, maize has a lower carbon saturation point than C3 plants like soybean¹⁵¹ due to the high affinity (to CO₂) of the key enzyme, phosphoenolpyruvate carboxylase^{152,153}. These physiological and biochemical responses of maize to CO₂ indicated that further increases in CO₂ levels may not increase assimilation production^{150,151}. Increased CO₂ level have been shown

to benefit other crops^{154–157}. However, the response of C4 plants (maize) to elevated CO₂ levels is complex, as it is influenced by various factors such as air temperature, water availability, light intensity, vapor pressures, and nitrogen availability^{158,159}. Nevertheless, predicted rise in CO₂ levels by the years 2050 and 2100 may diminish the beneficial effect of CO₂ in row crops, like maize^{150,151}. Further research is therefore required to determine the influence of elevated CO₂ in C4 plants at different growth stages^{150,152,160,161}.

Even though PT is a crucial crop growth factor, the current findings revealed that, at a 1% level of significance, PT patterns were determined to pose a negative and significant effect on maize yields in both the short- and long-term (Table 4A). More specifically, every 1 mm change in PT had reduced maize yield in the short- and long-term, by 0.64% and 2.70%, respectively (Table 4A). These results are consistent with the observations of Rosenzweig et al.¹⁶², Chen et al.¹⁶³, and Xiang and Solaymani⁵⁸ who also noted the negative effect of the ongoing PT trends on maize yield. A crop yield decline due to prevailing PT trends was also documented in the study by Shammil and Meng³⁶ in MS. These results are attributable to the excessive PT (1504.44 mm annually) in MS¹⁶⁴. Excessive PT, in addition to directly or physically harming the crop, results in prolonged wet conditions that lead to soil saturation and are averse to crop development, particularly in conditions of inadequate drainage¹⁶⁵. This yield-reducing effect of excess moisture is attributable to (i) root growth hindrance impairing plants ability of nutrients and water uptake^{166,167}, (ii) increased nitrate leaching, leading to nutrient depletion¹⁶⁸, (iii) anoxic conditions in soil, leading to the risk of toxic substances development, diseases, and insect infestation¹⁶⁹, and (iv) delayed planting or harvesting, owing to the difficulty of driving the machinery in wet fields^{149,170,171}. On account of the aforementioned factors, the US as a whole suffers a 3% yield loss annually^{162,172}, and significant yield decline has been seen over the past two decades in various parts of the US *i.e.*, Iowa^{173,174}. When the analysis was further scaled down to a monthly level, it was discovered that the most significant month correlated with the MS maize yield was August, and the association was negative (Table 4B). This indicates that the August PT had the most significant negative effect on MS maize, and Eck et al.⁸² also deduced similar results documenting increased PT to be detrimental in the latter part of the MGS. This is because the uptake of nitrogen, phosphorus, and potassium in maize plants continues up until the R3–R4 stage in August, when the plant can still transpire to the extent of 0.25–0.30 inches of water, according to Lauer¹⁷⁵, who claimed that by this time, the two (ear and kernel number) of three key yield parameters are determined, but the kernel size/weight is still yet to be determined. Furthermore, low PT is required during the ripening period (August) of maize⁹⁶, nonetheless, the current study found that the MGS month with the highest PT growth rate (2.69 mm/decade) was August (Table 3). However, Rosenzweig et al.¹⁶² had a different perspective on the negative association of August–maize yield, according to them it probably has less to do with plant itself and more primarily linked with the harvesting challenges arising from overly moist conditions, for growers. Delayed harvesting degrades the quality of maize, rendering it unsalvageable, in some instances, due to rotting in the field⁸². Overall, such scenarios of delayed harvesting could lead to a yield loss to the extent of 10%¹⁴⁹.

Pearson's correlation matrix revealed that the RH of any month of MGS had no correlation but DTR of June, July, and August months had negative and strong correlation with the maize yield (Table 4B). These results are consistent with those of Muhammad et al.¹⁷⁶ who found a weak correlation of RH and HA with yields, as well as with that of Lobell⁸⁹ who examined the impact of DTR on maize yield.

The coefficient of ECM was determined to be -0.302 (Table 4A), which signifies that every year, 30.20% of the immediate climatic impact cumulatively transfers to form the permanent basis for the long-term effects. A 30.20% is equivalent to the results of Warsame et al.⁵⁵ and Jan et al.⁴⁴. The ARDL model estimated the adjusted R² value of 0.766, indicating that 76.60% of the total variations in maize yield due to the studied variables are explained by the study model.

Study limitations

Each research has its unique set of limitations, which forms the base for further advancement in the research field. The factors such as maize evapotranspiration, sunshine durations/hours, irrigation intensity, and vapor pressure deficit that could interact to determine the climatic effects for better insights on crop–climate link, were not included in the present study due to data unavailability. Hence, future research is suggested incorporating the aforesaid variables along with the variables considered in the present study for more practicable and accurate estimations.

Concluding remarks

This study demonstrated a markedly rising trend in Tmax, Tmin, and CO₂, with Tmin majorly contributing to the overall warming trend in the MGS of MS. The Tmin progressed at a faster rate (0.14°C decade⁻¹) than the Tmax, causing a considerably lowering trend in the DTR. The month-wise analysis determined the most correlated month for Tmax (June and July), Tmin and DTR (June, July, and August), and PT (August) in significantly impacting maize yield in MS, indicating the varied sensitivity of maize yield to within season variability for different climatic parameters. The crop–climate link assessment revealed a significantly negative effect of Tmax and PT on maize yield in both short and long run, whereas Tmin and CO₂ emissions posed a significantly positive effect on maize yield in long run and no effect in short run. Overall, the study model explained the 76.60% variations in maize yield due to climate change in MS. As shown by the ECM coefficient of the study model, the short-term immediate climatic effects on maize progressively transfer to permanent long-term effects by 30.2% every year, making the crop–climate link more prominent in the long run than in the short run. As the water and nutrient usage efficiencies are climate driven and based on the current findings, it is suggested to reassess the agronomic optimum management strategies in the face of MS crop–climate link. Also, the research efforts need to be intensified to test crop varieties that might be more resistant to elevated Tmax, perform better under delayed planting circumstances, and continue to interact favorably with elevated CO₂ and Tmin scenarios under

the local climatic conditions of the MS. Moreover, it is recommended to test current findings at the field or in controlled settings using the locally prevalent climatic indices with a focus on agronomic optimum management strategies as they react to the climatic variations.

Data availability

The data used in this study is accessed from National Agricultural Statistics Service's repository (USDA-NASS), US Climate Divisional Database (NOAA), PRISM database, and US energy information administration. The online links for these data sources are mentioned in Section "Data" (data) of methodology chapter. However, for more information on data, rs2564@msstate.edu (Ramandeep Kumar Sharma) can be contacted. No separate field study on plants was carried out because all the data used in the study was accessible online.

Received: 12 June 2023; Accepted: 25 September 2023

Published online: 03 October 2023

References

- García-Lara, S., & Serna-Saldivar, S. O. Corn history and culture. *Corn*, 1–18 (2019).
- FAO. FAOSTAT—Crops and Livestock Products. *Food and Agriculture Organization (FAO)*. 2020. Available online: <https://www.fao.org/faostat/en/#data/QCL> (accessed on 14 March 2023).
- MAC 2021. <https://www.mdac.ms.gov/agency-info/mississippi-agriculture-snapshot/>
- USDA-national Agricultural Statistics Service (2021) https://www.nass.usda.gov/Publications/Todays_Reports/reports/fcdat_e10.pdf
- Cox, M. S. The Lancaster soil test method as an alternative to the Mehlich 3 soil test method1. *Soil Sci.* **166**(7), 484–489 (2001).
- Kebede, H., Fisher, D. K., Sui, R. & Reddy, K. N. Irrigation methods and scheduling in the Delta region of Mississippi: Current status and strategies to improve irrigation efficiency. *Am. J. Plant Sci.* **5**(20), 2917 (2014).
- Dhillon, J., Li, X., Bheemanahalli, R. & Reed, V. Mississippi state and county level yield gap in corn production. *Agric. Environ. Lett.* **7**(2), e20092 (2022).
- Snyder, K. A., Miththapala, S., Sommer, R. & Braslow, J. The yield gap: Closing the gap by widening the approach. *Expe. Agric.* **53**(3), 445–459 (2017).
- Licker, R. *et al.* Mind the gap: how do climate and agricultural management explain the 'yield gap' of croplands around the world?. *Global Ecol. Biogeogr.* **19**(6), 769–782 (2010).
- Kukal, M. S. & Irmak, S. Climate-driven crop yield and yield variability and climate change impacts on the US Great Plains agricultural production. *Sci. Rep.* **8**(1), 1–18 (2018).
- Oglesby, C. *et al.* Discrepancy between the crop yield goal rate and the optimum nitrogen rates for maize production in Mississippi. *Agron. J.* **115**(1), 340–350 (2023).
- Ray, D. K., Gerber, J. S., MacDonald, G. K. & West, P. C. Climate variation explains a third of global crop yield variability. *Nat. Commun.* **6**(1), 1–9 (2015).
- Li, S. *et al.* The observed relationships between wheat and climate in China. *Agric. For. Meteorol.* **150**(11), 1412–1419 (2010).
- de Cárcer, P. S., Sinaj, S., Santonja, M., Fossati, D. & Jeangros, B. Long-term effects of crop succession, soil tillage and climate on wheat yield and soil properties. *Soil Tillage Res.* **190**, 209–219 (2019).
- Faghih, H., Behmanesh, J., Rezaei, H. & Khalili, K. Climate and rainfed wheat yield. *Theor. Appl. Climatol.* **144**(1), 13–24 (2021).
- Schierhorn, F., Hofmann, M., Gagalyuk, T., Ostapchuk, I. & Müller, D. Machine learning reveals complex effects of climatic means and weather extremes on wheat yields during different plant developmental stages. *Clim. Change* **169**(3), 1–19 (2021).
- Kucharik, C. J. & Serbin, S. P. Impacts of recent climate change on Wisconsin maize and soybean yield trends. *Environ. Res. Lett.* **3**(3), 034003 (2008).
- Durdu, Ö. F. Evaluation of climate change effects on future maize (*Zea mays* L.) yield in western Turkey. *Int. J. Climatol.* **33**(2), 444–456 (2013).
- Sun, L., Li, H., Ward, M. N. & Moncunill, D. F. Climate variability and maize yields in semiarid Ceará, Brazil. *J. Appl. Meteorol. Climatol.* **46**(2), 226–240 (2007).
- Oguntunde, P. G., Lischeid, G. & Dietrich, O. Relationship between rice yield and climate variables in southwest Nigeria using multiple linear regression and support vector machine analysis. *Int. J. Biometeorol.* **62**(3), 459–469 (2018).
- Islam, A. R. M. *et al.* Variability of climate-induced rice yields in northwest Bangladesh using multiple statistical modeling. *Theor. Appl. Climatol.* **147**(3), 1263–1276 (2022).
- Frieler, K. *et al.* Understanding the weather signal in national crop-yield variability. *Earth's Future* **5**(6), 605–616 (2017).
- Lobell, D. B. & Field, C. B. Global scale climate–crop yield relationships and the impacts of recent warming. *Environ. Res. Lett.* **2**(1), 014002 (2007).
- Jägermeyr, J. & Frieler, K. Spatial variations in crop growing seasons pivotal to reproduce global fluctuations in maize and wheat yields. *Sci. Adv.* **4**(11), eaat4517 (2018).
- Iizumi, T. & Ramankutty, N. Changes in yield variability of major crops for 1981–2010 explained by climate change. *Environ. Res. Lett.* **11**(3), 034003 (2016).
- Rizzo, G. *et al.* Climate and agronomy, not genetics, underpin recent maize yield gains in favorable environments. *Proc. Natl. Acad. Sci.* **119**(4), e2113629119 (2022).
- Urban, D., Roberts, M. J., Schlenker, W. & Lobell, D. B. Projected temperature changes indicate significant increase in interannual variability of US maize yields. *Clim. Change* **112**(2), 525–533 (2012).
- Shen, X., Liu, B., Henderson, M., Wang, L., Jiang, M., & Lu, X. Vegetation greening, extended growing seasons, and temperature feedbacks in warming temperate grasslands of China. *J. Clim.*, 1–51 (2022).
- Apata, T. G. Effects of global climate change on Nigerian agriculture: An empirical analysis. *CBN J. Appl. Stat.* **2**(1), 31–50 (2011).
- Asseng, S. (2013). Agriculture and climate change in the southeast USA. In *Climate of the Southeast United States* (pp. 128–164). Island Press, Washington, DC.
- Sharma, R. K., Dhillon, J., Kumar, S., Vatta, K. & Reddy, K. N. Crop-climate link in the southeastern USA: A case study on Oats and Sorghum. *J. Agric. Food Res.* **12**, 100626 (2023).
- Ciscel, D. H. Creating economic growth in rural Mississippi Delta Counties. Federal Reserve Bank of St. Louis (1999).
- Sobel, R. S., & Hall, J. C. The sources of economic growth. *Promot. Prosper. Mississippi*, 15 (2018).
- Reddy, K. R. *et al.* Simulating the impacts of climate change on cotton production in the Mississippi Delta. *Clim. Res.* **22**(3), 271–281 (2002).
- Anapalli, S. S. *et al.* Vulnerabilities and adapting irrigated and rainfed cotton to climate change in the Lower Mississippi Delta Region. *Climate* **4**(4), 55 (2016).
- Shammi, S. A. & Meng, Q. Modeling the Impact of Climate Changes on Crop Yield: Irrigated vs Non-Irrigated Zones in Mississippi. *Remote Sens* **13**(12), 2249 (2021).

37. Sun, W. *et al.* Evaluation of models for simulating soybean growth and climate sensitivity in the US Mississippi Delta. *Eur. J. Agron.* **140**, 126610 (2022).
38. Anapalli, S. S., Pinnamaneni, S. R., Fisher, D. K. & Reddy, K. N. Vulnerabilities of irrigated and rainfed maize to climate change in a humid climate in the lower Mississippi delta. *Clim. Change* **164**(1), 1–18 (2021).
39. Parajuli, P. B., Jayakody, P., Sassenrath, G. F. & Ouyang, Y. Assessing the impacts of climate change and tillage practices on stream flow, crop and sediment yields from the Mississippi River Basin. *Agric. Water Manag.* **168**, 112–124 (2016).
40. Chandio, A. A., Jiang, Y., Fatima, T., Ahmad, F., Ahmad, M., & Li, J. (2022). Assessing the impacts of climate change on cereal production in Bangladesh: evidence from ARDL modeling approach. *International Journal of Climate Change Strategies and Management*.
41. Ranghuwal, S. *et al.* Quantifying the energy use efficiency and greenhouse emissions in Punjab agriculture India. *Energy Nexus* **11**, 100238 (2023).
42. Singh, P., Arora, K., Kumar, S., Gohain, N. & Sharma, R. K. Indian millets trade potential-cum-performance: Economic perspective. *Indian J. Agric. Sci.* **93**(2), 200–204 (2023).
43. Burroughs, W., & Burroughs, W. S. (Eds.). *Climate: Into the 21st century*. Cambridge University Press (2003).
44. Jan, I., Ashfaq, M. & Chandio, A. A. Impacts of climate change on yield of cereal crops in northern climatic region of Pakistan. *Environ. Sci. Pollut. Res.* **28**(42), 60235–60245 (2021).
45. Daly, C. *et al.* Physiographically sensitive mapping of climatological temperature and precipitation across the conterminous United States. *Int. J. Climatol.: A J. Royal Meteorol. Soc.* **28**(15), 2031–2064 (2008).
46. Yun, S. D. & Gramig, B. M. Agro-climatic data by county: A spatially and temporally consistent US dataset for agricultural yields, weather and soils. *Data* **4**(2), 66 (2019).
47. Marshall, M. *et al.* Field-level crop yield estimation with PRISMA and Sentinel-2. *ISPRS J. Photogramm. Remote Sens* **187**, 191–210 (2022).
48. Duan, L., Petroski, R., Wood, L. & Caldeira, K. Stylized least-cost analysis of flexible nuclear power in deeply decarbonized electricity systems considering wind and solar resources worldwide. *Nat. Energy* **7**(3), 260–269 (2022).
49. Adams, R. M., Hurd, B. H., Lenhart, S. & Leary, N. Effects of global climate change on agriculture: An interpretative review. *Clim. Res.* **11**(1), 19–30 (1998).
50. Ahmed, M. *et al.* Impact of climate change on dryland agricultural systems: A review of current status, potentials, and further work need. *Int. J. Plant Prod.* **16**(3), 341–363 (2022).
51. West, J. S., Townsend, J. A., Stevens, M. & Fitt, B. D. Comparative biology of different plant pathogens to estimate effects of climate change on crop diseases in Europe. *Eur. J. Plant Pathol.* **133**, 315–331 (2012).
52. Brevik, E. C. The potential impact of climate change on soil properties and processes and corresponding influence on food security. *Agriculture* **3**(3), 398–417 (2013).
53. Schneider, L., Rebetz, M., & Rasmann, S. The effect of climate change on invasive crop pests across biomes. *Current Opinion Insect Sci.*, 100895 (2022).
54. Pesaran, M. H., Shin, Y. & Smith, R. J. Bounds testing approaches to the analysis of level relationships. *J. Appl. Econom.* **16**(3), 289–326 (2001).
55. Warsame, A. A., Sheik-Ali, I. A., Ali, A. O. & Sarkodie, S. A. Climate change and crop production nexus in Somalia: Empirical evidence from ARDL technique. *Environ. Sci. Pollut. Res.* **28**(16), 19838–19850 (2021).
56. Asfew, M., & Bedemo, A. (2022). Impact of climate change on cereal crops production in Ethiopia. *Adv. Agric.*, 2022.
57. Agbenyo, W., Jiang, Y., Ding, Z., Titriku, J. K. & Ntim-Amo, G. Impact of climate change on cocoa production in Africa: An approach of cross-sectional ARDL. *Int. J. Environ. Res.* **16**(5), 1–12 (2022).
58. Xiang, X. & Soleymani, S. Change in cereal production caused by climate change in Malaysia. *Ecolog. Inform.* **70**, 101741 (2022).
59. Nkoro, E. & Uko, A. K. Autoregressive Distributed Lag (ARDL) cointegration technique: application and interpretation. *J. Stat. Econom. Methods* **5**(4), 63–91 (2016).
60. Babbhulkar, P. S., Wandile, R. M., Badole, W. P. & Balpande, S. S. Residual effect of long-term application of FYM and fertilizers on soil properties (Vertisols) and yield of soybean. *J. Indian Soc. Soil Sci.* **48**(1), 89–92 (2000).
61. Sieling, K., Brase, T. & Svib, V. Residual effects of different N fertilizer treatments on growth, N uptake and yield of oilseed rape, wheat and barley. *European J. Agron.* **25**(1), 40–48 (2006).
62. Chandio, A. A. *et al.* Assessment of formal credit and climate change impact on agricultural production in Pakistan: A time series ARDL modeling approach. *Sustainability* **12**(13), 5241 (2020).
63. Waiswa, D. Climate change and production of cereal crops in East Africa: Role of temperature, Precipitation, *Ecol. Carbon Footprint* (2023).
64. Nakamura, A. & Nakamura, M. Model specification and endogeneity. *J. Econom.* **83**(1–2), 213–237 (1998).
65. Wang, F., Zhan, C. & Zou, L. Risk of crop yield reduction in China under 15°C and 2°C global warming from CMIP6 models. *Foods* **12**(2), 413 (2023).
66. Mann, H. B. Nonparametric tests against trend. *Econom. J. Econom. Soc.*, 245–259 (1945).
67. Kendall, M. G. Rank correlation methods; Griffin: London, UK, 1975. Google Scholar (1975).
68. Sen, P. K. Estimates of the regression coefficient based on Kendall's tau. *J. Am. Stat. Assoc.* **63**(324), 1379–1389 (1968).
69. WMO. World Meteorological Organization 2018 Guide to climatological practices, second edition (2018).
70. Portney, L. G. Correlation. *Foundations of Clinical Research* (2000).
71. Raina, K. D., Callaway, C., Rittenberger, J. C. & Holm, M. B. Neurological and functional status following cardiac arrest: Method and tool utility. *Resuscitation* **79**(2), 249–256 (2008).
72. Prematunga, R. K. Correlational analysis. *Aust. Crit. Care* **25**(3), 195–199 (2012).
73. Gocic, M. & Trajkovic, S. Analysis of changes in meteorological variables using Mann-Kendall and Sen's slope estimator statistical tests in Serbia. *Global Planet. Change* **100**, 172–182 (2013).
74. Gujree, I., Ahmad, I., Zhang, F. & Arshad, A. Innovative trend analysis of high-altitude climatology of Kashmir Valley North-West Himalayas. *Atmosphere* **13**(5), 764 (2022).
75. DeJong, D. N., Nankervis, J. C., Savin, N. E. & Whiteman, C. H. The power problems of unit root test in time series with autoregressive errors. *J. Econom.* **53**(1–3), 323–343 (1992).
76. Patterson, K. Unit root tests in time series volume 1: Key concepts and problems. Springer (2011).
77. Dickey, D. A. & Fuller, W. A. Distribution of the estimators for autoregressive time series with a unit root. *J. Am. Stat. Assoc.* **74**(366a), 427–431 (1979).
78. Phillips, P. C. & Perron, P. Testing for a unit root in time series regression. *Biometrika* **75**(2), 335–346 (1988).
79. Gujarati, D., & Porter, D. (2003). Multicollinearity: What happens if the regressors are correlated. *Basic Econometr.*, 363.
80. Daoud, J. I. (2017). Multicollinearity and regression analysis. In *Journal of Physics: Conference Series* (Vol. 949, No. 1, p. 012009). IOP Publishing.
81. Brown, R. L., Durbin, J. & Evans, J. M. Techniques for testing the constancy of regression relationships over time. *J. Royal Stat. Soc. Ser. B (Methodol.)* **37**(2), 149–163 (1975).
82. Eck, M. A., Murray, A. R., Ward, A. R. & Konrad, C. E. Influence of growing season temperature and precipitation anomalies on crop yield in the southeastern United States. *Agric. For. Meteorol.* **291**, 108053 (2020).

83. Rosenzweig, C. & Tubiello, F. N. Effects of changes in minimum and maximum temperature on wheat yields in the central USA simulation study. *Agric. For. Meteorol.* **80**(2–4), 215–230 (1996).
84. Peng, S. *et al.* Asymmetric effects of daytime and night-time warming on Northern Hemisphere vegetation. *Nature* **501**(7465), 88–92 (2013).
85. Screen, J. A. Arctic amplification decreases temperature variance in northern mid- to high-latitudes. *Nat. Clim. Change* **4**(7), 577–582 (2014).
86. Sharma, R. K., Kumar, S., Vatta, K., Dhillon, J. & Reddy, K. N. Impact of recent climate change on cotton and soybean yields in the southeastern United States. *J. Agric. Food Res.* **9**, 100348 (2022).
87. Sharma, R. K. *et al.* Impact of recent climate change on maize, rice, and wheat in southeastern USA. *Sci. Rep.* **12**(1), 1–14 (2022).
88. Braganza, K., Karoly, D. J., & Arblaster, J. M. (2004). Diurnal temperature range as an index of global climate change during the twentieth century. *Geophys. Res. Lett.*, 31(13).
89. Lobell, D. B. Changes in diurnal temperature range and national cereal yields. *Agric. For. Meteorol.* **145**(3–4), 229–238 (2007).
90. Sun, X. *et al.* Global diurnal temperature range (DTR) changes since 1901. *Clim. Dynam.* **52**(5), 3343–3356 (2019).
91. Rahman, M. M. Environmental degradation: The role of electricity consumption, economic growth and globalisation. *J. Environ. Manag.* **253**, 109742 (2020).
92. Wu, J. Z. *et al.* Impact of climate change on maize yield in China from 1979 to 2016. *J. Integr. Agric.* **20**(1), 289–299 (2021).
93. Ainsworth, E. A., Lemonnier, P. & Wedow, J. M. The influence of rising tropospheric carbon dioxide and ozone on plant productivity. *Plant Biol.* **22**, 5–11 (2020).
94. Raju, B. R. *et al.* Root traits and cellular level tolerance hold the key in maintaining higher spikelet fertility of rice under water limited conditions. *Funct. Plant Biol.* **41**(9), 930–939 (2014).
95. Chen, J. J., Zhen, S. & Sun, Y. Estimating leaf chlorophyll content of buffaloberry using normalized difference vegetation index sensors. *HortTechnology* **31**(3), 297–303 (2021).
96. Hu, Q. & Buyanovsky, G. Climate effects on maize yield in Missouri. *J. Appl. Meteorol. Climatol.* **42**(11), 1626–1635 (2003).
97. Lobell, D. B. & Asner, G. P. Climate and management contributions to recent trends in US agricultural yields. *Science* **299**(5609), 1032–1032 (2003).
98. Wilson, J. H., Clowes, M. S. J. & Allison, J. C. S. Growth and yield of maize at different altitudes in Rhodesia. *Ann. Appl. Biol.* **73**(1), 77–84 (1973).
99. Mourtzinis, S., Ortiz, B. V. & Damianidis, D. Climate change and ENSO effects on Southeastern US climate patterns and maize yield. *Sci. Rep.* **6**(1), 1–7 (2016).
100. Sanchez, B., Rasmussen, A. & Porter, J. R. Temperatures and the growth and development of maize and rice: a review. *Global Change Biol.* **20**(2), 408–417 (2014).
101. Hoffman, A. L., Kemanian, A. R. & Forest, C. E. The response of maize, sorghum, and soybean yield to growing-phase climate revealed with machine learning. *Environ. Res. Lett.* **15**(9), 094013 (2020).
102. Butler, E. E. & Huybers, P. Adaptation of US maize to temperature variations. *Nat. Clim. Change* **3**(1), 68–72 (2013).
103. Commuri, P. D. & Jones, R. J. High temperatures during endosperm cell division in maize: A genotypic comparison under in vitro and field conditions. *Crop Sci.* **41**(4), 1122–1130 (2001).
104. Begcy, K. *et al.* Male sterility in maize after transient heat stress during the tetrad stage of pollen development. *Plant Physiol.* **181**(2), 683–700 (2019).
105. Bheemanahalli, R., Vennam, R. R., Ramamoorthy, P. & Reddy, K. R. Effects of post-flowering heat and drought stresses on physiology, yield, and quality in maize (*Zea mays* L.). *Plant Stress* **6**, 100106 (2022).
106. Bheemanahalli, R. *et al.* Effects of drought and heat stresses during reproductive stage on pollen germination, yield, and leaf reflectance properties in maize (*Zea mays* L.). *Plant Direct* **6**(8), e434 (2022).
107. Alsajri, F. A. *et al.* Morpho-physiological, yield, and transgenerational seed germination responses of soybean to temperature. *Front. Plant Sci.* **13**, 839270 (2022).
108. Hatfield, J. L. & Prueger, J. H. Temperature extremes: Effect on plant growth and development. *Weather Clim. Extremes* **10**, 4–10 (2015).
109. Stooksbury, D. E. & Michaels, P. J. Climate change and large-area Maize Yield in the Southeastern United States. *Agron. J.* **86**(3), 564–569 (1994).
110. Chen, C. *et al.* Will higher minimum temperatures increase maize production in Northeast China? An analysis of historical data over 1965–2008. *Agric. Forest Meteorol.* **151**(12), 1580–1588 (2011).
111. Zhang, Q., Zhang, J., Guo, E., Yan, D. & Sun, Z. The impacts of long-term and year-to-year temperature change on corn yield in China. *Theor. Appl. Climatol.* **119**(1), 77–82 (2015).
112. Shu, T. (2021). Soybean Phenotypic Variation Under High Night Temperature Stress.
113. Song, J. *et al.* The positive effects of increased light intensity on growth and photosynthetic performance of tomato seedlings in relation to night temperature level. *Agronomy* **12**(2), 343 (2022).
114. Magrin, G. O., Travasso, M. I. & Rodríguez, G. R. Changes in climate and crop production during the 20th century in Argentina. *Clim. Change* **72**(1), 229–249 (2005).
115. Tao, F., Yokozawa, M., Liu, J. & Zhang, Z. Climate–crop yield relationships at provincial scales in China and the impacts of recent climate trends. *Clim. Res.* **38**(1), 83–94 (2008).
116. Liu, Z., Yang, X., Hubbard, K. G. & Lin, X. Maize potential yields and yield gaps in the changing climate of northeast China. *Global Change Biol.* **18**(11), 3441–3454 (2012).
117. Ruane, A. C. *et al.* Multi-factor impact analysis of agricultural production in Bangladesh with climate change. *Global Environ. Change* **23**(1), 338–350 (2013).
118. Petersen, L. K. Impact of climate change on twenty-first century crop yields in the US. *Climate* **7**(3), 40 (2019).
119. Ding, R. & Shi, W. Contributions of climate change to cereal yields in Tibet, 1993–2017. *J. Geograph. Sci.* **32**(1), 101–116 (2022).
120. Zahoor, Z., Shahzad, K., & Mustafa, A. U. (2022). Do climate changes influence the agriculture productivity in Pakistan? Empirical Evidence from ARDL Technique. *Forman J. Econ. Stud.*, 18(1).
121. Bekuma Abdisa, T., Mamo Diga, G. & Regassa Tolessa, A. Impact of climate variability on rain-fed maize and sorghum yield among smallholder farmers. *Cogent Food Agric.* **8**(1), 2057656 (2022).
122. Cabas, J., Weersink, A. & Olale, E. Crop yield response to economic, site and climatic variables. *Clim. Change* **101**(3), 599–616 (2010).
123. Gobin, A. Modelling climate impacts on crop yields in Belgium. *Clim. Res.* **44**(1), 55–68 (2010).
124. Guo, H. *et al.* Annual ecosystem respiration of maize was primarily driven by crop growth and soil water conditions. *Agric. Ecosyst. Environ.* **272**, 254–265 (2019).
125. Paul, M. J. & Foyer, C. H. Sink regulation of photosynthesis. *J. Exp. Bot.* **52**(360), 1383–1400 (2001).
126. Wan, S., Xia, J., Liu, W. & Niu, S. Photosynthetic overcompensation under nocturnal warming enhances grassland carbon sequestration. *Ecology* **90**(10), 2700–2710 (2009).
127. Badu-Apraku, A., Hunter, R. B. & Tollenaar, M. Effect of temperature during grain filling on whole plant and grain yield in maize (*Zea mays* L.). *Can. J. Plant Sci.* **63**(2), 357–363 (1983).
128. Cairns, J. E. *et al.* Adapting maize production to climate change in sub-Saharan Africa. *Food Secur.* **5**(3), 345–360 (2013).

129. Kettler, B. A. *et al.* High night temperature during maize post-flowering increases night respiration and reduces photosynthesis, growth and kernel number. *J. Agron. Crop Sci.* **208**(3), 335–347 (2022).
130. Wang, Y. *et al.* Reduction in seed set upon exposure to high night temperature during flowering in maize. *Physiologia Plantarum* **169**(1), 73–82 (2020).
131. Liu, M. *et al.* Dissecting heat tolerance and yield stability in maize from greenhouse and field experiments. *J. Agron. Crop Sci.* **208**(3), 348–361 (2022).
132. Suwa, R. *et al.* High temperature effects on photosynthate partitioning and sugar metabolism during ear expansion in maize (*Zea mays* L.) genotypes. *Plant Physiol. Biochem.* **48**(2–3), 124–130 (2010).
133. Wilhelm, E. P., Mullen, R. E., Keeling, P. L. & Singletary, G. W. Heat stress during grain filling in maize: Effects on kernel growth and metabolism. *Crop Sci.* **39**(6), 1733–1741 (1999).
134. Reilly, J. M. (Ed.). *Agriculture: The potential consequences of climate variability and change for the United States.* Cambridge University Press (2002).
135. Izaurralde, R. C., Rosenberg, N. J., Brown, R. A. & Thomson, A. M. Integrated assessment of Hadley Center (HadCM2) climate-change impacts on agricultural productivity and irrigation water supply in the conterminous United States: Part II. Regional agricultural production in 2030 and 2095. *Agric. For. Meteorol.* **117**(1–2), 97–122 (2003).
136. Reilly, J. *et al.* US agriculture and climate change: New results. *Clim. Change* **57**(1), 43–67 (2003).
137. Schlenker, W. & Roberts, M. J. Nonlinear temperature effects indicate severe damages to US crop yields under climate change. *Proc. Natl. Acad. Sci.* **106**(37), 15594–15598 (2009).
138. Lobell, D. B., Bänziger, M., Magorokosho, C. & Vivek, B. Nonlinear heat effects on African maize as evidenced by historical yield trials. *Nat. Clim. Change* **1**(1), 42–45 (2011).
139. Lobell, D. B. *et al.* The critical role of extreme heat for maize production in the United States. *Nat. Clim. Change* **3**(5), 497–501 (2013).
140. Ahsan, F., Chandio, A. A. & Fang, W. Climate change impacts on cereal crops production in Pakistan: Evidence from cointegration analysis. *Int. J. Clim. Change Strateg. Manag.* **12**(2), 257–269 (2020).
141. Mahrous, W. Dynamic impacts of climate change on cereal yield in Egypt: An ARDL model. *J. Econ. Financ. Res.* **5**(1), 886–908 (2018).
142. Islam, A. *et al.* Modeling the impacts of climate change on irrigated maize production in the central great plains. *Agric. Water Manag.* **110**, 94–108 (2012).
143. Lobell, D. B. & Gourdj, S. M. The influence of climate change on global crop productivity. *Plant Physiol.* **160**(4), 1686–1697 (2012).
144. Kimball, B. A. *et al.* Productivity and water use of wheat under free-air CO₂ enrichment. *Global Change Biol.* **1**, 429–442 (1995).
145. Tubiello, F. N. & Ewert, F. Simulating the effects of elevated CO₂ on crops: Approaches and applications for climate change. *Eur. J. Agron.* **18**, 57–74 (2002).
146. Ziska, L. H. Rising atmospheric carbon dioxide and plant biology: the overlooked paradigm. *DNA Cell Biol.* **27**(4), 165–172 (2008).
147. DaMatta, F. M., Grandis, A., Arenque, B. C. & Buckeridge, M. S. Impacts of climate changes on crop physiology and food quality. *Food Res. Int.* **43**(7), 1814–1823 (2010).
148. Hatfield, J. L. & Dold, C. Water-use efficiency: Advances and challenges in a changing climate. *Front. Plant Sci.* **10**, 103 (2019).
149. Urban, D. W., Sheffield, J. & Lobell, D. B. The impacts of future climate and carbon dioxide changes on the average and variability of US maize yields under two emission scenarios. *Environ. Res. Lett.* **10**(4), 045003 (2015).
150. Leakey, A. D. *et al.* Elevated CO₂ effects on plant carbon, nitrogen, and water relations: Six important lessons from FACE. *J. Exp. Bot.* **60**(10), 2859–2876 (2009).
151. Von Caemmerer, S. & Furbank, R. T. The C₄ pathway: An efficient CO₂ pump. *Photosynth. Res.* **77**, 191–207 (2003).
152. Bowes, G. Photosynthetic responses to changing atmospheric carbon dioxide concentration. *Photosynth. Environ.*, 387–407 (1996).
153. Wedin, D. A. C₄ grasses: Resource use, ecology, and global change. *Warm-season (C₄) Grasses*, 45, 15–50 (2004).
154. Kimball, B. A. Carbon dioxide and agricultural yield: An assemblage and analysis of 430 prior observations I. *Agron. J.* **75**(5), 779–788 (1983).
155. Ejemeyovwi, J., Obindah, G. & Doyah, T. Carbon dioxide emissions and crop production: Finding a sustainable balance. *Int. J. Energy Econ. Policy* **8**(4), 303 (2018).
156. Ahmed, M., & Ahmad, S. Carbon dioxide enrichment and crop productivity. *Agronomic Crops: Volume 2: Management Practices*, 31–46 (2019).
157. Rehman, A., Ma, H. & Ozturk, I. Decoupling the climatic and carbon dioxide emission influence to maize crop production in Pakistan. *Air Qual., Atmos. Health* **13**, 695–707 (2020).
158. Seneweera, S. P., Ghannoum, O. & Conroy, J. High vapour pressure deficit and low soil water availability enhance shoot growth responses of a C₄ grass (*Panicum coloratum* cv. Bambatsi) to CO₂ enrichment. *Funct. Plant Biol.* **25**(3), 287–292 (1998).
159. Ghannoum, O. & Conroy, J. P. Nitrogen deficiency precludes a growth response to CO₂ enrichment in C₃ and C₄ Panicum grasses. *Funct. Plant Biol.* **25**(5), 627–636 (1998).
160. Ghannoum, O., Caemmerer, S. V., Ziska, L. H. & Conroy, J. P. The growth response of C₄ plants to rising atmospheric CO₂ partial pressure: A reassessment. *Plant, Cell Environ.* **23**(9), 931–942 (2000).
161. Ziska, L. H., & Bunce, J. A. Plant responses to rising atmospheric carbon dioxide. *Plant Growth Clim. Change*, 17–47 (2006).
162. Rosenzweig, C., Tubiello, F. N., Goldberg, R., Mills, E. & Bloomfield, J. Increased crop damage in the US from excess precipitation under climate change. *Global Environ. Change* **12**(3), 197–202 (2002).
163. Chen, C., Baethgen, W. E. & Robertson, A. Contributions of individual variation in temperature, solar radiation and precipitation to crop yield in the North China Plain, 1961–2003. *Clim. Change* **116**(3), 767–788 (2013).
164. MPR. (<http://coolweather.net/staterainfall/mississippi.htm>) (2022).
165. Li, Y., Guan, K., Schnitkey, G. D., DeLucia, E. & Peng, B. Excessive rainfall leads to maize yield loss of a comparable magnitude to extreme drought in the United States. *Global Change Biol.* **25**(7), 2325–2337 (2019).
166. Wenkert, W., Fausey, N. R. & Watters, H. D. Flooding responses in *Zea mays* L. *Plant Soil* **62**(3), 351–366 (1981).
167. Parent, C., Capelli, N., Berger, A., Crèvecoeur, M. & Dat, J. F. An overview of plant responses to soil waterlogging. *Plant Stress* **2**(1), 20–27 (2008).
168. Jabloun, M., Schelde, K., Tao, F. & Olesen, J. E. Effect of temperature and precipitation on nitrate leaching from organic cereal cropping systems in Denmark. *Eur. J. Agron.* **62**, 55–64 (2015).
169. Evans, R. O. & Fausey, N. R. Effects of inadequate drainage on crop growth and yield. In *Agricultural drainage* Vol. Monograph 9 (eds Skaggs, R. W. & van Schilfhaar, J.) 13–54 (The American Society of Agronomy and Academic Press, 1999).
170. Ashraf, M. Interactive effects of nitrate and long-term waterlogging on growth, water relations, and gaseous exchange properties of maize (*Zea mays* L.). *Plant Sci.* **144**(1), 35–43 (1999).
171. Kozdrój, J. & van Elsas, J. D. Response of the bacterial community to root exudates in soil polluted with heavy metals assessed by molecular and cultural approaches. *Soil Biol. Biochem.* **32**(10), 1405–1417 (2000).
172. FEMA. Federal Emergency Management Agency. <https://www.fema.gov/emergency-managers/risk-management/risk-capability-assessment> (2021).

173. Herbold, J. New approaches to agricultural insurance in developing economies. In: D. Köhn (ed.), *Finance for food: Towards new agricultural and rural finance*, pp. 199–217. https://doi.org/10.1007/978-3-642-54034-9_9 (2014).
174. RHIS. Rain and Hail Insurance Service, Inc. historic database, <http://www.rainhail.com> 2023.
175. Lauer, J. Integrated pest and crop management. News and resources for Wisconsin agriculture from the university of Wisconsin-Madison <https://ipcm.wisc.edu/blog/2016/08/what-is-happening-in-the-corn-plant-during-the-month-of-august/> (2016).
176. Muhammad, S., Alkali, M., Abdullahi, U. & Haruna, S. Exploring the effect of climate variability on the outputs of some selected crop in Gombe, Nigeria: A bound test approach. *Int. J. Intellect. Discourse* 5(2), 141–157 (2022).

Acknowledgements

Authors acknowledge Dr. Yen-Heng Lin at Mississippi State University's Northern Gulf Institute for helping with the relative humidity data collection.

Author contributions

R.S.: Conceptualization; Data curation; Visualization; Writing – original draft, J.D.: Conceptualization; Funding acquisition; Supervision; Project administration; Writing – review & editing, P.K.: Formal analysis; Methodology; Writing – review & editing, RB: Writing – review & editing, X.L.: Writing – review & editing, M.C.: Writing – review & editing, and K.R.: Writing – review & editing.

Funding

This publication is a contribution of the Mississippi Agricultural and Forestry Experiment Station.

Competing interests

The authors declare no competing interests.

Additional information

Correspondence and requests for materials should be addressed to J.D.

Reprints and permissions information is available at www.nature.com/reprints.

Publisher's note Springer Nature remains neutral with regard to jurisdictional claims in published maps and institutional affiliations.



Open Access This article is licensed under a Creative Commons Attribution 4.0 International License, which permits use, sharing, adaptation, distribution and reproduction in any medium or format, as long as you give appropriate credit to the original author(s) and the source, provide a link to the Creative Commons licence, and indicate if changes were made. The images or other third party material in this article are included in the article's Creative Commons licence, unless indicated otherwise in a credit line to the material. If material is not included in the article's Creative Commons licence and your intended use is not permitted by statutory regulation or exceeds the permitted use, you will need to obtain permission directly from the copyright holder. To view a copy of this licence, visit <http://creativecommons.org/licenses/by/4.0/>.

© The Author(s) 2023



Applied Mathematics in Science and Engineering >

Volume 31, 2023 - Issue 1

Open access

442 | 2

Views | CrossRef citations to date | 1 | Altmetric



Research Article

Analysis and estimation of the COVID-19 pandemic by modified homotopy perturbation method

Garima Agarwal, Man Mohan Singh, D. L. Suthar & S. D. Purohit

Article: 2279170 | Received 24 May 2023, Accepted 28 Oct 2023, Published online: 27 Nov 2023

Cite this article <https://doi.org/10.1080/27690911.2023.2279170>



Full Article

Figures & data

References

Citations

Metrics

Licensing

Reprints & Permissions

View PDF

View EPUB



Formulae display: **MathJax**

The Bernoulli equation is useful to assess the motility and recovery rate with respect to time in order to measure the COVID-19 outbreak. The homotopy perturbation method was applied in the current article to compute the Bernoulli equation. For the existence and uniqueness of solutions, we also used the Caputo–Fabrizio Integral and differential operators. Additionally, we conducted a corresponding investigation for derivatives of integer and fractional orders on the estimated motility and recovery rate.

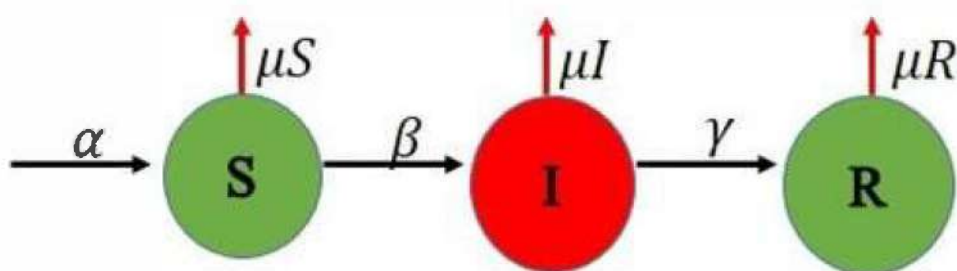
Q Keywords: SARS-CoV-2 homotopy decomposition method (HDM) ODE COVID-19 mathematical modelling

1. Introduction

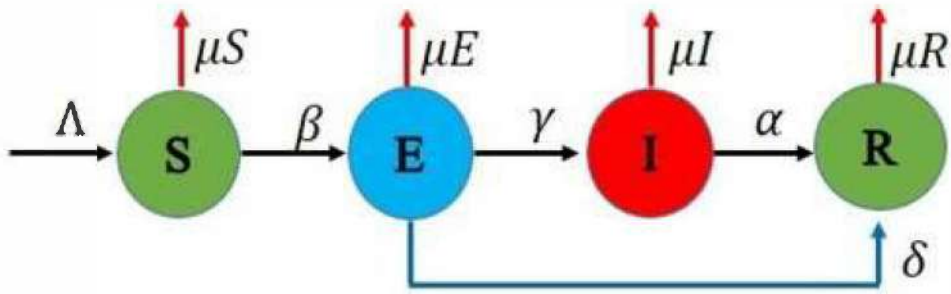
Globally, the coronavirus COVID-19 has spread. There are numerous mathematical models available for analysing the patterns and rough solutions to this epidemic. This virus originated in Wuhan, China, as is well known. The worldometer website, which is accessible online, states that the number of infected people in China is at an all-time high in the month of May. There are over 4 million instances of the coronavirus in the final week of May. Cherniha [1] proposed a Mathematical Model for the Corona.

The first model of this pandemic is known as the SIR (Susceptible-Infectious-Recovered) model which includes three ODE's is the most common model defined by Cooper [2] and the dynamic chart of the behaviour is given in Figure 1. After this model [3] gives the SEIR model for the outbreak of COVID-19 with the appropriate parameters as shown in Figure 2. In the continuation of getting the approximate solutions of the COVID-19 model, Pang [4] studied SEIQRD Model (Susceptible-Exposed-Infectious-Quarantine-Recovered-Death) with the more generalization of types of infected people as given in Figure 3. Similarly, Cherniha [1] proposed the SEAIRQF (Susceptible-Exposed-Asymptomatic-Infectious-Recovered-Quarantined-Fatality class) Model using the asymptomatic exposed behaviour given in Figure 4. Anirudh [5] described the outcome and the challenges of these models mentioned above using the study of corona behaviour.

Figure 1. The progression of the dynamic of SIR model.

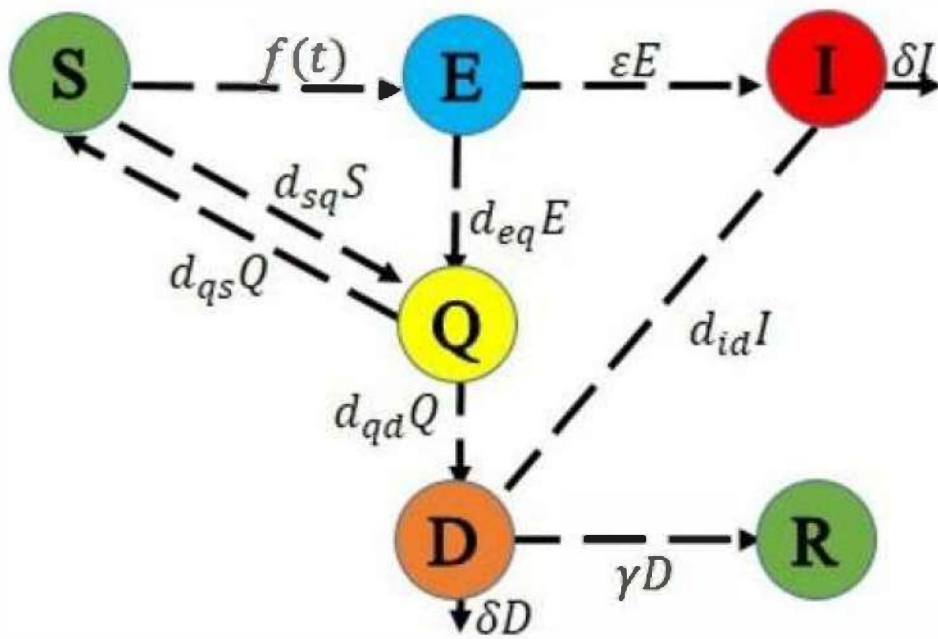


Display full size



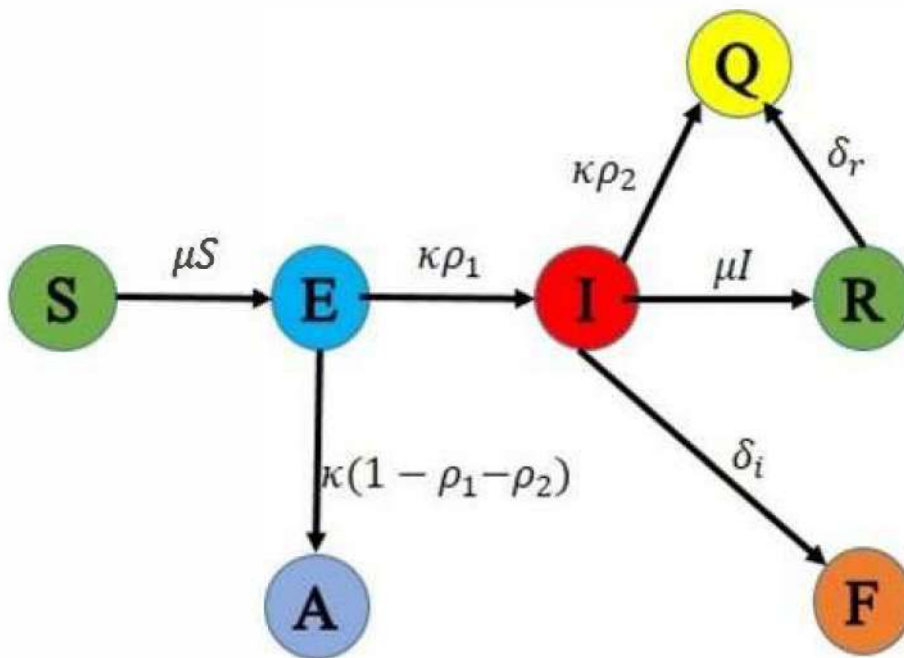
Display full size

Figure 3. The progression of the dynamic of SEIQDR model.



Display full size

Figure 4. The progression of the dynamic of SEAIQRF model.



Display full size

The flow chart of these mathematical models is given as:

In the year of 2020, Nisar [6,7] studied a Bats-hosts-reservoir People transmission fractional order COVID-19 model which was controlled and measured by the government.

Also, Thabet [8] proposed a mathematical model of COVID-19 under nonsingular derivative of fractional order.

For the prediction of this pandemic in different states of India, Jaspreet [9] also gave a preprint-based mathematical model of prediction of COVID-19. In May 2020, Ning [10] developed reliable epidemiological models to forecast the evolution of the virus and estimate the effectiveness of various intervention measures and their impacts on the economy. This was the first model based on the impact on economic conditions.

The numerical solution using Runge Kutta fourth-order method for this epidemic [11] gave a mathematical model with a nonstandard finite difference (NSFD) scheme and the wavelet based numerical scheme for fractional order SEIR epidemic is discussed by Kumar et al. [12].

Ali et al. [13] also introduced a mathematical model for the study of the HIV-1 virus.

In the same manner, Izhan [14] used a hybrid model and Ghosh et al. [15] studied the fractional model for population dynamics.

In the fractional order analysis with the comparison of this work in COVID, more study was also done [16–18].

The relationship of the mentioned model with the literature and comparison results are also reflected in the papers, in which Yavuz et al. studied about diabetes and hereditary and COVID-10 treatment rate [18–20].

Also in the cure of cancer, Altun [21] analysed Quantitative and numerical simulation. In the field of plant-pathogen herbivore interaction, Rahman [22] did a piecewise fractional analysis of the migration effect. In a similar manner, Joshi [17] analysed the stability of a non-singular fractional-order COVID-19 model with nonlinear incidence and treatment rate and Laxmi [16] studied on the vaccinal model for incorporating environmental transmission.

For the loss of immunity and quarantined class, Arif [23] gave models and numerical simulations and non-linear Burgers' equations via a semi-analytical technique [24].

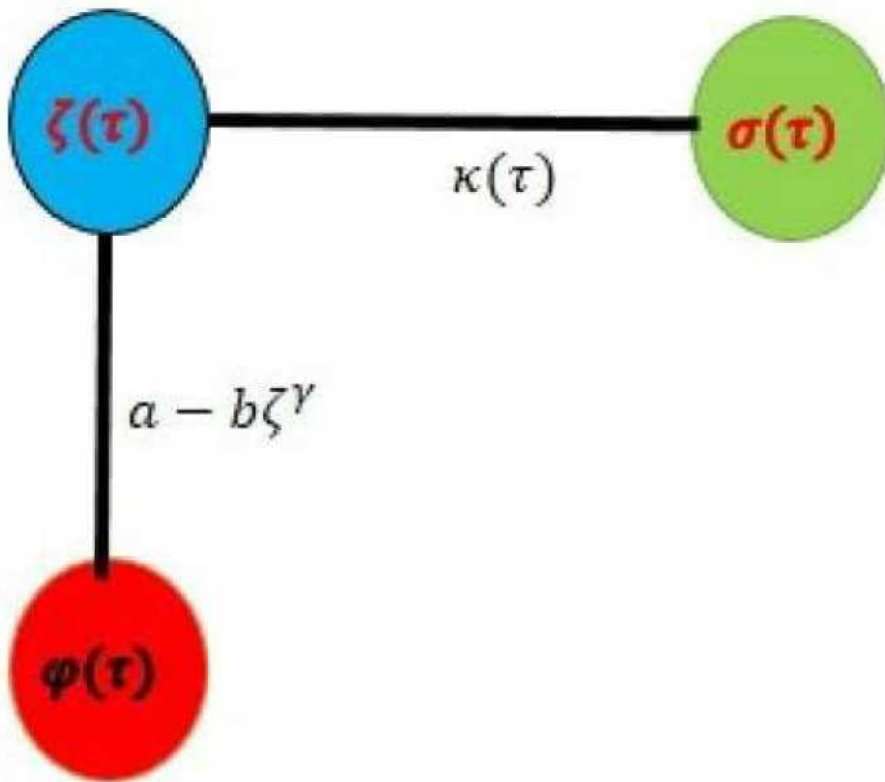
A Modified Homotopy Perturbation Transform Method (Fractional-Order Newell-Whitehead-Segel Equation) is also analysed by N. Iqbal, A.M. Albalahi, M.S. Abdo and W. Mohammed [25].

In this direction the studies are also relatable to the comparison of this method given by Zeb et al. [26], Evirgin et al. [27], Ozkose [28], Jha [29], Naik [18,30]

In this paper, we applied the first nontrivial biological model (Logistic model) given by Verhulst [31] in the proposition of COVID-19 mathematical model by two smooth function $\zeta(\tau)$ (total arised cases) and $\varphi(\tau)$ (total deaths) so that the study of behaviour of these graphs with the comparison of fractional order, Integer order and exact solution could be analysed.

The flow chart of this model is given in Figure 5.

Figure 5. Flow chart of total cases $\zeta(\tau)$ including total recovered $\sigma(\tau)$ and deaths



Display full size

2. Methodology

2.1. Homotopy decomposition method and modified homotopy perturbation method

It is the most practical technique to utilize recently in fractional calculus. This method of fractional derivatives provides numerous general instances of the fractional derivative model. Its use in the area of fractional calculus in applied mathematics is therefore more pertinent.

Atangana and Botha (2012) were the first to develop the Homotopy Decomposition Method (HDM) to solve partial differential equations, which are frequently encountered in problems involving heat diffusion, time fraction, groundwater flow, etc.

Since the modified Homotopy perturbation method is used in this paper along with Adomian polynomials, it is technically a modified Homotopy perturbation approach.

Baleanu et al. [32] also presented a fractional order model.

2.2. The mathematical model

In 1838, Verhulst [31] developed the first nontrivial biological model. This model is also known as the Logistic Model. The ODE of this model is given by

$$\frac{d\Psi}{d\tau} = \Psi(1 - \Psi), \quad \Psi(0) = \Psi_0. \quad (1)$$

It is the classical example of Mathematical Biology. The exact solution of this model is

$$\Psi(\tau) = \frac{\Psi_0 e^{\tau}}{1 + \Psi_0(e^{\tau} - 1)}. \quad (2)$$

Its curve is sigmoid (logistic) and useful for fractional value $\Psi_0 < 1/2$. In this paper, we used HDM to find the approximate solution for the total people and death people and compare to integer and fractional order solution with the general function $\zeta(\tau)$ that denotes the number of the Corona cases identifying to day τ (for some integer). The initial cases at $\tau = 0$ is $\zeta(0) = \zeta_0$. Now let the general equation of this model be

$$\frac{d\zeta}{d\tau} = \zeta(a - b\zeta^\gamma), \quad \zeta(0) = \zeta_0 > 0. \quad (3)$$

a and b are here positive constants and τ is the exponent which confirms the number of Corona cases that bounds in time τ .

Ayala, Gilpin and Ehrenfeld in Ref. [33] introduced nonlinearity of (3) for describing the competition between species, while the logistic equation here shows some common assumptions by Brauer [34]. There are two possibilities for the infected person during the epidemic first one is φ which shows the population of dead persons and the other one is σ which represents the population of recovered persons from the corona.

$\zeta = \varphi + \sigma$. (4) Now the φ which is directly proportional to total number ζ is

$$\frac{d\varphi}{d\tau} = k(\tau)\zeta, \quad \varphi(0) = \varphi_0 > 0. \quad (5)$$

Where $k(\tau)$ is the effectiveness coefficient of the system of health care in the process of epidemic and related to the expression

$k(\tau) = k_0 \exp(-s\tau)$, $s > 0$. All the parameters and defined functions are listed in Table 1:

Table 1. Table 1.



Display Table

The model (3)–(5) is used under essential simplifications of the epidemic process where it is assumed that $\zeta \gg \varphi$. Also, it is known that this pandemic is so severe that the rate

this epidemic not useful. For example, $v \cong 0.14u$ in Italy [35]. In that type of case, the above-mentioned mathematical model (3)–(5) would be more specified using the difference factor $(\zeta - \varphi)$ [since $\zeta \gg \varphi$] instead of a single function as follows

$$\frac{d\zeta}{d\tau} = (\zeta - \varphi) \left(a - b(\zeta - \varphi)^\gamma \right), \quad \zeta(0) = \zeta_0, \quad (6)$$

$$\frac{d\varphi}{d\tau} = k(\tau) (\zeta - \varphi), \quad \varphi(0) = \varphi_0. \quad (7) \text{ Now from (4) it is clear that } \sigma = (\zeta - \varphi), \text{ so}$$

$$\frac{d\sigma}{d\tau} = \frac{d\zeta}{d\tau} - \frac{d\varphi}{d\tau}, \quad (8) \text{ using (6) and (7) in (8), we get}$$

$$\frac{d\zeta}{d\tau} = \sigma (a - b\sigma^\gamma). \quad \zeta(0) = \zeta_0, \quad (9) \text{ And}$$

$$\frac{d\varphi}{d\tau} = k(\tau) \sigma, \quad \varphi(0) = \varphi_0. \quad (10) \text{ This equation (9) is called Bernoulli equation.}$$

These Equations (9) and (10) are time evolution equations of total cases and dead people. Now our aim is to compare these equations solutions by plotting the graphs between integer and fractional order.

For this first of all applying fractional order derivative [36] on (9) and (10)

$$D_t^\alpha [\zeta(\tau)] = \sigma(\tau) [a - b\sigma(\tau)^\gamma], \quad (11)$$

$$D_t^\beta [\varphi(\tau)] = k(\tau) \sigma(\tau). \quad (12) \text{ And the solutions are given by}$$

$$\zeta(\tau) = \zeta(0) + \frac{1}{\Gamma(\alpha)} \int_0^\tau (\tau - \theta)^{\alpha-1} \left[\sigma(\theta) [a - b\sigma(\theta)^\gamma] \right] d\theta, \quad (13)$$

$$\varphi(\tau) = \varphi(0) + \frac{1}{\Gamma(\beta)} \int_0^\tau (\tau - \theta)^{\beta-1} \left[k(\theta) \sigma(\theta) \right] d\theta. \quad (14) \text{ Here the sets of}$$

kernels are

$$k_1(\tau, \zeta) = \sigma(\tau) [a - b\sigma(\tau)^\gamma], \text{ and}$$

$$k_2(\tau, \varphi) = k(\tau) \sigma(\tau).$$

2.3. Existence and uniqueness of model solution

The Lipschitz conditions give the existence and uniqueness condition for mathematical models, which are studied by Moore et al. [37] for HIV/AIDS, which is given with a treatment compartment.

In this section, we studied the existence and uniqueness condition by applying Caputo–Fabrizio fractional operators in (11) and (12) on both sides, we get

$$\zeta(\tau) - \zeta(0) = {}^{CF}I_t^{\rho_1} [\sigma(\tau) a - b\sigma(\tau)^\gamma], \quad (15)$$

$\varphi(\tau) - \varphi(0) = {}^{CF}I_t^{\rho_2}[\kappa(\tau)\sigma(\tau)]$. (16) Where ${}^{CF}I_t^{\rho}$ is defined as the Caputo-fractional operator [38].

Then for simplicity, we define two kernels as follows:

$$k_1(\tau, \zeta) = \sigma(\tau) [a - b\sigma(\tau)^\gamma], \text{ and}$$

$k_2(\tau, \varphi) = k(\tau)\sigma(\tau)$. For proving the theorems, we will suppose that ζ and φ are nonnegative bounded functions, that means $\|\zeta(\tau)\| \leq \theta_1$, $\|\varphi(\tau)\| \leq \theta_2$. Where θ_1 and θ_2 are positive constants. Now represent

$\Gamma_1 = a - b\sigma(\tau)^\gamma$, $\Gamma_2 = \kappa(\tau)$. (17) Applying the definition of the Caputo-Fabrizio fractional integral in (11) and (12), we get

$$\begin{aligned} \zeta(\tau) - \zeta(0) &= \Omega(\rho_1)k_1(\tau, \zeta) + \omega(\rho_1) \int_0^\tau k_1(y, \zeta) dy, \\ \varphi(\tau) - \varphi(0) &= \Omega(\rho_2)k_2(\tau, \varphi) + \omega(\rho_2) \int_0^\tau k_2(y, \varphi) dy. \end{aligned} \quad (18) \text{ where the integral}$$

function is defined as:

$$\Omega(\rho) = \frac{2(1-\rho)}{(2-\rho)M(\rho)}, \text{ and}$$

$$\omega(\rho) = \frac{2\rho}{(2-\rho)M(\rho)}. \quad (19) \text{ in which } \rho \text{ is known as the order parameter.}$$

2.4. Theorem 1

If the following inequality holds

$0 \leq M = \max(\Gamma_1, \Gamma_2) < 1$. (20) Then the kernels k_1 , and k_2 satisfy Lipschitz conditions and are contraction mappings.

Proof: We consider the kernels k_1 . Let ζ and ζ_1 are any two functions, then we have $\|k_1(\tau, \zeta) - k_1(\tau, \zeta_1)\| = \|a[\sigma(\tau) - \sigma_1(\tau)] - b[\sigma(\tau)^\gamma - \sigma_1(\tau)^\gamma]\|$. (21) With the help of the norms of triangle inequality on the right side of the above equation, we get

$$\begin{aligned} \|k_1(\tau, \zeta) - k_1(\tau, \zeta_1)\| &\leq \|a[\sigma(\tau) - \sigma_1(\tau)]\| + \|b[\sigma(\tau)^\gamma - \sigma_1(\tau)^\gamma]\| \\ &\leq (a - b\sigma(\tau)^\gamma) \|\zeta(\tau) - \zeta_1(\tau)\| \\ &= \Gamma_1 \|\zeta(\tau) - \zeta_1(\tau)\|. \end{aligned} \quad (22)$$

Similarly, we can get

$\|k_2(\tau, \varphi) - k_2(\tau, \varphi_2)\| \leq \Gamma_2 \|\varphi(\tau) - \varphi_2(\tau)\|$. (23) where Γ_1 and Γ_2 are defined in (17). Therefore for k_1 and k_2 the Lipschitz conditions are satisfied. From (19) the variables are written in kernel terms as follows:

$$\begin{aligned}\zeta(\tau) &= \zeta(0) + \Omega(\rho_1)k_1(\tau, \zeta) + \omega(\rho_1) \int_0^\tau k_1(y, \zeta) dy, \\ \varphi(\tau) &= \varphi(0) + \Omega(\rho_2)k_2(\tau, \varphi) + \omega(\rho_2) \int_0^\tau k_2(y, \varphi) dy.\end{aligned}\quad (24) \text{ From these}$$

equations, the following recursive formulas be:

$$\begin{aligned}\zeta_n(\tau) &= \Omega(\rho_1)k_1(\tau, \zeta_{n-1}) + \omega(\rho_1) \int_0^\tau k_1(y, \zeta_{n-1}) dy, \\ \varphi_n(\tau) &= \Omega(\rho_2)k_2(\tau, \varphi_{n-1}) + \omega(\rho_2) \int_0^\tau k_2(y, \varphi_{n-1}) dy.\end{aligned}\quad (25) \text{ The initial conditions}$$

are as follows:

$\zeta_0(\tau) = \zeta(0), \quad \varphi_0(\tau) = \varphi(0)$. (26) In the recursive formulae, the differences between the successive terms are given as:

$$\begin{aligned}\phi_n(\tau) &= \zeta_n(\tau) - \zeta_{n-1}(\tau) = \Omega(\rho_1) \left[k_1(\tau, \zeta_{n-1}) - k_1(\tau, \zeta_{n-2}) \right] \\ &\quad + \omega(\rho_1) \int_0^\tau \left[k_1(y, \zeta_{n-1}) - k_1(y, \zeta_{n-2}) \right] dy,\end{aligned}\quad (27)$$

$$\begin{aligned}\psi_n(\tau) &= \varphi_n(\tau) - \varphi_{n-1}(\tau) = \Omega(\rho_2) \left[k_2(\tau, \varphi_{n-1}) - k_2(\tau, \varphi_{n-2}) \right] \\ &\quad + \omega(\rho_2) \int_0^\tau \left[k_2(y, \varphi_{n-1}) - k_2(y, \varphi_{n-2}) \right] dy.\end{aligned}\quad (28) \text{ It is noticeable that:}$$

$$\zeta_n(\tau) = \sum_{i=1}^n \phi_i(\tau), \quad \varphi_n(\tau) = \sum_{i=1}^n \psi_i(\tau). \quad (29)$$

Next, we arrange the recursive inequalities of the differences $\phi_n(\tau), \psi_n(\tau)$ as follows:

$$\begin{aligned}\|\phi_n(\tau)\| &= \|\zeta_n(\tau) - \zeta_{n-1}(\tau)\| \\ &= \left\| \Omega(\rho_1) \left(k_1(\tau, \zeta_{n-1}) - k_1(\tau, \zeta_{n-2}) \right) \right. \\ &\quad \left. + \omega(\rho_1) \int_0^\tau \left(k_1(y, \zeta_{n-1}) - k_1(y, \zeta_{n-2}) \right) dy \right\|.\end{aligned}\quad (30) \text{ solving the last equation, we}$$

get

$$\begin{aligned}\|\zeta_n(\tau) - \zeta_{n-1}(\tau)\| &\leq \Omega(\rho_1) \left\| k_1(\tau, \zeta_{n-1}) - k_1(\tau, \zeta_{n-2}) \right\| \\ &\quad + \omega(\rho_1) \int_0^\tau \left\| k_1(y, \zeta_{n-1}) - k_1(y, \zeta_{n-2}) \right\| dy.\end{aligned}\quad \text{Then, since the}$$

Lipschitz condition is satisfied by the kernel k_1 with Lipschitz constant Γ_1 , we have

$$\begin{aligned}\|\zeta_n(\tau) - \zeta_{n-1}(\tau)\| &\leq \Omega(\rho_1) \Gamma_1 \|\zeta_{n-1} - \zeta_{n-2}\| \\ &\quad + \omega(\rho_1) \Gamma_1 \int_0^\tau \|\zeta_{n-1} - \zeta_{n-2}\| dy.\end{aligned}\quad \text{Hence we get}$$

$\|\phi_n(\tau)\| \leq \Omega(\rho_1) \Gamma_1 \|\phi_{n-1}(\tau)\| + \omega(\rho_1) \Gamma_1 \int_0^\tau \|\phi_{n-1}(y)\| dy$, (31) similarly, the second result would be

$\|\psi_n(\tau)\| \leq \Omega(\rho_2) \Gamma_2 \|\psi_{n-1}(\tau)\| + \omega(\rho_2) \Gamma_2 \int_0^\tau \|\psi_{n-1}(y)\| dy$. (32) Hence the existence and similarly the uniqueness is governed by these equations.

2.5. Solution by modified homotopy perturbation method

Writing these variables in summation form and using the Homotopy Perturbation Method (HPM) [39] steps:

$$\sum_{n=0}^{\infty} p^n \zeta_n(\tau) = \zeta(0) + \frac{p}{\Gamma(\alpha)} \int_0^\tau (\tau - \theta)^{\alpha-1} \left[\sum_{n=0}^{\infty} p^n \sigma_n(\theta) \left[a - b \sum_{n=0}^{\infty} p^n \sigma_n(\theta)^\gamma \right] \right] d\theta, \quad (33)$$

$$\sum_{n=0}^{\infty} p^n \varphi_n(\tau) = \varphi(0) + \frac{p}{\Gamma(\beta)} \int_0^\tau (\tau - \theta)^{\beta-1} \left[k(\theta) \sum_{n=0}^{\infty} p^n \sigma_n(\theta) \right] d\theta. \quad (34) \text{ Where}$$

$0 < \alpha \leq 1, 0 < \beta \leq 1$. On computing the coefficient of the same powers of, we get the following integral equations

$$p^0: \zeta_0(\tau) = \zeta(0) = \zeta_0, \quad (35) \text{ Similarly,}$$

$$p^0: \varphi_0(\tau) = \varphi(0) = \varphi_0.$$

$$p^1: \zeta_1(\tau) = \frac{1}{\Gamma(\alpha)} \int_0^\tau (\tau - \theta)^{\alpha-1} \left[\sigma_0 \left(a - b \sigma_0^\gamma \right) \right] d\theta, \quad (36) \text{ And,}$$

$$p^1: \varphi_1(\tau) = \frac{1}{\Gamma(\beta)} \int_0^\tau (\tau - \theta)^{\beta-1} \left[k(\theta) \sigma_0 \right] d\theta.$$

$$p^2: \zeta_2(\tau) = \frac{1}{\Gamma(\alpha)} \int_0^\tau (\tau - \theta)^{\alpha-1} \left[\sigma_1(\theta) \left(a - b \sigma_1^\gamma(\theta) \right) \right] d\theta,$$

$$p^2: \varphi_2(\tau) = \frac{1}{\Gamma(\beta)} \int_0^\tau (\tau - \theta)^{\beta-1} \left[k(\theta) \sigma_1(\theta) \right] d\theta. \quad (37) \text{ Continuing this}$$

process up to n times, we get

$$p^n: \zeta_n(\tau) = \frac{1}{\Gamma(\alpha)} \int_0^\tau (\tau - \theta)^{\alpha-1} \left[\sigma_{n-1}(\theta) \left(a - b \sigma_{n-1}^\gamma(\theta) \right) \right] d\theta,$$

$$p^n: \varphi_n(\tau) = \frac{1}{\Gamma(\beta)} \int_0^\tau (\tau - \theta)^{\beta-1} \left[k(\theta) \sigma_{n-1}(\theta) \right] d\theta. \quad (38) \text{ Now since the}$$

Bernoulli equation gives the general form of the equation by taking the exponent of boundness $\gamma = 1$, so on solving the last set of equations

$$\zeta_1(\tau) = \frac{\alpha' \tau^\alpha}{\Gamma(\alpha + 1)}; \alpha' = \sigma_0 \left(a - b \sigma_0 \right), \quad (39)$$

$$\varphi_1(\tau) = \frac{\beta' \tau^\beta}{\Gamma(\beta + 1)}; \beta' = k \sigma_0. \quad (40) \text{ Similarly, in solving}$$

$\zeta(\tau) = \frac{1}{\Gamma(\alpha)} \int_0^\tau (\tau - \theta)^{\alpha-1} \left[\zeta(\theta) - m(\theta) \right] \left[a - b \left[\zeta(\theta) - m(\theta) \right] \right] d\theta$ after

$$\zeta_2(\tau) = (a - b) \left[\frac{\alpha' \tau^{2\alpha}}{\Gamma(2\alpha + 1)} - \frac{\beta' \tau^{\alpha + \beta}}{\Gamma(\alpha + \beta + 1)} \right]. \quad (41) \text{ and}$$

$$\varphi_2(\tau) = \frac{1}{\Gamma(\beta)} \int_0^\infty (\tau - \theta)^{\beta - 1} k \left[\zeta_1(\theta) - \varphi_1(\theta) \right] d\theta. \text{ after simplification}$$

$$\varphi_2(\tau) = k \left[\frac{\alpha' \tau^{\alpha + \beta}}{\Gamma(\alpha + \beta + 1)} - \frac{\beta' \tau^{2\beta}}{\Gamma(2\beta + 1)} \right]. \quad (42) \text{ Finally, the generalized series solution is given}$$

by

$$\zeta(\tau) = \zeta_0 + \zeta_1(\tau) + \zeta_2(\tau) + \dots \text{ and}$$

$$\varphi(\tau) = \varphi_0 + \varphi_1(\tau) + \varphi_2(\tau) + \dots \text{ Putting the above values, we get}$$

$$\zeta(\tau) = \zeta_0 + \frac{\alpha' \tau^\alpha}{\Gamma(\alpha + 1)} + (a - b) \left[\frac{\alpha' \tau^{2\alpha}}{\Gamma(2\alpha + 1)} - \frac{\beta' \tau^{\alpha + \beta}}{\Gamma(\alpha + \beta + 1)} \right] + \dots \quad (43) \text{ and}$$

$$\varphi(\tau) = \varphi_0 + \frac{\beta' \tau^\beta}{\Gamma(\beta + 1)} + k \left[\frac{\alpha' \tau^{\alpha + \beta}}{\Gamma(\alpha + \beta + 1)} - \frac{\beta' \tau^{2\beta}}{\Gamma(2\beta + 1)} \right] + \dots \quad (44)$$

2.6. Fractional order (0.5)

For this putting $\alpha = \beta = 1/2$ Also the required coefficient in the case of China Population [35] the following data are helpful

$$\zeta_0 = 571; \varphi_0 = 17; a = 28; b = 3.5 * 10^{-6}; k \approx k_0 = 0.0094; \quad \text{From these}$$

$$\sigma_0 = \zeta_0 - \varphi_0 = 571 - 17 = 554.$$

$$\alpha' = \sigma_0 [a - b\sigma_0] = 554 [0.28 - 554 (3.5 * 10^{-6})]. \text{ Hence } \alpha' = 154.04 \text{ and similarly}$$

$$\beta' = 5.2076 \text{ Using all these coefficients in (39) and (40), we get}$$

$$\zeta(\tau) = 571 + \frac{154.04}{\Gamma(3/2)} \tau^{1/2} + (0.2799) \left[\frac{154.04}{\Gamma(2)} \tau^{1/2} - \frac{5.2076}{\Gamma(2)} \tau^{1/2} \right] \tau^{1/2} + \dots \text{ Which in}$$

simplification gives

$$\zeta(\tau) = 571 + (173.86) \tau^{1/2} + (41.6581) \tau + \dots \quad (45) \text{ and}$$

$$\varphi(\tau) = 17 + \frac{5.2076}{\Gamma(3/2)} \tau^{1/2} + (0.0094) \left[\frac{154.04}{\Gamma(2)} - \frac{5.2076}{\Gamma(2)} \right] \tau + \dots \text{ which in simplification gives}$$

$$\varphi(\tau) = 17 + (5.8776) \tau^{1/2} + (1.3990) \tau + \dots \quad (46)$$

2.7. Fractional order (0.9)

For this putting $\alpha = \beta = 0.9$ and remaining all the same data and simplifying, we get

$$\zeta(\tau) = 571 + (154.03) \tau^{0.9} + (20.8176) \tau^{1.8} + \dots \quad (47)$$

$$\varphi(\tau) = 17 + (5.2075) \tau^{0.9} + (0.5978) \tau^{1.8} + \dots \quad (48)$$

2.8. Integer order (1)

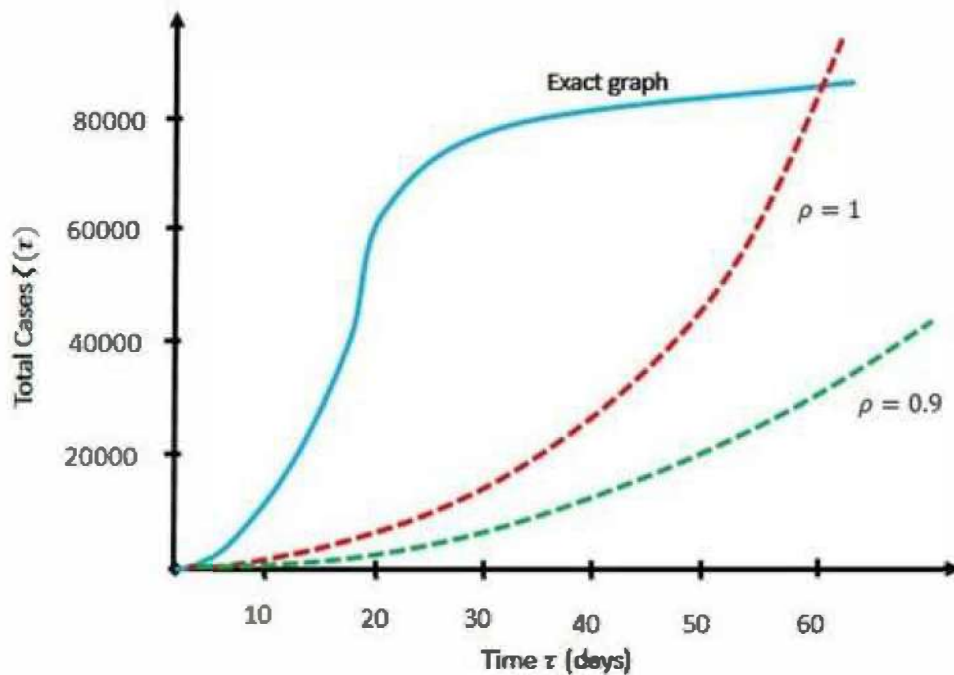
For this putting $\alpha = \beta = 1$ and remaining all the same data and simplifying, we get

$$\varphi(\tau) = 17 + (5.2076)\tau + (0.69951)\tau^2 + \dots \quad (50)$$

3. Conclusion

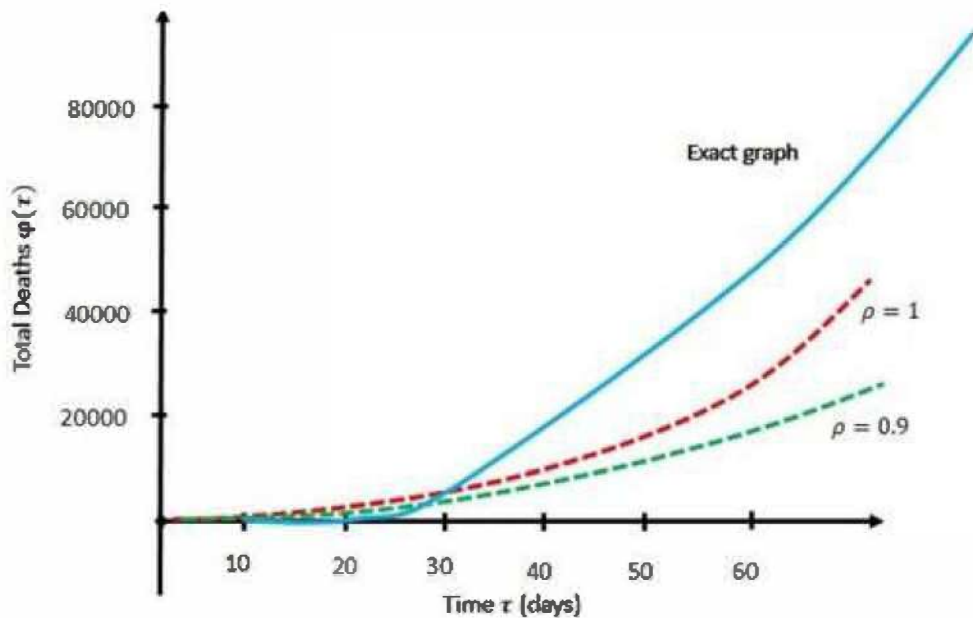
Figure 6 from the graphical study illustrates how the graph varies in integer order versus fractional order. In fractional order ($\rho = 0.9$), the total number of cases starts at 571 and rises to 2500 (about) after 60 days (here, x stands for time τ), which is more important and treatable than in integer order, where the cases rise to more than 80000 after 60 days. Figure 7 depicts how the graph's integer-order changes about fractional order. In fractional order ($\rho = 0.9$), the overall death toll starts at 17, and after 60 days (here, x stands for time τ), it rises to 70 (about). This is more significant and results in fewer deaths than in integer order ($\rho = 0.9$), where the cases rise to more than 3000 after 60 days. The data leads to the conclusion that fractional order performs better than integer order. This type of analysis will be more useful for the analysis and prediction of further improvements and future studies of such types of pandemics and diseases.

Figure 6. Graphs of $\zeta(\tau)$ fractional order (0.9) [green], integer order (1) [red], and exact solution [blue] with respect to time τ (x-axis).



Display full size

Figure 7. Graphs of $\rho(t)$ fractional order (0.9) [green], integer order (1) [red], and exact



Display full size

Disclosure statement

No potential conflict of interest was reported by the author(s).

References

1. Cherniha R, Davydovych V. A mathematical model for the COVID-19 outbreak. arXiv Vol. 2, 2020.
[Google Scholar](#)
2. Cooper I, Mondal A. A SIR model assumption for the spread of COVID-19 in different communities. NCBI. 2020;139:139–148.
[Google Scholar](#)
3. Efimov D, Ushirobira U. On interval prediction of COVID-19 development based on a SEIR epidemic model. Vol. 32, Lille, France: CRISTAL-University de; 2020.

4. Pang L, Yang W, Zhang D, et al. Epidemic analysis of COVID-19 in China by dynamical modeling. arXiv. Vol. 2002, 2020.
[Google Scholar](#)
5. Anirudh A. Mathematical modeling and the transmission dynamics in predicting the COVID-19-What next in combating the pandemic. Infect Dis Model. 2020;5:366–374.
[PubMed](#) | [Google Scholar](#)
6. Shaikh AS, Shaikh IN, Nisar KS. A mathematical model of COVID-19 using fractional derivative: outbreak in india with dynamics of transmission and control. preprints Not Peer-Reviewed. Vol. 1, 2020.
[Google Scholar](#)
7. Nisar KS, Kumar S, Kumar R. A new Robotnov fractional-ewponential function based fractional derivative for diffusion equation under external force. Math Methods Appl Sci. 2020;43:1–11.
[Web of Science ®](#) | [Google Scholar](#)
8. Shah K, Abdeljawed T, Mahariq I. Qualitative analysis of a mathematical model in the time of COVID-19. Hindawi BioMed Res Int. 2020;2020:145–149.
[Web of Science ®](#) | [Google Scholar](#)
9. Singh J, Ahluwalia PK, Kumar A. Spread of COVID-19 in india: a mathematical model based COVID-19 prediction in India and its different states. medRxiv. Vol. 10, 2020.
[Google Scholar](#)
10. Wang N., Fu Y., Zhang H., et al. An evaluation of mathematical models for the outbreak of COVID-19. Precis Clin Med. 2020;3(2):85–93. doi: 10.1093/pcmedi/pbaa016
[PubMed](#) | [Google Scholar](#)
11. Zeb A, Alzahrani E, Erturk VS, et al. Mathematical model for coronavirus disease 2019

12. Kumar S, Kumar R, Osman MS, et al. A wavelet based numerical scheme for fractional order SEIR epidemic of measles by using Genocchi polynomials. *Numer Methods Partial Differ Equ.* 2021;**37**(2):1250–1268. doi:10.1002/num.v37.2.

13. Ali KK, Osman MS. Analytical and numerical study of the HIV-1 infection of CD4+ T-cells conformable fractional mathematical model that causes acquired immunodeficiency syndrome with the effect of antiviral drug therapy. *Math Methods Appl Sci.* 2023;**46**(7):7654–7670. doi: 10.1002/mma.v46.7

14. Izhan M, Yusoff M. The use of system dynamics methodology in building a COVID-19 confirmed case model. *Com Math Med.* 2020:2020:321–337.

15. Ghosh S, Kumar S, Kumar R. A fractional model for population dynamics of two interacting species by using spectral and hermite wavelets methods. *Numer Methods Partial Differ Equ.* 2020;**37**(2):1652–1672.

16. Vijayalaxmi GM, Besi R. A fractional order vaccination model for COVID-19 incorporating environmental transmission. *Bull Math Biol.* 2022;**1**:78–110.

17. Joshi H, Yavuz M, Townley S, et al. Stability analysis of a non-singular fractional-order covid-19 model with nonlinear incidence and treatment rate. *Phys Scr.* 2023;**98**(4):045216. doi: 10.1088/1402-4896/acbe7a

18. Naik PA, Yavuz M, Qureshi S, et al. Modeling and analysis of COVID-19 epidemics with

2020;135(1):1–42. doi: 10.1140/epjp/s13360-019-00059-2

[Google Scholar](#)

19. Yavuz M, Cosar FO, Usta F. A novel modeling and analysis of fractional-order COVID-19 pandemic having a vaccination strategy. In: AIP Conference Proceedings, Vol. 2483, AIP Publishing LLC; 2022.

[Google Scholar](#)

20. Yavuz M, Hader W. A new mathematical modelling and parameter estimation of COVID-19: a case study in Iraq. AIMS Bioeng. 2022;9(4):420–446. doi: 10.3934/bioeng.2022030

[Web of Science ®](#) | [Google Scholar](#)

21. Ucar E, Ozdemir N, Altun E. Qualitative analysis and numerical simulations of new model describing cancer. J Comput Appl Math. 2023;422:114899. doi: 10.1016/j.cam.2022.114899

[Web of Science ®](#) | [Google Scholar](#)

22. Rahman M, Arfan M, Baleanu D. Piecewise fractional analysis of the migration effect in plant-pathogen-herbivore interactions. Bull Math Biol. 2023;1:1–23.

[Google Scholar](#)

23. Arif F, Majeed Z, Rahman JU, et al. Mathematical modeling and numerical simulation for the outbreak of COVID-19 involving loss of immunity and quarantined class. Math Stat Aspects Health Sci. 2022;2022:89–94.

[Google Scholar](#)

24. Iqbal N, Chughtai MT, Ullah R. Fractional study of the non-linear Burgers' equations via a semi-analytical technique. Fractal Fract. 2023;7(2):103. doi: 10.3390/fractalfract7020103

[Web of Science ®](#) | [Google Scholar](#)

25. Iqbal N, Albalahi AM, Abdo MS, et al. Analytical analysis of fractional-order Newell-Whitehead-Segel equation: a modified homotopy perturbation transform method. *Adv Nonlinear Anal Appl.* 2022;2022:1–10.
[Google Scholar](#)
26. Naim M, Sabbar Y, Zeb A. Stability characterization of a fractional-order viral system with the non-cytolytic immune assumption. *Math Model Numer Simul Appl.* 2022;2:164–176.
[Google Scholar](#)
27. Evirgin F, Ucar E, Ucar S, et al. Modelling influenza a disease dynamic under Caputo-Fabrizio fractional derivative with distinct contact rates. *Math Model Numer Simul Appl.* 2023;3:58–73.
[Google Scholar](#)
28. Ozkose F, Yavuz M. Investigation of interactions between COVID-19 and diabetes with hereditary traits using real data: a case study in Turkey. *Comput Biol Med.* 2022;141:105044. doi: 10.1016/j.compbimed.2021.105044
[PubMed](#) | [Web of Science ®](#) | [Google Scholar](#)
29. Joshi H, yavuz M, Jha BK. Modelling and analysis of fractional-order vaccination model for control of COVID-19 outbreak using real data. *Math Biosci Eng.* 2023;20(1):213–240. doi: 10.3934/mbe.2023010
[PubMed](#) | [Web of Science ®](#) | [Google Scholar](#)
30. Kumar S., Ghosh S., Samet B., et al. An analysis for heat equations arises in diffusion process using new Yang–Abdel–Aty–Cattani fractional operator. *Math Methods Appl Sci.* 2020;43(9):6062–6080. doi: 10.1002/mma.v43.9.
[Web of Science ®](#) | [Google Scholar](#)
31. Verhulst P. nitice sur la loi que la population suit dans son accroissement. *Corr Math Phys.* 1838;10:113–129.

32. Baleanu D, Mohammadi H, Rezapour S. A fractional differential equation model for the COVID-19 transmission by using the Caputo-Fabrizio derivative. *Adv Differ Equ.* 2020;299:552–561.
[Google Scholar](#)
33. Ayala FJ, Gilpin ME, Ehrenfeld JG. Competition between species: theoretical models and experimental tests. *Theor Pop Biol.* 1973;4(3):331–356. doi: 10.1016/0040-5809(73)90014-2
[PubMed](#) | [Web of Science®](#) | [Google Scholar](#)
34. Brauer F, Castillo Chavez C. *Mathematical models in populations biology and epidemiology.* Vol. 6, New York (NY): Springer; 2012.
[Google Scholar](#)
35. <https://www.worldometers.info/coronavirus/> (accessed on 1 May 2020).
[Google Scholar](#)
36. Matlob MA, Jamali Y. The concepts and applications of fractional order differential calculus in modeling of viscoelastic systems: a primer. *arxiv.org.* Vol. 6, 2017.
[Google Scholar](#)
37. Moore EJ, Sirisubtawee S. A Caputo-Fabrizio fractional differential equation model for HIV/AIDS with treatment compartment. Vol. 9. Cham: Springer; 2019. doi: 10.1186/s13662-019-2138-9.
[Google Scholar](#)
38. Nosheen A, Tariq M, Khan KA. On Caputo fractional derivatives and Caputo-Fabrizio integral operators via (s,m) -convex functions. *MDPI.* 2023;7(2):187.
[Google Scholar](#)
39. Srivastava HM, Dubey RS, Jain M. A study of the fractional-order mathematical model of diabetes and its resulting complications. Vol. 26, London: Wiley publication; 2019.

doi: 10.1002/mma.5681.

Google Scholar

Download PDF

Related research

People also read

Recommended articles

Cited by
2

[Homotopy decomposition method to analysis fractional hepatitis B virus infection model](#) >

M. M. Gour et al.

Applied Mathematics in Science and Engineering

Published online: 24 Sep 2023



[Mathematical modelling with computational fractional order for the unfolding dynamics of the communicable diseases](#) >

Mati ur Rahman et al.

Applied Mathematics in Science and Engineering

Published online: 16 Jan 2024



[Predicting COVID-19 outbreak in India using modified SIRD model](#) >

Sakshi Shringi et al.

Applied Mathematics in Science and Engineering

Published online: 2 Feb 2024



[View more](#)

Information for

Authors

R&D professionals

Editors

Librarians

Societies

Opportunities

Reprints and e-prints

Advertising solutions

Accelerated publication

Corporate access solutions

Open access

Overview

Open journals

Open Select

Dove Medical Press

F1000Research

Help and information

Help and contact

Newsroom

All journals

Books

Keep up to date

Register to receive personalised research and resources
by email



Sign me up



Copyright © 2024 **Informa UK Limited** [Privacy policy](#) [Cookies](#) [Terms & conditions](#) [Accessibility](#)

Registered in England & Wales No. 3099067
5 Howick Place | London | SW1P 1WG

Rotary International President
Rtn Jennifer Jones

District Governor
Rtn Dr Balwant Singh Chirana

President
PHF Rtn Radhey Shyam Gupta
D-13, Indra Puri Colony, Lal Kothi,
Jaipur, Rajasthan 302015 (India)
Mobile: +91-9414779184
eMail: rsgupta9414@gmail.com

Secretary
PHF Rtn Meeta Mathur
G-2, Janpath, Shyam Nagar,
Jaipur Rajasthan 302019 (India)
Mobile: +91-9982659532
eMail: alokmeeta@yahoo.com

Treasurer
Rtn Brajesh Kumar Gupta
D-28, Indra Puri Colony, Lal Kothi,
Jaipur, Rajasthan 302015 (India)
Mobile: +91-9829072271
eMail: brajeshgupta24@gmail.com

Club Patron
Maj Donor Rtn Dr Sudhir Kumar Calla

President Elect (2024-25)
PHF Rtn CFP Shalini

Immediate Past President
MPHF Rtn Er Narendra Mal Mathur

Vice Presidents
MPHF Rtn Adv Ashok Goyal
PHF Rtn Desh Deepak Goyal

Jt. Secretary
Rtn Er Nand Kishore Maheshwari

Director – Club Administration
PHF Rtn Rajendra Tiwari

Director – Service Projects
Rtn Er Sudesh Roop Rai

Director – Environment Service
Rtn Shyam Sunder Gupta

Director – Foundation
MPHF Rtn Vipin Bahl

Director – Literacy & T.E.A.C.H.
PHF Rtn Dr Arun Kumar Arya

Director – Membership
PHF Rtn Jwala Prasad Sharma

Director – Public Image & Fellowship
PHF Rtn Chander Mohan Mahajan

Director – Publications
PHF Rtn Basant Jain

Director – Youth Service
Rtn Prof Anil Dutt Vyas

Executive Secretary - I.T.
PHF Rtn Prof Raj Kishor Pareek

Club Trainer
MPHF Rtn Ravi Shanker Sharma

Sergeant at Arms
PHF Rtn Er Satish Goyal

Date: 31 Oct 23

TO WHOMSOEVER IS CONCERN

Rotaract Club, Directorate of Students' Welfare along with Rotary Club Jaipur, Bapu Nagar conducted a Awareness on Environmental Protection at Dehmi Kalan Village by planting the 15 plants in village on 31st Oct 2023. It was a physical activity involving the students from NSS, DSW and the Rotaract Club MUJ. Event was well coordinated by the Department of Business Administration

We would like to appreciate Rotaract Club, Directorate of Students' Welfare, Manipal University Jaipur for the efforts and express our gratitude towards them.

Regards



Rtn Meeta Mathur
Secretary

Rotary International President
Rtn Jennifer Jones

President
PHF Rtn **Radhey Shyam Gupta**
D-13, Indra Puri Colony, Lal Kothi,
Jaipur, Rajasthan 302015 (India)
Mobile: +91-9414779184
eMail: rsgupta9414@gmail.com

Secretary
PHF Rtn **Meeta Mathur**
G-2, Janpath, Shyam Nagar,
Jaipur Rajasthan 302019 (India)
Mobile: +91-9982659532
eMail: alokmeeta@yahoo.com

Treasurer
Rtn **Brajesh Kumar Gupta**
D-28, Indra Puri Colony, Lal Kothi,
Jaipur, Rajasthan 302015 (India)
Mobile: +91-9829072271
eMail: brajeshkgupta24@gmail.com

Club Patron
Maj Donor Rtn Dr **Sudhir Kumar Calla**

President Elect (2024-25)
PHF Rtn CFP **Shalini**

Immediate Past President
MPHF Rtn Er **Narendra Mal Mathur**

Vice Presidents
MPHF Rtn Adv **Ashok Goyal**
PHF Rtn **Desh Deepak Goyal**

Jt. Secretary
Rtn Er **Nand Kishore Maheshwari**

Director – Club Administration
PHF Rtn **Rajendra Tiwari**

Director – Service Projects
Rtn Er **Sudesh Roop Rai**

Director – Environment Service
Rtn **Shyam Sunder Gupta**

Director – Foundation
MPHF Rtn **Vipan Bahl**

Director – Literacy & T.E.A.C.H.
PHF Rtn Dr **Arun Kumar Arya**

Director – Membership
PHF Rtn **Jwala Prasad Sharma**

Director – Public Image & Fellowship
PHF Rtn **Chander Mohan Mahajan**

Director – Publications
PHF Rtn **Basant Jain**

Director – Youth Service
Rtn Prof **Anil Dutt Vyas**

Executive Secretary - I.T.
PHF Rtn Prof **Raj Kishor Pareek**

Club Trainer
MPHF Rtn **Ravi Shanker Sharma**

Sergeant at Arms
PHF Rtn Er **Satish Goyal**

Date: 03/10/23

TO WHOMSOEVER IS CONCERN

Rotaract Club, Directorate of Students' Welfare along with Rotary Club Jaipur, Bapu Nagar conducted a Plantation Drive at Mahatma Gandhi Government School (English Medium), Begas on 3rd October 2023. It was a physical activity involving the students from NSS, DSW and the Rotaract Club MUJ.

We would like to appreciate Rotaract Club, Directorate of Students' Welfare, Manipal University Jaipur for the efforts and express our gratitude towards them.

Regards



Rtn Meeta Mathur
Secretary



Rotary International President
Rtn Jennifer Jones

District Governor
Rtn Dr Balwant Singh Chirana

President
PHF Rtn Radhey Shyam Gupta
D-13, Indra Puri Colony, Lal Kothi,
Jaipur, Rajasthan 302015 (India)
Mobile: +91-9414779184
eMail: rsgupta9414@gmail.com

Secretary
PHF Rtn Meeta Mathur
G-2, Janpath, Shyam Nagar,
Jaipur Rajasthan 302019 (India)
Mobile: +91-9982659532
eMail: alokmeeta@yahoo.com

Treasurer
Rtn Brajesh Kumar Gupta
D-28, Indra Puri Colony, Lal Kothi,
Jaipur, Rajasthan 302015 (India)
Mobile: +91-9829072271
eMail: brajeshgupta24@gmail.com

Club Patron
Maj Donor Rtn Dr Sudhir Kumar Calla

President Elect (2024-25)
PHF Rtn CFP Shalini

Immediate Past President
MPHF Rtn Er Narendra Mal Mathur

Vice Presidents
MPHF Rtn Adv Ashok Goyal
PHF Rtn Desh Deepak Goyal

Jt. Secretary
Rtn Er Nand Kishore Maheshwari

Director – Club Administration
PHF Rtn Rajendra Tiwari

Director – Service Projects
Rtn Er Sudesh Roop Rai

Director – Environment Service
Rtn Shyam Sunder Gupta

Director – Foundation
MPHF Rtn Vipin Bahl

Director – Literacy & T.E.A.C.H.
PHF Rtn Dr Arun Kumar Arya

Director – Membership
PHF Rtn Jwala Prasad Sharma

Director – Public Image & Fellowship
PHF Rtn Chander Mohan Mahajan

Director – Publications
PHF Rtn Basant Jain

Director – Youth Service
Rtn Prof Anil Dutt Vyas

Executive Secretary - I.T.
PHF Rtn Prof Raj Kishor Pareek

Club Trainer
MPHF Rtn Ravi Shanker Sharma

Sergeant at Arms
PHF Rtn Er Satish Goyal

Date: 26 Oct 23

TO WHOMSOEVER IS CONCERN

Dept of Chemistry and Rotaract Club, Directorate of Students' Welfare along with Rotary Club Jaipur, Bapu Nagar conducted Plantation Drive at Dadar ki Dhani Village. Event was well coordinated by the Department of Chemistry and DSW.

We would like to appreciate Rotaract Club, Directorate of Students' Welfare, Manipal University Jaipur for the efforts and express our gratitude towards them.

Regards

Rtn Meeta Mathur
Secretary

Rotary International President
Rtn Jennifer Jones

District Governor
Rtn Dr Balwant Singh Chirana

President
PHF Rtn Radhey Shyam Gupta
D-13, Indra Puri Colony, Lal Kothi,
Jaipur, Rajasthan 302015 (India)
Mobile: +91-9414779184
eMail: rsgupta9414@gmail.com

Secretary
PHF Rtn Meeta Mathur
G-2, Janpath, Shyam Nagar,
Jaipur Rajasthan 302019 (India)
Mobile: +91-9982659532
eMail: alokmeeta@yahoo.com

Treasurer
Rtn Brajesh Kumar Gupta
D-28, Indra Puri Colony, Lal Kothi,
Jaipur, Rajasthan 302015 (India)
Mobile: +91-9829072271
eMail: brajeshkgupta24@gmail.com

Club Patron
Maj Donor Rtn Dr Sudhir Kumar Calla

President Elect (2024-25)
PHF Rtn CFP Shalini

Immediate Past President
MPHF Rtn Er Narendra Mal Mathur

Vice Presidents
MPHF Rtn Adv Ashok Goyal
PHF Rtn Desh Deepak Goyal

Jt. Secretary
Rtn Er Nand Kishore Maheshwari

Director – Club Administration
PHF Rtn Rajendra Tiwari

Director – Service Projects
Rtn Er Sudesh Roop Rai

Director – Environment Service
Rtn Shyam Sunder Gupta

Director – Foundation
MPHF Rtn Vipin Bahl

Director – Literacy & T.E.A.C.H.
PHF Rtn Dr Arun Kumar Arya

Director – Membership
PHF Rtn Jwala Prasad Sharma

Director – Public Image & Fellowship
PHF Rtn Chander Mohan Mahajan

Director – Publications
PHF Rtn Basant Jain

Director – Youth Service
Rtn Prof Anil Dutt Vyas

Executive Secretary - I.T.
PHF Rtn Prof Raj Kishor Pareek

Club Trainer
MPHF Rtn Ravi Shanker Sharma

Sergeant at Arms
PHF Rtn Er Satish Goyal

Date: 06/09/23

TO WHOMSOEVER IS CONCERN

Rotaract Club, Directorate of Students' Welfare along with Rotary Club Jaipur, Bapu Nagar conducted a Plantation Drive at Mahatma Gandhi Government School (English Medium), Begas on 6th September 2023. It was a physical activity involving the students from NSS, DSW and the Rotaract Club MUJ. Event was well coordinated, where more than 30 samplings of plants were planted in the schools.

We would like to appreciate Rotaract Club, Directorate of Students' Welfare, Manipal University Jaipur for the efforts and express our gratitude towards them.

Regards



Rtn Meeta Mathur
Secretary

Rotary International President
Rtn Jennifer Jones

District Governor
Rtn Dr Balwant Singh Chirana

President
PHF Rtn Radhey Shyam Gupta
D-13, Indra Puri Colony, Lal Kothi,
Jaipur, Rajasthan 302015 (India)
Mobile: +91-9414779184
eMail: rsgupta9414@gmail.com

Secretary
PHF Rtn Meeta Mathur
G-2, Janpath, Shyam Nagar,
Jaipur Rajasthan 302019 (India)
Mobile: +91-9982659532
eMail: alokmeeta@yahoo.com

Treasurer
Rtn Brajesh Kumar Gupta
D-28, Indra Puri Colony, Lal Kothi,
Jaipur, Rajasthan 302015 (India)
Mobile: +91-9829072271
eMail: brajeshgupta24@gmail.com

Club Patron
Maj Donor Rtn Dr Sudhir Kumar Calla

President Elect (2024-25)
PHF Rtn CFP Shalini

Immediate Past President
MPHF Rtn Er Narendra Mal Mathur

Vice Presidents
MPHF Rtn Adv Ashok Goyal
PHF Rtn Desh Deepak Goyal

Jt. Secretary
Rtn Er Nand Kishore Maheshwari

Director – Club Administration
PHF Rtn Rajendra Tiwari

Director – Service Projects
Rtn Er Sudesh Roop Rai

Director – Environment Service
Rtn Shyam Sunder Gupta

Director – Foundation
MPHF Rtn Vipin Bahl

Director – Literacy & T.E.A.C.H.
PHF Rtn Dr Arun Kumar Arya

Director – Membership
PHF Rtn Jwala Prasad Sharma

Director – Public Image & Fellowship
PHF Rtn Chander Mohan Mahajan

Director – Publications
PHF Rtn Basant Jain

Director – Youth Service
Rtn Prof Anil Dutt Vyas

Executive Secretary - I.T.
PHF Rtn Prof Raj Kishor Pareek

Club Trainer
MPHF Rtn Ravi Shanker Sharma

Sergeant at Arms
PHF Rtn Er Satish Goyal

Date: 25 Oct 23

TO WHOMSOEVER IS CONCERN

Rotaract Club, Directorate of Students' Welfare along with Rotary Club Jaipur, Bapu Nagar conducted campaign on Swachh Bharat Abhiyan on October 25 2023 at Dehmi Kalan. An awareness session is taken by Team MUJ physically involving the students from NSS, DSW and the Rotaract Club MUJ. Event was well coordinated by the Department of Business Administration.

We would like to appreciate Rotaract Club, Directorate of Students' Welfare, Manipal University Jaipur for the efforts and express our gratitude towards them.

Regards



Rtn Meeta Mathur
Secretary

Rotary International President
Rtn Jennifer Jones

District Governor
Rtn Dr Balwant Singh Chirana

President
PHF Rtn Radhey Shyam Gupta
D-13, Indra Puri Colony, Lal Kothi,
Jaipur, Rajasthan 302015 (India)
Mobile: +91-9414779184
eMail: rsgupta9414@gmail.com

Secretary
PHF Rtn Meeta Mathur
G-2, Janpath, Shyam Nagar,
Jaipur Rajasthan 302019 (India)
Mobile: +91-9982659532
eMail: alokmeeta@yahoo.com

Treasurer
Rtn Brajesh Kumar Gupta
D-28, Indra Puri Colony, Lal Kothi,
Jaipur, Rajasthan 302015 (India)
Mobile: +91-9829072271
eMail: brajeshkgupta24@gmail.com

Club Patron
Maj Donor Rtn Dr Sudhir Kumar Calla

President Elect (2024-25)
PHF Rtn CFP Shalini

Immediate Past President
MPHF Rtn Er Narendra Mal Mathur

Vice Presidents
MPHF Rtn Adv Ashok Goyal
PHF Rtn Desh Deepak Goyal

Jt. Secretary
Rtn Er Nand Kishore Maheshwari

Director – Club Administration
PHF Rtn Rajendra Tiwari

Director – Service Projects
Rtn Er Sudesh Roop Rai

Director – Environment Service
Rtn Shyam Sunder Gupta

Director – Foundation
MPHF Rtn Vipin Bahl

Director – Literacy & T.E.A.C.H.
PHF Rtn Dr Arun Kumar Arya

Director – Membership
PHF Rtn Jwala Prasad Sharma

Director – Public Image & Fellowship
PHF Rtn Chander Mohan Mahajan

Director – Publications
PHF Rtn Basant Jain

Director – Youth Service
Rtn Prof Anil Dutt Vyas

Executive Secretary - I.T.
PHF Rtn Prof Raj Kishor Pareek

Club Trainer
MPHF Rtn Ravi Shanker Sharma

Sergeant at Arms
PHF Rtn Er Satish Goyal

Date: 24/08/23

TO WHOMSOEVER IS CONCERN

Rotaract Club, Directorate of Students' Welfare along with Rotary Club Jaipur, Bapu Nagar conducted a Plantation Drive at Mahatma Gandhi Government School (English Medium), Dehmi Kalan on 24th August 2023. It was a physical activity involving the students from NSS, DSW and the Rotaract Club MUJ.

We would like to appreciate Rotaract Club, Directorate of Students' Welfare, Manipal University Jaipur for the efforts and express our gratitude towards them.

Regards



Rtn Meeta Mathur
Secretary




**MANIPAL UNIVERSITY
JAIPUR**

FACULTY OF DESIGN

**International Conference on Sustainable Development for
Heritage and Built Environment**

22/06/2023 – 23/06/2023


Head, Department of Interior Design
SD&A, Faculty of Design
Manipal University Jaipur



Content of Report

1. Introduction of the Event
2. Objective of the Event
3. Beneficiaries of the Event
4. Brief Description of the event
5. Photographs
6. Poster of an Event
7. Schedule of the Event
8. Attendance of the Event



1. Introduction of the Event

The conference is inspired from the critical challenge of human, environmental, heritage and built sustainability concerning the present and future generations in a global-scale context. This theme emphasizes the strong foundation that is provided by using research to inform our everyday practices, policies, and analytical approaches. This interdisciplinary forum is for scholars, teachers, and practitioners from the built environment professional discipline who share an interest in—and concern for— sustainability in an holistic perspective, where environmental, cultural, economic and social concerns intersect. It will provide a platform for various individuals to connect the past and present and develop solutions to a more universal and environmentally friendly approach towards built environment.

The conference will include topics such as

- (i) Sustainable approach to design in built environment,
- (ii) Sustainability & built Heritage,
- (iii) Conserving Built Heritage,
- (iv) Sustainable Policies for Environmental and Infrastructure Planning,
- (v) Earth and Environmental Planning & Design

2. Objective of the Event

This conference was a gathering of minds dedicated to addressing the pressing challenges of sustainability that affect our world today and tomorrow. It recognized that sustainability is a multifaceted concept that requires interdisciplinary collaboration and rigorous research. By bringing together scholars, educators, and practitioners, the conference facilitated the exchange of ideas and the development of solutions that promote a more sustainable, resilient, and environmentally friendly built environment.

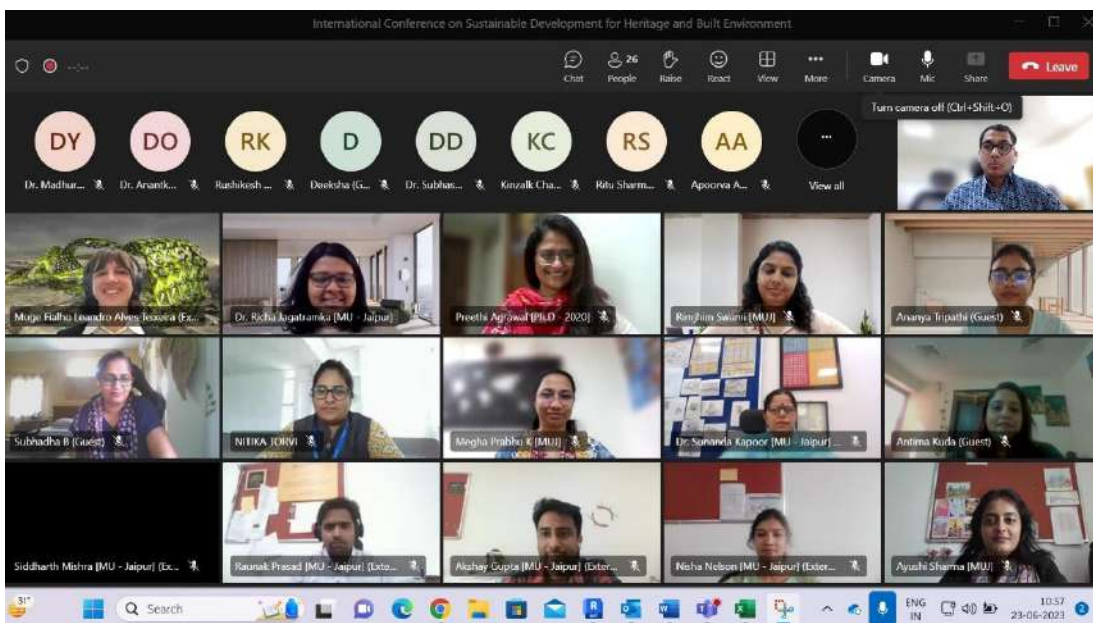
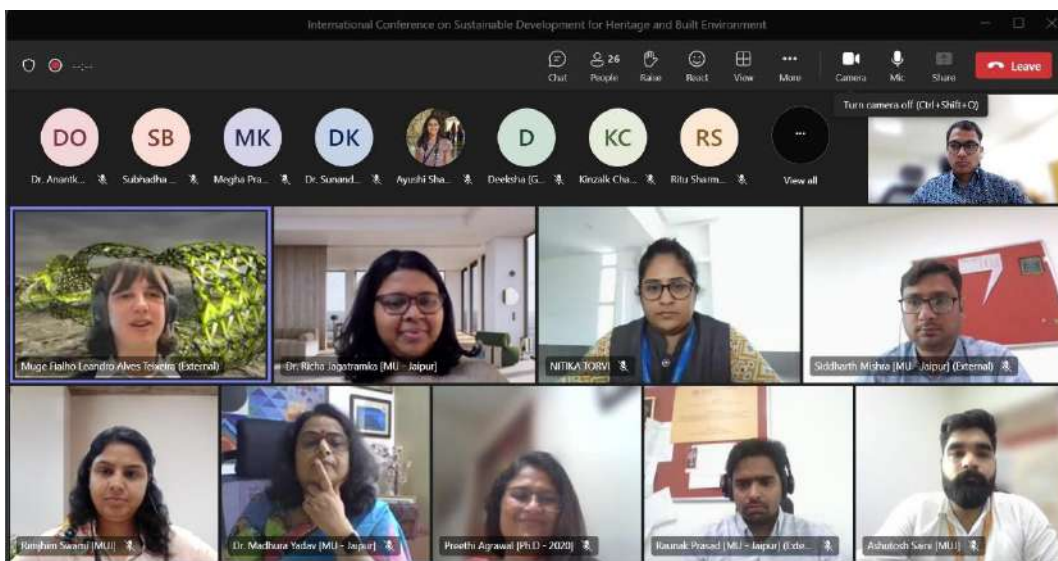
3. Beneficiary of the event

This interdisciplinary forum is for scholars, teachers, and practitioners from the built environment professional discipline who share an interest in—and concern for— sustainability in an holistic perspective, where environmental, cultural, economic and social concerns intersect.

4. Brief Description of the event

The conference was hosted by Department of Interior Design and School of Architecture and Design, Faculty of Design at Manipal University Jaipur. This interactive and engaging event is tailored exclusively for our researchers, as part of our commitment to foster continuous learning, future research opportunities. The presentations focused on sustainability as the prime agenda and paved way for the researchers to present their work at an international level.

5. Photographs of the Event



Snippets of the Conference

6. Poster of the event



**MANIPAL UNIVERSITY
JAIPUR**
(University under Section 2(i) of the UGC Act)

School of Architecture and
Design and Department of
Interior Design

International Conference
on
**“Sustainable
Development for
Heritage and Built
Environment”**

22nd June – 23rd June 2023

Venue:
Manipal University Jaipur/ Hybrid
Mode

About the University
The Manipal Education Group, with its heritage of excellence in higher education for over 60 years, launched Manipal University Jaipur (MUJ) in 2011. MUJ is affiliated by University Grants Commission, Association of Indian Universities, Council of Architecture, Bar Council of India and All India Council of Technical Education. MUJ is the first university in the state of Rajasthan, accredited as A+ (3.28) grade by NAAC. The university offers courses in different disciplines like Architecture, Interior Design, Fashion Design, Applied arts, Engineering, Management, Hospitality, Humanities & Social Sciences, Journalism and Mass communication, Basic Sciences, Law, Business & Commerce.

Organizing Committee
Patron:
Dr. G. K. Prabhu (President, MUJ)
Co - Patrons
Dr. Thammaiah Chekkera (Pro-President, MUJ)
Dr. Nitu Bhatnagar (Registrar, MUJ)
Chairs:
Dr. Madhura Yadav (Dean, FoD, MUJ)
Dr. J.P. Sampath Kumar (Director, SD&A, MUJ)
Convenors:
Dr. Richa Jagatramka (Assist. Prof., ID-SD&A)
Ar. Raunak Prasad (Assist. Prof., SA&D)
Coordinators:
Ar. Megha Prabhu (Assist. Prof., ID-SD&A)
Ar. Himangshu Kedia (Assist. Prof., ID-SD&A)
Ar. Akshay Gupta (Assist. Prof., SA&D)
Ar. Ashutosh Saini (Assist. Prof., SA&D)

About the Conference
The conference will include topics such as

- (i) Sustainable approach to design in built environment,
- (ii) Sustainability & built Heritage,
- (iii) Conserving Built Heritage,
- (iv) Sustainable Policies for Environmental and Infrastructure Planning,
- (v) Earth and Environmental Planning & Design.

Participants will gain exposure and insight To various sustainable approaches to sustain the heritage as well as define the built environment. It will provide a platform for various individuals to connect the past and present and develop solutions to a more universal and environmentally friendly approach towards built environment.

Submission Deadline:
Call for Papers – 23rd Feb 2023
Abstract Submission – 30th March 2023
Acceptance Notification – 7th April 2023
Full paper Submission – 23rd April 2023

Publication –
Conference proceedings with IOP
Conference Series: Earth and Environmental Science (SCOPUS Indexed)

Notable Speakers

1. Dr. Ranjith Dayaranthe , Associate Professor, Asian School of Architecture, Australia
2. Dr. Muge Belek Fialho Teixeira, Queensland University of Technology.
3. Dr. Shikha Jain, Director, DRONAH
4. Dr. Rajat Gupta, Oxford Brookes, Director, Dept. of sustainable development
5. Ar. Chitra Vishwanath, Biome Bangalore.

Conference Fees :
Students 9500 INR
Academicians & professional 10500 INR

For International Participants
Students - 150 USD
Academicians & professional – 180 USD

For additional information contact –
richa.jagatramka@jaipur.manipal.edu
raunak.prasad@jaipur.manipal.edu

7. Schedule of the event

Time	Event	Speaker
11:00 – 11:30 AM	Opening speech	Dr Richa Jagatramka
11: 30 – 11:35 AM	Welcome address	Dr Madhura Yadav
11: 35 – 11:45 AM	Introduction of international speaker	Ar Himangshu Kedia
11: 45 AM – 12:45 PM	Presentation by Dr Muge	Dr Muge
12: 45 – 01:00 PM	Q & A session	
01:00 – 01:05PM	Vote of Thanks	Ar. Himangshu Kedia



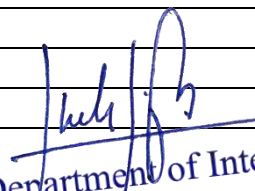
Meeting Link :

https://teams.microsoft.com/l/meetup-join/19%3ameeting_MmRjNjZiN2ltMTc1NS00YmJlTkwMTltMzBiYTVjNTIOYTRh%40thread.v2/0?context=%7b%22Tid%22%3a%227d0726e8-bf4b-4ac1-99f1-010fb11f1d3f%22%2c%22Oid%22%3a%2216be8839-914f-456c-9836-e6b3ba8fa2f9%22%7d

8. Attendance of the Event

Total attendees – 28 participants from MUJ and outside

Sl.no	Name	Organisation
1	Dr. Richa Jagatramka	FOD
2	Megha Prabhu K	FOD
3	Dr. Sampath Kumar Padmanabha Jinka	FOD
4	Dr. Madhura Yadav	FOD
5	Dr. Anantkumar Dada Ozarkar	FOD
6	Dr. Subhash Chandra Devrath	FOD
7	Nisha Nelson	FOD
8	Preethi Agrawal	Practicing Architect and PhD scholar
9	NITIKA TORVI	Christ University
10	Subhadha B	Christ University
11	Himangshu Kedia	FOD
12	Rushikesh Kolte	MNIT
13	Dr. Sunanda Kapoor	FOD
14	Ananya Tripathi	AKTU - GCA
15	Kinzalk Chauhan	FOD
16	Ritu Sharma	FOS – Phd Scholar
17	Rimjhim Swami	FOD
18	Ayushi Sharma	FOD
19	Apoorva Agarwal	FOD
20	Muge Fialho Leandro Alves Teixeira	QUT Australia
21	Deeksha	MNIT
22	Siddharth Mishra	FOD
23	Akshay Gupta	FOD
24	Ritu Sharma	FOD
25	Neha Saxena	FOD
26	Antima Kuda	MAHE Dubai
27	Raunak Prasad	FOD
28	Ashutosh Saini	FOD


Head, Department of Interior Design
SD&A, Faculty of Design
Manipal University Jaipur



Applied Mathematics in Science and Engineering >

Volume 31, 2023 - Issue 1

Open access

442 | 2

Views | CrossRef citations to date | 1 | Altmetric



Research Article

Analysis and estimation of the COVID-19 pandemic by modified homotopy perturbation method

Garima Agarwal, Man Mohan Singh, D. L. Suthar & S. D. Purohit

Article: 2279170 | Received 24 May 2023, Accepted 28 Oct 2023, Published online: 27 Nov 2023

Cite this article <https://doi.org/10.1080/27690911.2023.2279170>



Full Article

Figures & data

References

Citations

Metrics

Licensing

Reprints & Permissions

View PDF

View EPUB



Formulae display: **MathJax**

The Bernoulli equation is useful to assess the motility and recovery rate with respect to time in order to measure the COVID-19 outbreak. The homotopy perturbation method was applied in the current article to compute the Bernoulli equation. For the existence and uniqueness of solutions, we also used the Caputo–Fabrizio Integral and differential operators. Additionally, we conducted a corresponding investigation for derivatives of integer and fractional orders on the estimated motility and recovery rate.

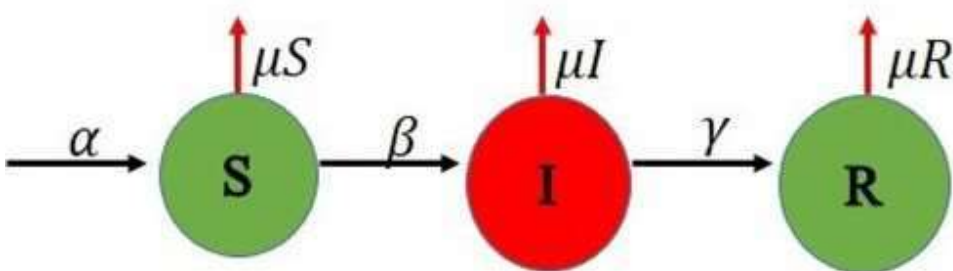
Q Keywords: SARS-CoV-2 homotopy decomposition method (HDM) ODE COVID-19 mathematical modelling

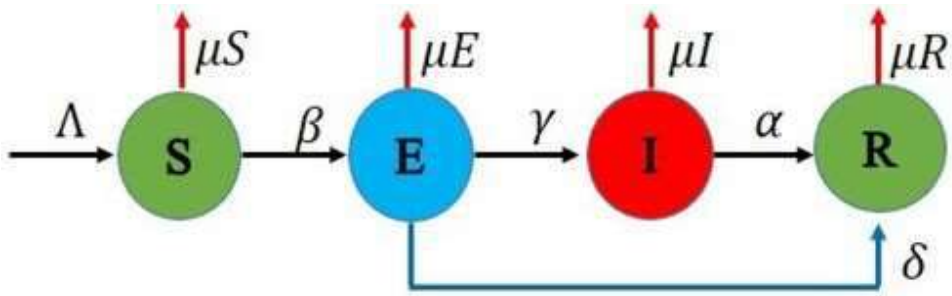
1. Introduction

Globally, the coronavirus COVID-19 has spread. There are numerous mathematical models available for analysing the patterns and rough solutions to this epidemic. This virus originated in Wuhan, China, as is well known. The worldometer website, which is accessible online, states that the number of infected people in China is at an all-time high in the month of May. There are over 4 million instances of the coronavirus in the final week of May. Cherniha [1] proposed a Mathematical Model for the Corona.

The first model of this pandemic is known as the SIR (Susceptible-Infectious-Recovered) model which includes three ODE's is the most common model defined by Cooper [2] and the dynamic chart of the behaviour is given in Figure 1. After this model [3] gives the SEIR model for the outbreak of COVID-19 with the appropriate parameters as shown in Figure 2. In the continuation of getting the approximate solutions of the COVID-19 model, Pang [4] studied SEIQRD Model (Susceptible-Exposed-Infectious-Quarantine-Recovered-Death) with the more generalization of types of infected people as given in Figure 3. Similarly, Cherniha [1] proposed the SEAIRQF (Susceptible-Exposed-Asymptomatic-Infectious-Recovered-Quarantined-Fatality class) Model using the asymptomatic exposed behaviour given in Figure 4. Anirudh [5] described the outcome and the challenges of these models mentioned above using the study of corona behaviour.

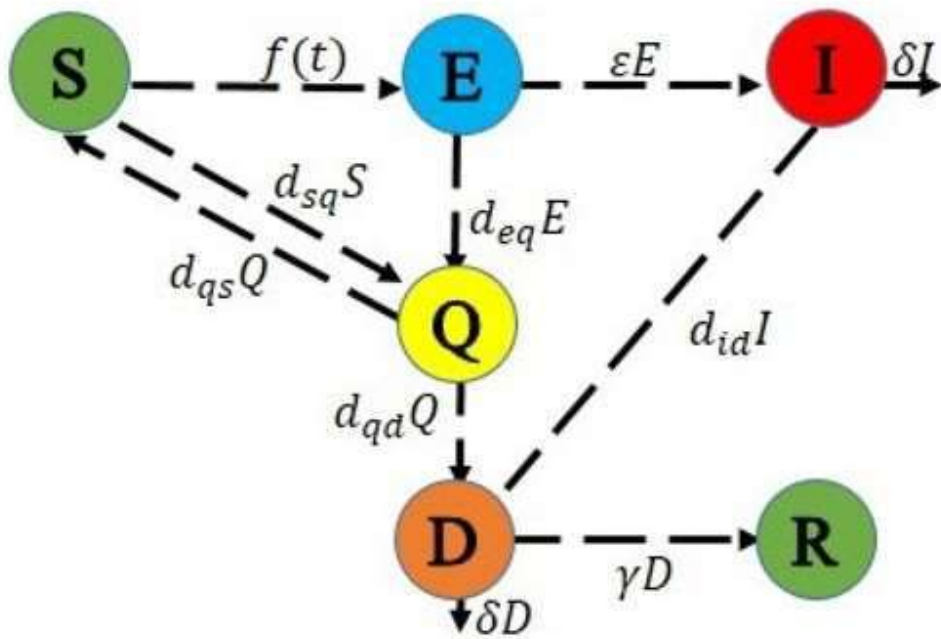
Figure 1. The progression of the dynamic of SIR model.





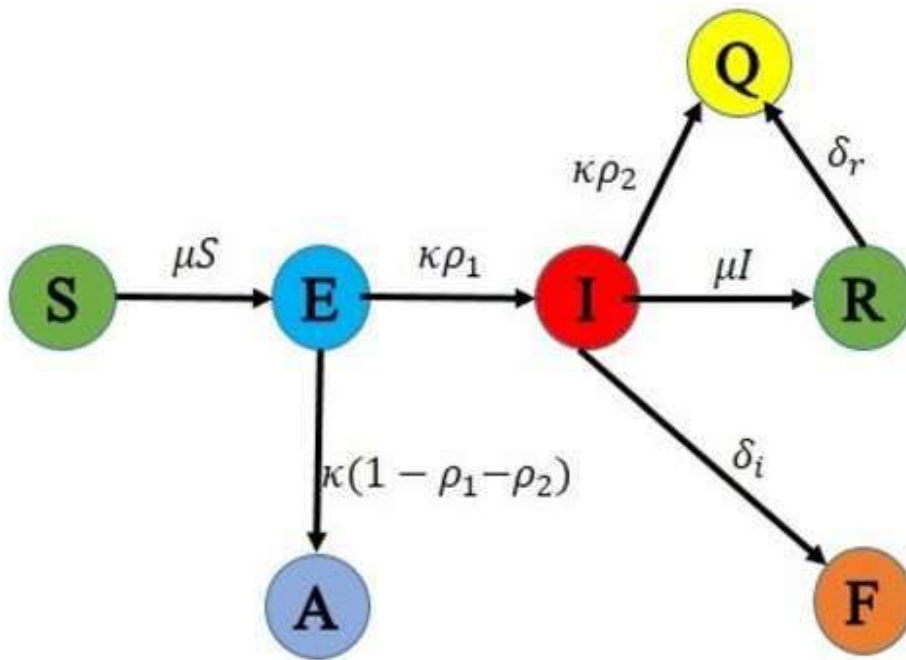
Display full size

Figure 3. The progression of the dynamic of SEIQDR model.



Display full size

Figure 4. The progression of the dynamic of SEAIQRF model.



Display full size

The flow chart of these mathematical models is given as:

In the year of 2020, Nisar [6,7] studied a Bats-hosts-reservoir People transmission fractional order COVID-19 model which was controlled and measured by the government.

Also, Thabet [8] proposed a mathematical model of COVID-19 under nonsingular derivative of fractional order.

For the prediction of this pandemic in different states of India, Jaspreet [9] also gave a preprint-based mathematical model of prediction of COVID-19. In May 2020, Ning [10] developed reliable epidemiological models to forecast the evolution of the virus and estimate the effectiveness of various intervention measures and their impacts on the economy. This was the first model based on the impact on economic conditions.

The numerical solution using Runge Kutta fourth-order method for this epidemic [11] gave a mathematical model with a nonstandard finite difference (NSFD) scheme and the wavelet based numerical scheme for fractional order SEIR epidemic is discussed by Kumar et al. [12].

Ali et al. [13] also introduced a mathematical model for the study of the HIV-1 virus.

In the same manner, Izhan [14] used a hybrid model and Ghosh et al. [15] studied the fractional model for population dynamics.

In the fractional order analysis with the comparison of this work in COVID, more study was also done [16–18].

The relationship of the mentioned model with the literature and comparison results are also reflected in the papers, in which Yavuz et al. studied about diabetes and hereditary and COVID-10 treatment rate [18–20].

Also in the cure of cancer, Altun [21] analysed Quantitative and numerical simulation. In the field of plant-pathogen herbivore interaction, Rahman [22] did a piecewise fractional analysis of the migration effect. In a similar manner, Joshi [17] analysed the stability of a non-singular fractional-order COVID-19 model with nonlinear incidence and treatment rate and Laxmi [16] studied on the vaccinal model for incorporating environmental transmission.

For the loss of immunity and quarantined class, Arif [23] gave models and numerical simulations and non-linear Burgers' equations via a semi-analytical technique [24].

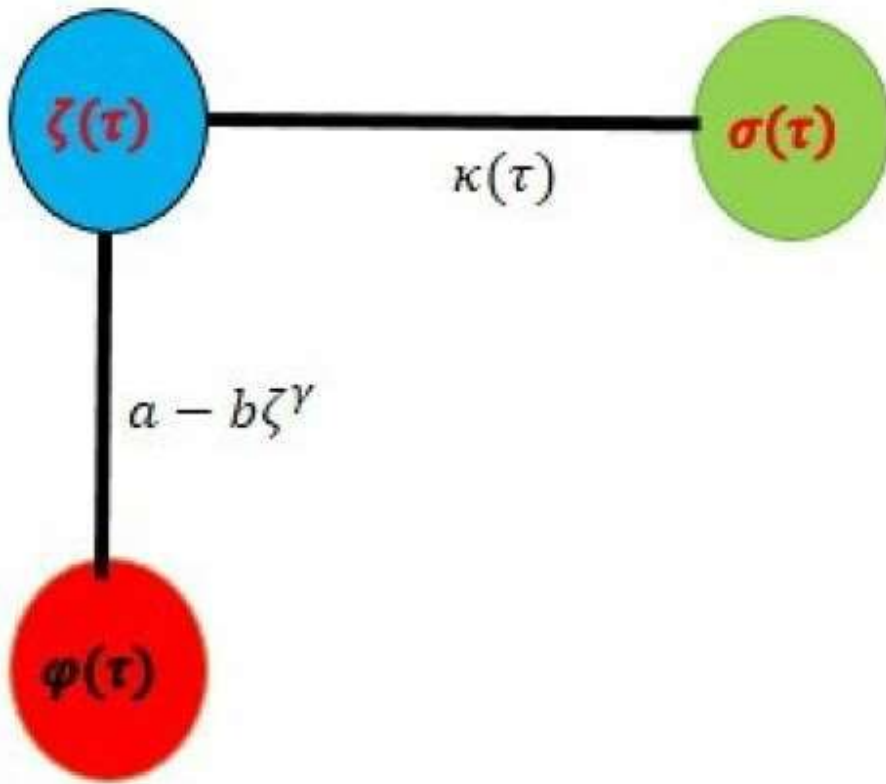
A Modified Homotopy Perturbation Transform Method (Fractional-Order Newell-Whitehead-Segel Equation) is also analysed by N. Iqbal, A.M. Albalahi, M.S. Abdo and W. Mohammed [25].

In this direction the studies are also relatable to the comparison of this method given by Zeb et al. [26], Evirgin et al. [27], Ozkose [28], Jha [29], Naik [18,30]

In this paper, we applied the first nontrivial biological model (Logistic model) given by Verhulst [31] in the proposition of COVID-19 mathematical model by two smooth function $\zeta(\tau)$ (total arised cases) and $\varphi(\tau)$ (total deaths) so that the study of behaviour of these graphs with the comparison of fractional order, Integer order and exact solution could be analysed.

The flow chart of this model is given in Figure 5.

Figure 5. Flow chart of total cases $\zeta(\tau)$ including total recovered $\sigma(\tau)$ and deaths



Display full size

2. Methodology

2.1. Homotopy decomposition method and modified homotopy perturbation method

It is the most practical technique to utilize recently in fractional calculus. This method of fractional derivatives provides numerous general instances of the fractional derivative model. Its use in the area of fractional calculus in applied mathematics is therefore more pertinent.

Atangana and Botha (2012) were the first to develop the Homotopy Decomposition Method (HDM) to solve partial differential equations, which are frequently encountered in problems involving heat diffusion, time fraction, groundwater flow, etc.

Since the modified Homotopy perturbation method is used in this paper along with Adomian polynomials, it is technically a modified Homotopy perturbation approach.

Baleanu et al. [32] also presented a fractional order model.

2.2. The mathematical model

In 1838, Verhulst [31] developed the first nontrivial biological model. This model is also known as the Logistic Model. The ODE of this model is given by

$$\frac{d\Psi}{d\tau} = \Psi(1 - \Psi), \quad \Psi(0) = \Psi_0. \quad (1)$$

It is the classical example of Mathematical Biology. The exact solution of this model is

$$\Psi(\tau) = \frac{\Psi_0 e^{\tau}}{1 + \Psi_0(e^{\tau} - 1)}. \quad (2)$$

Its curve is sigmoid (logistic) and useful for fractional value $\Psi_0 < 1/2$. In this paper, we used HDM to find the approximate solution for the total people and death people and compare to integer and fractional order solution with the general function $\zeta(\tau)$ that denotes the number of the Corona cases identifying to day τ (for some integer). The initial cases at $\tau = 0$ is $\zeta(0) = \zeta_0$. Now let the general equation of this model be

$$\frac{d\zeta}{d\tau} = \zeta(a - b\zeta^\gamma), \quad \zeta(0) = \zeta_0 > 0. \quad (3)$$

a and b are here positive constants and τ is the exponent which confirms the number of Corona cases that bounds in time τ . Ayala, Gilpin and Ehrenfeld in Ref. [33] introduced nonlinearity of (3) for describing the competition between species, while the logistic equation here shows some common assumptions by Brauer [34]. There are two possibilities for the infected person during the epidemic first one is φ which shows the population of dead persons and the other one is σ which represents the population of recovered persons from the corona.

$\zeta = \varphi + \sigma$. (4) Now the φ which is directly proportional to total number ζ is

$$\frac{d\varphi}{d\tau} = k(\tau)\zeta, \quad \varphi(0) = \varphi_0 > 0. \quad (5)$$

Where $k(\tau)$ is the effectiveness coefficient of the system of health care in the process of epidemic and related to the expression $k(\tau) = k_0 \exp(-s\tau)$, $s > 0$. All the parameters and defined functions are listed in Table 1:

Table 1. Table 1.



Display Table

The model (3)–(5) is used under essential simplifications of the epidemic process where it is assumed that $\zeta \gg \varphi$. Also, it is known that this pandemic is so severe that the rate

this epidemic not useful. For example, $v \cong 0.14u$ in Italy [35]. In that type of case, the above-mentioned mathematical model (3)–(5) would be more specified using the difference factor $(\zeta - \varphi)$ [since $\zeta \gg \varphi$] instead of a single function as follows

$$\frac{d\zeta}{d\tau} = (\zeta - \varphi) \left(a - b(\zeta - \varphi)^\gamma \right), \quad \zeta(0) = \zeta_0, \quad (6)$$

$$\frac{d\varphi}{d\tau} = k(\tau) (\zeta - \varphi), \quad \varphi(0) = \varphi_0. \quad (7) \text{ Now from (4) it is clear that } \sigma = (\zeta - \varphi), \text{ so}$$

$$\frac{d\sigma}{d\tau} = \frac{d\zeta}{d\tau} - \frac{d\varphi}{d\tau}, \quad (8) \text{ using (6) and (7) in (8), we get}$$

$$\frac{d\zeta}{d\tau} = \sigma (a - b\sigma^\gamma). \quad \zeta(0) = \zeta_0, \quad (9) \text{ And}$$

$$\frac{d\varphi}{d\tau} = k(\tau) \sigma, \quad \varphi(0) = \varphi_0. \quad (10) \text{ This equation (9) is called Bernoulli equation.}$$

These Equations (9) and (10) are time evolution equations of total cases and dead people. Now our aim is to compare these equations solutions by plotting the graphs between integer and fractional order.

For this first of all applying fractional order derivative [36] on (9) and (10)

$$D_t^\alpha [\zeta(\tau)] = \sigma(\tau) [a - b\sigma(\tau)^\gamma], \quad (11)$$

$$D_t^\beta [\varphi(\tau)] = k(\tau) \sigma(\tau). \quad (12) \text{ And the solutions are given by}$$

$$\zeta(\tau) = \zeta(0) + \frac{1}{\Gamma(\alpha)} \int_0^\tau (\tau - \theta)^{\alpha-1} \left[\sigma(\theta) [a - b\sigma(\theta)^\gamma] \right] d\theta, \quad (13)$$

$$\varphi(\tau) = \varphi(0) + \frac{1}{\Gamma(\beta)} \int_0^\tau (\tau - \theta)^{\beta-1} \left[k(\theta) \sigma(\theta) \right] d\theta. \quad (14) \text{ Here the sets of}$$

kernels are

$$k_1(\tau, \zeta) = \sigma(\tau) [a - b\sigma(\tau)^\gamma], \text{ and}$$

$$k_2(\tau, \varphi) = k(\tau) \sigma(\tau).$$

2.3. Existence and uniqueness of model solution

The Lipschitz conditions give the existence and uniqueness condition for mathematical models, which are studied by Moore et al. [37] for HIV/AIDS, which is given with a treatment compartment.

In this section, we studied the existence and uniqueness condition by applying Caputo–Fabrizio fractional operators in (11) and (12) on both sides, we get

$$\zeta(\tau) - \zeta(0) = {}^{CF}I_t^{\rho_1} [\sigma(\tau) a - b\sigma(\tau)^\gamma], \quad (15)$$

$\varphi(\tau) - \varphi(0) = {}^{CF}I_t^{\rho_2}[\kappa(\tau)\sigma(\tau)]$. (16) Where ${}^{CF}I_t^{\rho}$ is defined as the Caputo-fractional operator [38].

Then for simplicity, we define two kernels as follows:

$$k_1(\tau, \zeta) = \sigma(\tau) [a - b\sigma(\tau)^\gamma], \text{ and}$$

$k_2(\tau, \varphi) = k(\tau)\sigma(\tau)$. For proving the theorems, we will suppose that ζ and φ are nonnegative bounded functions, that means $\|\zeta(\tau)\| \leq \theta_1$, $\|\varphi(\tau)\| \leq \theta_2$. Where θ_1 and θ_2 are positive constants. Now represent

$\Gamma_1 = a - b\sigma(\tau)^\gamma$, $\Gamma_2 = \kappa(\tau)$. (17) Applying the definition of the Caputo-Fabrizio fractional integral in (11) and (12), we get

$$\begin{aligned} \zeta(\tau) - \zeta(0) &= \Omega(\rho_1)k_1(\tau, \zeta) + \omega(\rho_1) \int_0^\tau k_1(y, \zeta) dy, \\ \varphi(\tau) - \varphi(0) &= \Omega(\rho_2)k_2(\tau, \varphi) + \omega(\rho_2) \int_0^\tau k_2(y, \varphi) dy. \end{aligned} \quad (18) \text{ where the integral}$$

function is defined as:

$$\Omega(\rho) = \frac{2(1-\rho)}{(2-\rho)M(\rho)}, \text{ and}$$

$$\omega(\rho) = \frac{2\rho}{(2-\rho)M(\rho)}. \quad (19) \text{ in which } \rho \text{ is known as the order parameter.}$$

2.4. Theorem 1

If the following inequality holds

$0 \leq M = \max(\Gamma_1, \Gamma_2) < 1$. (20) Then the kernels k_1 , and k_2 satisfy Lipschitz conditions and are contraction mappings.

Proof: We consider the kernels k_1 . Let ζ and ζ_1 are any two functions, then we have

$\|k_1(\tau, \zeta) - k_1(\tau, \zeta_1)\| = \|a[\sigma(\tau) - \sigma_1(\tau)] - b[\sigma(\tau)^\gamma - \sigma_1(\tau)^\gamma]\|$. (21) With the help of the norms of triangle inequality on the right side of the above equation, we get

$$\begin{aligned} \|k_1(\tau, \zeta) - k_1(\tau, \zeta_1)\| &\leq \|a[\sigma(\tau) - \sigma_1(\tau)]\| + \|b[\sigma(\tau)^\gamma - \sigma_1(\tau)^\gamma]\| \\ &\leq (a - b\sigma(\tau)^\gamma) \|\zeta(\tau) - \zeta_1(\tau)\| \\ &= \Gamma_1 \|\zeta(\tau) - \zeta_1(\tau)\|. \end{aligned} \quad (22)$$

Similarly, we can get

$\|k_2(\tau, \varphi) - k_2(\tau, \varphi_2)\| \leq \Gamma_2 \|\varphi(\tau) - \varphi_2(\tau)\|$. (23) where Γ_1 and Γ_2 are defined in (17). Therefore for k_1 and k_2 the Lipschitz conditions are satisfied. From (19) the variables are written in kernel terms as follows:

$$\begin{aligned}\zeta(\tau) &= \zeta(0) + \Omega(\rho_1)k_1(\tau, \zeta) + \omega(\rho_1) \int_0^\tau k_1(y, \zeta) dy, \\ \varphi(\tau) &= \varphi(0) + \Omega(\rho_2)k_2(\tau, \varphi) + \omega(\rho_2) \int_0^\tau k_2(y, \varphi) dy.\end{aligned}\quad (24) \text{ From these}$$

equations, the following recursive formulas be:

$$\begin{aligned}\zeta_n(\tau) &= \Omega(\rho_1)k_1(\tau, \zeta_{n-1}) + \omega(\rho_1) \int_0^\tau k_1(y, \zeta_{n-1}) dy, \\ \varphi_n(\tau) &= \Omega(\rho_2)k_2(\tau, \varphi_{n-1}) + \omega(\rho_2) \int_0^\tau k_2(y, \varphi_{n-1}) dy.\end{aligned}\quad (25) \text{ The initial conditions}$$

are as follows:

$$\zeta_0(\tau) = \zeta(0), \quad \varphi_0(\tau) = \varphi(0). \quad (26) \text{ In the recursive formulae, the differences between the successive terms are given as:}$$

$$\begin{aligned}\phi_n(\tau) &= \zeta_n(\tau) - \zeta_{n-1}(\tau) = \Omega(\rho_1) \left[k_1(\tau, \zeta_{n-1}) - k_1(\tau, \zeta_{n-2}) \right] \\ &\quad + \omega(\rho_1) \int_0^\tau \left[k_1(y, \zeta_{n-1}) - k_1(y, \zeta_{n-2}) \right] dy,\end{aligned}\quad (27)$$

$$\begin{aligned}\psi_n(\tau) &= \varphi_n(\tau) - \varphi_{n-1}(\tau) = \Omega(\rho_2) \left[k_2(\tau, \varphi_{n-1}) - k_2(\tau, \varphi_{n-2}) \right] \\ &\quad + \omega(\rho_2) \int_0^\tau \left[k_2(y, \varphi_{n-1}) - k_2(y, \varphi_{n-2}) \right] dy.\end{aligned}\quad (28) \text{ It is noticeable that:}$$

$$\zeta_n(\tau) = \sum_{i=1}^n \phi_i(\tau), \quad \varphi_n(\tau) = \sum_{i=1}^n \psi_i(\tau). \quad (29)$$

Next, we arrange the recursive inequalities of the differences $\phi_n(\tau), \psi_n(\tau)$ as follows:

$$\begin{aligned}\|\phi_n(\tau)\| &= \|\zeta_n(\tau) - \zeta_{n-1}(\tau)\| \\ &= \left\| \Omega(\rho_1) \left(k_1(\tau, \zeta_{n-1}) - k_1(\tau, \zeta_{n-2}) \right) \right. \\ &\quad \left. + \omega(\rho_1) \int_0^\tau \left(k_1(y, \zeta_{n-1}) - k_1(y, \zeta_{n-2}) \right) dy \right\|.\end{aligned}\quad (30) \text{ solving the last equation, we}$$

get

$$\begin{aligned}\|\zeta_n(\tau) - \zeta_{n-1}(\tau)\| &\leq \Omega(\rho_1) \left\| k_1(\tau, \zeta_{n-1}) - k_1(\tau, \zeta_{n-2}) \right\| \\ &\quad + \omega(\rho_1) \int_0^\tau \left\| k_1(y, \zeta_{n-1}) - k_1(y, \zeta_{n-2}) \right\| dy.\end{aligned}\quad \text{Then, since the}$$

Lipschitz condition is satisfied by the kernel k_1 with Lipschitz constant Γ_1 , we have

$$\begin{aligned}\|\zeta_n(\tau) - \zeta_{n-1}(\tau)\| &\leq \Omega(\rho_1) \Gamma_1 \|\zeta_{n-1} - \zeta_{n-2}\| \\ &\quad + \omega(\rho_1) \Gamma_1 \int_0^\tau \|\zeta_{n-1} - \zeta_{n-2}\| dy.\end{aligned}\quad \text{Hence we get}$$

$$\|\phi_n(\tau)\| \leq \Omega(\rho_1) \Gamma_1 \|\phi_{n-1}(\tau)\| + \omega(\rho_1) \Gamma_1 \int_0^\tau \|\phi_{n-1}(y)\| dy, \quad (31) \text{ similarly, the second result would be}$$

$$\|\psi_n(\tau)\| \leq \Omega(\rho_2) \Gamma_2 \|\psi_{n-1}(\tau)\| + \omega(\rho_2) \Gamma_2 \int_0^\tau \|\psi_{n-1}(y)\| dy. \quad (32) \text{ Hence the existence and similarly the uniqueness is governed by these equations.}$$

2.5. Solution by modified homotopy perturbation method

Writing these variables in summation form and using the Homotopy Perturbation Method (HPM) [39] steps:

$$\sum_{n=0}^{\infty} p^n \zeta_n(\tau) = \zeta(0) + \frac{p}{\Gamma(\alpha)} \int_0^\tau (\tau - \theta)^{\alpha-1} \left[\sum_{n=0}^{\infty} p^n \sigma_n(\theta) \left[a - b \sum_{n=0}^{\infty} p^n \sigma_n(\theta)^\gamma \right] \right] d\theta, \quad (33)$$

$$\sum_{n=0}^{\infty} p^n \varphi_n(\tau) = \varphi(0) + \frac{p}{\Gamma(\beta)} \int_0^\tau (\tau - \theta)^{\beta-1} \left[k(\theta) \sum_{n=0}^{\infty} p^n \sigma_n(\theta) \right] d\theta. \quad (34) \text{ Where}$$

$0 < \alpha \leq 1, 0 < \beta \leq 1$. On computing the coefficient of the same powers of, we get the following integral equations

$$p^0: \zeta_0(\tau) = \zeta(0) = \zeta_0, \quad (35) \text{ Similarly,}$$

$$p^0: \varphi_0(\tau) = \varphi(0) = \varphi_0.$$

$$p^1: \zeta_1(\tau) = \frac{1}{\Gamma(\alpha)} \int_0^\tau (\tau - \theta)^{\alpha-1} \left[\sigma_0 \left(a - b \sigma_0^\gamma \right) \right] d\theta, \quad (36) \text{ And,}$$

$$p^1: \varphi_1(\tau) = \frac{1}{\Gamma(\beta)} \int_0^\tau (\tau - \theta)^{\beta-1} \left[k(\theta) \sigma_0 \right] d\theta.$$

$$p^2: \zeta_2(\tau) = \frac{1}{\Gamma(\alpha)} \int_0^\tau (\tau - \theta)^{\alpha-1} \left[\sigma_1(\theta) \left(a - b \sigma_1^\gamma(\theta) \right) \right] d\theta,$$

$$p^2: \varphi_2(\tau) = \frac{1}{\Gamma(\beta)} \int_0^\tau (\tau - \theta)^{\beta-1} \left[k(\tau) \sigma_1(\theta) \right] d\theta. \quad (37) \text{ Continuing this}$$

process up to n times, we get

$$p^n: \zeta_n(\tau) = \frac{1}{\Gamma(\alpha)} \int_0^\tau (\tau - \theta)^{\alpha-1} \left[\sigma_{n-1}(\theta) \left(a - b \sigma_{n-1}^\gamma(\tau) \right) \right] d\theta,$$

$$p^n: \varphi_n(\tau) = \frac{1}{\Gamma(\beta)} \int_0^\tau (\tau - \theta)^{\beta-1} \left[k(\theta) \sigma_{n-1}(\theta) \right] d\theta. \quad (38) \text{ Now since the}$$

Bernoulli equation gives the general form of the equation by taking the exponent of boundness $\gamma = 1$, so on solving the last set of equations

$$\zeta_1(\tau) = \frac{\alpha' \tau^\alpha}{\Gamma(\alpha + 1)}; \alpha' = \sigma_0 \left(a - b \sigma_0 \right), \quad (39)$$

$$\varphi_1(\tau) = \frac{\beta' \tau^\beta}{\Gamma(\beta + 1)}; \beta' = k \sigma_0. \quad (40) \text{ Similarly, in solving}$$

$\zeta(\tau) = \frac{1}{\Gamma(\alpha)} \int_0^\tau (\tau - \theta)^{\alpha-1} \left[\zeta(\theta) - \omega(\theta) \right] \left[a - b \left[\zeta(\theta) - \omega(\theta) \right] \right] d\theta$. after

$$\zeta_2(\tau) = (a - b) \left[\frac{\alpha' \tau^{2\alpha}}{\Gamma(2\alpha + 1)} - \frac{\beta' \tau^{\alpha + \beta}}{\Gamma(\alpha + \beta + 1)} \right]. \quad (41) \text{ and}$$

$$\varphi_2(\tau) = \frac{1}{\Gamma(\beta)} \int_0^\infty (\tau - \theta)^{\beta - 1} k \left[\zeta_1(\theta) - \varphi_1(\theta) \right] d\theta. \text{ after simplification}$$

$$\varphi_2(\tau) = k \left[\frac{\alpha' \tau^{\alpha + \beta}}{\Gamma(\alpha + \beta + 1)} - \frac{\beta' \tau^{2\beta}}{\Gamma(2\beta + 1)} \right]. \quad (42) \text{ Finally, the generalized series solution is given}$$

by

$$\zeta(\tau) = \zeta_0 + \zeta_1(\tau) + \zeta_2(\tau) + \dots \text{ and}$$

$$\varphi(\tau) = \varphi_0 + \varphi_1(\tau) + \varphi_2(\tau) + \dots \text{ Putting the above values, we get}$$

$$\zeta(\tau) = \zeta_0 + \frac{\alpha' \tau^\alpha}{\Gamma(\alpha + 1)} + (a - b) \left[\frac{\alpha' \tau^{2\alpha}}{\Gamma(2\alpha + 1)} - \frac{\beta' \tau^{\alpha + \beta}}{\Gamma(\alpha + \beta + 1)} \right] + \dots \quad (43) \text{ and}$$

$$\varphi(\tau) = \varphi_0 + \frac{\beta' \tau^\beta}{\Gamma(\beta + 1)} + k \left[\frac{\alpha' \tau^{\alpha + \beta}}{\Gamma(\alpha + \beta + 1)} - \frac{\beta' \tau^{2\beta}}{\Gamma(2\beta + 1)} \right] + \dots \quad (44)$$

2.6. Fractional order (0.5)

For this putting $\alpha = \beta = 1/2$ Also the required coefficient in the case of China Population [35] the following data are helpful

$$\zeta_0 = 571; \varphi_0 = 17; a = 28; b = 3.5 * 10^{-6}; k \approx k_0 = 0.0094; \quad \text{From these}$$

$$\sigma_0 = \zeta_0 - \varphi_0 = 571 - 17 = 554.$$

$$\alpha' = \sigma_0 [a - b\sigma_0] = 554 \left[0.28 - 554 (3.5 * 10^{-6}) \right]. \text{ Hence } \alpha' = 154.04 \text{ and similarly}$$

$$\beta' = 5.2076 \text{ Using all these coefficients in (39) and (40), we get}$$

$$\zeta(\tau) = 571 + \frac{154.04}{\Gamma(3/2)} \tau^{1/2} + (0.2799) \left[\frac{154.04}{\Gamma(2)} \tau^{1/2} - \frac{5.2076}{\Gamma(2)} \tau^{1/2} \right] \tau^{1/2} + \dots \text{ Which in}$$

simplification gives

$$\zeta(\tau) = 571 + (173.86) \tau^{1/2} + (41.6581) \tau + \dots \quad (45) \text{ and}$$

$$\varphi(\tau) = 17 + \frac{5.2076}{\Gamma(3/2)} \tau^{1/2} + (0.0094) \left[\frac{154.04}{\Gamma(2)} - \frac{5.2076}{\Gamma(2)} \right] \tau + \dots \text{ which in simplification gives}$$

$$\varphi(\tau) = 17 + (5.8776) \tau^{1/2} + (1.3990) \tau + \dots \quad (46)$$

2.7. Fractional order (0.9)

For this putting $\alpha = \beta = 0.9$ and remaining all the same data and simplifying, we get

$$\zeta(\tau) = 571 + (154.03) \tau^{0.9} + (20.8176) \tau^{1.8} + \dots \quad (47)$$

$$\varphi(\tau) = 17 + (5.2075) \tau^{0.9} + (0.5978) \tau^{1.8} + \dots \quad (48)$$

2.8. Integer order (1)

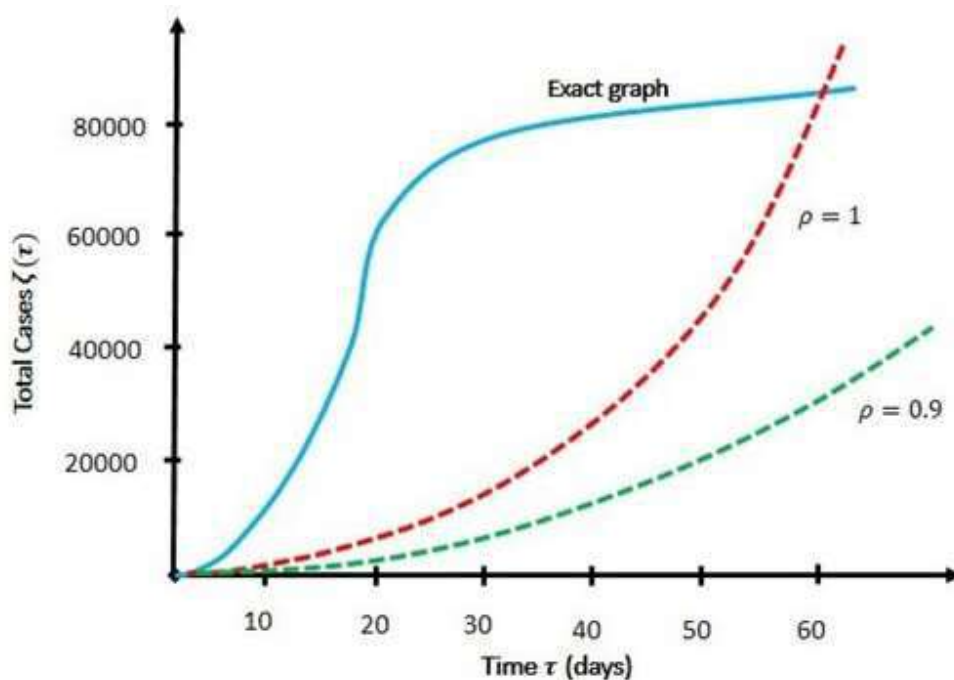
For this putting $\alpha = \beta = 1$ and remaining all the same data and simplifying, we get

$$\varphi(\tau) = 17 + (5.2076)\tau + (0.69951)\tau^2 + \dots \quad (50)$$

3. Conclusion

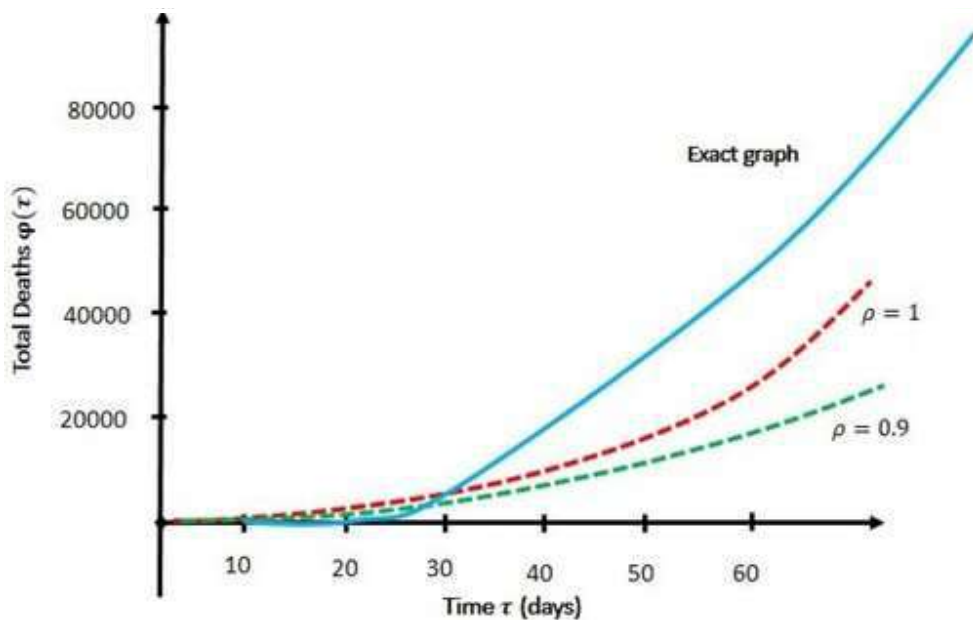
Figure 6 from the graphical study illustrates how the graph varies in integer order versus fractional order. In fractional order ($\rho = 0.9$), the total number of cases starts at 571 and rises to 2500 (about) after 60 days (here, x stands for time τ), which is more important and treatable than in integer order, where the cases rise to more than 80000 after 60 days. Figure 7 depicts how the graph's integer-order changes about fractional order. In fractional order ($\rho = 0.9$), the overall death toll starts at 17, and after 60 days (here, x stands for time τ), it rises to 70 (about). This is more significant and results in fewer deaths than in integer order ($\rho = 0.9$), where the cases rise to more than 3000 after 60 days. The data leads to the conclusion that fractional order performs better than integer order. This type of analysis will be more useful for the analysis and prediction of further improvements and future studies of such types of pandemics and diseases.

Figure 6. Graphs of $\zeta(\tau)$ fractional order (0.9) [green], integer order (1) [red], and exact solution [blue] with respect to time τ (x-axis).



Display full size

Figure 7. Graphs of $\varphi(t)$ fractional order (0.9) [green], integer order (1) [red], and exact



Display full size

Disclosure statement

No potential conflict of interest was reported by the author(s).

References

1. Cherniha R, Davydovych V. A mathematical model for the COVID-19 outbreak. arXiv Vol. 2, 2020.
[Google Scholar](#)
2. Cooper I, Mondal A. A SIR model assumption for the spread of COVID-19 in different communities. NCBI. 2020;139:139–148.
[Google Scholar](#)
3. Efimov D, Ushirobira U. On interval prediction of COVID-19 development based on a SEIR epidemic model. Vol. 32, Lille, France: CRISTAL-University de; 2020.

4. Pang L, Yang W, Zhang D, et al. Epidemic analysis of COVID-19 in China by dynamical modeling. arXiv. Vol. 2002, 2020.
[Google Scholar](#)
5. Anirudh A. Mathematical modeling and the transmission dynamics in predicting the COVID-19-What next in combating the pandemic. *Infect Dis Model.* 2020;5:366–374.
[PubMed](#) | [Google Scholar](#)
6. Shaikh AS, Shaikh IN, Nisar KS. A mathematical model of COVID-19 using fractional derivative: outbreak in india with dynamics of transmission and control. preprints Not Peer-Reviewed. Vol. 1, 2020.
[Google Scholar](#)
7. Nisar KS, Kumar S, Kumar R. A new Robotnov fractional-ewponential function based fractional derivative for diffusion equation under external force. *Math Methods Appl Sci.* 2020;43:1–11.
[Web of Science ®](#) | [Google Scholar](#)
8. Shah K, Abdeljawed T, Mahariq I. Qualitative analysis of a mathematical model in the time of COVID-19. *Hindawi BioMed Res Int.* 2020;2020:145–149.
[Web of Science ®](#) | [Google Scholar](#)
9. Singh J, Ahluwalia PK, Kumar A. Spread of COVID-19 in india: a mathematical model based COVID-19 prediction in India and its different states. *medRxiv.* Vol. 10, 2020.
[Google Scholar](#)
10. Wang N., Fu Y., Zhang H., et al. An evaluation of mathematical models for the outbreak of COVID-19. *Precis Clin Med.* 2020;3(2):85–93. doi: 10.1093/pcmedi/pbaa016
[PubMed](#) | [Google Scholar](#)
11. Zeb A, Alzahrani E, Erturk VS, et al. Mathematical model for coronavirus disease 2019

12. Kumar S, Kumar R, Osman MS, et al. A wavelet based numerical scheme for fractional order SEIR epidemic of measles by using Genocchi polynomials. Numer Methods Partial Differ Equ. 2021;**37**(2):1250–1268. doi:10.1002/num.v37.2.

13. Ali KK, Osman MS. Analytical and numerical study of the HIV-1 infection of CD4+ T-cells conformable fractional mathematical model that causes acquired immunodeficiency syndrome with the effect of antiviral drug therapy. Math Methods Appl Sci. 2023;**46**(7):7654–7670. doi: 10.1002/mma.v46.7

14. Izhan M, Yusoff M. The use of system dynamics methodology in building a COVID-19 confirmed case model. Com Math Med. 2020:2020:321–337.

15. Ghosh S, Kumar S, Kumar R. A fractional model for population dynamics of two interacting species by using spectral and hermite wavelets methods. Numer Methods Partial Differ Equ. 2020;**37**(2):1652–1672.

16. Vijayalaxmi GM, Besi R. A fractional order vaccination model for COVID-19 incorporating environmental transmission. Bull Math Biol. 2022;**1**:78–110.

17. Joshi H, Yavuz M, Townley S, et al. Stability analysis of a non-singular fractional-order covid-19 model with nonlinear incidence and treatment rate. Phys Scr. 2023;**98**(4):045216. doi: 10.1088/1402-4896/acbe7a

18. Naik PA, Yavuz M, Qureshi S, et al. Modeling and analysis of COVID-19 epidemics with

2020;135(1):1–42. doi: 10.1140/epjp/s13360-019-00059-2

| [Google Scholar](#)

19. Yavuz M, Cosar FO, Usta F. A novel modeling and analysis of fractional-order COVID-19 pandemic having a vaccination strategy. In: AIP Conference Proceedings, Vol. 2483, AIP Publishing LLC; 2022.

[Google Scholar](#)

20. Yavuz M, Hader W. A new mathematical modelling and parameter estimation of COVID-19: a case study in Iraq. AIMS Bioeng. 2022;9(4):420–446. doi: 10.3934/bioeng.2022030

| [Web of Science ®](#) | [Google Scholar](#)

21. Ucar E, Ozdemir N, Altun E. Qualitative analysis and numerical simulations of new model describing cancer. J Comput Appl Math. 2023;422:114899. doi: 10.1016/j.cam.2022.114899

| [Web of Science ®](#) | [Google Scholar](#)

22. Rahman M, Arfan M, Baleanu D. Piecewise fractional analysis of the migration effect in plant-pathogen-herbivore interactions. Bull Math Biol. 2023;1:1–23.

[Google Scholar](#)

23. Arif F, Majeed Z, Rahman JU, et al. Mathematical modeling and numerical simulation for the outbreak of COVID-19 involving loss of immunity and quarantined class. Math Stat Aspects Health Sci. 2022;2022:89–94.

[Google Scholar](#)

24. Iqbal N, Chughtai MT, Ullah R. Fractional study of the non-linear Burgers' equations via a semi-analytical technique. Fractal Fract. 2023;7(2):103. doi: 10.3390/fractalfract7020103

| [Web of Science ®](#) | [Google Scholar](#)

25. Iqbal N, Albalahi AM, Abdo MS, et al. Analytical analysis of fractional-order Newell-Whitehead-Segel equation: a modified homotopy perturbation transform method. *Adv Nonlinear Anal Appl.* 2022;2022:1–10.
[Google Scholar](#)
26. Naim M, Sabbar Y, Zeb A. Stability characterization of a fractional-order viral system with the non-cytolytic immune assumption. *Math Model Numer Simul Appl.* 2022;2:164–176.
[Google Scholar](#)
27. Evirgin F, Ucar E, Ucar S, et al. Modelling influenza a disease dynamic under Caputo-Fabrizio fractional derivative with distinct contact rates. *Math Model Numer Simul Appl.* 2023;3:58–73.
[Google Scholar](#)
28. Ozkose F, Yavuz M. Investigation of interactions between COVID-19 and diabetes with hereditary traits using real data: a case study in Turkey. *Comput Biol Med.* 2022;141:105044. doi: 10.1016/j.compbimed.2021.105044
[PubMed](#) | [Web of Science ®](#) | [Google Scholar](#)
29. Joshi H, yavuz M, Jha BK. Modelling and analysis of fractional-order vaccination model for control of COVID-19 outbreak using real data. *Math Biosci Eng.* 2023;20(1):213–240. doi: 10.3934/mbe.2023010
[PubMed](#) | [Web of Science ®](#) | [Google Scholar](#)
30. Kumar S., Ghosh S., Samet B., et al. An analysis for heat equations arises in diffusion process using new Yang–Abdel–Aty–Cattani fractional operator. *Math Methods Appl Sci.* 2020;43(9):6062–6080. doi: 10.1002/mma.v43.9.
[Web of Science ®](#) | [Google Scholar](#)
31. Verhulst P. nitice sur la loi que la population suit dans son accroissement. *Corr Math Phys.* 1838;10:113–129.

32. Baleanu D, Mohammadi H, Rezapour S. A fractional differential equation model for the COVID-19 transmission by using the Caputo-Fabrizio derivative. *Adv Differ Equ.* 2020;299:552–561.
[Google Scholar](#)
33. Ayala FJ, Gilpin ME, Ehrenfeld JG. Competition between species: theoretical models and experimental tests. *Theor Pop Biol.* 1973;4(3):331–356. doi: 10.1016/0040-5809(73)90014-2
[PubMed](#) | [Web of Science®](#) | [Google Scholar](#)
34. Brauer F, Castillo Chavez C. *Mathematical models in populations biology and epidemiology.* Vol. 6, New York (NY): Springer; 2012.
[Google Scholar](#)
35. <https://www.worldometers.info/coronavirus/> (accessed on 1 May 2020).
[Google Scholar](#)
36. Matlob MA, Jamali Y. The concepts and applications of fractional order differential calculus in modeling of viscoelastic systems: a primer. *arxiv.org.* Vol. 6, 2017.
[Google Scholar](#)
37. Moore EJ, Sirisubtawee S. A Caputo-Fabrizio fractional differential equation model for HIV/AIDS with treatment compartment. Vol. 9. Cham: Springer; 2019. doi: 10.1186/s13662-019-2138-9.
[Google Scholar](#)
38. Nosheen A, Tariq M, Khan KA. On Caputo fractional derivatives and Caputo-Fabrizio integral operators via (s,m) -convex functions. *MDPI.* 2023;7(2):187.
[Google Scholar](#)
39. Srivastava HM, Dubey RS, Jain M. A study of the fractional-order mathematical model of diabetes and its resulting complications. Vol. 26, London: Wiley publication; 2019.

Download PDF

Related research

People also read

Recommended articles

Cited by
2

[Homotopy decomposition method to analysis fractional hepatitis B virus infection model >](#)

M. M. Gour et al.

Applied Mathematics in Science and Engineering

Published online: 24 Sep 2023



[Mathematical modelling with computational fractional order for the unfolding dynamics of the communicable diseases >](#)

Mati ur Rahman et al.

Applied Mathematics in Science and Engineering

Published online: 16 Jan 2024



[Predicting COVID-19 outbreak in India using modified SIRD model >](#)

Sakshi Shringi et al.

Applied Mathematics in Science and Engineering

Published online: 2 Feb 2024



[View more >](#)

Information for

Authors

R&D professionals

Editors

Librarians

Societies

Opportunities

Reprints and e-prints

Advertising solutions

Accelerated publication

Corporate access solutions

Open access

Overview

Open journals

Open Select

Dove Medical Press

F1000Research

Help and information

Help and contact

Newsroom

All journals

Books

Keep up to date

Register to receive personalised research and resources
by email



Sign me up



Copyright © 2024 **Informa UK Limited** [Privacy policy](#) [Cookies](#) [Terms & conditions](#) [Accessibility](#)

Registered in England & Wales No. 3099067
5 Howick Place | London | SW1P 1WG



Bioprospecting of novel ligninolytic bacteria for effective bioremediation of agricultural by-product and synthetic pollutant dyes

Devendra Jain^{a,*}, Jitendra Kumar Navariya^a, Ali Asger Bhojiya^{a,b}, Abhijeet Singh^c, Santosh Ranjan Mohanty^d, Sudhir K. Upadhyay^{e,*}

^a All India Network Project on Soil Biodiversity and Biofertilizers, Department of Molecular Biology and Biotechnology, Rajasthan College of Agriculture, Maharana Pratap University of Agriculture and Technology, Udaipur 313001, India

^b Faculty of Science, US Ostwal Science, Arts and Commerce College, Mangalwad, Chittorgarh, Rajasthan 302024, India

^c Department of Biosciences, Manipal University Jaipur, Jaipur 303007, India

^d All India Network Project on Soil Biodiversity-Biofertilizers, ICAR-Indian Institute of Soil Science, Bhopal 462038, India

^e Department of Environmental Science, V.B.S. Purvanchal University, Jaunpur 222003, India

ARTICLE INFO

Keywords:

Lignin
Methylene blue
Lignin degradation bacteria
Ligninolytic enzymes
16 S rRNA gene sequencing
Biodegradation

ABSTRACT

Lignin is a significant renewable carbon source that needs to be exploited to manufacture bio-ethanol and chemical feedstocks. Lignin mimicking methylene blue (MB) dye is widely used in industries and causes water pollution. Using kraft lignin, methylene blue, and guaiacol as a full carbon source, 27 lignin-degrading bacteria (LDB) were isolated from 12 distinct traditional organic manures for the current investigation. The ligninolytic potential of 27 lignin-degrading bacteria was assessed by qualitative and quantitative assay. In a qualitative plate assay, the LDB-25 strain produced the largest zone, measuring 6.32 ± 0.297 , on MSM-L-kraft lignin plates, while the LDB-23 strain produced the largest zone, measuring 3.44 ± 0.413 , on MSM-L-Guaiacol plates. The LDB-9 strain in MSM-L-kraft lignin broth was able to decolorize lignin to a maximum of $38.327 \pm 0.011\%$ in a quantitative lignin degradation assay, which was later verified by FTIR assay. In contrast, LDB-20 produced the highest decolorization ($49.633 \pm 0.017\%$) in the MSM-L-Methylene blue broth. The highest manganese peroxidase enzyme activity, measuring $6322.314 \pm 0.034 \text{ U L}^{-1}$, was found in the LDB-25 strain, while the highest laccase enzyme activity, measuring $1.5105 \pm 0.017 \text{ U L}^{-1}$, was found in the LDB-23 strain. A preliminary examination into the biodegradation of rice straw using effective LDB was carried out, and efficient lignin-degrading bacteria were identified using 16SrDNA sequencing. SEM investigations also supported lignin degradation. LDB-8 strain had the highest percentage of lignin degradation (52.86%), followed by LDB-25, LDB-20, and LDB-9. These lignin-degrading bacteria have the ability to significantly reduce lignin and lignin-analog environmental contaminants, therefore they can be further researched for effective bio-waste management mediated breakdown.

1. Introduction

Plant biomass naturally decomposes over time and is mostly triggered by enzymatic activity of neighboring bacterial and fungal species (Janusz et al., 2017; da Costa et al., 2018; Jimenez et al., 2018; Lee et al., 2019; Riyadi et al., 2020). Numerous microorganisms, such as bacteria and fungi, have been the focus of the most thorough investigations on lignin alteration and breakdown (Lee et al., 2019; Atiwesh et al., 2022). When lignocellulosic organic wastes are processed for use in the

production of bioethanol and the paper industry, respectively, powerful lignin-degrading microorganisms or their ligninolytic enzymes can be used successfully (Fang et al., 2018; Brink et al., 2019; Li et al., 2022). Plants' rigidity and tensile strength come from lignin, a complex, chemically heterogeneous polymer made up of 4-hydroxyl phenylpropanoid units (Hasanin et al., 2018). Biomass is essentially resistant because lignin acts as a physical barrier to stop cellulose from being hydrolyzed by biological or chemical processes (Wu et al., 2022).

For the production of biofuels, lignocellulosic biomass is highly

* Corresponding authors.

E-mail addresses: devendrajain@mpuat.ac.in, devroshan@gmail.com (D. Jain), sku.env.lko@gmail.com (S.K. Upadhyay).

¹ ORCID: <https://orcid.org/0000-0002-4345-1536>

² ORCID: <https://orcid.org/0000-0002-2228-8063>

desirable as a raw component (Malode et al., 2021). Lignin and cellulose make up the majority of 80% of crop residue/biomass (Chen et al., 2018). Large volumes of lignocellulosic waste are produced by forestry and agricultural activities, paper-pulp companies, wood industries etc. and burning is a common method of decreasing this waste, which otherwise may contribute to pollution (Haile et al., 2021). Therefore, enhancing lignin breakdown has enormous promise to save the environment and build new beneficial products (Gupta et al., 2022). Chemical contaminants like synthetic dyes are significant contributors to water pollution. Methylene blue (MB) dye is one of these and is frequently used in various industries such as dyeing, textile, tannery, and paper, etc. (Bhat et al., 2022; Pham et al., 2022). Using promising microbial isolates, a biological strategy giving a more affordable and sustainable alternative method has been used to remove MB. Microorganisms, which can degrade MB, come from a wide range of taxa, including *Acinetobacter*, *Aspergillus*, *Bacillus*, *Pseudomonas*, *Staphylococcus* etc. (Eslami et al., 2017; Karim et al., 2018; Bharti et al., 2019; Ogunlaja et al., 2020; Kishor et al., 2021b; Haque et al., 2021). To participate in central carbon metabolism, bacteria that degrade lignin and lignin-imitating dyes secrete extracellular enzymes that break down lignin into smaller components (Beckham et al., 2016). A range of extracellular oxidative enzymes, such as laccases, lignin peroxidases (LiPs), manganese peroxidases (MnPs), and multifunctional peroxidases, are released by the lignin-degrading organisms (Kumar and Chandra, 2020).

Several bacteria, in addition to wood-rot fungus, can degrade lignin (Haq et al., 2022). Pretreatments may become economically viable if lignin is removed selectively using lignin-degrading enzymes (Lee et al., 2019; Wu et al., 2022). A biological (or primarily biological) approach to removing lignin could overcome these limitations, enabling the generation of bio-fuel at a cheaper cost and with less impact on the environment. Microorganisms can produce metabolites and enzymes that hasten the breakdown of organic waste and raise the caliber of soil humus (Singh et al., 2017).

The breakdown of rice straw into smaller products so they can be digested by microorganisms occurs through a microbial process (Goodman, 2020). In the past, the majority of these lignin-degrading bacteria were found in soil and the intestines of insects that fed wood (Zhang et al., 2021). This research was focused on identifying and characterizing the microbial inoculants that causes rice straw to break down so quickly. In this study, we identify new lignin-degrading bacteria from a variety of organic sources, characterize them, and assess their potential for lignin degradation.

2. Material and methods

2.1. Isolation and screening of lignin-degrading bacteria

The isolation of LDB was carried out using the method reported by Rahman et al. (2013). The minimal salt media-Luria agar (MSM-L agar) medium supplemented with 1% Kraft lignin (KL) as the primary carbon and energy source was used for the isolation of ligninolytic bacteria from freshly prepared organic manures (Jain et al., 2021) (Table 1). The bacterial strains that showed proper growth were purified on fresh MSM-L agar plates and stored at 4 °C. Screening of LDB was carried out on MSM-L agar plate containing Kraft lignin (0.5%) (Chen et al., 2012b) and guaiacol (10%) (Atalla et al., 2010) and methylene blue indicator dye (50 mg/L) (Bandounas et al., 2011) and incubated at 30 ± 2° C for 4–5 days for the development of the de-colorization zone. After growth, the plates were taken out and flooded with 10 ml of a ferric chloride/potassium ferricyanide solution [1% (w/v)]. After 10 min, the solution was drained off, leaving the agar where the aromatic compounds were present stained blue or green. It was assumed that a yellowish zone where growth had been eradicated was proof of lignin breakdown (McCarthy and Broda, 1984). The degrading of indicator dye is considered a positive test for lignin degradation (Bandounas et al.,

Table 1

Determination of lignolytic activities of lignin degrading bacteria isolated from traditional organic manures.

S. N.	Source	Strain Name	Growth and de-colorization of ligninolytic substrates		
			Kraft Lignin	Guaiacol	Methylene blue
1	JeevaAmrat	SBD-LDB-1	+	+	-
2	BhabhutAmritPani	SBD-LDB-2	+	+	+
3	PanchGavya	SBD-LDB-3	+	+	+
4	MatkaKhad	SBD-LDB-4	+	+	+
5	Vermiwash (Silica enriched)	SBD-LDB-5	+	+	-
6	BeejaAmrat	SBD-LDB-6	+	-	+
7	Vermi Wash	SBD-LDB-7	+	+	+
8	Silica enriched Compost tea	SBD-LDB-8	+	+	+
9	Compost Tea	SBD-LDB-9	+	+	+
10	BD500	SBD-LDB-10	+	+	-
11	BD500	SBD-LDB-11	+	+	+
12	JeevaAmrat	SBD-LDB-12	+	+	-
13	BhabhutAmritPani	SBD-LDB-14	+	+	+
14	PanchGavya	SBD-LDB-15	+	+	-
15	MatkaKhad	SBD-LDB-16	+	+	-
16	Silica enriched vermi wash	SBD-LDB-17	+	+	-
17	BeejaAmrat	SBD-LDB-18	+	-	-
18	Vermi Wash	SBD-LDB-19	+	+	+
19	Compost tea (Silica enriched)	SBD-LDB-20	+	+	+
20	Compost Tea	SBD-LDB-21	+	-	-
21	BD 501	SBD-LDB-22	+	+	+
22	BD 501	SBD-LDB-23	+	+	+
23	PanchGavya	SBD-LDB-24	+	+	+
24	MatkaKhad	SBD-LDB-25	+	+	+
25	Silica enriched vermi wash	SBD-LDB-26	+	+	+
26	BeejaAmrat	SBD-LDB-28	+	+	-
27	Vermi Wash	SBD-LDB-29	+	+	+

2011).

3. Ligninolytic enzyme activity assay

A 50 ml conical flask filled with MSM-L medium was used to inoculate the chosen positive isolates for screening assays. These inoculated flasks were incubated for 6 days per the procedures outlined by Rahman et al. (2013), during which time culture samples were collected for manganese peroxidase (MnP) and laccase activity were assessed using the oxidation of Guaiacol (2-methoxyphenol) and ABTS (2, 2'-azinobis-(3-ethylbenzothiazoline-6-sulphonate) method respectively (Rahman et al., 2013; Bourbonnais et al., 1995).

3.1. Decolorization activity of bacteria on liquid MSM containing MB dye and Kraft lignin

Decolorization of lignin-mimicking dyes i.e. Methylene Blue (MB) was assessed in test tubes as liquid-phase assays. For broth assays, the individual bacterial strains were grown in MSM containing methylene blue indicator dye (50 mg/L) at 30 °C with shaking at 200 rpm. Control without inoculation was also maintained. The samples were centrifuged and dye de-colorization was absorbance was measured at λ_{663} (Saratale et al., 2009).

All the test bacterial cultures were inoculated in 10 ml of MSM-L agar medium containing 0.5% lignin in 25 ml capacity screwed cap tubes with the maintenance of un-inoculated control for comparison. All the tubes were incubated at $30 \pm 2^{\circ}$ C at 120 rpm for 5 days in a shaker incubator and color change was measured by spectrophotometer on the 5th day at 465 nm. The decolorization percentage of 0.5% lignin by respective bacteria was calculated using the formula given by (Sani and Banerjee, 1999).

$$\% \text{ decolorization} = \frac{\text{Initial absorbance} - \text{observed absorbance}}{\text{Initial absorbance}} \times 100$$

Additionally, Fourier transform infrared (FTIR) spectroscopy study was done to verify that the isolates had degraded and depolymerized kraft lignin (Khan et al., 2022).

3.2. In vitro efficacy of ligninolytic bacteria for degradation of agro-waste residues

After being treated with 1% NaOH for 24 h at room temperature, deionized water was used to adjust the pH to 7, and then the rice straw was dried at 80 °C (Yu et al., 2009). The 3 g quantity of pretreated rice straw was immersed in 100 ml flasks in triplicate and steam sterilized and then 5 ml of selected lignin-degrading bacteria were inoculated in each flask incubated for 21 days at ambient temperature (room temperature) and assayed for lignin degradation and the observations of weight reduction and consistency were also monitored (Bakar et al., 2018). After the end of the incubation period, the acid detergent fiber (ADF) and acid detergent lignin (ADL) methods (Thimmaiah, 2009) were used to determine the amount of lignin in rice straw.

4. Effects of bio-pretreatment on the structure of the rice straw

Using a freeze drier, untreated and bio-pretreated rice straw was dehydrated. Using a scanning electron microscope (SEM), the various surface morphologies of the untreated and bio-pretreated rice stover were observed (Dong et al., 2019).

5. Sequencing and Phylogenetic Analysis of 16 S rDNA of Potent LDB Isolates

The five most effective LDB isolates' PCR-amplified 16 S rDNA region was sequenced using an automated DNA sequencer (ABI model 377, Applied Biosystems, USA) in accordance with the normal technique utilizing universal 16 S rDNA primers (27 F and 1492 R; amplicons size \approx 1465 bp). Prior to BLAST, the 16 S rDNA sequences were modified using the Bio Edit software. Utilizing the nucleotide BLASTn programme, the sequences collected during the investigation were compared to previously submitted sequences in the nucleotide database GenBank at the National Center for Biotechnology (NCBI) (Altschul et al., 1990). The online programme CLUSTAL-W was used to align the 16 S rDNA consensus sequences (Thompson et al., 1994). Phylogenetic trees were constructed using this alignment and the greatest likelihood technique using MEGA 6.06 software (Tamura et al., 2013).

6. Statistical analyses

Using SPSS-20, the statistical analysis known as the standard

deviation (SD) was performed on all the observed data. Additionally, correlation functional interaction between all chosen bacterial isolates' production of the enzymes that break down Kraft lignin and Methylene Blue was performed using Past3 software, and correlation heat maps were created using TB tools.

7. Result and discussion

7.1. Isolation and screening of lignin degrading bacteria

The isolation and screening of lignin-degrading bacteria were carried out on the MSM-L agar medium supplemented with Kraft lignin (0.5%), Guaiacol (10%), and Methylene blue (50 mg/L). In the present study, 27 lignin-degrading bacteria were isolated and purified from 12 different organic produces and are summarized in Table 1. All the strains were able to grow on MSM-L containing Kraft lignin (0.5%), whereas 24 strains and 18 strains were able to grow and utilize Guaiacol (10%) and Methylene blue (50 mg/L) respectively. The 16 strains along with the positive culture showed positive growth and de-colorization on all three different ligninolytic substrates. The decolorization zone was measured to determine the lignin degradation index (LDI), and the findings are shown in Table 2. This is the first report that we are aware of lignin-degrading microbial strains being isolated from conventional liquid organic manures.

The various lignin-degrading bacteria were identified in rotting oil palm, empty fruit bunches, rotten wood, textile effluent, and sludge etc. (Faisal et al., 2021; Kishor et al., 2021a). While Harith et al. (2014) isolated 8 strains with lignin degradation ability from agro-industrial waste, Sharifi-Yazdi et al. (2001) isolated 22 LDB strains from decayed plants, Falade et al. (2017) isolated 30 potential strains of ligninolytic bacteria from water and sediment samples, and Couger et al. (2020) isolated lignin-degrading bacteria from the termite gut. Nahrowi et al. (2018) previously reported a correlation between ligninolytic activities of bacterial isolates and the lignin degradation index (LDI), and they

Table 2

Determination of lignolytic activities of lignin degrading bacteria using plate assay by measuring decolourisation zone.

S.NO	Strain Name	Lignin degradation index by measuring decolourisation zone after 72 h	
		Kraft Lignin (0.5%)	Guaiacol (10%)
1	SBD-LDB-1	3.24 ± 0.035	2.86 ± 0.125
2	SBD-LDB-2	2.1 ± 0.10	2.21 ± 0.257
3	SBD-LDB-3	3.6 ± 0.200	2.28 ± 0.145
4	SBD-LDB-4	3.46 ± 0.351	1.31 ± 0.162
5	SBD-LDB-5	1.01 ± 0.11	1.83 ± 0.175
6	SBD-LDB-6	1.04 ± 0.12	ND
7	SBD-LDB-7	3.38 ± 0.325	1.63 ± 0.126
8	SBD-LDB-8	5.23 ± 0.321	3.01 ± 0.225
9	SBD-LDB-9	5.47 ± 0.240	3.21 ± 0.256
10	SBD-LDB-10	3.48 ± 0.141	1.65 ± 0.200
11	SBD-LDB-11	4.53 ± 0.251	3.02 ± 0.087
12	SBD-LDB-12	5.15 ± 0.160	2.21 ± 0.256
13	SBD-LDB-14	2.35 ± 0.100	2.01 ± 0.225
14	SBD-LDB-15	0.94 ± 0.18	1.78 ± 0.257
15	SBD-LDB-16	4.32 ± 0.192	2.26 ± 0.205
16	SBD-LDB-17	5.57 ± 0.222	2.41 ± 0.272
17	SBD-LDB-18	0.98 ± 0.08	ND
18	SBD-LDB-19	1.24 ± 0.250	1.52 ± 0.087
19	SBD-LDB-20	5.17 ± 0.210	3.30 ± 0.174
20	SBD-LDB-21	0.84 ± 0.14	ND
21	SBD-LDB-22	3.34 ± 0.262	2.36 ± 0.127
22	SBD-LDB-23	6.14 ± 0.161	3.44 ± 0.413
23	SBD-LDB-24	6.31 ± 0.298	2.88 ± 0.247
24	SBD-LDB-25	6.32 ± 0.297	3.29 ± 0.187
25	SBD-LDB-26	3.61 ± 0.135	2.09 ± 0.085
26	SBD-LDB-28	1.04 ± 0.13	1.93 ± 0.081
27	SBD-LDB-29	3.42 ± 0.186	2.84 ± 0.177

*ND: Not Detected; Data (Mean of triplicate value ± SD)

demonstrated that lignin-degrading bacterial isolates had LDI values ranging from 2.6 to 1.22, validating the results of the Lignin degradation index by lignin-degrading bacterial strains. Falade et al. (2017) assessed the lignin-degrading activity of bacterial strains using guaiacol decolorization and found that only 5 strains out of 30 displayed decolorization zone, which validates our current findings.

8. Ligninolytic enzyme activity assay

The quantification of ligninolytic enzymes viz. Manganese peroxidase enzyme and Laccase enzyme in the lignin-degrading bacteria were conducted further to understand the mechanism of their ligninolytic activities. The results of the Manganese peroxidase enzyme and Laccase enzyme were summarized in Fig. 1.

Fig. 1 shows the correlation between the percentage of KL and MB elimination and the bacterial enzymes (MnP and laccase). The lines in the graph below indicate the ligninolytic bacteria, while the columns stand in for the enzymes. The level of enzymatic activity was indicated by the colour of the tiles. The bacterial strains SBD-LDB-9, SBD-LDB-8, SBD-LDB-20, SBD-LDB-23, and SBD-LDB-25 that significantly reduce KL and MB were determined to have the highest enzymatic activity, as depicted in Fig. 1.

The highest Manganese peroxidase enzyme activity of $6322.314 \pm 0.034 \text{ U L}^{-1}$ was observed in the strain SBD-LDB-25 whereas the minimum activity of $2630.854 \pm 0.031 \text{ U L}^{-1}$ was observed in SBD-LDB-3 strain. In the case of Laccase enzyme, the maximum degradation activity was observed in SBD-LDB-23 strain of $1.510 \pm 0.017 \text{ U ml}^{-1}$ whereas minimum activity was reported in SBD-LDB-18

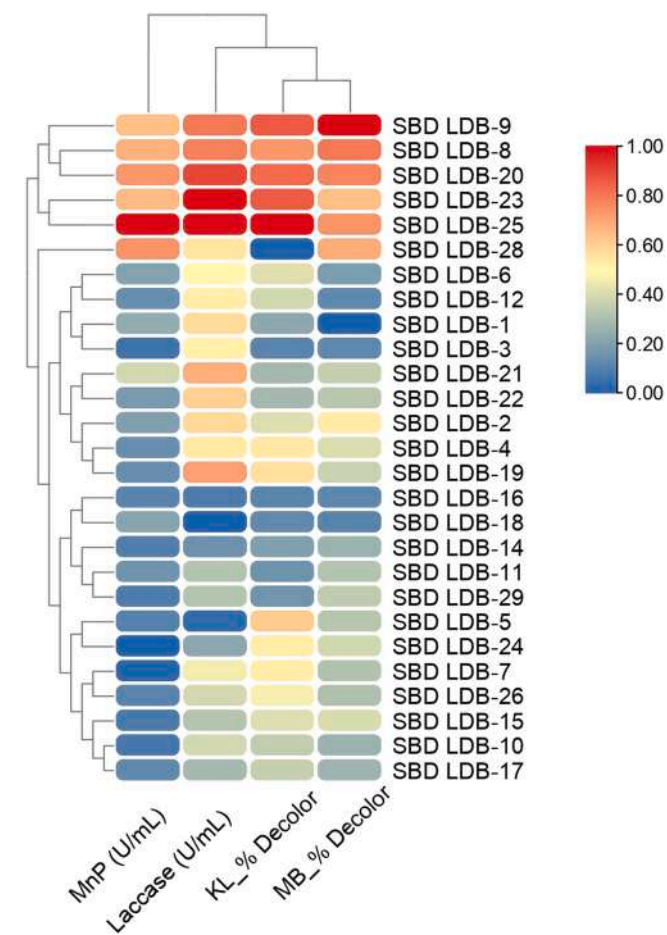


Fig. 1. Heatmap correlation analysis of the percentage of KL (Kraft Lignin) and MB (Methylene Blue) removed by several bacterial isolates producing the enzymes MnP and laccase.

strain of $0.825 \pm 0.026 \text{ U ml}^{-1}$. Shamseldin and Abdelkhalek (2015) studied Manganese peroxidase enzyme activities and reported that MnP activity was found as 1720 U L^{-1} and 1750 U L^{-1} after the third day whereas the Laccase enzymes were found as 810 U L^{-1} and 915 U L^{-1} after six days in two examined LDB strains. The enzyme activities reported by Shamseldin, Abdelkhalek (2015) were lower compared to the results obtained in the present studies. The results observed by Chen et al. (2012a) and Yang et al. (2017) were in close agreement with the result obtained in the present study. Chen et al. (2012b) revealed the maximum Manganese peroxidase activity was 3229.8 U L^{-1} on the 4th day and the highest Laccase activity of 1275 U L^{-1} was recorded at the 5th day of the growth of the bacteria. Yang et al. (2017) reported that the Laccase activity of most LDB increased significantly from 24 to 48 h, with a maximum of 2250 U L^{-1} in the bacterial strain H2 at 60 h incubation. In the case of the Manganese peroxidase enzyme, the highest activity of 1119 U L^{-1} was observed in strain J12 at 24 h.

8.1. Decolorization activity of bacteria on liquid MSM containing MB dye and Kraft lignin

The quantitative determination of the ligninolytic activities of the LDB was identified by measuring of percent decolorization of MSM-L broth medium supplemented with kraft lignin (0.5%) and Methylene blue indicator dye (50 mg/L) after 72hrs of incubation. All the strains showed significant activity and the results of the % degradation of Kraft lignin and methylene blue indicator dye were summarized in Table 3.

The data of the % decolorization is displayed in heat map graph format in Fig. 1. It is a method of condensing information, with the lines denoting the investigated ligninolytic bacteria and the columns denoting Kraft Lignin and Methylene Blue decolorization. The degree of the % decolorization is shown by the colored tiles. Fig. 1 demonstrates that the bacterial strains SBD-LDB-9, SBD-LDB-8, SBD-LDB-20, SBD-LDB-23, and SBD-LDB-25 achieved the highest % decolorization.

The maximum percent decolorization of $38.327 \pm 0.011\%$ was observed by the SBD-LDB-9 strain in MSM-L broth containing Kraft

Table 3
Quantitative determination of Ligninolytic activity of bacteria.

S.N.	Percent decolourisation		
	Strain Name	Kraft lignin (0.25%)	Methylene blue (50 mg/L)
1	SBD-LDB-1	19.566 ± 0.010	17.866 ± 0.013
2	SBD-LDB-2	21.025 ± 0.005	30.250 ± 0.016
3	SBD-LDB-3	23.587 ± 0.025	23.495 ± 0.018
4	SBD-LDB-4	19.771 ± 0.027	21.684 ± 0.012
5	SBD-LDB-5	19.809 ± 0.012	22.222 ± 0.017
6	SBD-LDB-6	24.429 ± 0.021	26.383 ± 0.015
7	SBD-LDB-7	23.419 ± 0.020	28.732 ± 0.012
8	SBD-LDB-8	37.298 ± 0.013	46.256 ± 0.020
9	SBD-LDB-9	38.327 ± 0.011	48.458 ± 0.015
10	SBD-LDB-10	24.317 ± 0.021	29.613 ± 0.007
11	SBD-LDB-11	20.819 ± 0.014	30.886 ± 0.016
12	SBD-LDB-12	30.134 ± 0.028	38.228 ± 0.017
13	SBD-LDB-14	22.409 ± 0.031	29.662 ± 0.019
14	SBD-LDB-15	19.0422 ± 0.012	21.390 ± 0.013
15	SBD-LDB-16	22.858 ± 0.011	23.201 ± 0.014
16	SBD-LDB-17	29.985 ± 0.012	44.542 ± 0.019
17	SBD-LDB-18	17.385 ± 0.015	22.663 ± 0.014
18	SBD-LDB-19	18.387 ± 0.011	30.299 ± 0.012
19	SBD-LDB-20	35.185 ± 0.030	49.633 ± 0.017
20	SBD-LDB-21	23.943 ± 0.016	29.075 ± 0.012
21	SBD-LDB-22	23.228 ± 0.007	32.795 ± 0.006
22	SBD-LDB-23	35.652 ± 0.005	46.941 ± 0.022
23	SBD-LDB-24	22.521 ± 0.019	31.082 ± 0.012
24	SBD-LDB-25	33.558 ± 0.017	47.969 ± 0.007
25	SBD-LDB-26	25.065 ± 0.009	39.452 ± 0.020
26	SBD-LDB-28	16.666 ± 0.009	26.258 ± 0.017
27	SBD-LDB-29	23.251 ± 0.014	30.299 ± 0.010

Data (Mean of triplicate value ± SD)

lignin whereas the minimum activity was observed in the SBD-LDB-28 strain with $16.666 \pm 0.009\%$ decolorization. A similar percent decolorization was observed in MSM-L broth containing Methylene blue dye and after 72 hrs incubation, the maximum percent decolorization ($49.633 \pm 0.017\%$) was observed in the SBD-LDB-20 strain whereas the minimum percent decolorization ($17.866 \pm 0.013\%$) was observed in SBD-LDB-1 strain. It has been speculated that the depolymerization of lignin polymers by bacterial ligninolytic systems, which consists of several enzymes secreted by these bacteria, is what causes the reduction in a color that results from lignin biodegradation. *Bacillus amyloliquefaciens* (SL-7) bacteria produced manganese peroxidase, lignin peroxidase, Laccase activity, and degraded 28.55% of tobacco straw lignin (Mei et al., 2020). Xiong et al. (2013) reported that *Panteoa* spp. strain Sd-1 effectively reduced lignin color (52.4%) after 4 days of incubation. The ligninolytic bacterial strain, *Bacillus velezensis*, was used by Verma et al. (2020) and found that under ideal conditions, this strain had a maximum capacity for KL decolorization and degradation of 56.16% and 40.39%, respectively. These findings were in close agreement with those of the current study.

9. FTIR analysis

The lignin-degrading bacterial isolates were evaluated using FT-IR to determine how they had altered the structural and chemical properties of kraft lignin (Fig. 2). Lignin degradation was evident from the FTIR spectra of untreated and treated kraft lignin using lignin degrading bacteria depicted discrete changes, especially in the FTIR absorbance range from 1350 to 1715 cm^{-1} correlated to the stretching of C=C bonds in the aromatic skeleton of lignin when incubated in the broth for 5 days (Wang et al., 2021). The C=C bonds in the aromatic skeleton of lignin are the primary targets of the ligninolytic enzymes, resulting in lignin structural depolymerization (Zeng et al., 2014). Further, the decrease in absorbance around wave number 3500 – 3000 cm^{-1} corresponds to –OH bonds in alcohol and phenol in lignin in treated samples also indicating lignin degradation (Khan et al., 2022). Kraft lignin's FTIR spectrum underwent significant changes at 3210 cm^{-1} (OH stretching

vibration), 2927 cm^{-1} (stretching vibration of C–H band in CH_2 , CH_3 , and CH_3O groups of the lignin structure), 2860 cm^{-1} (C–H stretching in aromatic methoxyl groups), 1715 cm^{-1} (C=O stretching), 1650 cm^{-1} (Absorbed O–H and conjugated C–O), 1635 cm^{-1} (C=C stretching vibration in benzene ring), 1580 cm^{-1} , 1511 cm^{-1} (attributed to the stretching vibration of aromatic rings), 1420 cm^{-1} (O– CH_3 stretching vibration), 1330 cm^{-1} (–CH stretching vibration), 1042 cm^{-1} (C–O vibrations) and 618 cm^{-1} (stretching vibrations of the C–S bond linked to the aromatic ring) (Kumar et al., 2015; Xu et al., 2018; Ma et al., 2021). The absorbance at 1335 cm^{-1} (S) significantly decreased during biodegradation, but the absorbance at 1275 cm^{-1} (G) barely changed. Significant differences between the FTIR spectra of the treated samples and the control samples showed that the lignin structure was largely destroyed by the different enzymes secreted by LDB used in the present study.

9.1. In vitro screening of lignin-degrading bacteria using rice straw bio-waste as substrate

Furthermore, research was conducted to determine the optimal strain for in vitro degradation of agricultural waste. The consistency of rice straw altered when the lignin content in the straw was broken down by lignin-degrading bacteria, as shown in Fig. 3. The results of the decomposition of rice straw by using lignin degrading bacteria were summarized in Table 4. In rice straw that had been exposed to lignin-degrading bacteria, the amount of lignin was substantially reduced after 20 days after inoculation compared to the control rice straw. Among all LDB strains, the maximum percent lignin degradation were obtained in the SBD-LDB-8 strain (52.86%) followed by SBD-LDB-25 (52.69%), and SBD-LDB-20 (48.01%) and SBD-LDB-9 (45.99%) whereas the minimum percent lignin degradation was observed in SBD-LDB-17 strain (17.98%).

In a comparison of three bacterial isolates for lignin degradation on rice straw, Bakar et al. (2018) found that the rice straw treated with the AMB1 bacterial strain had significantly less lignin, at 4.97% compared to the lignin content of the control which was 8.89 ± 1.0 . Similarly,

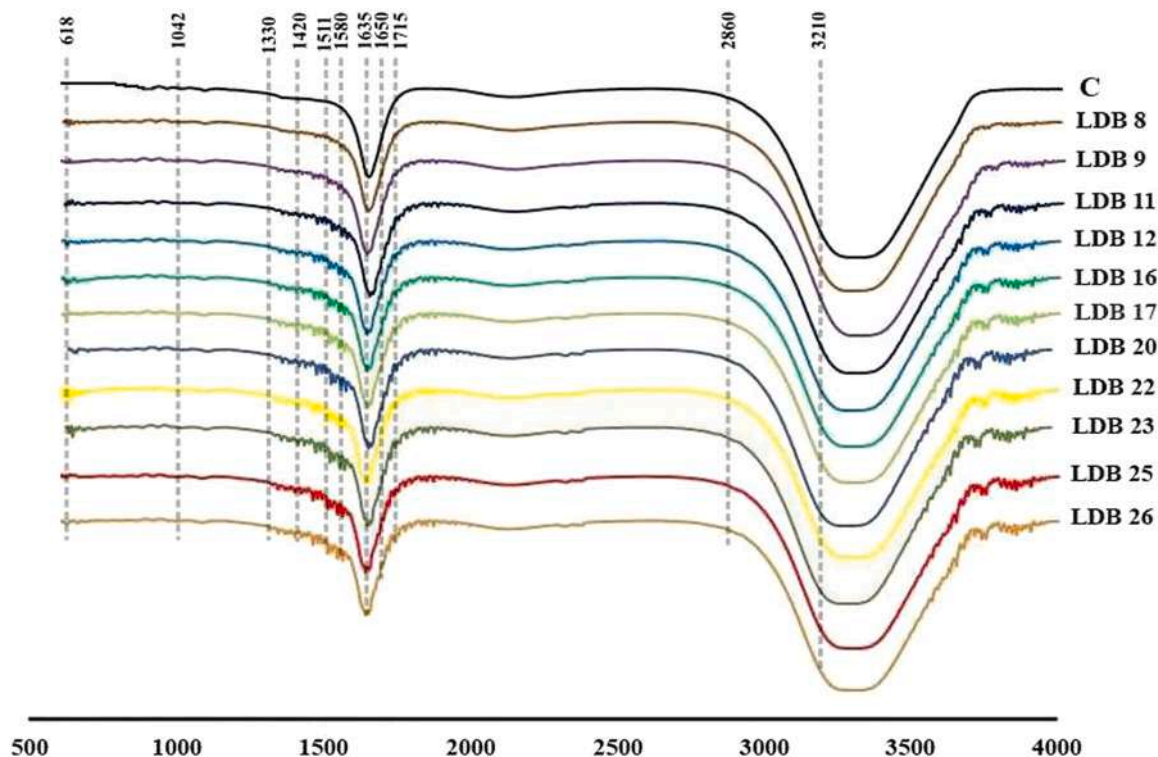


Fig. 2. FTIR spectrum of LDB treated and untreated kraft lignin.



Fig. 3. *In vitro* efficacy evaluation of lignin degrading bacteria for rice-straw degradation.

Table 4

Effect of effective lignin degrading bacteria pretreatment on the composition of rice straw.

Strain Name	ADF %*	ADL %* *	ASH %	Lignin%	% Lignin degradation
CONTROL	88.04	25.35	7	18.35 ± 0.014	100
SBD-LDB-8	68.43	13.98	5.3	8.65 ± 0.018	52.86
SBD-LDB-9	69.55	13.91	4	9.91 ± 0.016	45.99
SBD-LDB-11	76.03	18.73	4.6	14.06 ± 0.044	23.37
SBD-LDB-12	74.06	15.03	4	11.03 ± 0.027	39.89
SBD-LDB-16	75.44	16.55	4.6	11.08 ± 0.045	39.61
SBD-LDB-17	78.14	18.72	3.6	15.05 ± 0.023	17.98
SBD-LDB-20	72.46	13.87	4.3	9.54 ± 0.023	48.01
SBD-LDB-22	77.72	17.73	4.6	13.06 ± 0.015	28.82
SBD-LDB-23	69.42	13.57	3.6	9.91 ± 0.008	45.99
SBD-LDB-25	66.53	12.02	3.3	8.68 ± 0.038	52.69
SBD-LDB-26	76.16	16.78	4	12.78 ± 0.016	30.35

* Acid Detergent Lignin: Lignin+Ash (Data recorded after 21 days pretreatment)

* Acid Detergent Fiber (Cellulose+Hemi-cellulose+Lignin+Mineral);

Ochrobactrum oryzae BMP03 strain-treated rice straw's chemical makeup was investigated by Tsegaye et al. (2018) and reported that the BMP03 treatment degraded and mineralized 53.74% lignin after 14 days of pretreatment. According to Chandra et al. (2007), *Novosphingobium* sp. B-7 bacteria were responsible for 37% of the breakdown of Kraft lignin. Shi et al. (2017) found that after 7 days of pretreatment with the *Cupriavidus basilensis* B-8 bacterial strain, 41.5% of kraft lignin was eliminated, which was quite similar to the findings of the current study.

9.2. Effects of bio-pretreatment on the structure of the rice straw using SEM

The morphological modification of the rice straw that was treated by lignin-degrading bacterial isolates was analysed by scanning electron microscopy. The original rice straw displayed smooth, well-organized, and complete frameworks (Fig. 4). It was noticed that the surface was fairly smooth. It became fragmented and porous after being treated with lignin-degrading bacterial isolates. The rice straw developed some holes. After bacterial treatment, the rice straw's morphology showed that its linkages had been broken, and its lignin contents had been noticeably reduced. Various researchers observed the change in morphology of lignin using SEM which confirm the degradation of lignin visually (Xu et al., 2018; Ma et al., 2021). Dong et al. (2019) analyzes the lignin degradation by SEM technique and they observed that the microbial treated lignin sample became cracked and porous as compared to

ordered and intact structures of untreated lignin samples which further supports the observation in the present study.

9.3. Sequencing and phylogenetic analysis of 16 S rDNA of potent LDB isolates

Based on *in vitro* rice straw degradation efficacy, the comprehensive sequences of the 16 S rDNA genes of the most effective lignin-degrading bacterial strains were sequenced and examined using the nucleotide BLASTn programme. These strains were identified as LDB-8: *Enterobacter ludwigii* (MW264070), LDB-25: *Klebsiella variicola* (MW265009), LDB-20: *Rahnella aquatilis* (MW264333), LDB-9: *Bacillus paramycoides* (MW264994), and LDB-23: *Bacillus paramycoides* (MW423733) as shown in Fig. 5. Table 5 lists the molecular details and NCBI GeneBank accession number associated with these strains. Similar approach was adopted by Upadhyay et al. (2009, 2011) for identification of salt tolerant rhizobacterial isolates. Rahman et al. (2013) characterized lignin-degrading bacteria using 16 SrRNA gene sequencing analysis and identified the bacterial strains as *Bacillus* sp., *Ochrobactrum* sp., and *Leucobactersp.*, with 99% sequence similarity to the strains from NCBI-Gene bank databases. El-Hanafy et al. (2008) isolated two lignin-degrading bacterial strains from Egyptian soils and identified them as *Bacillus* sp. (EU344809) and *Bacillus subtilis* based on the partial 16 S rRNA sequencing (EU344808). From a decomposing empty fruit bunch of an oil palm, Riyadi et al. (2020) isolated and described a lignin-degrading bacterial strain. Based on 16S rDNA sequencing, the isolated strain was identified as *Streptomyces* sp. S6.

10. Conclusion

The current investigation was based on the isolation of 27 lignin-degrading bacteria from 12 conventional manures. These strains were strong in ligninolytic enzymes such laccase and MnP, which can degrade KL and MB. SBD-LDB-8, SBD-LDB-25, SBD-LDB-20, SBD-LDB-9, and SBD-LDB-23 were shown to be the best LDB isolates based on their *in vitro* lignin degradation capacity using rice straw as the substrate. SEM images indicating changes in surface morphological properties linked with lignin breakdown backed up this claim. Despite tremendous progress in the isolation and characterization of lignin-degrading microbes to date, appropriate and effective formulations for waste breakdown and biodegradation of synthetic dyes like MB must be developed. According to these results, the isolated LDB strains from the current study would make a good choice for lignin valorization. Therefore, more thorough research is needed to establish their capacity to degrade waste biomass on the ground and in certain environmental conditions.

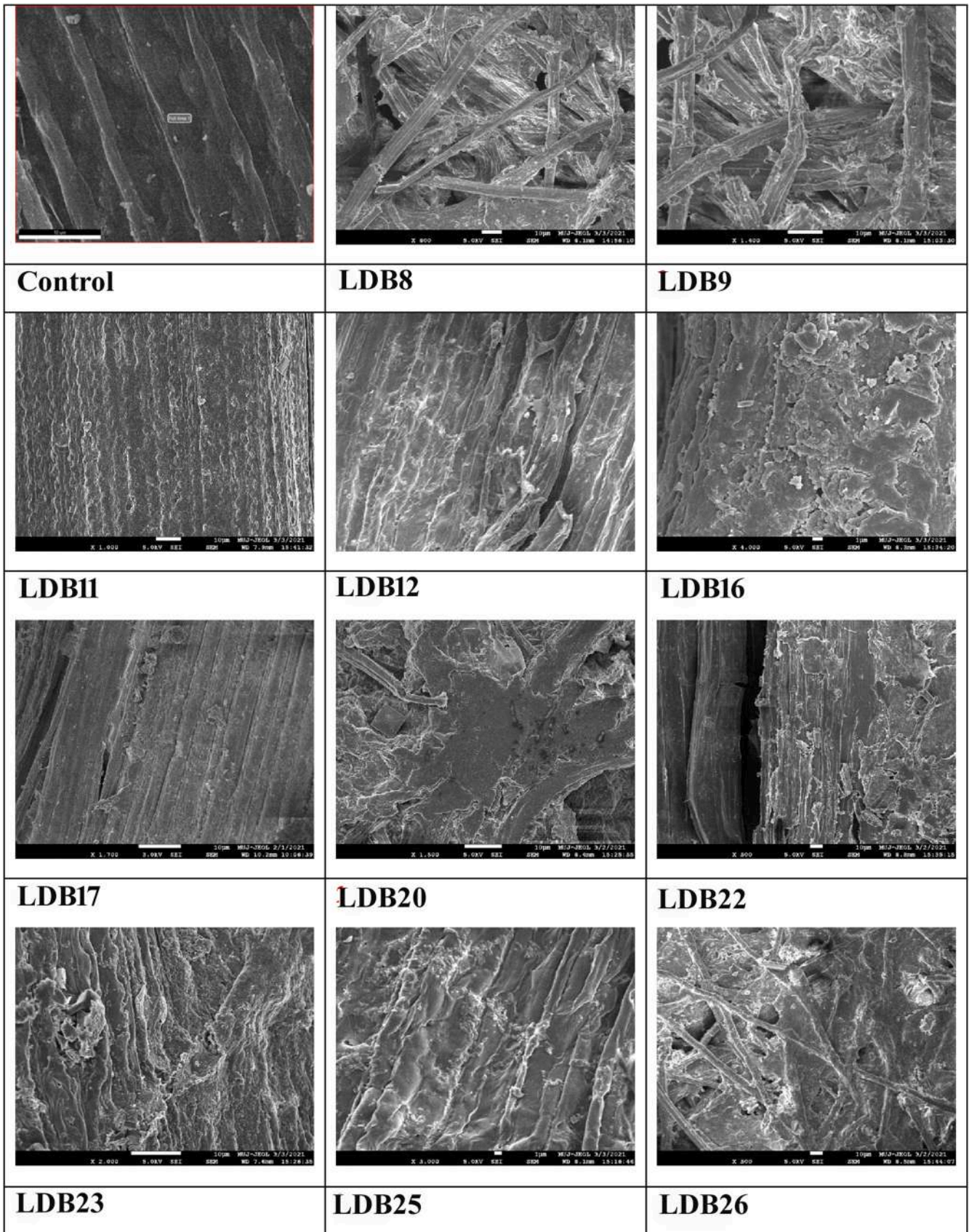


Fig. 4. Scanning electron micrographs of the control and LDB treated rice straw for 21 days.

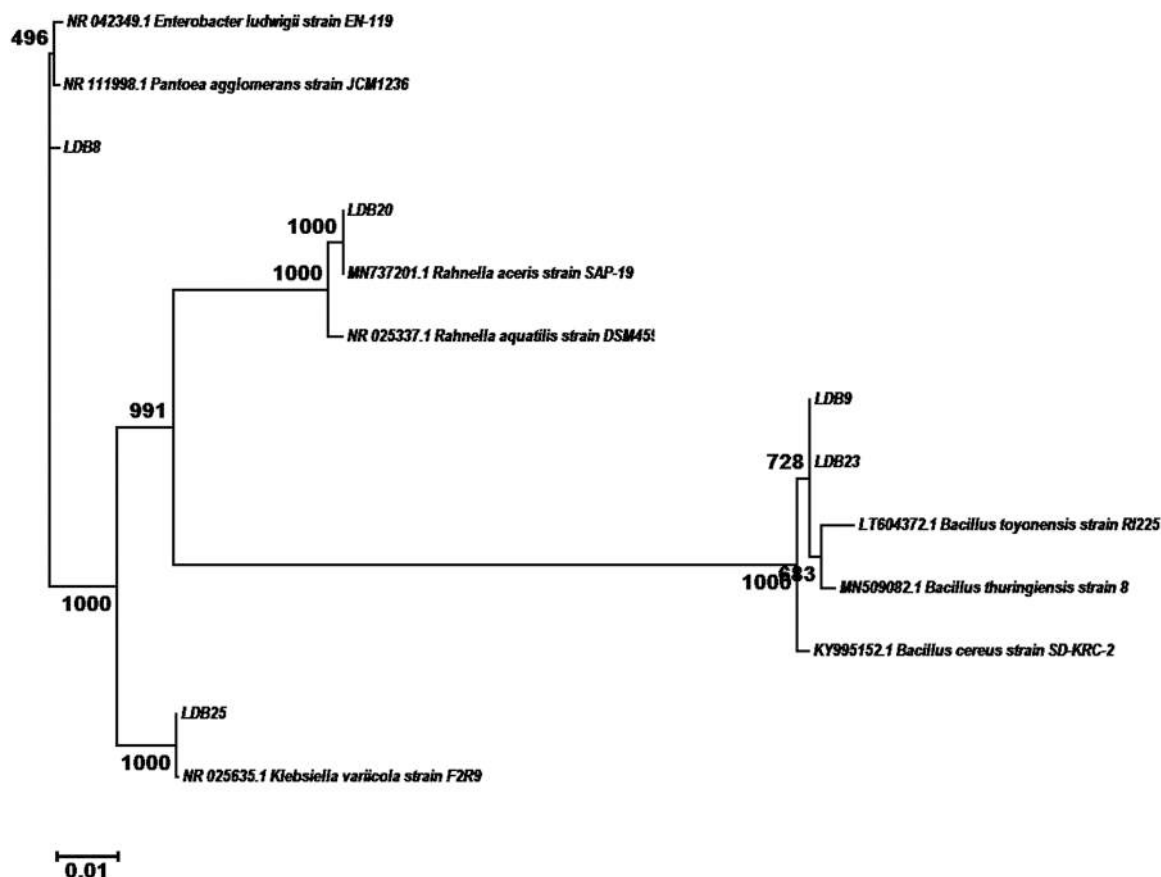


Fig. 5. Phylogenetic analysis of potent lignin degrading bacteria.

Table 5
Molecular identification of potent Lignin Degrading Bacteria.

Strains	Identification/ Accession number	Closest type strain			
		Molecular identity	Strain	Accession number	% Similarity/ Query Coverage
LBD-8	<i>Enterobacter ludwigii</i> / MW264070	<i>Enterobacter ludwigii</i>	EN-119	NR_042349.1	99.71/100
LDB-9	<i>Bacillus paramycooides</i> / MW264994	<i>Bacillus paramycooides</i>	MCCC 1A04098	NR_157734.1	99.00/99.09
LBD-20	<i>Rahnella aquatilis</i> / MW264333	<i>Rahnella aquatilis</i>	DSM 4594	NR_025337.1	99.57/100
LDB-23	<i>Bacillus paramycooides</i> / MW423733	<i>Bacillus paramycooides</i>	MCCC 1A04098	NR_157734.1	99.00/99.09
LBD-25	<i>Klebsiella variicola</i> / MW265009	<i>Klebsiella variicola</i>	F2R9	NR_025635.1	99/100

CRedit authorship contribution statement

DJ conceived and designed the experiments; JKN, AAB performed laboratory experiments; AS performed FTIR and SEM analysis; DJ, AAB, SKU, and SRM wrote the manuscript. All authors read and approved the final manuscript.

Declaration of Competing Interest

The authors declare that they have no known competing financial interests or personal relationships that could have appeared to influence the work reported in this paper.

Data Availability

Data will be made available on request.

Acknowledgments

The financial assistance from the All India Network Project on soil biodiversity and biofertilizers is highly acknowledged.

Disclosure statement

No potential conflict of interest was reported by the authors.

References

- Altschul, S.F., Gish, W., Miller, W., Myers, E.W., Lipman, D.J., 1990. Basic local alignment search tool. *J. Mol. Biol.* 215 (3), 403–410.
- Atalla, M.M., Zeinab, H.K., Eman, R.H., Amani, A.Y., Abeer, A.A.E.A., 2010. Screening of some marine-derived fungal isolates for lignin degrading enzymes (LDEs) production. *Agric. Biol. J. North Am.* 1 (4), 591–599.
- Atiweh, G., Parrish, C.C., Banoub, J., Le, T.T., 2022. Lignin degradation by microorganisms: a review. *Biotechnol. Prog.* 38 (2), e3226 <https://doi.org/10.1002/btpr.3226>.

- Bakar, N.A.A., Rahman, M.H.A., Shakri, N.A., Bakar, S.A., Hamid, A.A., 2018. Preliminary study on rice straw degradation using microbial inoculant under shake flask condition. *Afr. J. Biotechnol.* 17 (49), 1377–1382.
- Bandounas, L., Wierckx, N.J., de Winde, J.H., Ruijsenaars, H.J., 2011. Isolation and characterization of novel bacterial strains exhibiting ligninolytic potential. *BMC Biotechnol.* 11 (1), 94.
- Beckham, G.T., Johnson, C.W., Karp, E.M., Salvachua, D., Vardon, D.R., 2016. Opportunities and challenges in biological lignin valorization. *Curr. Opin. Biotechnol.* 42, 40–53.
- Bharti, V., Vikrant, K., Goswami, M., Tiwari, H., Sonwani, R.K., Lee, J., Tsang, D.C.W., Kim, K.H., Saeed, M., Kumar, S., et al., 2019. Biodegradation of methylene blue dye in a batch and continuous mode using biochar as packing media. *Environ. Res.* 1, 356–364.
- Bourbonnais, R., Paice, M.G., Reid, I.D., Lanthier, P., Yaguchi, M., 1995. Lignin oxidation by laccase isozymes from *Trametes versicolor* and role of the mediator 2,2-azino-bis(3-ethylbenzothiazoline-6-sulfonate) in kraft lignin depolymerization. *Appl. Environ. Microbiol.* 61, 1876–1880.
- Brink, D.P., Ravi, K., Lidén, G., et al., 2019. Mapping the diversity of microbial lignin catabolism: experiences from the eLignin database. *Appl. Microbiol. Biotechnol.* 103, 3979–4002. <https://doi.org/10.1007/s00253-019-09692-4>.
- Chandra, R., Raj, A., Purohit, H.J., Kapley, A., 2007. Characterisation and optimisation of three potential aerobic bacterial strains for kraft lignin degradation from pulp paper waste. *Chemosphere* 67 (4), 839–846.
- Chen, X., Hu, Y., Feng, S., et al., 2018. Lignin and cellulose dynamics with straw incorporation in two contrasting cropping soils. *Sci. Rep.* 8, 1633. <https://doi.org/10.1038/s41598-018-20134-5>.
- Chen, Y.H., Chai, L.Y., Zhu, Y.H., Yang, Z.H., Zheng, Y., Zhang, H., 2012a. Biodegradation of Kraft lignin by a bacterial strain *Comamonas* sp. B-9 isolated from eroded bamboo slips. *J. Appl. Microbiol.* 112 (5), 900–906.
- Chen, Y.H., Chai, L.Y., Tang, C., Yang, Z.H., Zheng, Y., Shi, Y., Zhang, H., 2012b. Kraft lignin biodegradation by *Novosphingobium* sp. B-7 and analysis of the degradation process. *Bioresour. Technol.* 123, 682–685.
- da Costa, R.R., Hu, H., Pilgaard, B., Vreeburg, S.M.E., Schückel, J., Pedersen, K.S.K., Kracún, S.K., Busk, P.K., Harholt, J., Sapountzis, P., Lange, L., Aanen, D.K., Poulsen, M., 2018. Enzyme activities at different stages of plant biomass decomposition in three species of fungus-growing termites. *Appl. Environ. Microbiol.* 84 (5), e01815–e01817. <https://doi.org/10.1128/AEM.01815-17>.
- Couger, M.B., Graham, C., Fathepure, B.Z., 2020. Genome sequence of lignin-degrading *Arthrobacter* sp. Strain RT-1, isolated from termite gut and rumen fluid. *Microbiol. Resour. Annu.* 9, 3.
- Dong, S.-J., Zhang, B.-X., Wang, F.-L., Xin, L., Gao, Y.-F., Ding, W., He, X.-M., Liu, D., Hu, X.-M., 2019. Efficient lignin degradation of corn stalk by *Trametes* with high Laccase activity and Enzymatic stability in salt and ionic liquid. *BioResources* 14 (3), 5339–5354.
- El-Hanafy, A.A., Abd-Elsalam, H.E., Hafez, E.E., 2008. Molecular characterization of two native Egyptian ligninolytic bacterial strains. *J. Appl. Sci. Res.* 4 (10), 1291–1296.
- Eslami, H., Khavivad, S.S., Salehi, F., Khosravi, R., Ali Fallahzadeh, R., Peirovi, R., Sadeghi, S., 2017. Biodegradation of methylene blue from aqueous solution by bacteria isolated from contaminated soil. *J. Adv. Environ. Health Res.* 5, 10–15.
- Faisal, U.H., Sabri, N.S.A., Yusof, N., Tahir, A.A., Said, N.N.M., Riyadi, F.A., Akhir, F.N.M., Othman, N., Hara, H., 2021. Draft genome sequence of lignin-degrading *Agrobacterium* sp. strain S2, isolated from a decaying oil palm empty fruit bunch. *Microbiol. Resour. Annu.* 10, e00259–21. <https://doi.org/10.1128/MRA.00259-21>.
- Falade, A.O., Eyisi, O.A., Mabinya, L.V., Nwodo, U.U., Okoh, A.I., 2017. Peroxidase production and ligninolytic potentials of fresh water bacteria *Raoultella ornithinolytica* and *Ensifer adhaerens*. *Biotechnol. Rep.* 16, 12–17.
- Fang, X., Li, Q., Lin, Y., Lin, X., Dai, Y., Guo, Z., Pan, D., 2018. Screening of a microbial consortium for selective degradation of lignin from tree trimmings. *Bioresour. Technol.* 254, 247–255.
- Goodman, B.A., 2020. Utilization of waste straw and husks from rice production: a review. *J. Bioresour. Bioprod.* 5 (3), 143–162. <https://doi.org/10.1016/j.jobab.2020.07.001>.
- Gupta, J., Kumari, M., Mishra, A., Swati, Akram, M., Thakur, I.S., 2022. Agro-forestry waste management-A review. *Chemosphere* 287 (3), 132321. <https://doi.org/10.1016/j.chemosphere.2021.132321>.
- Haile, A., Gelebo, G.G., Tesfaye, T., Mengie, W., Mebrate, M.A., Abuhay, A., Limeneh, D. Y., 2021. Pulp and paper mill wastes: utilizations and prospects for high value-added biomaterials. *Bioresour. Bioprocess* 8, 35. <https://doi.org/10.1186/s40643-021-00385-3>.
- Haq, I.U., Hillmann, B., Moran, M., et al., 2022. Bacterial communities associated with wood rot fungi that use distinct decomposition mechanisms. *ISME COMMUN* 2, 26. <https://doi.org/10.1038/s43705-022-00108-5>.
- Haque, M.M., Haque, M.A., Mosharaf, M.K., Marcus, P.K., 2021. Decolorization, degradation and detoxification of carcinogenic sulfonated azo dye methyl orange by newly developed biofilm consortia. *Saudi. J. Biol. Sci.* 28, 793–804.
- Harith, Z.T., Ibrahim, N.A., Yusoff, N., 2014. Isolation and identification of locally isolated lignin degrading bacteria. *J. Sustain. Sci. Manag* 9 (2), 114–118.
- Hasanin, M.S., Mostafa, A.M., Mwafy, E.A., Darwesh, O.M., 2018. Eco-friendly cellulose nano fibers via first reported Egyptian *Humicolafulvicoaratra* X4: Isolation and characterization. *Environ. Nanotechnol. Monit. Manag.* 10, 409–418.
- Jain, D., Ravina, Bhojiya, A.A., Chauhan, S., Rajpurohit, D., Mohanty, S.R., 2021. Polyphasic characterization of plant growth promoting cellulose degrading bacteria isolated from organic manures. *Curr. Microbiol.* 78, 739–748. <https://doi.org/10.1007/s00284-020-02342-3>.
- Janusz, G., Pawlik, A., Sulej, J., Swiderska-Burek, U., Jarosz-Wilkolazka, A., Paszczynski, A., 2017. Lignin degradation: microorganisms, enzymes involved, genomes analysis and evolution. *FEMS Microbiol. Rev.* 41 (6), 941–962.
- Jimenez, D.J., Chaib, De Mares, M., Salles, J.F., 2018. Temporal expression dynamics of plant biomass-degrading enzymes by a synthetic bacterial consortium growing on sugarcane bagasse. *Front Microbiol* 9, 299. <https://doi.org/10.3389/fmicb.2018.00299>.
- Karim, M.E., Dhar, K., Hossain, M.T., 2018. Decolorization of textile reactive dyes by bacterial monoculture and consortium screened from textile dyeing effluent. *J. Genet. Eng. Biotechnol.* 16, 375–380.
- Khan, S.I., Zarin, A., Ahmed, S., Hasan, F., Belduz, A.O., Çanakçı, S., Khan, S., Badshah, M., Farman, M., Shah, A.A., 2022. Degradation of lignin by *Bacillus altitudinis* SL7 isolated from pulp and paper mill effluent. *Water Sci. Technol.* 8 (1), 420. <https://doi.org/10.2166/wst.2021.610>.
- Kishor, R., Purchase, D., Saratale, G.D., Saratale, R.G., Ferreira, L.F.R., Bilal, M., Chandra, R., Bharagava, R.N., 2021a. Ecotoxicological and health concerns of persistent coloring pollutants of textile industry wastewater and treatment approaches for environmental safety. *J. Environ. Chem. Eng.* 9, 105012.
- Kishor, R., Saratale, G.D., Saratale, R.G., Ferreira, L.F.R., Bilal, M., Iqbal, H.M.N., Bharagava, R.N., 2021b. Efficient degradation and detoxification of methylene blue dye by a newly isolated ligninolytic enzyme producing bacterium *Bacillus AlbusMW407057*. *Coll. Surf. B Biointerfaces*, 111947. <https://doi.org/10.1016/j.colsurfb.2021.111947>.
- Kumar, A., Chandra, R., 2020. Ligninolytic enzymes and its mechanisms for degradation of lignocellulosic waste in environment. *Heliyon* 6 (2), e03170. <https://doi.org/10.1016/j.heliyon.2020.e03170>.
- Kumar, M., Singh, J., Singh, M.K., Singhal, A., Thakur, I.S., 2015. Investigating the degradation process of kraft lignin by β -proteobacterium, *Pandoraea* sp. ISTRKB. *Environ. Sci. Pollut. Res.* 22, 15690–15702. <https://doi.org/10.1007/s11356-015-4771-5>.
- Lee, S., Kang, M., Bae, J.-H., Sohn, J.-H., Sung, B.H., 2019. Bacterial valorization of lignin: strains, enzymes, conversion pathways, biosensors, and perspectives. *Front. Bioeng. Biotechnol.* 7, 209. <https://doi.org/10.3389/fbioe.2019.00209>.
- Li, X., Shi, Y., Kong, W., Wei, J., Song, W., Wang, S., 2022. Improving enzymatic hydrolysis of lignocellulosic biomass by bio-coordinated physicochemical pretreatment—A review. *Energy Rep.* 8, 696–709. <https://doi.org/10.1016/j.egyr.2021.12.015>.
- Ma, J., Li, Q., Wu, Y., Yue, H., Zhang, Y., Zhang, J., Shi, M., Wang, S., Liu, G.-Q., 2021. Elucidation of ligninolysis mechanism of a newly isolated white-rot basidiomycete *Trametes hirsute* X-13. *Biotechnol. Biofuels.* 14, 189. <https://doi.org/10.1186/s13068-021-02040-7>.
- Malode, S.J., Prabhu, K.K., Mascarenhas, R.J., Shetti, N.P., Aminabhavi, T.M., 2021. Recent advances and viability in biofuel production. *Energy Convers. Manag.* X 10, 100070. <https://doi.org/10.1016/j.ecmc.2020.100070>.
- McCarthy, A.J., Broda, P., 1984. Screening for lignin-degrading actinomycetes and characterization of their activity against [¹⁴C] lignin-labelled wheat lignocellulose. *Microbiology* 130 (11), 2905–2913.
- Mei, J., Shen, X., Gang, L., Xu, H., Wu, F., Sheng, L., 2020. A novel lignin degradation bacteria-Bacillus amyloliquefaciens SL-7 used to degrade straw lignin efficiently. *Bioresour. Technol.* 310, 123445. <https://doi.org/10.1016/j.biortech.2020.123445>.
- Nahrowi, B., Susilowati, A., Setyaningsih, R., 2018. Screening and identification of lignolytic bacteria from the forest at eastern slope of Lawu Mountain. *AIP Conf. Proc.* 2002 (1), 020–042. <https://doi.org/10.1063/1.5050138>.
- Ogunlaja, A., Nwankwo, I.N., Omaliko, M.E., Olukanni, O.D., 2020. Biodegradation of Methylene Blue as an evidence of synthetic dyes mineralization during textile effluent biotreatment by *Acinetobacter pittii*. *Environ. Process.* 7, 931–947.
- Pham, V.H.T., Kim, J., Chang, S., Chung, W., 2022. Biodegradation of methylene blue using a novel lignin peroxidase enzyme producing bacteria, named *Bacillus* sp. React3, as a promising candidate for dye-contaminated wastewater treatment. *Fermentation* 8, 190. <https://doi.org/10.3390/fermentation8050190>.
- Rahman, N.H.A., Abd Aziz, S., Hassan, M.A., 2013. Production of ligninolytic enzymes by newly isolated bacteria from palm oil plantation soils. *Bio Resour.* 8 (4), 6136–6150.
- Riyadi, F.A., Tahir, A.A., Yusof, N., Sabri, N.S.A., Noor, M.J.M.M., Akhir, F.N.M., Zakaria, Z., Hara, H., 2020. Enzymatic and genetic characterization of lignin depolymerization by *Streptomyces* sp. S6 isolated from a tropical environment. *Sci. Rep.* 10, 7813. <https://doi.org/10.1038/s41598-020-64817-4>.
- Sani, R.K., Banerjee, U.C., 1999. Decolorization of triphenylmethane dyes and textile and dye-stuff effluent by *Kurthia* sp. *Enzym. Microb. Technol.* 24 (7), 433–437.
- Saratale, R.G., Saratale, G.D., Kalyani, D.C., Chang, J.S., Govindwar, S.P., 2009. Enhanced decolorization and biodegradation of textile azo dye Scarlet R by using developed bacterial consortium-GR. *Bioresour. Technol.* 100 (9), 2493–2500.
- Shamseldin, A., Abdelkhalak, A.A., 2015. Isolation and identification of newly effective bacterial strains exhibiting great ability of lignin and Rice straw biodegradation. *Int. J. Curr. Microbiol. Appl. Sci.* 4 (6), 1039–1049.
- Sharif-Yazdi, M.K., Azimi, C., Khalili, M.B., 2001. Isolation and identification of bacteria present in the activated sludge unit, in the treatment of industrial waste water. *Iran. J. Public Health* 91–94.
- Shi, Y., Yan, X., Li, Q., Wang, X., Xie, S., Chai, L., Yuan, J., 2017. Directed bioconversion of Kraft lignin to polyhydroxy alkanolate by *Cupriavidusbasilensis* B-8 without any pretreatment. *Process Biochem.* 52, 238–242.
- Singh, R., Kumar, M., Mittal, A., Mehta, P.K., 2017. Microbial metabolites in nutrition, healthcare and agriculture. *3 Biotech* 7 (1), 15. <https://doi.org/10.1007/s13205-016-0586-4>.
- Tamura, K., Stecher, G., Peterson, D., Filipiński, A., Kumar, S., 2013. MEGA6: molecular evolutionary genetics analysis version 6.0. *Mol. Biol. Evol.* 30 (12), 2725–2729.
- Thimmaiah, S.K., 2009. Standard Methods Of Biochemical Analysis. Kalyani Publishers.

- Thompson, J.D., Higgins, D.G., Gibson, J., 1994. CLUSTAL W: improving the sensitivity of progressive multiple sequence alignment through sequence weighting, position-specific gap penalties and weight matrix choice. *Nucleic Acid. Res* 22 (22), 4673–4680.
- Tsegaye, B., Balomajumder, C., Roy, P., 2018. Biodegradation of wheat straw by *Ochrobactrumoryzae* BMP03 and *Bacillus* sp. BMP01 bacteria to enhance biofuel production by increasing total reducing sugars yield. *Environ. Sci. Pollut. Res.* 25 (30), 30585–30596.
- Upadhyay, S.K., Singh, D.P., Saikia, R., 2009. Genetic diversity of plant growth promoting rhizobacteria isolated from rhizospheric soil of wheat under saline condition. *Curr. Micro* 59, 489–496. <https://doi.org/10.1007/s00284-009-9464-1>.
- Upadhyay, S.K., Singh, J.S., Singh, D.P., 2011. Exopolysaccharide-producing plant growth-promoting rhizobacteria under salinity condition. *Pedosphere* 21, 214–222. [https://doi.org/10.1016/S1002-0160\(11\)60120-3](https://doi.org/10.1016/S1002-0160(11)60120-3).
- Verma, M., Ekka, A., Mohapatra, T., Ghosh, P., 2020. Optimization of kraft lignin decolorization and degradation by bacterial strain *Bacillus velezensis* using response surface methodology. *J. Environ. Chem. Eng.* 8 (5), 104–270.
- Wang, M., Dessie, W., Li, H., 2021. Chemically modified lignin: correlation between structure and biodegradability. *J. Renew. Mater.* 9, 2119.
- Wu, Z., Peng, K., Zhang, Y., Wang, M., Yong, C., Chen, L., Qu, P., Huang, H., Sun, E., Pan, M., 2022. Lignocellulose dissociation with biological pretreatment towards the biochemical platform: a review. *Mater. Today Bio* 16, 100445. <https://doi.org/10.1016/j.mtbio.2022.100445>.
- Xiong, X.Q., Liao, H.D., Ma, J.S., Liu, X.M., Zhang, L.Y., Shi, X.W., Yang, X.L., Lu, X.N., Zhu, Y.H., 2013. Isolation of a rice endophytic bacterium, *Pantoea* sp. S d-1, with ligninolytic activity and characterization of its rice straw degradation ability. *Lett. Appl. Microbiol.* 58 (2), 123–129.
- Xu, Z., Qin, L., Cai, M., Hua, W., Jin, M., 2018. Biodegradation of kraft lignin by newly isolated *Klebsiella pneumoniae*, *Pseudomonas putida*, and *Ochrobactrum tritici* strains. *Environ. Sci. Pollut. Res.* 25, 14171–14181. <https://doi.org/10.1007/s11356-018-1633-y>.
- Yang, C.X., Wang, T., Gao, L.N., Yin, H.J., Lu, X., 2017. Isolation, identification and characterization of lignin-degrading bacteria from Qinling, China. *J. Appl. Microbiol.* 123 (6), 1447–1460.
- Yu, G., Wen, X., Li, R., Qian, Y., 2009. In vitro degradation of a reactive azo dye by crude ligninolytic enzymes from non immersed liquid culture of *Phanerochaete chrysosporium*. *Process Biochem.* 41 (9), 1987–1993.
- Zeng, Y., Zhao, S., Yang, S., Ding, S.Y., 2014. Lignin plays a negative role in the biochemical process for producing lignocellulosic biofuels. *Curr. Opin. Biotechnol.* 27, 98–45.
- Zhang, W., Ren, X., Lei, Q., Wang, L., 2021. Screening and comparison of lignin degradation microbial consortia from wooden antiques. *Molecules* 26, 2862 <https://doi.org/10.3390/molecules26102862>.



Comparative evaluation of native *Trichoderma* species from groundnut rhizosphere against stem rot caused by *Sclerotium rolfsii* Sacc.

M. Raja^{1,4} · Rakesh Kumar Sharma¹ · Prashant Prakash Jambhulkar² · R. Thava Prakasa Pandian³ · Pratibha Sharma⁴

Received: 12 November 2022 / Revised: 20 January 2023 / Accepted: 27 February 2023
© Indian Phytopathological Society 2023

Abstract

Sclerotium rolfsii Sacc. is one of the important soil borne pathogen causing stem rot of groundnut prevalent in all growing area worldwide. The present study aimed on the identification of native *Trichoderma* isolates, and its efficacy against the stem rot pathogen in groundnut at field level. Thirty-five isolates of *Trichoderma* spp. isolated from the groundnut rhizosphere were comparatively evaluated for their biocontrol potential against *S. rolfsii* Sacc. and growth promoting traits in groundnut. The morphological studies of the 35 isolates were supported molecularly by amplifying of ITS region and classified into four species namely, *T. asperellum*, *T. citrinoviride*, *T. longibrachiatum* and *T. harzianum* which were further subjected to biocontrol efficacy tests. The highly efficient representative isolates namely, *T. harzianum* Thar23, *T. asperellum* Tasp49, *T. longibrachiatum* Tlongi5 and *T. citrinoviride* Tcitr2 were evaluated to produce lytic enzymes and growth promoting traits. The comparative study of these isolates revealed that, *T. harzianum* Thar23 produced significant ($P < 0.05$) amount of lytic enzymes viz., chitinase (31.36 U/ml), β 1, 3 glucanase (4.1 U/ml) and protease (2.76 U/ml). *T. harzianum* Thar23 promotes plant growth traits namely germination efficacy (31.48%), increase in the shoot length (42%) and root length (42.43%), improved vigor index, and increased relative water content (25.56%). Soil application, seed treatment and drenching with the powder formulation of Thar23 in field for the years 2019 and 2020 significantly ($P < 0.05$) reduced stem rot disease incidence to 59.45% and 53.79% and increased pod yield to 2.85 t/ha and 2.68 t/ha respectively. *T. harzianum* isolate Thar23 will help the groundnut growers for eco-friendly management of stem rot disease and increased yield.

Keywords Groundnut · Lytic enzymes · *S. rolfsii* · Stem rot · *Trichoderma* spp.

Introduction

Groundnut (*Arachis hypogaea* L.) is an important food and oil seed crop due to its high protein and oil content. Several biotic and abiotic factors are responsible for dismal

productivity. Diseases like stem rot, collar rot, root rot, leaf spot, bud necrosis, etc., are critical. Stem rot is also known as sclerotium blight caused by soil borne fungi *S. rolfsii* causes yield loss over 20–25 percent (Annual Report 2015–16). Under warm and high moisture conditions, white mycelium spread over the plant debris, soil and infect the host. The dark brown sclerotia of the pathogen are hard, spherical and 0.5–1.5 mm in size often found in the infected are of host and soil (Aycock 1966). Though fungicides are effective against pathogens, but they cause adverse effect on the environment thus can be replaced by biocontrol agents.

Trichoderma spp. (Teleomorph: *Hypocrea*) is an omnipresent ascomycetous fungus known for its biocontrol and industrial properties. This fungi were named *Trichoderma* in 1794 (Persoon 1794) and years later in 1865, the sexual stage *Hypocrea* species was suggested (Tulasne and Tulasne 1865). Diverse species of *Trichoderma* namely, *T. harzianum*, *T. asperellum*, *T. viride*, *T. virens*, *T. hamatum*

✉ Pratibha Sharma
psharma032003@yahoo.co.in

¹ Department of Biosciences, Manipal University Jaipur, Dehmi Kalan, Jaipur, Rajasthan 303007, India

² Department of Plant Pathology, Rani Lakshmi Bai Central Agricultural University, Jhansi, Uttar Pradesh 284003, India

³ Division of Plant Protection, ICAR-Central Plantation Crops Research Institute, Regional Station, Vittal, Karnataka 574 243, India

⁴ Department of Plant Pathology, Sri Karan Narendra Agriculture University, Jobner, Jaipur, Rajasthan 303328, India

and *T. atroviride* have been reported as biocontrol agents. *T. reesei*, *T. parareesei* and *T. longibrachiatum* are known for industrial enzyme production. *Trichoderma* species are widely present in the soil rhizosphere and documented for symbiotic relationship with the host roots. Due to the importance of the application of *Trichoderma* spp. as biocontrol agent in field condition, it is necessary to explore its biogeography. There are different studies conducted by the researchers to decipher the diversity of the native *Trichoderma* spp. and its application against major plant pathogens at national (Kumar et al. 2012; Agrawal and Kotasthane 2012; Devi et al. 2021; Manzar et al. 2021; Jambhulkar et al. 2022) and global (Li et al. 2016; Boat et al. 2020; Ma et al. 2020; Nofal et al. 2021). However, there is a need to explore the diversity of the native species at groundnut growing area of Jaipur, a semi-arid eastern plain zone of Rajasthan (Agro-climatic Zone- III-A), India.

There are various biocontrol mechanisms viz., mycoparasitism, antibiosis, induced systemic resistance in *Trichoderma* spp. and also known for production of many lytic enzymes viz., chitinases, glucanases, xylanase and proteases etc., as their primary weapons against the fungal pathogens (Sharma et al. 2014) and induce the systemic defence response by activating defence enzymes like peroxidases (PODs), polyphenol oxidases (PPO) and phenylalanine ammonia lyase (PAL) (Malolepsza et al. 2017). Plant growth promotion is crucial component of *Trichoderma* spp. which helps in improvement of plant growth in terms of increased plant biomass, root and shoot length and grain yield. *Trichoderma* colonizes fully on root tissues and triggers various mechanisms which induce plant growth promotion, facilitate nutrient uptake, induce plant defence mechanisms, helps in rhizosphere construction, increase carbohydrate metabolism, induce of phytohormones, root exudates and photosynthesis in host (Sallam et al. 2019). Among the genus of *Trichoderma* spp., *T. harzianum* is the most researched biocontrol species followed by others such as *T. viride*, *T. asperellum*, *T. hamatum*, *T. virens* and *T. koningii* (Keswani et al. 2014). Species like *T. longibrachiatum* and *T. citrinoviride* needs to be studied for its biocontrol and plant growth promoting capabilities. Therefore, the comparative evaluation of biocontrol efficacy and plant growth promoting traits of native isolates of *Trichoderma* spp. will be helpful in the characterization of biocontrol control agents and potential strains can be utilized at field conditions.

In the present study, we have isolated and characterized native isolates of *Trichoderma* from groundnut rhizosphere and potent isolates were comparatively evaluated to assess biocontrol and plant growth promoting potential against groundnut stem rot pathogen *S. rolfsii* under field conditions.

Materials and methods

Collection and isolation of *Trichoderma* isolates

The 60 rhizospheric soil samples were collected from groundnut growing areas of Jaipur (Agro-climatic Zone- III-A), a semi-arid eastern plain zone of Rajasthan, India. The longitude and latitude of collection locations were recorded and are given Table 1. For the isolation of *Trichoderma* spp., the rhizospheric soil samples were serially diluted on *Trichoderma* selective medium (TSM) (Elad et al. 1981) and incubated at $28 \pm 1 \text{ }^\circ\text{C}$ for 4 days. The newly emerging mycelia of fungal colonies were subcultured to fresh potato dextrose agar (PDA) plates and incubated at $28 \pm 1 \text{ }^\circ\text{C}$ for 7 days and maintained in potato dextrose agar (PDA) slants at $4 \text{ }^\circ\text{C}$ for further use in experiment. Culture of *S. rolfsii* was available at Department of Plant Pathology, SKN Agriculture University, Jobner- Jaipur.

Identification of *Trichoderma* isolates

Morphological identification

The purified 35 isolates were identified based on the different morphological characters viz., cultural characters like colour, growth and texture, microscopic features branching of conidiophores, phialides disposition, size and shape of conidia were identified based on the Rifai (1969), Bissett (1984) and Samuels et al. (1999).

Molecular identification

Actively growing *Trichoderma* isolates (5 mm disc) were inoculated into 50 mL potato dextrose broth (PDB) (HIMEDIA Labs, India) and incubated at $28 \pm 2 \text{ }^\circ\text{C}$ for 5–6 days at 180 rpm. The fungal mycelia were harvested using Whatman No. 1 filter paper and washed three times with sterile distilled water. Collected mycelium was grounded finely with liquid nitrogen and stored at $-80 \text{ }^\circ\text{C}$ till further use. Cetyltrimethyl ammonium bromide (CTAB) method was followed for total fungal DNA extraction (Culling 1992). The internal transcribed spacer (ITS) region was amplified by using universal primers ITS1 (5'-TCCGTAGGTGAACCTGCGG-3')/ITS4 (5'-TCCTCCGCTTATTGATATGC3') (White et al. 1990).

PCR reaction mixture was prepared in the final volume of 25 μL containing 2.5 μL of 10X PCR buffer with MgCl_2 , 1 μL of forward and reverse primer each (10 pM), 0.5 μL of 10 mM dNTP's, 0.5 μL of DyNAzyme II DNA Polymerase (2 U/ μL), 2 μL of genomic DNA (50 ng/ μL) and 17.5 μL of Molecular biology grade water and amplified by following

Table 1 List of *Trichoderma* isolates along with NCBI accession numbers and morphological specifications

S. no.	Isolate code	Location	Latitude and longitude	NCBI accession number	<i>Trichoderma</i> spp.	Morphological characteristics
1	Tasp1	Jobner, Jaipur	26° 58' 33.6" N 75° 22' 10.7" E	KT426888	Group I— <i>Trichoderma asperellum</i>	Colony: dark green Conidiophores: regularly branched, with lateral branches and paired Phialides: whorls of 2–4 phialides, straight, slightly wider in middle than base and ampulliform Conidia: globose to subglobose
2	Tasp2	Durgapura, Jaipur	26° 50' 41.0" N 75° 46' 52.5" E	KT426889		
3	Tasp3	Bagru, Jaipur	26° 49' 02.3" N 75° 33' 09.8" E	KT426890		
4	Tasp4	Samod Jaipur	27° 14' 01.5" N 75° 46' 53.1" E	KT426891		
5	Tasp5	Sambhar, Jaipur	27° 00' 12.3" N 75° 11' 24.7" E	KT426892		
6	Tasp6	Chaksu Jaipur	26° 35' 55.6" N 75° 56' 27.1" E	KU170973		
7	Tasp46	Jobner, Jaipur	26° 58' 59.3" N 75° 32' 35.1" E	MT065825		
8	Tasp47	Chaksu Jaipur	26° 36' 14.7" N 75° 55' 33.1" E	MT065826		
9	Tasp48	Durgapura, Jaipur	26° 55' 51.8" N 75° 45' 14.2" E	MT065827		
10	Tasp49	Samod Jaipur	27° 12' 32.6" N 75° 46' 57.5" E	MT065828		
11	Tasp50	Jobner, Jaipur	26° 59' 54.9" N 75° 22' 06.5" E	MT065829		
12	Tasp51	Bagru, Jaipur	26° 50' 08.7" N 75° 33' 19.1" E	MT065830		
13	Thar1	Durgapura, Jaipur	26° 55' 35.0" N 75° 42' 06.1" E	KT426893	Group II— <i>Trichoderma harzianum</i>	Colony: whitish green to pale green Conidiophores: flexuous, branches almost right angled Phialides: whorls of 2–6, ampulliform to lageniform, subulate, short, skittle-shaped, narrower at the base Conidia: globose to subglobose to short obovoid
14	Thar2	Samod Jaipur	27° 11' 08.5" N 75° 46' 59.9" E	KT426894		
15	Thar3	Jobner, Jaipur	26° 57' 56.3" N 75° 22' 35.9" E	KT426895		
16	Thar4	Durgapura, Jaipur	26° 50' 30.0" N 75° 47' 00.2" E	KT426896		
17	Thar5	Jobner, Jaipur	26° 58' 46.2" N 75° 22' 21.1" E	KT426897		
18	Thar20	Samod Jaipur	27° 11' 08.5" N 75° 46' 59.9" E	MT065754		
19	Thar21	Durgapura, Jaipur	26° 50' 46.1" N 75° 46' 46.4" E	MT065755		
20	Thar22	Bagru, Jaipur	26° 50' 08.7" N 75° 33' 19.1" E	MT065756		
21	Thar23	Jobner, Jaipur	26° 58' 33.6" N 75° 22' 10.7" E	MT065757		
22	Thar24	Sambhar, Jaipur	26° 52' 26.2" N 75° 07' 38.4" E	MT065758		
23	Thar25	Chaksu Jaipur	26° 35' 55.6" N 75° 56' 27.1" E	MT065759		

Table 1 (continued)

S. no.	Isolate code	Location	Latitude and longitude	NCBI accession number	<i>Trichoderma</i> spp.	Morphological characteristics
24	Tlongi1	Jobner, Jaipur	26° 93' 21.6" N 75° 37' 73.1" E	KT426898	Group III— <i>Trichoderma longibrachiatum</i>	Colony: dark olive green with yellow tinge Conidiophores: long main branches produce only a few side short branches Phialides: lageniform or bottle shaped Conidia: sub-cylindrical with distinct truncate base
25	Tlongi2	Bagru, Jaipur	26° 49' 02.3" N 75° 33' 09.8" E	KT426899		
26	Tlongi3	Chaksu Jaipur	26° 36' 14.7" N 75° 55' 33.1" E	KT426900		
27	Tlongi4	Samod Jaipur	27° 12' 32.7" N 75° 51' 31.3" E	KT426901		
28	Tlongi5	Sambhar, Jaipur	27° 00' 12.3" N 75° 11' 24.7" E	KT426902		
29	Tlongi25	Durgapura, Jaipur	26° 55' 35.0" N 75° 42' 06.1" E	MT052706	Group IV— <i>Trichoderma citrinoviride</i>	Colony: dusky yellowish green Conidiophores: main branches long and relatively straight Phialides: more elongate, lageniform or narrowly shaped Conidia: less ellipsoidal, apex broadly rounded
30	Tcetri1	Bagru, Jaipur	26° 48' 20.4" N 75° 33' 05.6" E	MT065795		
31	Tcetri2	Chaksu Jaipur	26° 34' 58.2" N 75° 59' 48.2" E	MT065796		
32	Tcetri3	Samod Jaipur	27° 12' 32.7" N 75° 51' 31.3" E	MT065797		
33	Tcetri4	Sambhar, Jaipur	27° 01' 58.6" N 75° 18' 48.0" E	MT065798		
34	Tcetri5	Jobner, Jaipur	26° 59' 40.4" N 75° 20' 49.4" E	MT065799		
35	Tcetri6	Durgapura, Jaipur	26° 50' 24.1" N 75° 46' 51.2" E	MT065800		

protocol: initial denaturation for 1 min at 95 °C, 30 cycles of denaturation for 30 s at 95 °C, primer annealing for 1 min at 60 °C, extension at 72 °C for 1 min and a final extension period for 7 min at 72 °C. The amplified PCR products were electrophoretically separated using 1.2% agarose gel in 1X TAE buffer at 80 V for 1 h. Amplified PCR fragments were visualized in UV light and gel documented. The desired amplified products were gel eluted (GeneJET Gel Extraction Kit, Thermo Scientific™, USA) and sequenced through the Sanger sequencing method (Eurofins Pvt. Ltd). The sequence contig was prepared using CAP3 sequence assembly program and aligned sequence were confirmed with nBLAST (www.ncbi.nlm.nih.gov/BLAST) and submitted to NCBI (<http://www.ncbi.nlm.nih.gov/>).

Phylogenetic analysis

The phylogenetic tree was constructed by aligning the generated sequences using ClustalW multiple sequence alignment program (Thompson et al. 1994) and MEGA7 software program (Kumar et al. 2016). Maximum Composite Likelihood (MCL) method was used to estimate the pairwise distances and bootstrap method was used to study the nodal robustness with a replication of 1000. The Kimura 2-parameter

distance model (Kimura 1980) was used for the construction of maximum-likelihood (ML) tree (Kumar et al. 2016).

Screening for antagonistic activity of *Trichoderma* isolates

Antagonistic activity of different 35 *Trichoderma* isolates against groundnut stem rot pathogen *S. rolfisii* was done by dual culture plate method (Dennis and Webster 1971). Seven days old actively growing mycelial disc (5 mm) of *Trichoderma* isolates and *S. rolfisii* were placed on PDA plates opposite from the periphery and plates without *Trichoderma* served as a control and plates were incubated at 28 ± 2 °C for 5–7 days. The percentage of inhibition was calculated by following formula

$$\text{Percentage of inhibition (PI)} = \frac{C-T}{C} \times 100$$

where 'C' is the radial growth of pathogen in the control PDA plate in cm and 'T' is the radial growth pathogen in test plate in cm.

The antagonism level of these isolates was evaluated according to Bell et al. (1982). *Trichoderma* isolates with significant antagonistic potential against *S. rolfisii* were

evaluated for production of lytic enzymes and plant growth promoting traits in groundnut.

Lytic enzymes assay of selected isolates of four *Trichoderma* spp.

Preparation of cell-free culture filtrate

The cell-free culture filtrate from selected isolates *T. harzianum* Thar23, *T. asperellum* Tasp49, *T. longibrachiatum* Tlongi5 and *T. citrinoviride* Tcitr2 were prepared using freeze-dried mycelia of *S. rolfsii* as a sole carbon source. Actively grown mycelial mat of *S. rolfsii* was harvested from 7 days old PDB broth and homogenized by using liquid nitrogen. The freeze dried pathogen mycelial powder was stored at $-20\text{ }^{\circ}\text{C}$. A 5 mm mycelial disc of actively growing selected *Trichoderma* isolates was inoculated in autoclaved 250 ml of minimal synthetic broth (MSB) containing (g/l) $\text{FeSO}_4\text{-}0.01$, $\text{MnSO}_4\text{-}0.01$, $\text{ZnSO}_4\text{-}0.01$, $\text{KCl}\text{-}0.5$, $\text{MgSO}_4\text{-}0.5$, $\text{K}_2\text{HPO}_4\text{-}1.0$, $\text{NaNO}_3\text{-}3.0$; pH 5.5 amended with 1% freeze dried mycelia of *S. rolfsii* and flasks were kept at $28\pm 2\text{ }^{\circ}\text{C}$ at 180 rpm and filtered through Whatman no. 1 filter paper at different time interval from day 1 to 10.

Estimation of chitinase (EC 3.2.1.14)

Dinitrosalicylic acid (DNSA) method was used to estimate the chitinase production from *Trichoderma* isolates. One millilitre of culture filtrate with 0.5 ml of colloidal chitin and 0.5 ml of 1 M sodium acetate buffer was mixed and incubated at $40\text{ }^{\circ}\text{C}$ for 6 h and centrifuged at 12,000 rpm for 5 min at $4\text{ }^{\circ}\text{C}$. One millilitre of supernatant was mixed with 0.5 ml of DNSA in 1 M NaOH and 0.1 ml of 10 M NaOH and kept at $100\text{ }^{\circ}\text{C}$ for 5 min. The assay mixture was recorded spectrophotometrically at 582 nm and N-acetylglucosamine (GlcNAc) was used as standard. Specific chitinolytic activity was defined as unit of GlcNAc released by 1 ml of enzyme solution under assay conditions.

Estimation of β -1,3-glucanase (EC 3.2.1.39)

β -1,3-Glucanase activity was determined using laminarin as a substrate. The assay mixture contains 0.5 ml of culture filtrate with 1 ml of laminarin in 50 mM acetate buffer (pH 4.8) and was incubated at $50\text{ }^{\circ}\text{C}$ for 10 min. One ml of dinitrosalicylic acid was added to the reaction mixture and kept at $95\text{ }^{\circ}\text{C}$ for 5 min and total amount of reducing sugar was recorded at 540 nm. One unit of β -1,3-glucanase activity was defined as the amount of enzyme required to release one μmol of reducing sugar per minute.

Estimation of protease (EC 3.4.21.4)

Protease activity was determined using 1% casein as substrate in 50 mM phosphate buffer (pH 7.0) was denatured at $100\text{ }^{\circ}\text{C}$ for 15 min in the water bath. The reaction mixture containing 1 ml of casein substrate was added with 3 ml of 10% trichloroacetic acid (TCA) and kept at $4\text{ }^{\circ}\text{C}$ for 1 h. This mixture was centrifuged at 8000 rpm for 15 min at $4\text{ }^{\circ}\text{C}$, and supernatant was recorded at 280 nm. One unit of protease activity was defined as the amount of enzyme solution equivalent to release 1 μmol of tyrosine under assay conditions.

Plant growth promoting traits of selected isolates of four *Trichoderma* spp. in groundnut

The plant growth promoting ability of the selected *Trichoderma* isolates in groundnut (RG-510 Spreading variety) was studied under pot conditions. Groundnut seeds were treated with spore suspensions of each selected *Trichoderma* isolates containing 2×10^8 spores ml^{-1} and were soaked for one hour. Spore suspensions from selected isolates were prepared from PDA plates containing 7 days old cultures of *Trichoderma* by scraping gently on the surface of the plates with sterile distilled water containing 0.01% Tween 20 and filtered through two layers of sterile muslin cloth. The spore concentration was adjusted with the aid of haemocytometer.

Efficacy on seed germination, root, and shoot length and relative water content (RWC)

The germination efficacy of selected *Trichoderma* isolates in groundnut seeds was studied by treating with *Trichoderma* spore suspension (2×10^8 spores ml^{-1}) and transferred to respective pots containing sterile soil along with farm yard manure (FYM) in 10:1 ratio. Seeds treated with sterile water served as control. After 10 days, the number of germinated seedlings in each replication was counted and the germination was calculated and expressed by using the following formula

$$\begin{aligned} &\text{Germination percentage (\%)} \\ &= \frac{\text{Number of germinated seeds}}{\text{Total number of seeds}} \times 100 \end{aligned}$$

Groundnut plants (30 days old) were harvested from each treatment and washed three times with sterile distilled water. The root and shoot length were observed and based on the root and shoot length with germination percentage, the vigour index was calculated by using formula given by Abdul Baki and Anderson (1973).

$$\text{Vigour Index (VI)} = (\text{Mean shoot length} + \text{Mean root length}) \times \text{Germination (\%)}$$

To determine relative water content, the harvested plants were air dried and weighed (fresh weight). For dry weight, the plants were kept in hot air oven at 100 °C for 20 min, and then kept at 80 °C for 24 h at oven then weighed and recorded (Tian et al. 2015). Each control and treatment were repeated three times. The following formula was used to determine RWC of shoots and roots.

$$\text{RWC (\%)} = \frac{\text{FW} - \text{DW}}{\text{FW}} \times 100$$

where, RWC is relative water content, FW: fresh weight, and DW: dry weight.

Groundnut stem rot management by application of selected isolates of four *Trichoderma* spp. under field conditions

The field experiment was conducted in the randomized block design with three replications in the kharif season of 2019 and 2020 at Agronomy Farm, S.K.N. College of Agriculture, Jobner situated 26° 05' N-latitude and 75° 28' E-longitudes and at an altitude of 427 m above mean sea level in Jaipur district of Rajasthan. The region falls in agroclimatic zone III-a (semi-arid eastern plain), and variety RG 510 was used for both experimental years. The seeds were treated with talc-based bioformulation of different *Trichoderma* isolates at 8 g/kg. The spore concentration of the bioformulation was maintained 2×10^8 CFU/g. The treatment schedule is as follows.

T1—Soil application with *T. asperellum* Tasp49 enriched FYM (10: 200) + seed treatment with *T. asperellum* Tasp49 at 8 g/kg seeds + drenching with *T. asperellum* Tasp49 at 8 ml/l at 40 days after sowing.

T2—Soil application with *T. harzianum* Thar23 enriched FYM (10: 200) + seed treatment with *T. harzianum* Thar23 at 8 g/kg seeds + drenching with *T. harzianum* Thar23 at 8 ml/l at 40 days after sowing.

T3—Soil application with *T. longibrachiatum* Tlongi5 enriched FYM (10: 200) + seed treatment with *T. longibrachiatum* Tlongi5 at 8 g/kg seeds + drenching with *T. longibrachiatum* Tlongi5 at 8 ml/l at 40 days after sowing.

T4—Soil application with *T. citrinoviride* Tcetri2 enriched FYM (10: 200) + seed treatment with *T. citrinoviride* Tcetri2 at 8 g/kg seeds + drenching with *T. citrinoviride* Tcetri2 at 8 ml/l at 40 days after sowing.

T5—Untreated control.

Disease incidence was monitored on a weekly basis by observation of symptoms and was calculated by the following formula

$$\text{Disease incidence (DI) (\%)} = \frac{\text{Number of infected plants}}{\text{Total number of plants}} \times 100$$

Shelling of the well dried 100 g pods from each treatment was done and recorded weight of kernels and the shelling percentage was calculated by following formula

$$\text{Shelling percentage} = \frac{\text{Kernel weight}}{\text{Pod weight}} \times 100$$

The pod yield was calculated from each treatment separately after threshing, winnowing, and cleaning the produce was weighed and converted in terms of Tones/ha.

Statistical analysis

The normality of the data was checked and found that data are treatment-wise normally distributed. All the treatments replicated thrice in a completely randomized design and the descriptive statistics of the data are presented as mean value \pm SD. Significance of mycelial growth inhibition, enzyme production and growth promotion were tested by a one-way analysis of variance (ANOVA). The data were analysed by ANOVA using R-programming language and treatment means were compared using Fisher's Protected LSD test at $p=0.05$ (Gomez and Gomez 1984).

Results

Morphological characteristics of *Trichoderma* isolates

Thirty-five isolates of *Trichoderma* spp. were collected from the rhizospheric soil of groundnut growing area of Jaipur District (26.9706° N, 75.3791° E) of Rajasthan, India, which were further morphologically characterized through microscopic studies. Based on morphological features the isolates were classified into four groups I *T. asperellum*, group II *T. harzianum*, group III *T. longibrachiatum* and group IV *T. citrinoviride* (Table 1). The group I consisted of 12 isolates of *T. asperellum* showed dark green and compact colonies on PDA medium with the typically paired and regularly branched conidiophores (Table 1). The conidia were globose to sub-globose in shape with the size of 2.5–3 μ m (Fig. 1). A total of 11 isolates of *T. harzianum* in grouped exhibited whitish green to pale green on PDA surface with short branched and irregular conidiophores at right angle. The shape of conidia was globose to sub-globose to short obovoid with size of 1.5–2 μ m (Fig. 1). The 6 isolates of group III were yellowish green or dark olive green on PDA plates with short, branched conidiophores, lageniform or bottle shaped conidia on long main branches with the size of

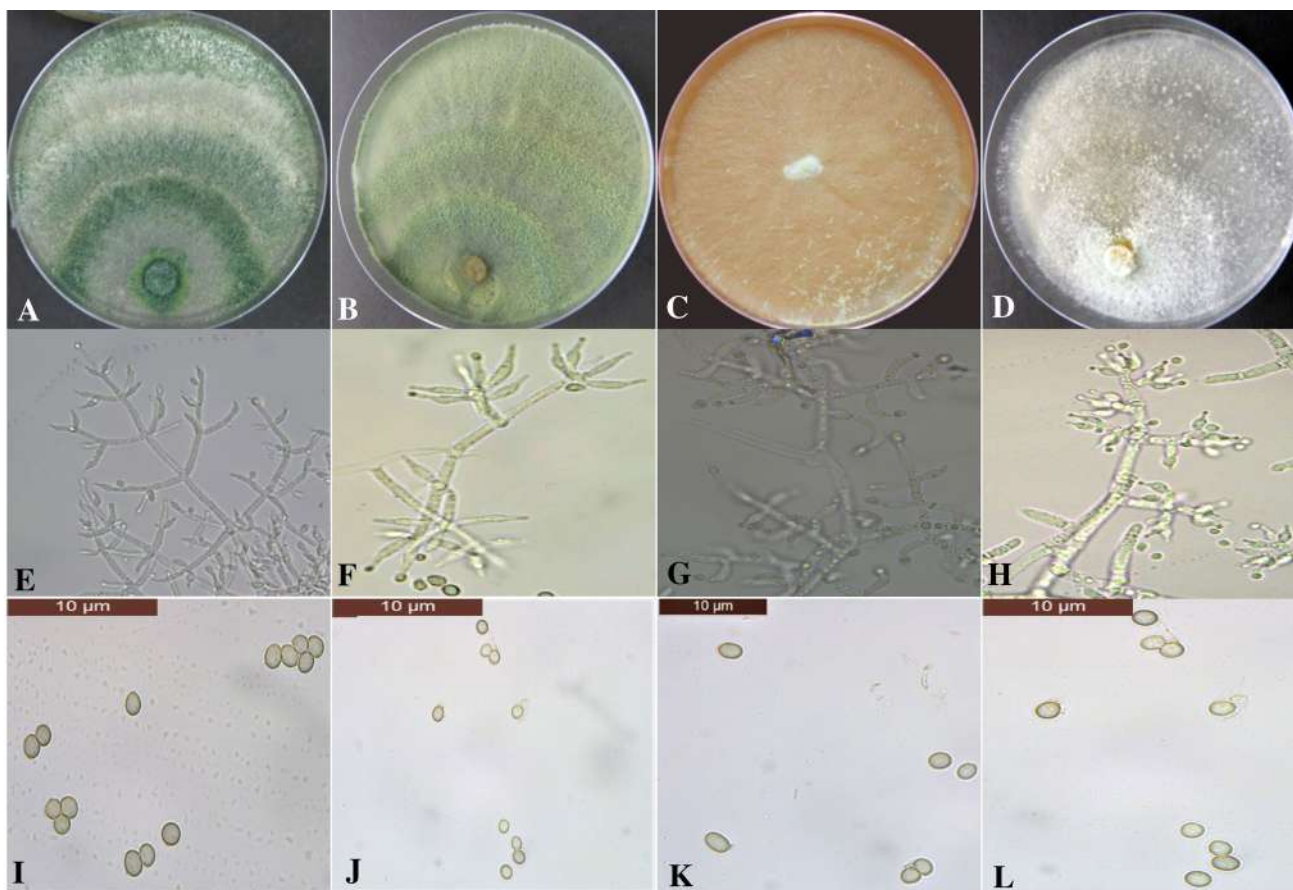


Fig. 1 PDA culture plates showing 7 days old representative isolates of *Trichoderma* spp. **a, e, i** Showing the growth on PDA, branching pattern of phialides and conidia of *T. asperellum* Tasp49. **b, f, j** Showing the growth on PDA, branching pattern of phialides and

conidia of *T. harzianum* Thar23. **c, f, k** Showing growth on PDA, branching pattern of phialides and conidia of *T. longibrachiatum* Tlongi5. **d, h, l** Showing growth on PDA, branching pattern of phialides and conidia of *T. citrinoviride* Tcitr2 (scale bar 10 µm)

2–2.5 µm were classified as *T. longibrachiatum*. The group IV was classified as *T. citrinoviride* consisted of 6 isolates which showed dusky yellowish green colony on PDA with less ellipsoidal, broadly rounded apex conidia with size of 2–2.5 µm, with relatively straight long branched conidiophores, relatively elongate, lageniform or narrowly shaped phialides (Fig. 1).

Molecular characterization of *Trichoderma* isolates and phylogenetic analysis

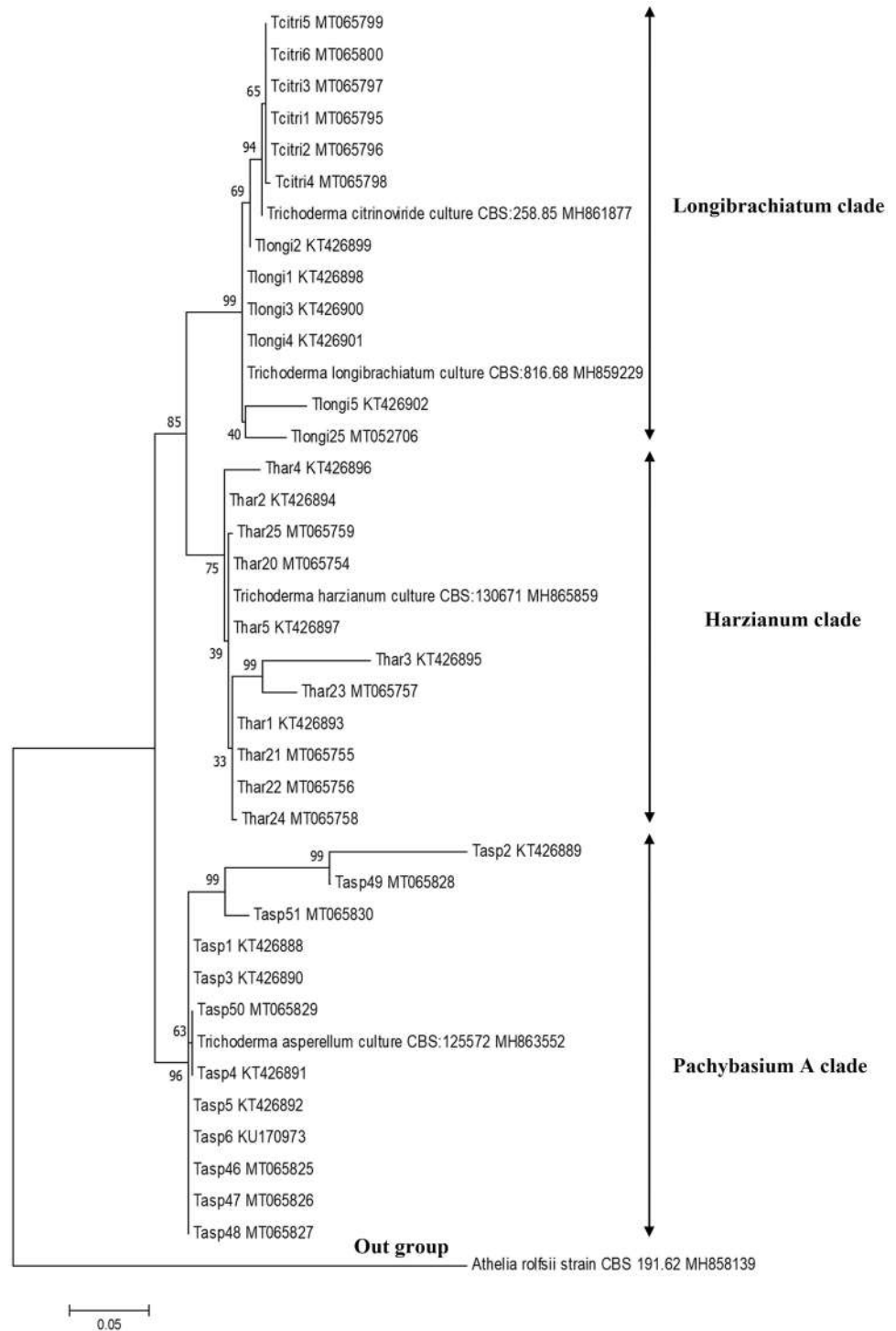
A single amplified product around 550–650 bp of all 35 isolates of *Trichoderma* spp. were sequenced and confirmed with BLAST search tool and submitted to NCBI (Table 1). The BLAST analysis was differentiating at species level with homology percentage of 95–99%, and results obtained from phylogenetic analysis of ITS sequences showed that the 35 *Trichoderma* isolates can be separated into four different species with three distinct clades of *Trichoderma* namely (Fig. 2), the Pachybasium A clade (*T. asperellum*), the

Harzianum clade (*T. harzianum*), and the Longibrachiatum clade (*T. longibrachiatum* and *T. citrinoviride*). The Pachybasium A clade consists of 12 isolates of *T. asperellum* with a bootstrap value of 98%, the clade Harzianum consisting of 11 isolates of *T. harzianum* supported by bootstrap value of 81%. The closely associated species both *T. longibrachiatum* (6 isolates) and *T. citrinoviride* (6 isolates), fall in the section Longibrachiatum clade with 96% bootstrap value indicating the close relationship of both species (Fig. 2).

Antagonistic activity of *Trichoderma* isolates against *S. rolfsii*

The antagonistic activity of 35 isolates of *Trichoderma* spp. against *S. rolfsii* was evaluated by dual culture assay. Two groups of *T. asperellum* and *T. harzianum* exhibited higher antagonistic activity with the range of 62% to 81.7% against *S. rolfsii*. Group III *T. longibrachiatum* and Group IV *T. citrinoviride* recorded moderate or lower mycelial inhibition from 51.43 to 67.5% (Fig. 3). The degree of antagonism was

Fig. 2 Phylogenetic relationships of *Trichoderma* isolates inferred by analysis of ITS region and constructed using two parameter model implemented in the MEGA7 inferred by using the Maximum Likelihood method and Tamura-Nei model. Analysis was conducted in MEGA 7 and the percentage of replicate trees in which the associated taxa clustered together in the bootstrap test



measured by the scale described by Bell et al. (1982). Isolates from *T. asperellum* group namely *Tasp*1, *Tasp*3, *Tasp*6, *Tasp*46 and *Tasp*49, from *T. harzianum* group namely, *Thar*1, *Thar*3, *Thar*4, *Thar*5, *Thar*20, *Thar*21, *Thar*22, *Thar*23, *Thar*24 and *Thar*25 exhibited class 1 level of antagonism, whereas isolates like *Tasp*2, *Tasp*4, *Tasp*5, *Tasp*47, *Tasp*48, *Tasp*50 and *Tasp*51 from *T. asperellum* group, one

isolate from *T. harzianum* *Thar*2, some of the isolates from *T. longibrachiatum* group namely *Tl*ongi1, *Tl*ongi2, *Tl*ongi4, *Tl*ongi5 and *Tc*itri2, *Tc*itri4 and *Tc*itri6 from *T. citrinoviride* group expressed the class 2 level of antagonism. Class 3 level of antagonism was observed in *Tl*ongi3 and *Tl*ongi25 from *T. longibrachiatum* and *Tc*itri1, *Tc*itri3 and *Tc*itri5 from *T. citrinoviride* against *S. rolfsii*. Among 35 isolates,

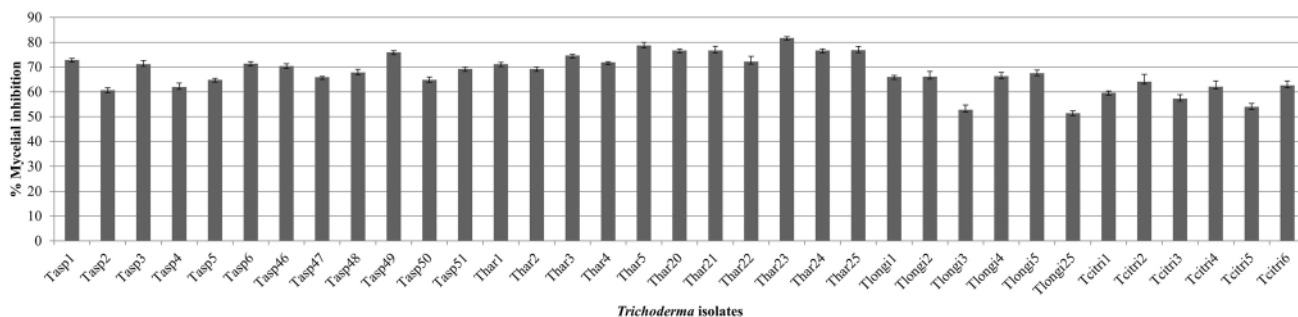


Fig. 3 Per cent mycelial inhibition of *S. rolfii* by different *Trichoderma* isolates in dual culture assay. Treatment means were compared using Fisher’s Protected LSD test ($p=0.05$)

the potential isolate from each group namely *T. asperellum* Tasp49 from group I, *T. harzianum* Thar23 from group II, *T. longibrachiatum* Tlongi5 from group III and *T. citrinoviride* Tcetri2 from group IV were selected for the study of lytic enzyme production and plant growth promoting traits in groundnut.

Lytic enzymes assay of selected isolates of four *Trichoderma* spp.

The lytic enzymes like chitinase, β -1,3-glucanase and protease from selected *Trichoderma* isolates were studied by using freeze dried mycelia of *S. rolfii* in MSB as a source of enzyme production. The enzyme activity from the isolates were gradually increased from day 1 to 7 for chitinase and day 1–6 for β -1,3-glucanase and protease and decreased after day 7. Among the selected isolates, *T. harzianum* Thar23 (31.36 U/ml) significantly produced higher amount of chitinase on day 7 followed by *T. asperellum* Tasp49 (25.26 U/ml) (Fig. 4). The other selected isolates *T. longibrachiatum* Tlongi5 (20.1 U/ml) and *T. citrinoviride* Tcetri2 (17.3 U/ml)

exhibited lesser amount of chitinase enzyme activity as compared to other isolates (Fig. 4). Similarly, another lytic enzymes β -1, 3-glucanase and protease are also produced significantly higher 4.1 U/ml and 2.76 U/ml on day 6 by *T. harzianum* Thar23 followed by *T. asperellum* Tasp49 (2.6 U/ml and 2.13 U/ml). The other two selected isolates *T. longibrachiatum* Tlongi5 (1.33 U/ml and 1.16 U/ml) and *T. citrinoviride* Tcetri2 (0.8 U/ml and 0.83 U/ml) showed lesser production of these enzymes compared to other isolates (Fig. 4).

Plant growth promoting traits of selected isolates of four *Trichoderma* spp. in groundnut

The selected isolates were comparatively tested for their growth promoting ability in groundnut under greenhouse conditions. The seeds treated with *T. harzianum* Thar23 and *T. asperellum* Tasp49 significantly increased the germination efficacy to 31.48 and 24.47% and increased the shoot length by 42 and 21.44% and root length by 73.72 and 62.76% compared to control with vigour index of 3598.25 and 3030.65

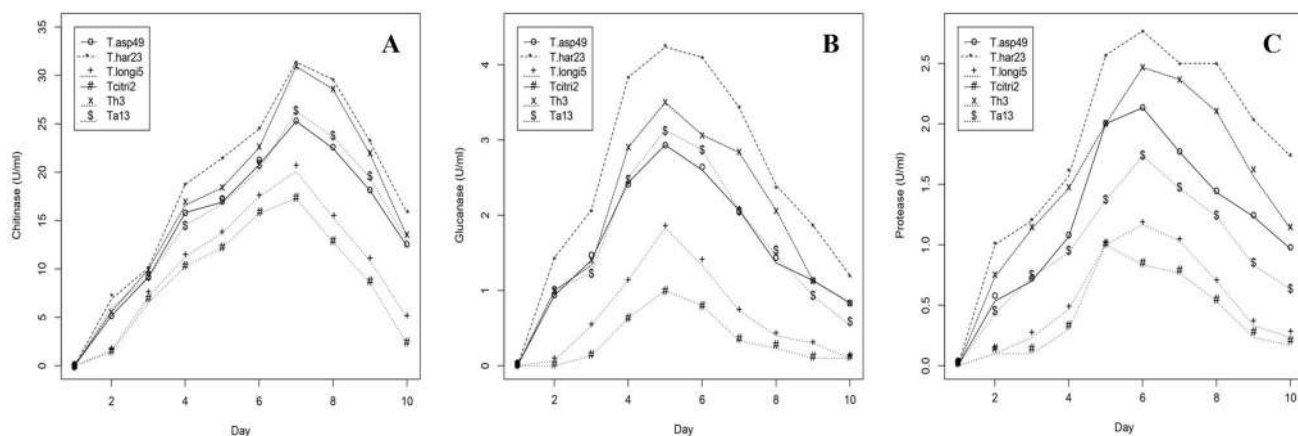


Fig. 4 Lytic enzymes **a** chitinase, **b** β -1,3-glucanase and **c** protease secretion (U/ml) from selected *Trichoderma* isolates at different time intervals

Table 2 Plant growth promoting efficacy of selected *Trichoderma* isolates in groundnut under glasshouse conditions

<i>Trichoderma</i> isolates	Shoot length (in cm)	Root length (in cm)	Germination (%)	Plant vigour index	Relative water content of shoot (%)	Relative water content of root (%)
Tasp49	22.27 ± 1.36 ^c	15.3 ± 0.1 ^c	80.67 ± 0.29 ^d	3030.65 ± 128.31 ^d	75.77 ± 0.02 ^d	77.73 ± 2.38 ^d
Thar23	26.03 ± 0.71 ^d	16.33 ± 0.23 ^d	85.2 ± 0.2 ^e	3598.25 ± 58.05 ^e	78.36 ± 0.27 ^e	81.23 ± 0.59 ^e
Tlongi5	20.36 ± 0.47 ^b	10.8 ± 0.26 ^b	70.33 ± 0.42 ^c	2191.98 ± 35.51 ^c	71.40 ± 0.84 ^c	70.47 ± 0.82 ^c
Tcetri2	19.4 ± 0.46 ^{ab}	9.37 ± 0.15 ^a	68.23 ± 0.25 ^b	1962.78 ± 20.64 ^b	67.55 ± 0.77 ^b	67.25 ± 1.02 ^b
Control	18.33 ± 0.21 ^a	9.4 ± 0.17 ^a	64.8 ± 0.529 ^a	1797.17 ± 26.98 ^a	66.46 ± 0.64 ^a	60.65 ± 2.71 ^a

Values given in the column are the average of three replications followed by standard deviation. The different small letters (a–e) superscripts within the column are significantly difference at $P \leq 0.05$

(Table 2) and increase in plant biomass in terms of the fresh and dry weight of shoot and root. The RWC of shoot and root treated with Thar23 shown higher (81.23%) than control (60.65%) (Table 2). However, the moderate effect on germination efficacy and plant growth promoting traits was observed in seed treatment with *T. citrinoviride* Tcetri2 as compared to other selected isolates (Table 2).

Groundnut stem rot management by application of selected isolates of four *Trichoderma* spp. under field conditions

Field experiments were conducted to evaluate the efficacy of native *Trichoderma* isolates on stem rot disease incidence, shelling percent and pod yield for the year of 2019 and 2020 kharif season. Soil application, seed treatment and drenching with *T. harzianum* Thar23 and *T. asperellum* Tasp49 significantly ($P < 0.05$) reduced stem rot disease incidence up to 59.45%, 52.01% in 2019 and 53.79%, 48.74% for the year of 2020 and increased pod yield in *T. harzianum* Thar23 (2.85 t/ha and 2.68 t/ha) and *T. asperellum* Tasp49 (2.62 t/ha and 2.55 t/ha) treated plots with increased shelling percent (Table 3). However, treatment with *T. longibrachiatum* Tlongi5 and *T. citrinoviride* Tcetri2 shows moderate reduction in disease incidence up to 35.11%, 34.16% in 2019 and 34.16%, 33.21% in 2020 with pod yield of 2.13 t/ha, 2.05 t/ha in 2019 and 2.05 t/ha and 1.95 t/ha in 2020 (Table 3). The results obtained from field experiments that indicate the effect of application of *T. harzianum* Thar23 in improvement of the pod yield up to 51.59% and 38.58% during 2019 and 2020 kharif seasons, respectively.

Discussion

The present study was focused on morphological and molecular characterization, antagonistic ability, and plant growth promoting traits in the potential native *Trichoderma* isolates tested against stem rot pathogen *S. rolfisii* of groundnut. The isolates from rhizosphere soil of groundnut were collected

and characterized based on the morphological characteristics to identify the species level by using the reference of Rifai (1969), Bissett (1984) and Samuels et al. (1999) and classified in to four groups, namely *T. asperellum* (12), *T. harzianum* (11), *T. longibrachiatum* (6) and *T. citrinoviride* (6). Morphological characterization of native *Trichoderma* isolates has earlier been taken up by several researchers (Rifai 1969; Bissett 1984; Pandian et al. 2016; Devi et al. 2021; Jambhulkar et al. 2022). In addition to supporting the reliability of morphological identification, isolates were further characterized molecularly by amplifying ITS region. Kullnig-Gradinger et al. (2002) described the multigene phylogeny approaches for the evolution of *Trichoderma* spp. by using the ITS1 and ITS2, 28S rDNA, mitSSU, *tef* 1 and *ech42* genes. Indian researchers have widely surveyed in different locations of the country and have reported from the different geographical locations like New Delhi (Muthu and Sharma 2011), South Andaman Island (Kumar et al. 2012), Chhattisgarh (Agrawal and Kotasthane 2012), Manipur (Kamala et al. 2015) and Uttarakhand (Manzar et al. 2021), different states of India (Devi et al. 2021). The present study revealed the presence of diverse *Trichoderma* spp. in the rhizosphere of groundnut growing area of Jaipur District of Rajasthan. Mainly *T. asperellum* and *T. harzianum* were found to be dominant species with greater antagonistic potential against a wide range of phytopathogens. Till now, 375 species of *Trichoderma* spp. have been identified and their DNA barcoding information was deposited in the International Subcommittee on Taxonomy of *Trichoderma* (ICTT) (<http://www.trichoderma.info>). The modern *Trichoderma* taxonomy methods help in the precise identification and reorganization of 50 new species of *Trichoderma* per year (Cai and Druzhinina 2021). Similar studies by Manzar et al. (2021) highlighted the phylogenetic relationship among the *Trichoderma* spp. based on the ITS and *tef-1α* sequences. Out of 20 isolates, nineteen isolates belonged to *T. asperellum* as compared to *T. harzianum* (one isolate). With the upcoming trend of development of potential native strains of *Trichoderma* spp. characterization

Table 3 Effect of soil application, seed treatment and drenching with selected *Trichoderma* isolates against *S. rolfisii* in groundnut under field conditions during 2019 and 2020 kharif season

<i>Trichoderma</i> isolates	Per cent disease incidence (PDI)		Reduction over control		Pods per plant		Shelling per cent		Pod yield (t/ha)	
	2019	2020	2019	2020	2019	2020	2019	2020	2019	2020
Tasp49	18.66 ± 0.50 ^c	20.66 ± 0.66 ^c	52.01 ^b	48.74 ^b	25.33 ± 0.57 ^b	29.00 ± 1.00 ^a	61.43 ± 0.37 ^b	58.76 ± 0.51 ^b	2.62 ± 0.03 ^b	2.55 ± 0.04 ^a
Thar23	15.76 ± 0.66 ^d	18.63 ± 0.51 ^d	59.45 ^a	53.79 ^a	31.00 ± 1.00 ^a	22.33 ± 1.15 ^b	66.06 ± 0.15 ^a	62.16 ± 0.25 ^a	2.85 ± 0.04 ^a	2.68 ± 0.02 ^a
Tlongi5	25.23 ± 0.20 ^b	26.46 ± 0.45 ^b	35.11 ^c	34.37 ^c	20.00 ± 1.00 ^c	15.66 ± 0.05 ^c	54.93 ± 0.56 ^c	51.00 ± 0.20 ^c	2.13 ± 0.03 ^c	2.07 ± 0.05 ^b
Tcetri2	25.6 ± 0.43 ^b	26.93 ± 0.47 ^b	34.16 ^c	33.21 ^c	19.33 ± 1.15 ^c	16.00 ± 0.00 ^c	54.66 ± 0.23 ^c	50.50 ± 0.45 ^c	2.05 ± 0.03 ^c	1.95 ± 0.03 ^b
Control	38.9 ± 0.65 ^a	40.33 ± 0.41 ^a	–	–	18.66 ± 0.57 ^c	15.33 ± 0.57 ^c	50.7 ± 0.41 ^d	48.76 ± 0.23 ^d	1.88 ± 0.03 ^d	1.84 ± 0.43 ^c

Values given in the column are the average of three replications followed by standard deviation. The different small letters (a–e) superscripts within the column are significantly difference at P ≤ 0.05

through molecular and morphological tools have become very important step in research.

To further utilize the native strains for biological control, antagonism tests are required to understand the mechanism under in vitro and in vivo conditions. The antagonistic ability of the *Trichoderma* isolates was tested against *S. rolfisii* showed significant reduction in the mycelial growth of pathogen. Significant variation was observed in the isolates from *T. asperellum* and *T. harzianum* while *T. longibrachiatum* and *T. citrinoviride* exhibited moderate efficacy. The CWDEs are specialized group (glycosyl-hydrolases, oxidoreductases, lyases, and esterases) of enzymes produced by *Trichoderma* spp. which are key component against wide range of phytopathogens. Recently Kaur et al. 2021 reported purified proteins both endochitinase and β-1,3-glucanase from *T. viride* isolate T1#3 degrade the hyphae of *R. solani* causing sheath blight in rice. Several research findings stated that the genus of *Trichoderma* is known to produce CDWs like chitinase, β-1,3-glucanase and protease are playing key role in the suppression of the growth of major soil borne pathogens (Guigon-Lopez et al. 2015; Li et al. 2016; Elamathi et al. 2018; Boat et al. 2020; Macena et al.2020). In recent years, green synthesis of nanoparticles by these species made an impact in the agricultural and food sector due to the secretion of bioactive enzymes, metabolites and accumulation of metals are responsible for reduction of metal ions and helping in the formation nanoparticles. Raja et al. 2021 reported that biologically synthesized nanoparticles by using cell free culture filtrate of *T. harzianum* Th3 inhibits the mycelial growth of groundnut root rot complex pathogens by 60–65%. Production of secondary metabolites during mycoparasitism also a pivotal key of *Trichoderma* spp. in the antagonistic mechanism. For example, secondary metabolites like harzianic acid (HA), 6-pentyl-α-pyrone (6PP), koniginin, harzianopyridone and etc. can be correlated with biocontrol mechanisms (Vinale and Sivasithamparam 2020).

Plant growth promoting fungi (PGPF) are majorly associated with wide range of hosts and helps in transformation of soil nutrients, alter the niche of rhizosphere, elucidate the systemic resistance, and improve the plant growth. *Trichoderma* spp. are one of major beneficial fungal community present in the soil environment which directly create an impact on plants such as increased in number lateral roots and length, cumulative root length and root tips, germination efficacy and seeding growth, improved surface area of roots and leaves, wet and dry weight of plant biomass, and positive effect on flowering. And also responsible for elucidation of plant immunity through increasing jasmonic acid (JA), salicylic acid (SA), ethylene (ET), phytoalexin levels and root exudates in plants, soil nutrients solubilization, and nutrient uptake. Some of the *Trichoderma* spp. are rhizospheric competent in nature that can be able to colonize the plant

roots and enter the epidermis and outer cortex of root system (Harman et al. 2004). Recently Nofal et al. (2021) reported that seedling treatment with 10% cell free culture filtrate of *T. atroviride* from rhizosphere of tomato could improve the plant growth and decreased wilt incidence percentage (8%) caused by *Fusarium oxysporum* f. sp. *lycopersici*. The current study also revealed the impact of seed inoculation with selected native *Trichoderma* isolates which helps in improvement of germination efficacy, root, and shoot length in groundnut. The RWC of the root and shoot in treated plants has been increased which indicates the acceleration in the plant growth. Based on the obtained results, the highly efficient strain *T. harzianum* Thar23 exhibits excellent mycelial growth inhibition of pathogen, lytic enzymes production and improve the plant growth could be used against biotic and abiotic stress at greenhouse and field level in pest management practices.

Performance of microbial antagonistic under field condition is one of the important key factors in commercialization of the product at market level. The present findings were in accordance with several research findings stated that the importance of performance of *Trichoderma* spp. against reduction of different pathogen population at field level (Sharma et al. 2012; Jambhulkar et al. 2022). In this present study, there are differences in performance of *Trichoderma* isolates, however treatment with *T. harzianum* Thar23 enhanced groundnut growth, reduction in *S. rolfisii* disease incidence, significant increase in shelling percentage and pod yield among other isolates.

Conclusion

Based on morpho and molecular characterization 35 native *Trichoderma* isolates were grouped into four different *Trichoderma* spp. namely, *T. asperellum* (12), *T. harzianum* (11), *T. Longibrachiatum* (6) and *T. citrinoviride* (6) from rhizosphere of groundnut and screened based on the antagonistic activity against *S. rolfisii*. The potential isolates from each group viz., *T. harzianum* Thar23, *T. asperellum* Tasp49, *T. longibrachiatum* Tlongi5 and *T. citrinoviride* Tcetri2 were selected for lytic enzyme production and plant growth promoting studies in groundnut. The highly efficient isolate *T. harzianum* Thar23 exhibits excellent mycelial growth inhibition of pathogen, lytic enzymes production and improves the plant growth which could be used in biotic and abiotic stress management in groundnut at both green house and field level.

Acknowledgements The authors are thankful to Head, Department of Plant Pathology, Sri Karan Narendra Agriculture University, Jobner for providing research facilities. This present study is part of first author's Ph.D. programme and thankful to Head, Department of Biosciences,

Manipal University Jaipur for necessary support during the research work.

Funding Funding was provided by Indian Council of Agricultural Research (F. No. Agril. Edn. /9/11/2016/ES/HRD).

Declarations

Conflict of interest The authors declare no competing of interest.

References

- Abdul-Baki AA, Anderson JD (1973) Vigour determination in soybean seed by multiple criteria 1. *Crop Sci* 13(6):630–633
- Agrawal T, Kotasthane AS (2012) Chitinolytic assay of indigenous *Trichoderma* isolates collected from different geographical locations of Chhattisgarh in Central India. *Springerplus* 1(1):1–10
- Annual Report (2015–16) ICAR-directorate of groundnut research, Junagadh-362001, Gujarat, India
- Aycock R (1966) Stem rot and other diseases caused by *Sclerotium rolfisii* or the status of Rolfs' fungus after 70 years. Raleigh (NC): North Carolina Agricultural Experiment Station Bulletin, pp 132–202
- Bell DK, Wells HD, Markham CR (1982) In vitro antagonism of *Trichoderma* spp. against six fungal plant pathogens. *Phytopathology* 72:379–382
- Bissett J (1984) A revision of the genus *Trichoderma* I sect. *Longibrachiatum* sect. nov. *Can J Bot* 2:924–931
- Boat MAB, Sameza ML, Iacomini B, Tchameni SN, Boyom FF (2020) Screening, identification and evaluation of *Trichoderma* spp. for biocontrol potential of common bean damping-off pathogens. *Biocontrol Sci Technol* 30(3):228–242
- Cai F, Druzhinina IS (2021) In honour of John Bissett: authoritative guidelines on molecular identification of *Trichoderma*. *Fungal Divers* 107(1):1–69
- Culling KW (1992) Design and testing of a plant specific PCR primer for ecological evolutionary studies. *Mol Ecol* 1:233–240
- Dennis L, Webster J (1971) Antagonistic properties of some species of *Trichoderma*. III. Hyphal production. *Trans Br Mycol Soc* 57:363–369
- Devi P, Prabhakaran N, Kamil D, Choudhary SP (2021) Polyphasic taxonomy of Indian *Trichoderma* species. *Phytotaxa* 502(1):1–27
- Elad Y, Chet I, Henis Y (1981) A selective medium for improving quantitative isolation of *Trichoderma* spp. from soil. *Phytoparasitica* 9:59–67
- Elamathi E, Malathi P, Viswanathan R, Sundar AR (2018) Expression analysis on mycoparasitism related genes during antagonism of *Trichoderma* with *Colletotrichum falcatum* causing red rot in sugarcane. *J Plant Biochem Biotechnol* 27:351–361
- Gomez KA, Gomez AA (1984) Statistical procedures for agricultural research. Wiley, New York
- Guigon-Lopez C, Vargas-Albores F, Guerrero-Prieto V, Ruocco M, Lorito M (2015) Changes in *Trichoderma asperellum* enzyme expression during parasitism of the cotton root rot pathogen *Phymatotrichopsis omnivora*. *Fungal Biol* 119(4):264–273
- Harman GE, Howell CR, Viterbo A, Chet I, Lorito M (2004) *Trichoderma* species: opportunistic, avirulent plant symbionts. *Nat Rev Microbiol* 2:43–56
- Jambhulkar PP, Raja M, Singh B, Katoch S, Kumar S, Sharma P (2022) Potential native *Trichoderma* strains against *Fusarium verticillioides* causing post flowering stalk rot in winter maize. *Crop Prot* 152:105838

- Kamala T, Devi SI, Sharma KC, Kennedy K (2015) Phylogeny and taxonomical investigation of *Trichoderma* spp. from Indian region of Indo-Burma biodiversity hot spot region with special reference to Manipur. *BioMed Res Int* 1–21
- Kaur R, Kalia A, Lore JS, Kaur A, Yadav I, Sharma P, Sandhu JS (2021) *Trichoderma* sp. endochitinase and β -1,3-glucanase impede *Rhizoctonia solani* growth independently, and their combined use does not enhance impediment. *Plant Pathol* 70:1388–1396
- Keswani C, Mishra S, Sarma BK, Singh SP, Singh HB (2014) Unraveling the efficient applications of secondary metabolites of various *Trichoderma* spp. *Appl Microbiol Biotechnol* 98:533–544
- Kimura MA (1980) Simple method for estimating evolutionary rates of base substitutions through comparative studies of nucleotides sequences. *J Mol Evol* 2:87–90
- Kumar K, Amarasan N, Bhagat S, Madhuri K, Srivastava RC (2012) Isolation and characterization of *Trichoderma* spp. for antagonistic activity against root rot and foliar pathogens. *Indian J Microbiol* 52(2):137–144
- Kullnig-Gradinger CM, Szakacs G, Kubicek CP (2002) Phylogeny and evolution of the fungal genus *Trichoderma*—a multigene approach. *Mycol Res* 106:757–767
- Kumar S, Stecher G, Tamura K (2016) MEGA7: molecular evolutionary genetics analysis version 7.0 for bigger datasets. *Mol Biol Evol* 33:1870–1874
- Li Y, Sun R, Yu J, Saravanakumar K, Chen J (2016) Antagonistic and biocontrol potential of *Trichoderma asperellum* ZJSX5003 against the maize stalk rot pathogen *Fusarium graminearum*. *Indian J Microbiol* 56(3):318–327
- Ma J, Tsegaye E, Li M, Wu B, Jiang X (2020) Biodiversity of *Trichoderma* from grassland and forest ecosystems in Northern Xinjiang, China. *3 Biotech* 10(8):1–13
- Macena AMF, Kobori NN, Mascarin GM, Vida JB, Hartman GL (2020) Antagonism of *Trichoderma*-based biofungicides against Brazilian and North American isolates of *Sclerotinia sclerotiorum* and growth promotion of soybean. *Biocontrol* 65:235–246
- Malolepsza U, Nawrocka J, Szczech M (2017) *Trichoderma virens* 106 inoculation stimulates defense enzyme activities and enhances phenolics levels in tomato plants leading to lowered *Rhizoctonia solani* infection. *Biocontrol Sci Technol* 27(2):180–199
- Manzar N, Singh Y, Kashyap AS, Sahu PK, Rajawat MVS, Bhowmik A, Sharma PK, Saxena AK (2021) Biocontrol potential of native *Trichoderma* spp. against anthracnose of great millet (*Sorghum bicolor* L.) from Tarai and hill regions of India. *Biol Control* 152:104474
- Muthu KA, Sharma P (2011) Molecular and morphological characters: an appurtenance for antagonism in *Trichoderma* spp. *Afr J Biotechnol* 10(22):4532–4543
- Nofal AM, El-Rahman MA, AbdelghanyTM A-M, M, (2021) Mycoparasitic nature of Egyptian *Trichoderma* isolates and their impact on suppression Fusarium wilt of tomato. *Egypt J Biol Pest Control* 31:103
- Pandian RTP, Raja M, Kumar A, Sharma P (2016) Morphological and molecular characterization of *Trichoderma asperellum* strain Ta13. *Indian Phytopathol* 69:297–303
- Persoon CH (1794) *Dispositamethodicafungorum*. *RomersneuesMagazin der Botanik* 1:81–128
- Raja M, Sharma RK, Jambhulkar PP, Sharma KR, Sharma P (2021) Biosynthesis of silver nanoparticles from *Trichoderma harzianum* Th3 and its efficacy against root rot complex pathogen in groundnut. *Mater Today Proc* 43(5):3140–3143
- Rifai MA (1969) A revision of the genus *Trichoderma*. *Mycol Papers* 116:1–56
- Sallam N, Eraky AM, Sallam A (2019) Effect of *Trichoderma* spp. on Fusarium wilt disease of tomato. *Mol Biol Rep* 46(4):4463–4470
- Samuels GJ, Lieckfeldt E, Nirenberg HI (1999) *Trichoderma asperellum*, a new species with warted conidia, and redescription *T. viride*. *Sydowia* 51:71–88
- Schuster A, Schmoll M (2010) Biology and biotechnology of *Trichoderma*. *Appl Microbiol Biotechnol* 87(3):787–799
- Sharma P, Saini MK, Deep S, Kumar V (2012) Biological control of groundnut root rot in farmer's field. *J Agric Sci* 4(8):48–59
- Sharma P, Sharma M, Raja M, Shanmugam V (2014) Status of *Trichoderma* research in India: a review. *Indian Phytopathol* 67(1):1–19
- Thompson JD, Higgins DG, Gibson TJ (1994) CLUSTALW: improving the sensitivity of progressive multiple sequence alignment through sequence weighting, position-specific gap penalties and weight matrix choice. *Nucleic Acids Res* 22:4673–4680
- Tian X, He M, Wang Z, Zhang J, Song Y, He Z, Dong Y (2015) Application of nitric oxide and calcium nitrate enhances tolerance of wheat seedlings to salt stress. *Plant Growth Regul* 77(3):343–356
- Tulasne LR, Tulasne C (1865) *Selecta fungorumcarpologia*. Jussu, Paris
- Vinale F, Sivasithamparam K (2020) Beneficial effects of *Trichoderma* secondary metabolites on crops. *Phytother Res* 34(11):2835–2842
- White TJ, Bruns T, Lee SJWT, Taylor J (1990) Amplification and direct sequencing of fungal ribosomal RNA genes for phylogenetics. In: Innis MA, Gelfand DH, Sninsky JJ, White TJ (eds) *PCR protocols: a guide to methods and applications*. Academic Press, New York, pp 315–322

Publisher's Note Springer Nature remains neutral with regard to jurisdictional claims in published maps and institutional affiliations.

Springer Nature or its licensor (e.g. a society or other partner) holds exclusive rights to this article under a publishing agreement with the author(s) or other rightsholder(s); author self-archiving of the accepted manuscript version of this article is solely governed by the terms of such publishing agreement and applicable law.



OPEN ACCESS

EDITED BY

Sirikanjana Thongmee,
Kasetsart University, Thailand

REVIEWED BY

Ramzan Ahmed,
University of Science and Technology,
Meghalaya, India
Mithun Kumar Ghosh,
Govt College Hatta, India

*CORRESPONDENCE

Devendra Jain,
✉ devroshan@gmail.com,
✉ devendrajain@mpuat.ac.in

SPECIALTY SECTION

This article was submitted to
Nanoscience,
a section of the journal
Frontiers in Chemistry

RECEIVED 30 January 2023

ACCEPTED 23 March 2023

PUBLISHED 07 April 2023

CITATION

Singh D, Jain D, Rajpurohit D, Jat G,
Kushwaha HS, Singh A, Mohanty SR,
Al-Sadoon MK, Zaman W and
Upadhyay SK (2023), Bacteria assisted
green synthesis of copper oxide
nanoparticles and their potential
applications as antimicrobial agents and
plant growth stimulants.
Front. Chem. 11:1154128.
doi: 10.3389/fchem.2023.1154128

COPYRIGHT

© 2023 Singh, Jain, Rajpurohit, Jat,
Kushwaha, Singh, Mohanty, Al-Sadoon,
Zaman and Upadhyay. This is an open-
access article distributed under the terms
of the [Creative Commons Attribution
License \(CC BY\)](https://creativecommons.org/licenses/by/4.0/). The use, distribution or
reproduction in other forums is
permitted, provided the original author(s)
and the copyright owner(s) are credited
and that the original publication in this
journal is cited, in accordance with
accepted academic practice. No use,
distribution or reproduction is permitted
which does not comply with these terms.

Bacteria assisted green synthesis of copper oxide nanoparticles and their potential applications as antimicrobial agents and plant growth stimulants

Deepak Singh¹, Devendra Jain^{1*}, Deepak Rajpurohit¹,
Gajanand Jat², Himmat Singh Kushwaha³, Abhijeet Singh⁴,
Santosh Ranjan Mohanty⁵, Mohammad Khalid Al-Sadoon⁶,
Wajid Zaman⁷ and Sudhir K. Upadhyay⁸

¹Department of Molecular Biology and Biotechnology, Maharana Pratap University of Agriculture and Technology, Udaipur, India, ²Department of Soil Science and Agricultural Chemistry, Maharana Pratap University of Agriculture and Technology, Udaipur, India, ³Material Research Centre, Malviya National Institute of Technology, Jaipur, India, ⁴Department of Biosciences, Manipal University Jaipur, Jaipur, India, ⁵All India Network Project on Soil Biodiversity-Biofertilizers, ICAR-Indian Institute of Soil Science, Bhopal, India, ⁶Department of Zoology, College of Science, King Saud University, Riyadh, Saudi Arabia, ⁷Department of Life Sciences, Yeungnam University, Gyeongsan, Republic of Korea, ⁸Department of Environmental Science, V. B. S. Purvanchal University, Jaunpur, India

Copper oxide nanoparticles (CuO-NPs) have piqued the interest of agricultural researchers due to their potential application as fungicides, insecticides, and fertilizers. The *Serratia* sp. ZTB29 strain, which has the NCBI accession number MK773873, was a novel isolate used in this investigation that produced CuO-NPs. This strain can survive concentrations of copper as high as 22.5 mM and can also remove copper by synthesizing pure CuO-NPs. UV-VIS spectroscopy, DLS, Zeta potential, FTIR, TEM, and XRD techniques were used to investigate the pure form of CuO-NPs. The synthesized CuO-NPs were crystalline in nature (average size of 22 nm) with a monoclinic phase according to the XRD pattern. CuO-NPs were found to be polydisperse, spherical, and agglomeration-free. According to TEM and DLS inspection, they ranged in size from 20 to 40 nm, with a typical particle size of 28 nm. CuO-NPs were extremely stable, as demonstrated by their zeta potential of -15.4 mV. The ester (C=O), carboxyl (C=O), amine (NH), thiol (S-H), hydroxyl (OH), alkyne (C-H), and aromatic amine (C-N) groups from bacterial secretion were primarily responsible for reduction and stabilization of CuO-NPs revealed in an FTIR analysis. CuO-NPs at concentrations of 50 $\mu\text{g mL}^{-1}$ and 200 $\mu\text{g mL}^{-1}$ displayed antibacterial and antifungal activity against the plant pathogenic bacteria *Xanthomonas* sp. and pathogenic fungus *Alternaria* sp., respectively. The results of this investigation support the claims that CuO-NPs can be used as an efficient antimicrobial agent and nano-fertilizer, since, compared to the control and higher concentrations of CuO-NPs (100 mg L⁻¹) considerably improved the growth characteristics of maize plants.

KEYWORDS

novel bacterial isolate, 16s-rDNA sequencing, CuO-NPs-green synthesis, confirmatory tests, antimicrobial and plant growth-promoting activity

1 Introduction

Nanotechnology research is the most active research region in contemporary materials science (Singh et al., 2018; Rajput et al., 2021a; Bhavyasree and Xavier, 2022). Nanomaterials synthesis through conventional physical and chemical methods has several adverse features *viz.*, critically high pressure and temperature conditions, utilization of expensive and hazardous chemicals, a longer reaction time and absorbance of toxic by-products on nanomaterial surface (Buazar et al., 2019; Sukumar et al., 2020). Properties of NPs determined by their size, shape, composition, crystalline, and structure (Sharma et al., 2020; Hidangmayum et al., 2022; Rajput et al., 2022). Recent years have seen a significant increase in the significance of green synthesis techniques for nanomaterials, making it one of the very popular methods in modern material sciences (Sukhwal et al., 2017; Mahboub et al., 2022).

Green synthesis has become one of the most preferred methods to overcome the adverse effects physical and chemical synthesis such as critical conditions of temperature and pressure, expensive and toxic chemicals, long reflux time of reaction, toxic by-products *etc.* (Sukhwal et al., 2017; Jain et al., 2020). Metal-tolerant bacteria are important nano-factories that not only accumulates and also detoxify heavy metals due to the various mechanism, *i.e.*, reductase enzymes, EPS, *etc.*, to reduce metal salts to nanomaterials (Jain et al., 2012; Jain et al., 2020; Garg et al., 2022). The nanomaterial synthesis using plant extracts may be easier than microbial synthesis however the microbial synthesis is more cost-effective and freer from any seasonal and plant growth stage variation.

Inorganic metal oxide NPs, *viz.*, CuO, ZnO, MgO, TiO₂, SiO₂, *etc.*, with significant antimicrobial features as well as their selective toxicity, point to potential applications of these materials in medical devices and diagnostics, therapeutics, and nanomedicine against human pathogens (Mohsen and Zahra, 2008; Sobha et al., 2010; Jain D. et al., 2022). These inorganic oxide NPs are beneficial as antibacterial agents because they are more effective against resistant pathogens. According to Makhluaf et al. (2005), crystalline structure and particle shape of nanomaterials have relatively little effect on antibacterial behavior, but a high concentration of smaller-size nanoparticles with a higher surface area does.

The simplest copper compound in the family is copper oxide, which has a variety of possibly practical physical characteristics (Buazar et al., 2019). Copper oxide (CuO) has drawn more interest than other nanomaterials because of its distinctive qualities, which include stability, conductivity, catalytic activity, and anticancer and antibacterial activities. Copper oxide nanoparticles (CuO-NPs) are receiving more attention owing to their availability and lower cost when compared to more costly and noble metals like gold and silver, as well as their effective potential for application as microbial agents (Sankar et al., 2014). Among them, CuO-NPs has drawn a lot of attention in research areas including solar cells, biodiesel, photocatalysis, water pollutant removal, supercapacitors, and electrocatalysis owing to their desired qualities, such as cheap cost, non-toxicity, and ease of manufacturing (Grigore et al., 2016).

By preventing the growth of bacteria, fungi, viruses, and algae, CuO-NPs have important antimicrobial qualities (Amin et al., 2021; Bukhari et al., 2021). Furthermore, compared to other organic antimicrobials like silver and gold, nanoscale copper oxide has a

longer shelf life. According to Keabadile et al. (2020) green synthesis of CuO-NPs with acceptable physio-chemical characteristics has previously been performed with several microbial precursors as reductants. However, very little study has been done on the synthesis of CuO-NPs employing bacteria that are copper-resistant. Hence, the current investigation was conducted to tackle this issue and build a bacteria-assisted synthesis of CuO-NPs and assessment of their antimicrobial and plant growth stimulating activities.

2 Materials and methods

2.1 Source, minimum inhibitory concentration, and molecular identification of copper-tolerant bacteria

The maximum copper tolerance concentration (MTC) was determined on LB agar medium (in triplicate) having an increased concentration of CuSO₄ (2.5–25 mM), and the MTCs were noted from the concentration of CuSO₄ at which the isolate failed to demonstrate growth. The different bacterial isolates were utilized in this study taken from our lab, which were isolated from Zn-Pb ore mine tailings areas of Zawar mines in Udaipur, Rajasthan, India (Jain et al., 2020). According to a previously illustrated method, the 16S rDNA region was amplified and sequenced to perform molecular characterization of copper-tolerant bacteria (Janda and Abbott, 2007).

2.2 Bacterial-assisted synthesis of copper oxide nanoparticles

The synthesis of CuO-NPs was borne out by using copper (Cu) tolerant bacterial isolate (ZTB29) with little modification technique of earlier published (John et al., 2021). The bacterial strain that showed the highest tolerance against copper ion, was inoculated in LB medium (100 mL) and incubated at 28°C with 150 rpm. After 24 h, 5 mM CuSO₄·5H₂O was dropped into the bacterial culture and incubated for 48 h at 28°C until the solution color changed from blue to green. This combination was then centrifuged at 4,000 rpm for 20 min at 4°C to separate the bacterial cell pellet, and the CuO-NPs were produced by centrifuging the residual supernatant at 14,000 rpm for 15 min at 4°C. The obtained CuO-NP pellet was washed twice with deionized water, dried at 80°C in an oven and used for further characterization. A control experiment without copper-tolerant bacteria was also done and upon inclusion of 5 mM CuSO₄·5H₂O, the color change was not seen which states no nanoparticles formation.

2.3 Characterization of CuO-NPs

CuO-NPs were primarily characterized using UV-Vis absorption scanning at 200–1,000 nm using a nanophotometer (Make: Implen, Germany) as the method outlined by Davaeifar et al. (2019). Dynamic Light Scattering (DLS) and Zeta potential were performed by the earlier described method (Rajput et al., 2021b) by using Malvern zeta-sizer nanoseries (United Kingdom). The FTIR spectroscopy (Perkin Elmer)

was performed for CuO-NPs (in KBr pellets) in the 4,100–400 cm^{-1} range (Garg et al., 2022). Around 10 μL of CuO-NPs dispersed in milli Q water were placed onto carbon-coated copper TEM grid for transmission electron microscopy (Tecnai G220 (FEI) S-Twin 200kv) (Sukhwal et al., 2017). The dried powder of CuO-NPs was further characterized by XRD (X'Pert Pro X-ray diffractometer, PAN analytical BV) with Cu K α radiation set with 40 kV and 30 mA (Sukhwal et al., 2017).

2.4 Antimicrobial activities of CuO nanoparticles

Antibacterial activities of bacterial-assisted CuO-NPs were studied by both disc diffusion method and well diffusion using LB agar medium against plant pathogenic bacteria *Xanthomonas* sp. Briefly, 1 mL bacterial suspension ($>10^7$ CFU mL^{-1}) was spread by spreader on LB agar Petri-plates, and in disc diffusion method, the sterile filter paper disk, dipped in a known concentration of CuO-NPs was placed on LB agar plates whereas, in well diffusion method, 5 mm wells (prepared by sterile cork-borer on LB agar Petri-plates) were loaded with CuO-NPs and incubated for inhibition zone development (Jain et al., 2020). The antifungal activities of CuO-NPs were investigated by using the poisoned food technique and spore germination test. The radial mycelia growth of test fungi *Alternaria* sp. was recorded on PDA containing different concentrations of CuO-NPs (50, 75, 100, 150, and 200 $\mu\text{g mL}^{-1}$). PDA plates without CuO-NPs were used as a control. These plates were kept for incubation at 25°C until full radical growth was observed in the control. The different concentration of CuO-NPs was used as per the CRD design in triplicate and the significant difference among treatment were determined by Turkey–Kramer HSD test at $p = 0.05$.

2.5 *In vitro* studies of CuO-NPs on the growth of maize

The experimental pot was filled with agricultural soil supplemented with sterile planting mixture, seeded with maize seed (PRATAP-3), and placed inside the plant growth chamber (humidity: 60%, light intensity: 750 $\mu\text{mol/m}^2\text{s}$ with 15 h light and 9 h dark conditions at 25°C–20°C). Seven days old maize seedlings were treated with CuO-NPs concentrations *viz.* 0, 25, 50, 75, 100, 200, and 300 mg L^{-1} (in Hoagland solution) as foliar spray. The shoot length (cm), root length (cm), chlorophyll content (SPAD-502 + Chlorophyll Meter, Spectrum Technologies, India), Copper content [atomic absorption spectroscopy (AAS), Make: Electronics co. India Ltd. Modal no. AAS4141] was studied in 21 days old seedlings (Garg et al., 2022).

3 Result

3.1 Source, screening of MTC against copper and molecular identification of potent copper-tolerant bacteria

The bacterial isolates ZTB15, ZTB24, ZTB28, and ZTB29 were tested for their maximum copper (CuSO_4) tolerance levels in

nutritional broth and observed Minimum inhibitory concentration (MIC). The bacterial isolate ZTB29 had a very maximum MIC of 22.5 mM copper in the medium and was able to withstand high doses of copper in the current experiment (Supplementary Table S1). A further selection of the ZTB29 strain was made for the bacterially aided synthesis of copper oxide CuO-NPs. The ZTB-29 isolate's 16S rRNA gene was sequenced in its entirety and put into nucleotide-nucleotide BLAST analysis. The strains' similarity and matches to previously published bacterial rDNA sequences allowed scientists to identify them as *Serratia* sp. (Figure 1). The ZTB29 nucleotide sequence was deposited to NCBI with the accession MK773873. The detailed biochemical, plant growth promoting and other physiological attributes of the ZTB29 strain were summarized in (Supplementary Table S2) which enables the ZTB29 strain to not only bioremediate excess copper but also to promote plant growth.

3.2 ZTB29 assisted copper oxide nanoparticles synthesis and its confirmatory examination

The easily observed synthetic bacterial growth in the bottom of the flask demonstrated the reaction between the bacterium and copper sulfate, the precursor salt. The starting solution's color changed from light blue to green when 5 mM copper sulfate was added drop by drop to the bacterial suspension, indicating the production of CuO-NPs. The greatest absorbance of 285 nm by using UV-visible spectroscopy was observed, indicating that copper sulfate (which does not produce any absorbance at 285 nm: Supplementary Figure S1), the starting material, was converted to CuO-NPs, as shown in (Figure 2).

The surface charge, size distribution, and potential stability of the nanoparticles contained in a liquid were characterized using dynamic light scattering (DLS) and zeta potential, respectively. Particles in the solution ranged in size from 15 nm to 30 nm and were homogeneous in size. The average CuO-NPs particle size was 21 ± 5.4 nm which was created with a homogenous dispersion (Figure 3A). The TEM investigations provided strong support for the DLS findings. The presence of bacterial cell artifacts or the agglomeration of nanoparticles may be responsible for the second large-size distribution peak at about 1,000 nm. The zeta potential's magnitude (–30 mV to +30 mV) determines the stability and primarily depends upon the surface charge of the generated nanomaterials. The produced nanoparticles have a Zeta potential of –15.4 mV, which demonstrates that they were quite stable at ambient temperature (Figure 3B). The similar zeta potential value was observed even after 1 year of synthesis with CuO-NPs suggesting CuO-NPs were stable for 1 year or more. Zeta potential with a negative value indicates a strong repelling force between the particles, which inhibits agglomeration.

Fourier transform infrared spectroscopy (FTIR) technique was utilized to recognize the occurrence of different functional groups found in a sample. Depending on the infrared absorption range 600–4,000 cm^{-1} in FTIR analysis, the absorbance range 3,200–3,550 cm^{-1} is indicated for O-H stretching, 2,371 cm^{-1} observance for O=C=O stretching, 1,624 cm^{-1} observance for C=C stretching, 1,058 cm^{-1} observance for C-OH stretching,

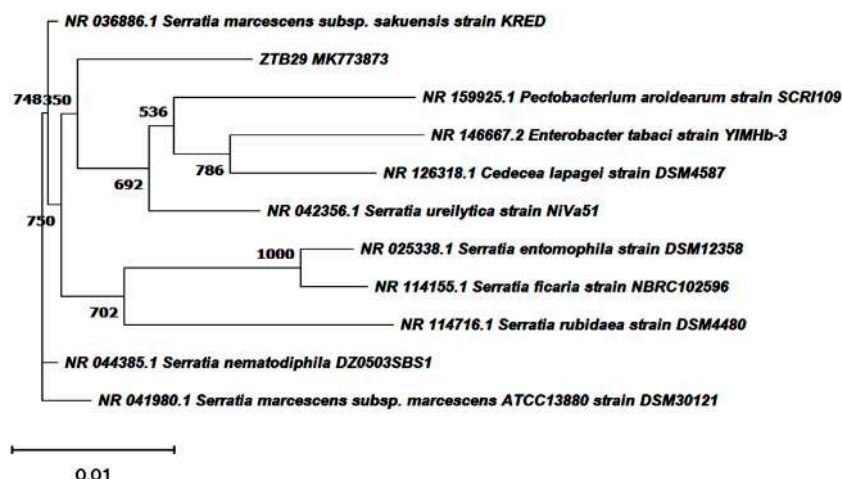


FIGURE 1

Neighbourhood joining tree showing the polygenetic relationship of copper tolerant bacterial strain ZTB29 *Serratia* sp. (NCBI Accession: MK773873).

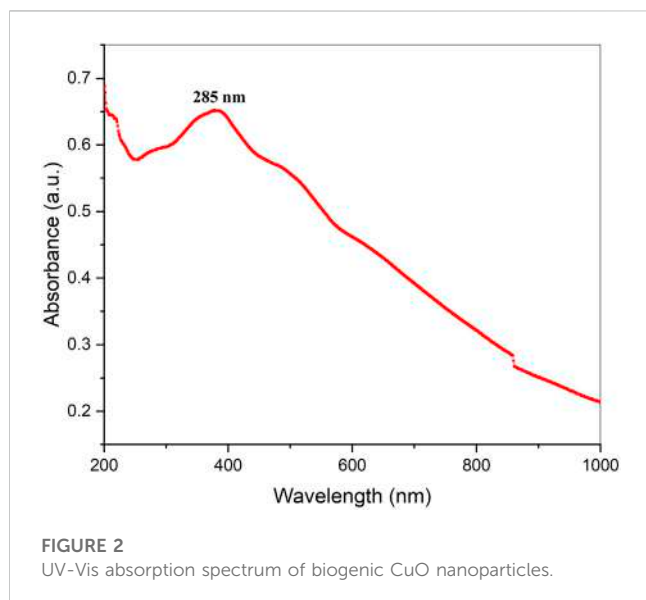


FIGURE 2

UV-Vis absorption spectrum of biogenic CuO nanoparticles.

$1,377\text{ cm}^{-1}$ observance for the existence of CO_2 when compared with the standard database. The 608 cm^{-1} vibration attributed to CuO formation confirms the synthesis of pure CuO nanostructures. FTIR study revealed that the carboxyl (C=O), hydroxyl (OH), amine (NH), alkyne (C-H), thiol (S-H), ester (C=O) and aromatic amine (C-N) groups from the bacterial secretion are responsible for the copper reduction and CuO-NPs stabilization (Figure 4). The details of the different FTIR peaks observed in bacteria assisted CuO-NPs and the bacterial extract used for CuO-NPs synthesis were described in the Supplementary Table S3 and Supplementary Figure S2. The CuO-NP's size and shape were studied using TEM. TEM analysis revealed the formation of different shapes of copper oxide nanostructures (Figure 5). It was evident from TEM studies that CuO-NPs were polydisperse and spherical which were free from agglomeration. The particles were in the size range of 20–40 nm with 28 nm average particles size.

X-ray diffraction (XRD) was performed to study the phase (structure) and purity (composition) of the biosynthesized CuO-NPs using copper-tolerant bacteria. The XRD pattern (Figure 6) depicted the creation of pure and crystalline CuO-NPs. The peaks at $2\theta = 32.548$, 35.466 , and 38.769 were assigned to the (110) (002) and (111) reflection lines of monoclinic CuO-NPs compared to JCPDS file No. 01-080-1268. The average crystallite size calculated based on the Scherrer technique for synthesized CuO-NP was 22 nm.

3.3 Antimicrobial activities of CuO-NPs

The CuO-NPs ($50\text{ }\mu\text{g mL}^{-1}$) showed significant antibacterial activity by generating an inhibition zone in well diffusion assay (Figure 7A). The disc contacting $50\text{ }\mu\text{g mL}^{-1}$ CuO-NPs demonstrated antibacterial activity against *Xanthomonas* sp. as it showed a clear inhibition zone (Figure 7B), which was higher compare to Neomycin ($30\text{ }\mu\text{g mL}^{-1}$) and lower compare to Rifampicin ($5\text{ }\mu\text{g mL}^{-1}$). The highest inhibition of 91% in fungal mycelia and 88% spore germination was detected at the $200\text{ }\mu\text{g mL}^{-1}$ CuO-NPs concentration (Table 1). The rate of mycelia inhibition and spore germination was proportional to CuO-NPs concentration (Figure 8). The results observed in the present study revealed CuO-NP can be used as an efficient nano fungicide against soil-born fungus.

3.4 Influence of CuO-NPs on maize seedling

The shoot and root length, plant biomass, total chlorophyll and copper content were considerably high in the maize plantlet (21 days old) compared to the untreated control plantlet (Table 2). The maximum shoot and root length, biomass and chlorophyll content were observed in 100 mg L^{-1} CuO-NPs application and contributed to plant growth significantly as efficient nano-fertilizers. The CuO-NPs ($<100\text{ mg L}^{-1}$) caused significant toxicity to maize seedlings and resulted in decreased growth parameters.

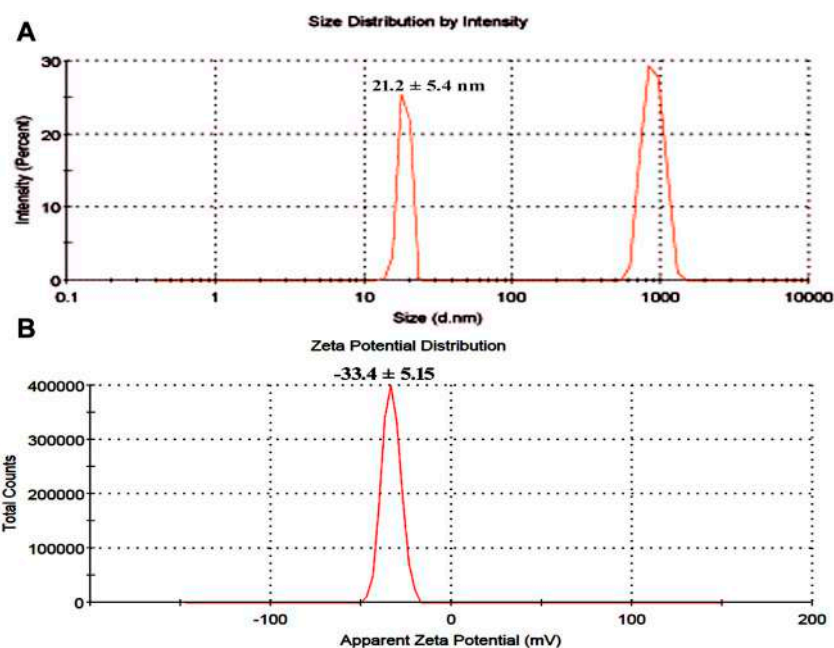


FIGURE 3 (A) Particle size determination using dynamic light scattering (B) Zeta potential analysis of bacterial assisted CuO nanoparticles.

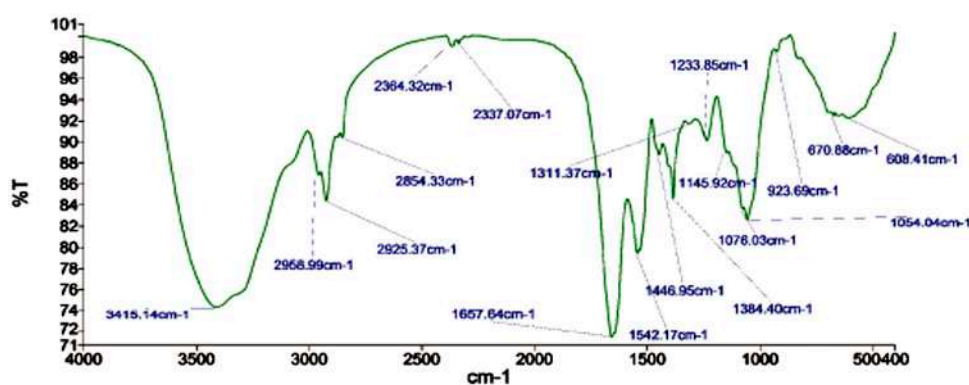


FIGURE 4 FTIR analysis of biogenic CuO nanoparticles.

4 Discussions

The new study could pave the way for bioprospecting for metal-tolerant microorganisms for the quick and easy synthesis of nanoparticles with a variety of applications (Jain et al., 2012; Jain et al., 2020). John et al. (2021) investigated bacterial strain copper tolerance at various CuSO_4 concentrations, and the bacterial strain *Marinomonas*, which tolerated 5 mM CuSO_4 , was employed to produce copper and CuO-NPs. Similar findings were found in the current investigation. Tiwari et al. (2016) synthesized CuO-NPs from a copper-resistant *Bacillus cereus* isolate that tolerated >10 mM of copper. The *B. cereus* isolate was able to and was identified as *B. cereus* using 16S rDNA amplification and sequencing. The change of color depends on the surface plasmon vibration of the

nanoparticles (Abdulhameed et al., 2019). Shantkriti and Rani (2014) observed that the color of the reaction changed from blue to dark green when CuSO_4 was added to the *Pseudomonas fluorescens* solution, which corroborated the findings. The bacteria-assisted green synthesis of metal and metal oxide nanoparticles is dependent on the bacteria's ability to remediate harmful metal concentrations by reducing metal ions to nanoparticles (Jain et al., 2020). As a result, copper-tolerant bacteria produce copper and copper oxide nanomaterials by mimicking the natural biomineralization processes that these microbes have adapted to under dangerous copper concentrations (John et al., 2021).

UV-visible absorption spectroscopy can be used to characterize metallic nanoparticles based on surface plasmon resonance (SPR) (Upadhyay et al., 2023). UV-visible spectroscopy (wavelength scan

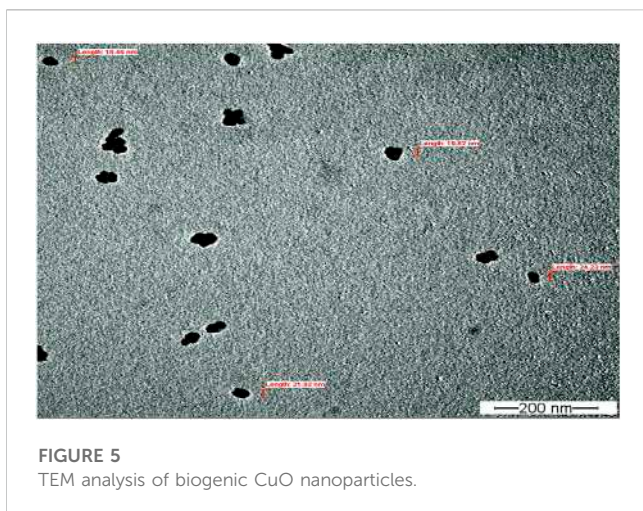


FIGURE 5
TEM analysis of biogenic CuO nanoparticles.

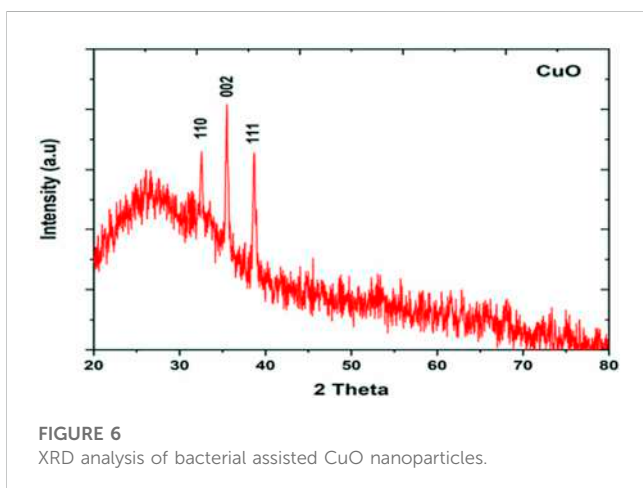


FIGURE 6
XRD analysis of bacterial assisted CuO nanoparticles.

between 200 and 1,000 nm) was used to observe the solution resulting from the bluish-to-greenish color alterations of copper-tolerant bacteria (Zhao et al., 2022). The spectra of CuO-NPs generated employing copper-tolerant bacteria showed pronounced absorption at 285 nm wavelength, confirming the conversion of the starting material (copper sulfate) to the final product (CuO nanoparticles) as shown in Figure 3. Tshireletso et al. (2021) revealed that the UV-VIS absorption spectra of green-produced CuO-NPs from citrus peel extracts resulted in a notable absorbance at 290 nm. Due to surface plasmon resonance, Sankar et al. (2014) found that the UV-Vis spectra of papaya leaf extract medicated CuO-NPs spanned between 250–300 nm. In contrast, the different experiments revealed distinct absorption peaks and spectrums, which could be attributable to different forms of copper and copper oxide nanomaterials and the technology employed for nanomaterial fabrication.

DLS confirmed that the produced CuO-NPs had a homogeneous particle size distribution (15 nm–30 nm) and an average particle size of 21 ± 5.4 nm (Figure 4A), which TEM investigations also validated. The CuO-NPs' -15.4 mV zeta value clearly demonstrated their fairly stable character, as illustrated in Figure 4B. Nardella et al. (2022) conducted DLS investigations of biosynthesized CuO-NPs and reported a 24.4 nm Z-average diameter, while the zeta potential value, which frequently analyses the stability of nanoparticles, was found to be -16.1 mV, confirming the nanoparticles' stability. Nagaraj et al. (2019) reported

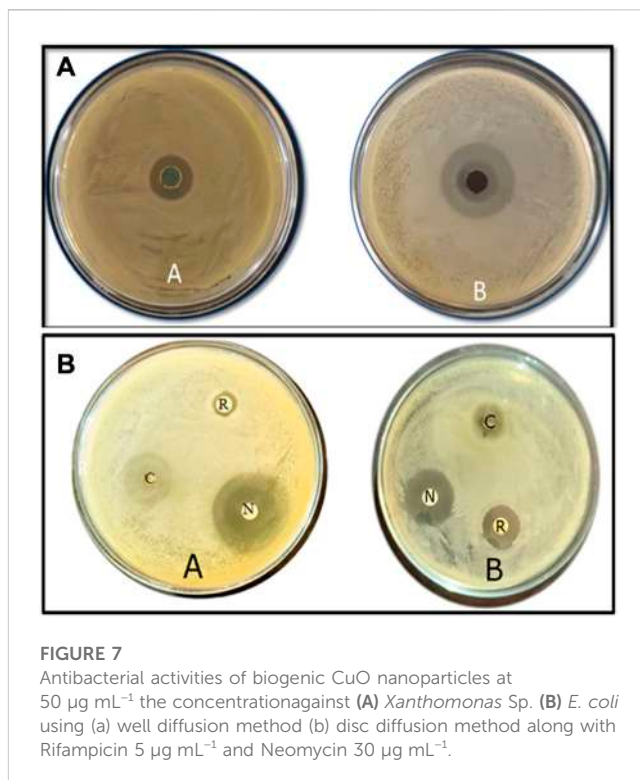


FIGURE 7
Antibacterial activities of biogenic CuO nanoparticles at $50 \mu\text{g mL}^{-1}$ the concentration against (A) *Xanthomonas* Sp. (B) *E. coli* using (a) well diffusion method (b) disc diffusion method along with Rifampicin $5 \mu\text{g mL}^{-1}$ and Neomycin $30 \mu\text{g mL}^{-1}$.

the *Pterolobium hexapetalum* leaf extract-mediated synthesized CuO-NPs and the synthesized nanoparticles were extensively distributed and highly dispersed in the 10–76 nm size range, however, the associated zeta potential was -27.6 mV attributed to moderate stability of nanoparticles.

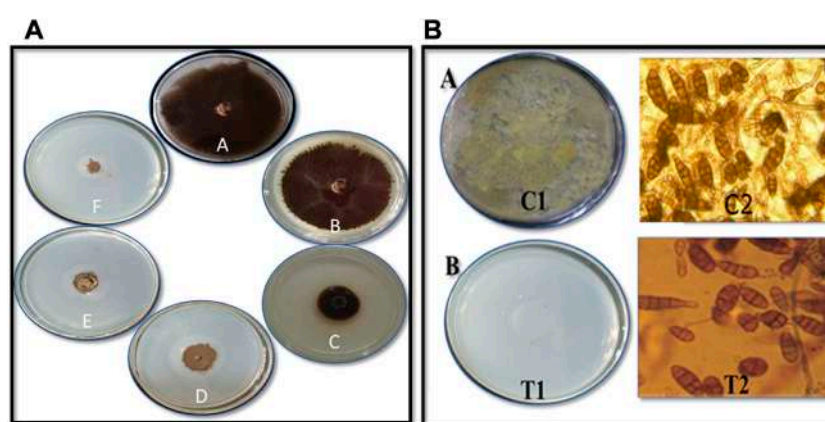
FTIR study indicated the presence of different compounds from the bacterial secretion involved in the reduction and stabilization of CuO-NPs. Amin et al. (2021) observed the FTIR peaks at 518.4 and 600.1 cm^{-1} (formation of CuO nanostructure and Cu–O stretching), $1,021.14$ and 800.58 cm^{-1} (assigned to C–O and C–H bending) and $1,412.3$ and $1,636.4 \text{ cm}^{-1}$ (O–H bending and C=C stretching). John et al. (2021) studied FTIR spectroscopy of CuO-NPs synthesized from marine bacteria indicating the presence of $-\text{C}=\text{O}$, $-\text{OH}$, $-\text{NH}$, $-\text{CH}_2$ scissor vibrations of aliphatic compounds and C=C bonds inside the biomolecules suggesting the interaction of these biomolecules with CuO-NPs also observed in the present study.

TEM analysis revealed the formation of polydisperse and roughly spherical CuO-NPs which were free from agglomeration with the 20–40 nm size range (average particle size is 28 nm). The CuO-NPs as water suspension are slightly agglomerated due to their interaction with water and due to such inter-particle interactions viz. van der Waals, electrostatic and magnetic forces, etc. Previously, similar results of biogenic CuO-NPs were reported by several studies (Ida et al., 2010; Cheng and Walker, 2010; Chandra et al., 2014; Sagadevan and Koteswari, 2015; Kimber et al., 2020; Singh et al., 2019) as observed in TEM. John et al. (2021) reported the TEM micrographs of CuO-NPs from marine bacteria and reported the synthesis of monodispersed, spherical/ovoidal NPs of 10 nm–70 nm size with ~ 40 nm average size. The irregular shape can be attributed to bacterial metabolites on the surface of nanoparticles as stabilizing and reducing agents. Bukhari et al. (2021) reported the *Streptomyces* sp. mediated Cu-NPs synthesis of uniform and spherical nanoparticles (1.72–13.49 nm) in the TEM

TABLE 1 Effect of varying concentrations of CuO nanoparticles on *in vitro* mycelial growth and spore germination of phytopathogenic fungi *Alternaria* sp.

Treatment (CuO nanoparticles)	Percent inhibition mycelia growth	Percent inhibition spore germination
Control	0.0 ± 0.0 _A	5.33 ± 1.52 _A
50 µg mL ⁻¹	15.0 ± 1.53 _B	15.0 ± 2.0 _B
75 µg mL ⁻¹	70.0 ± 1.53 _C	55.0 ± 2.0 _C
100 µg mL ⁻¹	77.0 ± 5.7 _{CD}	64.3 ± 2.51 _D
150 µg mL ⁻¹	81.0 ± 2.0 _D	74.0 ± 1.0 _E
200 µg mL ⁻¹	91.0 ± 1.52 _E	88.0 ± 2.0 _F

*Each value is mean of 3 replicates from 2 experiments. Mean ± SE, followed by same letter in column of each treatment is not significant difference at $p = 0.05$ by Tukey–Kramer HSD, test, % inhibition rate was calculated compared to the germination of the control (0%).

**FIGURE 8**

Antifungal activity of CuO nanoparticles against *Alternaria* sp. on (A) mycelial growth inhibition by poisoned food technique (A) Control (B) 50 µg mL⁻¹ (C) 75 µg mL⁻¹ (D) 100 µg mL⁻¹ (E) 150 µg mL⁻¹ and (F) 200 µg mL⁻¹ CuO nanoparticles (B) Spore germination inhibition by (A) Pour plate technique C1 - Crude spore suspension and T1 - 200 µg mL⁻¹ CuO nanoparticles (B) Microscopic studies C2: Control, T2: 200 µg mL⁻¹ CuO nanoparticles.

TABLE 2 *In vitro* studies on the effect of CuO-NPs on growth of maize seedling (Data are means of three replicates ±SD. Data are recorded after 21 days of germination).

Treatment	Average shoot length (cm)	Shoot dry weight (g)	Average root length (cm)	Chlorophyll index (SPAD)	Copper content in maize seedling (ppm)
Control	18.4 ± 1.7	4.4 ± 1.1	12.8 ± 2.1	10.03 ± 2.11	0.041 ± 0.02
T 1	24.5 ± 2.4	7.8 ± 2.3	14.8 ± 3.2	12.33 ± 2.65	0.055 ± 0.08
T 2	28.8 ± 2.8	8.3 ± 1.6	21.6 ± 2.4	13.63 ± 2.49	0.088 ± 0.06
T 3	32.4 ± 2.2	8.4 ± 2.1	24.1 ± 1.9	14.14 ± 2.43	0.092 ± 0.08
T 4	34.2 ± 3.1	10.6 ± 1.8	24.8 ± 2.3	16.86 ± 4.5	0.098 ± 0.09
T 5	29.4 ± 2.3	9.1 ± 1.5	22.7 ± 2.1	13.93 ± 2.8	0.012 ± 0.05
T 6	21.1 ± 1.9	7.5 ± 1.2	15.1 ± 1.7	11.26 ± 2.3	0.015 ± 0.05

images. Krishna et al. (2020) synthesized CuO nanoparticles from *Cinnamomum malabratrum* aqueous leaf extract and the TEM revealed spherically shaped CuO-NPs with 11 nm–24 nm size range which was also in close agreement with the present study.

The XRD pattern revealed the pure CuO-NPs were crystalline in nature. Ali et al. (2021) performed XRD of CuO-NPs and the detected peaks in their study confirmed the monoclinic phase of CuO compared to JCPDS card 000021040 which was also seen in the present study. Further, the characteristic crystallite size measured

using the Scherrer equation was found to be 24.7 nm also supports the finding of the present study. Buazaret al. (2019) reported that clear and sharp peaks in XRD can be ascribed to the highly crystalline structure of nanomaterials. Similar results of the crystallite size of CuO-NPs in the range of 9–23 nm were solely dependent on the precursor conditions (Tavakoli et al., 2019).

The CuO-NPs exhibited superior antimicrobial activities and have a significant potential to control phytopathogens. Krishna et al. (2020) reported significant antibacterial activities of CuO-NPs against human pathogenic bacteria viz., *Escherichia coli*, *Staphylococcus aureus*, *Pseudomonas aeruginosa* and *Proteus mirabilis* using well diffusion method and similar results were also observed against plant pathogenic bacteria in the present study. Abboud et al. (2014) reported significant antimicrobial activities of CuO-NPs synthesized from the alga extract against *Enterobacter aerogenes* and *S. aureus* and the observed radial diameter of the inhibition zone was 14 and 16 mm, respectively. Bhavyasree and Xavier (2022) extensively reviewed the copper and CuO nanomaterial and their antimicrobial properties and demonstrated the mechanism of antibacterial action which includes mechanical damage, gene toxicity, and oxidative stress injury. The bio-molecules absorbed on the surface may also help in the antimicrobial activities of CuO-NPs.

The CuO-NPs (200 g mL⁻¹ concentration) exhibited superior antifungal activities. Qamar et al. (2020) showed reasonable results for the antifungal activity of CuO-NPs against *Trichophyton rubrum*. Rabiee et al. (2020) synthesized *Achillea millefolium* extract-mediated CuO-NPs and reported significant *in vitro* antifungal activities against four different fungi. The biosynthesized CuO-NPs showed effective antifungal activities owing to the entering of CuO-NPs on fungal membranes and negatively effect the cell divisions *via* strong interaction on the respiratory chains.

The use of CuO-NPs (100 mg L⁻¹) resulted in the improvement of plant growth attributes as copper-based nano-fertilizer. The specific doses of CuO-NPs can play a remarkable role in plant growth promotion are advocated by several researchers (Singh et al., 2018; Rajput et al., 2022) due to the increase bio-availability of Cu²⁺ which led to accelerating the mobilization of food reserves during germination, greater activation of copper enzymes such as cytochrome C oxidase, etc. CuO-NPs in the optimum dose can significantly influence the plant growth and act as efficient nano-fertilizers.

5 Conclusion

In conclusion, we present a straightforward, quick, and environmentally friendly method for producing CuO-NPs with exceptional antibacterial properties. Different approaches have been applied to clarify the size, shape, composition, and stability, and the findings demonstrate that the synthesized nanoparticles are very stable and monoclinic, with the largest particles falling within the size range of 28 nm in diameter. The CuO-NPs may function as a potent bactericide and fungicide that may be employed to combat plant infections as a result of the positive results. With the right toxicological information, the greenly produced CuO-NPs have a large potential and may be used for a variety of tasks, including food processing and control, biomedical forms, product packaging, and more. According to the observations of this study, CuO-NPs are a novel class of antimicrobial agents that may be developed and applied in sustainable agriculture.

Data availability statement

The datasets presented in this study can be found in online repositories. The names of the repository/repositories and accession number(s) can be found below: <https://www.ncbi.nlm.nih.gov/>-, MK773873.

Author contributions

DJ designed the research. DS, DR, GJ performed the experiments. SM, SU interpreted the data. HK and AS performed TEM, DLS, Zeta, FTIR and XRD. DJ and SU wrote manuscript. MS and WZ revised and proofread manuscript. All authors reviewed the manuscript.

Funding

Gratefully acknowledge the support by Researchers Supporting Project Number (RSP2023R410), King Saud University, Riyadh, Saudi Arabia. The financial assistance from All India Network Project on soil biodiversity and Bio-fertilizer project and MPUAT, India.

Acknowledgments

The authors would like to extend their sincere appreciation to the Researchers Supporting Project Number (RSP2023R410), King Saud University, Riyadh, Saudi Arabia. The financial assistance from All India Network Project on soil biodiversity & Bio-fertilizer project and the equipment support from IDP, NAHEP project are gratefully acknowledged.

Conflict of interest

The authors declare that the research was conducted in the absence of any commercial or financial relationships that could be construed as a potential conflict of interest.

Publisher's note

All claims expressed in this article are solely those of the authors and do not necessarily represent those of their affiliated organizations, or those of the publisher, the editors and the reviewers. Any product that may be evaluated in this article, or claim that may be made by its manufacturer, is not guaranteed or endorsed by the publisher.

Supplementary material

The Supplementary Material for this article can be found online at: <https://www.frontiersin.org/articles/10.3389/fchem.2023.1154128/full#supplementary-material>

References

- Abdoud, Y., Saffaj, T., Chagraoui, A., Bouari, A. El., Brouzi, K., and Tanane, O. (2014). Biosynthesis, characterization and antimicrobial activity of copper oxide nanoparticles (CONPs) produced using Brown alga extract (*Bifurcariabifurcata*). *Appl. Nanosci.* 4, 571–576. doi:10.1007/s13204-013-0233-x
- Abdulhameed, A. S., Jawad, A. H., and Mohammad, A. K. T. (2019). Synthesis of chitosan-ethylene glycol diglycidyl ether/TiO₂ nanoparticles for adsorption of reactive orange 16 dye using a response surface methodology approach. *Bioresour. Technol.* 293, 122071. doi:10.1016/j.biortech.2019.122071
- Ali, M., Ijaz, M., Ikram, M., Ul-Hamid, A., Avais, M., and Anjum, A. A. (2021). Biogenic synthesis, characterization and antibacterial potential evaluation of copper oxide nanoparticles against *Escherichia coli*. *Nanoscale Res. Lett.* 16, 148. doi:10.1186/s11671-021-03605-z
- Amin, F., Khattak, B., Alotaibi, A., Qasim, M., Ahmad, I., Ullah, R., et al. (2021). Green synthesis of copper oxide nanoparticles using *Aerjavanica* leaf extract and their characterization and investigation of *in vitro* antimicrobial potential and cytotoxic activities. *Evidence-Based Complement. Altern. Med.* 5589703, 1–12. doi:10.1155/2021/5589703
- Bhavysree, P. G., and Xavier, T. S. (2022). Green synthesised copper and copper oxide-based nanomaterials using plant extracts and their application in antimicrobial activity: Review. *Curr. Res. Green Sustain. Chem.* 5, 100249. doi:10.1016/j.crgsc.2021.100249
- Buazar, F., Sweidi, S., Badri, M., and Kroushawi, F. (2019). Biofabrication of highly pure copper oxide nanoparticles using wheat seed extract and their catalytic activity: A mechanistic approach. *Green Process. Synthesis* 8, 691–702. doi:10.1515/gps-2019-0040
- Bukhari, S. I., Hamed, M. M., Al-Agamy, M. H., Gazwi, H. S. S., Radwan, H. H., and Youssif, A. M. (2021). Biosynthesis of copper oxide nanoparticles using *Streptomyces* MHM38 and its biological applications. *Hindawi J. Nanomater.* 6693302, 1–16. doi:10.1155/2021/6693302
- Chandra, S., Kumar, A., and Kumar, T. (2014). Synthesis and characterization of copper nanoparticles by reducing agent. *J. Saudi Chem. Soc.* 18 (2), 149–153. doi:10.1016/j.jscs.2011.06.009
- Cheng, G., and Walker, A. R. H. (2010). Transmission electron microscopy characterization of colloidal copper nanoparticles and their chemical reactivity. *Anal. Bioanal. Chem.* 396, 1057–1069. doi:10.1007/s00216-009-3203-0
- Davaeifar, S., Modarresi, M. H., Mohammadi, M., Hashemi, E., Shafiei, M., Maleki, H., et al. (2019). Synthesizing, characterizing, and toxicity evaluating of phycocyanin-ZnO nanorod composites: A back to nature approaches. *Colloids Surfaces B Biointerfaces* 175, 221–230. doi:10.1016/j.colsurfb.2018.12.002
- Garg, K. K., Jain, D., Rajpurohit, D., Kushwaha, H. S., Daima, H. K., Stephen, B. J., et al. (2022). Agricultural significance of silica nanoparticles synthesized from a silica Solubilizing Bacteria. *Comments Inorg. Chem.* 42 (4), 209–225. doi:10.1080/02603594.2021.1999234
- Grigore, M. E., Biscu, E. R., Holban, A. M., Gestal, M. C., and Grumezescu, A. M. (2016). Methods of synthesis, properties and biomedical applications of CuO nanoparticles. *Pharm. (Basel)* 9 (4), 75. doi:10.3390/ph9040075
- Hidangmayum, A., Debnath, A., Guru, A., Singh, B. N., Upadhyay, S. K., and Dwivedi, P. (2022). Mechanistic and recent updates in nano-bioremediation for developing green technology to alleviate agricultural contaminants. *Int. J. Environ. Sci. Technol.*, 1–26. doi:10.1007/s13762-022-04560-7
- Ida, K., Sugiyama, Y., YukiChujyo, Y., Tomonari, M., Tomoharu Tokunaga, T., Sasaki, K., et al. (2010). *In-situ* TEM studies of the sintering behavior of copper nanoparticles covered by biopolymer nanoskin. *J. Electron Microsc.* 59, 75–80. doi:10.1093/jmicro/dfq055
- Jain, N., Bhargava, A., Tarafdar, J. C., Singh, S. K., and Panwar, J. (2012). A biomimetic approach towards synthesis of zinc oxide nanoparticles. *Appl. Microbiol. Biotechnol.* 97 (2), 859–869. doi:10.1007/s00253-012-3934-2
- Jain, D., Kour, R., Bhojjiya, A. A., Meena, R. H., Singh, A., Mohanty, S. R., et al. (2020). Zinc tolerant plant growth promoting bacteria alleviates phytotoxic effects of zinc on maize through zinc immobilization. *Sci. Rep.* 10, 13865. doi:10.1038/s41598-020-70846-w
- Jain, D., Kushwaha, H. S., Rathore, K. S., Stephen, B. J., Daima, H. K., Jain, R., et al. (2022). Fabrication of iron oxide nanoparticles from ammonia vapor and their importance in plant growth and dye degradation. *Part. Sci. Technol.* 40, 97–103. doi:10.1080/02726351.2021.1929601
- Jain, R., Bohra, N., Singh, R. K., Upadhyay, S. K., Srivastava, A. K., and Rajput, V. D. (2022). “Nanomaterials for plants: From ecophysiology to signaling mechanisms and nutrient uptake,” in *The role of nanoparticles in plant nutrition under soil pollution. Sustainable plant nutrition in a changing world*. Editors V. D. Rajput, K. K. Verma, N. Sharma, and T. Minkina (Cham: Springer). doi:10.1007/978-3-030-97389-6_8
- Janda, J. M., and Abbott, S. L. (2007). 16S rRNA gene sequencing for bacterial identification in the diagnostic laboratory: Pluses, perils, and pitfalls. *J. Clin. Microbiol.* 45 (9), 2761–2764. doi:10.1128/JCM.01228-07
- John, M. S., Nagoth, J. A., Zannotti, M., Giovannetti, R., Mancini, A., Ramasamy, K., P., et al. (2021). Biogenic synthesis of copper nanoparticles using bacterial strains isolated from an antarctic consortium associated to a psychrophilic marine ciliate: Characterization and potential application as antimicrobial agents. *Mar. Drugs* 19 (5), 263. doi:10.3390/md19050263
- Keabadile, O. P., Aremu, A. O., Elugoke, S. E., and Fayemi, O. E. (2020). Green and traditional synthesis of copper oxide nanoparticles-comparative study. *Nanomater. (Basel)* 10 (12), 2502. doi:10.3390/nano10122502
- Kimber, R. L., Bagshaw, H., Smith, K., Buchanan, D. M., Coker, V. S., Cavet, J. S., et al. (2020). Biomineralization of Cu 2S nanoparticles by geobactersulfurreducens. *Appl. Environ. Microbiol.* 86, 009677–e1020. doi:10.1128/AEM.00967-20
- Krishna, B. A., Kumar, P. N., and Prema, P. (2020). Green synthesis of copper oxide nanoparticles using *Cinnamomum malabratrum* leaf extract and its antibacterial activity. *Indian J. Chem. Technol.* 27, 525–530.
- Mahboub, H. H., Rashidian, G., Hoseinifar, S. H., Kamel, S., Zare, M., Ghafarifarsani, H., et al. (2022). Protective effects of *Allium hirtifolium* extract against foodborne toxicity of Zinc oxide nanoparticles in Common carp (*Cyprinus carpio*). *Comp. Biochem. Physiol. Part C Toxicol. Pharmacol.* 257, 109345. doi:10.1016/j.cbpc.2022.109345
- Makhluif, S., Dror, R., Nitzan, Y., Abramovich, R. J., and Gedanken, A. (2005). Microwave-assisted synthesis of nanocrystalline MgO and its use as a bactericide. *Adv. Funct. Mater.* 15, 1708–1715. doi:10.1002/adfm.200500029
- Mohsen, J., and Zahra, B. (2008). Protein nanoparticle: A unique system as drug delivery vehicles. *Afr. J. Biotechnol.* 7, 4926.
- Nagaraj, E., Karuppanan, K., Shanmugam, P., and Venugopal, S. (2019). Exploration of biosynthesized copper oxide nanoparticles using *pterolobiumhexapetalum* leaf extract by photocatalytic activity and biological evaluations. *J. Clust. Sci.* 30, 1157–1168. doi:10.1007/s10876-019-01579-8
- Nardella, M. I., Fortino, M., Barbanente, A., Natile, G., Pietropaolo, A., and Arnesano, F. (2022). Multinuclear metal-binding ability of the N-terminal region of human copper transporter Ctr1: Dependence upon pH and metal oxidation state. *Front. Mol. Biosci.* 9, 897621. doi:10.3389/fmolb.2022.897621
- Qamar, H., Rehman, S., Chauhan, D. K., Tiwari, A. K., and Upmanyu, V. (2020). Green synthesis, characterization and antimicrobial activity of copper oxide nanomaterial derived from *momordica charantia*. *Int. J. Nanomed.* 15, 2541–2553. doi:10.2147/IJN.S240232
- Rabiee, N., Bagherzadeh, M., Kiani, M., Ghadiri, A. M., Etesamifar, F., Jaberzadeh, A. H., et al. (2020). Biosynthesis of copper oxide nanoparticles with potential biomedical applications. *Int. J. Nanomed.* 15, 3983–3999. doi:10.2147/IJN.S255398
- Rajput, V. D., Minkina, T., Fedorenko, A., Chernikova, N., Hassan, T., Mandzhieva, S., et al. (2021a). Effects of zinc oxide nanoparticles on physiological and anatomical indices in spring barley tissues. *Nanomaterials* 11, 1722. doi:10.3390/nano11071722
- Rajput, V. D., Singh, A., Minkina, T., Rawat, S., Mandzhieva, S., Sushkova, S., et al. (2021b). Nano-enabled products: challenges and opportunities for sustainable agriculture. *Plants* 10, 2727. doi:10.3390/plants10122727
- Rajput, V. D., Minkina, T., Upadhyay, S. K., Kumari, A., Ranjan, A., Mandzhieva, S., et al. (2022). Nanotechnology in the restoration of polluted soil. *Nanomaterials* 12, 769. doi:10.3390/nano12050769
- Sagadevan, S., and Koteeswari, P. (2015). Analysis of structure, surface morphology, optical and electrical properties of copper nanoparticles. *J. Nanomed. Res.* 2 (5), 133–136. doi:10.15406/jnmr.2015.02.00040
- Sankar, R., Manikandan, P., Malarvizhi, V., Fathima, T., and ShivashangariRavikumar, K. S. V. (2014). Green synthesis of colloidal copper oxide nanoparticles using *Carica papaya* and its application in photocatalytic dye degradation. *Spectrochim. Acta Part A Mol. Biomol. Spectrosc.* 121, 746–750. doi:10.1016/j.saa.2013.12.020
- Shantkriti, S., and Rani, P. (2014). Biological synthesis of Copper nanoparticles using *Pseudomonas fluorescens*. *Int. J. Curr. Microbiol. Appl. Sci.* 3 (9), 374–383.
- Sharma, M., Sharma, A., and Majumder, S. (2020). Synthesis, microbial susceptibility and anti-cancerous properties of copper oxide nanoparticles-review. *Nano Express* 1 (1), 012003. doi:10.1088/2632-959x/ab9241
- Singh, J., Dutta, T., Kim, K. H., Rawat, M., Samddar, P., and Kumar, P. (2018). ‘Green’ synthesis of metals and their oxide nanoparticles: Applications for environmental remediation. *J. Nanobiotechnol.* 16 (1), 84. doi:10.1186/s12951-018-0408-4
- Singh, J., Kumar, V., Kim, K. H., and Rawat, M. (2019). Biogenic synthesis of copper oxide nanoparticles using plant extract and its prodigious potential for photocatalytic degradation of dyes. *Environ. Res.* 177, 108569. doi:10.1016/j.envres.2019.108569
- Sobha, K., Surendranath, K., Meena, V. K., Jwala, T., Swetha, N., and Latha, K. S. M. (2010). Emerging trends in nanobiotechnology. *J. Biotechnol. Mol. Rev.* 5, 01–12.
- Sukhwai, A., Jain, D., Joshi, A., Rawal, P., and Kushwaha, H. S. (2017). Biosynthesized silver nanoparticles using aqueous leaf extract of *Tagetuspatala* L. and evaluation of their antifungal activity against phytopathogenic fungi. *IET Nanobiotechnol.* 11, 531–537. doi:10.1049/iet-nbt.2016.0175
- Sukumar, S., Rudrasenan, A., and PadmanabhanNambiar, D. (2020). Green-Synthesized rice-shaped copper oxide nanoparticles using *Caesalpinia bonducella*

seed extract and their applications. *ACS-Omega* 5 (2), 1040–1051. doi:10.1021/acsomega.9b02857

Tavakoli, S., Kharaziha, M., and Ahmadi, S. (2019). Green synthesis and morphology dependent antibacterial activity of copper oxide nanoparticles. *J. Nanostruct.* 9 (1), 163–171. doi:10.22052/JNS.2019.01.018

Tiwari, M., Jain, P., Hariharapura, R., Kashinathan, N., Bhat, B., Nayanabhirama, U., et al. (2016). Biosynthesis of copper nanoparticles using copper-resistant *Bacillus cereus*, a soil isolate. *Process Biochem.* 51, 1348–1356. doi:10.1016/j.procbio.2016.08.008

Tshireletso, P., Ateba, C. N., and Fayemi, O. E. (2021). Spectroscopic and antibacterial properties of CuONPs from orange, lemon and tangerine peel

extracts: Potential for combating bacterial resistance. *Molecules* 26, 586. doi:10.3390/molecules26030586

Upadhyay, S. K., Devi, P., Kumar, V., Pathak, H. K., Kumar, P., Rajput, V. D., et al. (2023). Efficient removal of total arsenic ($As^{3+}/5+$) from contaminated water by novel strategies mediated iron and plant extract activated waste flowers of marigold. *Chemosphere* 313, 137551. doi:10.1016/j.chemosphere.2022.137551

Zhao, H., Maruthupandy, M., Al-mekhlafi, F. A., Chackaravathi, G., Ramachandran, G., and Chelliah, C. K. (2022). Biological synthesis of copper oxide nanoparticles using marine endophytic actinomycetes and evaluation of biofilm producing bacteria and A549 lung cancer cells. *J. King Saud Univ. - Sci.* 34 (3), 101866. doi:10.1016/j.jksus.2022.101866

RESEARCH ARTICLE

Efficacy evaluation of newly isolated zinc solubilizing bacteria for their potential effect on maize (*Zea mays* L.) under zinc deficient soil conditions

Aradhana Sukhwai¹ | Devendra Jain^{1,2}  | Vimal Sharma¹ | S. N. Ojha³ | Gajanand Jat⁴ | Sudhir K. Mohanty⁵  | Abhijeet Singh⁶ | Santosh Ranjan Mohanty⁷

¹Department of Molecular Biology and Biotechnology, Rajasthan College of Agriculture, Maharana Pratap University of Agriculture and Technology, Udaipur, India

²Southern Insect Management Research Unit, USDA-ARS, Stoneville, MS, USA

³Department of Extension Education, Rajasthan College of Agriculture, Maharana Pratap University of Agriculture and Technology, Udaipur, India

⁴Department of Soil Science and Agricultural Chemistry, Rajasthan College of Agriculture, Maharana Pratap University of Agriculture and Technology, Udaipur, India

⁵Department of Environmental Science, V. B. S. Purvanchal University, Jaunpur, India

⁶Department of Biosciences, Manipal University Jaipur, Jaipur, India

⁷All India Network Project on Soil Biodiversity-Biofertilizers, ICAR-Indian Institute of Soil Science, Bhopal, India

Correspondence

Devendra Jain, Department of Molecular Biology and Biotechnology, Rajasthan College of Agriculture, Maharana Pratap University of Agriculture and Technology, Udaipur-313001, India.

Email: devendrajain@mpuat.ac.in and devroshan@gmail.com

Abstract

Zinc solubilizing bacteria (ZSB) induces the conversion of fixed and unavailable soil zinc to readily available zinc contributes plant zinc nutrition and fortification. The present research intended to determine the screening of plant growth-promoting (PGP) traits of potent ZSB, biochemical and molecular characterization of ZSB, and assessment of potent ZSB for crop yield at the field level. Therefore, in the present study, molecular and functional characterization of native ZSB isolates was done to examine their response to plant growth performance and yield, mobilization of zinc, and acquisition by maize plants. Zinc solubilizing bacterial isolates namely, ZSB1, and ZSB 17 were solubilized insoluble zinc namely, ZnCO₃, ZnO, Zn₃(PO₄)₂ and significantly induced growth performance of maize crop at field conditions. A biochemical study revealed that both ZSB isolates were positive for catalase and urease production. Isolates ZSB1 & ZSB17 showed different PGP attributes like production of Indole-3-acetic acid (IAA), siderophore, NH₃, and HCN. Both isolates were solubilized phosphate, potassium, and silica and showed 1-aminocyclopropane-1-carboxylate (ACC)-deaminase activity. 16S rRNA amplification and sequence study of ZSB1 and ZSB17 revealed that both the isolates were *Cupriavidus* sp. and *Pantoea agglomerans*, respectively, and novel. The results elucidated from pot studies demonstrated that both ZSB1 & ZSB17 were the more suitable isolates than other ZSB isolates, and these isolates were further tested for field studies. *Cupriavidus* sp. and *Pantoea agglomerans* strains increased Zn-translocation toward grains and yield of Maize (cv: P3441) by 19.01% and 17.64%, respectively. We conclude that the novel indigenous ZSB strains substantially heightened zinc mobilization, the yield of maize crop, restore soil health, and can be suitable for biofortification and biofertilizers technology.

KEYWORDS

16S rDNA sequencing, field experiment, PGP attributes, zinc solubilizing bacteria, zinc translocation index

1 | INTRODUCTION

The availability of plant necessary elements has a direct impact on soil fertility and agricultural crop productivity. The availability of plant

essential elements may change as a result of the buildup of higher concentrations of metals and metalloids in contaminated soil (Alengebawy et al., 2021). A mediated metabolic pathway requires minimal metalloids and heavy metals at appropriate concentrations

for root microbiota, soil fertility, and plant growth (Barra & Terenzi, 2021; Upadhyay et al., 2022). Few metalloids and heavy metals, on the other hand, are even at low concentrations hazardous to plant development and soil fertility (Chibuiké & Obiora, 2014). Man-made activities such as mining, developing industrial zones, chemicals and pesticides, waste disposal, and so forth are increasing the prevalence of these contaminants (Alengebawey et al., 2021; Upadhyay & Edrisi, 2021).

Essential elements such as Zn (zinc), Cu (copper), Fe (iron), Mg (magnesium), and so forth are necessary to plant growth at an optimum concentration (White & Brown, 2010). Plant growth and soil fertility are also reduced by (i) a higher concentration of essential elements, and (ii) incompatible form of essential elements in the soil (Baldantoni et al., 2019), hence optimum concentration of essential micronutrients is required for soil productivity. Microbes can mobilize or solubilize trapped essential elements in contaminated soil by releasing extra-cellular enzymes; these enzymes may be facilitated by redox reactions (García-Arellano et al., 2004).

Plant growth promoting rhizobacteria (PGPR) plays remarkable and promising role in phyto-stimulation by releasing plant hormones like Indole-3-acetic acid (IAA), Gibberellins and so forth (Upadhyay & Chauhan, 2022), and other solubilized trapped essential elements of soil and increasing essential element uptake in plants (Singh et al., 2022; Upadhyay et al., 2009). These procedures are known as PGPR direct mechanisms (Mahmud et al., 2021; Singh et al., 2022). The production of exo-polysaccharides (Upadhyay et al., 2011), antibiotics, antioxidants (Upadhyay & Singh, 2015), biocontrol action to reduce phytopathogens, and so forth are indirect mechanisms of PGPRs (Mahmud et al., 2021). Mobilization and solubilization of trapped essential elements by rhizobacteria can be effective sustainable approaches to improving plant growth performance and enhancing soil fertility in zinc-contaminated soil (Bhojiya et al., 2022).

The ZSB (zinc solubilizing bacteria) are renowned for their effectiveness in the solubilization of zinc when combined with plant root exudates, which function as a chemo-attractant and improve the availability of native rhizobacteria promotes plant growth (Upadhyay et al., 2022). ZSB thus facilitate native zinc for plant assimilation, leading to plant growth promotion (Shakeel et al., 2015). Previously, studies on the utilization of ZSB to enhance the Zn acquisition in crops such as wheat, mung-bean etc. and correcting Zn deficiency in soil by increasing over 50% available Zn levels in the harvest soil samples has been reported (Dinesh et al., 2018; Mumtaz et al., 2017; Sirohi et al., 2015). In more than 300 enzymes, zinc and zinc ion plays a vital biological role by maintaining protein structure & stability and is found in many metalloenzymes as essential cofactor (Sarathambal et al., 2010).

Zinc deficiency leads to biomass and fertility reduction directly reduces crop plant yield, chlorosis in leaves which negatively impact photosynthesis, increased iron accumulation causing cellular toxicity, and increased oxidative stress with reduced Cu/Zn SOD activities (Thiébaud & Hanikenne, 2022). Zinc deficiency in maize is very likely to result in stunting, acute chlorosis, reduced pollen viability, and male sterility (Brown, 2008). Due to the selective cultivation of high-yield maize varieties with synthetic fertilizers to boost cropping and quality

over the past few decades, zinc deficiency has ravaged into the soil-crop environment, making maize the most susceptible cereal crop to Zn deficiency (Fageria et al., 2002).

Fifty percent of global and Indian soils are zinc deficient which is projected to increase to an estimated 63% by 2025 leading to reductions not only in crop yield but also in food quality (Hussain et al., 2022; Shukla et al., 2021). In India, 51.2% soils from the states Andhra Pradesh, Assam, Bihar, Chhattisgarh, Goa, Gujarat, Karnataka, Madhya Pradesh, Maharashtra, Odisha, Rajasthan, Telangana, and Uttar Pradesh were deficient in available Zn (Shukla et al., 2021). Zn solubilization and mobilization by soil microbes has sustainable perspectives in comparison to chemical fertilizers. Therefore, the intent of current investigation was focused on (i) isolation and screening of potent ZSB and its plant growth-promoting (PGP) attributes, (ii) 16SrRNA characterization of potent screened bacterial isolates, (iii) Influence of potent isolates on plant growth and soil health in zinc infested soil at field level.

2 | MATERIALS AND METHODS

2.1 | Physico-chemical properties of rhizospheric soil samples

The rhizospheric soils of chickpea plant were obtained from the Durgapur (23.85° N; 73.68° E) and Pratapgarh (23.56° N; 73.74° E) districts of Rajasthan (Figure 1), both the sites were adjacent to ZAWAR mines (Latit-24.3540034; Long-73.733064). Physico-chemical properties such as EC (Electrical conductivity), OC (Organic Carbon), Av. N (available nitrogen), Av. P (available phosphorus), Av. K (available potassium), and diethylenetriaminepentaacetic acid (DTPA) extracted zinc were analyzed as per standard procedures (Jain, Kour, et al., 2020; Vance et al., 1987).

2.2 | Isolation of ZSB and screening of its zinc solubilizing potential

The ZSB isolation was done with serial dilution plate method on specific media namely, Mineral salt media (Saravanan et al., 2007) and Bunt & Rovira medium (Bunt & Rovira, 1955) supplemented with different insoluble zinc source such as ZnO, ZnCO₃, and Zn₃(PO₄)₂ to produce a clear halo zone after 48 h incubation at 28°C ± 2°C were purified and considered as ZSB. To evaluate zinc solubilization efficiency of the isolates, the halo zone forming bacterial isolates were put on Bunt and Rovira agar and MSM media plates with a 0.1% insoluble zinc-source and at 28°C ± 2°C plates were incubated for 48 h. Zn solubilization efficiency was calculated as given equation.

$$\text{Solubilization efficiency} = \frac{\text{Zone diameter}}{\text{Diameter of colony growth}} \times 100$$

Further, for quantitative estimation (broth assay) of zinc solubilizing potential of ZSB strains were determined by following Gandhi

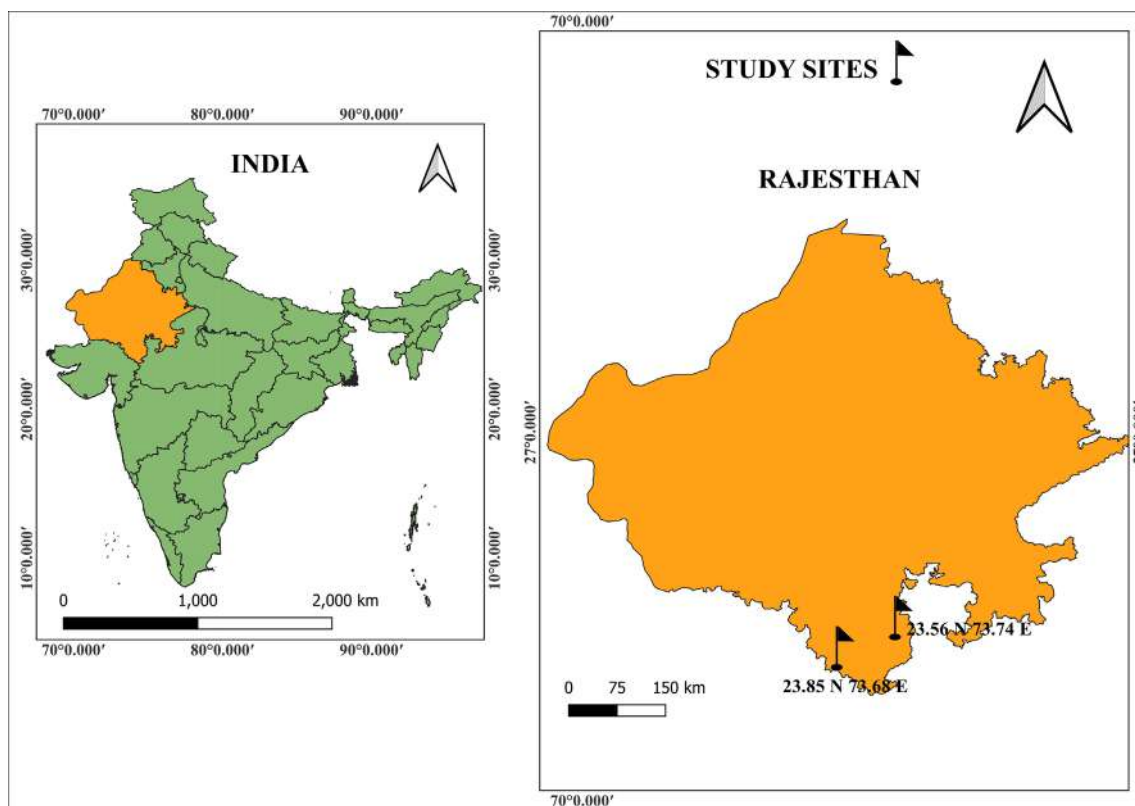


FIGURE 1 Map of the state of Rajasthan showing the geographic locations of collection of soil samples for the isolation of zinc solubilizing bacteria. [Colour figure can be viewed at wileyonlinelibrary.com]

et al. (2014). Briefly, the available zinc concentration was measured using atomic absorption spectrophotometer (AAS 4141 model, Electronics Corp. of India Ltd., India) in the culture filtrate of ZSB grown in MSM broth containing different insoluble zinc source (0.1%) at 4th, 8th, and 16th day of incubation (Gandhi et al., 2014). The pH shift of culture filtrate and uninoculated medium were also analyzed using pH meter.

2.3 | Morphological, biochemical, and molecular identification of potent ZSB

Morphological characteristics namely, form, elevation, margin, cell form, colony color, appearance colony morphology, growth, Gram staining (Gram, 1884) and basic biochemical test namely, Catalase test, Urease test, and Gelatin Liquification test were studied using the standard procedure (Blazevic & Ederer, 1975). Molecular identification of the screened ZSB isolates was carried out through 16S rRNA PCR amplification by using universal primers according to Weisburg et al. (1991) and Jain, Sanadhya, et al. (2020) and sequenced. The 16S rDNA sequences of ZSB isolates were subjected to a BLAST analysis (Altschul et al., 1990) in order to retrieve closely related sequences of type strains and further aligned using online tool CLUSTAL-W (Thompson et al., 1994). The MEGA 6.06 software was employed to construct phylogenetic tree (Tamura et al., 2013).

2.4 | HPLC and GCMS analysis for gluconic acid

The production of gluconic acid by ZSB isolates were tested by injecting the 5 days pre incubated culture filtrate in to a RP-HPLC (Agilent) having C18 column and the mobile phase acetonitrile: water (30:70 v/v) with a flow-rate @ 1.0 mL/min was used with an isocratic flow to detect gluconic acid at 210 nm through UV/Vis-detector (Jain, Kour, et al., 2020). The culture filtrates were further evaluated for the presence of various organic acids and other moieties using GCMC (GCMSQP2020, Shimadzu). Briefly, the methanol extracts (500 μ L) of lyophilized culture filtrate 100 μ L of N-Methyl-N-(trimethylsilyl) trifluoroacetamide and 100 μ L of pyridine were added and the reactions were heated (60°C for 30 min gently) in a water bath and left 12 h for stabilization. These processed samples were analyzed through GC-MS (source temperature 200°C, ionizing voltage 70 eV) and operated with scan mode (50–700 m/z) with temperature ranged 70–260°C and data was compared with NIST library.

2.5 | Physiological and PGP attributes of potent ZSB

Physiological attributes of potent ZSB isolates such as tolerance of pH (Graham, 1992), tolerance of salinity (Upadhyay et al., 2009) tolerance of temperature (Graham, 1992), tolerance of drought (Abolhasani

et al., 2010), antibiotic resistance (Li & Ramakrishna, 2011) was performed by using standard protocols. Zinc solubilizing bacterial isolates were examined for their multiple PGP traits such as production of IAA, siderophore-production, 1-aminocyclopropane-1-carboxylate (ACC) deaminase activity, phosphate-solubilization, potassium and silica solubilization, HCN, ammonia and exopolysaccharides production with standard published methodologies (Jain, Kour, et al., 2020; Naureen et al., 2015; Siddiqui et al., 2021; Upadhyay et al., 2011; Yadav et al., 2022). Hydrolytic enzymes (α amylase, cellulase, pectinase, and protease) was measured by the method of Cappuccino and Sherman (1992) & lipase (Ertugrul et al., 2007), chitinase activity (Kumar et al., 2012), and glucanase activity (Fawzy and Monaim, 2016) were screened by using standard protocols.

2.6 | Bio efficacy evaluation of potent ZSB

2.6.1 | Pot experiment

Bio efficacy and plant growth promotion ability of selected ZSB1 and ZSB17 strains as liquid microbial inoculants was evaluated under pot culture in triplicate following complete randomized design according to our previously published research (Jain et al., 2021). The maize seeds (5–10) were treated with ZSB liquid inoculants ($>8.5 \times 10^8$ cfu mL⁻¹) and placed in 4.0–5.0 cm deep in each pot. All the pots were given uniform recommended dose of fertilizers (RDF) namely, N (@ 120 kg N: P@ 60 kg P₂O₅ and K @ 40 kg K₂Oha⁻¹; Omara et al., 2016). After 30 days of sowing, plant growth parameters namely, average shoots, root-length, root-number, leaf-number, and leaf chlorophyll content (Ronen & Galun, 1984) were analyzed using standard protocols.

2.6.2 | Field experiment

The field studies were undertaken at Krishi Vigyan Kendra, Dungarpur and Instructional farm, Rajasthan College of Agriculture (RCA), (composite soil analysis reports of both experimental fields were summarized in Supplementary data sheet Table S1.1), where the DTPA extractable zinc content is low (<0.6 PPM) in 2 years of kharif seasons to differentiate the effect of two ZSB isolates on growth and yield of Maize variety P3441. The field experiment was laid out in a RBD (randomized block design) with 15 treatments in three replications including two ZSB isolates and uninoculated control (S₁: 100% RDF, T₁: ZSB1 ONLY, T₂: ZSB1+ 100% RDF, T₃: ZSB1 + 75% RDF, T₄: ZSB1 + 50% RDF, T₅: ZSB1 + 100% RDF + ZnSO₄, T₆: ZSB1 + 75% RDF + ZnSO₄, T₇: ZSB1 + 50% RDF + ZnSO₄, T₈: ZSB17 ONLY, T₉: ZSB17 + 100% RDF, T₁₀: ZSB17 + 75% RDF, T₁₁: ZSB17 + 50% RDF, T₁₂: ZSB17 + 100% RDF + ZnSO₄, T₁₃: ZSB17 + 75% RDF + ZnSO₄, T₁₄: ZSB17 + 50% RDF + ZnSO₄) as similar approach was adopted by earlier reported work of Upadhyay et al. (2019). The sowing was done by manual dibbling the seeds at a distance of 60 cm × 40 cm row to plant (Fahad et al., 2016).

ZSB liquid biofertilizer @ 5 mL kg⁻¹ treated to seed before sowing. To enhance the health of cropping over the crop season,

all recommended agronomical practices namely, sowing, weeding, manuring, harvesting, and so forth were taken. Ten plants were randomly selected from every plot at physiological maturity of the crop (106–110 days from sowing), the parameters of yield and harvest including cob length (cm); number of grains per row; number of rows per cob; weight of cobs per plot; weight of grain (g); thousand grain weight (g); biological yield per plot (g); harvest index (%) were evaluated manually (Supplementary data sheet: experimental details) (Gheith et al., 2022). Data analysis was accomplished by using the analysis of variance determining levels of significance.

2.7 | Analysis of Zn-content and Zn-translocation index (ZTI)

The powdered sample (shoot and grain) from all 15 treatments were digested using a triacid mixture (HNO₃: H₂SO₄: HClO₃ in the ratio of 9:2:1) and the Zn-content were measured using AAS to quantify the Zn translocation index (ZTI) (Rengel & Graham, 1996).

$$ZTI = \frac{\text{Zn concentration in grains}}{\text{Zn concentration in shoot}} \times 100$$

3 | RESULTS

In the present study, the physico-chemical characteristics of Dungarpur and Pratapgarh soil samples are described in Table S1.2. The soil samples textured with clay loam and sandy loam, while the soil pH ranged from acidic to neutral. The rhizospheric soils contains moderate to high range of ECe, OC, Av. N, Av. P, and Av. K. The DTPA extractable concentrations of Zn-soil (available Zn) were observed as 0.572 and 0.686 ppm.

3.1 | Isolation and assay (qualitative and quantitative) for zinc solubilization by ZSB

Microorganisms have varied solubilization response with different insoluble form of zinc hence, in the present study, ZSB isolates ZSB1 and ZSB17 were selected based on their capabilities in solubilizing multiple forms of insoluble zinc namely, ZnO, ZnPO₄, and ZnCO₃ in plate assay. Qualitative screening of zinc solubilization was carried out in MSM media and R&B media plates supplemented with different insoluble Zn compounds (Table 1). Zn solubilization zone with ZSB1 was observed in MSM media plates was 3.78 mm, 5.46 mm and 4.10 mm with ZnCO₃, ZnO, and Zn₃(PO₄)₂, respectively, and by ZSB17 was 3.09 mm, 3.79 mm, and 6.56 mm with ZnCO₃, ZnO, and Zn₃(PO₄)₂, respectively whereas in R&B media maximum zone of solubilization was observed with ZSB1 was 3.78 mm, 5.43 mm, and 4.10 mm with ZnCO₃, ZnO, and Zn₃(PO₄)₂, respectively, and by ZSB17 (3.09 mm, 2.85 mm, and 6.56 mm with ZnCO₃, ZnO, and Zn₃(PO₄)₂, respectively). Higher solubilization of Zn was observed in plates containing MSM media.

TABLE 1 Qualitative and quantitative assay for Zinc solubilization by ZSB strains on different insoluble Zn compounds.

Qualitative assay for zinc solubilization by measuring solubilizing index (SI)						
	SI ON R&B (ZNO)	SI ON R&B (ZNC)	SI ON R&B (ZNP)	SI ON MSM (ZNO)	SI ON MSM (ZNC)	SI ON MSM (ZNP)
ZSB-1	5.43 ± 0.05	3.78 ± 0.02	4.1 ± 0.02	5.46 ± 0.05	3.78 ± 0.02	4.10 ± 0.02
ZSB-17	2.85 ± 0.04	3.09 ± 0.08	6.56 ± 0.01	3.79 ± 0.02	3.09 ± 0.08	6.56 ± 0.01
Qualitative assay (broth assay) by measuring soluble Zinc (µg/mL) using AAS						
	4th day (µg/mL)	8th day (µg/mL)	16th day (µg/mL)	pH		
ZSB-1	5.1800 ± 0.0436	14.5767 ± 0.0416	17.3033 ± 0.0603	30.2		
ZSB-17	6.1100 ± 0.0201	14.2500 ± 0.0657	14.6533 ± 0.6240	40.1		

Abbreviations: MSM, mineral salt media; R&B, bunt & Rovira medium; ZNO, Zinc oxide; ZNC, Zinc carbonate; ZNP, Zinc phosphate.

Both ZSB strains were further evaluated for quantitative Zn-solubilization at different time intervals in MSM broth (broth assay). The results revealed that the amount of Zn solubilized from insoluble zinc-oxide, zinc-carbonate, and zinc-phosphate by both the ZSB isolates, and Zn solubilization rate was proportional with incubation time (Table 1). Maximum available Zn registered by ZSB1 was 5.18 µg mL⁻¹ on the fourth day, which peaked to 14.57 µg mL⁻¹ during the eighth day, followed by 17.30 µg mL⁻¹ during the 16th day whereas zinc solubilization by ZSB17 was 6.11 µg mL⁻¹ on the 4th day, which peaked to 14.25 µg mL⁻¹ during the eighth day, followed by 14.65 µg mL⁻¹ during the 16th day. Zn solubilization and reduction in pH of the culture medium showed positive correlation for both the ZSB isolates.

3.2 | Morphological, biochemical, and molecular characterization of ZSB isolates

The shape of ZSB1 and ZSB17 isolate was rod and cocci respectively, while both were gram negative. Colony characteristics as colony color, form, elevation, margin and appearance were also noted along with key biochemical tests and described in Supplementary data sheet Table S2. Biochemical analysis revealed that both ZSB isolates were negative for gelatin liquification test, while both were positive for catalase and urease production. The 16S rRNA gene sequence of isolate ZSB1 showed 95.49% homology with 16S rRNA sequence of *Cupriavidus campinensis* strain BT HNGU56 (Accession number KY010351) already submitted to GenBank data repository of the NCBI. The sequence of 16S rRNA gene of isolate ZSB17 showed 99.68% homology with 16S rRNA sequence of *Pantoea* sp. strain AS-43 (Accession number OL604306) already submitted to GenBank data repository of the NCBI [ZSB1: *Cupriavidus* sp. (Accession number: KY244144); ZSB17: *Pantoea agglomerans* strain ZSB17 (Accession number: MK773870)]. The phylogenetic position of the species is shown in Figure 2.

3.3 | Gluconic acid production by potent ZSB isolates

The reduction of pH from in broth assays was validated by measuring gluconic acid from the chosen ZSB isolates using HPLC

(Supplementary data sheet Figure S1). Both the ZSB isolates showed the secretion of gluconic acid on comparison with the standard gluconic acid and ZSB 1 and ZSB17 produced 286.14 and 102.74 mg/mL gluconic acid respectively after 5 days of incubation in Zn-supplemented MSM media. Further the culture filtrates were subjected to GCMS analysis which also revealed the secretion of different organic acids (Supplementary data sheet Figures S2 and S3).

3.4 | Physiological and PGP attributes of potent ZSB

The isolates ZSB1 and ZSB17 was screened primarily for physiological attributes that includes pH tolerance, salinity tolerance, temperature tolerance, drought tolerance, antibiotic sensitivity (Supplementary data sheet Table S3). Strain ZSB1 was able to tolerate at 1% salt concentration while ZSB17 strain were able to tolerate 2% salt concentration. Both isolates were exposed to temperature stress and ZSB1 was able to grow at various temperatures ranging from 25°C to -40°C while strain ZSB17 showed growth at temperature ranging from 20°C to -45°C. Further the drought tolerant capacities of ZSB were assessed using varying concentration of PEG on MSM-broth and ZSB1 were able to grow upto 40% PEG whereas ZSB17 were tolerated upto 10% PEG. The zinc solubilizing isolates resisted the antibiotics peniciline (µg) and ampicillin (µg) and sensitive toward kanamycin (µg), cefixime (µg), and rifampicin (µg).

Multiple PGPR activities of both ZSB isolates (Table 2) revealed that strain ZSB1 and ZSB17 were suitable plant growth promoting candidates. In the presence of L-tryptophan ZSB1 and ZSB17 produced 64.49 µg/mL IAA and 66.81 µg/mL IAA respectively. Phosphate solubilization by strain ZSB1 was 2.63 ± 0.4 and by strain ZSB17 2.97 ± 0.7 mm diameter around the colonies. Both ZSB isolates were also found positive for potassium solubilization. Both ZSB isolates were able to solubilize potash as forming clear zones in Aleksandrov agar media supplemented with mica. Zone of potash solubilization by strain ZSB1 was 2.86 ± 0.3 mm and by ZSB17 was 3.53 ± 0.02. Both isolates were also subjected for silica solubilization test. Silica solubilization by ZSB1 was 3.83 ± 0.17 and by strain ZSB17 2.64 ± 0.04 mm diameter around the colonies. These selected ZSB isolates have evaluated for different enzymes production by conducting enzyme assays. Research findings showed that both ZSB isolates

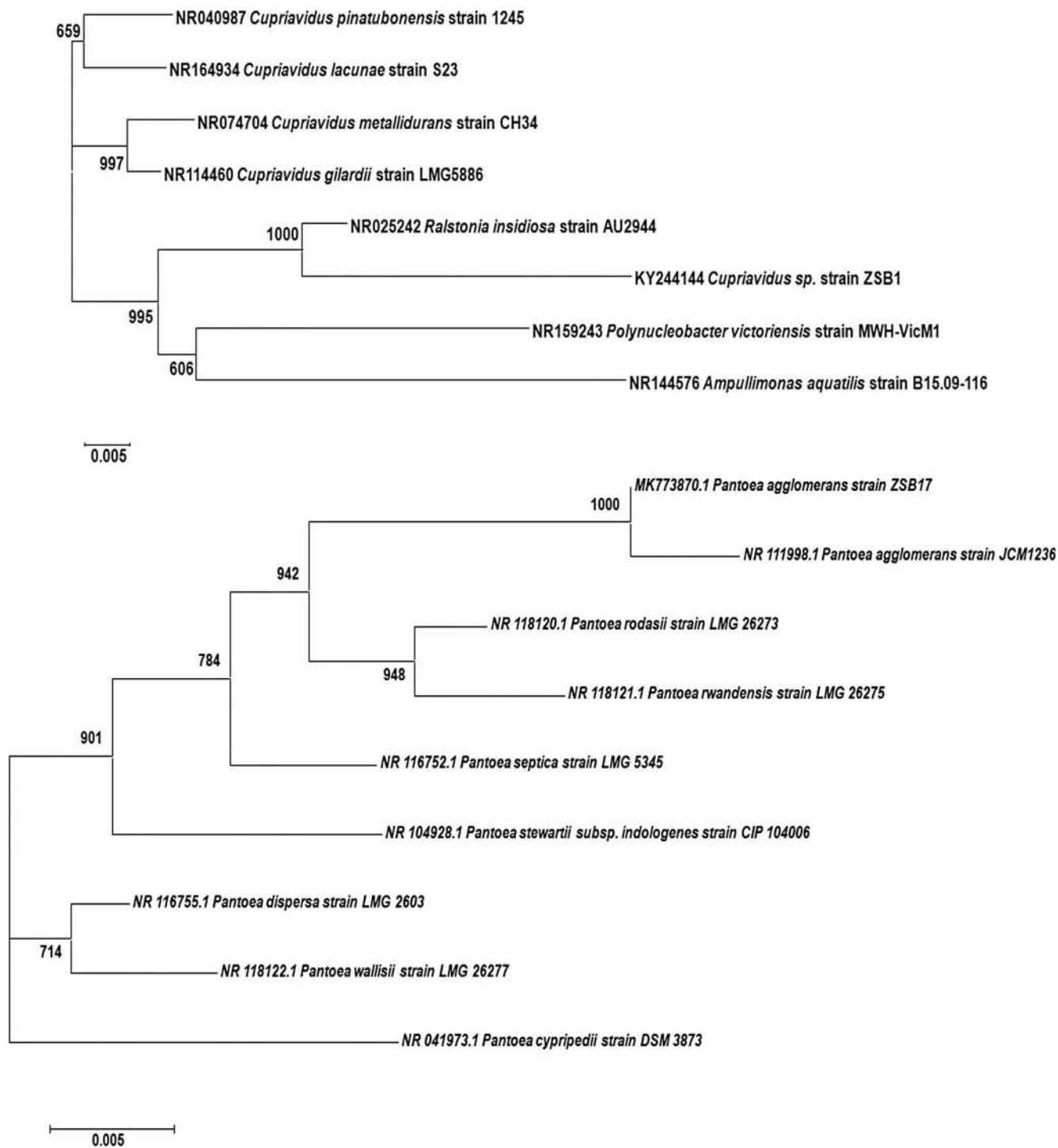


FIGURE 2 Phylogenetic analysis of potent ZSB isolates.

were positive for amylase, lipase, protease, and cellulase production and negative for chitinase and glucanase production with respect to hydrolytic enzymes.

3.5 | Bio efficacy evaluation: Pot and field study

The results from pot experiments revealed that both the ZSB isolates significantly induces maize plant growth-performance. Zinc

solubilizing isolates inoculation showed substantial growth in leaf no., leaf-length, shoots-length as compared to uninoculated control and significantly enhanced the root-length, root-number, and leaf chlorophyll content (Supplementary data sheet Table S4). The untreated control showed minimum value in all studied plant growth parameters.

Field experiment was conducted following in-vitro authentication for both selected ZSB isolates ZSB1 and ZSB17 on 13 selected growth and yield related attributes were recorded in Table 3

TABLE 2 PGP and hydrolytic enzyme production traits in ZSB isolates.

Plant growth promoting traits	ZSB1	ZSB17
ACC Deaminase	+	+
Ammonia production	+	+++
Sidero-phore	+	+
HCN	+	+
EPS	–	–
IAA ($\mu\text{g/mL}$)	640.49	668.17
P solubilization index (cm)	2.63 ± 0.04	2.97 ± 0.07
K solubilization index (cm)	2.86 ± 0.03	3.53 ± 0.02
Si solubilization index (cm)	3.8367 ± 0.17	2.6467 ± 0.04
Lipase activity	+	+++
Amylase activity	+	+
Protease activity	+	+
Cellulase activity	+	+
Chitinase activity	–	–
Glucanase activity	–	–

Note: Value (mean of triplicate) \pm standard deviation.

(Supplementary data sheet). In the present research, the preferred maize variety P3441 was used with implementing all favored SAP (standard-agronomic-practices). For field experiment 15 treatments along with control were designed with combination of RDF and ZnSO_4 . Among all the treatments, the highest biological yield (q/ha) was observed in treatment T_5 ($143.82 \pm 5.65\text{q/ha}$) which were combination of 100% RDF, ZSB1 isolates and ZnSO_4 followed by treatment T_{12} , T_6 , T_{13} , T_2 , T_{14} , T_3 , T_7 , T_9 , T_{10} , T_4 , T_{11} , T_1 , T_8 over the control. The maize plant growth and production have been significantly increased through seed bacterization with ZSB isolates. The difference was significant on yield was recorded in treated than control. Table 3 presents data on the parameters of crop growth and yield trend for maize.

The impact of ZSB isolates on the maize grain Zn content & ZTI are summarized in Table 4. In treatment T_5 (ZSB1+ 100% RDF + ZnSO_4) highest ZTI was observed (ZTI = 55.21%) followed by the maize plants treated with treatment T_{12} (ZSB17 + 100% RDF + ZnSO_4 ; ZTI = 53.4%). This clearly illustrates the role of ZSB isolates in translocating Zn toward maize grains. Zinc translocation analysis revealed that zinc acquisition in grain and shoot was significantly enhanced with strain ZSB1 than strain ZSB17 and un-inoculated control.

4 | DISCUSSION

The growth and productivity of crops were significantly impacted by a zinc shortage in the soil ultimately lead to low zinc contents in crops (Hafeez et al., 2013; Hussain et al., 2022). Following previously published studies, the ZSB isolates were obtained from rhizospheric soil

in this research (Bhatt & Maheshwari, 2020; Sunithakumari et al., 2016). *Cupriavidus* sp. and *Pantoea agglomerans* were identified as the effective ZSB strains ZSB1 and ZSB17 by 16S rRNA gene sequencing. The biochemical characterization represents the intrinsic biochemical and structural properties of the bacteria to adopt in the specific environment. In medium supplied with zinc phosphate and zinc carbonate, ZSB1 shown higher solubilization efficiency, but ZSB17 demonstrated higher solubilization in medium supplemented with zinc oxide. Ramesh et al. (2014) showed that the findings of the current investigation are supported by the ZSB strains MDSR7 and MDSR14 solubilizing all three zinc compounds (zinc, zinc-phosphate, and zinc-oxide). The current study reports that the higher Zn-solubilization zone was observed in ZnO supplemented medium compared to ZnCO_3 amended medium (Goteti et al., 2013; Mishra et al., 2017). In this work, a broth test was used to quantitatively evaluate the solubilization of zinc. As zinc solubilization increased over time, the highest amount of zinc was registered in ZSB17 on day 16 at 14.65 g mL^{-1} . Similar findings with isolated ZSB solubilized insoluble ZnO (40.81 mL^{-1} to 62.48 mL^{-1} soluble Zn) were also reported by Mishra et al. (2017). One important mechanism for the solubilization of metals and minerals is the secretion of OA (organic acids) by PGPRs, and gluconic acid is thought to be the main OA involved in the solubilization of insoluble minerals in soil (Sunithakumari et al., 2016). This will be the primary intermediary for solubilization due to the presence of 2-ketogluconic acid as a main product in cultures altered with the solubilization of insoluble zinc source (Gontia-Mishra et al., 2017) and likely as a result of increased acidity (Dinesh et al., 2018).

More or less every organism has a different active mechanism of zinc solubilization, which relies on the type of bacteria present. The ability of the ZSB strains in the current study to withstand stress, including pH, temperature, salt, and drought, is an inherent biochemical characteristic that aids in their survival in challenging rhizosphere conditions (Upadhyay et al., 2019). If a PGPR displays a variety of PGP properties, it might be a good candidate for microbial inoculants (Singh et al., 2022; Upadhyay & Chauhan, 2022). The ZSB1 and ZSB17 strains were positive for multiple PGP traits namely, ACC-deaminase-activity, siderophore-production, HCN-production, and ammonia-production. Rhizobacterial isolates are well established organisms, which may be remarkable assets for plant growth promotion through different mechanisms (Nadeem et al., 2010; Upadhyay et al., 2022; Upadhyay & Singh, 2015). ACC, a precursor for the ethylene stress hormone as the only source of nitrogen plays an important role for plant growth promotion (Mishra et al., 2017). HCN is a secondary metabolite of bacteria that inhibits growth of pathogenic microorganisms (Siddiqui, 2006). Similarly, recently Jain et al. (2020a) demonstrated that zinc tolerant PGPR produce siderophores and induced growth of plants. Ramesh et al. (2014) demonstrated that strong ammonia-producing bacterial isolates can be beneficial as a source of nitrogen for plant growth-performance.

This study, the IAA production capacities of ZSB isolates is consistent with other researchers' findings (Abaid-Ullah et al., 2015; Zhao et al., 2011). Gandhi & Muralidharan (2016) demonstrated that

TABLE 3 Effect of ZSB strains on growth and yield parameters of maize under field experiment.

Treatment	Biological yield (kg)	Cob length (cm)	Weight of cob/plot (kg)	No of cobs/plot	No of rows/cob	No of grains/row	Weight of grain/plot (kg)	Grain yield (q/ha)	Weight of fodder/plot (kg)	Stover yield (q/ha)	Biological yield (q/ha)	Harvest index (%)	1000 grain wt (g)
S ₁	60.40	20.00	40.20	24.00	14.00	40.00	20.59	54.00	30.81	79.31	133.31	40.48	210.65
T ₁	40.80	18.00	20.92	22.00	12.00	36.00	20.30	48.00	20.50	51.98	99.98	48.28	245.66
T ₂	60.10	22.00	40.10	27.00	16.00	42.00	3.12	65.00	20.98	62.06	127.06	51.26	289.82
T ₃	50.90	20.20	30.90	25.00	14.00	36.00	2.83	59.00	30.07	63.90	122.90	48.58	253.00
T ₄	50.40	19.00	30.40	24.00	14.00	36.00	20.54	53.00	20.86	59.48	112.48	47.45	254.00
T ₅	60.90	23.00	4.58	29.00	18.00	44.00	30.26	68.00	30.64	75.82	143.82	47.23	292.65
T ₆	60.40	21.50	40.30	28.00	16.00	40.00	20.98	62.00	30.42	71.31	133.31	46.62	268.00
T ₇	50.80	20.00	40.00	26.00	14.00	38.00	20.69	56.00	30.11	64.81	120.81	46.35	278.00
T ₈	40.40	17.70	20.46	20.00	12.00	34.00	2.21	46.00	20.19	45.65	91.65	50.19	269.00
T ₉	50.80	20.60	30.50	26.00	16.00	40.00	3.02	63.00	20.78	57.81	120.81	52.35	285.00
T ₁₀	50.50	19.80	30.20	24.00	14.00	38.00	20.74	57.00	20.76	57.57	114.57	50.03	269.00
T ₁₁	50.10	18.40	30.10	23.00	14.00	36.00	20.50	52.00	20.60	54.23	106.23	49.05	288.00
T ₁₂	60.60	22.00	40.30	28.00	16.00	41.58	30.07	64.00	30.53	73.48	137.48	47.11	288.51
T ₁₃	60.30	21.00	40.10	25.00	16.00	40.00	20.78	58.00	30.52	73.23	131.23	44.50	285.48
T ₁₄	60.10	20.50	30.80	23.00	14.00	38.00	20.54	53.00	30.56	74.06	127.06	41.71	255.00
SEm±	00.270	00.937	00.169	10.160	00.638	10.632	00.113	20.362	00.286	50.962	50.602	20.794	90.111
CD at 5%	00.780	20.705	00.488	30.351	10.841	40.712	00.328	60.823	00.827	17.221	16.180	80.069	26.313
CD at 1%	10.051	30.643	00.658	40.513	20.480	60.345	00.441	90.187	10.113	23.188	21.787	10.866	35.431

Note: The data express the pooled value of the triplicate data collected in two sessions.

TABLE 4 Effect of ZSB isolates on Zinc translocation from shoot to grain; Zinc Translocation Index.

Treatment	Zn in grain	Zn in Stover	Zinc translocation index (%)
S ₁	25.93	78.60	32.9
T ₁	23.20	78.37	29.62
T ₂	35.33	68.03	51.9
T ₃	33.70	70.79	47.6
T ₄	30.30	73.47	41.14
T ₅	38.20	68.77	55.21
T ₆	34.77	70.00	49.5
T ₇	32.97	70.83	46.4
T ₈	21.47	79.00	27
T ₉	34.60	71.23	48.5
T ₁₀	31.83	69.80	45.5
T ₁₁	27.50	70.33	39.11
T ₁₂	35.50	66.33	53.4
T ₁₃	31.50	65.73	47.9
T ₁₄	29.17	69.03	42.1
SEm±	0.961	1.227	
CD at 5%	2.777	3.543	
CD at 1%	3.739	4.771	

Note: The data express the pooled value of the triplicate data collected in two sessions.

phytohormone IAA (auxin) was produced by AGM3 (an isolate) at 45.61 g mL⁻¹, followed by the AGM9 37.27 g mL⁻¹ in IAA broth medium. The capability of PGP isolates to solubilize insoluble P form to a plant available P form significantly improves crop production under P limiting conditions (Majeed et al., 2015).

According to the findings of an experiment performed by Dinesh et al. (2018), *B. megaterium* (Strain CDK25) is capable of soluble and mobilized phosphate, both inorganic and organic. *Bacillus licheniformis* (BHU18) and *Pseudomonas azotoformans* (BHU21), two KSB isolates, demonstrated noticeably higher K-solubilization than the results seen in the current research, according to Saha et al. (2016). According to Naureen et al. (2015), 29 out of a total of 111 bacterial isolates can dissolve mineral silicates. Zhao et al. (2011) reported on the isolation and characterization of ZSB strains with multiple PGP traits and stated that *Bacillus* spp. exhibit numerous plant growth promoting attributes that support plant growth, including Zn and P solubilization, IAA production, oxidase activity, catalase activity, and phytohormone development. The increase in plant growth could be attributed to ZSB isolates' capacity to supply nutrients through nitrogen fixation, phosphate solubilization, siderophores synthesis, and the release of phytohormones (Mumtaz et al., 2017; Jain et al., 2017). Amylase, lipase, protease, and cellulase synthesis were found in zinc solubilizing isolates, and these enzymes indirectly aid plant growth by controlling soil-borne phytopathogens (Jha et al., 2012).

Zinc solubilizing isolates inoculation under pot conditions significantly improved the root length, root no., and leaf chlorophyll content and the results were well supported by Karnwal (2021) reported zinc solubilizing *Pseudomonas* spp. isolated from vermicompost significantly improves plant growth and maximum zinc content in Okra

fruit compared to uninoculated control. Application of ZSB substantially improves plant growth by increasing Zn bioavailability in soil to crop plants hence reduce the use of synthetic zinc fertilizers. The field experiment was conducted following in vitro authentication for ZSB1 and ZSB17 strains on 13 selected growth and yield-related attributes, among all the treatments, the highest biological yield (q/ha) was observed in treatment T5 (143.82 ± 5.65 q/ha) which were a mixture of 100% RDF, ZSB1 isolates and ZnSO₄. The maize plant growth and production have been significantly increased through seed bacterization with ZSB isolates. Hussain et al. (2015) recorded an increase in plant growth attributes primarily shoot length, root length, shoot fresh and dry biomass, and root fresh and dry biomass when Zn solubilizing *Bacillus* sp. (AZ6) was inoculated under field conditions. Sarathambal et al. (2010) have demonstrated that the dry weight of the maize is increased compared with control by the inoculation of zinc solubilizing *Gluconacetobacter diazotrophicus*. An experiment conducted by Goteti et al. (2013) in which they revealed that seed bacterization with zinc solubilizing PGP bacteria facilitates the growth of plant height (root and height of the shoot); leaf area; and dry mass.

The results of the study on the effect of ZSB isolates on zinc translocation index (ZTI) in maize plant are presented in Table 4. Zinc translocation index is used in this study as a similar notion to the translocation factor (TF) that can be viewed as the ratio of an element in a plant's shoots and roots (Upadhyay et al., 2021). The maize plant showed the highest ZTI (55.21%) in treatment T5 (ZSB1 + 100% RDF + ZnSO₄), followed by treatment T12 (ZSB17 + 100% RDF + ZnSO₄; 53.4%). This clearly shows ZSB isolates have role in translocation of Zn toward maize grains and similar finding was earlier

reported by Goteti et al. (2013) and Omara et al. (2016). In comparison to the control, the introduction of *B. aryabhatai* isolates to wheat and soybean crops dramatically boosted Zn uptake as well as shoot and seed weight (He et al., 2010). In addition to synergistic impact on plants' growth and yield, ZSBs have a strong capacity to enhance the Zn content of cereals which ultimately improves human health and immunity (Abaid-Ullah et al., 2015; Wang et al., 2014). Krithika and Balachandar (2016) reported that ZSB up-regulated the expression of Zn-regulated transporters and iron (Fe)-regulated transporter-like protein (ZIP) genes in rice suggested its important role in zinc fertilization and fortification. Uptake of micronutrients (Zn) by the plants from soil is a mutually dependent process (Bouain et al., 2014). Using microbial tools to enhance the availability of soil Zn to crop plants is one of the sustainable ways of reducing the Zn deficiency and improving Zn content of food crops grain in zinc deficient soils (Sirohi et al., 2015). Furthermore, such microbial tools will improve the zinc deficient soil and restore them to healthy soil by improving available zinc in soil. The ZSB isolates from the present study can be used for development of liquid biofertilizers to improve zinc acquisition in different crop plants cultivated in southern Rajasthan based on dedicated field studies.

5 | CONCLUSION

The primary issue that inhibits plant growth performance in degraded soil is the type of zinc that is not readily available to plants; zinc-deficient soil is frequently observed in the current research sites. Zn is a crucial micronutrient needed for healthy plant development and growth, and a deficiency does more than just harm human health and crop productivity. The findings of this research demonstrated that two distinct native bacteria, *Cupriavidus* sp. and *Pantoea agglomerans*, had the highest potential to solubilize insoluble zinc in the form of zinc that was readily available and to promote maize growth at the field level. Both isolates (*Cupriavidus* sp. and *P. agglomerans*) demonstrated a variety of PGP properties and produced catalase and urease, both of which promoted plant development. *Cupriavidus* sp. and *P. agglomerans* increased the yield of maize by 19.01% and 17.64%, respectively, and improved Zn translocation toward grains. We conclude that the *Cupriavidus* sp. and *P. agglomerans*, considerably improved soil health, maize crop production, and both unique strains could play a spectacular and promising role in bio-fertilizer technology.

AUTHOR'S CONTRIBUTION

Devendra Jain designed the research. Aradhana Sukhwil performed the experiments. Vimal Sharma interpreted the data. Gajanand Jat performed soil and AAS analysis. Aradhana Sukhwil performed HPLC and GCMS studies. Devendra Jain and Sudhir K. Udpadhyay wrote the manuscript. All authors reviewed the manuscript.

ACKNOWLEDGMENTS

The financial assistance from All India Network Project on soil biodiversity and International Zinc Association, USA are gratefully acknowledged. Dr. Devendra Jain acknowledges the financial support from

IDP, NAHEP, ICAR, New Delhi for International training. Dr. Udpadhyay acknowledges to the Department of Environmental Science, VBS Purvanchal University.

CONFLICT OF INTEREST STATEMENT

No potential conflict of interest was reported by the authors.

DATA AVAILABILITY STATEMENT

The data that support the findings of this study are available on request from the corresponding author. The data are not publicly available due to privacy or ethical restrictions.

ORCID

Devendra Jain  <https://orcid.org/0000-0002-4345-1536>

Sudhir K. Mohanty  <https://orcid.org/0000-0002-2228-8063>

REFERENCES

- Abaid-Ullah, M., Hassan, M. N., Jamil, M., Brader, G., Shah, M. K. N., Sessitsch, A., & Hafeez, F. Y. (2015). Plant growth promoting rhizobacteria: An alternate way to improve yield and quality of wheat (*Triticum aestivum* L.). *International Journal of Agriculture and Biology*, 17, 51–60.
- Abolhasani, M., Lakzian, A., Tajabadipour, A., & Haghnia, G. (2010). The study salt and drought tolerance of *Sinorhizobium* bacteria to the adaptation to alkaline condition. *Australian Journal of Basic and Applied Sciences*, 4, 882–886.
- Alengebawy, A., Abdelkhalek, S. T., Qureshi, S. R., & Wang, M. Q. (2021). Heavy metals and pesticides toxicity in agricultural soil and plants: Ecological risks and human health implications. *Toxics*, 9, 42. <https://doi.org/10.3390/toxics9030042>
- Altschul, S. F., Gish, W., Miller, W., Myers, E. W., & Lipman, D. J. (1990). Basic local alignment search tool. *Journal of Molecular Biology*, 215(3), 403–410.
- Baldantoni, D., Saviello, G., & Alfani, A. (2019). Nutrients and non-essential elements in edible crops following long-term mineral and compost fertilization of a Mediterranean agricultural soil. *Environmental Science and Pollution Research*, 26(35), 35353–35364. <https://doi.org/10.1007/s11356-018-3353-8>
- Barra, C. A., & Terenzi, V. (2021). Rhizosphere microbial communities and heavy metals. *Microorganisms*, 9, 1462. <https://doi.org/10.3390/microorganisms9071462>
- Bhatt, K., & Maheshwari, D. K. (2020). Zinc solubilizing bacteria (*Bacillus megaterium*) with multifarious plant growth promoting activities alleviates growth in *Capsicum annum* L. *3 Biotech*, 10(2), 36. <https://doi.org/10.1007/s13205-019-2033-9>
- Bhojjiya, A. A., Joshi, H., Udpadhyay, S. K., Srivastava, A. K., Pathak, V. V., Pandey, V. C., & Jain, D. (2022). Screening and optimization of zinc removal potential in *Pseudomonas aeruginosa*-HMR1 and its plant growth-promoting attributes. *The Bulletin of Environmental Contamination and Toxicology*, 108(3), 468–477. <https://doi.org/10.1007/s00128-021-03232-5>
- Blazevic, D. J., & Ederer, G. M. (1975). Principles of biochemical tests in diagnostic microbiology. *Wiley and Company, New York*, 2, 13–45.
- Bouain, N., Shahzad, Z., Rouached, A., Khan, G. A., Berthomieu, P., Abdelly, C., Poirier, Y., & Rouached, H. (2014). Phosphate and zinc transport and signalling in plants: Toward a better understanding of their homeostasis interaction. *The Journal of Experimental Botany*, 65, 5725–5741. <https://doi.org/10.1093/jxb/eru314>
- Brown, P. H. (2008). Micronutrient use in agriculture in the United States of America: Current practices, trends and constraints. In *Micronutrient deficiencies in global crop production, heavy metals in soils: Trace metals and metalloids in soils and their bioavailability* (Vol. 11, pp. 267–286). Springer.

- Bunt, J. S., & Rovira, A. D. (1955). Microbiological studies of some subantartic soils. *Journal of Soil Science*, 6, 119–128.
- Cappuccino, J. C., & Sherman, N. (1992). *Microbiology: A laboratory manual* (Vol. 3, third ed., pp. 125–179). Benjamin Cummings Publication company.
- Chibuikwe, G. U., & Obiora, S. C. (2014). Heavy metal polluted soils: Effect on plants and bioremediation methods. *Applied and Environmental Soil Science*, 2014, 752708 (1–12). <https://doi.org/10.1155/2014/752708>
- Dinesh, R., Srinivasan, V., Hamza, S., Sarathambal, C., Gowda, S. J. A., Ganeshamurthy, A. N., Gupta, S. B., Nair, V. A., Subila, K. P., Lijina, A., & Divya, V. C. (2018). Isolation and characterization of potential Zn solubilizing bacteria from soil and its effects on soil Zn release rates, soil available Zn and plant Zn content. *Geoderma*, 321, 173–186.
- Ertugrul, S., Donmez, G., & Takac, S. (2007). Isolation of lipase producing *Bacillus* sp. from olive mill waste water and improving its enzyme activity. *Journal of Hazardous Material*, 149, 720–724.
- Fageria, N., Baligar, V., & Clark, R. (2002). Micronutrients in crop production. *Advance Agronomy*, 77, 185–268.
- Fahad, S., Saud, S., Muhammad, H., Hassan, S., Shah, A., & Ullah, F. (2016). Effect of row spacing and methods of sowing on the performance of maize. *Austin Food Science*, 1(2), 1008.
- Fawzy, M., & Monaim, A. (2016). Efficacy of secondary metabolites and extracellular lytic enzymes of plant growth promoting rhizobacteria (PGPR) in controlling *Fusarium* wilt of chickpea. *Egyptian Journal of Agricultural Research*, 94, 573–589.
- Gandhi, A., & Muralidharan, G. (2016). Assessment of zinc solubilizing potentiality of *Acinetobacter* sp. isolated from rice rhizosphere. *European Journal of Soil Biology*, 76, 1–8.
- Gandhi, A., Muralidharan, G., Sudhakar, E., & Murugan, A. (2014). Screening for elite zinc solubilizing bacterial isolate from rice rhizosphere environment. *International Journal of Recent Scientific Research*, 5, 2201–2204.
- Garcia-Arellano, H., Alcalde, M., & Ballesteros, A. (2004). Use and improvement of microbial redox enzymes for environmental purposes. *Microbial Cell Factories*, 3, 10. <https://doi.org/10.1186/1475-2859-3-10>
- Gheith, E. M. S., El-Badry, O. Z., Lamlo, S. F., Ali, H. M., Siddiqui, M. H., Ghareeb, R. Y., El-Sheikh, M. H., Jebri, J., Abdelsalam, N. R., & Kandil, E. E. (2022). Maize (*Zea mays* L.) productivity and nitrogen use efficiency in response to nitrogen application levels and time. *Frontiers in Plant Science*, 13, 941343. <https://doi.org/10.3389/fpls.2022.941343>
- Gontia-Mishra, I., Sapre, S., & Tiwari, S. (2017). Zinc solubilizing bacteria from the rhizosphere of rice as prospective modulator of zinc biofortification in rice. *Rhizosphere*, 3, 185–190.
- Goteti, P. K., Emmanuel, L. D. A., Desai, S., & Shaik, M. H. A. (2013). Prospective zinc solubilizing bacteria for enhanced nutrient uptake and growth promotion in maize (*Zea mays* L.). *International Journal of Microbiology*, 10, 1155–1162.
- Graham, P. H. (1992). Stress tolerance in *Rhizobium* and *Bradyrhizobium* and nodulation under adverse soil conditions. *Canadian Journal of Microbiology*, 38, 475–484.
- Gram, H. C. (1884). Über die isolierte Färbung der Schizomyceten in Schnitt- und Trockenpräparaten. *Fortschritte der Medizin (in German)*, 2, 185–189.
- Hafeez, B., Khanif, Y. M., & Saleem, M. (2013). Role of zinc in plant nutrition—A review. *American Journal of Experimental Agriculture*, 3, 374–391.
- He, C. Q., Tan, G. E., Liang, X., Du, W., Chen, Y. L., Zhi, G. Y., & Zhu, Y. (2010). Effect of Zn-tolerant bacterial strains on growth and Zn accumulation in *Oryzophragmus violaceus*. *Applied Soil Ecology*, 44, 1–5.
- Hussain, A., Arshad, M., Ahmad, Z., & Asghar, M. (2015). Prospects of zinc solubilizing bacteria for enhancing growth of maize. *Pakistan Journal of Agricultural Sciences*, 52, 915–922.
- Hussain, A., Jiang, W., Wang, X., Shahid, S., Saba, N., Ahmad, M., Dar, A., Masood, S. U., Imran, M., & Mustafa, A. (2022). Mechanistic impact of zinc deficiency in human development. *Frontiers in Nutrition*, 9(1–11), 717064. <https://doi.org/10.3389/fnut.2022.717064>
- Jain, D., Kour, R., Bhojiya, A. A., Meena, R. H., Singh, A., Mohanty, S. R., Rajpurohit, D., & Ameta, K. D. (2020a). Zinc tolerant plant growth promoting bacteria alleviates phytotoxic effects of zinc on maize through zinc immobilization. *Scientific Reports*, 10, 13865. <https://doi.org/10.1038/s41598-020-70846-w>
- Jain, D., Sanadhya, S., Saheewala, H., Maheshwari, D., Shukwal, A., Singh, P. B., Meena, R. H., Choudhary, R., Mohanty, S. R., & Singh, A. (2020b). Molecular diversity analysis of plant growth promoting rhizobium isolated from groundnut and evaluation of their field efficacy. *Current Microbiology*, 77, 1550–1557. <https://doi.org/10.1007/s00284-020-01963-y>
- Jain, D., Sharma, J., Kaur, G., Bhojiya, A. A., Chauhan, S., Sharma, V., Suman, A., Mohanty, S. R., & Maharjan, E. (2021). Phenetic and molecular diversity of nitrogen fixing plant growth promoting *Azotobacter* isolated from semiarid regions of India. *BioMed Research International*, 2021, 6686283. <https://doi.org/10.1155/2021/6686283>
- Jain, D., Sunda, S. D., Sanadhya, S., Dhruva, J. N., & Khandelwal, S. K. (2017). Molecular characterization and PCR-based screening of cry genes from *Bacillus thuringiensis* strains. *3 Biotech*, 7, 4.
- Jha, B., Gontia, I., & Hartmann, A. (2012). The roots of the halophyte *Salicornia brachiata* are a source of new halotolerant diazotrophic bacteria with plant growth-promoting potential. *Plant and Soil*, 356, 265–277. <https://doi.org/10.1007/s11104-011-0877-9>
- Karnwal, A. (2021). Zinc solubilizing pseudomonas spp. from vermicompost bestowed with multifaceted plant growth promoting properties and having prospective modulation of zinc biofortification in *Abelmoschus esculentus* L. *Journal of Plant Nutrition*, 44, 1023–1038. <https://doi.org/10.1080/01904167.2020.1862199>
- Krithika, S., & Balachandrar, D. (2016). Expression of zinc transporter genes in rice as influenced by zinc-solubilizing *Enterobacter cloacae* strain ZSB14. *Frontiers in Plant Science*, 7, 446. <https://doi.org/10.3389/fpls.2016.00446>
- Kumar, P., Dubey, R. C., & Maheshwari, D. K. (2012). *Bacillus* strains isolated from rhizosphere showed plant growth promoting and antagonistic activity against phytopathogens. *Microbiology Research*, 167, 493–499.
- Li, K., & Ramakrishna, W. (2011). Effect of multiple metal resistant bacteria from contaminated lake sediments on metal accumulation and plant growth. *Journal of Hazardous Materials*, 189, 531–539.
- Mahmud, A. A., Upadhyay, S. K., Srivastava, A. K., & Bhojiya, A. A. (2021). Biofertilizers: A nexus between soil fertility and crop productivity under abiotic stress. *Current Research in Environmental Sustainability*, 3, 100063.
- Majeed, A., Abbasi, M. K., Hameed, S., Imran, A., & Rahim, N. (2015). Isolation and characterization of plant growth-promoting rhizobacteria from wheat rhizosphere and their effect on plant growth promotion. *Frontiers in Microbiology*, 6, 198.
- Mumtaz, M. Z., Ahmad, M., Jamil, M., & Hussain, T. (2017). Zinc solubilizing *Bacillus* spp. potential candidates for biofortification in maize. *Microbiological Research*, 202, 51–60.
- Nadeem, S. M., Zahir, Z. A., Naveed, M., Asghar, H. N., & Arshad, M. (2010). Rhizobacteria capable of producing ACC-deaminase may mitigate salt stress in wheat. *Soil Science Society of America Journal*, 74, 533–542. <https://doi.org/10.2136/sssaj2008.0240>
- Naureen, Z., Aqeel, M., Hassan, M. N., Gilani, S. A., Bouqellah, N., Mabood, F., Hussain, J., & Hafeez, F. Y. (2015). Isolation and screening of silicate bacteria from various habitats for biological control of phytopathogenic fungi. *American Journal of Plant Sciences*, 6, 2850–2859.
- Omara, A. A., Ghazi, A. A., & El-Akhdar, I. A. (2016). Isolation and identification of zinc dissolving bacteria and their potential on growth of *Zea mays*. *Egyptian Journal of Microbiology*, 51, 29–43.
- Ramesh, A., Sharma, S. K., Sharma, M. P., Yadav, N., & Joshi, O. P. (2014). Inoculation of zinc solubilizing *Bacillus aryabhatai* strains for improved growth, mobilization and biofortification of zinc in soybean and wheat cultivated in vertisols of central India. *Applied Soil Ecology*, 73, 87–96.

- Rengel, Z., & Graham, R. D. (1996). Uptake of zinc from chelate buffered nutrient solutions by wheat genotypes differing in Zn efficiency. *Journal of Experimental Biology*, 47, 217–226.
- Ronen, R., & Galun, M. (1984). Pigment extraction from lichens with dimethylsulfoxide (DMSO) and estimation of chlorophyll degradation. *Environmental and Experimental Botany*, 24, 239–245.
- Saha, M., Maurya, B. R., Bahadur, I., & Kumar, A. (2016). Identification and characterization of potassium solubilizing bacteria (KSB) from Indo-Gangetic Plains of India. *Biocatalysis and Agricultural Biotechnology*, 7, 202–209.
- Sarathambal, C., Thangaraju, M., Paulraj, C., & Gomathy, M. (2010). Assessing the zinc solubilization ability of *Gluconacetobacter diazotrophicus* in maize rhizosphere using labelled Zn compounds. *Indian Journal of Microbiology*, 50, 103–109.
- Saravanan, V. S., Madhaiyan, M., & Thangaraju, M. (2007). Solubilization of zinc compounds by the diazotrophic, plant growth promoting bacterium *Gluconacetobacter diazotrophicus*. *Chemosphere*, 66, 1794–1798.
- Shakeel, M., Rais, A., Hassan, M. N., & Hafeez, F. Y. (2015). Root associated *Bacillus* sp. improves growth, yield and zinc translocation for basmati rice (*Oryza sativa*) varieties. *Frontiers in Microbiology*, 6, 1286–1291.
- Shukla, A. K., Behera, S. K., Prakash, C., Tripathi, C., Patra, A. C., Dwivedi, B. S., Trivedi, V., Rao, C. S., Chaudhari, S. K., Das, S., & Singh, A. K. (2021). Deficiency of phyto-available Sulphur, zinc, boron, iron, copper and manganese in soils of India. *Scientific Reports*, 11, 19760. <https://doi.org/10.1038/s41598-021-99040-2>
- Siddiqui, A. R., Shahzad, S. M., Ashraf, M., Yasmeen, T., Kausar, R., Albasher, G., Alkahtani, S., & Shakoob, A. (2021). Development and characterization of efficient K-solubilizing rhizobacteria and mesorhizobial inoculants for chickpea. *Sustainability*, 13, 10240. <https://doi.org/10.3390/su131810240>
- Siddiqui, Z. A. (2006). PGPR: prospective bio-control agents of plant pathogens. In Z. A. Siddiqui (Ed.), *PGPR: Biocontrol and Biocontrol* (pp. 112–142). Springer.
- Singh, P., Chauhan, P. K., Upadhyay, S. K., Singh, R. K., Dwivedi, P., Wang, J., Jain, D., & Jiang, M. (2022). Mechanistic insights and potential use of siderophores producing microbes in rhizosphere for mitigation of stress in plants grown in degraded land. *Frontiers in Microbiology*, 13, 2415. <https://doi.org/10.3389/fmicb.2022.898979>
- Sirohi, G., Upadhyay, A., Srivastava, P. S., & Srivastava, S. (2015). PGPR mediated zinc biofertilization of soil and its impact on growth and productivity of wheat. *Journal of Soil Science and Plant Nutrition*, 15(1), 202–216.
- Sunithakumari, K., Devi, S. N. P., & Vasandha, S. (2016). Zinc solubilizing bacterial isolates from the agricultural fields of Coimbatore, Tamil Nadu, India. *Current Science*, 110, 196–205.
- Tamura, K., Stecher, G., Peterson, D., Filipiński, A., & Kumar, S. (2013). Molecular evolutionary genetics analysis version 6.0. *Molecular Biology and Evolution*, 30, 2725–2729.
- Thiébaud, N., & Hanikenne, M. (2022). Zinc deficiency responses: Bridging the gap between Arabidopsis and dicotyledonous crops. *Journal of Experimental Botany*, 73(6), 1699–1716. <https://doi.org/10.1093/jxb/erab491>
- Thompson, J. D., Higgins, D. G., & Gibson, J. (1994). CLUSTAL W: Improving the sensitivity of progressive multiple sequence alignment through sequence weighting, position-specific gap penalties and weight matrix choice. *Nucleic Acid Research*, 22, 4673–4680.
- Upadhyay, S. K., Saxena, A. K., Singh, J. S., & Singh, D. P. (2019). Impact of native ST-PGPR (*Bacillus pumilus*; EU927414) on PGP traits, antioxidants activities, wheat plant growth and yield under salinity. *Climate Change and Environmental Sustainability*, 7, 157–168. <https://doi.org/10.5958/2320-642X.2019.00021.8>
- Upadhyay, S. K., Ahmad, M., Srivastava, A. K., Abhilash, P. C., & Sharma, B. (2021). Optimization of eco-friendly novel amendments for sustainable utilization of Fly ash based on growth performance, hormones, antioxidant, and heavy metal translocation in chickpea (*Cicer arietinum* L.) plant. *Chemosphere*, 267, 129216. <https://doi.org/10.1016/j.chemosphere.2020.129216>
- Upadhyay, S. K., & Chauhan, P. K. (2022). Optimization of eco-friendly amendments as sustainable asset for salt-tolerant plant growth-promoting bacteria mediated maize (*Zea Mays* L.) plant growth, Na uptake reduction and saline soil restoration. *Environmental Research*, 211(113081), 1–10. <https://doi.org/10.1016/j.envres.2022.113081>
- Upadhyay, S. K., & Edrisi, S. A. (2021). Developing sustainable measures to restore fly-ash contaminated lands: Current challenges and future prospects. *Land Degradation and Development*, 32, 4817–4831. <https://doi.org/10.1002/ldr.4090>
- Upadhyay, S. K., & Singh, D. P. (2015). Effect of salt-tolerant plant growth-promoting rhizobacteria on wheat plants and soil health in a saline environment. *Plant Biology*, 17(1), 288–293. <https://doi.org/10.1111/plb.12173>
- Upadhyay, S. K., Singh, D. P., & Saikia, R. (2009). Genetic diversity of plant growth promoting rhizobacteria isolated from Rhizospheric soil of wheat under saline condition. *Current Microbiology*, 59, 489–496. <https://doi.org/10.1007/s00284-009-9464-1>
- Upadhyay, S. K., Singh, J. S., & Singh, D. P. (2011). Exopolysaccharide-producing plant growth-promoting rhizobacteria under salinity condition. *Pedosphere*, 21, 214–222. [https://doi.org/10.1016/S1002-0160\(11\)60120-3](https://doi.org/10.1016/S1002-0160(11)60120-3)
- Upadhyay, S. K., Srivastava, A. K., Rajput, V. D., Chauhan, P. K., Bhojija, A. A., Jain, D., Chaubey, G., Sharma, D. B., & Minkina, T. (2022). Root exudates: Mechanistic insight of plant growth promoting rhizobacteria for sustainable crop production. *Frontiers in Microbiology*, 13, 1–19. <https://doi.org/10.3389/fmicb.2022.916488>
- Vance, E. D., Brookes, P. C., & Jenkinson, D. S. (1987). An extraction method for measuring soil microbial biomass. *Soil Biology and Biochemistry*, 19, 703–707.
- Wang, L., Cai, Y., Zhu, L., Guo, H., & Yu, B. (2014). Major role of NAD-dependent lactate dehydrogenases in the production of L-lactic acid with high optical purity by the thermophile *Bacillus coagulans*. *Applied and Environmental Microbiology*, 80, 7134–7141.
- Weisburg, W. G., Barns, S. M., Pelletier, D. A., & Lane, D. J. (1991). 16S ribosomal DNA amplification for phylogenetic study. *Journal of Bacteriology*, 173(2), 697–703. <https://doi.org/10.1128/jb.173.2.697-703.1991>
- White, P. J., & Brown, P. H. (2010). Plant nutrition for sustainable development and global health. *Annals of Botany*, 105, 1073–1080. <https://doi.org/10.1093/aob/mcq085>
- Yadav, V. K., Bhagat, N., & Sharma, S. K. (2022). Modulation in plant growth and drought tolerance of wheat crop upon inoculation of drought-tolerant *Bacillus* species isolated from hot arid soil of India. *Journal of Pure and Applied Microbiology*, 16(1), 246–262.
- Zhao, Q., Shen, Q., Ran, W., Xiao, T., Xu, D., & Xu, Y. (2011). Inoculation of soil by *Bacillus subtilis* Y-IVI improves plant growth and colonization of the rhizosphere and interior tissues of muskmelon (*Cucumis melo* L.). *Biology and Fertility of Soils*, 47, 507–514.

SUPPORTING INFORMATION

Additional supporting information can be found online in the Supporting Information section at the end of this article.

How to cite this article: Sukhwai, A., Jain, D., Sharma, V., Ojha, S. N., Jat, G., K. Mohanty, S., Singh, A., & Mohanty, S. R. (2023). Efficacy evaluation of newly isolated zinc solubilizing bacteria for their potential effect on maize (*Zea mays* L.) under zinc deficient soil conditions. *Land Degradation & Development*, 1–12. <https://doi.org/10.1002/ldr.4818>



Geophysical and geostatistical assessment of groundwater and soil quality using GIS, VES, and PCA techniques in the Jaipur region of Western India

Jabbar Khan¹ · Govind Gupta¹ · Naveen Kumar Singh¹ · Vivek Narayan Bhawe² · Vinay Bhardwaj² · Pallavi Upreti³ · Rani Singh⁴ · Amarendra Kumar Sinha⁵

Received: 15 February 2023 / Accepted: 25 May 2023 / Published online: 1 June 2023
© The Author(s), under exclusive licence to Springer-Verlag GmbH Germany, part of Springer Nature 2023

Abstract

In present study, geophysical and geostatistical variability of ground water and agricultural soil investigated in the Jaipur region of Rajasthan (Western India) by applying the geographic information system (GIS), vertical electrical sounding (VES), and statistical analysis. Ground water and soil samples collected from different sites from the selected study area and variation pattern of quality parameters were assessed. A contour map analysis of distribution of metals and other contaminants in the samples was conducted using GIS. Maximum concentration of metals recorded in the soil samples in order of Fe, 11.25 mg kg^{-1} > Mn, 8.6 mg kg^{-1} > Zn, 7.2 mg kg^{-1} > Cu, 0.455 mg kg^{-1} ; however, maximum concentration of metals in the ground water samples was found as Zn, 2.64 mg L^{-1} > Cu, 0.86 mg L^{-1} > Fe, 0.39 mg L^{-1} > Mn, 0.18 mg L^{-1} > Pb, 0.065 mg L^{-1} > Ni, 0.016 mg L^{-1} . Observed data emphasis variability in groundwater and soil quality parameter by PCA technique indicated 84.60% and 66.98% of variance, respectively. Soil quality index (SQI) value was observed as 0.482 indicating that 46% of soil sampling sites deteriorated and shown poor quality. Similarly, water quality index (WQI) value indicates good water quality at the sampling sites TW1, TW8, TW10, and TW12; however, TW3, TW4, TW6, TW19, TW20, and TW22 sites showed very poor water quality. The present study concludes that overexploitation of groundwater and unregulated discharge of wastewater leads to depletion of water and soil quality. Further, applying geographical and geostatistical techniques in assessing water and soil quality could be more effective tools in environmental monitoring and management for environmental and health safety.

Keywords Bioaccumulation · Bioavailability · Biotransformation · Contamination · Groundwater · Metals · Principal component analysis (PCA) · Water quality

Responsible Editor: Wei Liu

✉ Naveen Kumar Singh
naveenenviro04@gmail.com

¹ Department of Chemistry, Environmental Science discipline, School of Basic Sciences, Manipal University Jaipur, Dehmi Kalan, Jaipur, Rajasthan 303007, India

² Ground Water Department, Jaipur, Rajasthan, India

³ Department of Geography, Dr. Nityanand Himalayan Research and Study Centre (DNHRSC), Dehradun, Uttarakhand, India

⁴ Subodh P.G. (Autonomous) College, Rambagh, Jaipur, Rajasthan, India

⁵ Chhatrapati Shivaji Maharaj University, (Panvel) Navi Mumbai, Maharashtra 410206, India

Introduction

Rapid urbanization leads to several environmental issues, including poor living conditions, changes in land use pattern, overexploitation of water and soil, transportation congestion, resettlement, disasters, and environmental pollution (Kalayci Onac et al. 2021; Aksoy et al. 2022; Tay and Ocansey 2022; Dogan et al. 2023). Fresh water including ground water is one of the most important components of the environment and essential for human survival and wellbeing (Gavrilescu 2021). However, extensive exploitation of water by human being leads to substantial environmental cost due to contamination, scarcity, and depletion of water resources affecting water supply and health safety (Tzanakakis et al. 2020; Singh et al. 2022). Scarcity of safe drinking water is now becoming a problem due to

extensive urbanisation, industrialization, agriculture, and climate change affecting about 40% of human population globally (Calzadilla et al. 2011; Bilge Ozturk et al. 2022). Groundwater found underground in cracks and crannies in rock, sand, and soil is the main source of drinking water supply. Exploitation of groundwater may result in dissolution of numerous contaminants as it passes through the rocks and soil during leaching and percolation (Saleem et al. 2018). Trace metals emanating from different industrial, transportation, construction, and agricultural activities affect soil and water quality as recalcitrant and toxic contaminants (Romic and Romic 2003; Cetin et al. 2022a; Sahin et al., 2022). Link between soil quality and socioeconomic well-being of humans, particularly, global food security and human health have been reported (Yu et al. 2018; Kopittke et al. 2019). Soil and water contamination occurs due to various anthropogenic activities and geological processes releasing metals and other elements; therefore, assessment of soil and water quality is becoming more crucial in adapting appropriate strategies to prevent and preserve the land and water resources for human wellbeing (Ahmet et al. 2006; Cesur et al. 2021). More common metal contaminants in soil and water are Pb, Cr, As, Zn, V, Cd, Cu, and Sn reported with high levels of toxicity for biota (Yang et al. 2016; Hanfi et al. 2020; Cetin et al. 2022b).

India is one of the emerging nations with more industrial and other developmental activities having wastewater generation and discharge on the land and in the aquatic ecosystems leads to soil and water contamination (Tiwari et al. 2011). Metals persist in the soil and water, accumulates in the plants by roots uptake, and biomagnifies in the animals through food chain, which causes detrimental impact to the biota (Luo et al. 2012; Ali et al. 2019; Cetin and Abo Aisha 2023). Certain metals easily enter the food chain due to their bioavailability in the rhizosphere, uptake, and accumulation in the plants and can reach to other animals and humans through food (Gu et al. 2016; Rajendran et al. 2022). It has been reported that excessive accumulation of trace elements like cadmium, lead, and nickel in the plants causes toxicity and slows down the growth and productivity (Pandey and Sharma 2002; Zouboulis et al. 2004). A substantial threat to aquatic and terrestrial biodiversity as well as health hazards for humans posed by contaminated water and soil (Olayinka-Olagunju et al. 2021). Types of rock, physicochemical characteristics of soil, atmospheric precipitation, and surface geochemical processes affect the groundwater quality parameters and contamination (Garg and Hassan 2007; Cesur et al. 2021). Groundwater is most reliable source even in India because it provides a significant proportion of the country's drinking and agricultural water requirements (Mahmood and Kundu 2005).

Physico-chemical characteristics of soil also affects the water quality of groundwater at a given regions (Griffiths

et al. 2010; Hermans et al. 2020). Different physio-chemical and biological indicators have been used in various studies to evaluate the soil quality (Filip 2002; Schloter et al. 2003). GIS has evolved into a trustworthy instrument for absorbing, analyzing, and displaying spatial data that can be utilized for environmental monitoring, planning, and resource management applications (Cetin 2015; Singha et al. 2015). The geographical information system (GIS) has become an important tool in research for resource management as it allows users to use geographical data in a variety of context and way in an integrated approach. Remote sensing (RS) and GIS studies in integration make it easier to work in relatively broad areas, particularly in environmental impact assessment for sustainable urban planning and resource utilization (Cetin 2019; Pekkan et al. 2021; Cetin et al. 2022c). Convergence of data concerning environmental assessment-related issues as well as the manipulation of spatial data into various forms in response to geosocial requirements may be accomplished using GIS (Cetin et al. 2022d). The principal component analysis (PCA) is a prominent statistical analysis tool for investigating data patterns thorough factor analysis approach. Basic purpose of PCA is to create new variables as principal components, from a set of existing original variables (Wu et al. 2020). Potential of geophysical information system-based geostatistical methodologies in assessing the region's groundwater and soil quality as well as its susceptibility to water-borne diseases reported (Ali and Ahmad 2020).

The Sanganer, Jaipur region of Rajasthan, Western India, having more industrial activities specially printing and dyeing operations leads to huge amount of wastewater generation and discharge in water and agricultural soil through unregulated disposal and irrigation practices. Very limited data are available related to using geographical information system and geostatistical techniques in the ground water and soil quality assessment. Therefore, the present study was conducted to assess ground water and soil quality at different sites based on a minimal set of interconnected geophysical and chemical criteria at Sanganer, Jaipur region of Rajasthan, Western India, and apply geophysical and geostatistical including GIS, VES, and PCA techniques to emphasize the water and soil quality parameters for environmental monitoring and assessment.

Materials and methods

Study area

The whole study conducted in the industrial and agricultural tracts in the north of Jaipur–Sanganer regions at different selected sampling sites, situated between 26° 49' and 26° 51' N and 75° 46' and 75° 51' E in the Jaipur district,

Rajasthan, Western India (Fig. 1). One selected study site, the Sanganer, is famous for its hand-printed textiles have land size of 78.24 square kilometres, situated on NH-12, 10 kilometres to the southwest of Jaipur City. The Sanganer is well-known for its distinctive type of printing “Sanganer Printing” basically in the small-scale industries of the

Chippas community, involving dyeing and printing of textiles (Dadhich et al. 2016). Dyeing and printing processes release wastewater during water-based color fixing procedure and discharged in the surrounding areas which pollutes water and soil. The chippas community either transport the textiles to a well dug on the bank of the Dravyawati River or

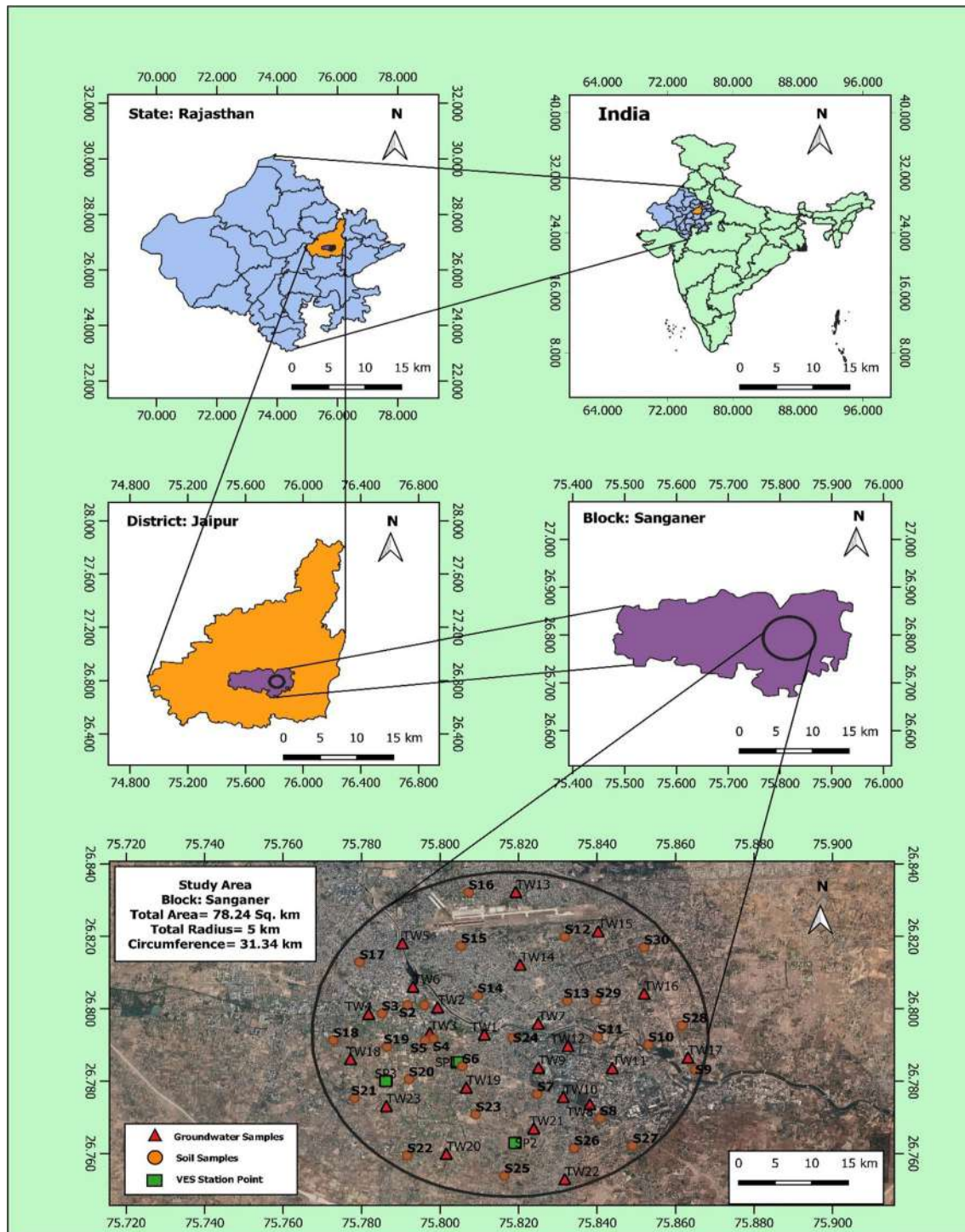


Fig. 1 Sampling sites of soil and ground water selected in the study area, Sanganer, Jaipur, Rajasthan, India

wash it at their wells in the city at various places randomly. Textile wastewater along with sewage from across the of Jaipur city discharged directly into the Dravyawati river in the selected study area is being polluted. Historically, Sanganer was primarily an agricultural region; however, during the last decade, the textile and dyeing industries have dramatically risen in the area and encroached the previously untapped agricultural land. With more than 250 separate printing units connected, it has emerged as one of the major centers of the printing and dyeing industries nowadays today in India. Growing demand and low production costs leads to the introduction of synthetic and chemical dyes, which have several environmental impacts. The regions of Jaipur–Sanganer with a high number of dyeing and printing industrial units releasing tonnes of waste into the aquatic environment, agricultural fields, and on open spaces nearby, polluting the water and soil (Sharma et al. 2014). Contamination of water and soil have negative impact on nutrition and human health due to deterioration of drinking water quality and food quality; however, at severe stage, poor quality may prevent soil from performing its natural physio-chemical and biological functions and deteriorate region's overall productivity of the terrestrial ecosystem.

Sampling sites and sampling

One-liter capacity plastic bottle rinsed with distilled water used to collect the groundwater samples. Grab sampling conducted for groundwater water sampling and samples preserved in the bottles with adjusted pH 2 and stored in refrigerator at 4 °C with slightly acidified with nitric acid (HNO₃) for analysis of water quality parameters including metals (Mn, Cu, Ni, Zn, Pb, and Cu). In Sanganer industrial region, having a new industrial area (RICCO) and an industrial zone (RSMDC), a quantitative soil and water sampling conducted to evaluate the water and soil quality parameters of the agricultural land as well as the degree of contamination in water due to industrial activities. Soil samples (250 g) taken from 30 randomly selected sites with a depth of 45 to 60 cm within a 5-kilometer radius of the Sanganer industrial zone and packed in fresh plastic zip-lock bag separately to determine the soil quality parameters (Fig. 2). All the sampling sites were precisely geotagged and labeled from S1 to S30 using a Garmin GPS device (model 68 s), allowing for the retrieval of a variety of location-specific data (Luo et al. 2011). Description of location and sampling sites are shown in the Table 1. The geoelectrical resistivity approach used to conduct field surveys in the study region which requires injecting a man-made current through several electrodes (AB) into the subsurface medium and observing the voltage changes at the potential electrodes (MN) to assess the variation in the ground's resistivity (Binley et al. 2015).

Analysis of soil and water quality parameters

Collected soil samples analyzed for 10 functional indicators parameters (i.e., pH, EC, OC, P, S, K, Zn, Fe, Cu, and Mn) for soil quality (YanBing et al. 2009). Similarly, collected water samples from different selected sites analyzed for water quality parameters in the laboratory. Average of all sets of triplicates calculated and values recorded into the data system (Juhos et al. 2019). All the analysis conducted following the procedure established by the American Public Health Association (Baird and Bridgewater 2017). A typical laboratory digital micro-processor pH meter used to estimate hydrogen ion concentration (pH) in the water samples (Salem et al. 2020). Similarly, electrical conductivity (EC) determined using an electrical conductivity meter (an EC probe and equipment that had been calibrated) by following the procedure of McNeill 1992. A digital water quality test kit used to evaluate total dissolved solids (TDS); however, EDTA titration method was used to calculate total hardness in the water samples. An argentometric titration used to quantify the amount of chloride in a water sample followed by alkalinity determined using the titrimetric method. UV-visible spectrophotometer used to determine the amount of fluoride in the collected water samples. Titration method used to estimate soil organic carbon (SOC) in the soil samples (Walkley and Black 1934) which involves oxidizing organic material in sulfuric acid with a predetermined quantity of chromate (Sato et al. 2014; Gelman et al. 2012). The Johnson–Nishita procedure used to measure sulfur content in the soil samples (Dean 1966). Sulfur and other minerals present in soil solution specially SO₄ ions adsorbed are the principal source of sulfur in soil. The replacement of SO₄ ions is of the utmost importance, and phosphate ions substituted wherever possible for adsorption and monocalcium phosphate, or phosphate ions, are present in the soil. The SO₄ ions are replaced with CaCl₂ ions in a more effective way throughout the extraction process and SO₄ extract turbulence determined by using a spectrophotometer. Potash content in soil samples estimated using a flame photometer following the procedure of Brondi et al. (2016).

Metal estimation

The concentration of Fe, Cu, Zn, Ni, Mn, and Pb in groundwater samples, whereas the metal Fe, Zn, Cu, and Mn analyzed in the soil samples estimated after complete digestion in HClO₄ and HNO₃ (3 : 1), using hollow cathode lamp at a certain wavelength into an atomic absorption spectrophotometer (AAS, Shimadzu) in comparison to standard metal solutions.

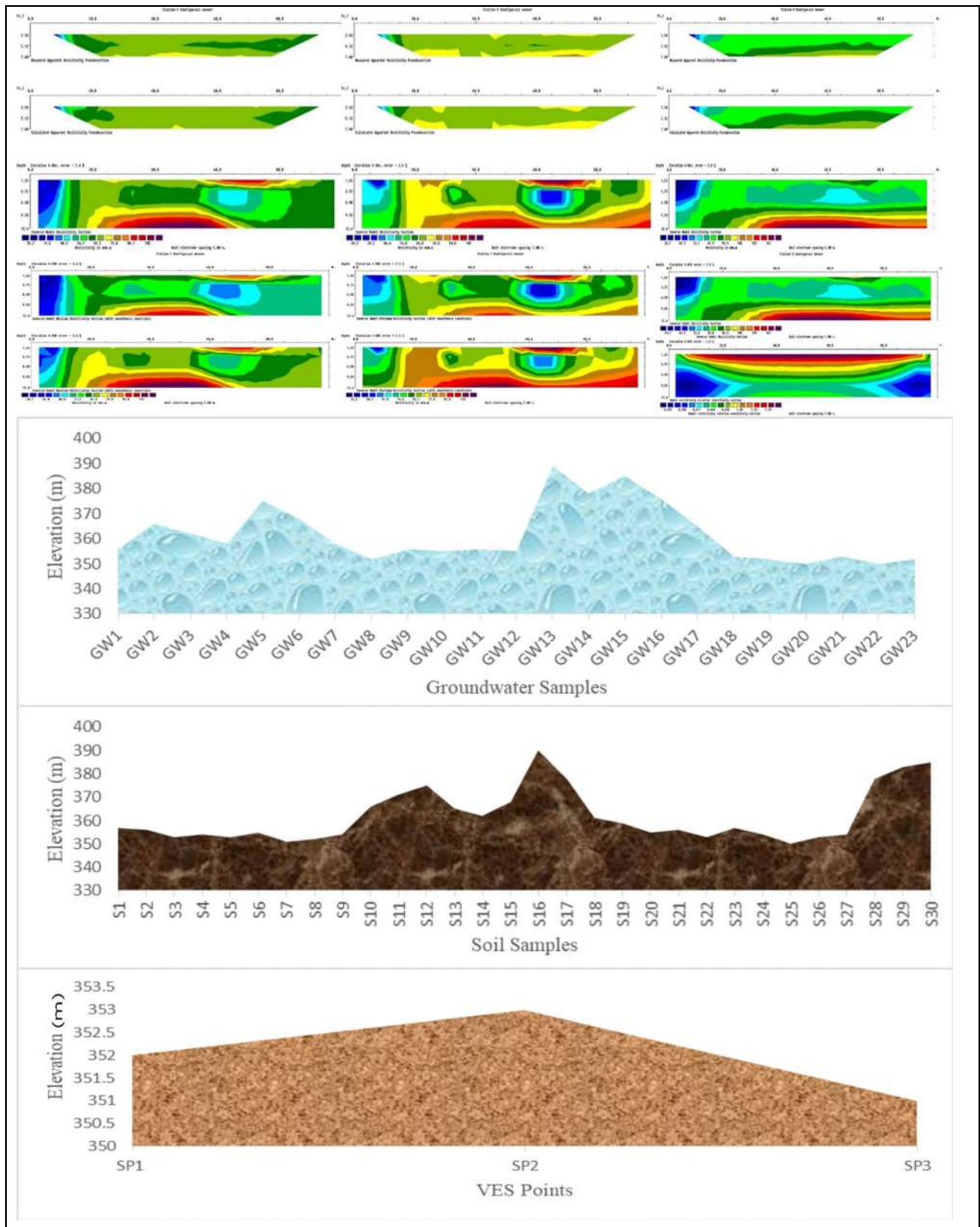


Fig. 2 Geoelectrical layers and elevation point of different sampling sites at the study area, Sanganer, Jaipur, Rajasthan, India

Table 1. Description of sampling sites of ground water samples, soil samples and VES station selected at Sanganer study area, Jaipur (Rajasthan), India

Ground water sample			Soil samples		
Sampling site	Latitudinal and longitudinal position	Elevation (m)	Sampling site	Latitudinal and longitudinal position	Elevation (m)
GW1	26.7929 N, 75.8113 E	357	S1	26.8010 N, 75.7960 E	354
GW2	26.8004 N, 75.7994 E	356	S2	26.8010 N, 75.7917 E	350
GW3	26.7933 N, 75.7974 E	353	S3	26.7987 N, 75.7852 E	353
GW4	26.7986 N, 75.7818 E	354	S4	26.7916 N, 75.7982 E	354
GW5	26.8181 N, 75.7904 E	353	S5	26.7912 N, 75.7962 E	378
GW6	26.8061 N, 75.7931 E	355	S6	26.7841 N, 75.8057 E	383
GW7	26.7959 N, 75.8250 E	351	S7	26.7764 N, 75.8248 E	385
GW8	26.7736 N, 75.8382 E	352	S8	26.7697 N, 75.8408 E	356
GW9	26.7837 N, 75.8251 E	354	S9	26.7832 N, 75.8650 E	366
GW10	26.7756 N, 75.8314 E	366	S10	26.7901 N, 75.8531 E	362
GW11	26.7836 N, 75.8439 E	371	S11	26.7923 N, 75.8402 E	358
GW12	26.7897 N, 75.8326 E	375	S12	26.8199 N, 75.8318 E	375
GW13	26.8323 N, 75.8193 E	365	S13	26.8022 N, 75.8324 E	368
GW14	26.8122 N, 75.8204 E	362	S14	26.8036 N, 75.8096 E	358
GW15	26.8214 N, 75.8403 E	368	S15	26.8174 N, 75.8054 E	352
GW16	26.8042 N, 75.8520 E	390	S16	26.8322 N, 75.8073 E	356
GW17	26.7865 N, 75.8632 E	378	S17	26.8129 N, 75.7795 E	355
GW18	26.7861 N, 75.7772 E	361	S18	26.7913 N, 75.7728 E	356
GW19	26.7782 N, 75.8067 E	359	S19	26.7895 N, 75.7865 E	355
GW20	26.7599 N, 75.8016 E	355	S20	26.7805 N, 75.7921 E	389
GW21	26.7669 N, 75.8239 E	356	S21	26.7753 N, 75.7782 E	378
GW22	26.7529 N, 75.8318 E	353	S22	26.7594 N, 75.7916 E	385
GW23	26.7731 N, 75.7863 E	357	S23	26.7708 N, 75.8091 E	376
	VES		S24	26.7920 N, 75.8186 E	365
SP1 (VES)	26.7852 N, 75.8044 E	352	S25	26.7538 N, 75.8164 E	353
SP2 (VES)	26.7629 N, 75.8191 E	353	S26	26.7615 N, 75.8342 E	352
SP3 (VES)	26.7800 N, 75.7862 E	351	S27	26.7621 N, 75.8491 E	350
			S28	26.7954 N, 75.8617 E	353
			S29	26.8023 N, 75.8397 E	350
			S30	26.8170 N, 75.8520 E	352

Geostatistical analysis

To assess overall quality of water and soil samples collected from the different sites in the study area, data of soil and water quality parameters analysed thoroughly by applying geostatistical tools. Quantitative evaluation's framework combines geotechnical and physicochemical analysis of water and soil samples with descriptive statistics and statistical modelling. Outcome data is gathered after the laboratory chemical analysis of selected soil and water samples, followed by review with analysis of data on SPSS software (version 22 for Windows). Discriminating analysis (correlation) of data performed using Statistical Package for the Social Sciences (SPSS) for Windows, version 23.0. (Ukah et al. 2019, 2020). Several statistical methods used in data

analysis and models including MV, SD, and CV (Li et al. 2016; Zhu et al. 2019). Further, water quality index (WQI) and soil quality index (SQI) evaluated to assess the region's overall variations and patterns of water and soil quality parameters using site-specific indicator evaluation outputs. Weighted arithmetic mean technique for WQI was used in this investigation (Tyagi et al. 2013).

$$WQI_A = \sum_{i=1}^n qi X Wi,$$

$$\sum_{i=1}^n Wi = 1,$$

where Wi is the unit weight of each parameter, qi is the 0–100 subindex rating for each variable, and n is the number


of subindices aggregated. Multivariate statistical technique, the principal component analysis (PCA), was used to reduce the dataset into new variables, create a minimum data set (MDS), and analyze relationships between different metal contents in the water and soil samples and other quality parameters including pH, TOC, and EC along with factor analysis (FA) to identify specific factor weight of a particular metal (Weissmannová and Pavlovský 2017). The SAS Systems for Windows 10 platform and Statistica 12.5® software used to perform principal component analysis (PCA), followed by a Varimax rotation used to rotate each PCA component. The Varimax rotation method of factor analysis and the principal component primary result analysis performed by following the procedure of Kaiser 1958 and Maiz et al. 2000. For the GIS-based evaluation, SQI and WQI maps, spatial distribution maps, area maps, and thematic maps for the region produced by using Sentinel 2 Satellite data (March 2021) in bands: 3, 4, 8 developed on ArcGIS software 10.8 (2020).

Results

Groundwater samples (23) and soil samples (30) collected from selected sampling sites of the study area, Jaipur regions of Rajasthan, Western India, analyzed for quality parameters. Based on the sounding data, the present study inferred with three geoelectrical layers comprising topsoil, unsaturated, and saturated zones (Fig. 2). For all the sections topmost layer assumed to be topsoil, above the water table and substantially drier more often reflects greater resistivity. Peat investigated in the topsoil layer by resistance correlation with soil lithology from neighboring boreholes. Regional lithology of Sanganer shown in the Table 2 which indicates formation depth range as alluvium, 0.0–95 m; weathered, 0.69–128 m; and hard rock, 9.2 m. In present study, the

third layer of all the sections represent highest concentration of geoelectrical sections with low resistivities (less than 10 m). Values and their variation pattern of water quality parameters in 23 groundwater samples at different sites of the study area depicted in Fig. 3. Maximum values of different parameters of groundwater samples recorded as pH, 8.0; electrical conductivity (EC), 3.01 S/m, TDS, 1501 mg/l; fluoride, 1.9 mg/l; total hardness, 273 mg/l; Ca, 88.1 mg/l; Mg, 12.67 mg/l; chloride, 227.42 mg/l; HCO₃, 61.87 mg/l; and CO₃, 58.29 mg/l. However, maximum metal concentration in groundwater samples recorded as Zn, 2.64 mg/l; Cu, 0.862 mg/l; Fe, 0.392 mg/l; Mn, 0.181 mg/l, Pb, 0.065 mg/l; and Ni, 0.016 mg/l. pH and TDS level in the ground water samples found in the range of 7.0 to 8.0 and 559 to 1501 mg/l, indicate that values are within the range of 6.5 to 8.5 and 500 to 1500 mg/l, respectively, as per WHO standard of water quality. Similarly, for 30 soil samples, maximum values of soil quality parameters recorded as pH, 8.4; electrical conductivity (EC), 0.27 μS/m; organic carbon, 0.23 %; phosphorous, 50.23 mg/kg; potash, 786 mg/kg; sulfur, 29.68 mg/kg. However, maximum metal concentration in the soil samples recorded as Fe, 11.25 mg/kg; Mn, 8.65 mg/kg; Zn, 7.26 mg/kg; and Cu, 0.45 mg/kg as shown in Fig. 4. Result shows that none of the parameters including pH have a strong correlation. Samples’ scores and loadings plots together showed physio-chemical characteristics of soil that affect each order on the score plots. Retained variables divided into groups using the factor analysis technique in accordance with statistical factors and correlation matrix (Table 3). As depicted in the Table 4, maximum WQI found in groundwater sample collected at sampling site TW22 and minimum in the sample collected from TW12. Results of PCA and FA analysis for groundwater revealed that the first component (PC1), which accounted for 39.12% of the total variance, included Mn, pH, and EC; however, S, OC, and P made the second component (PC2) with a total variance of 12.54%. Similarly, pH, Mn,

Table 2. Regional lithology of the study area, Sanganer, Jaipur (Rajasthan), India

Aquifers depth (m)	Aquifers	Geological formation	Depth (m)	Laboratory experiment model
0–95	Alluvium	Surface soil, sandy clay	0–4	
		Clayey sand	4–13	
		Clayey kankar	13–19	
0.6–128	Weathered	Sandy clay with kankar	19–29	
		Kankar and clay	29–38	
		Kankar and sand	38–47	
9.2	Hardrock	Weathered schist	47–73	
		Schist	73–150	

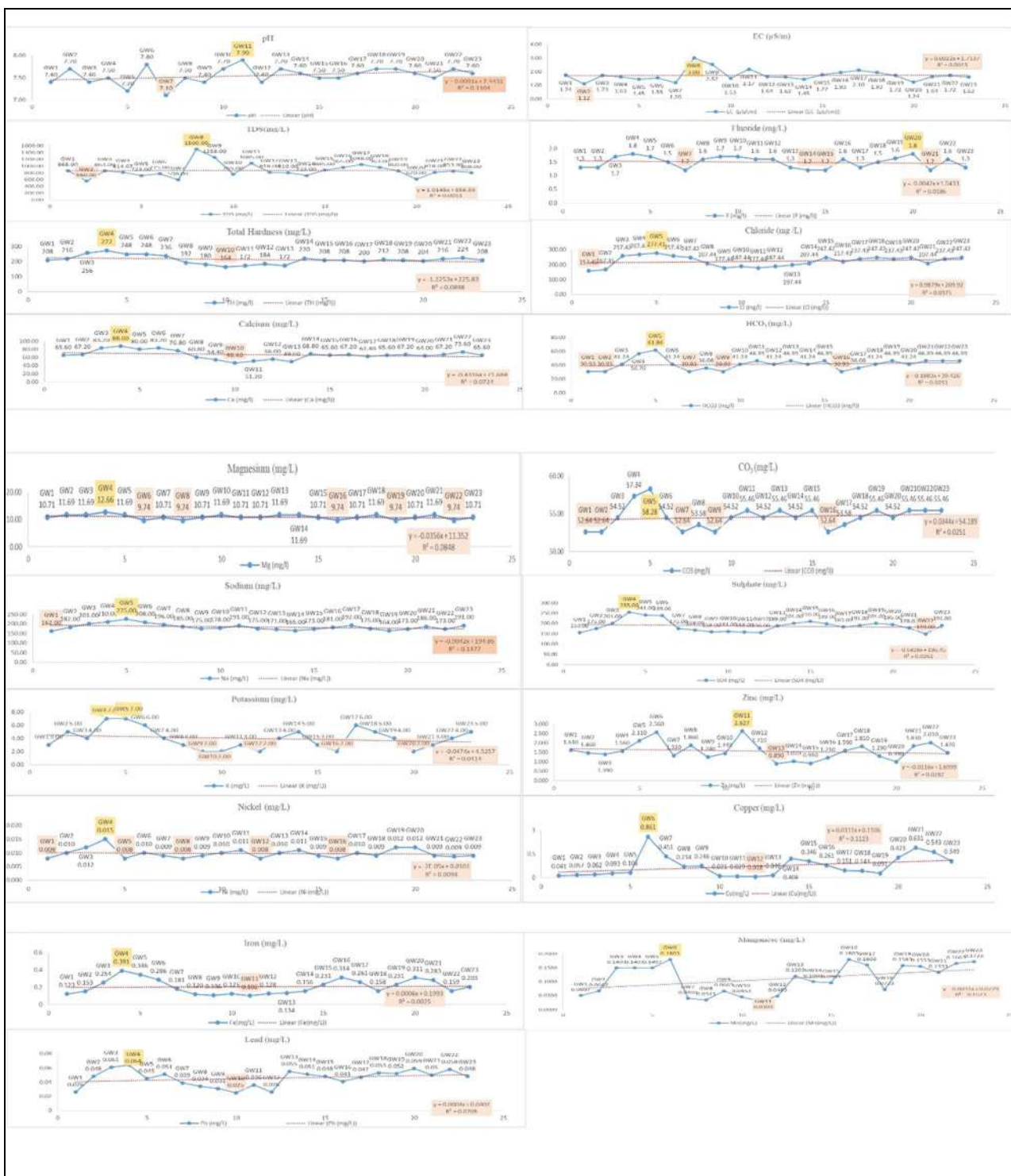


Fig. 3 Variations in water quality parameters of ground water samples collected from in different sites at the study area, Sangaran, Jaipur, Rajasthan, India

and Cu made PC3 with a total variance of 11.42% followed by phosphorous made PC4 a total variance of 9.06%, while all four extraction factors accounted for 72.15% of the overall variation. However, in case for soil samples Mn, pH, and

EC produced the first component (PC1) with 24.26% of the variance followed by the second component (PC2) produced included S, OC, and P with a total variation of 17.48%, while PC3 made up of pH, Cu, and Mn with a total variance of

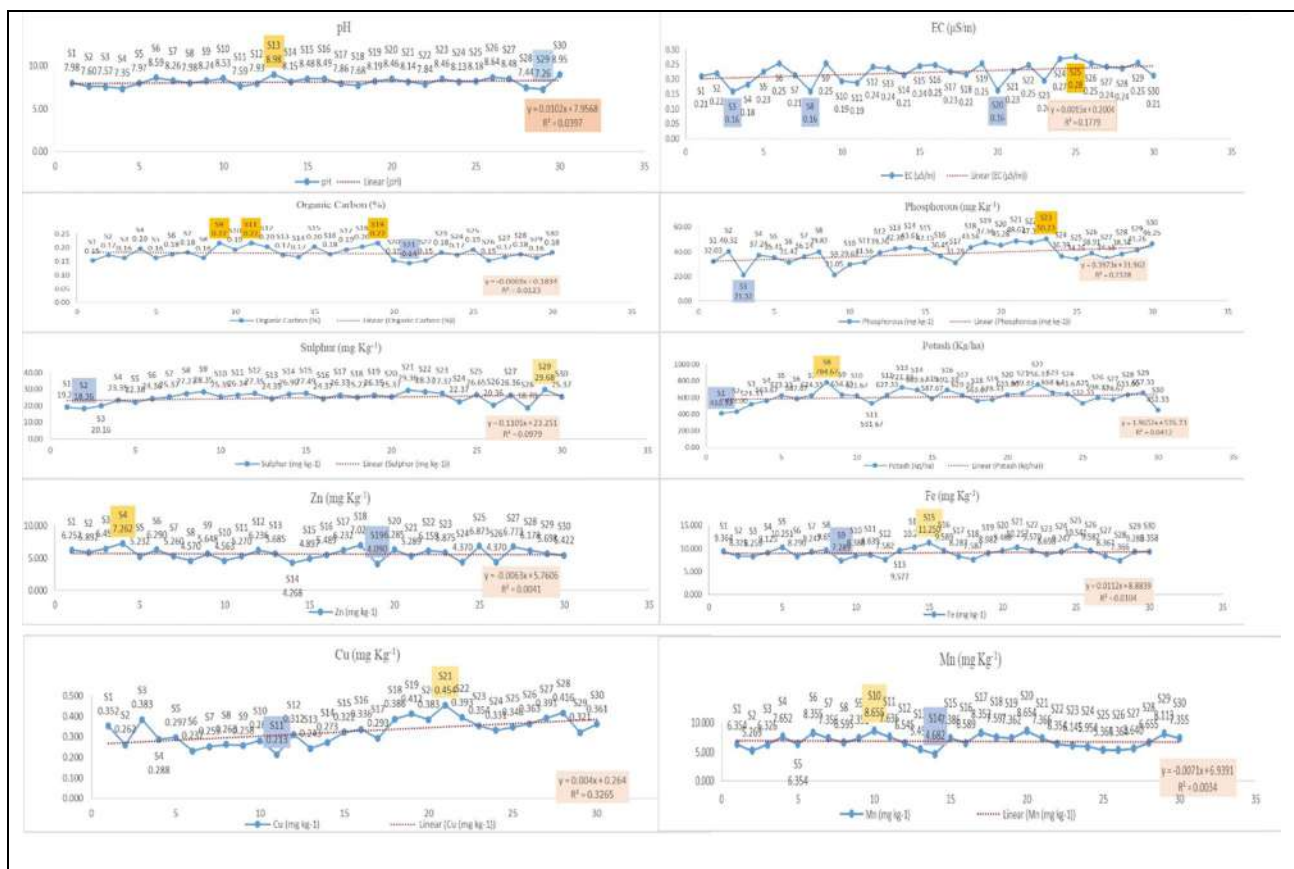


Fig. 4 Variations in soil quality parameters of soil samples collected from different sites at the study area, Sanganer, Jaipur, Rajasthan, India

13.65% and PC4 contained phosphorus with a total variance of 11.58% (Fig. 5A). Result shows that water quality of groundwater samples collected at TW1, TW8, TW10, and TW12 sampling sites in the Sanganer area are in very good quality category; however, groundwater samples from TW3, TW4, TW6, TW19, and TW22 sites recorded under very poor water quality category with high level of contaminants (Fig. 5B). Similarly, total 9 soil quality parameters including pH, EC, OC, P, S, K, Zn, Fe, and Mn used to evaluate the soil quality index (SQI), and an average soil quality index (SQI) value 0.517 recorded for the selected study area based on MDS, with a range of 0.341 to 0.635 (Fig. 5B). According to the suggested framework, the SQI values for the entire selected region divided into three categories viz; category 1 (C1), SQI value less than 0.4 (degraded); category 2 (C2), SQI value between 0.41 and 0.5 (moderately degraded); and category 3 (C3), SQI value greater than 0.51 (least degraded). SQI revealed that soil samples at S19 site showed highest SQI score, 0.636, followed by S6, S7, S12, S13, S15, S16, S17, S18, S20, S21, S22, S23, S25, S27, S29, and S30 more than average as shown in Fig. 5B. Data shows that 13.3% of the soil samples from the study area have low soil pollution with good soil health; however,

40% of the soil samples have moderate contamination with SQI values in the range of 0.41 to 0.5 and 46.6% of soil samples shown as degraded soil under the poor-quality category with SQI values more than 0.51. At 5 kilometers away from the Sanganer industrial regions, high-intensity farming techniques, and conventional farming practices, excessive fertilizer use may be responsible for the soil degradation in the selected sites. Based on SQI score, the S19 site showed highly contaminated soil in the study area; however, it is crucial to note that the high score may be due to increased chemical build-up and other components like sulfur rather than trace metals having low concentration; however, it may be useful in environmental health assessment. Results of the factor analysis (FA) recorded insufficient if the Kaiser–Meyer–Olkin (KMO) test result value found to be less than 0.5; however, KMO found less FA findings in the test’s outcome than the chemical examination of soil samples. FA did not alter KMO testing significantly because there is no related cut-off point, and the results for the sample given a less clear indication of the applicability of the FA as KMO values estimated 0.487 and 0.466 (less than 0.5) for the groundwater and soil samples, respectively. Percentage (%) of variance evaluated by placing three components out of

Table 3. Correlation matrix^a of ground water and soil samples collected from different sites at Sanganer study area, Jaipur, Rajasthan, India

Groundwater quality parameters		pH	EC	TDS	F	TH	Ca	Mg	Cl	HCO ₃	CO ₃	Na	K	SO ₄	Zn	Mn	Cu	Fe	Pb
Correlation	pH	1.000	.080	.082	.047	-.348	-.338	-.1	-.207	.078	.078	-.284	.008	-.087	.250	.121	.047	-.213	.219
	EC	.080	1.000	1.000	.217	-.366	-.327	-.371	-.211	-.185	-.185	-.088	-.251	-.282	.214	-.241	-.147	-.309	-.326
	TDS	.082	1.000	1.000	.217	-.367	-.328	-.370	-.212	-.185	-.185	-.088	-.252	-.279	.212	-.239	-.149	-.308	-.326
	F	.047	.217	.217	1.000	.068	.074	-.040	.194	.267	.267	.257	-.111	.155	.213	.337	.131	-.259	.240
	TH	-.348	-.366	-.367	.068	1.000	.993	.217	.695	.320	.320	.605	.671	.698	.153	.491	.322	.693	.599
	Ca	-.338	-.327	-.328	.074	.993	1.000	.096	.705	.282	.281	.586	.641	.676	.180	.517	.374	.687	.580
	Mg	-.132	-.371	-.370	-.040	.217	.096	1.000	.028	.361	.361	.241	.346	.280	-.190	.399	-.366	.156	.244
	Cl	-.207	-.211	-.212	.194	.695	.705	.028	1.000	.538	.538	.572	.569	.734	.044	.295	.345	.735	.659
	HCO ₃	.078	-.185	-.185	.267	.320	.282	.361	.538	1.000	1.000	.441	.480	.560	.242	.343	-.032	.462	.449
	CO ₃	.078	-.185	-.185	.267	.320	.281	.361	.538	1.000	1.000	.441	.480	.560	.242	.343	-.032	.462	.449
	Na	-.284	-.088	-.088	.257	.605	.586	.241	.572	.441	.441	1.000	.615	.590	.498	.154	.115	.582	.215
	K	.008	-.251	-.252	-.111	.671	.641	.346	.569	.480	.480	.615	1.000	.672	.284	.314	.074	.459	.529
	SO ₄	-.087	-.282	-.279	.155	.698	.676	.280	.734	.560	.560	.590	.672	1.000	-.010	.589	.185	.811	.590
	Zn	.250	.214	.212	.213	.153	.180	-.190	.044	.242	.242	.498	.284	-.010	1.000	-.145	.175	-.008	-.143
	Ni	.300	-.241	-.239	.337	.351	.307	.399	.295	.343	.343	.154	.314	.451	1.000	.281	-.117	.388	.604
	Mn	.121	-.241	-.242	.131	.491	.517	-.131	.645	.381	.381	.288	.411	.589	-.054	1.000	.393	.750	.695
	Cu	.047	-.147	-.149	-.259	.322	.374	-.366	.345	-.032	-.032	.115	.074	.185	.175	-.054	1.000	.270	.288
	Fe	-.213	-.309	-.308	.240	.693	.687	.156	.735	.462	.462	.582	.459	.811	-.008	.388	.750	1.000	.582
	Pb	.219	-.326	-.326	.036	.599	.580	.244	.659	.449	.449	.215	.529	.590	-.143	.604	.288	.582	1.000
	Soil quality parameter																		
	pH	1.000	.163	-.071	.166	.148	.111	-.324	.291	-.039	-.089								
Correlation	EC	.163	1.000	.125	.059	.113	.075	-.064	.079	.131	-.264								
	OC	-.071	.125	1.000	-.237	.226	-.174	.023	-.382	-.331	.288								
	Phosphorus	.166	.059	-.237	1.000	.290	.250	-.178	.385	.400	-.109								
	Sulfur	.148	.113	.226	.290	1.000	.493	-.101	.202	-.026	.314								
	Potash	.111	.075	-.174	.250	.493	1.000	-.291	.160	-.064	-.012								
	Zn	-.324	-.064	.023	-.178	-.101	-.291	1.000	-.362	.149	.110								
	Fe	.291	.079	-.382	.385	.202	.160	-.362	1.000	.054	-.234								
	Cu	-.039	.131	-.331	.400	-.026	-.064	.149	.054	1.000	-.059								
	Mn	-.089	-.264	.288	-.109	.314	-.012	.110	-.234	-.059	1.000								

Table 4. Water quality and soil quality Index

Groundwater quality index						
Parameters	Quantity of sample	WQI (mean)	Std. deviation	Std. error	Maximum	Minimum
pH	23	7.5522	.0035	.0020	8.0000	7.0000
EC ($\mu\text{S/m}$)	23	1.7400	.0027	.0015	3.0100	1.1100
TDS (mg/l)	23	868.7246	.7633	.4407	1501.0000	559.0000
Fluoride (mg/l)	23	1.4928	.0054	.0031	1.9000	1.1000
TH (mg/l)	23	211.1304	.5325	.3074	273.0000	163.0000
Ca (mg/l)	23	66.5043	.0035	.0020	88.1000	46.3000
Mg (mg/l)	23	10.9249	.0009	.0005	12.6700	9.7300
Cl (mg/l)	23	221.7787	.0025	.0014	277.4200	157.4400
HCO ₃ (mg/l)	23	41.6862	.0041	.0024	61.8700	30.9200
CO ₃ (mg/l)	23	54.6017	.0082	.0047	58.2900	52.6300
Na (mg/l)	23	184.0000	.6035	.3484	226.0000	161.0000
K (mg/l)	23	3.9565	.6745	.3894	8.0000	1.0000
SO ₄ (mg/l)	23	188.2609	.8165	.4714	256.0000	148.0000
Zn (mg/l)	23	1.5612	.0083	.0048	2.6400	1.6000
Ni (mg/l)	23	0.0098	.0010	.0006	.0160	.0011
Mn (mg/l)	23	0.1099	.0004	.0002	.1810	.0300
Cu (mg/l)	23	0.2442	.0008	.0005	.8620	.0170
Fe (mg/l)	23	0.2068	.0008	.0005	.3920	.1010
Pb (mg/l)	23	0.0456	.0008	.0004	.0650	.0240
Soil quality index						
Parameters	Quantity of sample	SQI (mean)	Std. deviation	Std. error	Maximum	Minimum
pH	30	8.11	.0064	.0037	8.40	7.98
EC ($\mu\text{S/m}$)	30	.2240	.0008	.0005	.2760	.1580
Organic carbon (%)	30	.1793	.0061	.0035	.2300	.1400
Phosphorous (mg kg ⁻¹)	30	38.1197	.0009	.0005	50.2310	21.0500
Sulfur (mg kg ⁻¹)	30	24.9634	.0006	.0004	29.6810	18.3620
Potash (kg/ha)	30	607.1889	.7385	.4264	786.00	410.00
Zn (mg kg ⁻¹)	30	5.6635	.0010	.0006	7.2630	4.0890
Fe (mg kg ⁻¹)	30	9.0579	.0006	.0003	11.2510	7.2890
Cu (mg kg ⁻¹)	30	.3261	.0005	.0003	.4550	.2130
Mn (mg kg ⁻¹)	30	6.8290	.0007	.0004	8.6560	4.6810

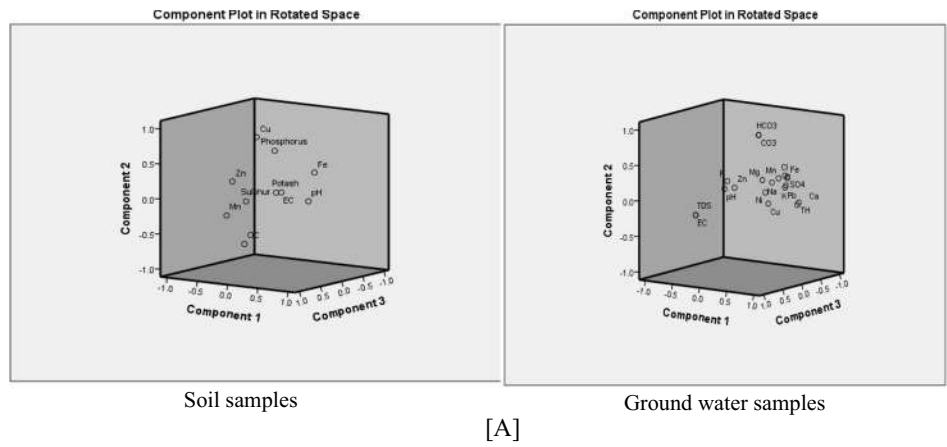
the four PC ranges (component based on Jolliffe's criterion) and recorded 84.60% and 66.98% for groundwater and soil samples, respectively (supplementary data).

Discussion

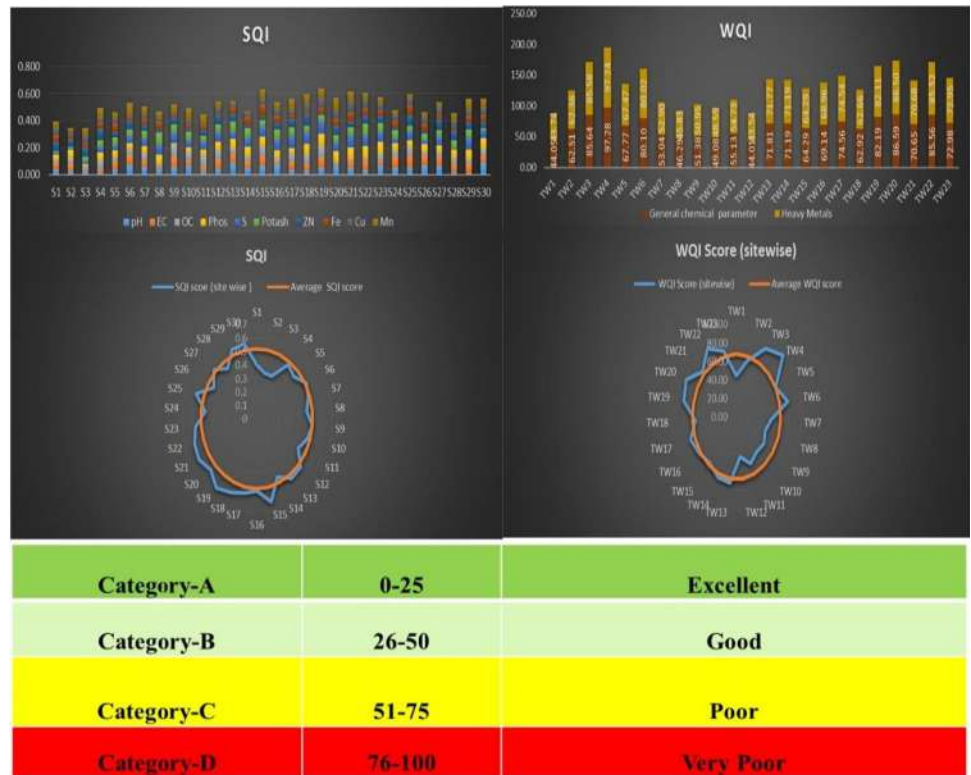
Collected samples from the selected study area, Jaipur regions of Rajasthan, Western India, evaluated for water and soil quality parameters which indicate slightly basic in nature as pH varied within the ranged of 7.0 to 8.0 in the samples. pH is one of the essentially functional parameters for evaluating the quality of soil and water (Filip 2002). Depending on the underlying geological units' actual resistivity, the geoelectrical characteristics utilized to create earth models which displayed as subsurface stratigraphy

and from which possible aquifer zones mapped for sampling and assessing the groundwater quality parameters at different sites in the selected region (Mogaji and Omobude 2017). Higher value of EC in groundwater samples indicates impurity as compared to pure water which is not an excellent conductor of electricity having a lower EC than the groundwater. According to previous studies, groundwater exhibits low resistivities between 10 and 100 Ωm in the context of sedimentary (Adagunodo et al. 2018). Kaiser's criterion replaced with Jolliffe's criterion since it is too high and allows for a graphic representation of the factor loading through a dipole using the first three components (Jolliffe 1972). However, soil solution's EC indicates total amount of salts and ions present in the soil (Bronson et al. 2005; Peralta and Costa 2013). A significant indicator of the soil quality is electrical conductivity, which reflects the salinity of the soil

Fig. 5 Component plot of ground water and soil samples (A). Soil quality index (SQI) and water quality index (WQI) of collected samples (B)



[A]



[B]

(Hardie and Doyle 2012). Studies revealed that low resistivity values inside the underlying strata likely caused by high ion concentrations and fine-grained sediments like silt and clay (Amaya et al. 2018). Another soil quality parameter of soil is known as soil organic carbon (SOC) contains organic remains of dead animals and plants at various stages of decomposition which affects physicochemical characteristics of the soil (Campbell 1978). Concentration of SOC in the soil samples is one of the fundamental criteria for soil quality (Unger 1997). Agricultural production, plant development, and soil fertility also depend on phosphorus content, which is the second-most important macronutrient

in soil after nitrogen (Malhotra et al. 2018). Similarly, soil fertility, pH levels, plant development, and efficient nitrogen fixation processes dependent on its existence in the soil (Jordan and Ensminger 1959). Potash content is another essential macronutrient for preserving soil fertility and pH homeostasis. Fertilizer used usually to supplement K into the soil in case of its deficiency because plants require K for their growth and development during the life cycle (Morgan and Connolly 2013). However, high concentration of potash in soil also effects soil quality and causes soil degradation (Sillanpaa 1982). Water and soil quality assessment studies have sparked interest on a global scale due to growing

attention on the depletion of water and soil quality to assess the environmental impact of anthropogenic activities for environmental sustainability (Raiesi and Kabiri 2016). Various attempts have been made to measure the quality of the soil and water using different indicators (Armenise et al. 2013; Seybold et al. 2018). Water quality index makes it possible to examine water quality in a variety of ways that affect a stream's ability to sustain by its processes and to ensure sustainable use of water resources to minimize risks and preserve aquatic ecosystems (Akkaraboyina and Raju 2012). WQI is an important distinctive grade which summarizes overall quality of water and helps in selecting the most effective treatment strategy for wastewater before its final discharge and disposal to prevent water contamination (Tyagi et al. 2013). Status and level of contamination of water has been evaluated by using water quality parameters and quality index (Shah and Joshi 2017). The WQI and SQI approach is one of the best and most widely used techniques for assessing the quality of soil and water for adapting treatment and conservation strategies (Arshad and Martin 2002; YanBing et al. 2009). Physio-chemical and biological characteristics of soil indicated by the soil quality which is crucial to its long-term functionality and productivity and sustainability. An encompassing view of the region's overall soil quality evaluated assessing the soil quality index (Bhattacharyya 2017). Similarly, minimum data set (MDS) for the data reflecting the soil's functional capacity used in evaluating the soil quality index (Klimkowitz-Pawlas et al. 2019). By using multivariate geostatistical techniques, contemporary data analysis and metal content estimation of four metals (Zn, Cu, Mn, and Fe) in the soil and six metals (Zn, Cu, Mn, Fe, Pb, and Ni) in groundwater emphasis water and soil quality (Lu et al., 2010). Metals Zn, Ni, Mn, Cu, Fe, and Pb chosen based on PCA, FA, and CA investigations as reference elements for soil and groundwater contamination. Several studies evaluated metal contamination of soil and water in the different urban and industrial regions using principal component analysis (Manta et al. 2002; Skrbic and Djurisc-Mladenovic, 2007, Guo et al., 2013). PCA technique used to show the relationship among metals concentration and other parameters (pH, EC, TOC) in the soil and water (Weissmannová and Pavlovský 2017). FA produced using a constant value for all the soil and water quality parameters with a correlation matrix to minimize the effect of varying units on the variables (Lin et al. 2002). Kaiser–Meyer–Olkin (KMO) test used to evaluate whether the sample is large enough to use factor analysis (Kaiser 1974). In principal component analysis (PCA), variables referred to as principal components (PC) used to illustrate the relation between two elements (Esbensen and Geladi 2010). In similar study, Tripathi and Singal (2019) evaluated water quality of the Ganga River using PCA technique. In contrast, Praus (2019) used primary component weighted

index (PCWI) for assessing the quality of both untreated and treated wastewater to evaluate WQI. Data indicate that unregulated discharge of wastewater including urban sewage contaminate water and soil by the process of seepage and leaching or irrigation with wastewater leads to depletion of groundwater and soil quality. High concentration of metals and other contaminants in the soil and groundwater may be due to continuous and long-term disposal of wastewater containing metals from industrial units leading to health hazards (Wuana and Okieimen 2011). Therefore, applying geographical and geostatistical techniques with an integrated approach could be more effective ways in environmental monitoring and assessment of soil and water contamination to ensure environmental and health safety.

Conclusion

Groundwater and soil quality parameters of water and soil samples varied with different sites of the selected study area, indicate about 13.3% of the sites found to have good soil health with minimum contamination level followed by 40% of sites with moderate contamination; however, 46.6% of sites shown high level of contamination of soil. Evaluating WQI and SQI values in the present study offers insightful information about site-wise variation pattern of quality parameters including metals identifying the sites with high level of contamination to opt appropriate strategies and mitigation measures to ensure preserving groundwater and soil quality. Further, a study concludes that contamination of water and soil with metals and other contaminants leads to depletion of quality parameters which affects nutrients cycling in the aquatic and terrestrial ecosystem with more imbalances in availability of NPK. GIS-based WQI maps provide more description of sites in categorizing contaminated regions to ensure safe water supply and developing wastewater treatment facilities for sustainable urban planning. Besides, water and soil quality assessment using GIS and geostatistical technique provide regional and spatial variability of contaminants with their correlation to establish standards of soil health and drinking for effective natural resource management in a particular region. Therefore, the present study could be a new insight in environmental monitoring involving quantitative and qualitative assessment of water and soil quality for sustainable resource utilization and conservation applying geographical and geostatistical techniques.

Supplementary Information The online version contains supplementary material available at <https://doi.org/10.1007/s11356-023-28004-y>.

Acknowledgments The authors are thankful to Manipal University Jaipur, India, for providing facilities and continuous encouragements and Ground Water Department, Jaipur, Rajasthan, India for support.

Author contribution All authors contributed to the study conception and design. Sampling of water and soil samples, analysis, and drafting of manuscript were performed by J. Khan and G. Gupta. All authors commented on previous versions of the manuscript. Hypothesis and designing of the experiment were done by N. K. Singh; data analysis and improving the manuscript were done by V.N. Bhave and V. Bhardwaj; map designing and statistical analysis were done by P. Upreti and R. Singh; and geophysical analysis and editing were done by A. K. Sinha. All authors read and approved the final manuscript.

Data availability This is not applicable.

Declarations

Ethical approval This is not applicable.

Consent to participate The authors mutually agreed to submit the manuscript in the esteemed journal ESPR.

Consent to publish All authors are mutually agreed to publish the manuscript in the journal ESPR.

Competing interests The authors declare no competing interests.

References

- Adagunodo TA, Akinloye MK, Sunmonu LA, Aizebeokhai AP, Oyeyemi KD, Abodunrin FO (2018) Groundwater exploration in Aaba residential area of Akure, Nigeria. *Front Earth Sci* 6
- Ahmet D, Fevzi Y, Tuna AL, Nedim O (2006) Heavy metals in water, sediment and tissues of *Leuciscus cephalus* from a stream in southwestern Turkey. *Chemosphere* 63:1451–1458
- Akkaraboyina MK, Raju PS (2012) A comparative study of water quality indices of River Godavari. *UJERT* 2:161–167
- Aksoy T, Dabanli A, Cetin M, Senyel Kurkcuoglu MA, Cengiz AE, Cabuk SN, Agacsapan B, Cabuk A (2022) Evaluation of comparing urban area land use change with Urban Atlas and CORINE data. *Environ Sci Pollut Res Int* 29:28995–29015
- Ali H, Khan E, Ilahi I (2019) Environmental chemistry and ecotoxicology of hazardous heavy metals: Environmental persistence, toxicity, and bioaccumulation. *J Chem* 6730305
- Ali SA, Ahmad A (2020) Analysing water-borne diseases susceptibility in Kolkata Municipal Corporation using WQI and GIS based Kriging interpolation. *Geo Journal* 85:1151–1174
- Amaya GA, Mårdh J, Dahlin T (2018) Delimiting a saline water zone in Quaternary fluvial–alluvial deposits using transient electromagnetic: a case study in Punata, Bolivia. *Environ Earth Sci* 77:46
- Armenise E, Redmile-Gordon MA, Stellacci AM, Ciccicarese A, Rubino P (2013) Developing a soil quality index to compare soil fitness for agricultural use under different managements in the Mediterranean environment. *Soil Tillage Res* 130:91–98
- Arshad MA, Martin S (2002) Identifying critical limits for soil quality indicators in agro-ecosystems. *Agric Eco Environ* 88:153–160
- Baird R, Bridgewater L (2017) Standard methods for the examination of water and wastewater. APHA, Washington, DC
- Bhattacharyya P (2017) Soil quality index under organic farming. *Organic farming in tropical islands of india*, 260–267
- Bilge Ozturk G, Ozenen Kavlak M, Cabuk SN, Cabuk A, Cetin M (2022) Estimation of the water footprint of kiwifruit: in the areas transferred from hazelnut to kiwi. *Environ Sci Pollut Res Int* 29:73171–73180
- Binley A, Hubbard SS, Huisman JA, Revil A, Robinson DA, Singha K, Slater LD (2015) The emergence of hydrogeophysics for improved understanding of subsurface processes over multiple scales. *Water Resour Res* 51:3837–3866
- Brondi AM, Daniel JSP, de Castro VXM, Bertoli AC, Garcia JS, Trevisan MG (2016) Quantification of humic and fulvic acids, macro- and micronutrients and C/N ratio in organic fertilizers. *Commun Soil Sci Plant Anal* 47:2506–2513
- Bronson KF, Booker JD, Officer SJ, Lascano RJ, Maas SJ, Searcy SW, Booker J (2005) Apparent electrical conductivity, soil properties and spatial covariance in the US Southern High Plains. *Precision Agriculture* 6:297–311
- Calzadilla A, Rehdanz K, Tol RSJ (2011) Trade liberalization and climate change: a computable general equilibrium analysis of the impacts on global agriculture. *Water* 3:526–550
- Campbell CA (1978) Soil organic carbon, nitrogen and fertility. In: Schnitzer M, Khan S.U. (Eds.). *Developments in soil science* 8:173–271
- Cesur A, Zeren Cetin I, Abo Aisha AES, Alrabiti OBM, Aljama AMO, Jawed AA, Cetin M, Sevik H, Ozel HB (2021) The usability of *Cupressus arizonica* annual rings in monitoring the changes in heavy metal concentration in air. *Environ Sci Pollut Res Int* 28:35642–35648
- Cetin M (2019) The effect of urban planning on urban formations determining bioclimatic comfort area's effect using satellitia imagines on air quality: a case study of Bursa city. *Air Qual Atmos Health* 12:1237–1249
- Cetin M, Abo Aisha AES (2023) Variation of AI concentrations depending on the growing environment in some indoor plants that used in architectural designs. *Environ Sci Pollut Res Int* 30:18748–18754
- Cetin M, Aksoy T, Bilge Ozturk G, Cabuk A (2022d) Developing a model for the relationship between vegetation and wind power using remote sensing and geographic information systems technology. *Water Air Soil Pollut* 233:450
- Cetin M, Aljama AMO, Alrabiti OBM, Adiguzel F, Sevik H, Cetin IZ (2022a) Determination and mapping of regional change of Pb and Cr pollution in Ankara City Center. *Water Air Soil Pollut* 233:163
- Cetin M, Aljama AMO, Alrabiti OBM, Adiguzel F, Sevik H, Cetin IZ (2022b) Using topsoil analysis to determine and map changes in Ni Co pollution. *Water Air Soil Pollut* 233:293
- Cetin M, Isik Pekkan O, Bilge Ozturk G, Anil Senyel Kurkcuoglu M, Kucukpehlivan T, Cabuk A (2022c) Examination of the change in the vegetation around the Kirka Boron Mine Site by using remote sensing techniques. *Water Air Soil Pollut* 233:254
- Cetin M (2015) Using GIS analysis to assess urban green space in terms of accessibility: case study in Kutahya. *Int J Sust Devel W Ecol* 22:420–424
- Dadhich PN, Jain H, Meena J, Meena H, Meena CS (2016) Water resource management based on GIS- a case study of municipality of Sanganer, Jaipur. *IJERT, NCACE* 4:23
- Dean GA (1966) A simple colorimetric finish for the Johnson-Nishita microdistillation of sulphur. *Analyst* 91:530
- Dogan S, Kilicoglu C, Akinci H, Sevik H, Cetin M (2023) Determining the suitable settlement areas in Alanya with GIS-based site selection analyses. *Environ Sci Pollut Res Int* 30:29180–29189
- Esbensen KH, Geladi P (2010) Principles of proper validation: use and abuse of re-sampling for validation. *J Chemom* 24:168–187
- Filip Z (2002) International approach to assessing soil quality by ecologically related biological parameters. *Agric Ecosys Environ* 88:169–174
- Garg NK, Hassan Q (2007) Alarming scarcity of water in India. *Curr Sci* 93:932–941
- Gąsiorek M, Kowalska J, Mazurek R, Pająk M (2017) Comprehensive assessment of heavy metal pollution in topsoil of historical urban park on an example of the Planty Park in Krakow (Poland). *Chemosphere* 179:148–158

- Gavrilescu M (2021) Water, Soil, and Plants Interactions in a Threatened Environment. *Water* 13:2746
- Gelman F, Binstock R, Halicz L (2012) Application of the Walkley–Black titration for the organic carbon quantification in organic rich sedimentary rocks. *Fuel* 96:608–610
- Griffiths BS, Ball BC, Daniell TJ, Hallett PD, Neilson R, Wheatley RE, Osler G, Bohanec M (2010) Integrating soil quality changes to arable agricultural systems following organic matter addition, or adoption of a ley-arable rotation. *Appl Soil Ecol* 46:43–53
- Gu YG, Gao Y, Lin Q (2016) Contamination, bioaccessibility and human health risk of heavy metals in exposed-lawn soils from 28 urban parks in southern China's largest city, Guangzhou. *Appl Geochem* 67:52–58
- Guo X, Yuan D, Jiang J, Zhang H, Deng Y (2013) Detection of dissolved organic matter in saline-alkali soils using synchronous fluorescence spectroscopy and principal component analysis. *Spectrochim Acta A* 104:280–286
- Hanfi MY, Mostafa MY, Zhukovsky MV (2020) Heavy metal contamination in urban surface sediments: sources, distribution, contamination control, and remediation. *Environ Monitor Assess* 192:1–21
- Hardie M, Doyle R (2012) Measuring soil salinity. In: *Methods in molecular biology (Clifton, N.J.)*, 913:415–425
- Hermans SM, Buckley HL, Case BS, Curran-Cournane F, Taylor M, Lear G (2020) Using soil bacterial communities to predict physico-chemical variables and soil quality. *Microbiome* 8:79
- Jolliffe IT (1972) Discarding variables in a principal component analysis. I: artificial data. *J R Stat Soc Ser C Appl Stat* 160–173
- Jordan HV, Ensminger LE (1959) The role of sulfur in soil fertility. In: *Normax AG (ed) Advances in agronomy*, vol 10. Academic Press, pp 407–434
- Juhos K, Czigány S, Madarász B, Ladányi M (2019) Interpretation of soil quality indicators for land suitability assessment—a multivariate approach for Central European arable soils. *Ecol Indic* 99:261–272
- Kaiser HF (1958) The varimax criterion for analytic rotation in factor analysis. *Psychometrika* 23:187–200
- Kaiser HF (1974) An index of factorial simplicity. *Psychometrika* 39:31–36
- Kalayci Onac A, Cetin M, Sevik H, Orman P, Karci A, Gonullu Sutcuoglu G (2021) Rethinking the campus transportation network in the scope of ecological design principles: case study of Izmir Katip Çelebi University Çiğli Campus. *Environ Sci Pollut Res* 28:50847–50866
- Klimkowicz-Pawlas A, Ukalska-Jaruga A, Smreczak B (2019) Soil quality index for agricultural areas under different levels of anthropopressure. *Inter Agrophys* 33:455–462
- Kopittke PM, Menzies NW, Wang P, McKenna BA, Lombi E (2019) Soil and the intensification of agriculture for global food security. *Environ Int* 132:105078
- Li D, Gao G, Shao M, Fu B (2016) Predicting available water of soil from particle-size distribution and bulk density in an oasis–desert transect in northwestern China. *J Hydrol* 538:539–550
- Lin YP, Teng TP, Chang TK (2002) Multivariate analysis of soil heavy metal pollution and landscape pattern in Changhua country in Taiwan. *Landsc Urban Plan* 62:19–35
- Lu X, Wang L, Li LY, Lei K, Huang L, Kang D (2010) Multivariate statistical analysis of heavy metals in street dust of Baoji, NW China. *J Hazard Mater* 173:744–749
- Luo XS, Ding J, Xu B, Wang YJ, Li HB, Yu S (2012) Incorporating bio accessibility into human health risk assessments of heavy metals in urban park soils. *Sci Total Environ* 424:88–96
- Luo Y, Su B, Yuan J, Li H, Zhang Q (2011) GIS techniques for watershed delineation of SWAT Model in Plain Polders. *Procedia Environ Sci* 10:2050–2057
- Mahmood A, Kundu (2005) “Status of water supply, sanitation and solid waste management in urban areas” New Delhi, National Institute of Urban Affairs (NIUA)
- Maiz I, Arambarri I, Garcia R, Millán E (2000) Evaluation of heavy metal availability in polluted soils by two sequential extraction procedures using factor analysis. *Environ Pollut* 110:3–9
- Malhotra H, Vandana Sharma S, Pandey R (2018) Phosphorus nutrition: plant growth in response to deficiency and excess. In: Hasanuzzaman M, Fujita M, Oku H, Nahar K, Hawrylak-Nowak B (eds) *Plant Nutrients and Abiotic Stress Tolerance*. Springer, pp 171–190
- Manta DS, Angelone M, Bellanca A, Neri R, Sprovieri M (2002) Heavy metals in urban soils: a case study from the city of Palermo (Sicily), Italy. *Sci Total Environ* 300:229–243
- McNeill JD (1992) Rapid, accurate mapping of soil salinity by electromagnetic ground conductivity meters. In: *Advances in measurement of soil physical properties: bringing theory into practice*. John Wiley & Sons, Ltd, pp. 209–229
- Mogaji KA, Omobude OB (2017) Modeling of geoelectric parameters for assessing groundwater potentiality in a multifaceted geologic terrain, Ipinsa Southwest, Nigeria – a GIS-based GODT approach. *NRIAG J Astron Geophys* 6:434–451
- Morgan JB, Connolly EL (2013) Plant-soil interactions: Nutrient uptake learn science at scitable. *National J Edu* 4:2
- Olayinka-Olagunju JO, Dosumu AA, Olatunji-Ojo AM (2021) Bio-accumulation of heavy metals in pelagic and benthic fishes of Ogbese River, Ondo State, South-Western Nigeria. *Water Air & Soil Pollut* 232:44
- Pandey N, Sharma CP (2002) Effect of heavy metals Co^{2+} , Ni^{2+} and Cd^{2+} on growth and metabolism of cabbage. *Plant Sci* 163:753–758
- Pekkan OI, Senyel Kurkcuoglu MA, Cabuk SN, Aksoy T, Yilmazel B, Kucukpehlivan T, Dabanli A, Cabuk A, Cetin M (2021) Assessing the effects of wind farms on soil organic carbon. *Environ Sci Pollut Res Int* 28:18216–18233
- Peralta NR, Costa JL (2013) Delineation of management zones with soil apparent electrical conductivity to improve nutrient management. *Comp Electron Agricul* 99:218–226
- Praus P (2019) Principal component weighted index for wastewater Quality Monitoring. *Water* 11:2376
- Raiesi F, Kabiri V (2016) Identification of soil quality indicators for assessing the effect of different tillage practices through a soil quality index in a semi-arid environment. *Ecol Indic* 71:198–207
- Rajendran S, Priya TAK, Khoo KS, Hoang TK, Ng HS, Munawaroh HSH, Show PL (2022) A critical review on various remediation approaches for heavy metal contaminants removal from contaminated soils. *Chemosphere* 287:132369
- Romic M, Romic D (2003) Heavy metals distribution in agricultural topsoils in urban area. *Environ Geol* 43:795–805
- Sahin G, Cabuk SN, Cetin M (2022) The change detection in coastal settlements using image processing techniques: a case study of Korfez. *Environ Sci Pollut Res Int* 29:15172–15187
- Saleem M, Hussain A, Mahmood G, Waseem M (2018) Hydro-geochemical assessment of groundwater in shallow aquifer of greater Noida region, Uttar Pradesh (U.P), India. *Appl Water Sci* 8:186
- Salem A, Dezső J, El-Rawy M, Lóczy D (2020) Hydrological modeling to assess the efficiency of groundwater replenishment through natural reservoirs in the Hungarian Drava River Floodplain. *Water* 12:250
- Sato JH, de Figueiredo CC, Marchão RL, Madari BE, Benedito LEC, Busato JG, de Souza DM (2014) Methods of soil organic carbon determination in Brazilian savannah soils. *J Agric Sci* 71:302–308
- Schlöter M, Dilly O, Munch JC (2003) Indicators for evaluating soil quality. *Agric Ecosys Environ* 98:255–262

- Seybold CA, Mansbach MJ, Karlen DL, Rogers HH (2018) Quantification of soil quality. In: Soil processes and the carbon cycle. CRC Press, pp 387–404
- Shah KA, Joshi GS (2017) Evaluation of water quality index for River Sabarmati, Gujarat, India. *Appl Water Sci* 7:1349–1358
- Sharma N, Sharma S, Gehlot A (2014) Influence of dyeing and printing industrial effluent on physicochemical characteristics of water – case study on the printing cluster of Bagru, Jaipur (Rajasthan), India. *IOSR J Appl Chem* 7:61–64
- Sillanpää M (1982) Micronutrients and the nutrient status of soils: a global study. *FAO Soil Bulletin No. 48*, Food and Agriculture Organization, Rome
- Singh R, Upreti P, Allemailam KS, Almatroudi A, Rahmani AH, Albalawi GM (2022) Geospatial assessment of ground water quality and associated health problems in the Western Region of India. *Water*. 14:296
- Singha SS, Devatha CP, Singha S, Verma MK (2015) Assessing ground water quality using GIS. *International J Eng Res Technol* 4:11
- Skrbic B, Djuricic-Mladenovic N (2007) Principal component analysis for soil contamination with organochlorine compounds. *Chemosphere* 68:2144–2152
- Tay DA, Ocansey RTA (2022) Impact of urbanization on health and well-being in Ghana. Status of research, intervention strategies and future directions: a rapid review. *Front Pub health* 10:877920
- Tiwari KK, Singh NK, Patel MP, Tiwari MR, Rai UN (2011) Metal contamination of soil and translocation in vegetables growing under industrial wastewater irrigated agricultural field of Vadodara, Gujarat, India. *Ecotoxicol Environ Saf* 74:1670–1677
- Tripathi M, Singal SK (2019) Allocation of weights using factor analysis for development of a novel water quality index. *Ecotoxicol Environ Saf* 183:109510
- Tyagi S, Sharma B, Singh P, Dobhal R (2013) Water quality assessment in terms of water quality index. *Am J Water Resour* 1:34–38
- Tzanakakis VA, Paranychianakis NV, Angelakis AN (2020) Water supply and water scarcity. *Water* 12:2347
- Ukah BU, Ameh PD, Egbueri JC, Unigwe CO, Ubido OE (2020) Impact of effluent-derived heavy metals on the groundwater quality in Ajao industrial area, Nigeria: an assessment using entropy water quality index (EWQI). *IJWREE* 4:231–244
- Ukah BU, Egbueri JC, Unigwe CO, Ubido OE (2019) Extent of heavy metals pollution and health risk assessment of groundwater in a densely populated industrial area, Lagos, Nigeria. *IJWREE* 3:291–303
- Unger PW (1997) Aggregate and organic carbon concentration interrelationships of a Torricite Paleustoll. *Soil and Tillage Res* 42:95–113
- Walkley A, Black IA (1934) An examination of the degtjareff method for determining soil organic matter, and a proposed modification of the chromic acid titration method. *Soil Sci* 37:29–38
- Weissmannová HD, Pavlovský J (2017) Indices of soil contamination by heavy metals—methodology of calculation for pollution assessment (minireview). *Environ Monit Assess* 189:616
- Wu J, Li P, Wang D, Ren X, Wei M (2020) Statistical and multivariate statistical techniques to trace the sources and affecting factors of groundwater pollution in a rapidly growing city on the Chinese Loess Plateau. *Hum Ecol Risk Assess* 26:1603–1621
- Wuana RA, Okieimen FE (2011) Heavy metals in contaminated soils: a review of sources, chemistry, risks and best available strategies for remediation. *ISRN Ecol* 402647
- Yanbing Q, Darilek JL, Huang B, Yongcun Z, Weixia S, Zhiquan G (2009) Evaluating soil quality indices in an agricultural region of Jiangsu Province, China. *Geoderma* 149:325–334
- Yang K, Nam T, Nam K, Kim YJ (2016) Characteristics of heavy metal contamination by anthropogenic sources in artificial lakes of urban environment. *KSCE J Civ Eng* 20:121–128
- Yu P, Han D, Liu S, Wen X, Huang Y, Jia H (2018) Soil quality assessment under different land uses in an alpine grassland. *CATENA* 171:280–287
- Zhu Y, Chen L, Wang K, Wang W, Wang C, Shen Z (2019) Evaluating the spatial scaling effect of baseflow and baseflow nonpoint source pollution in a nested watershed. *J Hydrol* 579:124221
- Zouboulis AI, Loukidou MX, Matis KA (2004) Biosorption of toxic metals from aqueous solutions by bacteria strains isolated from metal-polluted soils. *Process Biochem* 39:909–916

Publisher's note Springer Nature remains neutral with regard to jurisdictional claims in published maps and institutional affiliations.

Springer Nature or its licensor (e.g. a society or other partner) holds exclusive rights to this article under a publishing agreement with the author(s) or other rightsholder(s); author self-archiving of the accepted manuscript version of this article is solely governed by the terms of such publishing agreement and applicable law.

Research Article

Yogesh Dadhich, Reema Jain*, Karuppusamy Loganathan*, Mohamed Abbas, Kalyana Srinivasan Prabu, and Mohammed S. Alqahtani

Sisko nanofluid flow through exponential stretching sheet with swimming of motile gyrotactic microorganisms: An application to nanoengineering

<https://doi.org/10.1515/phys-2023-0132>
received July 19, 2023; accepted October 13, 2023

Abstract: The swimming of motile gyrotactic microorganism's phenomenon has recently become one of the most important topics in research due to its applicability in biotechnology, many biological systems, and numerous engineering fields. The gyrotactic microorganisms improve the stability of the nanofluids and enhance the mass/heat transmission. This research investigates the MHD fluid flow of a dissipative Sisko nanofluid containing microorganisms moving along an exponentially stretched sheet in the current framework. The mathematical model comprises equations that encompass the preservation of mass, momentum, energy, nanoparticle concentration, and microorganisms. The equations that govern are more complicated because of non-linearity, and therefore to obtain the combination of ordinary differential equations, similarity transformations are utilized.

The numerical results for the converted mathematical model are carried out with the help of the `bvp4c` solver. The resulting findings are compared to other studies that have already been published, and a high level of precision is found. The graphical explanations for velocity, temperature, and nanoparticles volume fraction distribution are shown with physical importance. Physical characteristics like Peclet number, Sisko fluid parameter, thermophoresis and Brownian motion parameter, and Hartmann number are taken into consideration for their effects. Based on the numerical outcomes, the bioconvection Peclet number enhances the density of mobile microorganisms, whereas thermal radiation contributes to an elevation in temperature. The velocity field decreases with the enhancement of magnetic parameter; however, the temperature field increases with increased magnetic parameter and thermophoresis parameter augmentation. Our numerical findings are ground breaking and distinctive, and they are used in microfluidic devices including micro instruments, sleeve electrodes, and nerve development electrodes. This study has various applications in nanoengineering, including nanomaterial synthesis, drug delivery systems, bioengineering, nanoscale heat transfer, environmental engineering.

Keywords: MHD, nanofluid, Sisko model, microorganisms, exponentially stretched sheet

* **Corresponding author: Reema Jain**, Department of Mathematics and Statistics, Manipal University Jaipur, Jaipur 303007, Rajasthan, India, e-mail: reemajain197@gmail.com

* **Corresponding author: Karuppusamy Loganathan**, Department of Mathematics and Statistics, Manipal University Jaipur, Jaipur 303007, Rajasthan, India, e-mail: loganathankaruppusamy304@gmail.com

Yogesh Dadhich: Department of Mathematics and Statistics, Manipal University Jaipur, Jaipur 303007, Rajasthan, India

Mohamed Abbas: Electrical Engineering Department, College of Engineering, King Khalid University, Abha 61421, Saudi Arabia, e-mail: mabas@kku.edu.sa

Kalyana Srinivasan Prabu: Department of Physics, Kongu Engineering College, Erode, Tamil Nadu, India, e-mail: kprabhush@kongu.edu

Mohammed S. Alqahtani: Radiological Sciences Department, College of Applied Medical Sciences, King Khalid University, Abha 61421, Saudi Arabia; BioImaging Unit, Space Research Centre, Michael Atiyah Building, University of Leicester, Leicester, LE1 7RH, United Kingdom, e-mail: mosalqhtani@kku.edu.sa

Nomenclature

A	material parameter (–)
B_0	magnetic field strength ($\text{kg s}^{-2} \text{A}^{-1}$)
C	concentration (kg m^{-3})
C_∞	ambient concentration (kg m^{-3})
C_w	sheet concentration (kg m^{-3})
c_p	specific heat ($\text{J kg}^{-1} \text{K}^{-1}$)
d	chemotaxis constant (m)
D_B	coefficient of Brownian diffusion ($\text{m}^2 \text{s}^{-1}$)

D_m	microorganism diffusion coefficient ($m^2 s^{-1}$)
D_T	coefficient of thermophoretic diffusion ($m^2 s^{-1}$)
E_c	Eckert number (–)
k	thermal conductivity ($W m^{-1} K^{-1}$)
L_b	bioconvection Lewis number (–)
L_e	Lewis parameter (–)
M	magnetic field parameter
N_b	Brownian diffusion parameter
N_t	thermophoresis parameter
Nu_x	local Nusselt number
N	concentration of microorganisms ($kg m^{-3}$)
N_w	sheet concentration of microorganisms ($kg m^{-3}$)
N_∞	ambient concentration of microorganisms ($kg m^{-3}$)
Pe	Peclet number
Pr	Prandtl number
q_r	radiative heat flux ($W m^{-2}$)
R	radiation parameter
Re_a, Re_b	local Reynolds numbers
Sh_x	Sherwood number
T	fluid temperature (K)
T_w	sheet temperature (K)
T_∞	ambient fluid temperature (K)
u, v	velocity components ($m s^{-1}$)
W_c	maximum cell swimming speed ($m s^{-1}$)
x, y	Cartesian coordinates (m)

Greek symbols

α	thermal diffusivity ($m^2 s^{-1}$)
δ	heat source/sink parameter
η	similarity parameter
θ	temperature similarity function
ϕ	concentration similarity function
χ	microorganism similarity function
λ	mixed convection parameter
ϑ	kinematic viscosity ($m^2 s^{-1}$)
ρ	density ($kg m^{-3}$)
τ	ratio of the effective heat capacity
σ	electrical conductivity (S/m)

Subscripts

∞	ambient condition
w	surface condition

1 Introduction

Numerous biological, industrial, and technical processes, such as the production of fibres, refinement of polymer, hot roll glass blasting, heat exchangers, extrusion of aerodynamics, MHD power generators, domestic refrigerator-freezers, rubber and plastic sheet manufacturing, cooling process of reactors, improving diesel generator efficiency, and cooling/drying of papers, the flow of nanofluid over stretching or shrinking sheets is extremely important [1]. Nanofluids may be useful in solar energy, nuclear reactors, medicine delivery, and cancer treatment. Nanoparticle scattering in common (base) fluids yields nanofluids. Polymer solutions can be utilized as base fluids in addition to normal fluids including oils and lubricants. Choi *et al.* [2] were the first to present the fundamental concept of such metallic nanoparticles by presenting a comprehensive model for improving the thermal characteristics of base fluid. Subsequently, Buongiorno [3] established a non-homogeneous equilibrium model by incorporating Brownian movement and thermophoresis properties to describe the slip mechanism of nanoparticles. Eastman *et al.* [4] explored the phenomena of heat transfer in the presence of copper oxide (CuO) particles made of water and Al_2O_3 particles made of ethylene glycol. Since then, Sheikholeslami *et al.* [5] have explored the properties of nanofluids. Pourfattah *et al.* [6] employed two-phase flow simulation to investigate the characteristics of microchannel heat sink. The processing methods and thermal characteristics of oil-based nanofluid were investigated by Asadi *et al.* [7]. Khan *et al.* [8] investigated the fluid flow of nanoparticles for the Jeffrey fluid. An experimental study on the effects of ultra-sonication of MWCNT- H_2O nanofluid was carried out by Asadi *et al.* [9]. Zeeshan *et al.* [10] conducted an analysis on the movement of two immiscible fluids within a lengthy, flexible tube. They formulated models for both the core and peripheral regions, making assumptions of long wavelength behaviour and creeping flow. Riaz *et al.* [11] explored the transportation of nanosized particles through a curved channel characterized by non-Darcy porous conditions. The flow in this channel is driven by a peristaltic wave. Riaz *et al.* [12] analyzed the effects of an applied magnetic field and entropy generation on Jeffrey nanofluid in the annular section between two micro non-concentric pipelines, with the inner pipe being rigid and moving at a constant speed. The researchers discovered that the magnetic field reduced the flow velocity and the rate of entropy production while increasing the temperature of the nanofluid. Following that, other researchers and technologists worked in the same field, and numerous publications have been published that

consider the existence of nanofluids and magnetic fields in addition to linear and nonlinear thermal radiation, chemical reactions, and other factors [13–15].

Bioconvection occurs when bacteria spread randomly in a single-celled and, in certain cases, colony-like pattern. Because of the gyrotactic microorganisms upstream, the buoyancy of the fluid significantly increases. The flow of microbes in nanofluids has recently drawn the attention of researchers due to wide applications in biosensors, microbial-enhanced oil recovery, engineering, biological, and chemical fields such as biofuels, cancer treatment, enzymes, biotechnological applications, production and manufacturing, industrial level, and others. Firstly, Kuznetsov [16] established the concept of nanofluid bioconvection. Later, using Navier–Stokes equations, Alloui *et al.* [17] examined the distribution of microorganisms in a cylinder. Waqas *et al.* [18] used the magnetic dipole effect to investigate the bioconvection effect that microbes produce in Jeffery nanofluid through an expanded surface. Waqas *et al.* [19] presented a computational investigation of nanofluid flow (Oldroyd-B Model) with mass and heat transport, gyrotactic microbes past a rotating disc using the MATLAB built-in function `bvp4c`. Uddin *et al.* [20] first described the blowing effect on bio-convection flow across a dynamic stretched sheet. Following that, Chamkha *et al.* [21] described the bio-convective fluid flow containing microbes through a radiating stretching plate. Using the help of a nanofluid model of Buongiorno's and the O-Boussinesq approximation, Rashad and Nabwey [22] examined the bio-convection flow containing microorganisms through a cylinder placed horizontally under convective boundaries. Alwatban *et al.* [23] investigated bioconvection using slip effects of Wu's at the surface. Aziz *et al.* [24] anticipated a bioconvective flow of microorganisms embedded in the porous medium. Shaw *et al.* [25] used a spectrum relaxation technique to derive the associated equations depicting the fluid nanoflow with microorganisms. Rashad and Nabwey [22] and Rashad *et al.* [26] recently addressed the subject of bioconvection over a vertical thin cylinder. Elboughdiri *et al.* [27] investigated radiating viscoelastic nanofluids in MHD mixed convective flows near a sucked impermeable surface with exponentially decreasing heat generation using Jeffery's model, convective mass transport, thermophoresis, and Brownian diffusion under boundary layer assumptions. The influence of nanoparticles on the thermosolutal sensitivity of non-Newtonian fluid flow is investigated by Sharma *et al.* [28], with numerical computations employing blood as the base liquid. Wakif [29] computed the two-dimensional mixed convective motion of a radiating mixture of an upper-convected Maxwell nanofluid and gyrotactic motile microorganisms along a convectively heated vertical surface with a uniform magnetic

field source, revealing the non-homogeneous appearance and dynamical properties of the system. Puneeth *et al.* [30] investigation focuses on analysing the impact of Brownian motion and thermophoresis on the flow of a tangent hyperbolic (pseudoplastic) nanofluid past a rotating cone in three-dimensional free stream conditions.

Observations from previous studies reveal the lack of evidence regarding the flow of dissipative magneto Sisko nanofluid with gyrotactic microorganisms along an exponentially stretching sheet. The goal of this study is to describe the heat transfer properties of bioconvection flow of Sisko nanofluid along an exponential stretched sheet. To obtain a simplified mathematical model, similarity transformations are employed. The computational analysis is completed using the `bvp4c` and coding MATLAB scripts. Graphical analysis is used to explore the behaviour of the relevant parameters, and results are compared with the earlier research. For designing equipment, such as electric ovens, electric heaters, microelectronics, and wind generators, the thermal industry uses these kinds of modelled problems. The study aims to analyse the behaviour of the nanofluid flow and the influence of the motile microorganisms, with potential applications in the field of nanoengineering.

2 Mathematical modelling

2.1 Rheological model

Consider a non-Newtonian fluid that is time independent and follows the Sisko rheological model; the Cauchy stress tensor for such fluids is defined as follows:

$$\mathbf{T} = -p\mathbf{I} + \mathbf{S},$$

where \mathbf{S} is the extra stress tensor and is expressed as follows:

$$\mathbf{S} = \left[\mathbf{a} + \mathbf{b} \left| \sqrt{\frac{1}{2}\text{tr}(\mathbf{A}_1^2)} \right|^{n-1} \right] \mathbf{A}_1,$$

where for “ $n > 0$ for various fluids,” a and b are the physical constants difference, $\mathbf{A}_1 = (\text{grad } V) + (\text{grad } V)^T$, V represents for the vector as velocity, and T stands for transposition and means the first Rivlin–Erickson tensor.

2.2 Governing equations and boundary conditions

The flow configuration of the current investigation is illustrated in Figure 1, which shows the movement of a two-dimensional laminar boundary layer dissipative Sisko

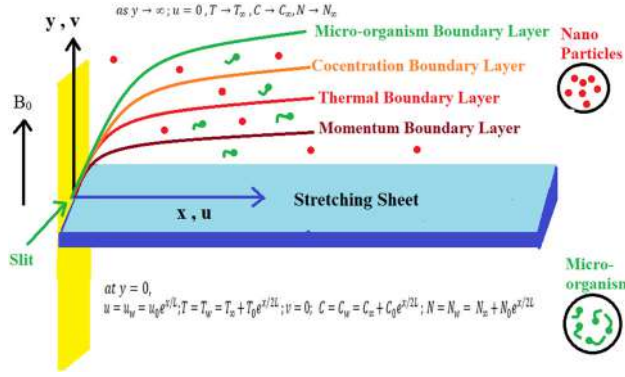


Figure 1: Physical model.

nanofluid containing microbes across an exponentially stretched surface, under steady conditions (independent of time). Here, the sheet was stretched exponentially along the x -axis with a stretching velocity $u_w(x) = u_0 e^{x/L}$ to initiate the flow of nanofluids. The effects of viscous dissipation, magnetic field, and Brownian motion are addressed in flow formulation. The x and y -axes are assumed perpendicular to each other. A fixed magnetic field, B_0 , is acted parallel to the y -direction upon. u and v represent the velocity components along the x and y axes, respectively. Furthermore, the assumption is made that the temperature, nanoparticle volume fraction, and density of motile microbes on the stretchable surface are T_w , C_w , and N_w , respectively. In addition, it is considered that these variables remain constant as T_∞ , C_∞ , and N_∞ when moving away from the stretchable surface.

Using the assumptions stated earlier, the fundamental equations for the present investigation can be addressed as follows [31]:

Continuity equation:

$$\frac{\partial u}{\partial x} + \frac{\partial v}{\partial y} = 0. \quad (1)$$

Momentum equation:

$$u \frac{\partial u}{\partial x} + v \frac{\partial u}{\partial y} = \frac{a}{\rho} \frac{\partial^2 u}{\partial y^2} - \frac{b}{\rho} \frac{\partial}{\partial y} \left(-\frac{\partial u}{\partial y} \right)^n - \frac{\sigma B_0^2 u}{\rho}. \quad (2)$$

Thermal energy equation:

$$\begin{aligned} u \frac{\partial T}{\partial x} + v \frac{\partial T}{\partial y} = & a \frac{\partial^2 T}{\partial y^2} + \tau \left[D_B \frac{\partial C}{\partial y} \frac{\partial T}{\partial y} + \frac{D_T}{T_\infty} \left(\frac{\partial T}{\partial y} \right)^2 \right] \\ & - \frac{1}{(\rho C_p)_f} \frac{\partial q_r}{\partial y} + \frac{Q}{(\rho C_p)_f} (T - T_\infty) \\ & + \frac{1}{(\rho C_p)_f} \left[a \left(\frac{\partial u}{\partial y} \right)^2 + b \left(-\frac{\partial u}{\partial y} \right)^{n+1} \right] \\ & + \frac{\sigma B_0^2 u^2}{(\rho C_p)_f}. \end{aligned} \quad (3)$$

Nanoparticle concentration equation:

$$u \frac{\partial C}{\partial x} + v \frac{\partial C}{\partial y} = D_B \frac{\partial^2 C}{\partial y^2} + \frac{D_T}{T_\infty} \frac{\partial^2 T}{\partial y^2}. \quad (4)$$

Conservation equation for microorganisms:

$$u \frac{\partial N}{\partial x} + v \frac{\partial N}{\partial y} - D_m \frac{\partial^2 N}{\partial y^2} + \frac{dW_c}{C_w - C_\infty} \left[\frac{\partial}{\partial y} \left(N \frac{\partial C}{\partial y} \right) \right] = 0. \quad (5)$$

The corresponding boundary conditions are as follows:

$$\text{at } y = 0 : u = u_w = u_0 e^{x/L}; v = 0; T = T_w; \quad (6)$$

$$C = C_w; N = N_w,$$

$$\text{at } y \rightarrow \infty; u = 0, T \rightarrow T_\infty, C \rightarrow C_\infty, N \rightarrow N_\infty. \quad (7)$$

The following transformations are used to convert the aforementioned equations into their non-dimensional forms [32]:

$$\begin{aligned} \eta &= y \sqrt{\frac{u_0}{2\partial L}} e^{x/2L} \\ u &= u_0 e^{x/L} f'(\eta) \\ v &= -\sqrt{\frac{u_0 \partial}{2L}} e^{x/2L} [f(\eta) + \eta f'(\eta)] \\ \theta(\eta) &= \frac{T - T_\infty}{T_w - T_\infty} \\ \phi(\eta) &= \frac{C - C_\infty}{C_w - C_\infty} \\ \chi(\eta) &= \frac{N - N_\infty}{N_w - N_\infty}. \end{aligned} \quad (8)$$

The radiative heat flux q_r is determined using the Rosseland diffusion approximation and is given by

$$q_r = -\frac{4\sigma^* \partial T^4}{3k^* \partial y}. \quad (9)$$

The Rosseland mean absorption coefficient is denoted as k^* , and the Stefan–Boltzmann constant is represented by σ^* . Assuming minimal temperature variations within the flow, T^4 can be expressed as a linear function of temperature.

$$T^4 = 4T_\infty^3 - 3T_\infty^4. \quad (10)$$

Using Eqs. (9) and (10)

$$\frac{\partial q_r}{\partial y} = -\frac{16\sigma^* T_\infty^3}{3k^*} \frac{\partial^2 T}{\partial y^2}, \quad (11)$$

where η shows similarity parameter; $f(\eta)$ indicates dimensionless stream function; $\theta(\eta)$ represents dimensionless temperature; and $f'(\eta)$ shows the dimensionless velocity profile (the derivative of $f(\eta)$).

By utilizing the non-dimensional similarity parameters given below, Eqs. (1)–(7) can be converted into

dimensionless equations. The given equations are converted into their non-dimensional forms using the following transformations:

$$Af''' + n(-f'')^{n-1}f''' - Mf' - 2f'^2 + ff'' = 0, \quad (12)$$

$$\left(1 + \frac{4R}{3}\right)\theta'' + P_r f\theta' + \delta P_r \theta + N_b \theta' \phi' + N_t \theta'^2 + MP_r E_c f'^2 + AP_r E_c (f'')^2 + P_r E_c (-f'')^{n+1} = 0, \quad (13)$$

$$\phi'' + P_r L_e f \phi' + \left(\frac{N_t}{N_b}\right)\theta'' = 0, \quad (14)$$

$$\chi'' + L_b f \chi' - [P_e(\phi'' \chi + \phi' \chi')] = 0. \quad (15)$$

Furthermore, the boundary conditions are modified as follows: at

$$\begin{aligned} \eta = 0 : f'(\eta) = 1; f(\eta) = 0; \theta(\eta) = 1; \\ \phi(\eta) = 1; \chi(\eta) = 1, \end{aligned} \quad (16)$$

for

$$\eta \rightarrow \infty : f'(\eta) = 0; \theta(\eta) = 0; \phi(\eta) = 0; \chi(\eta) = 0. \quad (17)$$

In Eqs. (12)–(17), the prime indicates the differentiation with respect to η (similarity parameter). The following non-dimensional parameters are used:

$$\begin{aligned} L_b &= \frac{\alpha}{D_m}; P_e = \frac{dW_c}{D_m}; N_b = \frac{\tau D_B (C_w - C_\infty)}{\vartheta}; \\ N_t &= \frac{\tau D_T (T_w - T_\infty)}{\vartheta T_\infty}; L_e = \frac{\alpha_f}{D_B}; R = \frac{4\sigma^* T_\infty^3}{k^* k}; \delta = \frac{Qx}{\rho c_p u_\infty}; \\ E_c &= \frac{(u_\infty)^2}{(c_p)_f (T_w - T_\infty)}; P_r = \frac{\vartheta}{\alpha_f}; A = \frac{(Re_b)^{2/(n+1)}}{Re_a}; Re_a = \frac{\rho x u_\infty}{a}; \\ Re_b &= \frac{\rho x (u_\infty)^{(2-n)}}{b} \end{aligned}$$

2.3 Coefficients of heat and mass transport

The main objective of this analysis is to determine the factors that engineers need to take into account when addressing heat and nanoparticle mass transfer. Defining

$$\text{these as follows: local Nusselt number } Nu_x = \left(\frac{xq_w}{k(T_w - T_\infty)} \right)_{y=0}$$

$$\text{and local nanofluid Sherwood number } Sh_x = \left(\frac{xq_w}{D_B(C_w - C_\infty)} \right)_{y=0},$$

where $q_w = -k \left(\frac{\partial T}{\partial y} \right)_{y=0}$ is wall heat flux. Using the aforementioned

transformations, these parameters will reduce to $(Re_b)^{-1/(n+1)}$

$$Nu_x = -\left(1 + \frac{4R}{3}\right)\theta'(0) \text{ and } (Re_b)^{-1/(n+1)} Sh_x = -\phi'(0).$$

3 Computational procedure

The examined physical problem is addressed by a system of partial differential equations that are reduced to a system of ordinary differential equations (ODEs) using appropriate similarity transformations. Furthermore, the converted system of nonlinear ODEs (12)–(17) is solved by using the `bvp4c` function. To achieve this, the system of ODEs (18)–(23) is converted to first-order ODEs, which can be summed up as follows:

Solution by `bvp4c`:

$$f = y_1; f' = y_2; f'' = y_3; f''' = y_4; \theta = y_5; \theta' = y_6; \theta'' = y_7; \phi = y_8; \phi' = y_9; \phi'' = y_{10}; \chi = y_{11}; \chi' = y_{12}; \chi'' = y_{13}$$

$$f''' = \frac{2y_2^2 + M^2 y_2 - y_1 y_3}{A + (-1)^{n-1} n (y_3)^{n-1}}, \quad (18)$$

$$\begin{aligned} \theta'' = y_7 \\ = \frac{[P_r y_1 y_5 + \delta P_r y_4 + P_r E_c (-y_3)^{n+1} + MP_r E_c y_2^2 + N_b y_5 y_7 + N_t y_5^2 + AP_r E_c (y_3)^2]}{-\left(1 + \frac{4R}{3}\right)}, \end{aligned} \quad (19)$$

$$y_7' = \phi'' = -\left[P_r L_e y_1 y_7 + \frac{N_t}{N_b} y_5 \right] \quad (20)$$

$$y_9' = \chi'' = P_e y_7 y_9 + P_e y_8 \phi'' - L_b y_1 y_9. \quad (21)$$

Using boundary conditions

$$\begin{aligned} \text{at } \eta = 0 : y_0(1) = 0, y_0(2) - 1 = 0, y_0(4) - 1 = 0, \\ y_0(6) - 1 = 0, y_0(8) - 1 = 0, \end{aligned} \quad (22)$$

$$\begin{aligned} \text{for } \eta \rightarrow \infty : y_1(2) = 1, y_1, y_1(4) = 0, \\ y_1(6) = 0, y_1(8) = 0. \end{aligned} \quad (23)$$

The convenience with which nonlinear issues in simple domains can be dealt with is an advantage of this approach. The method is proven effective and precise in a number of boundary value problems and iteratively refined to a range of 10^{-5} and a step size of 0.05.

4 Results and discussion

In this section, we will focus on explaining the flow regime, or the conditions under which the nanofluid moves and behaves in terms of its velocity temperature, micro-organism profile, and nanoparticle concentration. The scope of variables considered in this investigation is

$$0 \leq A \leq 1.5, 0 \leq M \leq 1.5, 0 \leq P_r \leq 1.5, 0 \leq E_c \leq 1.5, 0 \leq N_b \leq 1.5, 0 \leq N_t \leq 1.5, 0 \leq L_e \leq 1.5, 0 \leq R \leq 1.5, 0 \leq \delta \leq 1.5, 0 \leq L_b \leq 1.5, 0 \leq P_e \leq 1.5.$$

4.1 Effect of A on velocity, temperature, chemical reaction, motile density profiles

Figure 2(a) shows that the fluid velocity increases as Sisko fluid parameter (material parameter) increases. Due to the fact that the relationship between the material parameter and the fluid’s viscosity is inverse. The observations from this study indicated that when the value of A was increased, the viscosity of the fluid decreased, leading to a subsequent

reduction in the resistance encountered during fluid motion. The fluid velocity rises as a result. The effect of Sisko fluid parameter A (material parameter) on fluid temperature is shown in Figure 2(b). As the material parameter A is raised, a drop in the fluid temperature is seen.

4.2 Effect of M on velocity, temperature, nanoparticle concentration, and microorganism profiles

The purpose of Figure 3(a)–(d) is to explore how the velocity, temperature, volume proportion of nanoparticles, and

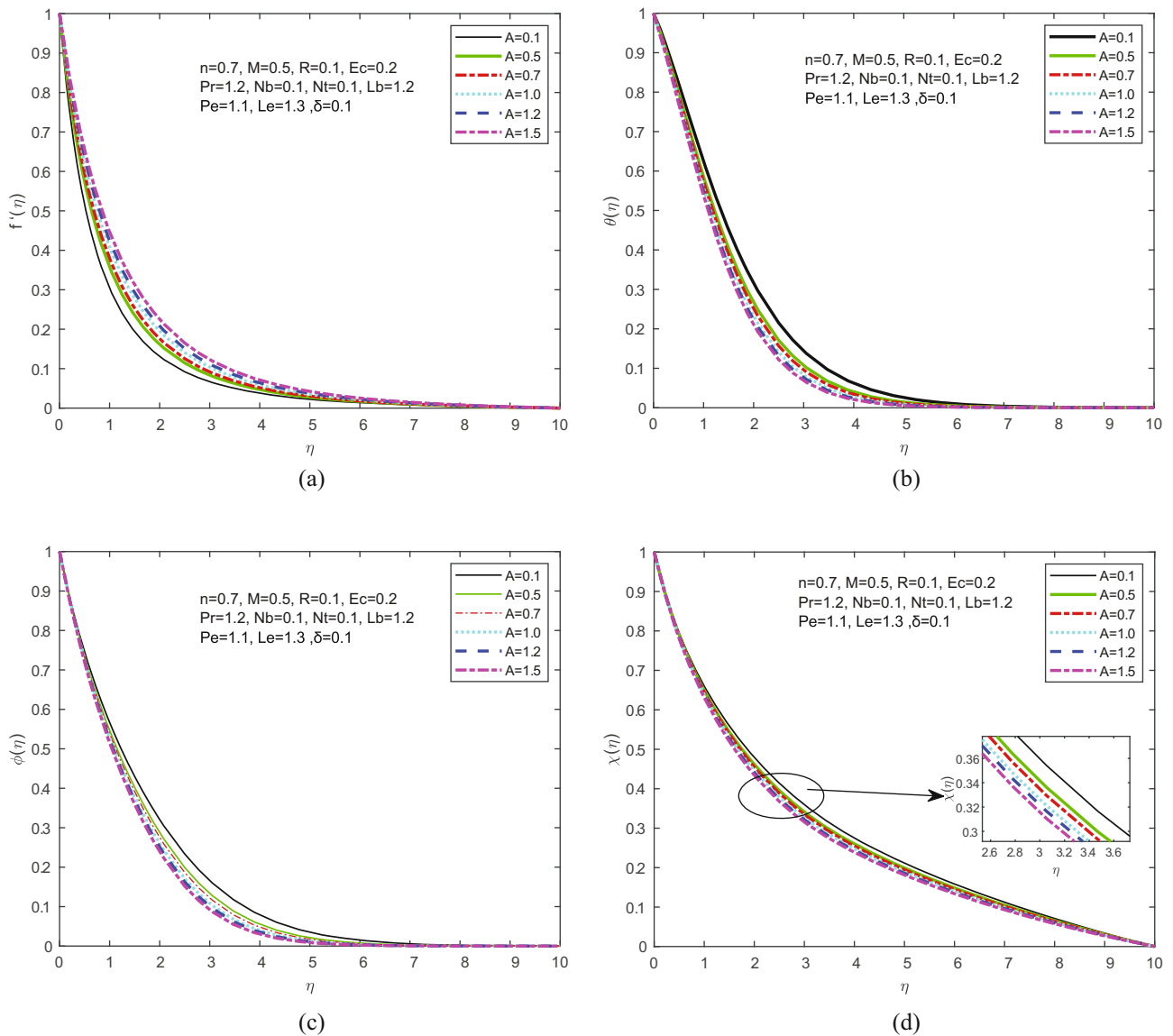


Figure 2: (a) f' vs A , (b) θ vs A , (c) ϕ vs A and (d) χ vs A .

microorganism density curves are influenced by the magnetic parameter (M). The velocity profile is observed to decrease as magnetic field strength estimates (M) increase, according to Figure 3(a), owing to the Lorentz force theorem, on which the magnetic field is established. The greater collisional impact between fluid atoms, as indicated by M , results in increased fluid flow resistance. Furthermore, the Lorentz force, which acts in opposition to the direction of flow, creates a resistance force that contributes to the thickness of the thermal boundary layer, as shown in Figure 3(b). The presence of a reversing force results in a decrease in the fluid flow, leading to a decline in the velocity field. Notably, Figure 3(c) and (d) demonstrate that the inclusion of magnetic parameters contributed to the enhancement of temperature and volume fraction

near the surface, as well as the thicknesses of the thermal and nanoparticle concentration boundary layers. These outcomes can be explained by the increased heat generation associated with higher magnetic parameter values (M), which led to the expansion of temperature, concentration, and gyrotactic microorganism boundary layers, as depicted in Figure 3(b)–(d).

4.3 Effect of P_r on temperature, nanoparticle concentration profile, and microorganism profiles

The curves for the temperature, nanoparticle volume fraction, and density of the motile microorganisms are

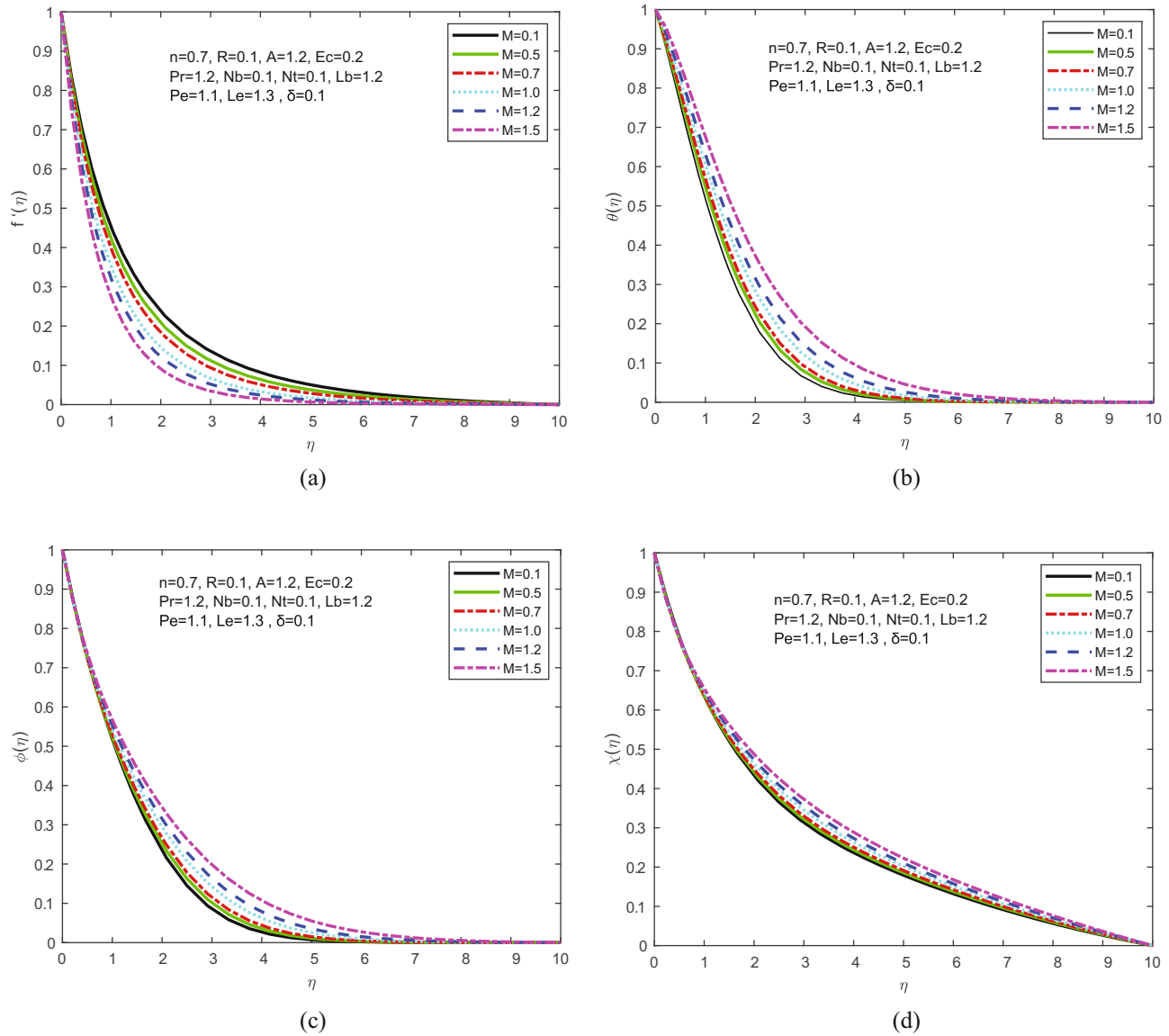


Figure 3: (a) f' vs M , (b) θ vs M , (c) ϕ vs M and χ vs M .

depicted in Figure 4(a)–(c), which illustrated the manner in which the Prandtl number Pr affected these curves. The Prandtl number had no effect on velocity, according to Eq. (9). As shown in Figure 4(a), the temperature and thickness of the thermal boundary layer decreased as Pr increased. In terms of physical significance, when Pr was raised, the thermal diffusivity dropped, leading to a reduction in the capability of energy to transfer across the thermal boundary layer. The thicknesses of the concentration boundary layer exhibited an upward trend as Pr increased as shown in Figure 4(b). The influence of the Prandtl number on the motile microorganism's density ($\chi(\eta)$) is shown in Figure 4(c), which indicates that the density of microorganisms increased with increasing

Pr . This is due to the fact that the boundary layer thicknesses of the motile microorganisms decreased with increasing Pr , causing their size to decrease. In other terms, the increase in Pr resulted in a reduction in the number of gyrotactic microbes.

4.4 Effect of E_c on temperature, nanoparticle concentration profile, and microorganism profiles

In Figure 5(a)–(c), temperature, concentration, and microorganism density variations are depicted for different

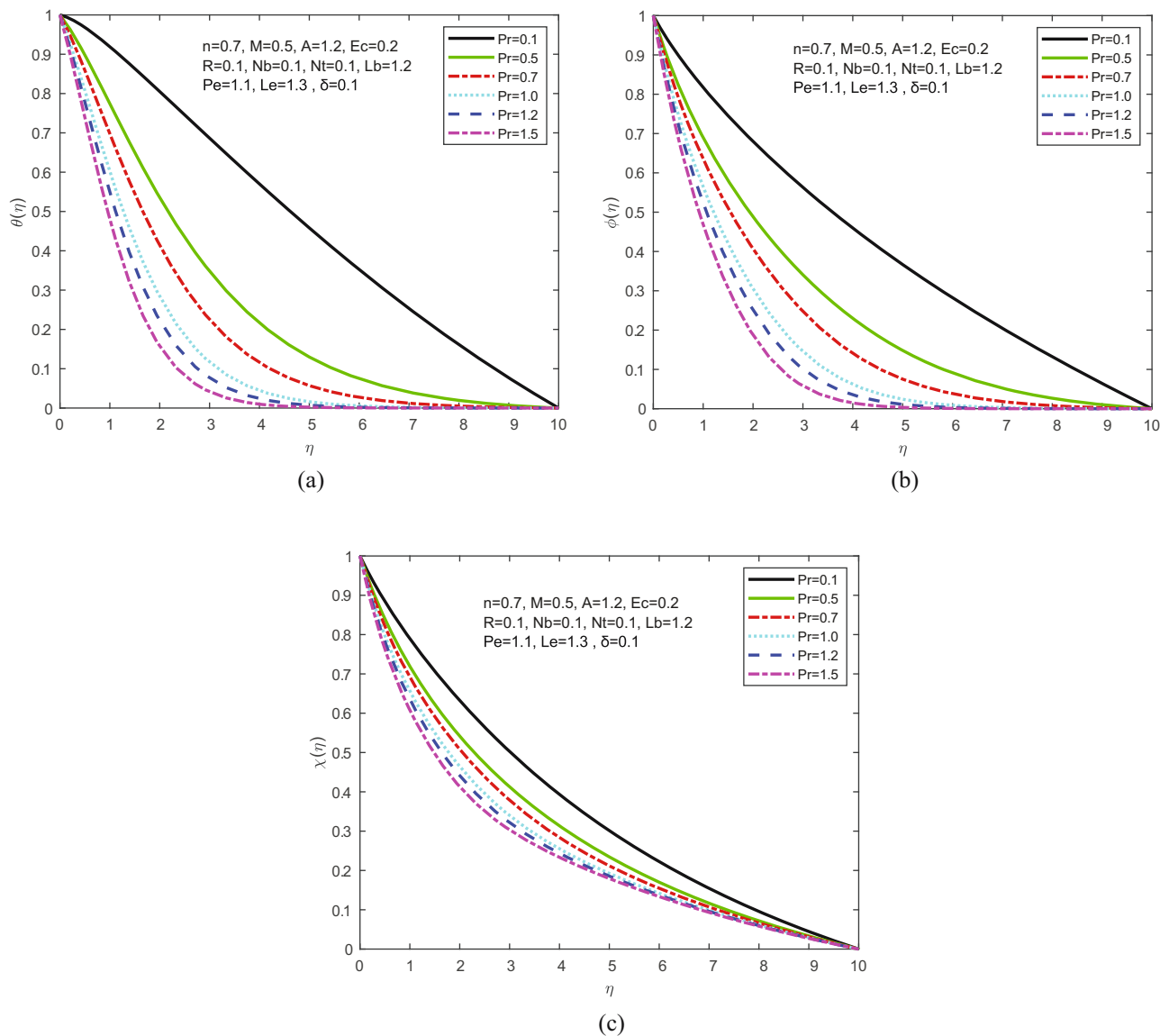


Figure 4: (a) θ vs Pr , (b) ϕ vs Pr , and (c) χ vs Pr .

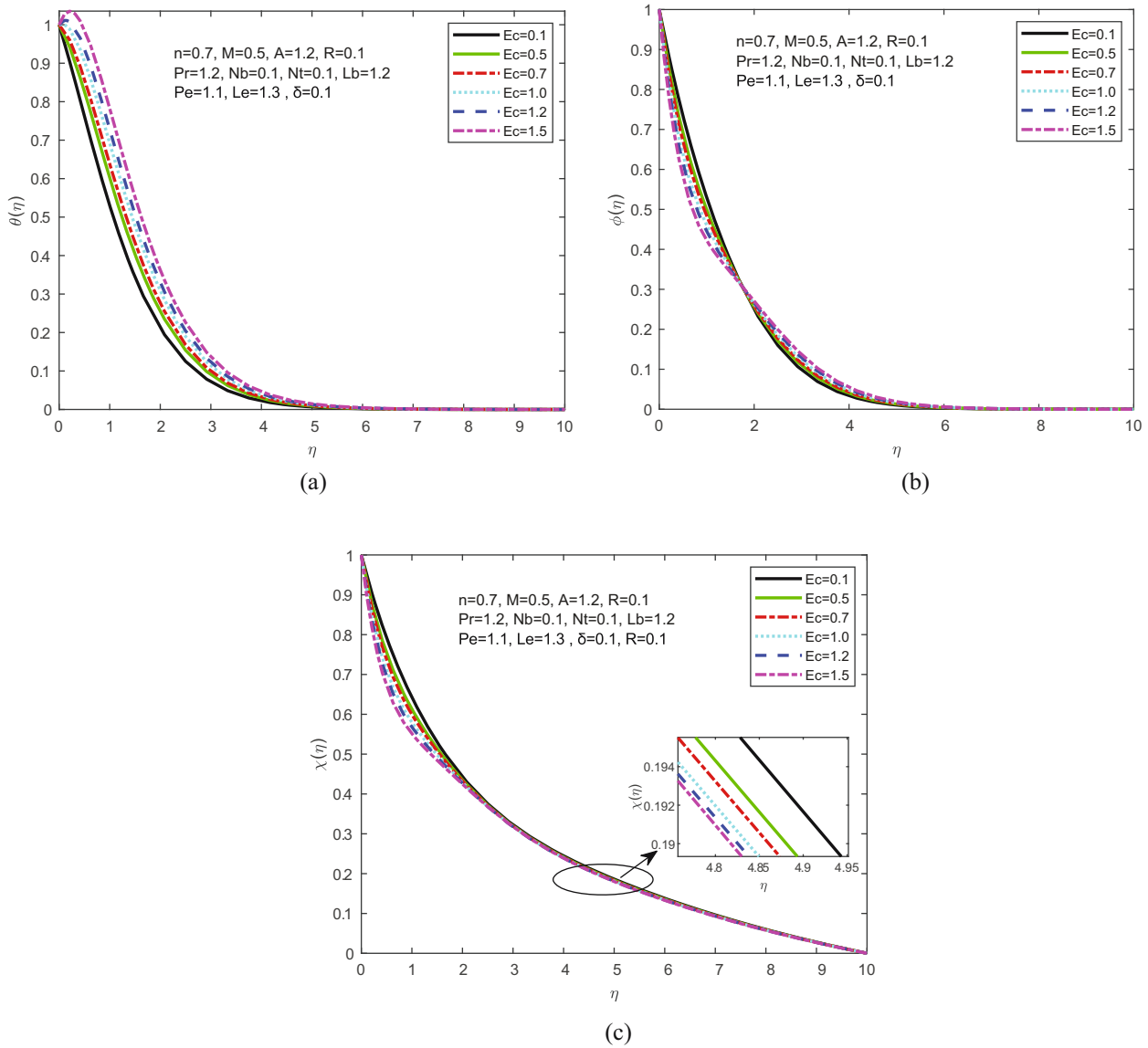


Figure 5: (a) θ vs E_c , (b) ϕ vs E_c and (c) χ vs E_c .

Eckert number (E_c) values. These figures illustrate that an elevated Eckert number leads to an increase in fluid temperature. This effect arises from the fact that E_c represents the ratio between kinetic energy and enthalpy, and as E_c increases, so does kinetic energy. Consequently, fluid particles collide more frequently, converting kinetic energy into thermal energy and resulting in higher fluid temperatures. It was observed that when E_c increased, the density of microorganism dropped. When the Eckert number increases in the fluid flow, it implies that there is a higher rate of heat transfer. Elevated temperatures resulting from increased heat transfer can be detrimental to microorganisms, leading to a drop in their density due to thermal stress.

4.5 Effect of N_b on temperature, nanoparticle concentration profile, and microorganism profiles

Figure 6(a) and (b) depict the impact of the N_b on the temperature and nanoparticle volume fraction trajectories. The temperature boundary layer was shown to be improved as N_b increased; however, the nanoparticle volume fraction boundary thickness had the reverse effect. Based on the information presented in Figure 6(b), it is evident that the Brownian motion parameter contributes to a decrease in the thickness of the concentration boundary layer, leading to a subsequent decline in the concentration. The particles travel

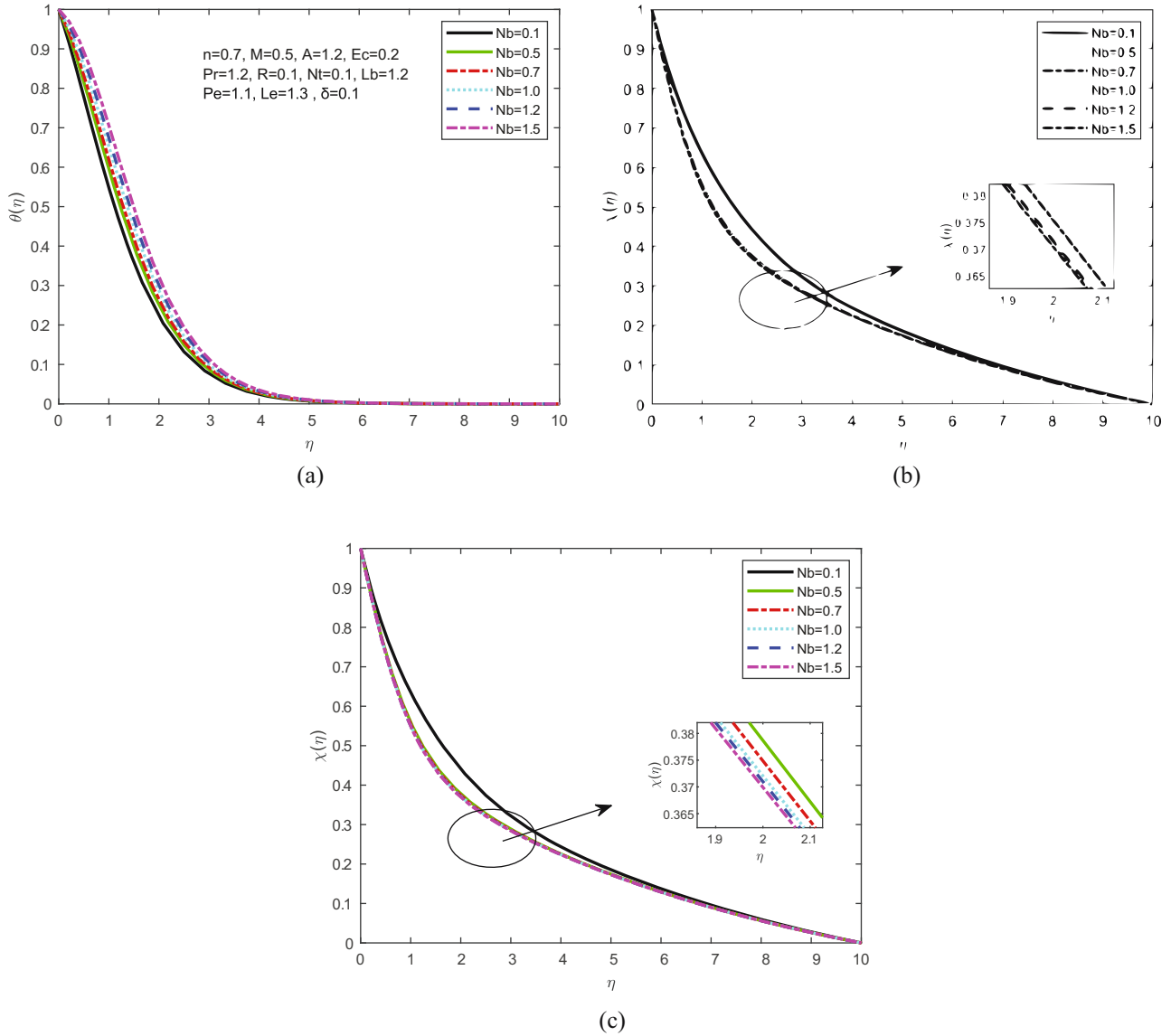


Figure 6: (a) θ vs N_b , (b) ϕ vs N_b and (c) χ vs N_b .

arbitrarily as a result of the greater Brownian motion, which is another physical explanation for the situation. This random movement results in additional heat being emitted. Hence, the formation of temperature curves was investigated. In addition, N_b has no effect on the motile microbe profiles' density and velocity.

4.6 Effect of δ on temperature, nanoparticle concentration profile, and microorganism profiles

Furthermore, the heat sink parameter (δ) represents the rate of heat removal or dissipation from a system. A higher

δ signifies more efficient cooling, leading to a lower temperature (Figure 7(a)). As shown in Figure 7(b), a higher δ indicates more efficient cooling and enhanced fluid motion, resulting in better nanoparticle dispersion and reduced concentration. An increase in the heat sink parameter (δ) leads to an increase in microorganism density profiles due to improved thermal regulation (Figure 7(c)).

4.7 Effect of L_e on nanoparticle concentration profile and microorganism profiles

By analysing Figure 8(a) and (b), it was evident that an elevated value of L_e led to a decline in concentration

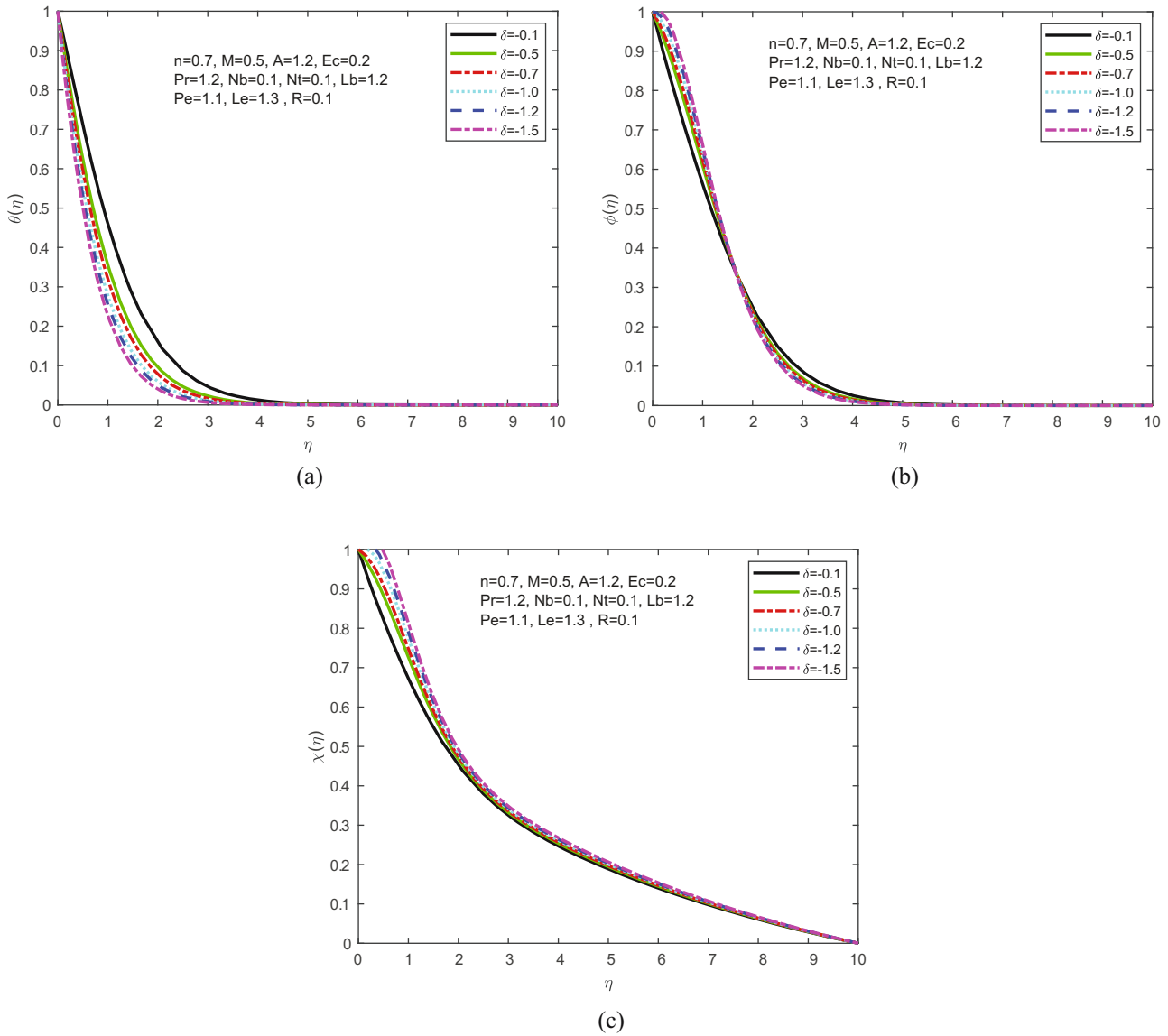


Figure 7: (a) θ vs δ , (b) ϕ vs δ , and (c) χ vs δ .

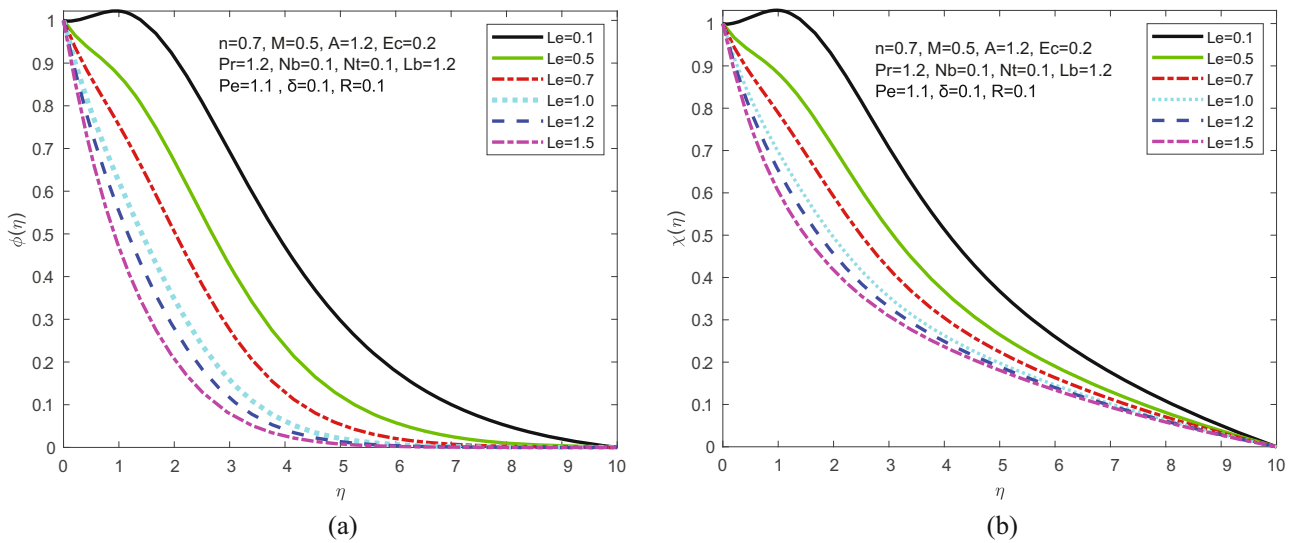


Figure 8: (a) ϕ vs Le and (b) χ vs Le .

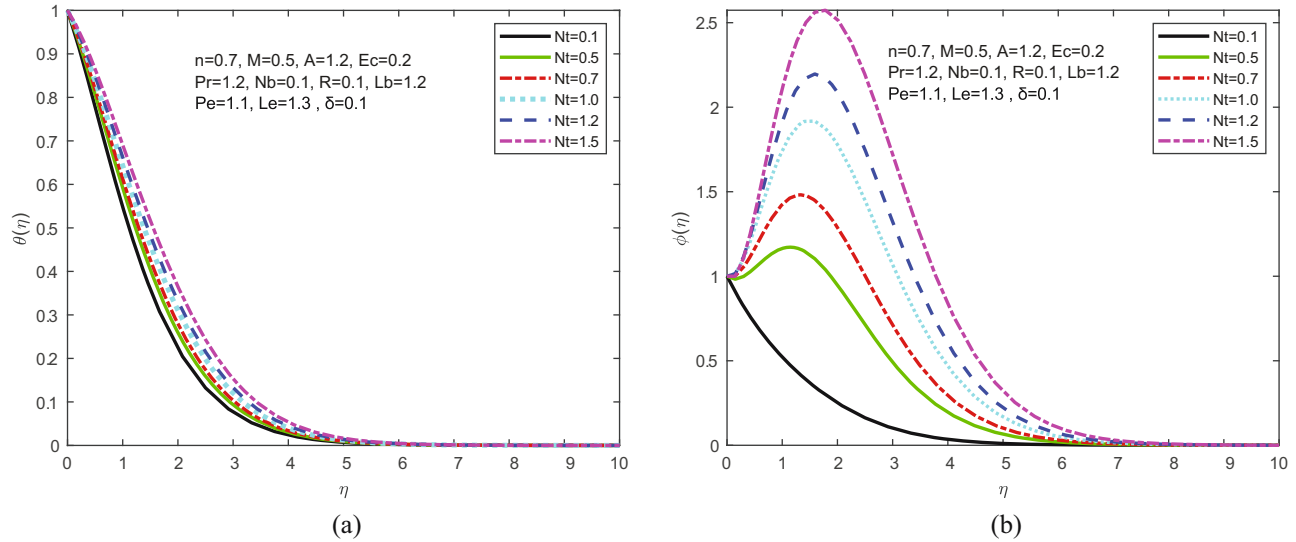


Figure 9: (a) θ vs N_t and (b) ϕ vs N_t .

profile, and on the other hand, the trend was reversed for the microorganism profile at $\eta \approx 1.2$. In the region where $\eta < 1.2$, the increase in L_e resulted in a decrease in the thickness of the microorganism boundary layers. while, for $\eta > 1.2$, the reverse trend was observed with increasing L_e . The effect of L_e on concentration is further illustrated in Figure 8(a), where it was observed that concentration decreased as L_e increased. The underlying explanation is that as L_e increases, mass diffusivity decreases, resulting in a reduction in the depth of penetration of the boundary layer.

4.8 Effect of N_t on temperature, nanoparticle concentration profile, and microorganism profiles

Variations in the thermophoresis parameter N_t are reflected in Figure 9(a) and (b), illustrating the impact on the

temperature and nanoparticle fraction curves. The results demonstrate that N_t has a significant impact on both temperature and nanoparticle fraction. This phenomenon occurs due to the increase in the thermal boundary layer density caused by the thermophoresis parameter. As observed in Figure 9(a), an increase in N_t results in an increase in temperature. The microscopic fluid particles involved in thermophoresis activities are drawn from the warm to the cold region, resulting in an improvement in temperature, thermal boundary layer, and nanoparticle volume fraction profiles. However, N_t has no impact on velocity and density curves of motile microorganism.

The local Nusselt number $[-\theta'(0)]$ for different parameters is compared with the results obtained by [15,33–35] in Table 1. It demonstrates excellent agreement between

Table 1: Comparison of local Nusselt number $-\theta'(0)$ for different values of P_T for $L_e = P_e = E_c = N_t = L_b = N_b = M = 0$

P_T	Ref. [15]	Ref. [33]	Ref. [34]	Ref. [35]	Current study
1	0.954782	0.954782	0.9547	0.954955	0.954779
1.5	1.234755				1.234823
2	1.471460		1.4714		1.471454
2.5	1.680229				1.680225
3	1.869073	1.869075	1.8691	1.869074	1.869072
5	2.500131	2.50013		2.500184	2.500139

Table 2: Comparison of Sherwood number $[-\phi'(0)]$ for different values of N_b , N_t , and P_T taking $L_e = P_e = E_c = L_b = 0$

N_b	N_t	P_T	$Sh_x n = 0$		$Sh_x n = 1$	
			Jawad <i>et al.</i> [36]	Current Study	Jawad <i>et al.</i> [36]	Current Study
0.1	0.5	1.5	-1.35820	-1.3479	-1.35938	-1.35859
0.5			-0.238811	-0.23792	-0.239002	-0.238092
1.0			-0.098888	-0.98742	-0.098954	-0.098879
1.5	0.1		0.0223188	0.022217	0.0223610	0.02228
	0.5		-1.35820	-1.35789	-1.35938	-1.35876
	1.0		-2.75366	-2.75306	-2.75610	-2.75532
	1.5		-4.14542	-4.14483	-4.14910	-4.14725
		3.0	-1.21912	-1.21754	-2.06224	-2.06212
		5.0	-1.53875	-1.53779	-2.45134	-2.45124

the current study and those obtained in the aforementioned studies.

Table 2 depicts the influence of Sherwood number due to various parameters. It is noticed that an elevation in the thermophoresis parameter causes an upward trend in local Sherwood number values, whereas an elevation in the Prandtl number results in a reduction in the Sherwood number.

5 Conclusions

In the current framework, this study investigates the MHD fluid flow of a dissipative Sisko nanofluid containing microorganisms moving along an exponentially stretched sheet. Using the *bvp4c* solver, numerical results for the converted mathematical model are calculated. The significant results are enumerated as follows:

- 1) Because of the inverse relationship between the material parameter (A) and the viscosity of the fluid. Observations from this study revealed that as the value of A increased, the fluid's viscosity decreased, resulting in a reduction in the resistance encountered during fluid motion. As a consequence, the fluid velocity increases.
- 2) Both temperature and nanoparticle fraction are significantly affected by the thermophoresis parameter (N_t). This phenomenon occurs because the increase in N_t increases the thermal boundary layer density.
- 3) When the Eckert number of a fluid increases, it indicates a higher rate of heat transfer. Microorganisms may experience a decrease in density as a consequence of thermal stress when exposed to elevated temperatures caused by increased heat transfer.
- 4) The increase in Prandtl number (P_r) resulted in a decrease in thermal diffusivity, hence causing a decline in the efficiency of energy transmission across the thermal boundary layer. The thickness of the concentration boundary layer demonstrated an increasing trend as the P_r grew.

Acknowledgments: The authors extend their appreciation to the Deanship of Scientific Research at King Khalid University (KKU) for funding this research through the Research Group Program under the grant number (R.G.P.2/453/44).

Funding information: This research is funded by the Deanship of Scientific Research at King Khalid University (KKU) for funding this research through the Research Group Program under the grant number (R.G.P.2/453/44).

Author contributions: All authors have accepted responsibility for the entire content of this manuscript and approved its submission.

Conflict of interest: The authors state no conflict of interest.

Data availability statement: All data generated or analysed during this study are included in this published article.

References

- [1] Shahid A, Huang H, Bhatti MM, Zhang L, Ellahi R. Numerical investigation on the swimming of gyrotactic microorganisms in nanofluids through porous medium over a stretched surface. *Mathematics*. 2020;8(3):380.
- [2] Choi SUS, Singer DA, Wang HP. Developments and applications of non-Newtonian flows. *ASME Fed*. 1995;66:99–105.
- [3] Buongiorno J. Convective transport in nanofluids. *J Heat Transf*. 2006;128:240–50.
- [4] Eastman JA, Choi US, Li S, Thompson LJ, Lee S. Enhanced thermal conductivity through the development of nanofluids. *MRS Proc*. 1996;457:3–11.
- [5] Sheikholeslami M, Ganji DD, Javed MY, Ellahi R. Effect of thermal radiation on magnetohydrodynamics nanofluid flow and heat transfer by means of two-phase model. *J Magn Magn Mater*. 2015;374:36–43.
- [6] Pourfattah F, Arani AAA, Babaie MR, Nguyen HM, Asadi A. On the thermal characteristics of a manifold microchannel heat sink subjected to nanofluid using two-phase flow simulation. *Int J Heat Mass Transf*. 2019;143:118518.
- [7] Asadi A, Aberoumand S, Moradikazerouni A, Pourfattah F, Żyła G, Estellé P, et al. Recent advances in preparation methods and thermophysical properties of oil-based nanofluids: A state-of-the-art review. *Powder Technol*. 2019;352:209–26.
- [8] Khan M, Shahid A, Malik MY, Salahuddin T. Thermal and concentration diffusion in Jeffery nanofluid flow over an inclined stretching sheet: A generalized Fourier's and Fick's perspective. *J Mol Liq*. 2018;251:7–14.
- [9] Asadi A, Alarifi IM, Ali V, Nguyen HM. An experimental investigation on the effects of ultrasonication time on stability and thermal conductivity of MWCNT-water nanofluid: Finding the optimum ultrasonication time. *Ultrason Sonochem*. 2019;58:104639.
- [10] Zeeshan A, Riaz A, Alzahrani F, Moqet A. Flow analysis of two-layer Nano/Johnson–Segalman fluid in a blood vessel-like tube with complex peristaltic wave. *Math Probl Eng*. 2022;2022:Article ID 5289401, 18.
- [11] Riaz A, Khan SU, Zeeshan A, Khan SU, Hassan M, Muhammad T. Thermal analysis of peristaltic flow of nanosized particles within a curved channel with second-order partial slip and porous medium. *J Therm Anal Calorim*. 2021;143:1997–2009.
- [12] Riaz A, Ellahi R, Sait SM, Muhammad T. Magnetized Jeffrey nanofluid with energy loss in between an annular part of two micro non-concentric pipes. *Energy Sources Part A: Recovery Util Environ Eff*. 2022;44(3):8314–33.
- [13] Tilili I, Nabwey HA, Ashwinkumar GP, Sandeep N. 3-D magnetohydrodynamic AA7072-AA7075/methanol hybrid nanofluid flow above an uneven thickness surface with slip effect. *Sci Rep*. 2020;10:1–13.

- [14] Chamkha AJ, Rashad AM, Alsabery AI, Abdelrahman ZMA, Nabwey HA. Impact of partial slip-on magneto-ferrofluids mixed convection flow in enclosure. *J Therm Sci Eng Appl.* 2020;12:051002.
- [15] Ferdows M, Nabwey HA, Rashad AM, Uddin MJ, Alzahrani F. Boundary layer flow of a nanofluid past a horizontal flat plate in a Darcy porous medium: A Lie group approach. *Proceedings of the Institution of Mechanical Engineers, Part C: Journal of Mechanical Engineering Science*; 2019.
- [16] Kuznetsov AV. Bio-thermal convection induced by two different species of microorganisms. *Int Commun Heat Mass Transf.* 2011;38:548–53.
- [17] Alloui Z, Nguyen TH, Bilgen E. Bioconvection of gravitactic microorganisms in a vertical cylinder. *Int Commun Heat Mass Transf.* 2005;32:739–47.
- [18] Waqas H, Hussain M, Alqarnib MS, Eid MR, Muhammad T. Numerical simulation for magnetic dipole in bioconvection flow of Jeffery nanofluid with swimming motile microorganisms. *Waves Random Complex Media.* 2021;3:1–18.
- [19] Waqas H, Imran M, Muhammad T, Salt SM, Ellahi R. Numerical investigation on bioconvection flow of Oldroyd-B nanofluid with non-linear thermal radiation and motile microorganisms over rotating disk. *J Therm Anal Calor.* 2021;145:523–39.
- [20] Uddin MJ, Kabir MN, Bég OA. Computational investigation of Stefan blowing and multiple-slip effects on buoyancy-driven bioconvection nanofluid flow with microorganisms. *Int J Heat Mass Transf.* 2016;95:116–30.
- [21] Chamkha AJ, Rashad AM, Kameswaran PK, Abdou MMM. Radiation effects on natural bioconvection flow of a nanofluid containing gyrotactic microorganisms past a vertical plate with streamwise temperature variation. *J Nanofluids.* 2017;6:587–95.
- [22] Rashad AM, Nabwey HA. Gyrotactic mixed bioconvection flow of a nanofluid past a circular cylinder with convective boundary condition. *J Taiwan Inst Chem Eng.* 2019;99:9–17.
- [23] Alwatban AM, Khan SU, Waqas H, Tlili I. Interaction of Wu's slip features in bioconvection of Eyring Powell nanoparticles with activation energy. *Process.* 2019;7:859.
- [24] Aziz A, Khan WA, Pop I. Free convection boundary layer flow past a horizontal flat plate embedded in porous medium filled by nanofluid containing gyrotactic microorganisms. *Int J Therm Sci.* 2012;56:48.
- [25] Shaw S, Sandile Motsa S, Sibanda P. Magnetic field and viscous dissipation effect on bioconvection in a permeable sphere embedded in a porous medium with a nanofluid containing gyrotactic micro-organisms. *Heat Transf – Asian Res.* 2018;47:718–34.
- [26] Rashad AM, Chamkha A, Mallikarjuna B, Abdou MMM. Mixed bioconvection flow of a nanofluid containing gyrotactic microorganisms past a vertical slender cylinder. *Front Heat Mass Transf.* 2018;10. <http://dx.doi.org/10.5098/hmt.10.21>.
- [27] Elboughdiri N, Reddy CS, Alshehri A, Eldin SM, Muhammad T, Wakif A. A passive control approach for simulating thermally enhanced Jeffery nanofluid flows nearby a sucked impermeable surface subjected to buoyancy and Lorentz forces. *Case Stud Therm Eng.* July 2023;47:103106.
- [28] Sharma J, Ahammad NA, Wakif A, Shah NA, Chung JD, Weera W. Solutal effects on thermal sensitivity of casson nanofluids with comparative investigations on Newtonian (water) and non-Newtonian (blood) base liquids. *Alex Eng J.* May 2023;71:387–400.
- [29] Wakif A. Numerical inspection of two-dimensional MHD mixed bioconvective flows of radiating Maxwell nanofluids nearby a convectively heated vertical surface. *Waves Random Complex Media.* 2023;1–22. doi: 10.1080/17455030.2023.2179853.
- [30] Puneeth V, Sarpabhusana M, Anwar MS, Aly EH, Gireesha BJ. Impact of bioconvection on the free stream flow of a pseudoplastic nanofluid past a rotating cone. *Heat Transf.* 2022;51(5):4544–61.
- [31] Jan A, Mushtaq M, Farooq U, Hussain M. Nonsimilar analysis of magnetized Sisko nanofluid flow subjected to heat generation/absorption and viscous dissipation. *J Magnetism Magnetic Mater.* 2022;564(2):170153.
- [32] Ferdows M, Zaimi K, Rashad AM, Nabwey HA. MHD bioconvection flow and heat transfer of nanofluid through an exponentially stretchable sheet. *Symmetry.* 2020;12:692.
- [33] Magyari E, Keller B. Heat and mass transfer in the boundary layers on an exponentially stretching continuous surface. *J Phys D Appl Phys.* 1999;32:577–85.
- [34] Biliana B, Nazar R. Numerical solution of the boundary layer flow over an exponentially stretching sheet with thermal radiation. *Eur J Sci Res.* 2009;33:710–7.
- [35] Loganathan P, Vimala C. MHD flow of nanofluids over an exponentially stretching sheet embedded in a stratified medium with suction and radiation effects. *J Appl Fluid Mech.* 2015;8:85–93.
- [36] Jawad M, Shah Z, Islam S, Khan W, Khan AZ. Nanofluid thin film flow of Sisko fluid and variable heat transfer over an unsteady stretching surface with external magnetic field. *J Algorithms Comput Technol.* 2019;1748301819832456.